

Reprint Compendium

Bio-protocol Cell Imaging

A Special Collection for Cell Bio 2023

bio-protocol

Bio-protocol Cell Imaging

A Special Collection for Cell Bio 2023

Collection Editor

Marion Hogg

Editor-in-chief

Caroline Shamu

Associate Editors

Alexandros Alexandratos
Pilar Villacampa Alcubierre
Chiara Ambrogio
Ralph Thomas Boettcher
Alessandro Didonna
Xi Feng
Gal Haimovich
Jan Huebinger
Aswad Khadilkar
David Paul
Rajesh Ranjan
Kristin L. Shingler
Giusy Tornillo
Zinan Zhou

Managing Editor

Marisa Rosa

Executive Editor

Rae Tian

Foreword

We are pleased to release *Bio-protocol Cell Imaging: A Special Collection for Cell Bio 2023*, featuring some of the most used cell imaging protocols published in *Bio-protocol* journal between 2021 and 2023. Timed for release at the start of the Cell Bio 2023 conference in Boston, this collection should be an excellent resource for cell biology researchers worldwide.

Bio-protocol was founded in 2011 by a group of researchers at Stanford University with a singular mission: Improving research reproducibility by publishing high-quality, step-by-step protocols. Since then, we have published more than 4,800 protocols, authored by 20,000+ scientists. Annual user surveys have shown that, for more than 3000 users who have followed a protocol published in *Bio-protocol*, 91% were able to successfully reproduce the protocol they tried. *Bio-protocol* articles are listed in PubMed Central and indexed in Web of Science (ESCI).

In this reprint collection, we have selected cell imaging protocols published in *Bio-protocol* recently that we consider the most highly used. We base this classification on metrics such as the number of times a protocol was viewed or downloaded by unique users, and the number of citations it has received in other publications.

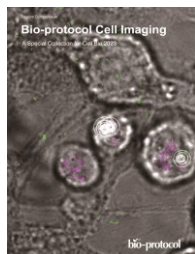
We hope that you will find this collection helpful and visit www.bio-protocol.org to check out our full protocol archive. Feel free to email us (eb@bio-protocol.org) with feedback, and please consider publishing a protocol in *Bio-protocol* in the future.

The *Bio-protocol* Editorial Team

Table of Contents

Preparation of Whole-mount Mouse Islets on Vascular Extracellular Matrix for Live Islet Cell Microscopy	1
Correlative Conventional and Super-resolution Photoactivated Localization Microscopy (PALM) Imaging to Characterize Chromatin Structure and Dynamics in Live Mammalian Cells.....	10
Protein Level Quantification Across Fluorescence-based Platforms.....	27
Intravital Imaging of Intestinal Intraepithelial Lymphocytes	44
Optogenetic Induction of Pyroptosis, Necroptosis, and Apoptosis in Mammalian Cell Lines.....	61
Visualizing Loss of Plasma Membrane Lipid Asymmetry Using Annexin V Staining.....	77
Quantifying Single and Dual Channel Live Imaging Data: Kymograph Analysis of Organelle Motility in Neurons.....	92
Dual-Color Live Imaging of Adult Muscle Stem Cells in the Embryonic Tissues of <i>Drosophila melanogaster</i>	103
Measuring Intracellular H ₂ O ₂ in Intact Human Cells Using the Genetically Encoded Fluorescent Sensor HyPer7	111
Visualization, Quantification, and Modeling of Endogenous RNA Polymerase II Phosphorylation at a Single-copy Gene in Living Cells.....	123
Patterned Substrate of Mobile and Immobile Ligands to Probe EphA2 Receptor Clustering	144
CRISPR/Cas9 Gene Editing of HeLa Cells to Tag Proteins with mNeonGreen	152
Single Molecule Tracking Nanoscopy Extended to Two Colors with MTT2col for the Analysis of Cell-Cell Interactions in Leukemia	170

Activation of Mitochondrial Ca ²⁺ Oscillation and Mitophagy Induction by Femtosecond Laser Photostimulation	183
High-speed Atomic Force Microscopy Observation of Internal Structure Movements in Living <i>Mycoplasma</i>	198
Laser Microirradiation and Real-time Recruitment Assays Using an Engineered Biosensor	206
Spherical Invasion Assay: A Novel Method to Measure Invasion of Cancer Cells.....	217
An Alternative Technique for Monitoring the Live Interaction of Monocytes and Tumor Cells with Nanoparticles in the Mouse Lung	230
A Multi-color Bicistronic Biosensor to Compare the Translation Dynamics of Different Open Reading Frames at Single-molecule Resolution in Live Cells.....	240
Monitoring Changes in the Oxidizing Milieu in the Endoplasmic Reticulum of Mammalian Cells Using HyPerER	261
Building a Total Internal Reflection Microscope (TIRF) with Active Stabilization (Feedback SMLM)	269
Retention Using Selective Hooks (RUSH) Cargo Sorting Assay for Live-cell Vesicle Tracking in the Secretory Pathway Using HeLa Cells.....	284
Generation and Implementation of Reporter BHK-21 Cells for Live Imaging of Flavivirus Infection	269
Carboxyfluorescein Dye Uptake to Measure Connexin-mediated Hemichannel Activity in Cultured Cells	316
Imaging of Human Cancer Cells in 3D Collagen Matrices	330



On the Cover:

Image from protocol “Single Molecule Tracking Nanoscopy Extended to Two Colors with MTT2col for the Analysis of Cell-Cell Interactions in Leukemia.”

DOI: 10.21769/BioProtoc.4390

Preparation of Whole-mount Mouse Islets on Vascular Extracellular Matrix for Live Islet Cell Microscopy

Kung-Hsien Ho¹, Guoqiang Gu^{1, 2, *} and Irina Kaverina^{1, *}

¹Department of Cell and Developmental Biology, Vanderbilt University, Nashville, TN, USA

²Program in Developmental Biology and Center for Stem Cell Biology, Vanderbilt University, Nashville, TN, USA

*For correspondence: guoqiang.gu@vanderbilt.edu; irina.kaverina@vanderbilt.edu

Abstract

Pancreatic islet β cells preferentially secrete insulin toward the plasma membrane, making contact with the capillary extracellular matrix (ECM). Isolated islets separated from the exocrine acinar cells are the best system for cell biology studies of primary β cells, whereas isolated islets lose their capillary network during ex vivo culture. Providing the appropriate extracellular signaling by attaching islets to vascular ECM-coated surfaces can restore the polarized insulin secretion toward the ECM. The guided secretion toward ECM-coated glass coverslips provides a good model for recording insulin secretion in real time to study its regulation. Additionally, β cells attached to the ECM-coated coverslips are suitable for confocal live imaging of subcellular components including adhesion molecules, cytoskeleton, and ion channels. This procedure is also compatible for total internal reflection fluorescence (TIRF) microscopy, which provides optimal signal-to-noise ratio and high spatial precision of structures close to the plasma membrane. In this article, we describe the optimized protocol for vascular ECM-coating of glass coverslips and the process of attachment of isolated mouse islets on the coverslip. This preparation is compatible with any high-resolution microscopy of live primary β cells.

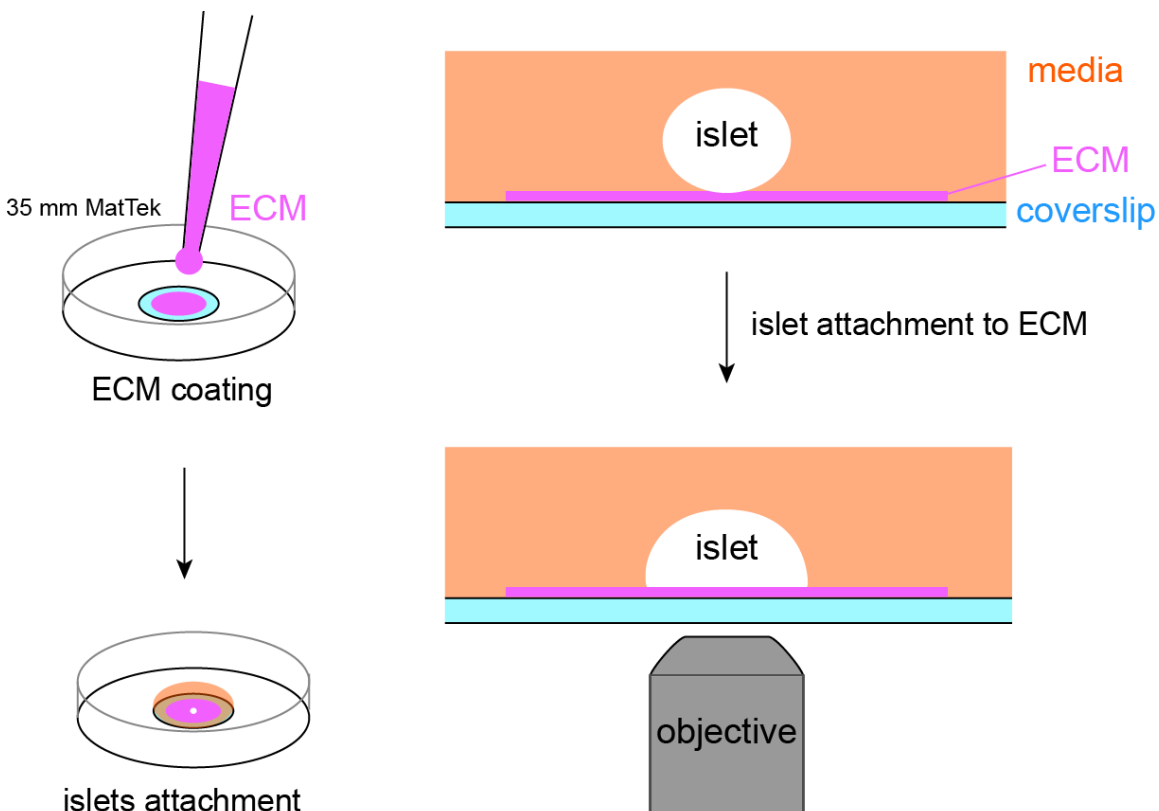
Key features

- Optimized coating procedure to attach isolated islets, compatible for both confocal and TIRF microscopy.
- The ECM-coated glass coverslip functions as the artificial capillary surface to guide secretion toward the coated surface for optimal imaging of secretion events.
- Shows the process of islets attachment to the ECM-coated surface in a 6-day ex vivo culture.

Keywords: Pancreatic β cells, Islet attachment, Islet ex vivo culture, Islet flattening, Human ECM, Live islet cells visualization

This protocol is used in: eLife (2021), DOI: 10.7554/eLife.59912

Graphical overview



Background

Pancreatic β cells regulate blood glucose homeostasis by secreting insulin to the blood stream in response to elevated glucose levels. The secretion of insulin is tightly regulated to prevent over-secretion, which causes hypoglycemia, or under-secretion, which in the long term leads to diabetes. Islet β cells preferentially secrete insulin toward the plasma membrane, making contact with the capillary extracellular matrix (ECM) or basement membrane (Low et al., 2014; Gan et al., 2018). Isolated islets lose their capillaries and the polarity of β cells during ex vivo culture. When studying β -cells secretion, recording secretion events on the plasma membrane making contact with the vascular ECM can better recapitulate the polarized insulin secretion of β cells in vivo. Coating coverslips with human ECM, derived from placenta and containing the main components of vascular ECM, is an ideal surface for islet attachment to study insulin secretion (Patterson et al., 2000; Arous and Wehrle-Haller, 2017; Barillaro et al., 2022). The coated coverslip functions as the artificial capillary surface to guide the secretion of attached islet β cells toward it and is suitable for high-resolution imaging to record secretion events.

Total internal reflection fluorescence (TIRF) microscopy is a powerful tool to study subcellular structures in attached β cells, such as adhesion molecules, cortical actin cytoskeleton, ion channels, and lipids in the plasma membrane. Another powerful application of TIRF microscopy is to record insulin secretion from individual β cells in real time. Multiple studies have reported different approaches to labeling insulin vesicles (Ma et al., 2004; Ivanova et al., 2013; Schifferer et al., 2017). Integration of an engineered insulin fusion probe to the genome of β cells in isolated rodent or human islets is usually technically challenging. Label-free approaches bypass this challenge and the possibility that a fluorescence probe may interfere with the maturation or secretion of insulin (Pouli et al., 1998; Schifferer et al., 2017). Successful label-free recording of insulin exocytosis has been reported using either two-photon microscopy or correlative scanning ion conductance microscopy-fluorescence confocal microscopy (Takahashi et al., 2002; Bednarska et al., 2021). Our lab has previously established a novel label-free approach to record insulin

secretion using TIRF microscopy and a cell-impermeable zinc-sensitive fluorescence dye, FluoZin™-3 (Gee et al., 2002; Zhu et al., 2015). The fusion of individual insulin vesicles to the plasma membrane transiently elevates local zinc concentration, which activates FluoZin™-3 to emit fluorescence upon excitation. This strategy allows visualization of insulin secretion at the cell–ECM interface with high spatial precision in real time. The conventional coating procedure for islet attachment and confocal microscopy includes a layer of matrigel between the coverslip and the ECM-coating. The matrigel layer provides a three-dimensional-like cushion to facilitate islet attachment but is not compatible with TIRF microscopy due to its thickness. In this article, we describe the details of an optimized ECM-coating and attachment of isolated islets on glass coverslips, which is compatible with TIRF microscopy and any high-resolution live-cell microscopy.

Materials and reagents

1. Mice [*GFP-Lifeact; Ins2^{Apple}*, 12–20 weeks (Riedl et al., 2008; Stancill et al., 2019)]
2. Human extracellular matrix (ECM) (Corning, catalog number: 354237)
3. Fetal bovine serum (FBS) (Atlanta Biologicals, catalog number: S11550)
4. RPMI 1640 (Gibco, catalog number: 11875)
5. Penicillin-Streptomycin solution (Pen-Strep) (Gibco, catalog number: 15140)
6. Nalgene™ Rapid-Flow™ Sterile Disposable Filter Units, 0.2 µm PES membrane (Thermo Fisher Scientific, catalog number: 569-0020)
7. Hanks' Balanced Salt Solution with calcium & magnesium (HBSS) (Gibco, catalog number: 21-020-CV)
8. Collagenase from *Clostridium histolyticum* (Millipore Sigma, catalog number: C5138, lot number: 0000164940)
9. Islet media (see Recipes)
10. Collagenase solution (see Recipes)
11. ECM coating solution (see Recipes)

Recipes

1. Islet media

RPMI-1640 (the media contains 11 mM glucose)

10% heat-inactivated FBS

100 U/mL penicillin-100 mg/mL streptomycin

Filter the media through a 0.2 µm PES membrane, store at 4 °C, and used within one month of preparation.

2. Collagenase solution

0.5 mg/mL collagenase in HBSS

Store aliquots (1 mL) of the prepared solution at -20 °C for up to one year.

3. ECM coating solution

9 µg/mL ECM in islet media

Store aliquots (100 µL) of the prepared solution at -20 °C for up to two years.

Equipment

1. Plasma cleaner (Harrick Plasma, model: PDC-001)
2. Nikon A1R laser scanning confocal microscope
3. CFI Apochromat TIRF 100×/1.45 oil objective (Nikon)
4. Olympus SZH10 dissection scope
5. MatTek glass bottom dishes, 35 mm dish, 10 mm microwell (MatTek, catalog number: P35G-1.5-10-C)
6. 150 mm dish (Corning, catalog number: 430599)

7. Tissue wipers (VWR, catalog number: 82003-820)
8. 5 mL syringe (BD, catalog number: 309646)
9. Needle [BD, catalog numbers: 305109 (27 G 1/2) and 305106 (30 G 1/2)]
10. 50 mL centrifuge tubes (VWR, catalog number: 525-1075)
11. Precision water bath (Precision Scientific, Model 182)
12. 60-mm polystyrene Petri dish (Thermo Fisher Scientific, catalog number: AS4052)
13. Water-jacked CO₂ incubator (NuAire, model: NU-8700 series 5)

Procedure

Day 0

1. The collagenase digestion of mouse pancreas and islet isolation follows the published procedure (Li et al., 2009; Ho et al., 2023). Briefly, mouse pancreata are injected with 2 mL of collagenase solution (see Recipes) using a 5 mL syringe and a 27 G 1/2 needle (or a 30 G 1/2 needle for smaller mice) through the common bile duct. The pancreata are digested in a 50 mL centrifuge tube in a water bath at 37 °C for 16 min with gentle shaking every 4 min. The digested homogenate is washed using 10 mL (per animal's pancreata) of chilled islet media (see Recipes) with vigorous shaking and centrifuged at 700×*g* for 2 min at 4 °C. Islets are hand-picked using a P20 pipette with 200 µL tips to a 60 mm Petri dish with islet media under a dissection scope. Repeat the picking three times to separate islets from pancreatic acinar cells (Note 1). The isolated islets are incubated in a water-jacked incubator with 5% CO₂ (Note 2).
2. Remove the lid and place the 35 mm MatTek dish with a 10 mm microwell in the plasma cleaner. Seal the chamber and establish vacuum. Set the RF (radio frequency) level to medium and initiate the cleaning for 1 min (Note 3). Place the lid back immediately after retrieving the dish from the cleaner. The plasma-cleaned MatTek dish can be stored in its packaging sleeve for six months at room temperature, but a coated dish is for immediate use.
3. Coat the coverslip of a plasma-cleaned MatTek dish by applying a small volume (~5 µL) of ECM coating solution (see Recipes) to the center of the coverslip (Figure 1A). When coating MatTek dishes, instead of measuring the exact volume of coating solution for each dish, we use a P100 pipette holding enough coating solution, push out a small amount of solution from the tip, smear it on the area to be coated, and suck excess solution back to the tip. This ensures the coating is not too thick to interfere with the downstream TIRF microscopy. We do not coat the entire coverslip to reduce the chance of an islet attaching to the edge of the microwell.

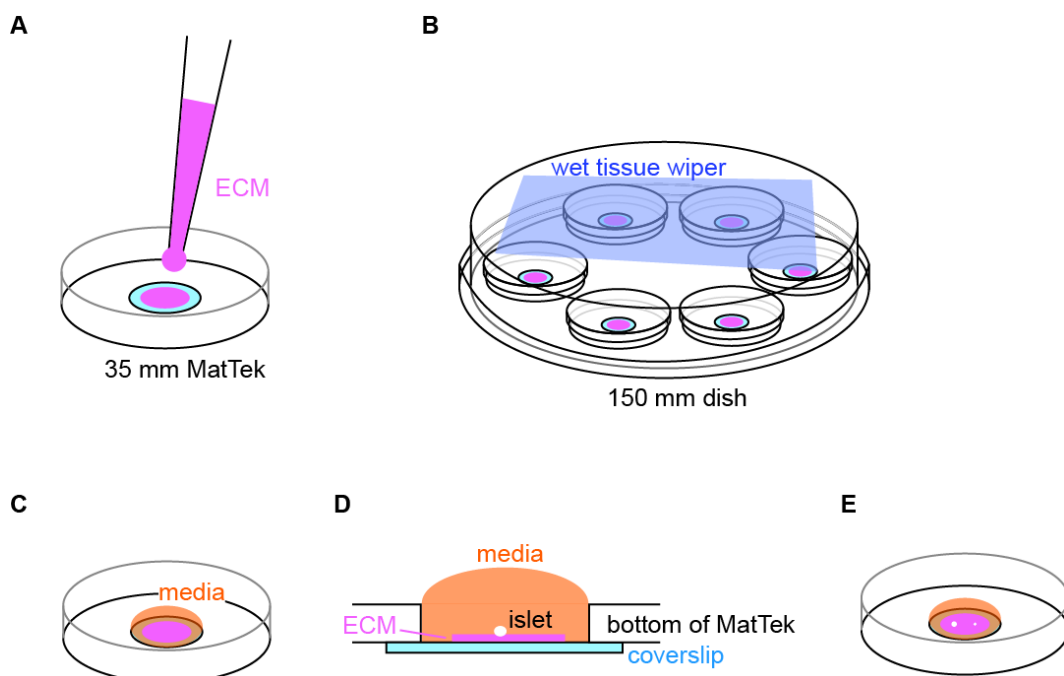


Figure 1. Illustration of coating and setup for islet attachment. (A) Schematic of coating of extracellular matrix (ECM) to the center of coverslip. (B) Schematic of MatTek dishes arrangement in a humidified 150 mm dish. (C) Schematic of media added and contained inside the microwell. (D) Side view of the MatTek dish showing the media contained inside the microwell. (E) Schematic showing two islets of different size plated per MatTek dish.

4. Cover the MatTek dish with its own lid and place it on the lid of a 150 mm dish. Create a humidified chamber by placing a sheet of tissue wiper wetted with distilled water on the bottom of the 150 mm dish and place the MatTek dish inside such that the tissue is at the top of the chamber (Figure 1B). Incubate at 37 °C in a water-jacketed incubator for 10 min to allow ECM coating on the coverslip.
5. Wash the coated coverslip once by pipetting 100 µL of islet media to the microwell and aspirate it from its edge that is not coated with ECM. Refill the microwell with 100 µL of islet media (Figure 1C). During washing and refilling, the media should be contained inside the microwell. This helps to retain the surface tension of islet media and constrain islet attachment inside the microwell (Figure 1D). If the media covers the plastic dish bottom, the planted islets may float out of the microwell and attach to the plastic.
6. Under a dissection scope, transfer 1–2 islets to the center of the microwell using a P20 pipette (Figure 1E) (Note 4).
7. Place the MatTek dish in the 150 mm dish (the humidified chamber) and carefully move it to the incubator (Figure 1B). Choose islets smaller than 120 µm in diameter for better dye penetration to the space between the islet attachment surface and the coverslip in downstream imaging. Without a wet tissue wiper inside the 150 mm dish, the small volume of 100 µL of islet media will dry out overnight even in a water-jacketed incubator (Note 5).
8. Incubate it for two days. There is no need to replace media or take the MatTek dish out to check the status of islets before day 2 (see below). To follow the attachment process on the ECM-coated coverslip, islets isolated from the *GFP-Lifeact; Ins2^{Apple}* mouse (Riedl et al., 2008; Stancill et al., 2019) are shown here. GFP-Lifeact labels cortical actin to delineate cell borders and *Ins2^{Apple}* (*Ins2* promoter driven H2B-mApple) marks β cells (Figure 2A). Approximately 70% of islets loosely attach to the ECM overnight (Figure 2B–2C). Taking the MatTek dish incubated overnight out for observation can easily stir up those loosely attached islets. Most islets (~90%) are firmly attached to the ECM after two nights.

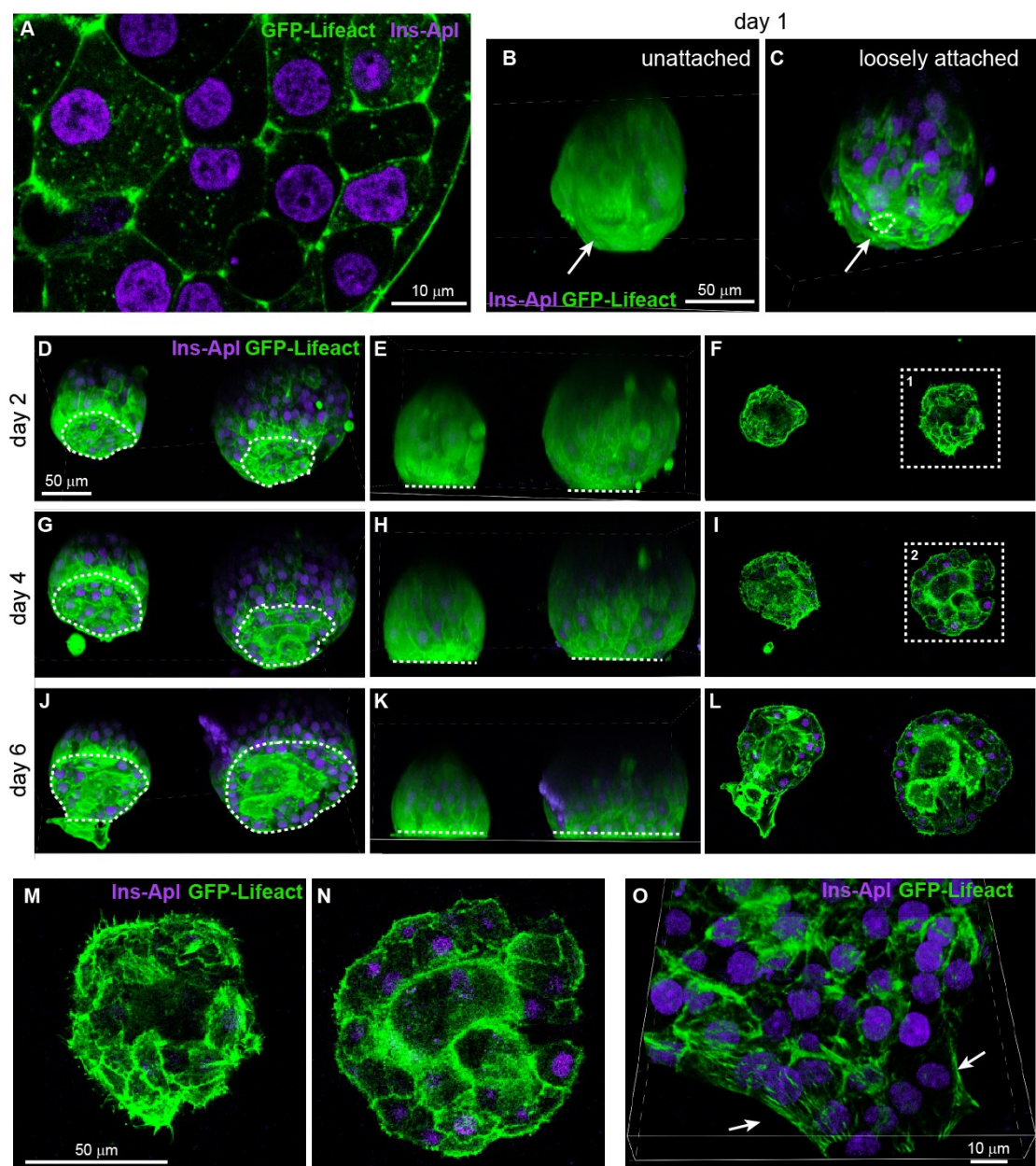


Figure 2. Attachment and flattening process of isolated mouse islets. (A) Single slice of confocal microscopy image of an islet isolated from the *GFP-Lifeact; Ins2^{Apple}* mouse. GFP-Lifeact (green) delineates cell borders and β -cells nuclei are labeled by *Ins2^{Apple}* (magenta). (B–C) Projected images of isolated islets incubated on extracellular matrix (ECM)-coated coverslip for one day. Dashed line delineates the attachment site of an islet. Arrow indicates the side in contact with the coverslip. (D–N) Confocal images of isolated islets incubated on ECM-coated coverslip for 2–6 days. D, G, and J show projected images. E, H, and K show the side view of the projected images. F, I, and L show single slice of confocal images at the z-plane of attachment. M and N show the enlargement of image at dashed square 1 and 2 respectively. Dashed lines delineate the attachment sites of islets (D, G, and J) or represent the location of coverslips (E, H, and K). (O) Projected image of an isolated islet attached to ECM-coated coverslip and flattened to single-cell-layer thickness at the periphery of the islet. Arrows indicate the periphery of the flattened islet.

Day 2

1. Take the dish out from the incubator and gently add 150 μ L of islet media from the edge of the microwell under a dissection scope. Because the majority of islets have now attached to the ECM on the coverslip, they are resistant to minor vibrations while moving the dish and it is okay to let the media exceed the microwell (Figure 2D–2F and 2M). Do not remove old media before adding the 150 μ L of fresh media. If the media is removed and then replaced, attached islets will be lifted up above the surface of media. For this reason, there should be no media change during the entire ex vivo culture of attached islets. Instead, we add more fresh media to the dish every other day.
2. Incubate the attached islets for two more days.

Day 4

Gently add 500 μ L of islet media from the edge of the microwell. The media will overflow from the microwell to the plastic dish bottom at this point. Islets are firmly attached to the ECM and will not float out of the microwell (Figure 2G–2I and 2N). The MatTek dish can hold 2 mL of media. The attached islets can be subjected to microscopy from day 4 to day 6.

Day 6

Islets attached firmly and further expanded their surfaces attached to the ECM. The area of attachment reaches 85%–90% of the hemispherical cross section area of an islet (Figure 2J–2L). It is noteworthy that the so-called “flattening” of isolated mouse islets refers only to the surface attached to the ECM-coated coverslip. The rest of the islet retains its spherical appearance even after 6 days of ex vivo culture. This is likely due to residual extracellular matrix (the peripheral capsule) surrounding an isolated mouse islet that maintains its spherical shape. Approximately 5% of attached islets can be fully flattened on a coated coverslip, likely due to incomplete peripheral capsule, and the islet periphery can reach single-cell-layer thickness (Figure 2O). The majority of attached islets with a hemispherical shape is suitable for live imaging using confocal or TIRF microscopy (Zhu et al., 2015; Trogden et al., 2021).

Validation of protocol

This protocol or parts of it has been used and validated in the following research article(s):

- Trogden, K.P., Lee, J., Bracey, K.M., Ho, K.H., McKinney, H., Zhu, X., Arpag, G., Folland, T.G., Osipovich, A.B., Magnuson, M.A., Zanic, M., Gu, G., Holmes, W.R., Kaverina, I. (2021). Microtubules regulate pancreatic β -cell heterogeneity via spatiotemporal control of insulin secretion hot spots. *eLife* (Figure 2).
- Zhu, X., Hu, R., Brissova, M., Stein, R.W., Powers, A.C., Gu, G., Kaverina, I. (2015). Microtubules Negatively Regulate Insulin Secretion in Pancreatic β Cells. *Dev. Cell.* (Figure 2, panel C–F).

Notes

1. A 10 μ L tip may injure large islets during picking and transferring. We usually can obtain 200–300 islets from one mouse using this procedure. Do not use cell culture dish to incubate isolated islets to prevent their attachment to the dish.
2. The isolated islets are incubated in 3 mL of islet media in a 60 mm Petri dish overnight for recovery. The islet number should not exceed 100 per dish to minimize the formation of hypoxia core (necrosis due to insufficient O₂) in larger islets.
3. The 10 mm microwell reduces the search time for an attached islet on a TIRF microscope and provides enough room for islets to attach to the glass coverslip instead of the edge of the microwell.

4. By choosing two islets with clear size difference, e.g., a mid-sized islet with a diameter of 100–120 μm and a small islet with a diameter of 60–80 μm , these two islets can be distinguished under the microscope without diamond pen marking on the coverslip.
5. Ideally, each 150 mm dish accommodates no more than six MatTek dishes to reduce the chance of knocking nearby MatTek dishes over while retrieving one.

Acknowledgments

This work is supported by National Institutes of Health, grants R01-DK106228 (to IK and GG), R35-GM127098 (to IK), and P30-DK020593-44S1 (to KHH). We thank Margret Fye for constructive feedback on the manuscript. This protocol was derived from the original work of Trogden et al. (2021).

Competing interests

The authors declare no competing interests.

References

- Arous, C. and Wehrle-Haller, B. (2017). [Role and impact of the extracellular matrix on integrin-mediated pancreatic \$\beta\$ -cell functions](#). *Biol. Cell* 109(6): 223–237.
- Barillaro, M., Schuurman, M. and Wang, R. (2022). [Collagen IV- \$\beta\$ 1-Integrin Influences INS-1 Cell Insulin Secretion via Enhanced SNARE Protein Expression](#). *Front. Cell Dev. Biol.* 10: e894422.
- Bednarska, J., Novak, P., Korchev, Y., Rorsman, P., Tarasov, A. I., and Shevchuk, A. (2021). [Release of insulin granules by simultaneous, high-speed correlative SICM-FCM](#). *J. Microsc.* 282(1): 21–29.
- Gan, W. J., Do, O. H., Cottle, L., Ma, W., Kosobrodova, E., Cooper-White, J., Bilek, M. and Thorn, P. (2018). [Local Integrin Activation in Pancreatic \$\beta\$ Cells Targets Insulin Secretion to the Vasculature](#). *Cell Rep.* 24(11): 2819–2826.e3.
- Gee, K. R., Zhou, Z. L., Qian, W. J. and Kennedy, R. (2002). [Detection and Imaging of Zinc Secretion from Pancreatic \$\beta\$ -Cells Using a New Fluorescent Zinc Indicator](#). *J. Am. Chem. Soc.* 124(5): 776–778.
- Ho, K. H., Jayathilake, A., Mahircan, Y., Nour, A., Osipovich, A. B., Magnuson, M. A., Gu, G. and Kaverina, I. (2023). [CAMSAP2 localizes to the Golgi in islet \$\beta\$ -cells and facilitates Golgi-ER trafficking](#). *iScience* 26(2): 105938.
- Ivanova, A., Kalaidzidis, Y., Dirkx, R., Sarov, M., Gerlach, M., Schroth-Diez, B., Müller, A., Liu, Y., Andree, C., Mulligan, B., et al. (2013). [Age-Dependent Labeling and Imaging of Insulin Secretory Granules](#). *Diabetes* 62(11): 3687–3696.
- Li, D. S., Yuan, Y. H., Tu, H. J., Liang, Q. L. and Dai, L. J. (2009). [A protocol for islet isolation from mouse pancreas](#). *Nat. Protoc.* 4(11): 1649–1652.
- Low, J. T., Zavortink, M., Mitchell, J. M., Gan, W. J., Do, O. H., Schwiening, C. J., Gaisano, H. Y. and Thorn, P. (2014). [Insulin secretion from beta cells in intact mouse islets is targeted towards the vasculature](#). *Diabetologia* 57(8): 1655–1663.
- Ma, L., Bindokas, V. P., Kuznetsov, A., Rhodes, C., Hays, L., Edwardson, J. M., Ueda, K., Steiner, D. F. and Philipson, L. H. (2004). [Direct imaging shows that insulin granule exocytosis occurs by complete vesicle fusion](#). *Proc. Natl. Acad. Sci. U. S. A.* 101(25): 9266–9271.
- Patterson, G. H., Knobel, S. M., Arkhammar, P., Thastrup, O. and Piston, D. W. (2000). [Separation of the glucose-stimulated cytoplasmic and mitochondrial NAD\(P\)H responses in pancreatic islet \$\beta\$ cells](#). *Proc. Natl. Acad. Sci. U. S. A.* 97(10): 5203–5207.
- Pouli, A. E., Kennedy, H. J., Schofield, J. G., and Rutter, G. A. (1998). [Insulin targeting to the regulated secretory pathway after fusion with green fluorescent protein and firefly luciferase](#). *Biochem. J.* 331(2): 669–675.

Cite as: Ho, K. H. et al. (2023). Preparation of Whole-Mount Mouse Islets on Vascular Extracellular Matrix for Live Islet Cell Microscopy. Bio-protocol 13(21): e4868. DOI: 10.21769/BioProtoc.4868.

- Riedl, J., Crevenna, A. H., Kessenbrock, K., Yu, J. H., Neukirchen, D., Bista, M., Bradke, F., Jenne, D., Holak, T. A., Werb, Z., et al. (2008). [Lifeact: a versatile marker to visualize F-actin](#). *Nat. Methods* 5(7): 605–607.
- Schifferer, M., Yushchenko, D. A., Stein, F., Bolbat, A. and Schultz, C. (2017). [A Ratiometric Sensor for Imaging Insulin Secretion in Single \$\beta\$ Cells](#). *Cell Chem. Biol.* 24(4): 525–531.e4.
- Stancill, J. S., Osipovich, A. B., Cartailler, J. P. and Magnuson, M. A. (2019). [Transgene-associated human growth hormone expression in pancreatic \$\beta\$ -cells impairs identification of sex-based gene expression differences](#). *Am. J. Physiol. Endocrinol. Metab.* 316(2): E196–E209.
- Takahashi, N., Kishimoto, T., Nemoto, T., Kadowaki, T. and Kasai, H. (2002). [Fusion Pore Dynamics and Insulin Granule Exocytosis in the Pancreatic Islet](#). *Science* 297(5585): 1349–1352.
- Trosgden, K. P., Lee, J., Bracey, K. M., Ho, K. H., McKinney, H., Zhu, X., Arpag, G., Folland, T. G., Osipovich, A. B., Magnuson, M. A., et al. (2021). [Microtubules regulate pancreatic \$\beta\$ -cell heterogeneity via spatiotemporal control of insulin secretion hot spots](#). *eLife* 10: e59912.
- Zhu, X., Hu, R., Brissova, M., Stein, R. W., Powers, A. C., Gu, G. and Kaverina, I. (2015). [Microtubules Negatively Regulate Insulin Secretion in Pancreatic \$\beta\$ Cells](#). *Dev. Cell* 34(6): 656–668.

Correlative Conventional and Super-resolution Photoactivated Localization Microscopy (PALM) Imaging to Characterize Chromatin Structure and Dynamics in Live Mammalian Cells

Dushyant Mehra^{1,2} and Elias M. Puchner^{1,*}

¹School of Physics and Astronomy, University of Minnesota, Twin Cities, MN, USA

²Department of Physiology and Biomedical Engineering, Mayo Clinic, Rochester, MN, USA

*For correspondence: epuchner@umn.edu

Abstract

A fundamental understanding of gene regulation requires a quantitative characterization of the spatial organization and dynamics of chromatin. The advent of fluorescence super-resolution microscopy techniques such as photoactivated localization microscopy (PALM) presented a breakthrough to visualize structural features with a resolution of ~20 nm in fixed cells. However, until recently the long acquisition time of super-resolution images prevented high-resolution measurements in living cells due to spreading of localizations caused by chromatin motion. Here, we present a step-by-step protocol for our recently developed approach for correlatively imaging telomeres with conventional fluorescence and PALM, in order to obtain time-averaged super-resolution images and dynamic parameters in living cells. First, individual single molecule localizations are assigned to a locus as it moves, allowing to discriminate between bound and unbound dCas9 molecules, whose mobilities overlap. By subtracting the telomere trajectory from the localization of bound molecules, the motion blurring is then corrected, and high-resolution structural characterizations can be made. These structural parameters can also be related to local chromatin motion or larger scale domain movement. This protocol therefore improves the ability to analyze the mobility and time-averaged nanoscopic structure of locus-specific chromatin with single-molecule sensitivity.

Keywords: Photoactivated localization microscopy, PALM, Single-molecule tracking, Nanoscale, Chromatin structure and dynamics, Live-cell chromatin imaging, CRISPR/dCas9 DNA-labeling, MS2 gRNA, Live-cell super-resolution imaging

This protocol is used in: Nucleic Acids Res. (2022), DOI: 10.1093/nar/gkac314

Background

Gene expression is thought to be regulated by the spatiotemporal organization of chromatin from the smallest length scale of individual nucleosomes (~10 nm) up to ~100 nm [1,2]. Even larger tertiary structures such as enhancer promoter contacts or topologically associated domains may exist that regulate gene expression [1,3]. The correlated movement between small chromatin structures and the large chromatin domains they are part of has been suggested as an important feature of nuclear phase condensates [4–6]. To understand these effects of chromatin structure and dynamics on gene regulation, imaging techniques are required that can characterize both the nanoscopic structure and the dynamics of chromatin in the larger context of chromatin domains they reside in.

Recently, two main breakthroughs facilitated research advances in this field: CRISPR/dCas9-based fluorescence labeling methods, to image specific sequences of chromatin, and super-resolution microscopy techniques such as photoactivated localization microscopy (PALM). By using programmable guide RNAs (gRNA), fluorophores can be targeted via CRISPR/dCas9 to specific sequences in the genome. Tens of fluorescent probes are required to be bound to a locus of interest to create a signal that is distinguishable from the background fluorescence of all other freely diffusing and searching probes [7]. To amplify the fluorescence signal of bound probes, repetitive RNA aptamers such as MS2 sequences have been attached to gRNAs that facilitate binding of multiple fluorophores. These labeling strategies facilitated conventional fluorescence timelapse imaging and yielded valuable insights into the slow and long-term dynamics of entire loci [7–9]. However, due to the optical diffraction limit, the structural characterization of smaller chromatin structures below ~250 nm has not been possible with conventional fluorescence microscopy. The development of PALM [10–12] enabled the tracking of single molecules in living cells (also referred to as single-particle tracking PALM, sptPALM) [13,14] and the acquisition of images of intracellular structures in fixed cells with ~20 nm resolution [15]. In PALM imaging, the spatiotemporal overlap of individual fluorophores is avoided by sparsely activating photoactivatable or photoswitchable fluorophores. In this way, the precise locations of individual fluorophores can be determined by Gaussian fitting of their intensity profile. By photoactivating and localizing many or all fluorophores over time, enough localizations are obtained to resolve structures below the optical diffraction limit in fixed cells or to link molecular trajectories to characterize their diffusion in live cells. CRISPR/dCas9-based DNA labeling has recently been applied in PALM to obtain structural information of chromatin compaction or condensation in chemically fixed cells or to characterize the dynamics of chromatin in live eukaryotic and prokaryotic cells [16]. However, until recently, it was not possible to simultaneously obtain such structural and dynamic information in living cells due to the motion of DNA during the long PALM data acquisition time. This motion spreads out the localizations of bound fluorophores along the trajectory of a locus and thus results in motion blurring.

Here, we present a protocol for our recently developed correlative conventional fluorescence and PALM imaging approach in living cells that overcomes these challenges [17]. This approach is based on labeling an intracellular structure or locus with a conventional fluorophore to track its location and motion during the entire PALM data acquisition time. Each structure or locus is, in addition, labeled with a spectrally distinct PALM-compatible fluorophore to record the single molecule localizations. The trajectory of the locus determined from the conventional fluorescence signal is then subtracted from the coordinates of its single molecule localizations to correct for motion blurring. As a result, high-resolution structural parameters such as the time-averaged size or the density of bound probes can be quantified to obtain new insights into the compaction of chromatin. In addition, the dynamics of the relative single molecule rearrangement or the motion of the entire locus can be related to its structural parameters, which has not been possible with existing techniques.

We demonstrate correlative conventional and PALM imaging using the well-characterized telomere sequences as a model system labeled via dCas9 and the MS2 coat proteins (MCP) that bind to a modified telomere-targeting gRNA scaffold. However, this imaging approach can be extended to single loci or other intracellular structures that can be labeled with a sufficient number of conventional and PALM-compatible fluorophores to create signals above background. Importantly, our presented data acquisition and analysis pipeline is a primary step to any downstream analysis to quantify structural or dynamic parameters. For instance, we demonstrate that determining the location and mobility of a locus relative to the single dCas9/MCP fluorophores classifies them more reliably as bound to a locus. The relative motion of single molecules compared to the entire locus furthermore reveals how small-scale chromatin rearrangements occur within the larger-scale chromatin movements. We also relate the compaction of telomeres to the local and global chromatin mobility to yield new insights. This protocol demonstrates that

correlative conventional fluorescence and PALM imaging accurately identifies Cas9 molecules bound to a locus and yields quantitative dynamic and time-averaged structural information about specific genomic loci at the nanoscale in living cells. The versatility of this protocol makes it applicable to other organelles and enables other existing or future downstream analysis techniques to extract and correlate high-resolution structural features with dynamic parameters.

Materials and reagents

1. Lab-Tek No. 1.5 8-well plates (Fisher Scientific, catalog number: 12-565-8)
2. Lipofectamine 3000 and p300 reagent (Invitrogen, catalog number: L3000001)
3. Opti-MEM media (Thermo Fisher, catalog number: 31985070)
4. MCP-HaloTag plasmid (Addgene, catalog number: 121937)
5. dCas9-GFP plasmid (Addgene, catalog number: 51023)
6. 2xMS2 gRNA plasmid (Addgene, catalog number: 75389)
7. PA-JF646 (Luke Lavis Lab, HHMI Janelia)
8. GIST-T1 Cells (gastrointestinal stromal tumor cells) (Cosmo Bio, catalog number: PMC-GIST01C)
Note: We used this cell line as it is hypothesized that this cancer phenotype is impacted by changes in chromatin structure and dynamics [18]. Furthermore, living GIST-T1 cells can be imaged for long periods of time and exhibit minimal auto-fluorescence and cell death.
9. T25 tissue culture flask (Thermo Fisher, catalog number: 156340)
10. Phenol-red free trypsin EDTA (Gibco, catalog number: 15400054)
11. Fetal bovine serum (FBS) (Gibco, catalog number: 10437028)
12. Fluorobrite DMEM (Gibco, catalog number: A1896701)
13. Penicillin/Streptomycin (Gibco, catalog number: 15140122)
14. L-Glutamine (Gibco, catalog number: 25030-081)
15. TetraSpeck microspheres (Invitrogen, catalog number: T7279)
16. 1.7 mL Eppendorf tubes (catalog number: 0030123611)
17. 37 °C 5% CO₂ incubator (Thermo Fisher, catalog number: 3110 or similar)
18. DI water (e.g., Thermo Fisher, catalog number: 751-610 or purified in house)
19. Distilled phosphate buffered saline (PBS) (Gibco, catalog number: 14040133)

Solutions

1. Fluorobrite media (see Recipes)
2. Serum-diluted Fluorobrite media (see Recipes)
3. DNA/lipid mixture (see Recipes)

Recipes

1. Fluorobrite media

10% FBS, 4 mM L-Glutamine, 1% penicillin/streptomycin, Fluorobrite DMEM. For 50 mL of media, add 5 mL of FBS, 500 µL of penicillin/streptomycin solution, 500 µL of L-Glutamine, and 44 mL of Fluorobrite DMEM.

2. Serum-diluted Fluorobrite media

1% FBS, 4 mM L-Glutamine, 1% penicillin/streptomycin, Fluorobrite DMEM solution. For 50 mL of media, add 500 µL of FBS, 500 µL of penicillin/streptomycin solution, 500 µL of L-Glutamine, and 48.5 mL of Fluorobrite DMEM.

3. DNA/lipid mixture

Mix 200 ng of telomere 2xMS2 gRNA along with 50 ng of MCP-HaloTag and 50 ng of dCas9-GFP plasmids with 10 µL of Opti-MEM, 1 µL of Lipofectamine 3000 reagent, and 0.5 µL of p300 reagent in a 1.7 mL Eppendorf tube in sterile cell culture environment.

Note: Telomere gRNA sequence was obtained from [7], and protocols from [8,19], and [9] were used to clone telomere gRNA sequence into 2xMS2 plasmid.

Equipment

1. Four OBIS lasers emitting 100 mW at 405 nm (Coherent, catalog number: 1178754), 50 mW at 488 nm (Coherent, catalog number: 1178764), 100 mW at 561 nm (Coherent, catalog number: 1253302) and 100 mW at 640 nm (Coherent, catalog number: 1178790)
2. Beam expander (Thor Labs, catalog number: GBE02-A)
3. Assorted lenses and mirrors (Thor Labs)
4. Inverted microscope (Eclipse Ti-E) equipped with a perfect focus system (Nikon, catalog number: MEA53100)
5. CFI 100× 1.49 NA oil immersion objective (Nikon, catalog number: MRD01991)
6. iXon 897 Ultra DU-897U EMCCD camera (Andor, catalog number: 77026047)
7. Quad band dichoric mirror (Chroma, catalog number: ZT405/488/561/640rpc)
8. Bandpass filters for the green (Chroma, catalog number: ET525/50), red (Chroma, catalog number: ET595/50), and far-red channel (Semrock, catalog number: FF731/137)
9. Dichroic long pass beam splitter for red/green channel experiments (Chroma, catalog number: T562lpxr BS)
10. Dichroic long pass beam splitter for far red/green channel experiments (Semrock, catalog number: FF652-Di01)
11. Motorized flat top stage for inverted microscope (ProScan II, catalog number: 77011328)
12. Heating insert P for Lab-TekTM S1 and temperature controller (Pecon, catalog number: 411860-9025-000 and 411860-9005-000)
13. Computer for microscope control and data acquisition (e.g., Dell, model: Optiplex 9020 Mini-Tower, Intel Core i7-4790 CPU @3.60GHz 4 cores, 16 GB RAM, 3.64 TB drive)
14. Computer for data analysis (e.g., Dell, model: PowerEdge T440, Intel Xeon Silver 4216 2.1G, 16C/32T, 9.6 GT/s, 22 M Cache, 16 GB RDIMM, 3,200 MT/s, Dual Rank, 8 TB 7.2K RPM SATA 6Gbps 512e 3.5 in Hot-plug Hard Drive)

Software

1. MATLAB 2018b
2. Insight3 Localization Software (Huang lab, UCSF or Zhuang lab, Harvard) or equivalent
3. Storm Control Software (<https://github.com/ZhuangLab/storm-control>) or equivalent
4. MATLAB-based trace linking and trace analysis (<https://osf.io/6n4ej/>)
5. MATLAB-based motion correction and trace separation code (<https://osf.io/6n4ej/>)
6. Python-based channel transformation code (<https://osf.io/6n4ej/>)

Procedure

A. GIST-T1 cell culture, seeding, and plasmid transfections

1. Seed GIST-T1 cells in 5 mL of Fluorobrite media at a density of 33% (~400,000–600,000 cells) in a T25 tissue culture flask.

Note: Fluorobrite media avoids fluorescence from phenol red.

2. Culture cells for ~1–2 days up to a density of 75%–80% in a humidified incubator at 37 °C and 5% CO₂. Split cells by aspirating media from the flask in a cell culture hood and washing cells with 37 °C PBS twice.
3. After removing PBS, add 0.5 mL of phenol-red free trypsin EDTA to the flask and make sure the entire surface area of the flask is covered.
4. Then, place flask in incubator for 2–3 min to allow cells to lift from flask. Verify that cells have lifted.
5. Add 2 mL of Fluorobrite media to trypsinized cells to neutralize trypsin and add cells at density mentioned in step A1 with 5 mL of Fluorobrite media or proceed with step A6.
6. Seed 50 μL of trypsinized cells in 8-well plates at a density of 50,000 cells/mL two days prior to imaging. Add 400 μL of media to each well after plating cells, and culture as in step A1.
Note: Cell concentration was measured using a hemocytometer, and Fluorobrite media was used to dilute cells to find appropriate concentration.
7. Approximately 15–17 h before imaging, mix 200 ng of telomere 2xMS2 gRNA plasmid to generate gRNA along with 50 ng of MCP-HaloTag and 50 ng of dCas9-GFP plasmids with 10 μL of Opti-MEM, 1 μL of Lipofectamine 3000 reagent, and 0.5 μL of p300 reagent in a 1.7 mL Eppendorf tube and incubate the DNA/lipid mixture for 15 min at room temperature in a sterile cell culture environment.
8. During incubation of step A7, aspirate media from GIST-T1 cells in a well plate and wash cells twice with 300 μL of Fluorobrite media heated to 37 °C. Then, add 100 μL of Fluorobrite media supplemented with 4 mM L-Glutamine, 1% FBS, 1% penicillin/streptomycin, and 200 μL of Opti-MEM. Then, place cells in an incubator at 37 °C with 5% CO₂ for 15 min.
9. After 15 min of incubation in step A8, remove cells from incubator, place in cell culture hood, and add all of the DNA/lipid mixture from the Eppendorf tube to cells in each well already supplemented with serum-diluted media by pipetting dropwise. If too much force is used, DNA/lipid complex may disassociate.
10. Place wells with transfecting cells in the incubator as in step A2 for 15–17 h.
11. Remove media from wells and wash cells twice with serum-diluted Fluorobrite media. Add 300 μL of serum-diluted Fluorobrite media with 100 nM of PA-JF646 dye and incubate for 15 min in a 37 °C incubator with 5% CO₂.
Note: PA-JF646 is a far-red fluorescent dye that is photoactivated by 405 nm light and contains a ligand that attaches to HaloTag [20,21]. This dye has a higher photon budget and longer on-times compared to other photoswitchable proteins, which results in improved detection, localization precision, and longer single molecule trajectories. This improves trace mobility analysis and diffusion coefficient estimation. This dye isn't fluorogenic and does fluoresce when not bound to HaloTag, which is why multiple rounds of washing are required before imaging.
12. After incubation, wash cells three times with Fluorobrite media and place in an incubator at 37 °C with 5% CO₂ for an additional 30 min.
13. Repeat step A12 three additional times prior to imaging to remove unbound PA-JF646 dye that is still able to fluoresce.
14. Keep samples in an incubator at 37 °C with 5% CO₂ until imaging.

B. Calibration and imaging experiments

Note: All experiments presented here were performed with a custom-built microscope, as recently described [22]; however, our protocol is applicable to data recorded with any microscope capable of simultaneous PALM and conventional fluorescence imaging in the respective channels. In short, a Nikon inverted microscope (Eclipse Ti-E) is equipped with a perfect focus system and an Andor iXon 897 Ultra DU-897U electron multiplying charge coupled detector (EMCCD), cooled to -70 °C and set to an amplifying gain of 30. The four 100 mW excitation lasers (405, 488, 561, and 640 nm OBIS-CW, Coherent Optics) are aligned, expanded, and focused into the back focal plane of the objective (Nikon CFI 100× 1.49 NA oil immersion) using various dichroic mirrors, beam expanders, and lenses. A quad band dichoric mirror (ZT405/488/561/640rpc; Chroma) separates fluorescence emission from excitation light. Fluorescence emission is further split into the far red and green signal using a dichroic long pass beam splitter (FF652-Di01; Semrock) and band pass filters FF731/137 (Semrock) for the far-red channel and ET525/50 (Chroma) for the green channel. Laser intensity

modulation and shutter sequences are synchronized with the camera and controlled digitally with a NI-DAQ board.

1. Mount microscope No. 1 cover glass or 8-well plates with 10 μL of TetraSpeck microspheres diluted 1:100 in DI water on microscope stage.
2. Excite microspheres separately using 640 and 488 nm excitation with approximately 1.75 mW power (power density $\sim 100 \text{ W/cm}^2$ in sample plane). Record a 100-frame movie with approximately 10 sparsely distributed microspheres over the entire field of view without moving the sample and use the first 50 frames to record 640 nm excited microspheres and the last 50 frames to record 488 nm excited microspheres.
3. Move the same microspheres to different positions in the camera to sample the entire field of view and repeat steps B2 and B3 at least five times. You can also image different microspheres placed in different regions across the field of view.

Note: The number of microspheres used depends on the field of view of the camera. Our field of view was 256 \times 256 pixels with a pixel size of 160 nm. You need at least 50 microspheres to create an accurate transformation with sub 20 nm registration error (see Figure 1). More microspheres or more images with microspheres shifted to different locations are necessary if your field of view is larger. Microsphere imaging can also be done after cellular imaging but should be done either before or after every imaging session, since registration parameters can change from session to session. This data will be used later to transform localizations from 640 nm channel to the 488 nm channel.

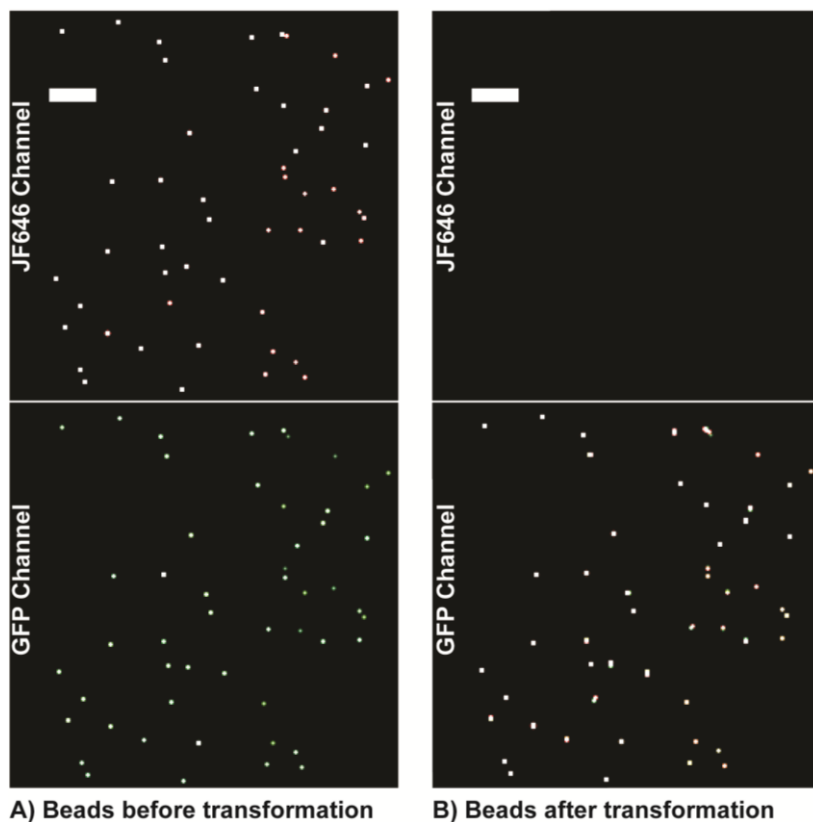


Figure 1. Example microsphere localization rendering. Example rendering of microsphere localizations across seven movies depicting the number and density of microspheres required to obtain an accurate transformation across the field of view. (A) Microspheres imaged in each channel to calculate the transformation matrix. (B) The transformation matrix is applied to transform bead localizations from the Jf646 channel to the GFP channel. This transformation matrix is then applied to single molecule localizations. Scale bars: 5 μm .

4. Remove microsphere sample and mount 8-well plate with transfected cells on microscope stage. Make sure the stage is heated to 37 °C and the CO₂ incubator on microscope stage reads 5%.
5. Using the Storm Control Software (or equivalent for a different microscope system), set up a 10-frame laser shutter sequence at 20 Hz with the first frame having 488 nm excitation for GFP imaging, the second having brightfield LED and 405 nm photoactivation, and frames 3–10 having 640 nm excitation for PALM imaging.

Note: The diffusion coefficient distributions of MCP-HaloTag with and without telomere gRNA taken at 20 Hz are statistically similar to the ones obtained at 60 Hz. While faster PALM imaging speeds in principle reduce motion blurring, the required higher excitation power reduces the length of single molecule traces, and thus lowers the precision for characterizing their motion. In our experience, a 20 Hz frame rate has been a good compromise between imaging speed, localization precision in each frame, and single molecule trace lengths.

6. Set the 488 nm laser power to 1.75 mW (power density ~100 W/cm² at sample plane) and the 640 nm to 17.5 mW (~1 kW/cm²). The 405 nm intensity will be adjusted to 1–251 μW (power density of ~0.06–15 W/cm²) during the experiment for constant photoactivation rates.
7. Turn on the 488 nm laser to visually identify cells with telomere puncta in cell nucleus prior to single molecule imaging. Keep 488 nm exposure to a minimum to reduce bleaching. Image telomere puncta conventionally using the 488 nm laser for at least 200 frames at 20 Hz for interpolation error analysis.

Note: Cells transfected with all three plasmids should show clear telomere puncta. Since cells are transiently transfected, some cells express all transfected plasmids while others do not. Look at cells that do not have gRNA but have MCP-HaloTag+PA-JF646 dye and dCas9-GFP expressed, and cells stained with only PA-JF646 dye and no transfected plasmids to characterize single molecule and conventional fluorescence background (see Figure 2).

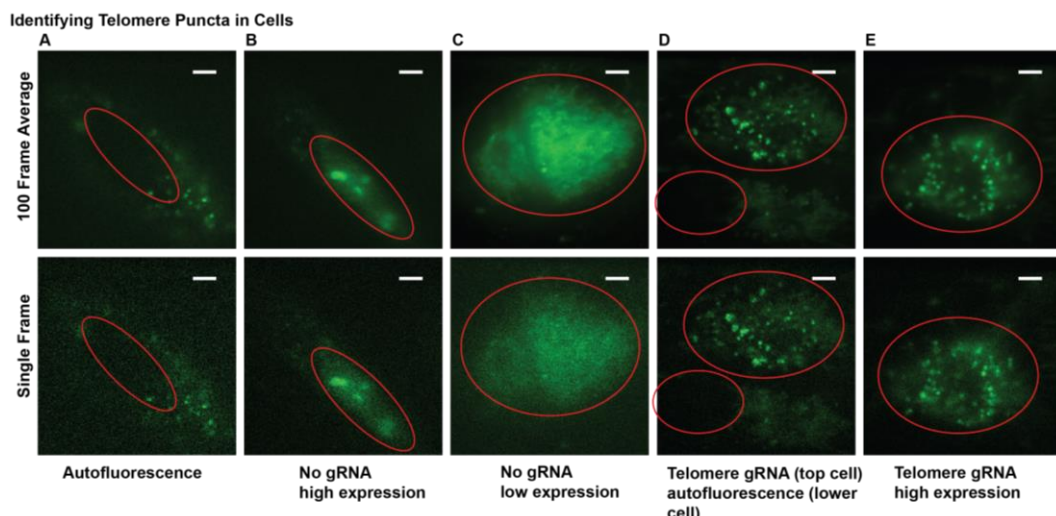


Figure 2. Examples of fluorescence images from transfected cells suitable and unsuitable for experiments. (A) Example of cellular autofluorescence. (B) and (C) Examples of cells expressing dCas9-GFP at various levels but without distinct telomere puncta due to the lack of gRNA. This can also occur with gRNA added. (D) and (E) Examples of telomere puncta at various expression levels suitable for imaging and analysis. Nuclei are marked with red line. Scale bars: 5 μm.

8. Once cells with telomere puncta are identified, begin 10-frame shutter and acquisition sequence. Start with 405 nm laser power of 1 μW (power density of ~0.06 W/cm²) and slowly increase at a rate of 5–10 μW every 1,000 frames until approximately 250 μW (power density of ~0.015 W/cm²) to ensure a sparse and consistent photoactivation rate (see Figure 3).

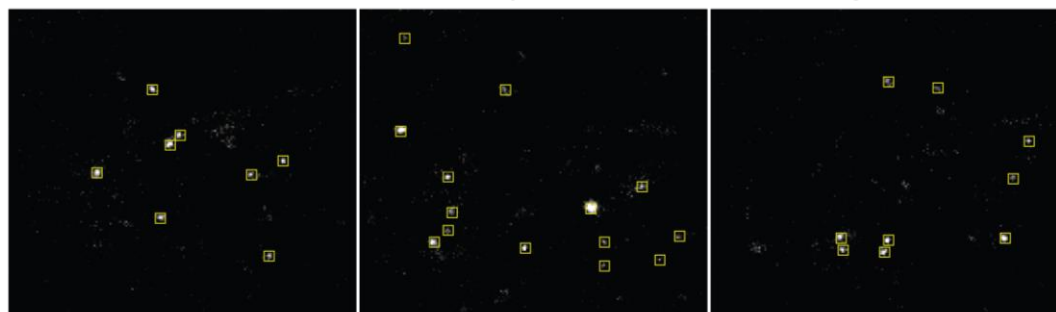
A) Examples of optimal activation density with low false linking rate**B) Examples of max allowable activation density with max allowable false linking rate****C) Examples of localizable data with high false linking rate**

Figure 3. Optimal photoactivation density. (A) Single frame of an optimal photoactivation density for single molecule tracking with low false linking rate. Yellow boxes are identified localizations from single-molecule emission events. (B) Example images of the maximal allowable localization density for single molecule tracking with acceptable false linking. (C) Examples of images with high-localization density that would result in a high false linking rate. False linking rates for example images are quantified in Figure 5. Scale bar: 5 μm .

9. Record data for 15,000–30,000 frames and stop sequence when cells start to change morphology indicating a decline of cell health (see Figure 4).

Note: Healthy GIST-T1 cells never change their morphology up to 15,000 frames. Only analyze and use frames up to 5,000 frames before morphology changes are detected, to exclude potential phototoxic effects prior to morphological changes. If cells start to change morphology sooner, cells are not healthy enough to begin with for imaging experiments (see Figure 4).

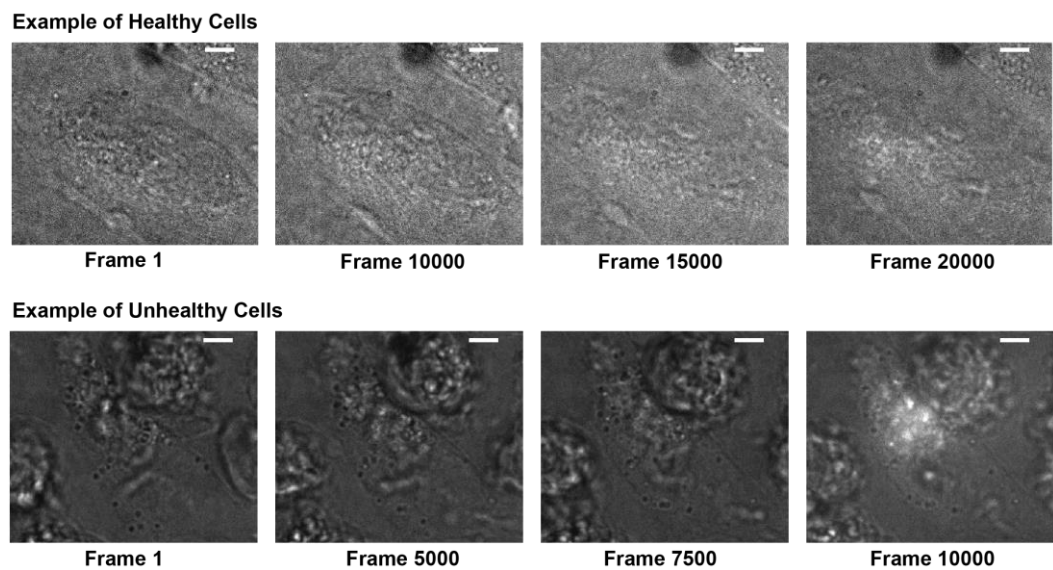


Figure 4. Cell morphology and health. LED + 405 nm photoactivation frames of healthy GIST-T1 cells (top) typically show retained morphology and size for at least 15,000 frames and show minimal autofluorescence upon 405 nm activation. Unhealthy cells (bottom) change morphology and become round within several thousand frames and show significant autofluorescence in response to 405 nm activation. Healthy cells also show much less contrast in the LED frame due to a more homogenous refractive index. Scale bars: 5 μ m.

10. Repeat steps B5–B9 to obtain more statistics from different cells. Typically, a number on the order of 10 cells is considered satisfactory.

Data analysis

A. Single molecule localization

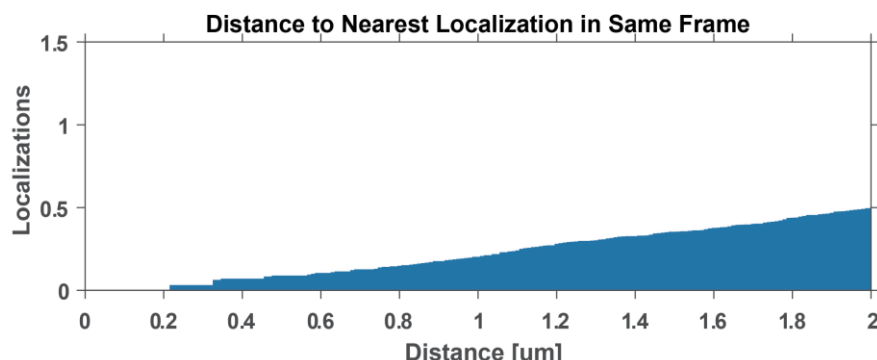
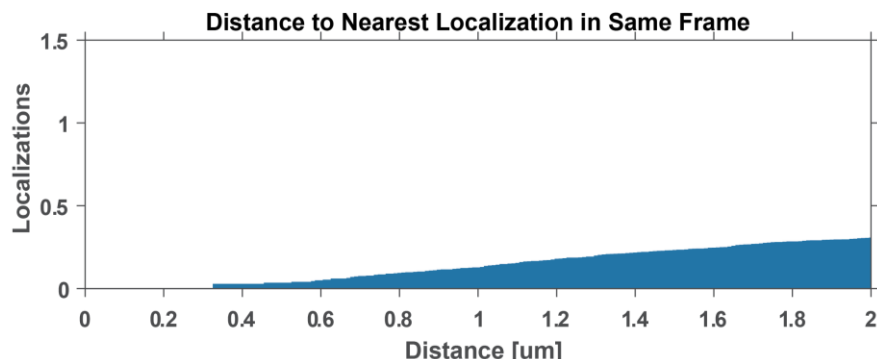
1. Use Insight3 localization software or a similar single molecule localization microscopy software to identify single molecule localizations and to fit them with 2D elliptical Gaussians with the following parameters: 7 \times 7 pixel ROI, widths between 250 and 700 nm, and minimum intensity of 100 photons. The x and y coordinate of each localization, along with the intensity, width, background, frame number, and other parameters are also stored in the single molecule list and outputted as a .txt file for further analysis.
Note: Other localization detection software, such as Thunderstorm or SMAP, can also be used with similar parameters [23,24]. Make sure to export localization list as .txt file and to include PSF widths.
2. Import molecule list into provided MATLAB analysis package or equivalent single particle tracking software. If using Insight3 for localization detection, insert file path into LoadMoleculeLList.m and execute function to generate a molecule list structure that will be used for subsequent analysis steps.
3. Use Thompson resolution formula or more accurate and updated version [25,26] to calculate localization precision of single molecule localizations. If using Insight3 to localize images, input molecule list into function ThompsonResolution.m to calculate localization resolution for each localization.
Note: The localization precision is provided in most localization software packages, such as Thunderstorm or SMAP along with localizations.

B. Single molecule trace linking and trace analysis

1. To perform trace-linking error analysis, execute the MATLAB function spatiotemporal_cc.m and provide the molecule list structure and desired frame range for the analysis. Use this function to measure pairwise distance of localizations in same frame (see Figure 5).

Note: This function normalizes the number of pairwise distances in each bin by the area and number of frame pairs. This modified pair correlation function quantifies the number of molecules found around each localization in the same frame. The number of localizations at your desired linking distance in the same frame will give you the estimate for the false linking rate.

A) Examples of optimal activation density with low false linking rate



B) Examples of localizable data with high false linking rate

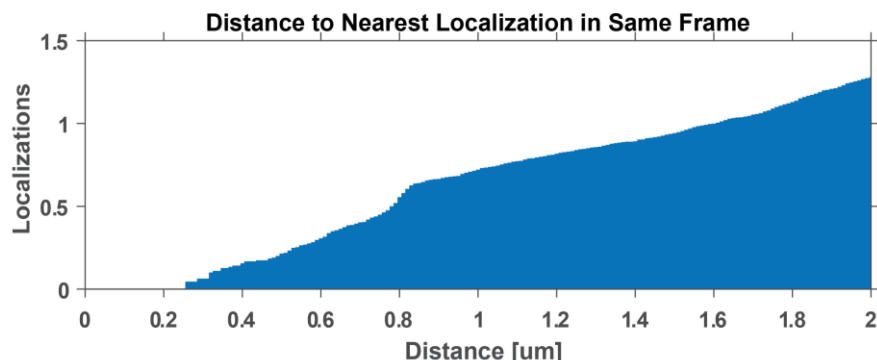


Figure 5. Localization density and false linking rate. False linking rate calculations for examples in Figure 3. These plots depict the average number of localizations as a function of distance away from a localization in the same frame. The false linking rate can be estimated by obtaining the number of localizations at a specific trace linking distance. (A) Optimal false linking rates for 0.48 μm linking

distance is between 0.01 and 0.05. (B) A linking error at 0.48 μm of approximately 0.1 is considered a high false linking rate and will lead to unreliable mobility measurements.

2. Exclude data from further analysis if localization density is too high and if the false linking rate is above 0.1. If false linking rate is too high throughout the duration of the experiment, record data with lower 405 nm photoactivation power in step B8.
Note: If you want to allow dark frames for linking a single molecule trace, incorporate the number of dark frames in the pair correlation metrics. For example, if you use one dark frame, then you need to calculate pairwise distances between every two frames to calculate false linking error.
3. Based on results from step 1, link localizations that are within the determined distance threshold. In the datasets presented here, a 0.48 μm linking distance was used. Only traces with a minimum of four localizations in consecutive frames are used for cross correlation and single trace fitting analysis. Input the data structure from LoadMoleculeList.m, linking distance (in μm), and number of dark frames into the MakeTraces.m function to link molecules across successive frames into traces. Any equivalent trace linking analysis package can also be used.
4. Calculate mean squared displacements (MSD) for each time step in all single molecule traces and average MSDs for each timestep of a single trace to obtain a time-averaged mean squared displacement (TAMSD) vs. time plot. If using the provided MATLAB code, input the output data structure from MakeTraces.m into function DiffusionDisplacement.m and execute DiffusionDisplacement.m.
5. Fit each TAMSD vs. time to the 2D diffusion equation $\langle r^2 \rangle = 4D\Delta t + 2\sigma^2$, where D is the diffusion coefficient, Δt is the time step, r^2 is the TAMSD, and σ is the localization precision (see Figure 6). Only use trajectories and diffusion coefficients from fits with a coefficient of determination value (R^2) of 0.7 or above and a diffusion coefficient above zero. If using the provided MATLAB code, execute DiffusionCoefficientAnalysis.m function, which calculates the diffusion coefficient and R^2 value for each input TAMSD calculated from DiffusionDisplacement.m.

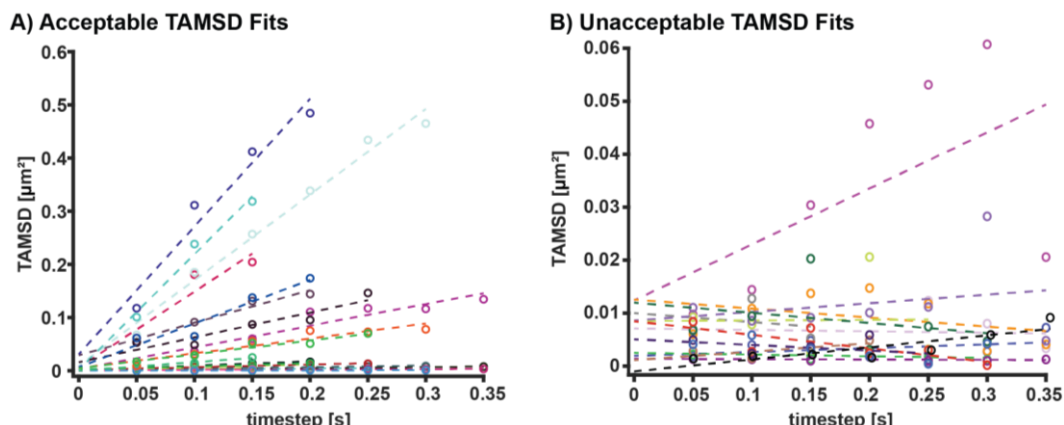


Figure 6. Time-averaged mean squared displacement (TAMSD) fitting. (A) Examples of acceptable TAMSD fits. These fits have R^2 values of above 0.7, positive slopes, and y intercepts above 0. The y intercept can be used to calculate localization precision. (B) Examples of excluded TAMSD fits. These fits have either R^2 values of below 0.7, negative slopes, or y intercepts at or below 0.

C. GFP cluster identification and trace linking analysis

1. Obtain GFP localizations by fitting GFP clusters with 2D Gaussians as in step A1 from Data analysis with the following parameters: 11 × 11 pixel ROI, widths between 250 and 7,000 nm, and a minimum of 200 photons. X and y coordinates of the GFP localization, along with the intensity, width, background, frame number, and other parameters will again be stored in the molecule list.

Note: Even though the width range is large, make sure widths from the same telomere do not deviate

significantly. If the GFP localization widths from the same telomere deviate by more than ~200 nm, it indicates that the telomere is moving along z too much and cannot be used for further analysis. If using other localization software such as SMAP or Thunderstorm, make sure PSF widths are included in the output molecule list.

2. To link telomere GFP localizations that are within 0.48 μm of each other in consecutive conventional imaging frames (every 10 frames), repeat steps B3–B5 with the GFP localization list.
3. Only use traces with a minimum of five localizations for downstream analysis. The widths of consecutive localizations in a trace should be within 200 nm to be included in downstream analysis. If using steps B3–B5, this will automatically be done in the motioncorrection.m function.

Note: An axial microsphere calibration [22] showed that PSFs width deviations of 200 nm corresponded to axial deviations of 450 nm, which is similar to the lateral trace linking threshold. In our analysis, we found that traces with below five localizations had insufficient single molecule localizations for downstream motion correction analysis.

4. Perform a linear interpolation between the x and y coordinates of GFP localizations in consecutive conventional image frames (frame 1 and frame 10) to obtain interpolated GFP coordinates during the frames that contained single molecule localizations. If using steps B3–B5, this will automatically be done in the motioncorrection.m function.
5. To estimate the upper limit of the interpolation error, analyze the data of step B7 of the calibration and imaging experiments in the same way as steps B1–B4 of Data analysis. Compare interpolated positions between frames nine frames apart to the actual position of the telomere.

Note: The median interpolation error of the presented data is $45 \pm 10 \text{ nm}$ and the mean interpolation error is constant up to 20 frames (Supplementary Figure 4 in reference [17]).

6. Calculate TAMSD and diffusion coefficients using the same procedure described in step B5 of Data analysis. Only use the first four time steps for fitting analysis to exclude nonlinear portions of the TAMSD that occur at later time steps. In this way, non-Brownian diffusion is approximated and sub-diffusive behavior at long times is not given too much weight in the fit.

D. Motion correction of single molecule localizations

1. Localize microspheres from calibration images recorded in steps B1–B3 in both channels using Insight3 localization software or equivalent with parameters used to localize single molecules in step A1 of Data analysis.
2. Fit the positions of the microspheres in both channels to a third order polynomial function to extract the coordinate transformation matrix between the two channels. If using the provided procedure, input the two molecule lists and execute the python polynomial transformation code bead_calibration.py [27,28].
3. Apply transformation to top channel to superimpose localizations from 640 nm channel to bottom channel. If using Insight3 localization software, go to STORM math in the STORM panel, click the custom math function, and copy the output transformation equations from the python transformation code into the *storm math* text box. Then, in *display layer options* under the *view* tab, click the drift correction box to view the transformed localizations. Transformed localizations will show up as XC and YC in the exported Insight3 localization software molecule list text file (see Figure 7).

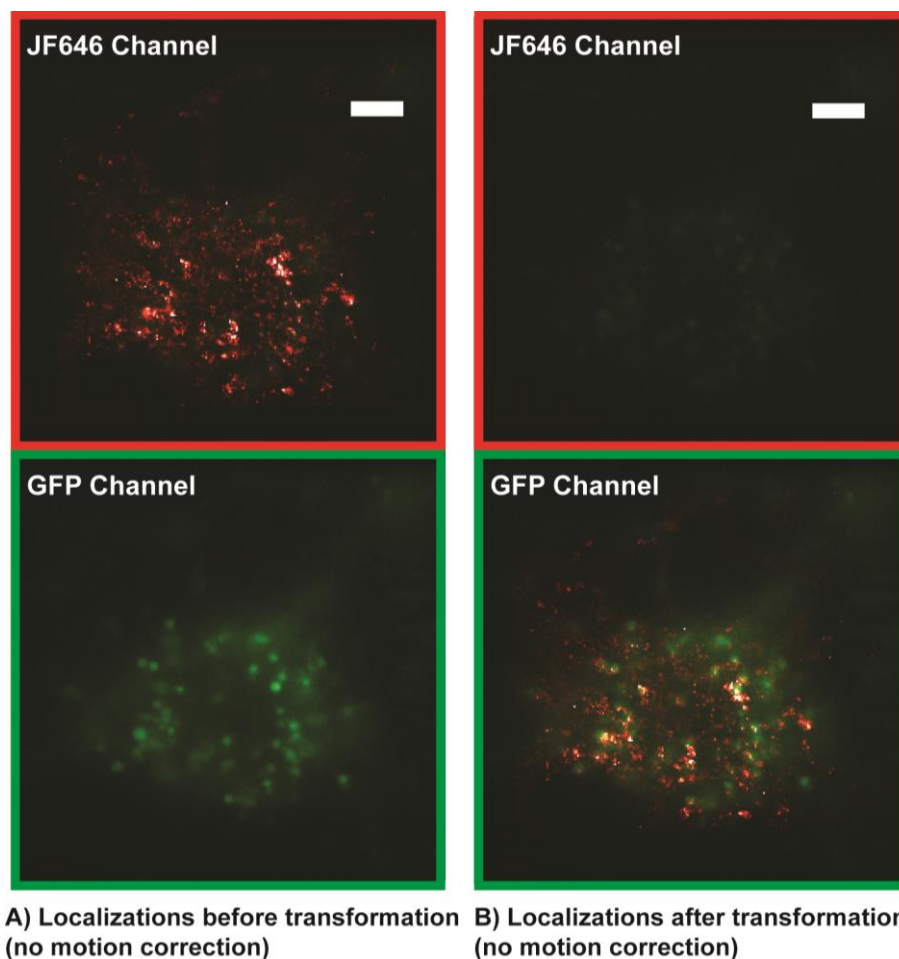


Figure 7. Single molecule localization microscopy (SMLM) localizations (red) before transformation (A) and after transformation (B) superimposed on GFP telomere cluster. The transformation is also used to correct for chromatic aberrations in the optical 4F emission path. Localizations that are not properly transformed cannot be accurately registered with GFP localizations and motion corrected. Apparent incomplete colocalization is due to telomere motion and is corrected during the motion correction analysis. Scale bars: 5 μm .

4. Calculate a distance matrix between the interpolated GFP localizations for a specific telomere and all single molecule localizations in that frame. If using the provided MATLAB code (`motioncorrection.m`) this will automatically be done in the cross-correlation section of the motion correction code. The code will loop through all accepted GFP trajectories.
5. The cross-correlation section of the provided motion correction MATLAB code (`motioncorrection.m`) identifies single molecule localizations whose distance to a GFP cluster is smaller than the radius of the cluster plus the localization precision of the cluster and the single molecule localizations. The radius of the last GFP localization prior to interpolation should be used as the radius of the interpolated GFP cluster coordinates. The motion correction code (`motioncorrection.m`) will classify single molecule traces with a minimum of four localizations and with all localizations residing within a GFP cluster as bound and will exclude single molecule traces where some but not all localizations or no localizations reside within a cluster.
6. To correct for motion of telomeres in PALM images, the motion correction section of provided MATLAB motion correction code (`motioncorrection.m`) will subtract the coordinates of GFP localizations at a

specific frame from the initial GFP localization in the trajectory and apply that subtraction to the single molecule localizations belonging to each GFP cluster and the same frame (see Figure 8).

Note: A minimum of four bound trajectories with a minimum of four localizations each should be used to obtain enough localizations to be able to motion correct localizations within a telomere trajectory and to calculate downstream metrics such as area and density.

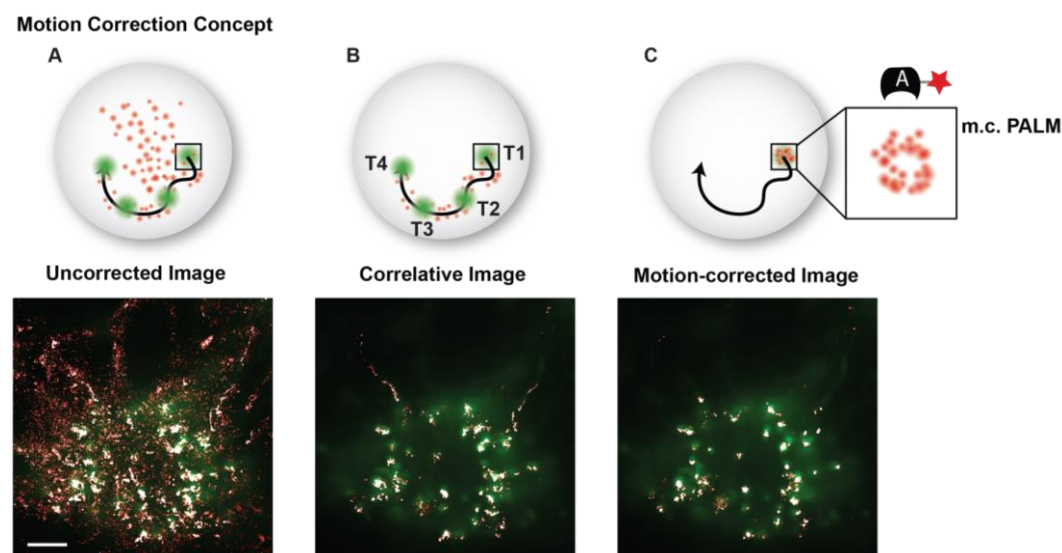


Figure 8. Motion correction example. (A) Superposition of a GFP image and conventional PALM image that includes a majority of freely diffusing and searching fluorescent probes. (B) The correlative conventional and PALM image only depicts PALM localizations that appear in proximity to a GFP cluster at any instance in time and suppresses background from freely diffusing and searching probes. (C) The motion-corrected PALM image super-resolves each moving telomere, which colocalizes with its GFP signal. Scale bar: 5 μm .

7. Apply a convex hull to the motion-corrected localizations in a cluster using the boundary function in MATLAB (`convhull.m`) to find the cluster boundary and use this boundary to calculate cluster area.
8. If calculating localization density, normalize the number of localizations by the cluster duration in the field of view to account for constant photoactivation rate.
9. Perform desired downstream analysis of structural and dynamic parameters. For instance, correlate cluster density or area with cluster mobility to correlate chromatin structural information with dynamic information. Since single molecule trajectories are assigned to specific GFP telomere trajectories, the diffusion coefficient of the single molecule trajectories can be compared to the mobility of GFP trajectories which provides meaningful information on chromatin rearrangements (see examples in Figure 9). Bulk trace analysis methods such as Gaussian mixture models, Bayesian inference techniques, or displacement analysis techniques can also be applied to trajectories.

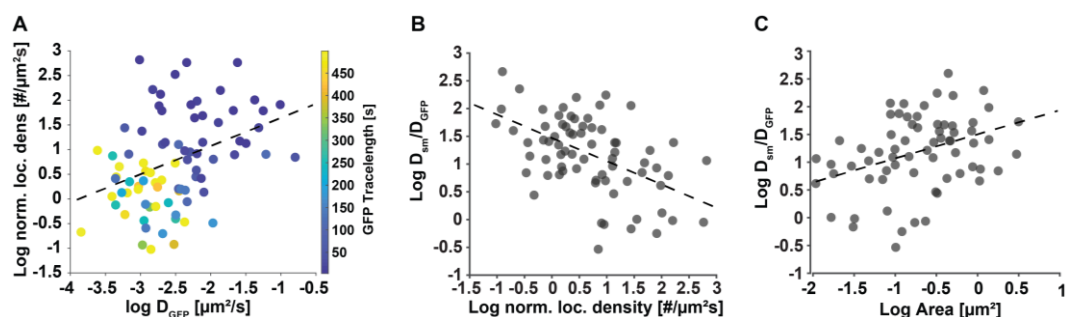


Figure 9. Secondary downstream analysis examples of motion-corrected data. (A) The localization density of individual telomeres has a slight correlation (correlation coefficient = 0.4) with their diffusion coefficient determined with the conventional GFP signal. This result is plausible, since denser, more compacted telomeres can diffuse more freely than less dense and more extended telomeres, whose motion is slowed down. (B) The ratio of average dCas9-MCP single molecule and the telomere diffusion coefficients they reside in presents a metric of relative single molecule re-arrangement and shows a negative correlation (correlation coefficient = -0.52) with the normalized localization density of the telomeres. (C) Likewise, the ratio of average dCas9-MCP diffusion coefficients show a positive correlation (correlation coefficient = 0.48) with the area of the telomeres they reside in. These results are plausible since denser, more compacted telomeres have less ability for relative motion or re-arrangement due to tighter packing compared to less dense, more extended telomeres, which exhibit more relative mobility. Data adapted from Mehra et al. (2022) [17].

Acknowledgments

The authors thank Angel Mancebo Jr for writing the two-channel microsphere calibration code and helpful discussions. The authors acknowledge Bo Huang for providing some of the PA-JF646 dye and helpful discussions. The authors acknowledge Tamas Ordog and Yujiro Hayashi for providing the GIST-T1 cells. The authors thank Stephen C. Ekker and Karl J. Clark for providing lab space, reagents, and guidance on molecular cloning. The authors thank Jacob Ritz for the helpful discussions. This work was supported by funding from the National Institutes of Health under award number R21GM127965 and from the Mayo Graduate School of Biomedical Sciences and Mayo Foundation. This protocol is used in Mehra et al. (2022) [17].

Competing interests

The authors declare that no competing interests exist.

Ethical considerations

GIST-T1 Cells were obtained from Dr. Tamas Ordog.

References

1. Szabo, Q., Bantignies, F. and Cavalli, G. (2019). Principles of genome folding into topologically associating domains. *Sci. Adv.* 5(4): eaaw1668. [doi: 10.1126/sciadv.aaw1668](https://doi.org/10.1126/sciadv.aaw1668)

2. Agbleke, A. A., Amitai, A., Buenrostro, J. D., Chakrabarti, A., Chu, L., Hansen, A. S., Koenig, K. M., Labade, A. S., Liu, S., Nozaki, T., et al. (2020). Advances in Chromatin and Chromosome Research: Perspectives from Multiple Fields. *Mol. Cell* 79(6): 881–901. [doi: 10.1016/j.molcel.2020.07.003](https://doi.org/10.1016/j.molcel.2020.07.003)
3. Li, J., Hsu, A., Hua, Y., Wang, G., Cheng, L., Ochiai, H., Yamamoto, T. and Pertsinidis, A. (2020). Single-gene imaging links genome topology, promoter-enhancer communication and transcription control. *Nature Structural & Molecular Biology* 27(11): 1032–1040. [doi: 10.1038/s41594-020-0493-6](https://doi.org/10.1038/s41594-020-0493-6)
4. Nozaki, T., Imai, R., Tanbo, M., Nagashima, R., Tamura, S., Tani, T., Joti, Y., Tomita, M., Hibino, K., Kanemaki, M. T., et al. (2017). Dynamic Organization of Chromatin Domains Revealed by Super-Resolution Live-Cell Imaging. *Mol. Cell* 67(2): 282–293.e7. [doi: 10.1016/j.molcel.2017.06.018](https://doi.org/10.1016/j.molcel.2017.06.018)
5. Ashwin, S. S., Nozaki, T., Maeshima, K. and Sasai, M. (2019). Organization of fast and slow chromatin revealed by single-nucleosome dynamics. *Proc. Natl. Acad. Sci. U. S. A.* 116(40): 19939–19944. [doi: 10.1073/pnas.1907342116](https://doi.org/10.1073/pnas.1907342116)
6. Nozaki, T., Shinkai, S., Ide, S., Higashi, K., Tamura, S., Shimazoe, M. A., Nakagawa, M., Suzuki, Y., Okada, Y., Sasai, M., et al. (2023). Condensed but liquid-like domain organization of active chromatin regions in living human cells. *Sci. Adv.* 9(14): eadfl488. [doi: 10.1126/sciadv.adf1488](https://doi.org/10.1126/sciadv.adf1488)
7. Chen, B., Gilbert, L. A., Cimini, B. A., Schnitzbauer, J., Zhang, W., Li, G. W., Park, J., Blackburn, E. H., Weissman, J. S., Qi, L. S., et al. (2013). Dynamic Imaging of Genomic Loci in Living Human Cells by an Optimized CRISPR/Cas System. *Cell* 155(7): 1479–1491. [doi: 10.1016/j.cell.2013.12.001](https://doi.org/10.1016/j.cell.2013.12.001)
8. Ma, H., Tu, L. C., Naseri, A., Huisman, M., Zhang, S., Grunwald, D. and Pederson, T. (2016). Multiplexed labeling of genomic loci with dCas9 and engineered sgRNAs using CRISPRainbow. *Nat. Biotechnol.* 34(5): 528–530. [doi: 10.1038/nbt.3526](https://doi.org/10.1038/nbt.3526)
9. Ma, H., Tu, L. C., Naseri, A., Chung, Y. C., Grunwald, D., Zhang, S. and Pederson, T. (2018). CRISPR-Sirius: RNA scaffolds for signal amplification in genome imaging. *Nat. Methods* 15(11): 928–931. [doi: 10.1038/s41592-018-0174-0](https://doi.org/10.1038/s41592-018-0174-0)
10. Huang, B., Wang, W., Bates, M. and Zhuang, X. (2008). Three-Dimensional Super-Resolution Imaging by Stochastic Optical Reconstruction Microscopy. *Science* 319(5864): 810–813. [doi: 10.1126/science.1153529](https://doi.org/10.1126/science.1153529)
11. Rust, M. J., Bates, M. and Zhuang, X. (2006). Sub-diffraction-limit imaging by stochastic optical reconstruction microscopy (STORM). *Nat. Methods* 3(10): 793–796. [doi: 10.1038/nmeth929](https://doi.org/10.1038/nmeth929)
12. Betzig, E., Patterson, G. H., Sougrat, R., Lindwasser, O. W., Olenych, S., Bonifacino, J. S., Davidson, M. W., Lippincott-Schwartz, J. and Hess, H. F. (2006). Imaging Intracellular Fluorescent Proteins at Nanometer Resolution. *Science* 313(5793): 1642–1645. [doi: 10.1126/science.1127344](https://doi.org/10.1126/science.1127344)
13. Manley, S., Gillette, J. M., Patterson, G. H., Shroff, H., Hess, H. F., Betzig, E. and Lippincott-Schwartz, J. (2008). High-density mapping of single-molecule trajectories with photoactivated localization microscopy. *Nat. Methods* 5(2): 155–157. [doi: 10.1038/nmeth.1176](https://doi.org/10.1038/nmeth.1176)
14. Lerner, J., Gomez-Garcia, P. A., McCarthy, R. L., Liu, Z., Lakadamalyali, M. and Zaret, K. S. (2020). Two-Parameter Mobility Assessments Discriminate Diverse Regulatory Factor Behaviors in Chromatin. *Mol. Cell* 79(4): 677–688.e6. [doi: 10.1016/j.molcel.2020.05.036](https://doi.org/10.1016/j.molcel.2020.05.036)
15. Otterstrom, J., Castells-Garcia, A., Vicario, C., Gomez-Garcia, P. A., Cosma, M. P. and Lakadamalyali, M. (2019). Super-resolution microscopy reveals how histone tail acetylation affects DNA compaction within nucleosomes in vivo. *Nucleic Acids Res.* 47(16): 8470–8484. [doi: 10.1093/nar/gkz593](https://doi.org/10.1093/nar/gkz593)
16. Neguembor, M. V., Sebastian-Perez, R., Aulicino, F., Gomez-Garcia, P. A., Cosma, M. P. and Lakadamalyali, M. (2018). (Po)STAC (Polycistronic SunTag modified CRISPR) enables live-cell and fixed-cell super-resolution imaging of multiple genes. *Nucleic Acids Res.* 46(5): e30. [doi: 10.1093/nar/glx1271](https://doi.org/10.1093/nar/glx1271)
17. Mehra, D., Adhikari, S., Banerjee, C. and Puchner, E. M. (2022). Characterizing locus specific chromatin structure and dynamics with correlative conventional and super-resolution imaging in living cells. *Nucleic Acids Res.* 50(13): e78–e78. [doi: 10.1093/nar/gkac314](https://doi.org/10.1093/nar/gkac314)
18. Flavahan, W. A., Drier, Y., Johnstone, S. E., Hemming, M. L., Tarjan, D. R., Hegazi, E., Shareef, S. J., Javed, N. M., Raut, C. P., Eschle, B. K., et al. (2019). Altered chromosomal topology drives oncogenic programs in SDH-deficient GISTs. *Nature* 575(7781): 229–233. [doi: 10.1038/s41586-019-1668-3](https://doi.org/10.1038/s41586-019-1668-3)
19. Ma, H., Naseri, A., Reyes-Gutierrez, P., Wolfe, S. A., Zhang, S. and Pederson, T. (2015). Multicolor CRISPR labeling of chromosomal loci in human cells. *Proc. Natl. Acad. Sci. U.S.A.* 112(10): 3002–3007. [doi: 10.1073/pnas.1420024112](https://doi.org/10.1073/pnas.1420024112)

Cite as: Mehra, D. and Puchner, E. M. (2023). Correlative Conventional and Super-resolution Photoactivated Localization Microscopy (PALM) Imaging to Characterize Chromatin Structure and Dynamics in Live Mammalian Cells. *Bio-protocol* 13(20): e4850. DOI: 10.21769/BioProtoc.4850.

20. Grimm, J. B., English, B. P., Choi, H., Muthusamy, A. K., Mehl, B. P., Dong, P., Brown, T. A., Lippincott-Schwartz, J., Liu, Z., Lionnet, T., et al. (2016). Bright photoactivatable fluorophores for single-molecule imaging. *Nat. Methods* 13(12): 985–988. [doi: 10.1038/nmeth.4034](https://doi.org/10.1038/nmeth.4034)
21. Grimm, J. B., English, B. P., Chen, J., Slaughter, J. P., Zhang, Z., Revyakin, A., Patel, R., Macklin, J. J., Normanno, D., Singer, R. H., et al. (2015). A general method to improve fluorophores for live-cell and single-molecule microscopy. *Nat. Methods* 12(3): 244–250. [doi: 10.1038/nmeth.3256](https://doi.org/10.1038/nmeth.3256)
22. Adhikari, S., Moscatelli, J. and Puchner, E. M. (2021). Quantitative live-cell PALM reveals nanoscopic Faa4 redistributions and dynamics on lipid droplets during metabolic transitions of yeast. *Mol. Biol. Cell* 32(17): 1565–1578. [doi: 10.1091/mbc.e20-11-0695](https://doi.org/10.1091/mbc.e20-11-0695)
23. Ovesný, M., Křížek, P., Borkovec, J., Švindrych, Z. and Hagen, G. M. (2014). ThunderSTORM: a comprehensive ImageJ plug-in for PALM and STORM data analysis and super-resolution imaging. *Bioinformatics* 30(16): 2389–2390. [doi: 10.1093/bioinformatics/btu202](https://doi.org/10.1093/bioinformatics/btu202)
24. Ries, J. (2020). SMAP: a modular super-resolution microscopy analysis platform for SMLM data. *Nat. Methods* 17(9): 870–872. [doi: 10.1038/s41592-020-0938-1](https://doi.org/10.1038/s41592-020-0938-1)
25. Thompson, R. E., Larson, D. R. and Webb, W. W. (2002). Precise Nanometer Localization Analysis for Individual Fluorescent Probes. *Biophys. J.* 82(5): 2775–2783. [doi: 10.1016/s0006-3495\(02\)75618-x](https://doi.org/10.1016/s0006-3495(02)75618-x)
26. Mortensen, K. I., Churchman, L. S., Spudich, J. A. and Flyvbjerg, H. (2010). Optimized localization analysis for single-molecule tracking and super-resolution microscopy. *Nat. Methods* 7(5): 377–381. [doi: 10.1038/nmeth.1447](https://doi.org/10.1038/nmeth.1447)
27. Mancebo, A., DeMars, L., Ertsgaard, C. T. and Puchner, E. M. (2020). Precisely calibrated and spatially informed illumination for conventional fluorescence and improved PALM imaging applications. *Methods Appl. Fluoresc.* 8(2): 025004. [doi: 10.1088/2050-6120/ab716a](https://doi.org/10.1088/2050-6120/ab716a)
28. Banerjee, C., Mehra, D., Song, D., Mancebo, A., Kim, D. H. and Puchner, E. M. (2020). ULK1 forms distinct oligomeric states and nanoscopic structures during autophagy initiation. *bioRxiv*: e187336. [doi: 10.1101/2020.07.03.187336](https://doi.org/10.1101/2020.07.03.187336)

Protein Level Quantification Across Fluorescence-based Platforms

Hector Romero*, Annika Schmidt, and M. Cristina Cardoso

Department of Biology, Technical University of Darmstadt, Darmstadt, Germany

*For correspondence: hector.romero@tu-darmstadt.de

Abstract

Biological processes are dependent on protein concentration and there is an inherent variability among cells even in environment-controlled conditions. Determining the amount of protein of interest in a cell is relevant to quantitatively relate it with the cells (patho)physiology. Previous studies used either western blot to determine the average amount of protein per cell in a population or fluorescence intensity to provide a relative amount of protein. This method combines both techniques. First, the protein of interest is purified, and its concentration determined. Next, cells containing the protein of interest with a fluorescent tag are sorted into different levels of intensity using fluorescence-activated cell sorting, and the amount of protein for each intensity category is calculated using the purified protein as calibration. Lastly, a calibration curve allows the direct relation of the amount of protein to the intensity levels determined with any instrument able to measure intensity levels. Once a fluorescence-based instrument is calibrated, it is possible to determine protein concentrations based on intensity.

Key features

- This method allows the evaluation and comparison of protein concentration in cells based on fluorescence intensity.
- Requires protein purification and fluorescence-activated cell sorting.
- Once calibrated for one protein, it allows determination of the levels of this protein using any fluorescence-based instrument.
- Allows to determine subcellular local protein concentration based on combining volumetric and intensity measurements.

Keywords: Quantification, Single-cell protein levels, FACS, Fluorescence, Microscopy, Western blotting

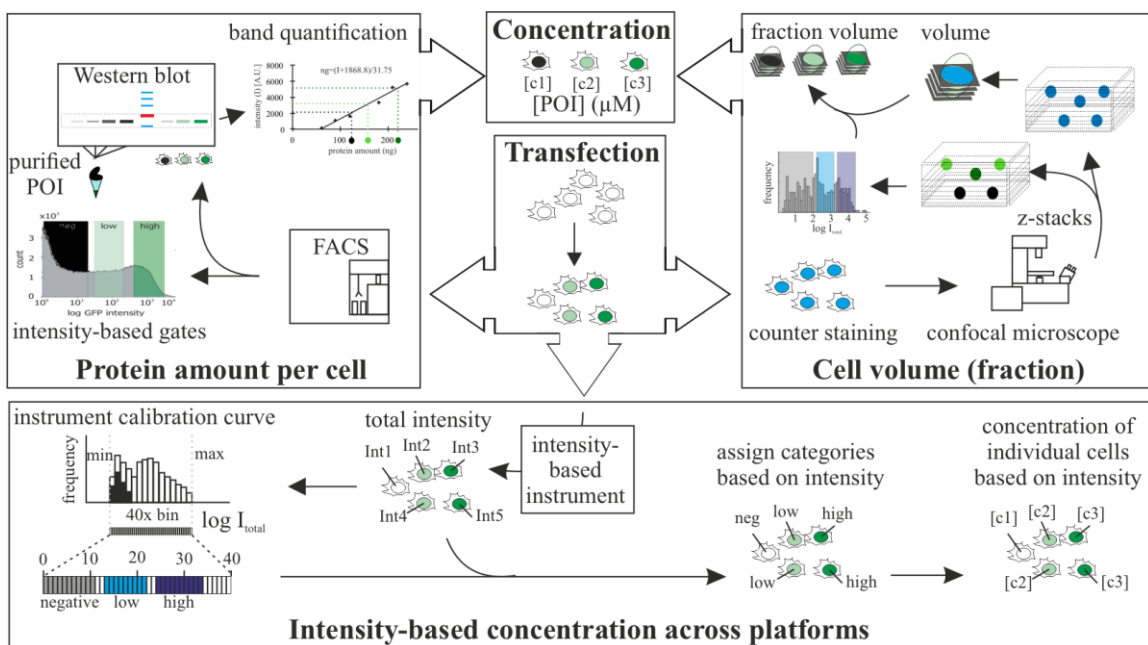
This protocol is used in: Nucleus (2022), DOI: 10.1080/19491034.2021.2024691

Cite as: Romero, H. et al. (2023). Protein Level Quantification Across Fluorescence-based Platforms. *Bio-protocol* 13(19): e4834. DOI: 10.21769/BioProtoc.4834.

Copyright: © 2023 The Authors; exclusive licensee Bio-protocol LLC.

This is an open access article under the CC BY-NC license (<https://creativecommons.org/licenses/by-nc/4.0/>).

Graphical overview



Protein level quantification across fluorescence-based platforms

Background

The use of fluorescently tagged proteins is a common tool in cell biology to study a variety of molecular processes. Although fluorescence is directly related to concentration of the fluorophore, the values of intensities do not translate directly into concentration of molecules. This is important to reproduce (patho)physiological concentrations of molecules including proteins. Western blots can be used to determine the average amount of proteins within a cell population. We performed fluorescence-activated cell sorting (FACS) prior to analysis by western blot to quantify protein levels within a cell population with defined fluorescence intensities and cell amounts. In addition, we developed a method that allows the direct relation of fluorescence intensities to get molecular concentration categories at the single-cell level. Furthermore, we expanded the method to allow concentration comparison between samples detected in different systems. Lastly, we extended the method to calculate average subcellular concentration variations. Other existing methods to determine protein concentrations are based on single-molecule imaging to calculate the number of molecules in beads (Chiu et al., 2001; Sugiyama et al., 2005) or, alternatively, use lipid or polymer layers in which the density of the fluorophore is known (Dustin, 1997; Zwier et al., 2004; Galush et al., 2008). These methods, although maybe more accurate in the estimation of concentration than ours, require calibration for each experiment and/or sophisticated equipment, whereas our method relies on equipment available in most molecular cell biology laboratories.

In the publication in which we utilized the method (Zhang et al., 2022), we used it to quantify ectopic protein concentrations in single cells and subcellular compartments. This allowed us to reproduce the same concentrations in cells and in *in vitro* experiments and to relate it to physiological tissue concentrations. Variations of the method can be used to quantify endogenous levels of tagged proteins (i.e., in cells with genetically engineered loci) or proteins labeled with antibodies.

Materials and reagents

Biological samples

1. Bovine serum albumin (BSA) (Sigma-Aldrich, catalog number: A8412); see General note 1
2. C2C12, mouse (*Mus musculus*) myoblasts (Yaffe and Saxel, 1977); see General note 1
3. Plasmid pc1208 (pEG-MeCP2) (Kudo et al., 2003); see General note 1
4. Rat IgG anti-MeCP2 4H7 antibody. Self-made, not commercial (Jost et al., 2011); see General note 1
5. Donkey anti-rat IgG-Cy3 antibody (Jackson ImmunoResearch, catalog number: 111560); see General notes 1 and 2

Reagents

1. 1,4-Diazabicyclo-[2.2.2]octane (DABCO) (Sigma-Aldrich, catalog number: D2522)
2. 2-propanol (AppliChem GmbH, catalog number: 131090.1212)
3. 4',6'-diamidine-2-phenylindole dihydrochloride (DAPI) (Carl Roth, catalog number: 6335.1)
4. Aluminum sulfate 14–18 hydrate (Carl Roth, catalog number: 3731.1)
5. Ammonium persulfate (Carl Roth, catalog number: 9592.3)
6. Bromophenol blue (Bio-Rad Laboratories, catalog number: 161-0404)
7. Coomassie, Brilliant Blue R (Sigma-Aldrich, catalog number: 1.12553)
8. Dimethylsulfoxide (DMSO) (Sigma-Aldrich, catalog number: D4540)
9. Di-sodium hydrogen phosphate 7-hydrate ($\text{Na}_2\text{HPO}_4 \cdot 7\text{H}_2\text{O}$) (Carl Roth, catalog number: X987.2)
10. Dithiothreitol (DTT) (Sigma-Aldrich, catalog number: D9779)
11. Ethanol absolute pure, pharma grade (AppliChem GmbH, catalog number: A4230)
12. Ethylenedinitrilotetraacetic acid (EDTA) (AppliChem GmbH, catalog number: 131026.1211)
13. Glucose (Sigma-Aldrich, catalog number: G5400)
14. Glycerol (Sigma-Aldrich, catalog number: G9422)
15. Hybond ECL membrane (nitrocellulose membrane) (VWR, catalog number: RPN3032D)
16. Low fat milk pulver (Sucofin)
17. Methanol for analysis EMPARTA® ACS (Sigma Aldrich, catalog number: 1070182511)
18. Mowiol® 4-88 (Sigma-Aldrich, catalog number: 81381)
19. Nonidet™ P-40 substitute (NP-40) (Roche, catalog number: 11332473001)
20. Pepstatin A (Sigma-Aldrich, catalog number: P5318)
21. Phenylmethylsulfonyl fluoride (PMSF) (Carl Roth, catalog number: 6367.1)
22. Potassium chloride (KCl) (Sigma-Aldrich, catalog number: P9541)
23. Potassium dihydrogen phosphate (KH_2PO_4) (Carl Roth, catalog number: 3904.1)
24. Tris (Sigma-Aldrich, catalog number: 93362)
25. Sodium chloride (NaCl) (Carl Roth, catalog number: 3957.1)
26. Sodium dodecyl sulfate (SDS) (Sigma-Aldrich, catalog number: 11667289001)
27. Trans-epoxysuccinyl-L-leucylamido(4-guanidino)butane (E64) (Sigma-Aldrich, catalog number: E3132)
28. Tween 20 (Carl Roth, catalog number: 131026.1211)
29. Whatman 3MM CHR (Whatman paper) (Cytiva, catalog number: 3030-672)

Solutions

1. Acrylamide/bis-acrylamide 30% (Polyacrylamide) (Sigma-Aldrich, catalog number: A3699)
2. Dulbecco's modified Eagle's medium, high glucose (Sigma-Aldrich, catalog number: D7777)
3. Fetal bovine serum advanced (Capricorn Scientific, catalog number: FBS-11A)
4. Formaldehyde solution, 36.5%–38% in H_2O (Sigma-Aldrich, catalog number: F8775)
5. Orthophosphoric acid (Carl Roth, catalog number: 6366.1)
6. Pierce™ 660 nm Protein Assay Reagent (Thermo Fisher, catalog number: 22660)

7. Pierce™ 10× Western Blot Transfer buffer, methanol-free (transfer buffer) (Thermo Fisher, catalog number: 35040)
8. Tetramethylethylenediamine (TEMED) (Sigma-Aldrich, catalog number: T9281)
9. Trypsin (Sigma-Aldrich, catalog number: T4049)
10. Ammonium persulfate 10% (see Recipes)
11. Coomassie destaining solution (see Recipes)
12. Coomassie staining solution (see Recipes)
13. DAPI solution (see Recipes)
14. E64 solution (see Recipes)
15. Loading buffer (see Recipes)
16. Low-fat milk 3% in PBS (see Recipes)
17. Low-fat milk 5% in PBS (see Recipes)
18. Lysis buffer (see Recipes)
19. Mounting media (see Recipes)
20. Pepstatin A solution (see Recipes)
21. Phosphate buffered saline (PBS) (see Recipes)
22. PBS-EDTA 0.02% (w/v) (see Recipes)
23. PMSF solution (see Recipes)
24. Polyacrylamide gel 5% (stacking) for 10 mL gel (see Recipes)
25. Polyacrylamide gel 8% (separating) for 10 mL gel (see Recipes)
26. Running buffer 10× (see Recipes)
27. Sodium dodecyl sulfate (SDS) 10% (see Recipes)
28. Tris 1 M pH 6.8 (see Recipes)
29. Tris 1 M pH 8.5 (see Recipes)
30. Tris 1.5 M pH 8.8 (see Recipes)

Recipes

1. Ammonium persulfate 10%

Reagent	Final concentration	Quantity
Ammonium persulfate	10% (w/v)	1 g
H ₂ O	n/a	to 10 mL
Total	n/a	10 mL

2. Coomassie destaining solution

Reagent	Final concentration	Quantity
Ethanol	10% (v/v)	40 mL
Orthophosphoric acid	2% (v/v)	2 mL
H ₂ O	n/a	58 mL
Total	n/a	100 mL

3. Coomassie staining solution

Reagent	Final concentration	Quantity
Coomassie	0.2% (w/v)	0.2 g
Orthophosphoric acid	2% (v/v)	2 mL
Ethanol	10% (v/v)	10 mL
H ₂ O	n/a	to 100 mL
Total	n/a	100 mL

4. DAPI solution

Reagent	Final concentration	Quantity
DAPI	1 mg/mL	10 mg
H ₂ O	n/a	to 10 mL
Total	n/a	10 mL

5. E64 solution

Reagent	Final concentration	Quantity
E64	1 mM	360 µg
Ethanol	50% (v/v)	500 µL
H ₂ O	n/a	500 µL
Total	n/a	1 mL

6. Loading buffer

Reagent	Final concentration	Quantity
Tris	50 mM	0.3 g
SDS	2% (v/v)	2 mL
Glycerol	10% (v/v)	10 mL
Bromophenol blue	0.01% (v/v)	100 µL
DTT	100 mM	1.5 g
H ₂ O	n/a	to 100 mL
Total	n/a	100 mL

7. Low-fat milk 3% in PBS

Reagent	Final concentration	Quantity
Low-fat milk pulver	3% (w/v)	0.3 g
PBS	n/a	to 10 mL
Total	n/a	10 mL

8. Low-fat milk 5% in PBS

Reagent	Final concentration	Quantity
Low-fat milk pulver	3% (w/v)	0.5 g
PBS	n/a	to 10 mL
Total	n/a	10 mL

9. Lysis buffer

Reagent	Final concentration	Quantity
Tris	25 mM	0.03 g
NaCl	1 M	0.6 g
Glucose	50 mM	0.09 g
EDTA	10 mM	0.03 g
Tween 20	0.2% (v/v)	20 µL
Nonidet™ P-40 substitute	0.2% (v/v)	20 µL
PMSF solution	1 mM	1 µL
E64 solution	10 µM	1 µL
Pepstatin A solution	29 µM	1 µL
H ₂ O	n/a	10 mL
Total	n/a	10 mL

10. Mounting media

Reagent	Final concentration	Quantity
Mowiol 4-88	13% (w/v)	8 g
Tris-HCl 1 M pH 8.5	133 mM	8 mL
H ₂ O	n/a	32 mL
Glycerol	33% (v/v)	20 mL
DABCO	2% (w/v)	1.2 g
Total	n/a	60 mL

- Add mowiol to Tris and H₂O and heat to 50–60 °C while stirring.
- Cool down to room temperature.
- Add glycerol and stir again.
- Add DABCO and dissolve it by stirring.
- Spin the solution at 5,000×g for 15 min.
- Aliquot the supernatant and store at -20 °C.

11. Pepstatin A solution

Reagent	Final concentration	Quantity
Pepstatin A	2.9 mM	2 mg
DMSO	n/a	1 mL
Total	n/a	1 mL

12. Phosphate buffered saline (PBS)

Reagent	Final concentration	Quantity
NaCl	1.37 M	80 g
KCl	27 mM	2 g
Na ₂ HPO ₄ ·7H ₂ O	10 mM	21.7 g
KH ₂ PO ₄	10 mM	2.4 g
H ₂ O	n/a	to 1 L
Total	n/a	1 L

13. PBS-EDTA 0.02% (w/v)

Reagent	Final concentration	Quantity
EDTA	0.02 % (w/v)	2 mg
PBS	n/a	to 100 mL
Total	n/a	100 mL

14. PMSF solution

Reagent	Final concentration	Quantity
PMSF	100 mM	17.42 mg
2-propanol	n/a	1 mL
Total	n/a	1 mL

15. Polyacrylamide gel 5% (stacking) for 10 mL gel

Reagent	Final concentration	Quantity
Polyacrylamide	5% (v/v)	0.33 mL
Tris 1 M pH 6.8	125 mM	0.25 mL
SDS 10%	0.1% (v/v)	0.02 mL
Ammonium persulfate 10%	0.1% (v/v)	0.02 mL
TEMED	0.001% (v/v)	0.002 mL
H ₂ O	n/a	1.4 mL
Total	n/a	2 mL

Cite as: Romero, H. et al. (2023). Protein Level Quantification Across Fluorescence-based Platforms. Bio-protocol 13(19): e4834. DOI: 10.21769/BioProtoc.4834.

16. Polyacrylamide gel 8% (separating) for 10 mL gel (see General note 1)

Reagent	Final concentration	Quantity
Polyacrylamide	8% (v/v)	2.7 mL
Tris 1.5 M pH 6.8	375 mM	2.5 mL
SDS 10%	0.1% (v/v)	0.1 mL
Ammonium persulfate 10%	0.1% (v/v)	0.1 mL
TEMED	0.0006% (v/v)	0.006 mL
H ₂ O	n/a	4.6 mL
Total	n/a	10 mL

17. Running buffer 10×

Reagent	Final concentration	Quantity
Tris base	25 mM	30 g
Glycin	1.92 M	144 g
SDS	1% (v/v)	100 mL
H ₂ O	n/a	to 1 L
Total	n/a	1 L

18. SDS 10%

Reagent	Final concentration	Quantity
SDS	10% (v/v)	10 mL
H ₂ O	n/a	90 mL
Total	n/a	100 mL

19. Tris 1 M pH 6.8

Reagent	Final concentration	Quantity
Tris	1 M	12.1 g
H ₂ O	n/a	to 100 mL
Total	n/a	100 mL

20. Tris 1 M pH 8.5

Reagent	Final concentration	Quantity
Tris	1 M	12.1 g
H ₂ O	n/a	to 100 mL
Total	n/a	100 mL

21. Tris 1.5 M pH 8.8

Reagent	Final concentration	Quantity
Tris	1.5 M	18.15 g
H ₂ O	n/a	to 100 mL
Total	n/a	100 mL

Equipment

- AMAXA nucleofector (Lonza) or equivalent. Required for transfection of cells. See General note 1
- Confocal microscope Leica TCS SPE-II (Leica) or equivalent. Required for imaging z-stacks to calculate volumes. See General note 1
- Imager AI600 (Amersham) or equivalent. Required for imaging of SDS-PAGE gels (Epi-white light of 470–635 nm, any appropriate filter to see Coomassie stained proteins) and western blots (fluorescence epi light: 460,

- 520, or 630 nm with corresponding emission filters Cy2-525BP20, Cy3-605BP40, or Cy5-705BP40, see General note 2)
4. Mini-PROTEAN Tetra Vertical Electrophoresis Cell (Bio-Rad Laboratories) or equivalent
 5. PowerPac Basic Power Supply (Bio-Rad Laboratories) or equivalent
 6. S3e Cell Sorter (Bio-Rad Laboratories) or equivalent. It requires an illumination source and filters fitting to the fluorescent tag fused to the protein of interest: for EGFP, a 488 nm laser with emission filter 525/30 nm can be used
 7. Single-molecule setup on a Nikon Eclipse Ti (Nikon). Used as example of fluorescence platforms. In the example given, EGFP images were taken using an OBIS 488 nm (100 mW) laser and a Quadbandpass (432/25 515/25 595/25 730/70 nm) filter from Nikon. See General note 1
 8. Trans-Blot[®] SD Semi-Dry Transfer Cell (Bio-Rad Laboratories) or equivalent
 9. Wide field microscope Axiovert 200 (Zeiss). Used as example of fluorescence platforms. In the example given, EGFP images were taken using a HBO100 bulb and a hard coated EGFP filter (ex: 482/18; bs: 495LP; em: 520/28). See General note 1
 10. 12 mm round coverslips (thickness 0.13–0.16 mm) (Diagonal, catalog number 41001112) or equivalent according to your microscope sample
 11. #1.5H 24 mm round coverslips (thickness 175 ± 5 µm) (Thor laboratories, catalog number: CG15XH1). Used for live-cell microscopy in single-molecule setup. See General note 1
 12. Widefield microscope Nikon Eclipse TiE2 (Nikon). Used for validation of the gate sorting across platforms. Spectra X LED 395 ± 25 nm (295 mW) and 370 ± 24 nm were used as illumination for DAPI and GFP respectively and a Quadbandpass (432 ± 25, 515 ± 25, 595 ± 25, 730 ± 70 nm) as emission filter. Images were acquired using a 20× SPlan Fluor LWD DIC objective with numerical aperture of 0.7

Software and datasets

1. S3 ProSortTM Software (Bio-Rad Laboratories) or equivalent. Used to analyze and sort the cells in the cell sorter
2. ImageJ (FIJI) (Schindelin et al., 2012). In the examples given, FIJI version 1.52q was used and the plugin BioFormats was required to open the images generated in the widefield and confocal microscopes
3. Velocity 6.3 (Perkin-Elmer). See General note 1. ImageJ plugin 3D suite can be used instead to calculate volumes and intensity in z-stacks

Procedure

A. Protein purification and concentration validation by SDS-polyacrylamide gel electrophoresis (PAGE)

1. Purify the protein. You will need a purified version of the protein of interest (POI) that you want to study. It can be either untagged or tagged (see General note 3). Due to the many possibilities in protein purification, we will not include a description of the protein purification that we used, which can be found in the manuscript (Zhang et al., 2022).
2. Analyze the purified protein using SDS-PAGE.
 - a. Prepare dilutions with known quantities (250, 500, 750, 1,000, 1,500, 2,000 ng) of a reference protein (i.e., BSA) for a final volume of 15 µL in H₂O.
 - b. Estimate the concentration of the purified protein by a colorimetric assay (e.g., PierceTM 660 nm Protein Assay Reagent).
 - c. Prepare specific quantities of the purified protein using the estimations (400, 600, 800, 1,000 ng) to a final volume of 15 µL in H₂O.
 - d. Mix the dilutions of reference protein with 5 µL of loading buffer 4× to a final concentration 1×, boil them in 95 °C for 5 min, and then keep on ice.

- e. Mix the different quantities of purified protein with 5 μ L of loading buffer 4 \times to a final concentration 1 \times , boil them at 95 °C for 5 min, and then keep on ice.
- f. Place a polyacrylamide gel in the electrophoresis chamber and fill it with 1 \times running buffer.
- g. Analyze the samples by polyacrylamide gel electrophoresis with constant 100 V.
- h. Incubate the gel in Coomassie staining solution overnight (~16 h).
- i. Incubate the gel in destaining solution (2 \times 10 min) and equilibrate in H₂O.
- j. Image the gel in the imager (Figure 1A).

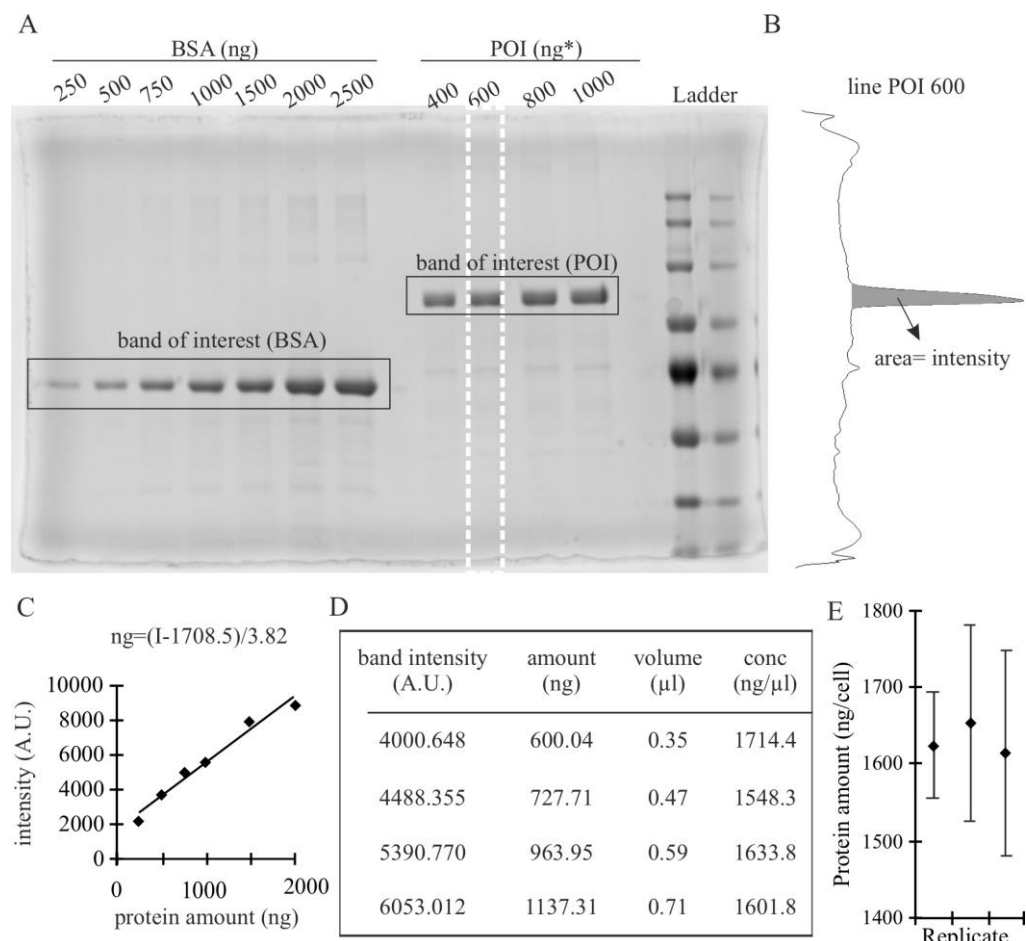


Figure 1. SDS-PAGE stained with Coomassie and analysis to validate the concentration of the purified protein. (A) Example of gel for validation. Known quantities of bovine serum albumin (BSA) are loaded together with different quantities of purified protein of interest (POI) estimated by colorimetric assay. Modified from Zhang et al. (2022). The white dashed line represents the selection used for quantification in B. (B) Intensity profile obtained in ImageJ using the gel analysis tool. Selections of the width of the band were done for individual bands and the area of the band of interest was calculated as the area under the peak. (C) Calibration curve based on the intensity measures obtained in B. The equation of the regression curve is described within the graph. (D) Calculations to obtain the corrected concentration (conc) of the POI, based on the intensity measurements of the POI bands using the equation of the regression curve from B, allow the determination of the corrected amount of POI from the calculated intensity of the band and the concentration in ng/ μ L as the average from the values obtained, 1624.6 ± 80.3 ng/ μ L. The values displayed are the calculation from left (POI 400 ng) to right (POI 1000) in the gel shown in A. The calculation of the error is described in the section data analysis. (E) Measurements and standard deviations for three technical replicates,

each of them taking four band intensities to calculate the average as shown in D (which corresponds to left replicate).

3. Validate the concentration of purified protein by image analysis of the gel using ImageJ.
 - a. Generate a rectangular selection that covers a complete band.
 - b. Create a region of interest using the function *Analyze* → *Gels* → *Select First Lane* (for the first lane) and *Analyze* → *Gels* → *Select Next Lane* (for the others) (Figure 1A, white dashed line).
 - c. Get the intensity measurements using the function *Analyze* → *Gels* → *Plot Lanes* (Figure 1B).
 - d. Quantify the intensity of the bands as the area under the peak (Figure 1B). To do so: i) draw a horizontal lane in the base of the peak using the tool *straight line* so the peak is closed; ii) use the tool *wand* to select the peak; iii) automatically, it will display the area of the region selected.
 - e. Plot the intensity (area) against the known concentration of the reference protein and generate a regression curve (Figure 1C).
 - f. The equation of the regression curve is $Y = a \times X + b$, being X the quantity of protein (in ng) and Y the intensity. Therefore, considering $X = (Y - b)/a$, you can calculate the protein amount based on intensity (Figure 1C). The parameter b corresponds to the background of the specific gel.
 - g. Use the intensity values obtained from the area under the peaks for each estimated amount of POI to get the actual values (Figure 1D).
 - h. You can get the concentration of the POI by dividing the amount of POI by the volume from the original solution added in each well (Figure 1D). The concentration of POI is the average of these values.

B. Calculation of protein amounts in cell fractions using fluorescence activated cell sorting and western blot

1. Sample preparation: grow the cells in the specific conditions required for its culture. You will need 10^6 – 10^7 cells in a 10 cm cell culture plate from wildtype (untransfected cells) and transfected cells. This step should be adapted to the specific cell line used. In the case of C2C12 using AMAXA electroporation:
 - a. Seed 50 cells/cm² in a 10 cm cell culture plate.
 - b. Grow overnight in growth media at 37 °C with 5% CO₂.
 - c. Remove media.
 - d. Wash cells with PBS-EDTA.
 - e. Add 2 mL of trypsin.
 - f. Incubate for 5 min at 37 °C.
 - g. Stop the trypsin with 4 mL of growth media.
 - h. Seed 0.5 mL of cells into a new 10 cm cell culture plate with 9 mL of growth media (untransfected sample).
 - i. Centrifuge 1 mL of cells at $0.3 \times g$ for 5 min and discard the supernatant.
 - j. Mix 2–5 µg of plasmid in 100 µL of room-temperature AMAXA M1 solution.
 - k. Resuspend the pellet in the AMAXA M1 solution containing the plasmid and collect in a cuvette.
 - l. Place the cuvette in the AMAXA nucleofector and select the program B-032.
 - m. Collect the cells and seed them in a new 10 cm cell culture plate with 10 mL of growth media (transfected sample).
 - n. Incubate the untransfected and transfected samples overnight at 37 °C with 5% CO₂.
2. Sample processing; the individual plates are processed individually:
 - a. Wash cells with PBS.
 - b. Add 2 mL of trypsin.
 - c. Incubate for 5 min at 37 °C.
 - d. Collect the cells in a 15 mL tube.
 - e. Centrifuge at $0.3 \times g$ for 5 min and discard the supernatant.
 - f. Resuspend the pellet in 2 mL of PBS.
 - g. Centrifuge at $0.3 \times g$ for 5 min and discard the supernatant.

- h. Resuspend the pellet in 3 mL of PBS.
3. Fluorescence-activated cell sorting (FACS)
 - a. Analyze the untransfected cells in analysis mode to determine the GFP intensity vs. the area and save the minimum and maximum intensity values. We recommend a count of approximately 10^6 cells for reproducibility. If the software of the FACS sorter does not provide the values, these can be inferred from the resulting graphs.
 - b. Analyze the transfected cells in analysis mode with the same settings as the untransfected cells and save the maximum intensity value. We recommend a count of approximately 10^6 cells for reproducibility. If the software of the FACS sorter does not provide the values, these can be inferred from the resulting graphs.
 - c. Use the acquired values for calculation of the gates (Table 1). See General note 4.

Table 1. Parameters for gate calculation based on intensities. *The use of logarithm is for presentation purposes and does not affect the following calculations.

Parameter	Description	Formula
MIN	Minimum value of intensity in the untransfected sample	$\log(\min \text{ int } \text{untransfected})^*$
NEG_MAX	Maximum value of intensity in the untransfected sample	$\log(\max \text{ int } \text{untransfected})^*$
POS_MAX	Maximum value of intensity in the transfected sample	$\log(\max \text{ int } \text{transfected})^*$
BIN	Reference interval (see General note 4)	$(\text{POS_MAX}-\text{NEG_MAX})/40$
POS_TH	Threshold to define a positive count	$\text{MIN} + 11 * \text{BIN}$
LOW_MIN	Minimum threshold for the category “low”	$\text{MIN} + 13 * \text{BIN}$
LOW_MAX	Maximum threshold for the category “high”	$\text{MIN} + 22 * \text{BIN}$
HIGH_MIN	Minimum threshold for the category “low”	$\text{MIN} + 24 * \text{BIN}$
HIGH_MAX	Maximum threshold for the category “high”	$\text{MIN} + 33 * \text{BIN}$

- d. Sort the transfected cells into “low” and “high” based on the intensity values defined by the gates (Figure 2). Collect the cells and save the cell number count.

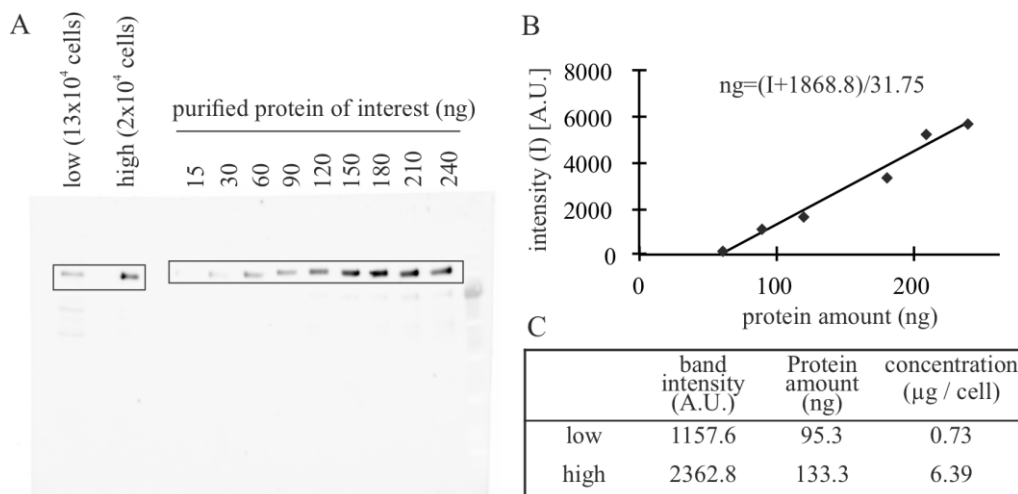


Figure 2. Example of western blot analysis to quantify the amount of protein of interest (POI) in FACS cell fractions. (A) Example of a gel for validation. Known quantities of purified POI are loaded together with lysates of known quantities of cells. Modified from Zhang et al. (2022). (B) Quantification of the bands of the gel using the gel tool analysis from ImageJ to determine the intensity of the purified POI and generate a calibration curve. (C) Combine the intensity measurements of the bands of lysates with the validation curve to obtain corrected amounts of total protein and, knowing the number of cells, the amount of protein per cell.

4. Extraction of total proteins from cells for western blot.
 - a. Centrifuge the cells from the sorted fractions at $0.3 \times g$ for 5 min and discard the supernatant.
 - b. Resuspend the pellet in 1 mL of lysis buffer with vigorous pipetting to disrupt the membranes.
5. Quantification of the amount of protein in sorted cells by western blot.
 - a. Prepare known quantities of purified POI (30, 60, 90, 120, 150, 180, 210, and 240 ng) according to the concentration calculated in A. See General note 5.
 - b. Mix the standard POI and the samples with a $4 \times$ loading buffer to a final concentration of $1 \times$ and boil them in 95 °C for 5 min. Clear the cell lysates by centrifugation at $10,000 \times g$ for 10 min and keep the supernatant on ice.
 - c. Analyze the fractions by SDS-PAGE as described before in steps A2e–A2f.
 - d. Prepare transfer buffer $1 \times$ by diluting 3 mL of transfer buffer $10 \times$ in 27 mL of H₂O.
 - e. Cut Whatman papers and nitrocellulose membrane in the size of the gel and soak them in transfer buffer $1 \times$ for 15 min.
 - f. Wash the gel in H₂O for 10 min.
 - g. Equilibrate the gel in transfer buffer $1 \times$ for 10 min.
 - h. Assemble the transfer unit into the transfer chamber (from down to up): 2× Whatman, nitrocellulose membrane, gel, 2× Whatman.
 - i. Remove the bubbles.
 - j. Transfer the proteins to a nitrocellulose membrane with constant 25 V for 20–45 min.
 - k. Incubate the membrane in 5% low-fat milk in PBS for 30–60 min at room temperature in a rotator.
 - l. Incubate with antibodies against your POI in the appropriate dilution overnight at 4 °C in a rotator.
 - m. Incubate with secondary antibodies linked to a fluorophore in the appropriate dilution in 3% low-fat milk in PBS for 1 h at room temperature in a rotator.
 - n. Detect the fluorescent signals using the imager (Figure 2A).
 - o. Measure the intensity in the bands using ImageJ as described before in steps A3a–A3d (Figure 1B).
 - p. Plot the intensity against the known concentrations to generate a regression curve.
 - q. Using the equation from the regression curve, calculate the protein amount for the “low” and “high” fractions of sorted cells. The intensities of the POI should be within the (linear) range of the calibration curve.
 - r. Divide the protein amount by the number of cells analyzed on the gel to obtain the number of molecules per cell.

C. Calculation of concentration (and use across imaging platforms)

1. Sample preparation. Grow the cells in the condition required in substrates suitable for imaging (i.e., chamber slides or coverslips). Follow the procedure described in step B1. See General note 6. The method is suitable for live or fixed cells. In case of fixed cells:
 - a. Remove media.
 - b. Wash the coverslips with PBS twice.
 - c. Incubate coverslips with formaldehyde solution 1:10 in PBS at room temperature for 10 min.
 - d. Wash the coverslips with PBS three times.
 - e. Add a 15 µL droplet of DAPI solution on parafilm and place the coverslips upside down. Incubate for 15 min at room temperature in darkness.
 - f. Turn the coverslips upside up.
 - g. Wash the coverslips with PBS three times.
 - h. Wash the coverslips once with H₂O.
 - i. Add a 10 µL droplet of mounting media on a glass slide and place the coverslips upside down on it.
 - j. Let it dry in darkness.
2. Generation of calibration curve. See General note 6.
 - a. Acquire images of the cells in both negative and transfected cells with the same settings for the channel of the POI. Additionally, one can acquire additional channels to facilitate segmentations. In

the examples given, we used a second channel with either DAPI (in fixed cells) or a protein that shows nuclear distribution (in live-cell imaging).

- b. Segment the cells (or nuclei, in our case) using ImageJ (Figure 3A). In the example given, cells were segmented using the following ImageJ protocol: i) *Process* → *Filters* → *Gaussian blur...*, applying 2 pixels sigma (radius); ii) *Process* → *Subtract background*, applying 15 pixels of Rolling ball radius, and all other options not selected; iii) *Image* → *Adjust* → *Threshold*, using “Li” as threshold method. Images were then revised to find nucleus that were too close together and recognized as one to either discard them (when they overlapped) or separate into two regions of interest (when possible).
- c. Calculate the total intensity in the channel of the POI for all cells. This value corresponds to the column “IntDen” in ImageJ result table and can be selected in *Analyze* → *Set measurements...* → *Integrated density*.
- d. Calculate the intensity values of the gates as described in Table 1 (Figure 3B).
- e. Plot the frequencies of cells in range of the logarithm of intensity (Figure 3C).

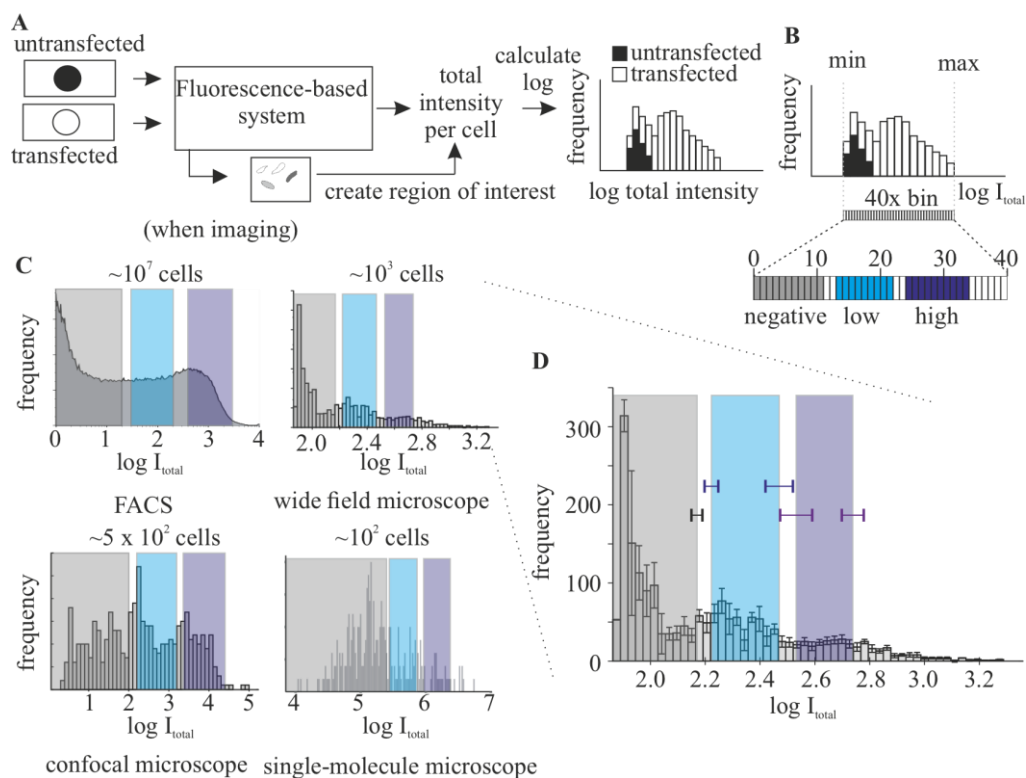


Figure 3. Generation of a calibration curve for different instruments. (A) Scheme of the minimal analysis required to generate a calibration curve in a new imaging system. (B) Calculation of the gates based on the values of intensity obtained. Bins are calculated as 1/40 of the difference between the minimal (min) and maximal (max) values observed. (C) Examples of curves for the same POI in different imaging systems: FACS (left panel), widefield (middle-left panel), confocal (right-left panel), and single-molecule microscope (right panel). Increasing the number of cells imaged leads to higher resemblance to the curve used for quantifying the protein of interest (POI) by western blot (FACS). FACS, widefield, and single molecule are modified from Zhang et al. (2022). (D) Depiction of the effects of replicates in the generation of the gates. The error bar corresponding to the three biological replicates (with $n > 500$ each) used to generate the widefield graph in C, including the standard deviation of the calculation of the gates using the single datasets.

- f. Check the quality of the calibration curve: all negative cells should be categorized as negative, and cells categorized as high should have a clear signal in the POI channel. See troubleshooting.

3. Calculation of concentration.
 - a. Acquire Z-stacks that contain the whole cellular structure where the POI is located, following the Nyquist sampling (i.e., in a confocal microscope), including the channel of the POI.
 - b. Segment the structure (additional channels can be used) and determine the intensity in the POI channel for the volume. See General note 8. In the example given, 3D segmentation was done in Volocity using the DAPI channel using the following protocol: I) Measure → Finding → Find objects; II) Measure → Processing → Dilate (iteration: 3); III) Measure → Processing → Fill holes in objects; IV) Measure → Processing → Erode (iteration: 3); V) Measure → Filtering → Exclude objects by size. The volume can be calculated from the Voxel count while the intensity is described in Sum, in the table that describes the ROIs.
 - c. Using the values for the gates of the calibration curve, classify the cells into *low* and *high*. See General note 7.
 - d. Calculate the average volume of the structure in the different categories.
 - e. The concentration of the POI for each category corresponds to the amount of protein per cell divided by the average volume of the structure for this category.

Data analysis

Note that, in the examples given, the protein concentration calculated for individual cells is classified in a broad category due to the selection of gates. However, the method can be as precise as it is possible to reduce the gate size and get enough cells to perform a measurable western blot. Even in this situation, there will be an error with three components: i) calculating the protein amount by western blot; ii) variability in cellular (or nuclear) volume; iii) error in the intensity measurements. Taking into account all these considerations, this method allows to assign single cells based on the POI fluorescence intensity to corresponding ranges of protein concentrations. To properly consider the mentioned errors in the final concentration number, error propagation should be taken into account at every step. In error propagation, given a function: $f = a \times b/y$, in which the errors of the variables a , b , and y are ∂_a , ∂_b , and ∂_c , respectively, the error of $f (\partial_f)$ can be calculated as follows:

$$\partial_f = f \times \sqrt{\frac{\partial_a^2}{a^2} + \frac{\partial_b^2}{b^2} + \frac{\partial_y^2}{y^2}}$$

Here, you can find the sources of error and how to obtain error values:

1. Protein concentration for the purified protein in ng/μL (Figure 1) and in the fractions in μg/cell (Figure 2).
 - a. Intensity measurements: can be estimated as the average standard deviation of the background signal. To calculate the background signal, generate several ROIs in the same size between lines and obtain the intensities. This value corresponds to the column “IntDen” in ImageJ result table and can be selected in Analyze → Set measurements... → Integrated density.
 - b. In replicate error: the standard deviation between the different lanes calculated (in the case of Figure 1).
 - c. Replicate error: standard deviation between technical and/or biological replicates plus the propagated error of the calculations.
2. Concentration of the protein in μM.
 - a. Protein concentration calculation as described above.
 - b. Volume calculation: standard deviation between cells.

In the example given in Figure 1, the background standard deviation, calculated as described in step 1a, is 15.793. Therefore, the concentrations in ng/μL for each line are $1,714.4 \pm 6.8$, 158.3 ± 5.5 , $1,633.8 \pm 4.8$, and $1,601.8 \pm 4.2$. The final concentration number is then the average of the values, 1624.6, and the error corresponds to the standard deviation of the replicates (69.5), to which is added the propagation error of the calculations (10.8), giving the final number of $1,624.6 \pm 80.3$ ng/μL.

Validation of protocol

This method was validated in Zhang et al. (2022), corresponding to figures 3, supplementary figure 3, and supplementary tables S9 and S10.

For quantification, three replicates of transfected cells were sorted and analyzed with western blot to obtain the number of molecules. At least 50 cells from two biological replicates were used to calculate the volumes for the concentration for each condition.

Different calibrating curves were used in widefield microscopy (three biological replicates with approximately 500 cells per experiment) with comparable results of intensity values (Figure 3D).

To validate the use across platforms, we prepared samples as described in step B1. One-third of the cells (transfected or untransfected) were grown on coverslips and two-thirds were grown on a tissue culture dish. After 24 h, coverslips were collected, fixed with ice-cold methanol for 6 min, counterstained with DAPI, and mounted as described in steps C1d to C1i. All coverslips were imaged using a widefield microscope (Figure 4A). The DAPI channel was used for segmentation by processing in ImageJ (Gaussian blur, sigma 5 pixels; Subtract background, rolling, 20 pixels). Only nuclei with areas between 90 and 140 μm^2 were considered based on our prior knowledge with C2C12 myoblasts. The calibration curve was done using the GFP intensities (Figure 4B, histogram) within the segmented nuclei. The cells grown on dishes were collected and sorted as described in steps B2 and B3, and the resulting fractions low and high were fixed with ice-cold methanol for 6 min, dried on to the coverslips by incubation at 37 °C overnight, and followed by counterstaining with DAPI and mounting as described before. These coverslips were imaged in the same conditions as the calibration (Figure 4A). The GFP intensity of the sorted cells was overlaid in the histogram (Figure 4B), resulting in segregation in the correct gates in most cases.

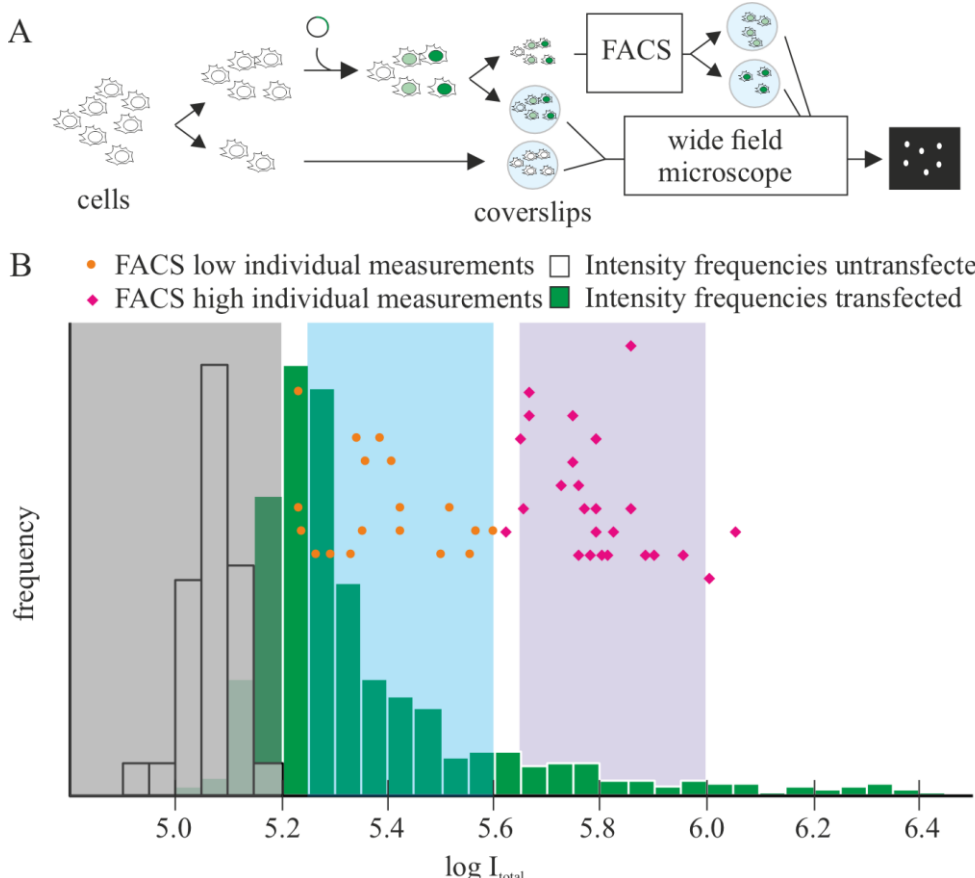


Figure 4. Validation of the reproducibility of the quantification across platforms. (A) Scheme of the validation process: cells (untransfected and transfected) were seeded in coverslips and, in parallel, a fraction of the transfected

cells was sorted using fluorescence-activated cell sorting (FACS) in the categories low and high. The resulting fractions were fixed on coverslips by dehydration. All coverslips were counterstained with DAPI and imaged using a widefield microscope. DAPI was used for segmenting cell nuclei and quantifying total intensity of the GFP channel in the nucleus. (B) Non-sorted cells were used for determining the calibration curve, based on the frequencies (n untransfected: 63, n transfected: 1,539). Orange dots and magenta diamonds represent individual intensity values for the sorted low and high fraction, respectively.

General notes and troubleshooting

General notes

1. This material is not specifically needed for the protocol but has been used in the examples given.
2. Fluorescent or radioactive coupled secondary antibodies should be used for western blot to ensure linearity of the signal intensities. Enzymatic reactions (i.e., antibodies coupled to horseradish peroxidase) are not recommended.
3. Use tagged purified protein in cases where the protein of interest does not have suitable antibodies for western blot.
4. The selection of 40 bins as reference interval is meant to be versatile to generate different gate outcomes (number of categories) without changing the reference interval but can be adapted to the concrete experimental settings. Please note that the number of bins determines the range of variability that is accepted when setting gates. This step is the most susceptible to optimization when using other fluorophores and/or proteins.
5. The amount of protein of interest analyzed on the gel should be similar to the amount expected for the number of cells loaded. When the band corresponding to the cells is not within the calibration curve, you can modify the amounts of purified protein loaded for calibration and/or use a different number of cells.
6. You will need untransfected wildtype cells without a tag as negative control and transfected cells in the same conditions as described in section B for generating the calibration curve for each platform. The system is suitable for both live and fixed-cell microscopy, including immunostaining. The only requirement is that any further fluorescence, antibody, or other component should not interfere with the measurement of the intensity of the POI (i.e., overlapping of emission spectra with detection).
7. Each imaging instrument will require its own calibration curve. The accuracy of the measurements is highly dependent on the number of cells used for the calibration curve (Figure 3C), being ~200 cells the minimum to get reproducible results. The calibration curve can be used in the same platform, as long as the acquisition conditions (i.e., laser power, exposure time) remain constant between experiments. Please note that calibration curves should be different if single plane and volumes are used. This method should not be affected by any additional processing method (i.e., different deconvolution algorithm). If additional processing is used to determine intensities during the analysis, the images used for calibration must be treated the same way.
8. This section can be used to determine subcellular concentration for the POI by segmenting the subcellular structure instead of the whole cell.

Troubleshoot in calibration curves

Problem 1: Negative cells are included in the low gate.

Possible causes: (a) Dead cells with high autofluorescence have been segmented; (b) two or more cells have been segmented as one. This can be detected by plotting intensities vs. cell area; (c) bins are not accurate enough due to insufficient number of cells.

Solutions: (a) Revise the images and eliminate these cells; (b) revise the segmentation process; or (c) acquire more images from the same sample in the same conditions or merge several experiments imaged in the same conditions.

Problem 2: Transfected cells are included in the negative category.

Possible cause: Inappropriate imaging conditions (i.e., laser power or acquisition time) lead to saturation of highly expressed cells.

Solution: Discard the dataset. If the dataset is extremely valuable, you can estimate the percentage of saturated cells compared to other datasets and displace the gates accordingly (note that this will add an imperfectible error!).

Acknowledgments

This work was financed by grants CA 198/10-1 project number 326470517 and CA 198/16-1 project number 425470807 to M.C.C. We thank Hui Zhang for his advice during the development of the method.

Competing interests

The authors declare no competing interests.

References

- Chiu, C. S., Kartalov, E., Unger, M., Quake, S. and Lester, H. A. (2001). [Single-molecule measurements calibrate green fluorescent protein surface densities on transparent beads for use with ‘knock-in’ animals and other expression systems](#). *J. Neurosci. Methods* 105(1): 55–63.
- Dustin, M. L. (1997). [Adhesive Bond Dynamics in Contacts between T Lymphocytes and Glass-supported Planar Bilayers Reconstituted with the Immunoglobulin-related Adhesion Molecule CD58](#). *J. Biol. Chem.* 272(25): 15782–15788.
- Galush, W. J., Nye, J. A. and Groves, J. T. (2008). [Quantitative Fluorescence Microscopy Using Supported Lipid Bilayer Standards](#). *Biophys. J.* 95(5): 2512–2519.
- Jost, K. L., Rottach, A., Milden, M., Bertulat, B., Becker, A., Wolf, P., Sandoval, J., Petazzi, P., Huertas, D., Esteller, M., et al. (2011). [Generation and Characterization of Rat and Mouse Monoclonal Antibodies Specific for MeCP2 and Their Use in X-Inactivation Studies](#). *PLoS One* 6(11): e26499.
- Kudo, S., Nomura, Y., Segawa, M., Fujita, N., Nakao, M., Schanen, C. and Tamura, M. (2003). [Heterogeneity in residual function of MeCP2 carrying missense mutations in the methyl CpG binding domain](#). *J. Med. Genet.* 40(7): 487–493.
- Schindelin, J., Arganda-Carreras, I., Frise, E., Kaynig, V., Longair, M., Pietzsch, T., Preibisch, S., Rueden, C., Saalfeld, S., Schmid, B., et al. (2012). [Fiji: an open-source platform for biological-image analysis](#). *Nat. Methods* 9(7): 676–682.
- Sugiyama, Y., Kawabata, I., Sobue, K. and Okabe, S. (2005). [Determination of absolute protein numbers in single synapses by a GFP-based calibration technique](#). *Nat. Methods* 2(9): 677–684.
- Yaffe, D. and Saxel, O. (1977). [Serial passaging and differentiation of myogenic cells isolated from dystrophic mouse muscle](#). *Nature* 270(5639): 725–727.
- Zwier, J. M., Van Rooij, G. J., Hofstraat, J. W. and Brakenhoff, G. J. (2004). [Image calibration in fluorescence microscopy](#). *J. Microsc.* 216(1): 15–24.
- Zhang, H., Romero, H., Schmidt, A., Gagova, K., Qin, W., Bertulat, B., Lehmkuhl, A., Milden, M., Eck, M., Meckel, T., et al. (2022). [MeCP2-induced heterochromatin organization is driven by oligomerization-based liquid–liquid phase separation and restricted by DNA methylation](#). *Nucleus* 13(1): 1–34.

Intravital Imaging of Intestinal Intraepithelial Lymphocytes

Sara McArdle¹, Goo-Young Seo¹, Mitchell Kronenberg^{1, 2, *}, and Zbigniew Mikulski^{1, *}

¹La Jolla Institute for Immunology, La Jolla, CA, USA

²Department of Molecular Biology, University of California San Diego, La Jolla, CA, USA

*For correspondence: mitch@lji.org; zmikulski@lji.org

Abstract

Intestinal intraepithelial lymphocytes (IEL) are a numerous population of T cells located within the epithelium of the small and large intestines, being more numerous in the small intestine (SI). They surveil this tissue by interacting with epithelial cells. Intravital microscopy is an important tool for visualizing the patrolling activity of IEL in the SI of live mice. Most IEL express CD8α; therefore, here we describe an established protocol of intravital imaging that tracks lymphocytes labeled with a CD8α-specific monoclonal antibody in the SI epithelium of live mice. We also describe data acquisition and quantification of the movement metrics, including mean speed, track length, displacement length, and paths for each CD8α⁺ IEL using the available software. The intravital imaging technique for measuring IEL movement will provide a better understanding of the role of IEL in homeostasis and protection from injury or infection *in vivo*.

Keywords: Intravital microscopy, Intraepithelial lymphocyte, Tracking, Cell labeling, Suction ring, Intestine, Confocal reflection

This protocol is used in: Sci. Immunol. (2022), DOI: 10.1126/sciimmunol.abm6931

Background

Intestinal intraepithelial lymphocytes (IEL), sometimes also known as intraepithelial T cells, are one of the largest populations of T lymphocytes in the body. They are located within the epithelium and interact extensively with intestinal epithelial cells by actively patrolling the basement membrane and migrating into the lateral intercellular space (Edelblum et al., 2012; Wang et al., 2014; Hoytema van Konijnenburg et al., 2017; Sumida et al., 2017). IEL are important for the maintenance of integrity of the intestinal barrier, repair of wounds, and protection from pathogenic invasion (Cheroutre et al., 2011). They include innate lymphoid cells but are mostly T lymphocytes. In previous work, we focused on the role of herpes virus entry mediator (HVEM) as a regulator of CD8 α^+ intraepithelial T cells in the small intestinal (SI) epithelium. We used intravital imaging to track lymphocytes labeled with a CD8 α -specific monoclonal antibody in the SI epithelium of live mice (Edelblum et al., 2012; Wang et al., 2014). In the previous work, by using mice with deficiency for HVEM expression exclusively in the intestine epithelium we showed that in the SI, epithelial HVEM expression is required for the normal patrolling movement of CD8 α^+ IEL. This correlated with a decreased response to bacterial infection (Seo et al., 2018). Here, we describe a protocol to analyze CD8 α^+ IEL in the SI epithelium using intravital imaging.

Materials and reagents

1. #1.5 12 mm round coverslips (Electron Microscopy Sciences, catalog number: 72230-01)
2. 31G 0.5 mL insulin syringe for retroorbital (RO) and anesthesia injection (BD, catalog number: 328447)
3. Vacuum grease, MOLYKOTE® High Vacuum Grease (McMaster-Carr, catalog number: 2966K52)
4. 10 mL syringe (BD, catalog number: 303134)
5. Lab tape (Fisher Scientific, catalog number: 15-950)
6. Antibodies: anti-CD8 α -AF488, clone 53-6.7 (eBioscience, catalog number: 53-0081-82); anti-CD8 α -AF647, clone 53-6.7 (BD Biosciences, catalog number: 557682); anti-EpCAM-AF647, clone G8.8 (BioLegend, catalog number: 118211)
7. Sterile phosphate buffered saline (PBS) (Thermo Fisher Scientific, catalog number: 10010023)
8. Isoflurane (Covetrus, National Drug Code: 11695-6777-2, 250 mL, catalog number: 029405)
9. Oxygen (100% compressed oxygen gas)
10. Ketamine, Ketaset, 100 mg/mL (Zoetis, National Drug Code: 54771-2013-1)
11. Xylazine, XylaMed, 100 mg/mL (VetOne, National Drug Code: 13985-612-50)
12. Vaseline (Fisher Scientific, catalog number: 17-986-496)
13. 70% isopropanol (Covetrus, National Drug Code: 11695-2178-6, reorder number 002498)
14. Mice on a C57BL/6 background, available from Jackson Laboratories, kept in specific pathogen-free conditions. We used *Hvem*^{fl/fl-neo/fl-neo} and *Hvem*^{fl/fl} mice (Seo et al., 2018)

Equipment

1. Animal heating controller and 15 cm × 10 cm heating plate (World Precision Instruments, catalog number: ATC2000 and 61830)
2. Rodent rectal temperature probe (World Precision Instruments, catalog number: RET-3)
3. Isoflurane vaporizer and mouse isoflurane mask
Link7 (Patterson Scientific, catalog number: 78919043)
Uniflow Single Manifold (Patterson Scientific, catalog number: 78924212)
4. Surgical scissors for skin, small surgical scissors, surgical forceps, Dumont #5/45 forceps
5. Hair clippers (Wahl, catalog number: 88420) or Nair hair remover sensitive formula
6. Thermal Cauterizer Unit (Geiger Instruments, model: 150-I or similar unit)
7. Suction ring assembly

- a. CNC-machined suction ring (parts Prototype Master, Angle Arm, Post, and Extension from *Zera Development Co.*, n.d., Santa Clara, CA)
 - b. Indicator swivel clamp with T-handle adjustment, 1/2" diameter × 3/8" diameter (McMaster-Carr, catalog number: 5148A28)
 - c. Polyethylene 160 tubing fitted with blunted 18G needle (Warner Instruments, catalog number: 64-0755)
 - d. Male Luer lock to 1/4" barb connector (Amazon, catalog number: B0BB649WM2)
 - e. Thick-walled vacuum tubing, internal diameter 3/8" or 9.7 mm (VWR, catalog number: MFLX06404-36)
 - f. Thick-walled vacuum tubing, internal diameter 5/16" or 7.9 mm (VWR, catalog number: MFLX06404-35)
 - g. Vacuum waste gate [can be repurposed from 2-way stopcock (Amazon, catalog number: B09P8GNP7S) or aquarium pump control valve (Amazon, catalog number: B08LGHWB77)]
 - h. 5/16" T-splitter (usplastic.com, catalog number: 62095)
 - i. Small vacuum trap with fittings for 7.9 mm ID tubing (SP Bel Art, catalog number: F19919-0000)
 - j. 1/4" NPT female to 3/8" barb connector (Amazon, catalog number: B09Q813WN1)
 - k. Coarse vacuum adjustment valve: 1/4" male-male NPT Valve (Amazon, catalog number: B07YFS1WFX)
 - l. 1/4" Barstock tee female adapter (Amazon, catalog number: B07MTWH2W9)
 - m. 2" male-male extension nipple (Amazon, catalog number: B000BOA2V2)
 - n. 1/4" NPT female-female coupler (Amazon, catalog number: B09651GMQ3)
 - o. Vacuum dry pressure gauge, lower mount, 1/4" NPT (Carbo Instruments, catalog number: D25-CSL-V00)
 - p. 1/4" NPT male to 5/16" barb connector (Amazon, catalog number: B07RKM6VR8)
 - q. Teflon tape (Amazon, catalog number: B095YCMHNX)
 - r. Hydrophobic filter, Millex-FG, 0.20 µm, hydrophobic PTFE, 50 mm (Millipore, catalog number: SLFG85010)
8. Upright Leica SP5 or SP8 confocal microscope or equivalent
 - a. Resonant scanner
 - b. 25× (0.95) water-dipping, coverslip-corrected objective (Leica 506375)
 - c. Piezo Z controller (Piezosystem Jena, catalog number: 0-350-01 or similar)
 - d. 488 and 638 nm laser lines
 - e. Motorized Movable Base Plate or equivalent for support of the animal stage (Scientifica, model: MMBP-7200-00)

Software

1. Leica SP8 software LAS X
2. Fiji (Schindelin et al., 2012) with the Bio-formats and MISTICA Image Alignment (Ray et al., 2016)
A version of Fiji packaged with MISTICA can be found at github.com/saramcardle/IEL. Otherwise, use the latest Fiji version.
3. Imaris (Bitplane, version 9.4 or higher)
4. MATLAB (Mathworks, version 2021a) or the compiled SpiderPlot application (github.com/saramcardle/IEL)

Procedure

A. Mouse preparation

Please consult your Institutional Animal Care Committee or equivalent body to ensure that all procedures were reviewed and approved according to the governing laws. All procedures described here were approved by the La Jolla Institute for Immunology Animal Care and Use Committee.

The guiding principle is to induce the least amount of stress on the animal. Handle animal cages with care so as not to startle the inhabitants. Avoid any strong scents, perfumes, and deodorants (*Mouse Room Conditions*,

n.d.). Practice handling of the mice to be confident, accurate, and gentle—this will minimize the stress to both animals and researchers. From the perspective of the mouse, repeated attempts to grab it are likely worse than a single successful capture. It is crucial to practice restraining the animal to deliver RO injections properly. In intravital microscopy, your biggest responsibility is to care for animals and to minimize the potential harm coming from your interventions. You will have a chance to glimpse the fascinating world of cellular behavior in their natural environment, but beware of false conclusions stemming from stressed, injured, damaged, hypoxic, unperfused, and photodamaged tissues.

1. For antibody-based cell labeling, inject the antibodies 4 h before imaging to allow for sufficient time for antibody penetration. With shorter incubations, a significant fraction of the antibody remains in the blood vessels. Over time, surface-bound antibodies will be internalized, and distinct membrane staining will be replaced by a more uniform labeling in the cytosol (Figure 1). In our hands, longer incubation times do not significantly improve cell labeling but are a cause of concern for biological actions mediated by antigen-antibody binding and other effects.

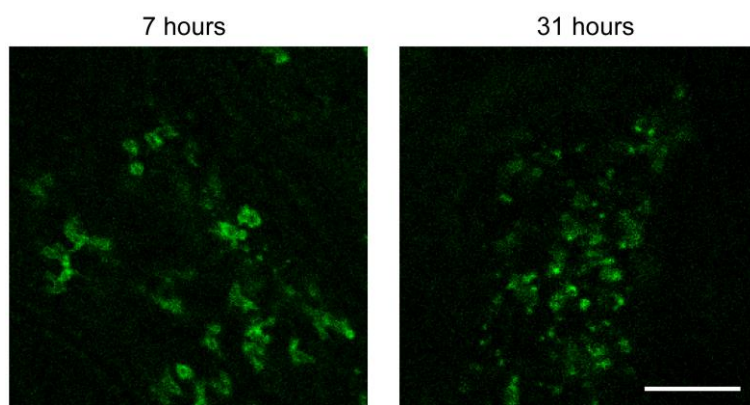


Figure 1. Effect of varying antibody penetration times. Seven hours after RO injection of CD8 α antibody (left), intestinal intraepithelial lymphocytes (IEL) show a classic membrane staining pattern. In contrast, 31 h after injection (right), IEL have internalized the CD8 α antibody, leading to smaller, punctate signals. Scale bar = 100 μ m. Brightness of each image was adjusted independently, and a green lookup table was used to improve visibility of the features.

2. If you are only using one antibody, we recommend choosing a far-red fluorophore (e.g., Alexa Fluor 647) due to that channel's lower autofluorescent background. For the two-channel imaging used here, we also used a green fluorophore (Alexa Fluor 488) to minimize channel bleed through. Use IgG antibodies directly conjugated to organic dyes, such as Alexa Fluor 488, 555, or 647. Avoid antibodies conjugated to bulky fluorescent proteins (such as phycoerythrin or allophycocyanin), as their large molecular weight impedes efficient diffusion into tissues and, while they are initially bright, they bleach quickly.
3. Dilute 15–20 μ g of antibody (here, anti-CD8 α and/or anti-EpCAM antibody) in 50 μ L of sterile PBS.
4. Anesthetize the mouse with isoflurane and inject the antibody solution retroorbitally (Yardeni et al., 2011). It is important to inject the full volume of labeled antibody for consistent labeling without introducing any air bubbles in the mouse's circulation.
5. Return mice to cages for recovery. Mice need to be fasted for 4 h to slow down peristalsis.

B. Suction ring setup

1. Suction rings, originally developed for lung imaging (Looney et al., 2011), offer a convenient way of stabilizing many mouse tissues. The rings we used were custom made at a CNC machine shop (see Notes for recommended supplier). An alternative design utilizes a resin 3D printer (Ahl et al., 2019) and contains an embedded electrical heater to provide more physiological thermal conditions during imaging. Ahl et al.

Cite as: McArdle, S. et al. (2023). Intravital Imaging of Intestinal Intraepithelial Lymphocytes. Bio-protocol 13(14): e4720. DOI: 10.21769/BioProtoc.4720.

(2019) provides an elegant description of the complete vacuum system and includes the 3D stereolithography [files for the 3D printer (in .stl format)]. An alternative device, which uses clamping instead of vacuum pressure, is described in Koike et al. (2021).

2. In this protocol, we based our part selection on United States American National Standard Pipe Thread (NPT). In this standard, fittings are based in inches. According to the standard, 3/8" barbed fitting will have a good fit for a 3/8" (9–10 mm) internal diameter vacuum tubing. The barb diameter is slightly larger than the tubing diameter to ensure a proper seal. You can modify the design to use materials available in your country or already existing in your laboratory. For the best performance of the vacuum system, you should try to maximize the internal diameter of the parts, minimize the total length of the circuit, and eliminate all leaks. Online suppliers such as Amazon, Fittings, Inc., or US Plastic Corporation offer a convenient source of parts. A local hardware or automotive stores can also serve as valuable resources for users who need additional help in procuring the parts or assembling the circuit.
3. Assemble the vacuum system (Figure 2). The suction ring is connected to a small vacuum trap to collect any biological fluids. From there, it is connected to a fine adjustment valve, a coarse adjustment valve, and a gauge to read the vacuum pressure. Finally, it is connected to the central building vacuum through a filter as a secondary method to prevent any contamination. Connect the pieces in the following order:
 - a. Connect the hydrophobic filter disk to the central vacuum shutoff valve with the 3/8" thick-walled vacuum tubing.
 - b. Attach the tubing to the barb of the 1/4" NPT female connector, and couple it to a male-male coarse adjustment valve using Teflon tape.
 - c. Couple the NPT connector with the female Tee connector.
 - d. Add the male-male extension nipple to the top of the Tee connector and fit the pressure gauge on top with the female-female 1/4" NPT coupling.
 - e. Attach the 1/4" NPT male to 5/16" barb connector to the Tee connector and fit the 5/16" vacuum tubing.
 - f. Add the plastic T-splitter and attach the 2-way stopcock fine adjustment valve on a length of tubing that will allow placement of the stopcock within reach of the surgeon. This valve can be opened to reduce the vacuum or closed to increase it. An alternative design can use an aquarium pump valve.
 - g. Attach the small vacuum trap with 5/16" vacuum tubing and secure it upright.
 - h. Add required length of the vacuum tubing to reach the microscope and connect the 1/4" barb to Luer lock connector. Add Teflon tape if needed to ensure proper seal.

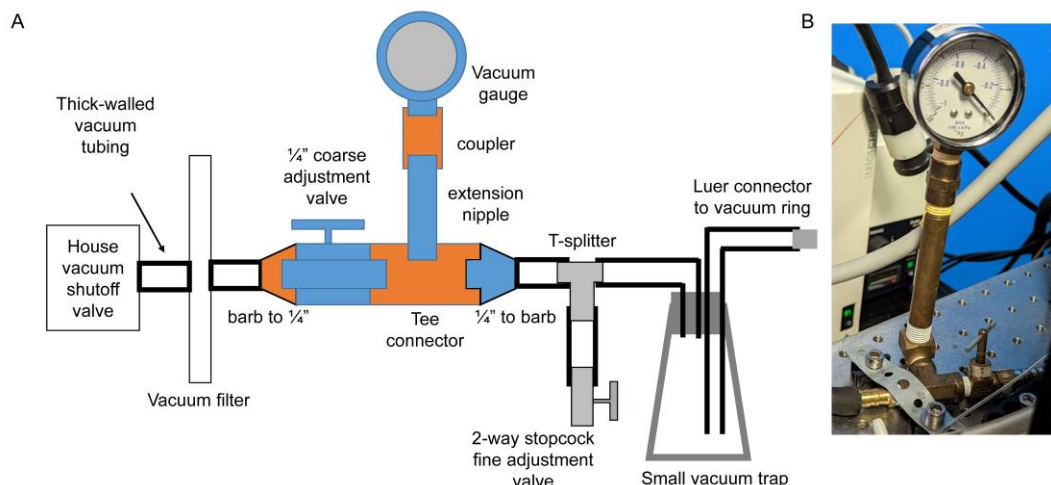


Figure 2. Schematics of vacuum circuit. A. Parts with female NPT connectors are indicated in orange; parts with male NPT connectors are indicated in blue. Grey parts are plastic luer-type or barbed connectors. B. Example build with vacuum gauge and adjacent parts.

4. Remove the plunger from a 10 mL syringe and squeeze a large bead of the vacuum grease into the syringe. Insert the plunger and apply a thin line of grease on the edge of the ring. Use Dumont #5/45 forceps to distribute the grease evenly on the rim of the ring. Remove any grease that got into the groove of the ring.
5. Clean a #1.5 12 mm diameter coverslip with 70% alcohol and wipe on lens paper to remove any traces of dust and lint. Place the coverslip on ring and press down to seal (Figure 3A).
6. Place the suction ring assembly on a post raised above the microscope stage and secure it with a right-angle post clamp or swivel clamp. We use a custom-made aluminum block with the post attached, screwed into the microscope stage for maximum stability, which can be requested at a machine shop. Make sure the cover glass is perpendicular to the optical axis of the microscope by aligning the ring parallel to the lens of the objective (Figure 3B).

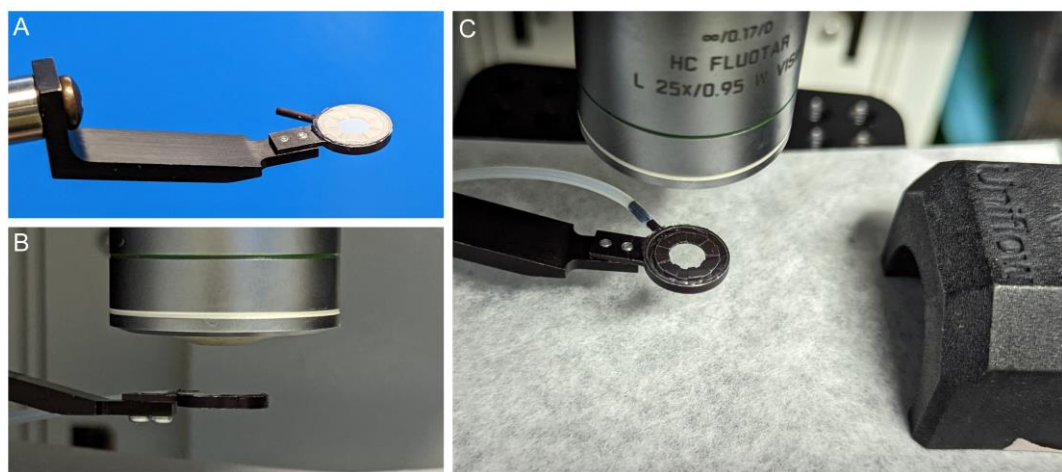


Figure 3. Assembling the suction ring. A. Attach a #1.5 coverslip to suction ring with vacuum grease and attach PE160 tubing. B. Adjust the ring to be parallel to the front lens of the objective. C. Position the suction ring and the nose cone on the heated platform.

7. Connect the suction ring via 18 G blunted needle end to the Luer lock of the vacuum circuit. Set the system to 5–20 mbar vacuum pressure. The exact value is dependent on the preparation and the way in which the system is integrated. Use the lowest vacuum pressure sufficient to stabilize the tissue.

C. Microscope setup

1. Insert the objective onto the piezo Z controller.
2. Open the acquisition software and initialize the resonant scanner.
3. Turn on appropriate laser lines and initially set the power to a low setting (~5%). In our case, we imaged using the 488 and 638 nm lines.
4. Select a dichroic filter that will give you the ability to switch between laser lines without needing to move any hardware. In our case, it was the 488/552/638 triple dichroic mirror for the SP8 system. For optimal use of confocal reflection microscopy for label-free detection of tissue structure, use the Reflection/Transmission mirror.
5. Set up the internal detector wavelengths, assigning the fluorescence gathered from antibody labeling on your most sensitive detectors (in our case, HyD detectors). These wavelengths were selected for AF488, AF647, and the confocal reflection channel:
 - AF488: 494–563 nm
 - Reflection: 619–651 nm
 - AF647: 651–722 nm
6. Either the tissue reflection or EpCAM staining for epithelium can be used to identify SI anatomy, although they provide slightly different information (Figure 4).

Cite as: McArdle, S. et al. (2023). Intravital Imaging of Intestinal Intraepithelial Lymphocytes. Bio-protocol 13(14): e4720. DOI: 10.21769/BioProtoc.4720.

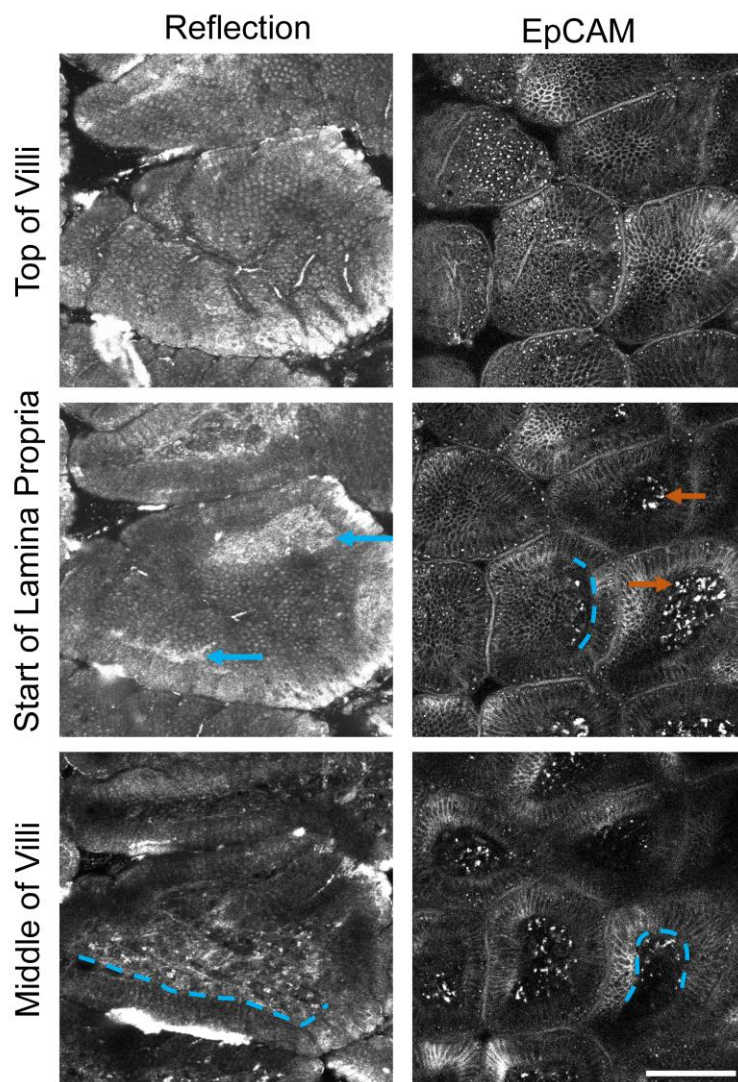


Figure 4. Comparison of visible structures from tissue reflection (left) and EpCAM staining (right) at three depths through the small intestinal (SI) villi. Brightness is adjusted in each image individually to accent details. Scale bar = 100 μm . Blue dotted lines = location of basal lamina. Blue arrows = basal lamina visible by reflection microscopy. Orange arrows = autofluorescent debris or non-specific binding of EpCAM antibody to macrophages.

7. Set the system to perform XYZT imaging, with the Z stepper controlled by the piezo element.
8. Adjust the pinhole size to two Airy units, enable bidirectional scanning, and find the appropriate phase correction. Enable line averaging during live acquisition setting and set the data acquisition mode to 8-bit. Set the zoom to the minimum allowed by the system for biggest field of view and adjust the line averaging to at least 8 \times . Our pixel size was set to approximately 0.6 μm with a corresponding field of view of approximately 370 μm .

D. Surgery and intravital microscopy

1. Please ensure all mouse handling and surgery steps are written in your Animal Care Committee-approved protocol. The following procedure is rather complex, with the scientist needing to simultaneously pay attention to the mouse anesthesia, the vacuum window pressure, and the image acquisition. We highly

- recommend practicing each part of the procedure slowly before attempting the full intravital imaging workflow. For example, a novice user can test the labeling, vacuum window, and image acquisition by practicing with a mouse that has been euthanized 4 h after antibody injection.
2. We found that preparations with isoflurane alone had too much movement (Video 1). Ketamine/xylazine anesthesia followed by isoflurane inhalation creates the best conditions for imaging with reduced motion artifacts (Figure 5, Video 2). Prepare the ketamine/xylazine mixture in sterile PBS (10 mg/mL ketamine and 1.5 mg/mL xylazine). Weigh the mouse and deliver 10 μ L of the prepared solution per gram of body weight (100 μ g of ketamine and 15 μ g of xylazine per gram of mouse weight) via intraperitoneal injection.

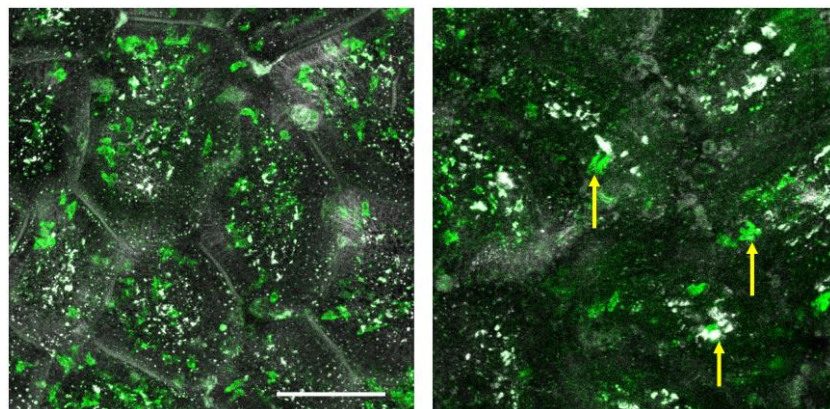
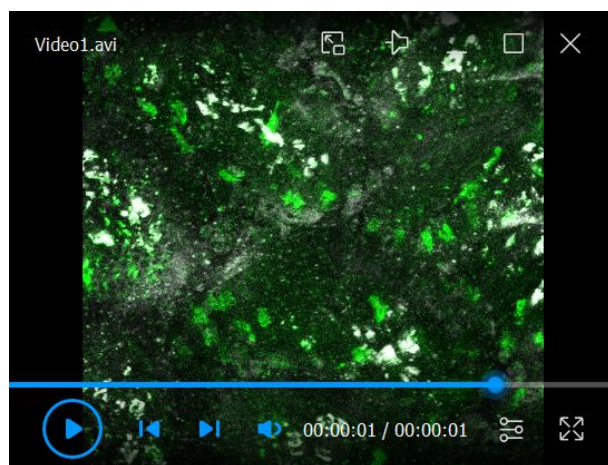
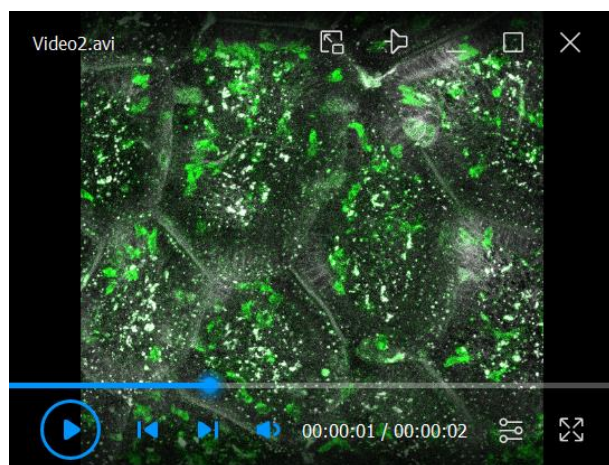


Figure 5. Example images from a well stabilized (left) and poorly stabilized (right) intravital movie. The image on the left was taken using a mouse anesthetized with both ketamine/xylazine and isoflurane; the image on the right was from a mouse anesthetized only with isoflurane. These are Z projections of single time points. Yellow arrows point to cell *shadows* that are caused by significant tissue motion between sequential Z steps, compromising the accuracy of the analysis. Green = CD8 α ; White = EpCAM. See also supplementary movies. Brightness was adjusted in each image. Scale bar = 100 μ m.



Video 1. Representative movie from an insufficiently stabilized preparation (isoflurane-only) that cannot be accurately quantified. Maximum intensity Z projection of a 10 min time series. Green = CD8 α ; White = EpCAM. Scale bar = 74 μ m. See also Figure 5.



Video 2. Representative example of a well stabilized movie from a mouse anesthetized with isoflurane and ketamine/xylazine. Maximum intensity Z projection of a 10 min time series. Green = CD8 α ; White = EpCAM. Scale bar = 74 μ m. See also Figure 5.

3. After anesthesia onset, shave the abdominal area with clippers or with hair removal lotion, followed by cleaning with 70% isopropanol.
4. Place the mouse ventral side up on heating pad and place the snout of the animal in isoflurane facemask. We place a thin steel plate over the ATC2000 heating pad, connected with thermal paste, to enable the use of a magnetic isoflurane mask. Alternatively, you can tape the isoflurane mask directly onto the heating pad.
5. Turn on isoflurane flow to face mask. Observe the breathing pattern of the animal and maintain a stable plane of anesthesia by delivering between 0.5% and 2% isoflurane. Labored breathing indicates the animal has been anesthetized too deeply.
6. Secure the limbs of the mouse with laboratory tape.
7. Insert a Vaseline-coated rectal thermometer and secure it by taping it to the tail. Set the feedback loop of the animal temperature controller to 37 °C.
8. Verify that a sufficient anesthesia level has been reached with a toe pinch (Figure 6A).
9. Position the ring assembly above the center of the abdomen and adjust it such that it is parallel to the front lens of the objective (Figures 3B and 6H). You might need to reposition the mouse to ensure that the ring has unobstructed access to the area. It is much safer to reposition the intact animal before incisions. Move the ring out of the way for surgery.
10. Make an approximately 2 cm midline incision in the skin with surgical scissors (Figure 6B). Locate the linea alba and make a 1.5 cm incision along it in the peritoneum to expose the small intestine, taking care to avoid inadvertently introducing hair in the surgical area or cutting through blood vessels (Figure 6C).
11. Using two wetted cotton tipped applicators, delicately move the intestine and position the antimesenteric side upwards. Look for areas that are free of food matter. Take care not to accidentally twist the gut and pinch the blood supply. Locate the stomach and find the piece of intestine distal to it. This will be the distal duodenum or jejunum. Exteriorize a small loop through the opening in the peritoneum (Figure 6D). Notice the blood vessels on both sides of the intestine and avoid cutting or damaging them. Using a cautery set to medium power, gently cauterize the antimesenteric surface of the intestine (Figure 6E). With small scissors, make an approximately 1 cm long opening along the cauterized edge (Figure 6F). Use cotton tipped applicators to gently open and flatten the gut, revealing the mucosal surface of the villi (Figure 6G). You may also use forceps but grab only the edges of the tissue.
 - a. Work quickly to avoid drying the tissue. If necessary, you can add a drop of PBS onto the mucosal surface to keep it moist. However, it is best not to disturb the mucus layer over the villi, because this will increase the amount of tissue movement.

- b. If you notice any bleeding, cauterize the wounded area immediately. If excess blood has pooled near the region of interest, add a drop of PBS and use gauze or a cotton tipped applicator to remove the excess. It is important to minimize blood loss because any blood on the imaged area will reduce the fluorescence intensity, but, as above, washing the tissue can damage the mucus and cause additional tissue motion.
12. Hold the suction ring in your dominant hand and lower it onto the exposed mucosal surface. Control the waste vacuum valve with your other hand and adjust the pressure to the lowest possible setting that achieves a complete seal against the tissue. You should see that the tissue is flattened against the coverslip (Figure 6H). Because the required pressure depends on how well the intestine seals to the ring, it is less important to keep the measured pressure consistent than ensuring the tissue is stable and undamaged in each preparation.

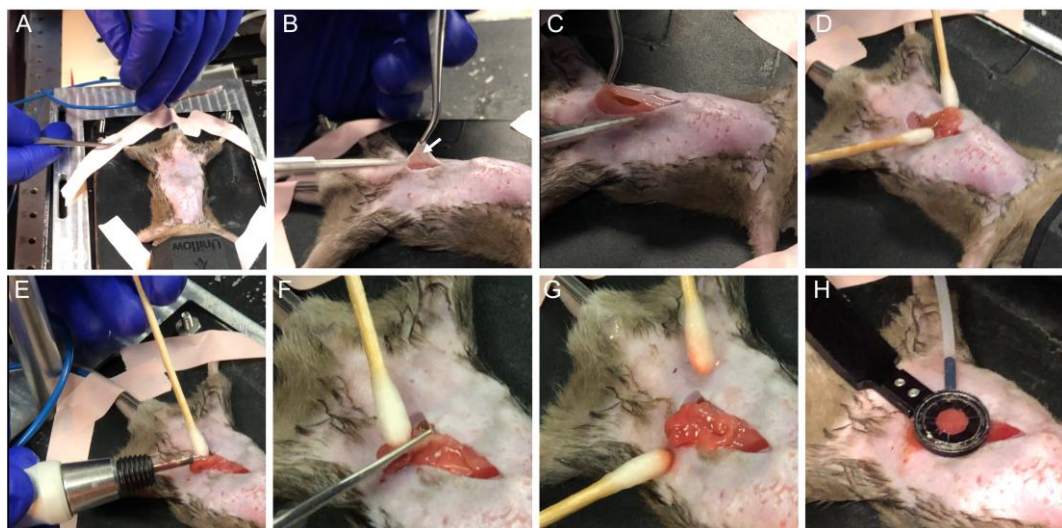


Figure 6. Overview of the surgical procedure. (A) Secure the animal and verify adequate anesthesia. (B) Make a midline incision taking care not to damage skin blood vessels (arrow). (C) Open peritoneum along linea alba and avoid major vessels. (D) Gently exteriorize the gut and find appropriate section free of food. (E) Cauterize the antimesenteric side. (F) Cut along the cauterized area to open the intestine. (G) Gently stretch and flatten mucosal surface. (H) Position suction ring above the exposed intestine and gently lower it onto the tissue while adjusting suction force to adhere the tissue to the coverslip.

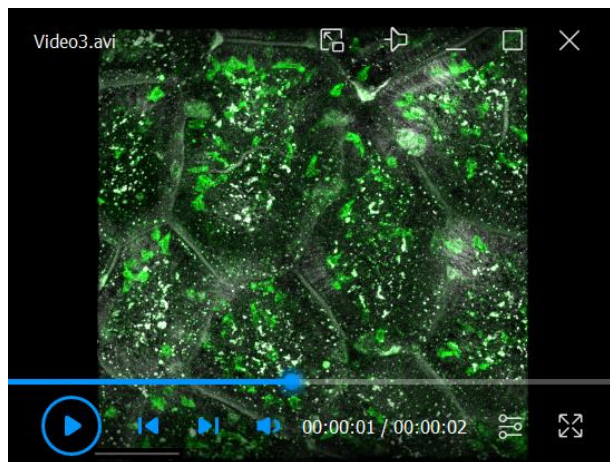
13. Add a drop of PBS on top of the coverslip for immersion and lower your objective to make contact with the fluid. With a long working distance objective, you will typically need to move the objective away from the ring to find the focus.
14. Using the 25 \times (0.95) objective and a green fluorescence filter cube, look through the eyepiece and observe the preparation under epifluorescence illumination. Erythrocytes in capillaries of the villi should be traveling at a high speed; you might see an occasional bigger immune cell moving through the blood stream. If the tissue is moving, gradually increase the pressure with the fine adjustment. Alternatively, inspect other areas within the vacuum ring to find a more stable location. You can further increase the stability of the preparation by gently lifting the ring by a few millimeters to isolate the attached tissue from the mouse's respiration (Move the objective out of the way before attempting this.). If you can see erythrocytes stopped in capillaries or moving in a backwards and forward motion, your vacuum pressure is too high, or you raised the preparation too much and the blood vessels have become pinched. Good preparations should show minimal movement of the villi and robust perfusion through the capillaries.
15. Start image acquisition in live mode and adjust the gain and laser power as necessary to utilize the full dynamic range without saturation. Image in simultaneous mode after calibrating the detectors' gains and wavelengths to avoid bleed through. Choosing optimal parameters for intravital imaging involves

balancing the need for high acquisition speed to track moving cells, high sensitivity to detect dimly labeled cells, and large field-of-view to make the most of every labor-intensive experiment. For more details on acquisition setup for intravital imaging, please see the review (McArdle et al., 2016).

16. Set the top and bottom of Z stack to encompass the top of the villus, the subepithelial area, and lamina propria. The basal lamina can be seen by reflection microscopy (Figure 4, blue arrows). If you use EpCAM labeling, the transition between the epithelium and lamina propria is visible as a distinct change in tissue texture (Figure 4, blue dotted lines showing some examples). Autofluorescent or non-specifically labeled macrophages are characteristic cells in the lamina propria that serve as a useful landmark (Figure 4, orange arrows).
17. Adjust the step size to 2.8 μm . Set the timelapse imaging to acquire Z stack every 30 s or faster, trimming the Z stack if needed. Acquire data for a minimum of 10 min per location. Save the data as .lif file.
18. Monitor the mouse plane of anesthesia throughout the experiment by observing the breathing pattern every 5–10 min and adjusting the amount of vaporized isoflurane as needed. Do a pinch test between the acquisitions to verify if the animal is fully anesthetized.
19. After completion of the imaging, euthanize the animal according to your approved protocol.
20. Clean the ring with PBS and 70% alcohol and remove the coverslip and any remaining vacuum grease.

E. Image processing

1. The suction ring often provides enough stability to the tissue to proceed with analysis without further motion removal. However, if necessary, small motion artifacts can be minimized after acquisition in Fiji (Schindelin et al., 2012). Whether the mechanical stabilization is sufficient for cell tracking is determined visually. Loosely, post-processing is necessary if there was gross tissue motion between Z steps or between sequential time steps of > 1/2 of a typical cell diameter (Figure 5).
 - a. Open the 1–3 channel .lif file in Fiji as a hyperstack using the Bioformats importer. Delete any Z steps that are entirely outside of the detectable tissue or region of interest because blank images without meaningful signal disrupt the alignment algorithm.
 - b. Change the color of each channel to either red, green, or blue, and then flatten the multichannel image to an RGB image. (This step can be skipped if there is only one channel.)
 - c. If each villus shows independent motion that ought to be corrected separately, create small crops of each villus. Each cropped region should be just large enough to capture the entire villus through all Z stacks and time points. Process all further steps independently for each region.
 - d. Apply the MSTHyperStackReg2 plugin (Ray et al., 2016). This software first aligns each Z step of each time point individually. Next, a maximum intensity Z projection is created to register the time series, and the calculated transform for each time step is applied to each Z position. At each stage, the entire sequence (either in Z or in T) is registered using minimum weighted spanning trees to choose a reference image and to ensure that outliers (images with particularly extreme motion artifacts) do not degrade the quality of the global alignment. This algorithm corrects lateral tissue movement in X and Y but does not correct vertical drift (Z motion).
 - i. First, perform coarse registration. We recommend using rigid body alignment using the *approximate* with a large graph width (the larger of half the number of Z steps per stack or half the number of time points) and allowing it to automatically choose the anchor image and add a border (Figure 7A). The automatically produced maximum intensity image can be used to visually check the alignment. Save the aligned Z stack as an intermediate step. High quality images with small non-linear tissue distortions can be successfully corrected using affine transformations, though affine transforms often produce very bad results from noisy or sparse images.
 - ii. Next, perform fine alignment on the results. We recommend using rigid body transforms, the *exact* method, a small (i.e., 5) graph width, automatic anchor selection, and no additional border (Figure 7A). This step can take a long time (hours), depending on the dimensions of your image and the graph width.
 - iii. The improvement in image quality using image registration is illustrated in Video 3 by comparison to Video 2.



Video 3. Improvement in image quality using image registration. The 3D data from Supplementary Video 2 was processed with MISTICA image alignment, which minimized jitter and drift. Maximum intensity Z projection of a 10 min time series. Green = CD8 α ; White = EpCAM. Scale bar = 74 μ m.

- e. In Fiji, adjust the image properties to set the voxel dimension and time step. Save the final result as a .tif hyperstack.
2. Immune surveillance of the epithelium can be measured by calculating the area covered by all labeled cells during a set amount of time in Fiji.
 - a. Load the raw .lif file or the aligned .tif hyperstack into Fiji.
 - b. Use the reflection signal or the EpCAM channel to identify the epithelial layer. At the top of each finger-like villus, there is a region approximately 10 μ m deep that is nearly exclusively epithelium. IEL often migrate along the basement membrane separating the SI epithelium from the lamina propria. Create a substack of the volume encompassing the epithelium at the top of the villus and the basement membrane and trim each video to a set amount of time (e.g., 10 min).
 - c. Using the polygon tool, draw a region of interest (ROI) encircling each villus and save each region to the ROI manager (Figure 7B).
 - d. Split the channels. On the CD8 α channel, use a median filter (2D, radius 2 pixels) to remove pixel noise.
 - e. Create a maximum intensity Z projection and then a maximum intensity T projection to combine all timepoints and Z locations into a single image, which has the location of every cell overlaid in the 10 min movie (Figure 7B).
 - f. Using the threshold tool, determine the intensity threshold that separates cells from background non-specific signal (Figure 7B). Ideally, this can be determined by performing one preliminary experiment with a labeled isotype control antibody. In the absence of this negative control sample, set the threshold to be just under the intensity of the dimmest labeled IEL. Use the same threshold for all samples by pressing the Set button and typing the determined threshold. Apply the threshold to binarize the image.
 - g. In Fiji, set the measurements to include area and area fraction; uncheck *limit to threshold*. Measure each ROI defining a villus. The results window will report the total area of the villus and the fraction that was visited by a cell in the time period (Figure 7C).
 - h. The movement of the cells can be displayed with a rainbow time projection (Figure 7D). Use the maximum intensity Z projection time series from step 2e and apply the Fiji plugin Temporal-Color Code (Miura, 2022) to show each time step as a unique color. Fast cells will appear as rainbow streaks while immobile cells appear white (all colors overlaid).

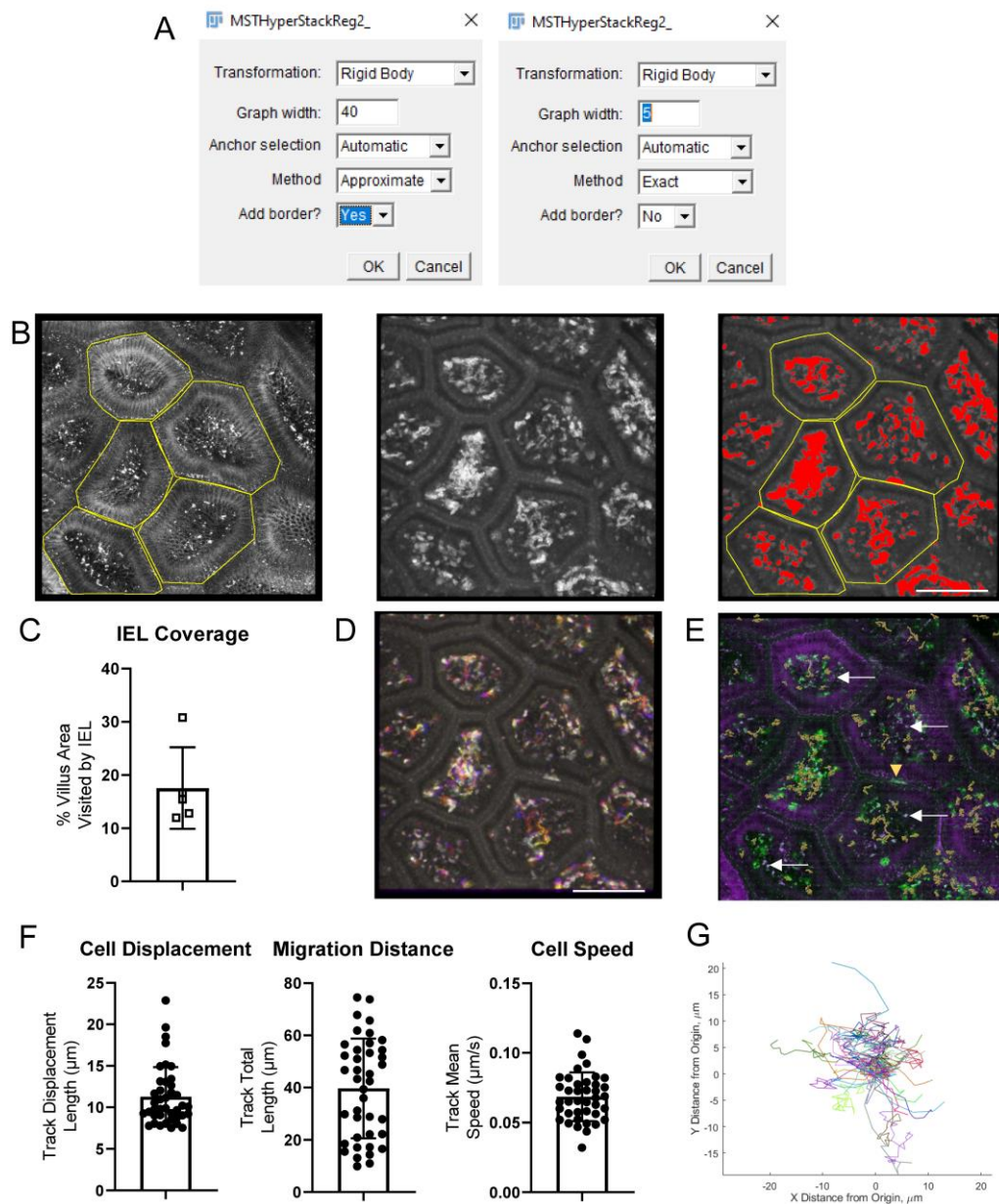


Figure 7. Examples of image processing steps and results. A. Screenshots of MSTHyperStackReg plugin parameters for an image with 85 Z-steps and 40 timepoints. Left: First round (approximate) settings, with graph width half of the Z stack. Right: second, more precise round of alignment. B. Screenshots of intermediate results during the calculation of villi coverage by intestinal intraepithelial lymphocytes (IEL). Left: Each villus is outlined using the EpCAM channel. Middle: median smoothing is applied to the CD8 α channel and a maximum intensity projection over all Z steps and all time points is applied to overlay the position of every IEL. Right: a threshold is applied to find the area visited by an IEL at least once during the 10 min movie and the villi outlines are overlaid (yellow). C. In each villus, the percentage of the area visited by an IEL is calculated. D. Alternatively, IEL movement can be displayed as a rainbow time projection. E. CD8 α -AF488 IEL (green) were tracked in Imaris. The tracks are shown as orange lines. EpCAM-AF647 (purple) marks the small intestinal (SI) epithelium. White arrows show a few of the many examples of artifacts that are visible in both the AF488 and AF647 channels. The yellow arrow shows a non-specifically labeled cell. F. Cell displacement, total movement distance, and speed were calculated from the Imaris tracks. G. The migration of each cell is shown as a spider plot. Scale bars = 100 μm .

Cite as: McArdle, S. et al. (2023). Intravital Imaging of Intestinal Intraepithelial Lymphocytes. Bio-protocol 13(14): e4720. DOI: 10.21769/BioProtoc.4720.

3. Movement statistics, such as mean speed, track length, and displacement demonstrate cell activation and patrolling behavior. Track the IEL in 3D in Imaris to quantify cell motility.
 - a. In Imaris, open the raw .lif files or tifs aligned in Fiji. If you are working with processed tifs, it is a good idea to check the voxel size and time step information in Image Properties.
 - b. If necessary, correct slow lateral and axial drift affecting the entire imaged volume in Imaris before cell tracking.
 - i. Use the Spots function to track bright, stable features, such as immobile cells, or autofluorescent or reflective debris. Please see below (step 3c) for details on the Spots function. Choose 3–10 spots that span the entire volume under analysis for the entire time series.
 - ii. In the Edit Tracks tab, select *Correct Drift*. Choose the options for correcting the image and objects, using translational and rotational drift, and include the entire result.
 - c. Tracking the movement of IEL can be performed semi-automatically with the Spots wizard (Figure 7E). The exact parameters need to be optimized for each project, but the overall process is similar in all cases. Detect round objects in your chosen channel (CD8α) and then apply quality, size, and intensity filters to remove debris and macrophages that have picked up the antibody. The most sensitive parameter is usually the expected object diameter; be sure to choose the typical diameter of the fluorescent spot, which may be smaller than the cell diameter if the antibodies have been internalized or if the cells are polarized. Add object filters to remove debris that is bright in multiple channels. Imaris then performs tracking of the segmented objects over time. For well-stabilized movies, the autoregressive motion algorithm usually produces the best results, although the Brownian motion algorithm can work in some cases. At this stage, adding track filters to remove stationary objects can improve performance.
 - d. There will nearly always be mistakes in the automatic tracking for intravital imaging data: single tracks inappropriately split, tracks jumping between neighboring cells, or nonIEL objects being included. Surface-labeled IEL can be distinguished from other objects by their shape (hollow, round), speed (greater than local tissue motion), and directionality (movement along basal lamina, as opposed to transverse). If multiple channels were imaged, autofluorescent objects can be seen in all channels, whereas antibody signals are usually much brighter in the proper channel (Figure 7E). Correct the centroid spots and connecting tracks manually in the Edit tab of the Spots object. It is important to use the same level of care and attention on all samples; manually correcting some images but not others can bias the final results. For further information on how to perform tracking in Imaris, please refer to Bitplane's extensive online tutorial library.
 - e. In the Statistics tab, export the track speed, track length, and track displacement metrics to a csv file. (Figure 7F). Use the *export data for plotting* to export the cell positions at each time point in a convenient three-column format.
 - f. Spider graphs are an informative way to visualize cell migration. In these graphs, each cell starts at position (0, 0) and its total path is drawn in a random color, demonstrating overall cell motility and directionality.
 - i. The spider plots can be generated from the exported cell position data using a simple script or stand-alone application found on GitHub (github.com/saramcardle/IEL) (Figure 7G).
 - ii. Alternatively, a spider graph can be generated in Imaris. First, select all the IEL tracks and duplicate the spots. In the new spots object, select all of the tracks and then apply the *Translate tracks* function in the Tools tab. This will move all of the tracks to originate at the same location. The newly adjusted position of each cell can be exported to a spreadsheet for plotting.
4. Limitations of image analysis
 - a. The cell-by-cell statistics produced here inherently have high variance due to natural biological variability (see plots in Figure 7). Additionally, each experiment only yields a small number of tracked cells (~20–40). Therefore, it is only possible to detect large differences between groups.
 - b. Even with tissue stabilization and drift correction, some tissue movement is usually still present. This tissue movement defines the lower limit of reliable quantification for cell speed and travel distance. To measure this for each dataset, track some autofluorescent spots that should not move during image acquisition, such as macrophages and food debris, using the Imaris spots wizard. Calculate their

- average speed and travel distance. The results show the sensitivity of your measurements; differences between cell groups smaller than typical gross tissue movement should be ignored, and preparations with unusually large tissue movement should be discarded.
- c. Sometimes, it can be difficult to distinguish antibody-labeled IEL from non-specific signals or autofluorescent objects. It is important to optimize the antibody concentration and injection time for your specific experimental protocol. Additionally, it can be helpful to perform a preliminary experiment using an isotype control antibody to visualize the intensity, location, and shape of artifacts as a negative control.
 - d. Please plan your experiments to minimize batch effects. If comparing two (or more) groups of mice, always image a mouse from each group back-to-back using the same batch of antibodies. Alternate which group is chosen to be run first each day, so that there is no systemic bias in the length of antibody incubation time or fasting time.
 - i. For projects comparing the activity of different cell populations, rather than different mouse conditions, it is possible to image two cell populations simultaneously with two different fluorophore-labeled antibodies. In this case, the movement characteristics of one population can be normalized to that of the other population in each mouse individually. This is an elegant way to minimize the differences in tissue motion in each preparation.

Notes

It is vital to consult your Institutional Animal Care Committee or equivalent body to ensure that all procedures were reviewed and approved according to the governing laws.

Intravital microscopy is a complex procedure. As each microscopy system is unique, it is best to seek advice from core facility staff or experienced users on how to establish the best parameters for imaging. Novice users should first master the handling of the microscope using an immobile object, such as a euthanized mouse injected with an antibody targeting the cells of interest. We encourage using untreated littermate control animals to understand the nature of autofluorescence in the tissue. Animals that received isotype control antibodies can serve as valuable controls for the specificity of antibodies targeting cells of interest. By comparing the images obtained from these kinds of samples, novice users can develop understanding of proper labeling and learn to distinguish it from artifacts and autofluorescence, which is often very strong in the lamina propria. For additional information on intravital microscopy in the gut, we refer readers to previous studies by Sujino et al. (2016), Chen et al. (2019), and Koike et al. (2021).

The suction ring assembly can be purchased from Zera Development Company; please see <https://www.zeradevelopment.com> for contact information. For the best performance of the vacuum circuit, make it as short as possible and seal all the leaks. Use Teflon tape to create a tight seal between metal parts of the system. Use large-bore vacuum tubing for connections between parts and minimize the volume of vacuum trap. Alternatively, the vacuum trap can be placed between the vacuum filter and the gauge assembly.

Acknowledgments

We wish to thank Dr. Grzegorz Chodaczek for sharing his expertise in intravital microscopy and for the development of suction ring techniques at La Jolla Institute for Immunology.

Funding: National Institutes of Health grants P01 DK46763, R01 AI61516, and MIST U01 AI125955 (MK); Chan-Zuckerberg Initiative Imaging Scientist Grant 2019-198153 (SM).

This protocol is derived from the original research paper (Seo et al., 2022; DOI: 10.1126/scimmunol.abm6931).

Competing interests

The authors have no conflicts or competing interests.

References

- Ahl, D., Eriksson, O., Sedin, J., Seignez, C., Schwan, E., Kreuger, J., Christoffersson, G. and Phillipson, M. (2019). [Turning Up the Heat: Local Temperature Control During in vivo Imaging of Immune Cells](#). *Front Immunol* 10: 2036.
- Chen, Y., Koike, Y., Chi, L., Ahmed, A., Miyake, H., Li, B., Lee, C., Delgado-Olguin, P. and Pierro, A. (2019). [Formula feeding and immature gut microcirculation promote intestinal hypoxia, leading to necrotizing enterocolitis](#). *Dis Model Mech* 12(12).
- Cheroutre, H., Lambolez, F. and Mucida, D. (2011). [The light and dark sides of intestinal intraepithelial lymphocytes](#). *Nat Rev Immunol* 11(7): 445-456.
- Edelblum, K. L., Shen, L., Weber, C. R., Marchiando, A. M., Clay, B. S., Wang, Y., Prinz, I., Malissen, B., Sperling, A. I. and Turner, J. R. (2012). [Dynamic migration of \$\gamma\delta\$ intraepithelial lymphocytes requires occludin](#). *Proc Nat Acad Sci U S A* 109(18): 7097-7102.
- Hoytema van Konijnenburg, D. P., Reis, B. S., Pedicord, V. A., Farache, J., Victora, G. D. and Mucida, D. (2017). [Intestinal Epithelial and Intraepithelial T Cell Crosstalk Mediates a Dynamic Response to Infection](#). *Cell* 171(4): 783-794.e13.
- Koike, Y., Li, B., Chen, Y., Ganji, N., Alganabi, M., Miyake, H., Lee, C., Hock, A., Wu, R., Uchida, K., et al. (2021). [Live Intravital Intestine with Blood Flow Visualization in Neonatal Mice Using Two-photon Laser Scanning Microscopy](#). *Bio Protoc* 11(5): e3937.
- Looney, M. R., Thornton, E. E., Sen, D., Lamm, W. J., Glenny, R. W. and Krummel, M. F. (2011). [Stabilized imaging of immune surveillance in the mouse lung](#). *Nat Methods* 8(1): 91-96.
- McArdle, S., Mikulski, Z. and Ley, K. (2016). [Live cell imaging to understand monocyte, macrophage, and dendritic cell function in atherosclerosis](#). *J Exp Med* 213(7): 1117-1131.
- Miura, K. (2022). [Temporal-Color Coder plugin for Fiji](#). Shell. Fiji. Retrieved from https://github.com/fiji/fiji/blob/847ee410deedda9ba1de673820a5fa63446aa2e1/plugins/Scripts/Image/Hypersacks/Temporal-Color_Code.ijm (Original work published 2011)
- Mouse Room Conditions. (n.d.). The Jackson Laboratory. Retrieved November 19, 2022, from <https://www.jax.org/jax-mice-and-services/customer-support/technical-support/breeding-and-husbandry-support/mouse-room-conditions>
- Ray, N., McArdle, S., Ley, K. and Acton, S. T. (2016). [MISTICA: Minimum Spanning Tree-Based Coarse Image Alignment for Microscopy Image Sequences](#). *IEEE J Biomed Health Inform* 20(6): 1575-1584.
- Schindelin, J., Arganda-Carreras, I., Frise, E., Kaynig, V., Longair, M., Pietzsch, T., Preibisch, S., Rueden, C., Saalfeld, S., Schmid, B., et al. (2012). [Fiji: an open-source platform for biological-image analysis](#). *Nat Methods* 9(7): 676-682.
- Seo, G.-Y., Shui, J.-W., Takahashi, D., Song, C., Wang, Q., Kim, K., Mikulski, Z., Chandra, S., Giles, D. A., Zahner, S., et al. (2018). [LIGHT-HVEM Signaling in Innate Lymphoid Cell Subsets Protects Against Enteric Bacterial Infection](#). *Cell Host Microbe* 24(2): 249-260.e4.
- Seo, G. Y., Takahashi, D., Wang, Q., Mikulski, Z., Chen, A., Chou, T. F., Marcovecchio, P., McArdle, S., Sethi, A., Shui, J. W., et al. (2022). [Epithelial HVEM maintains intraepithelial T cell survival and contributes to host protection](#). *Sci Immunol* 7(73): eabm6931.
- Sujino, T., London, M., Hoytema van Konijnenburg, D. P., Rendon, T., Buch, T., Silva, H. M., Lafaille, J. J., Reis, B. S. and Mucida, D. (2016). [Tissue adaptation of regulatory and intraepithelial CD4 \$^{+}\$ T cells controls gut inflammation](#). *Science* 352(6293): 1581-1586.
- Sumida, H., Lu, E., Chen, H., Yang, Q., Mackie, K. and Cyster, J. G. (2017). [GPR55 regulates intraepithelial lymphocyte migration dynamics and susceptibility to intestinal damage](#). *Sci Immunol* 2(18): eaao1135.

- Wang, X., Sumida, H. and Cyster, J. G. (2014). [GPR18 is required for a normal CD8 \$\alpha\alpha\$ intestinal intraepithelial lymphocyte compartment](#). *J Exp Med* 211(12), 2351-2359.
- Yardeni, T., Eckhaus, M., Morris, H. D., Huizing, M. and Hoogstraten-Miller, S. (2011). [Retro-orbital injections in mice](#). *Lab Anim (NY)* 40(5): 155-160.
- Zera Development Co. (n.d.). Zera development. Retrieved November 20, 2022, from <https://www.zeradevelopment.com>

Optogenetic Induction of Pyroptosis, Necroptosis, and Apoptosis in Mammalian Cell Lines

Kateryna Shkarina^{1,§,*} and Petr Broz^{1,*}

¹Department of Immunobiology, University of Lausanne, Lausanne, Switzerland

§Present address: Institute of Innate Immunity, University Hospital Bonn, Bonn, Germany

*For correspondence: petr.broz@unil.ch; kateryna.shkarina@uni-bonn.de

Abstract

Regulated cell death plays a key role in immunity, development, and homeostasis, but is also associated with a number of pathologies such as autoinflammatory and neurodegenerative diseases and cancer. However, despite the extensive mechanistic research of different cell death modalities, the direct comparison of different forms of cell death and their consequences on the cellular and tissue level remain poorly characterized. Comparative studies are hindered by the mechanistic and kinetic differences between cell death modalities, as well as the inability to selectively induce different cell death programs in an individual cell within cell populations or tissues. In this method, we present a protocol for rapid and specific optogenetic activation of three major types of programmed cell death: apoptosis, necroptosis, and pyroptosis, using light-induced forced oligomerization of their major effector proteins (caspases or kinases).

Keywords: Programmed cell death, Apoptosis, Pyroptosis, Necroptosis, Optogenetics

This protocol is used in: J. Cell Biol. (2022), DOI: 10.1083/jcb.202109038

Background

Regulated cell death is a common feature of multicellular organisms and plays a key role in development and tissue homeostasis and in protecting the host against malignant growth and various pathogens. Research over the last two decades has identified over 12 different forms of regulated cell death (Galluzzi et al., 2018); however, their study is often complicated by the complex crosstalk and interconnectivity between the different cell death pathways (Bedoui et al., 2020). Additionally, the consequences of different types of cell death in the tissue still remain insufficiently understood, which is at least partially due to the challenges of selectively targeting single cells in multicellular populations, as well as to the pleiotropic effects of commonly used *natural* cell death triggers both on the dying cells and their neighbors.

In recent years, multiple strategies have been developed to specifically ablate cells both in vitro and in living animals. However, some of these methods (such as laser ablation or photosensitization) still lack specificity regarding the type of cell death to be induced (Tirlapur et al., 2001; Qi et al., 2012), while others [such as chemically inducible dimerization of apoptotic or necroptotic effector proteins (Oberst et al., 2010; Wu et al., 2014)] suffer from a limited spatiotemporal control and require a delivery of soluble ligands, thus limiting their in vivo applications. To overcome these limitations and expand the scope of the tools available for programmed cell death induction, we recently developed a set of optogenetically activated cell death effectors (optoCDEs) (Shkarina et al., 2022), which enable selective induction of three major types of programmed cell death: apoptosis, pyroptosis, and necroptosis. These tools consist of three modules: 1) a photoactuator domain Cry2olig (Cry2 E490G), which responds to blue light by rapid homo-oligomerization, 2) an mCherry tag, which enables the detection of the cells expressing optoCDEs and estimation of the relative construct expression levels, and 3) an effector module (Figure 1A–1C). For opto-caspases, the effector module corresponds to the protease domain (p20 and p10 subunits) of corresponding caspases; the endogenous linkers and cleavage sites essential for the caspase activation are retained, while CARD (in caspase-1, -4, -5, -9, and -11) and DED (caspase-8) domains, responsible for the endogenous upper-level protein–protein interactions and homo-oligomerization, are removed. In opto-RIPK3, the design is similar, while the RHIM motif (responsible for the upstream interaction with the RIPK1) is mutated. In optoMLKL, the effector domain orientation in relation to Cry2olig and mCherry is reversed to keep the MLKL N-terminus (responsible for membrane binding and disruption) exposed. The considerations behind the construct design and testing of the different construct versions are described in more detail in the original paper (Shkarina et al., 2022). The blue light stimulation triggers the rapid activation and oligomerization of Cry2olig, which in turn results in the proximity-induced activation of effector domains and subsequent processing of downstream substrates, culminating in cell death. While Cry2olig alone responds to the blue light within seconds (Taslimi et al., 2014), the timing of cell death induction is defined by the kinetics of effector activation as well as availability and efficiency of the processing and activation of downstream substrates (such as apoptotic executioner caspases, necroptotic effector GSDMD, or pyroptotic effector MLKL); the first morphological features of cell death can usually be detected within minutes after the beginning of illumination.

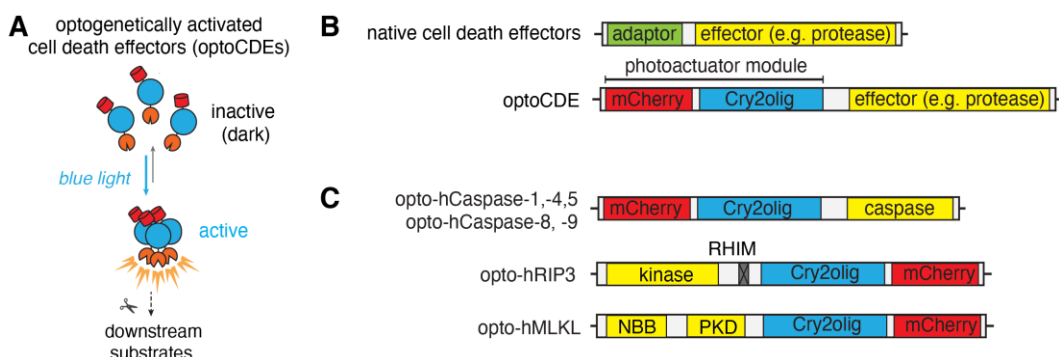


Figure 1. Schematic representation of the optogenetically activated cell death effectors (optoCDE) system. (A) OptoCDEs are inactive and monomeric in the dark state but are activated within seconds upon blue light illumination, which induces oligomerization of the Cry2olig photoactuator domain, activation of downstream substrates, and

Cite as: Shkarina, K. and Broz, P. (2023). Optogenetic Induction of Pyroptosis, Necroptosis, and Apoptosis in Mammalian Cell Lines. Bio-protocol 13(14): e4762. DOI: 10.21769/BioProtoc.4762.

induction of cell death. (B) General architecture of major cell death effectors and design of optoCDE constructs. Cell death effectors used in the study generally consist of an adaptor domain (CARD or DED for caspases and RHIM for RIPK3) and an effector domain bearing protease (caspases), kinase (RIPK3), or membrane-disrupting (MLKL) function. In the optoCDEs, the effector domain is retained, while the adaptor is replaced with the Cry2olig-mCherry photoactuator module (mCherry is used to visualize optoCDE expression and/or clustering). (C) Schematic representation of major types of optoCDE constructs used in the study. The detailed description and evaluation of the optoCDE tools is available in the original paper (Shkarina et al., 2022). Figure adapted from Shkarina et al. (2022).

The optoCDEs can be applied *in vitro*, as described in this protocol, as well as *in vivo* to selectively kill specific cells or cell populations in a highly controlled and specific manner (Shkarina et al., 2022). Additionally, the precise control over the illumination parameters, such as light intensity and duration, provides new means for cellular and mechanistic studies of these forms of cell death, as well as probing cell survival mechanisms that limit cellular damage downstream of these effectors.

Materials and reagents

A. Cell culture and lentiviral transduction

1. Sterile serological pipettes (Falcon, catalog number: 357543)
2. Sterile micropipette tips (Starlab TipOne, catalog number: S1120-8810)
3. Tissue culture–treated cell culture flasks (TPP, catalog number: 90076)
4. 10 cm Petri dishes (Falcon, catalog number: 351029)
5. Syringes (5 and 10 mL) (Braun Omnifix, catalog numbers: 4616103V and 4616057V)
6. Sterile tissue culture–treated 6-well flat-bottom plates (Eppendorf, catalog number: 0030720113)
7. Sterile 50 and 15 mL Falcon tubes (SPL life sciences, catalog numbers: 50015 and 50050)
8. Sterile 1.5 mL microcentrifuge tubes (Eppendorf, catalog number: 11.3817.01)
9. Aluminum foil (Sigma, catalog number: 326852)
10. 0.45 µm filters (Sarstedt, catalog number: 83.1826)
11. Polybrene (Merck, catalog number: TR-1003-G)
12. JetPRIME transfection reagent (Polyplus, catalog number: 101000027)
13. HEPES 1 M (Sigma, catalog number: H3375)
14. Dulbecco’s phosphate-buffered saline (DPBS) 1× (Thermo Fisher Scientific, catalog number: 10010023)
15. Dulbecco’s modified Eagle medium (DMEM) with GlutaMAX supplement (Thermo Fisher Scientific, catalog number: 10564011)
16. RPMI 1640 medium, with GlutaMAX supplement (Thermo Fisher Scientific, catalog number: 61870044)
17. Doxycycline hydrochloride (Sigma-Aldrich, catalog number: D3447)
18. Puromycin (Invivogen, catalog number: ant-pr-1)
19. Hygromycin B Gold (Invivogen, catalog number: ant-hg-1)
20. LPS-B5 ultrapure (Invivogen, catalog number: tlr1-b5lps)
21. PMA (Sigma-Aldrich, catalog number: P1585)
22. Fetal bovine serum (Bioconcept, catalog number: 2-01F10-I)

B. Live-cell imaging and cell death detection

1. 8-well tissue culture–treated µ slides (ibidi, catalog number: 80826)
2. Collagen solution from bovine skin (Sigma-Aldrich, catalog number: C4243)
3. Opti-MEM reduced serum medium (Gibco, catalog number: 11058021)
4. CellTox Green (Promega, catalog number: G8741)
5. DRAQ7 (BioLegend, catalog number: 424001)

6. Annexin V Pacific Blue (BioLegend, catalog number: 640918)
7. Annexin V FITC (BioLegend, catalog number: 640906)
8. Annexin V Alexa Fluor 647 (BioLegend, catalog number: 640912)
9. CellEvent caspase-3/7 green (Thermo Fisher Scientific, catalog number: R37111)

C. Cell lysis and cytokine secretion analysis

1. Vision Plate 24, 150 micron, TC-treated, sterile (Life Systems Design, catalog number: 4ti-0241)
2. 96-well flat-bottom plates
3. Lactate dehydrogenase (LDH) cytotoxicity detection kit (Sigma, catalog number: 11644793001)
4. Triton X-100 (Sigma, X100-500ML)
5. Human IL-1 β ELISA kit (R&D, catalog number: DY401)
6. ELISA plates (Sigma-Aldrich, catalog number: M9410-1CS)
7. LDH stop solution [2 M acetic acid (Sigma, catalog number: 64-19-7)] in dH₂O, store at 4 °C
8. Reagents and equipment for ELISA
9. Reagents and equipment for the Western Blot analysis
10. Fluorescence assay (Cisbio, catalog number: 62HIL1BPET)

Equipment

A. For cell culture

1. Tissue culture hood (such as HERASAFE™ KS, Thermo Scientific)
2. Cell incubator (Forma™ Steri-Cycle™ CO₂ Incubator, Thermo Scientific)
3. Centrifuge (Eppendorf 5810R)
4. Light microscope (such as Leica DMI6000B)
5. Pipettes

B. For imaging

1. Point-scanning confocal (such as Zeiss LSM800 or Leica SP8)

C. For cell population-level assays

1. Light plate apparatus (Gerhardt et al., 2016) equipped with double row of 450 nm light LEDs
2. Spectrophotometer/ELISA plate reader
3. Multichannel pipettes
4. Western blot imager

Software

1. ZEN (ZEISS, <https://www.zeiss.com/microscopy/en/products/software/zeiss-zen.html>)
2. Iris (Jeff Tabor laboratory, <http://taborlab.github.io/Iris/>)
3. Fiji (NIH, <https://imagej.net/software/fiji>) (Version 2.3.0)
4. Software for the plate reader
5. Microsoft Excel (Microsoft, version 16.69.1)
6. GraphPad Prism (version 9.3.1.)

Procedure

A. Generation of stable cell lines expressing optogenetically activated cell death effectors (optoCDEs)

1. Lentiviral particle production
 - a. Prepare stocks of purified lentiviral plasmids encoding optoCDE constructs. We recommend using endotoxin-free midi- or maxi-prep kits for plasmid purification.
 - b. Twenty-four hours prior to transfection, plate HEK293T cells in a tissue culture-treated 6-well plate at 5×10^5 cells/well in 2 mL of fresh cell culture medium.
 - c. For each well, prepare the transfection mix, as summarized in Table 1, in 1.5 mL tubes. Mix gently and incubate at room temperature for 15 min.

Table 1. Transfection mix per well of a 6-well plate

Components	Amount
pLVX-optoCDE	1.9 µg
PsPAX2	1.9 µg
VSVg	0.2 µg
JetPrime transfection reagent	5 µL
JetPrime Buffer	200 µL

- d. Add the transfection mix dropwise to the cells. Ensure that the whole surface of the well is evenly covered (this can be assessed by monitoring the transient change of the medium color). Incubate the cells at 37 °C and 5% CO₂.

- e. At 6–12 h post transfection, replace the transfection mix with 2 mL of fresh cell culture medium for virus collection.

Note: Use the appropriate cell culture medium for the cell line to be transduced.

- f. Incubate for an additional 36–48 h at 37 °C and 5% CO₂.

Note: Over the course of virus production, the transfected cells might change the morphology, round up, and lift, as a consequence of viral particle release.

- g. After 36–48 h, collect the virus-containing supernatants from transfected HEK293T cells into 15 mL Falcon tubes. At this step, the medium from the wells transfected with the same construct can be combined and further processed together.

- h. Using a 5 or 10 mL syringe, gently pass the supernatants through a 0.45 µm syringe filter to remove cell debris and collect the filtrate into the clean 15 mL Falcon tube. Supplement the virus-containing supernatants with 20 µM HEPES (final concentration) to facilitate viral particle stability.

- i. At this stage, the virus-containing supernatants can be either used directly or stored at -80 °C for several months.

2. Cell transduction

- a. Seed the appropriate number of cells to be transduced.

- i. For adherent cells: we recommend seeding 0.8×10^6 – 1×10^6 of cells per well of a 6-well plate, 6–24 h before transduction. Cells should be properly attached and cover 60%–70% of growth surface. The optimal seeding density can be adjusted to accommodate for the cell size and differences in the growth kinetics between different cell lines. We recommend using 2–5 mL/well of virus-containing medium for 6-well plates, 2 mL/well for 12-well plates, and 1 mL/well for 24-well plates.

- ii. For non-adherent cell lines: cells can be collected, centrifuged, and resuspended in the virus-containing medium immediately prior to transduction. The second centrifugation step (spinfection) can be performed either in plates or in 50 mL Falcon tubes (in this case, the cells need to be resuspended and transferred to the plates or flasks following the spinfection).

- iii. Include an additional well of mock-treated (polybrene-only treated) cells to control for cell viability and transduction efficiency.

- b. Replace the culture medium with the virus-containing medium supplemented with 5 µg/mL polybrene to facilitate viral particle adhesion.
 - c. To facilitate the infection, centrifuge the cells with the virus at 3,000×*g* for 1 h at 37 °C. For the plate centrifugation, seal the sides of the plates with tape to prevent the accidental spillover of the supernatants during plate transfer and centrifugation. Suspension cells can also be centrifuged in 50 mL Falcon tubes. After the completion of this step, move the cells to the cell culture incubator.
 - d. After 6–12 h, aspirate the virus medium, wash cells 1–2 times with the pre-warmed DPBS, and add the appropriate volume of fresh growth medium. If cell density is too high, cells can be transferred into the larger vessel at this step.
 - e. Let the cells recover for 24–48 h to increase the cell number and allow for the proper expression of the selection markers and/or antibiotic resistance genes.
 - f. To select successfully transduced cells, replace the medium with fresh medium containing the appropriate antibiotic concentration.
 - i. Use the non-transduced wells as the positive control for selection efficiency.
 - ii. The optimal antibiotic concentration for each cell line can vary and has to be determined using an antibiotic titration.
 - iii. For most cell lines, we have successfully used the selection medium containing 1–5 µg/mL of puromycin or 50–100 µg/mL of hygromycin B Gold.
 - g. After 3–5 days, remove the antibiotic-containing medium and expand the surviving cells.
3. Cell line validation
 - a. To confirm the transduction efficiency, induce optoCDE expression by incubating the cells with 1 µg/mL doxycycline for 24–48 h (at this stage, cells need to be protected from light to prevent the optoCDE activation and cell death). Include the non-treated control (without doxycycline) to control for the leaky expression.
 - b. The percentage of mCherry-positive cells can be quantified using fluorescent microscopy or FACS. The efficiency of cell death induction can then be tested as described in sections B and C.
Note: OptoCDEs are fused with mCherry allowing easy assessment of construct expression.
 - c. Following selection and validation, the stable lines can either be frozen away in liquid nitrogen for storage or directly used for experiments.

B. Optogenetic induction and visualization of pyroptosis, necroptosis, and apoptosis using confocal microscopy

1. Cell preparation for imaging
 - a. One day before the experiment, seed the cells into the 8-well tissue culture–treated µ-slides at the concentration of 0.5 × 10⁵–1 × 10⁵ cells/well.
 - i. If using other type of cell culture plates, the cell concentration should be adjusted to achieve 30%–70% of the density at the day of experiment. We recommend using a lower cell density for experiments focused on the high-resolution visualization of the dynamic cellular events during different types of cell death in adherent cells.
 - ii. For poorly adherent cell types (such as HEK293T, MCF7, or equivalent), the slides can be additionally pre-coated with 5% collagen.
 - 1) Prepare the appropriate volume of 5%–10% dilution of bovine skin collagen in sterile PBS. Mix thoroughly by inverting. Avoid vortexing, as this may lead to the collagen precipitation.
 - 2) Add 100–150 µL of collagen solution per well. The volume of liquid should be sufficient to fully cover the growth surface.
 - 3) Incubate the slides at room temperature for 5 min; then, aspirate the collagen and air dry the slides for 30–60 min in the hood. During aspiration, avoid touching the bottom of the slide (growth surface), as this might lead to the disruption of the collagen layer and reduce cell adhesion.
 - 4) The coated slides can be stored at room temperature for several weeks.
 - b. To induce the construct expression in the cells, supplement the cell culture medium with 1 µg/mL doxycycline and incubate for 16–24 h. The longer induction time can be used to achieve higher

Cite as: Shkarina, K. and Broz, P. (2023). Optogenetic Induction of Pyroptosis, Necroptosis, and Apoptosis in Mammalian Cell Lines. Bio-protocol 13(14): e4762. DOI: 10.21769/BioProtoc.4762.

- expression levels but can also result in increased cytotoxicity.
- c. To protect the cells from light following expression induction, construct a dark chamber by fully covering a petri dish with foil (Figure 2). Alternatively, cells can be placed in a plastic box or an alternative type of light-impermeable container, which allows air circulation and humidification.



Figure 2. Examples of the chambers that can be used to protect optogenetically activated cell death effectors (optoCDE)-expressing cells from light

- d. On the day of experiment: pre-heat the microscope to 37 °C. Ensure that the temperature is stabilized before the start of the imaging.
- e. Gently wash the cells with pre-warmed PBS and replace the cell culture medium with pre-warmed Opti-MEM or alternative imaging medium. At this stage, all the manipulations need to be performed under dim light or red-light conditions to avoid spontaneous optoCDE construct activation.
- f. Optional: for cell death detection, the following reagents can be directly added to imaging medium:
 - i. Visualization of membrane permeabilization:
 - 1) CellTox Green: 1:10,000
 - 2) DRAQ7: 1:1,000
 - ii. Visualization of PS exposure
 - 1) Annexin V Pacific Blue: 1:500
 - 2) Annexin V FITC 1:1,000
 - 3) Annexin V Alexa Fluor 647
 - iii. Apoptotic caspase activation
 - 1) CellEvent caspase-3/7 green—it is recommended to pre-load the cells with the dye for 1 h before an experiment.
 - 2) Alternatively, one can utilize genetically encoded fluorescent protein-based caspase-3/7 reporters, such as VC3AI or ZipGFP.
- 2. Microscope setup
 - a. Both 488 and 496 nm lasers can be used for Cry2olig activation. During continuous whole-field photoactivation experiments, Cry2olig stimulation can be coupled with simultaneous imaging of fluorophores in the green channel [in this case, it is preferable to set up this channel as the last in an acquisition sequence to obtain the *non-stimulated* ($t = 0$) images]. However, this is not possible when using pulsed activation and/or single-cell targeting; in this case, only red or far-red fluorescent dyes and proteins should be used for the visualization of cell death and other processes of interest.
 - b. Set up the time-lapse imaging. Keep in mind that Cry2olig activation will cumulatively depend on both the laser power and the frame rate, so both need to be adjusted accordingly (e.g., if using higher frame rate, it is recommended to decrease the 488 nm laser power, while longer frame intervals might require increased laser intensity for Cry2olig activation). As an example, Figure 3 shows the relationship between the blue laser intensity and the percentage of pyroptotic cells detected after 30 min of illumination.

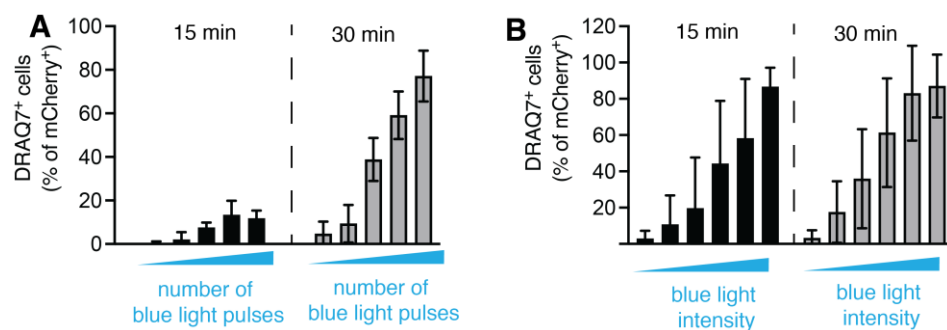


Figure 3. Relationship between opto-(h)caspase-1 activation and illumination parameters. (A) Quantification of pyroptotic (DRAQ7^+) cells at 15 and 30 min post transient blue light illumination, and (B) at continuous repetitive (every 15 s) stimulation with blue light of various intensity. The data corresponds to Figure 3A and 3B in the original paper (Shkarina et al., 2022).

- c. Acquire the time-lapse series. An example of the typical pyroptotic, necroptotic, and apoptotic cell morphology is shown in Figure 4. Note that the kinetics and morphological characteristics of each type of cell death vary among cell types and might also depend on the optoCDE construct expression level.

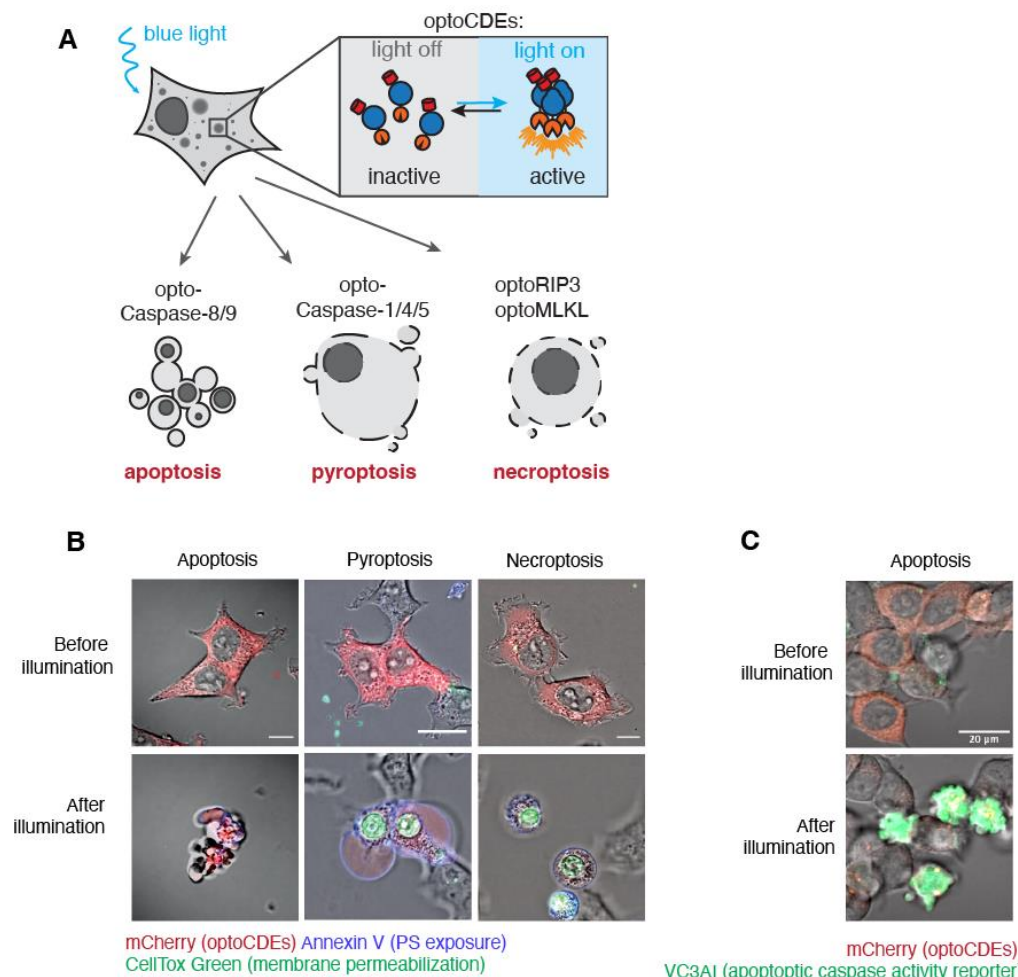


Figure 4. Assessment of optogenetically activated cell death effectors (optoCDE)-induced cell death

Cite as: Shkarina, K. and Broz, P. (2023). Optogenetic Induction of Pyroptosis, Necroptosis, and Apoptosis in Mammalian Cell Lines. Bio-protocol 13(14): e4762. DOI: 10.21769/BioProtoc.4762.

using microscopy. (A) Schematic representation of expected morphological changes in cells undergoing different types of cell death (apoptosis, pyroptosis, and necroptosis) in response to light-induced optoCDE activation. (B) Representative morphological features of HEK293T cells expressing pyroptotic [opto-(h)caspase-1], apoptotic [opto-(h)caspase-8], or necroptotic [opto-(h)RIPK3] effectors and stimulated with blue light. Red: mCherry-tagged optoCDEs; green: CellTox Green; blue: Annexin V. Due to the differences in cell death kinetics, the *after illumination* time point refers to 30 min for pyroptotic, 60 min for apoptotic, and 90 min for necroptotic cells. The images are derived from the original paper (Shkarina et al., 2022). (C) Representative images of cells expressing genetically encoded caspase-3/7 reporter VC3AI (green) and undergoing light-induced apoptosis approximately 1 h after illumination.

- d. Additionally, when doing this type of experiments for the first time, perform a similar experiment with the same cell type expressing Cry2olig alone and monitor the signs of cell death and/or abnormal changes in the cellular behavior related to the phototoxicity. If such changes are observed, decrease the laser power and/or the frame rate.
- 3. Optogenetic induction of pyroptosis in single cells
 - a. Set up the region of stimulation (ROI) corresponding to the specific cytoplasmic region in the cell to be targeted using ZEN “Bleaching” and “Regions” mode.
 - i. To account for the light diffusion and minimize the influence on the neighboring cells, the ROI should not exceed 5–10 μm^2 .
 - ii. The optimal laser intensity and number of scanning iterations varies depending on construct expression level, cell type, and type of cell death, and has to be determined empirically.
 - iii. If the signs of cell death (such as membrane blebbing, DRAQ7, or Annexin V positivity) are observed in the neighboring cells, reduce the ROI size and/or laser intensity or number of scanning iterations.
 - b. Set up the time-lapse experiment. This should include several frames before the photoactivation as the baseline, after which the ROI stimulation is performed, and additionally 30–60 min or more after.
 - c. Acquire the time lapse. To monitor for cell death, the imaging medium can be supplemented with the far-red cell death dyes (Annexin V or DRAQ7). The example of such experiment is shown at Figure 5.

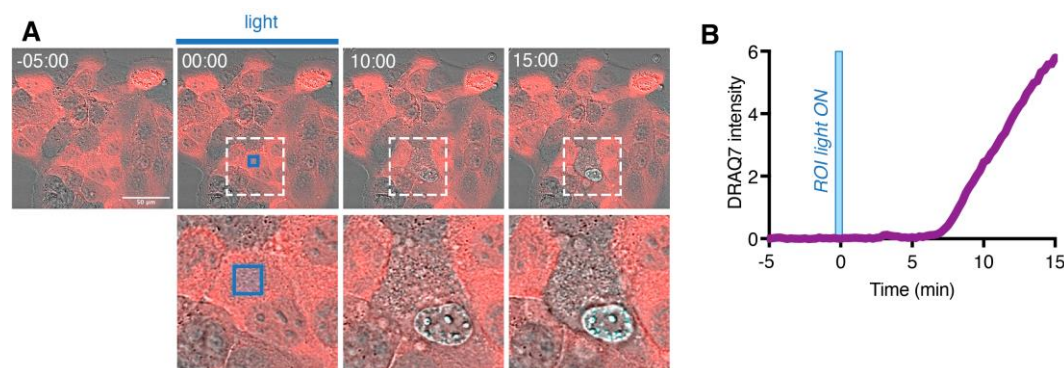


Figure 5. Single-cell optogenetic induction of pyroptosis. (A) Representative time-lapse images of HaCaT cells, where the cytoplasmic region of a selected single cell (inset) is selectively photoactivated with blue light [blue square represents region of illumination (ROI)] at 0 min. Note the morphological changes and gain of DRAQ7 signal (turquoise) in targeted cell but not in the neighboring cells. (B) Quantification of DRAQ7 intensity in the nucleus of the photoactivated cell. Figure adapted from Shkarina et al. (2022).

- d. If signs of optoCDE activation and cell death are also detected in the neighboring cells, repeat the experiment with the reduced laser power and/or number of pulses or decrease the ROI area.
- 4. Sub-lethal opto-caspase-1 activation

- a. Set up the ROI stimulation experiment as described above. In this experiment, the ROI can include the whole field of view or be limited to the single cell.
- b. Reduce the 488 nm laser power to 0.1%–0.2% and number of iterations to 1–3.
- c. To monitor membrane permeabilization, supplement the imaging medium with DRAQ7. Use higher dye concentration (1:100–1:500) and laser power/gain at this stage to detect low amount of membrane damage.
- d. Perform the imaging and photoactivation. The transient low-level optoCDE activation will likely lead to three phenotypes: 1) the cells that will undergo cell death (acquire “high” DRAQ7 staining); 2) the *survivor* cells (might acquire moderate DRAQ7 staining and transiently display some early features of cell death, such as membrane blebbing or nuclear condensation, but are able to revert to the normal morphology after), and 3) the cells that are not affected by the stimulation (not gaining DRAQ7 signal and no change in morphology) (Figure 6). The ratio of these cells in the population might depend on the optoCDE expression level, as well as additional cell-intrinsic factors (such as the variability in expression of the downstream effectors or activity of membrane repair systems).
- e. Adjust the stimulation parameters to achieve the desired optoCDE activation and cell survival ratio and repeat the experiment.

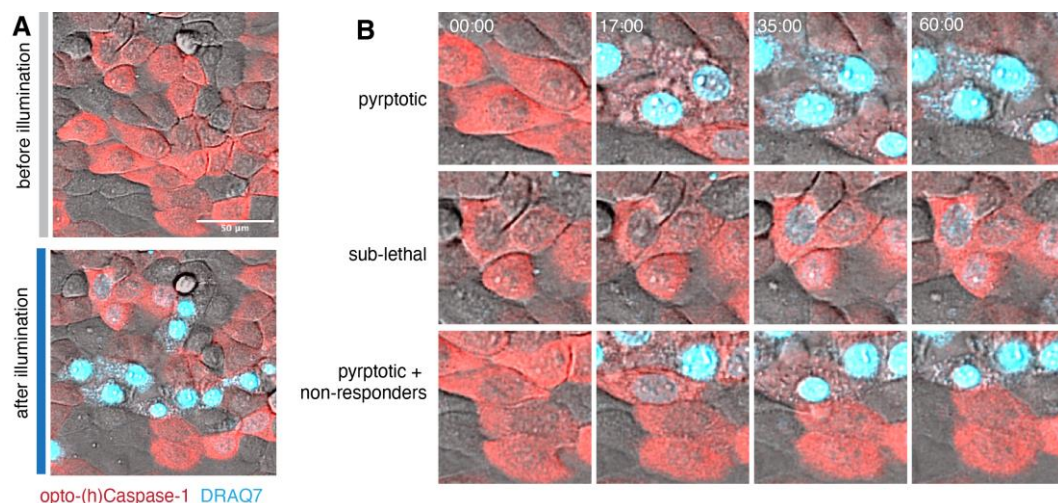


Figure 6. Sub-lethal induction of pyroptosis using transient opto-(h)caspase-1 activation in human keratinocytes. The confluent monolayer of HaCaT cells was transiently stimulated with low-intensity (0.2 mW/cm²/pulse, three pulses) blue light at 3 min after the beginning of time lapse, and the data was acquired for 60 min. (A) Representative images of the whole illuminated population before (at 0 min) and after (60 min). DRAQ7 (turquoise) is a membrane-impermeable DNA-binding dye used to visualize pyroptotic membrane permeabilization. (B) Close-up images of cells displaying three types of fates: pyroptotic (top), sub-lethal (middle), and both pyroptotic and non-responding cells (bottom). Note the strong DRAQ7 signal and loss of cytoplasmic mCherry in pyroptotic cells and low DRAQ7 positivity in the sub-lethally activated cells.

C. Optogenetic induction of pyroptosis in human macrophage-like cell lines

Important points

1. In this protocol, we utilize U937, human monocyte-like cell line, which can be differentiated into the macrophage-like phenotype using PMA treatment. However, a similar type of experiments can be performed with other cell lines.
2. Prior to seeding, transgenic U937 lines are grown in suspension in T75 flasks in complete RPMI medium. For optimal growth, the medium is exchanged every 2–3 days. Avoid growing the cells to too high density, as this will lead to the reduction of cell viability and might impact the differentiation.

Cite as: Shkarina, K. and Broz, P. (2023). Optogenetic Induction of Pyroptosis, Necroptosis, and Apoptosis in Mammalian Cell Lines. Bio-protocol 13(14): e4762. DOI: 10.21769/BioProtoc.4762.

3. The light plate apparatus was manufactured, assembled, and calibrated as described previously (Gerhardt et al., 2016). The programming of the devices is performed using Iris (<http://taborlab.github.io/Iris/>).
4. To determine the optimal illumination parameters for each type of cell death and for each cell type, we recommend testing a range of light intensities and illumination duration. When doing the experiment for the first time, always include the wild-type cells and/or cells expressing Cry2olig alone to control for the phototoxicity.
5. This protocol describes the analysis of pyroptosis induction using opto-(h)caspase-1; however, a similar procedure can be used to activate other optoCDE constructs.

Step-by-step protocol

1. Cell seeding and differentiation
 - a. Collect the desired volume of U937 cells into the 50 mL flasks and centrifuge at $300\times g$ at room temperature for 5 min. Discard the medium.
 - b. Resuspend the cells in fresh RPMI.
 - c. Count the cells and resuspend to the final density of 250,000 cells/mL.
 - d. Add PMA to the final concentration of 5 ng/mL.
 - e. Seed in 24-well black tissue culture–treated plates (4titude). Include additional wells for the non-illuminated cells and the positive (total lysis) control.
 - f. After 24 h, remove the PMA-containing medium, wash once with pre-warmed PBS, and add fresh growth medium.
 - g. After 48 h, replace the growth medium with the induction medium containing 2 $\mu\text{g}/\text{mL}$ doxycycline and incubate cells overnight to induce optoCDE expression.
2. Illumination
 - a. Set up the light plate apparatus in the cell incubator (Figure 6B). If using transient illumination times, these experiments can be performed on the bench before moving the plates to 37 °C.
 - b. Generate the custom illumination program using IRIS software. The example of an illumination layout is shown in Figure 7C. We recommend using duplicate wells for each illumination condition and including additional wells for the non-illuminated controls and total cell lysis (cells treated with 1% Triton X-100).

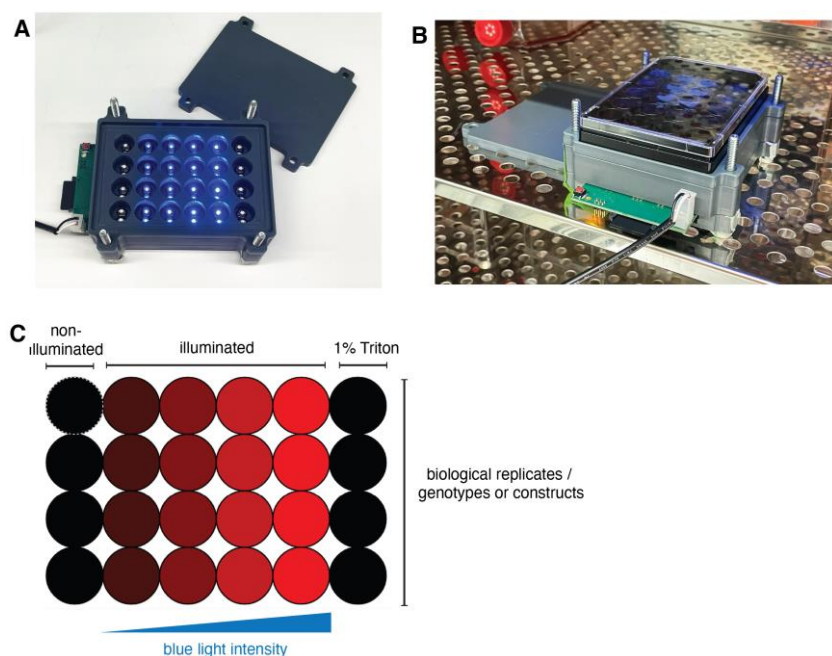


Figure 7. Light plate apparatus setup. (A) Photo of the self-made light plate apparatus device used for

Cite as: Shkarina, K. and Broz, P. (2023). Optogenetic Induction of Pyroptosis, Necroptosis, and Apoptosis in Mammalian Cell Lines. Bio-protocol 13(14): e4762. DOI: 10.21769/BioProtoc.4762.

the lactate dehydrogenase (LDH)/ELISA and western blot assays. (B) Setting up the device in the cell culture incubator for long-term experiments. (C) Example of the illumination layout used for determining the optimal illumination parameters.

- c. Download the program and transfer the files to the micro-SD card. Perform a short test illumination round to ensure that the device works properly.
 - d. Remove the cell culture medium from the cells and add 300 µL of pre-warmed Opti-MEM or equivalent serum-free phenol red free medium per well.
 - e. Place the plate into the light plate apparatus, cover the lid, and start the illumination. Upon the end of the program, the lights should turn off automatically.
 - f. Remove the plate from the light plate apparatus. Add 30 µL of 10% Triton X-100 to the positive control (total cell lysis) wells. Using a P1000 pipette, pipette 5–10 times to lyse the cells.
 - g. Centrifuge the plate at 500×*g* for 5 min at room temperature to pellet the cell debris.
 - h. Gently collect the supernatant from each well to the pre-labeled 1.5 mL microtubes. Avoid touching the well bottom to prevent debris collection. At this stage, 100 µL of supernatant can be used for lactate dehydrogenase (LDH) measurement, while the rest can be preserved at -20 °C for the cytokine measurement.
3. Assessment of cell lysis using LDH activity assay
 - a. Prepare the appropriate volume of the LDH reaction mix.
 - b. Using a multichannel pipette, add 30 µL of reaction mix per well of a flat-bottom 96-well plate. Avoid creating bubbles, as this will impact the assay efficiency and reading.
 - c. In each well, add 30 µL of the cell supernatants collected in the step 2h. Include two to three technical replicates per each experimental well. Minimize delays while pipetting, as this might impact the difference in the colorimetric reaction between the wells and lead to bias.
 - d. Mix by gently tapping the plate on the side. Avoid mixing by pipetting, as this will generate bubbles. If bubbles are produced during pipetting, they can be manually removed before reading the plates using either syringe needles or an inverted Bunsen burner.
 - e. Incubate the plate for 15–20 min at room temperature, protected from light.
 - f. Add 30 µL of stop solution per well and gently mix.
 - g. Measure the absorbance using a 490–492 nm filter.
 4. Assessment of the IL-1 β release
 - a. IL-1 β release quantification following illumination is typically quantified using ELISA, performed according to the manufacturer's protocol (available at R&D website).
 - b. We recommend using several dilutions (1:1, 1:2, 1:5) of the collected supernatants, as the amount of IL-1 β in undiluted supernatants frequently exceeds the dynamic range of assay.
 - c. Alternatively, a FRET-based no-wash homogeneous time resolved fluorescence assay can also be utilized for quicker single-step IL-1 β quantification.
 5. Western blot analysis of optoCDE activation and cell death
 - a. Before the start of the experiment, prepare the following reagents:
 - i. Pre-labeled 1.5 mL microtubes for supernatant and lysate collection.
 - ii. Cell lysis (RIPA or equivalent) and loading buffer.
 - iii. Reagents for phenol-chloroform protein precipitation.
 - iv. Reagents for the polyacrylamide gel preparation (or pre-cast gels).
 - v. Western blot running, transfer, and wash buffers.
 - b. Perform the illumination of the plates as described in step 5a. Ensure that the cells are in the good condition before the start of experiment and are mCherry-positive (this can be assessed using epifluorescent microscopy).
 - c. Centrifuge the plates at 300–500×*g* for 5 min at room temperature to pellet the dead cells and collect the supernatants from each well into 1.5 mL microcentrifuge tubes.
 - d. Immediately add 50–70 µL of hot (95 °C) loading buffer to the remaining adherent/pelleted cells. At this stage, plates can be processed immediately or sealed with parafilm and stored at -80 °C for later processing.

- e. Pipette the lysis buffer up and down 5–10 times and collect the lysates into the microtubes. If lysates become too viscous at this stage, they can be additionally sonicated.
- f. Incubate for 5 min at 95 °C.
- g. In parallel, perform the protein precipitation in the cell supernatants using the phenol-chloroform protein extraction method (Demarco et al. 2022). After the precipitation, the dried protein pellets can be either resuspended in 1× lysis/loading buffer and processed independently or combined with lysates of corresponding wells.
- h. Load samples on the 10%–12% polyacrylamide gels.
- i. Perform the gel running and western blot analysis of the samples following the protocol available in the host lab. The detailed protocol for western blot analysis of such samples can also be found in Demarco et al. (2022).
- j. For the detection of inflammatory opto-caspase activation, we recommend using the following primary antibodies: rabbit anti-cleaved IL-1 β (83186, CST; 1:1,000), which detects IL-1 β by activated opto-(h)caspase-1; mouse anti-IL-1 β (12242, CST; 1:1,000), which detects full-length unprocessed IL-1 β in non-activated cells; rabbit anti-GSDMD (ab210070; 1:1,000; Abcam), which detects non-activated GSDMD in resting cells; rabbit anti-cleaved N-terminal GSDMD (ab215203; 1:1,000; Abcam), which detects active GSDMD cleaved by opto-(h)caspase-1; mouse anti-caspase-1 (clone Bally-1 AG-20B-0048-C100; 1:1,000; AdipoGen); mouse anti-mCherry (ab125096; 1:2,000; Abcam); and HRP-conjugated mouse anti-tubulin (ab40742; 1:5,000; Abcam), used as a loading control. The secondary HRP-conjugated or fluorescently labeled antibodies can be used according to the lab's choice. A representative blot is shown in Figure 8.

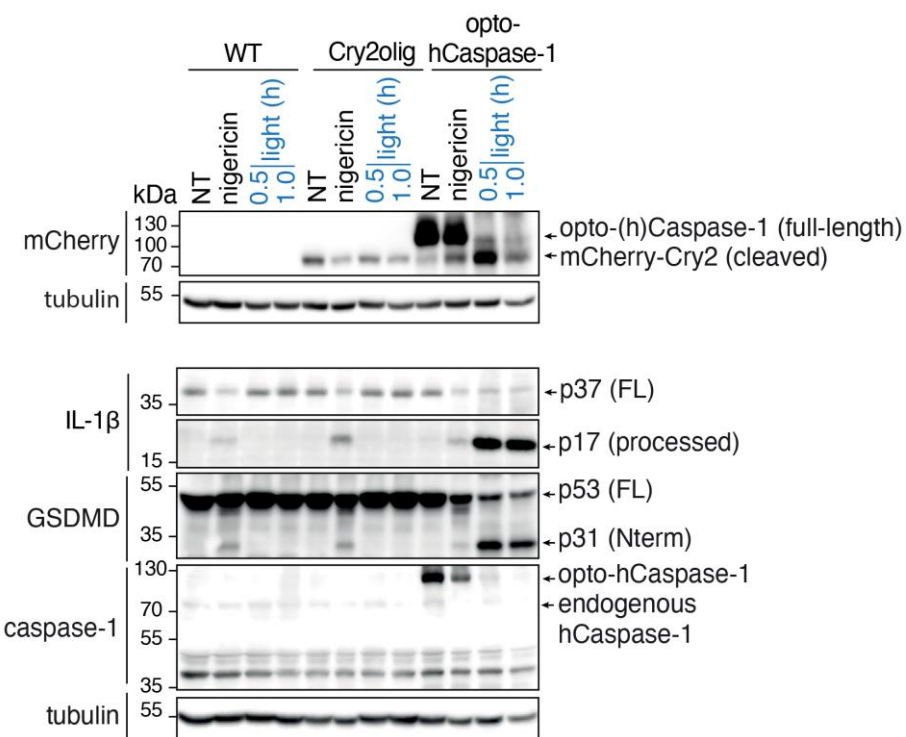


Figure 8. Example of the western blot analysis of opto-caspase-1-induced pyroptosis in U937 cells. Experiment was performed as described above and treatment with nigericin, an NLRP3 inflammasome activator, was used as a positive control to detect IL-1 β and GSDMD processing. Note the cleavage of opto-caspase-1 (as detected by the disappearance of full-length opto-caspase-1 band and accumulation of Cry2olig-mCherry), IL-1 β , and GSDMD upon illumination. Figure adapted from Shkarina et al. (2022).

Data analysis

1. Analysis of microscopy images

The analysis of the microscopy images is described in the Methods section of the original publication (Shkarina, et al., 2022). For quantification of different types of cell death, we assessed several parameters: a) appearance of the characteristic morphological changes associated with each type of cell death (cell rounding and swelling, nuclear condensation for pyroptosis and necroptosis, nuclear fragmentation and persistent membrane blebbing for apoptosis); b) Annexin V staining, as an indicator of membrane scrambling and phosphatidylserine exposure (for all three types of cell death); and c) uptake of specific dyes associated with the loss of membrane integrity, such as CellTox Green or DRAQ7 (for pyroptosis and necroptosis). Additionally, activation of the apoptotic caspases can be monitored using genetically encoded or chemical fluorogenic caspase reporters (such as VC3AI, described in the original paper, or CellEvent caspase-3/7 reporter system). The number of dying cells can be normalized to the total number of cells per field of view, or, alternatively, to the number of mCherry-positive cells in the population, to account for the construct expression and transduction efficiency.

2. Analysis of LDH assay and ELISA results

LDH release from pyroptotic (or generally necrotic) cells following illumination is quantified using the following equation:

$$(\text{LDH}_{\text{sample}} - \text{LDH}_{\text{negative control}})/(\text{LDH}_{\text{positive control}} - \text{LDH}_{\text{negative control}}) \times 100$$

Where negative control is assay medium (e.g., Opti-MEM or other phenol red free medium) and positive control corresponds to the cells lysed with the 1% Triton X-100.

Quantification of IL-1 β release is performed according to the manufacturer's protocol. Note that the variation in initial (pre-illumination) cell density between the cell lines or conditions can have a strong effect on the amount of detected IL-1 β . This can be corrected by normalizing IL-1 β values to the ratio of maximum LDH values from lysed cells. An example of the LDH and IL-1 β secretion data obtained from this type of experiments is shown in Figure 9.

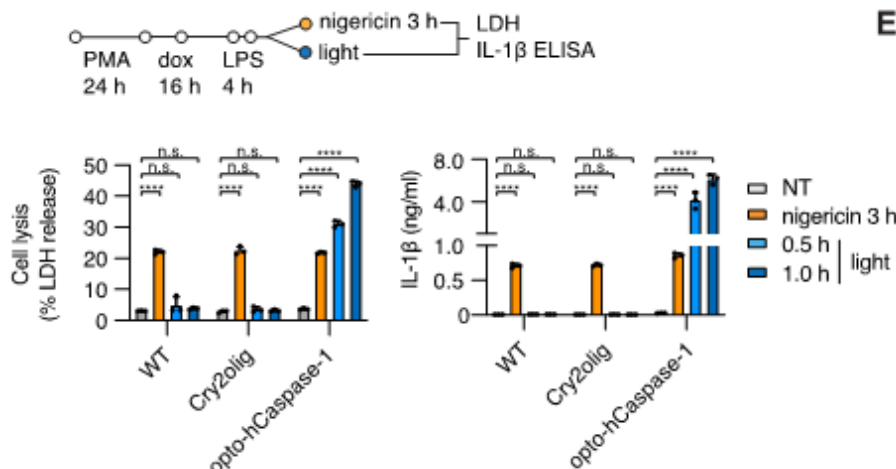


Figure 9. Example of lactate dehydrogenase (LDH) release and IL-1 β secretion upon illumination-induced opto-(h)caspase-1 activation. Nigericin (NLRP3 inflammasome activator) was used to monitor cell competency to endogenous inflammasome activation. Figure adapted from Shkarina et al. (2022).

Notes

General notes

1. When inducing different modes of cell death, it is important to take into consideration the selection of the appropriate cell line/type. We observed that the ability of cells to undergo different forms of cell death upon optoCDE activation varies among the different cell lines and cell types tested. This might depend on several factors:
 - a. Effector efficiency: we observed that, due to the differences in substrate processing kinetics and efficiency between different caspases, and also kinetic and mechanistic differences between separate cell death modalities, it might be necessary to adjust the levels of construct expression or stimulation to achieve similar cell death levels. As an example, in some cell lines, achieving an equal level of apoptosis might require higher expression of more prolonged stimulation for opto-caspase-8 than opto-caspase-9. Also, the same is applicable for opto-caspase-4 vs. opto-caspase-1 vs. opto-caspase-5, and for optoRIP3 vs. optoMLKL (although the last case can be explained by MLKL being the most distal cell death effector in necroptosis, while RIP3-induced necroptosis would be initiated more proximately and constrained by both endogenous MLKL levels and post-translational regulation).
 - b. Expression of downstream effectors, such as GSDMD for inflammatory (pyroptotic) caspases or MLKL for optoRIPK3. These proteins can be co-expressed with optoCDEs to achieve pyroptosis in the cell lines that are either naturally deficient (such as HEK cells) or express low levels (HeLa) of them endogenously.
 - c. Downstream regulatory mechanisms (such as phosphorylation or other types of post-translational modifications or protein–protein interactions), which might limit or promote optoCDE activation in some cell types.
2. Spontaneous or unwanted optoCDE activation due to overexpression or low-level activation due to visible light exposure might induce cytotoxicity or lead to the negative selection of expressing cells. Thus, it is essential to always protect the cells from visible light following the induction of optoCDE construct expression, or when using constitutive expression systems. All necessary cell handling, such as treatments or medium exchange, should be performed under dim light conditions, or using lab space and hoods equipped with red-light sources (lamps or LED strips). Additionally, we strongly recommend using inducible expression systems (such as Tet-ON) and tetracycline-free serum for stable cell line generation and maintenance.
3. Also, avoid checking the expressing cell lines under the microscope using violet, blue, or transmitted (white) light before the beginning of the experiment, as this will trigger the optoCDE construct activation. Usually, the mCherry expression in stable lines can be used as a good proxy measurement of the viability in unstimulated cells. Alternatively, visual assessment of cell density and morphology can be performed in separate wells, which can then be excluded from the experiment.
4. We recommend determining the optimal illumination parameters for each optoCDE construct and each cell line by testing several different blue light intensities and/or illumination duration. Additionally, it is essential to include wild-type cells and cells expressing Cry2olig alone to control for phototoxicity and potential non-specific effects of Cry2olig overexpression and photoactivation.

Acknowledgments

This work was supported by grants from the ERC (ERC2017-CoG-770988-InflamCellDeath), the Swiss National Science Foundation (175576 and 198005), the OPO Stiftung and Novartis to P.B. K.S. is a recipient of SNSF Postdoc.Mobility fellowship (P500PB_211096). This protocol was adapted from Shkarina et al. (2022).

Competing interests

The authors declare no competing interests.

References

- Bedoui, S., Herold, M. J. and Strasser, A. (2020). [Emerging connectivity of programmed cell death pathways and its physiological implications](#). *Nat Rev Mol Cell Bio* 21: 678–695.
- Demarco, B., Ramos, S. and Broz, P. (2022). [Detection of Gasdermin Activation and Lytic Cell Death During Pyroptosis and Apoptosis](#). In: Kufer, T.A., Kaparakis-Liaskos, M. (Eds.). *Effector-Triggered Immunity*. Methods in Molecular Biology. Humana Press, New York.
- Galluzzi, L., Vitale, I., Aaronson, S. A., Abrams, J. M., Adam, D., Agostinis, P., Alnemri, E. S., Altucci, L., Amelio, I., Andrews, D. W., et al. (2018). [Molecular mechanisms of cell death: recommendations of the Nomenclature Committee on Cell Death 2018](#). *Cell Death Differ* 25(3): 486–541.
- Gerhardt, K. P., Olson, E. J., Castillo-Hair, S. M., Hartsough, L. A., Landry, B. P., Ekness, F., Yokoo, R., Gomez, E. J., Ramakrishnan, P., Suh, J., et al. (2016). [An open-hardware platform for optogenetics and photobiology](#). *Sci. Rep* 6(1): e1038/srep35363.
- Oberst, A., Pop, C., Tremblay, A. G., Blais, V., Denault, J. B., Salvesen, G. S. and Green, D. R. (2010). [Inducible Dimerization and Inducible Cleavage Reveal a Requirement for Both Processes in Caspase-8 Activation](#). *J. Biol. Chem* 285(22): 16632–16642.
- Qi, Y. B., Garren, E. J., Shu, X., Tsien, R. Y. and Jin, Y. (2012). [Photo-inducible cell ablation in *Caenorhabditis elegans* using the genetically encoded singlet oxygen generating protein miniSOG](#). *Proc. Natl. Acad. Sci. U.S.A.* 109(19): 7499–7504.
- Shkarina, K., Hasel de Carvalho, E., Santos, J. C., Ramos, S., Leptin, M. and Broz, P. (2022). [Optogenetic activators of apoptosis, necroptosis, and pyroptosis](#). *J. Cell Biol* 221(6): e202109038.
- Taslimi, A., Vrana, J. D., Chen, D., Borinskaya, S., Mayer, B. J., Kennedy, M. J. and Tucker, C. L. (2014). [An optimized optogenetic clustering tool for probing protein interaction and function](#). *Nat. Commun* 5(1): e1038/ncomms5925.
- Tirlapur, U. K., Konig, K., Peuckert, C., Krieg, R. and Halbhuber, K. J. (2001). [Femtosecond near-infrared laser pulses elicit generation of reactive oxygen species in mammalian cells leading to apoptosis-like death](#). *Exp Cell Res* 263(1): 88–97.
- Wu, X. N., Yang, Z. H., Wang, X. K., Zhang, Y., Wan, H., Song, Y., Chen, X., Shao, J. and Han, J. (2014). [Distinct roles of RIP1–RIP3 hetero- and RIP3–RIP3 homo-interaction in mediating necroptosis](#). *Cell Death Differ* 21(11): 1709–1720.

Visualizing Loss of Plasma Membrane Lipid Asymmetry Using Annexin V Staining

Julia F. Baum^{1,2, #}, Huriye D. Uzun^{1,2, #}, and Thomas Günther Pomorski^{1,2, *}

¹Department of Molecular Biochemistry, Faculty of Chemistry and Biochemistry, Ruhr University Bochum, Bochum, Germany

²Department of Plant and Environmental Sciences, University of Copenhagen, Frederiksberg, Denmark

*For correspondence: Thomas.Guenther-Pomorski@ruhr-uni-bochum.de

#Contributed equally to this work

Abstract

Loss of plasma membrane lipid asymmetry contributes to many cellular functions and responses, including apoptosis, blood coagulation, and cell fusion. In this protocol, we describe the use of fluorescently labeled annexin V to detect loss of lipid asymmetry in the plasma membrane of adherent living cells by fluorescence microscopy. The approach provides a simple, sensitive, and reproducible method to detect changes in lipid asymmetry but is limited by low sample throughput. The protocol can also be adapted to other fluorescently labeled lipid-binding proteins or peptide probes. To validate the lipid binding properties of such probes, we additionally describe here the preparation and use of giant unilamellar vesicles as simple model membrane systems that have a size comparable to cells.

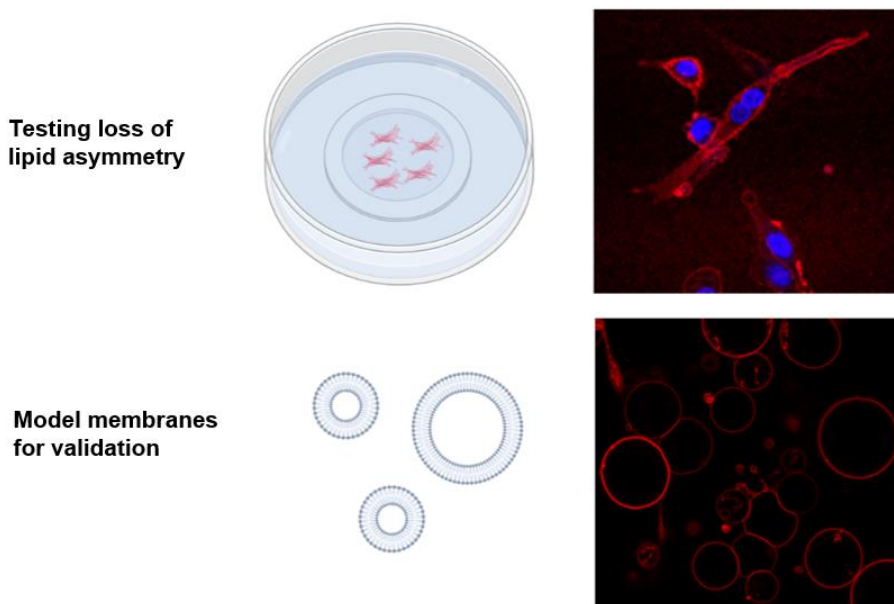
Key features

- Monitoring loss of lipid asymmetry in the plasma membrane via confocal microscopy.
- Protocol can be applied to any type of cell that is adherent in culture, including primary cells.
- Assay can be adapted to other fluorescently labeled lipid-binding proteins or peptide probes.
- Giant unilamellar vesicles serve as a tool to validate the lipid binding properties of such probes.

Keywords: Confocal microscopy, Giant vesicle, Lipid asymmetry, Lipid-binding protein, Mammalian cells, Plasma membrane

This protocol is used in: J. Cell. Sci. (2022), DOI: 10.1242/jcs.258649

Graphical overview



Imaging the binding of fluorescent annexin V to adherent mammalian cells and giant vesicles by confocal microscopy. Annexin V labeling is a useful method for detecting a loss of plasma membrane lipid asymmetry in cells (top image, red); DAPI can be used to identify nuclei (top image, blue). Giant vesicles are used as a tool to validate the lipid binding properties of annexin V to anionic lipids (lower image, red).

Background

A characteristic feature of many biological membranes is that their phospholipids are asymmetrically distributed across the lipid bilayer, a phenomenon known as transbilayer lipid asymmetry. A prominent example is the plasma membrane of animal cells, in which the phospholipids phosphatidylcholine and sphingomyelin are concentrated in the exoplasmic leaflet, whereas the aminophospholipids phosphatidylserine (PS) and phosphatidylethanolamine (PE) are restricted to the cytosolic leaflet (van Meer et al., 2008). Transbilayer lipid asymmetry is essential for several vital cellular functions, including the regulation of membrane protein activity, signaling, and vesicle formation in the secretory and endocytic pathways (Sprong et al., 2001; Ewers and Helenius, 2011; van Meer, 2011; Sebastian et al., 2012). In animals, loss of transbilayer lipid asymmetry has been linked to processes such as blood coagulation (Lentz, 2003; Jackson, 2011), cell adhesion (Schlegel et al., 1985; Malhotra et al., 1996; Wautier et al., 2011), macrophage recognition (Krahling et al., 1999), apoptosis (Bevers and Williamson, 2016), and myotube formation (van den Eijnde et al., 2001). The establishment and regulation of lipid asymmetry are therefore crucial for cells, and several membrane proteins have evolved to fulfill the function of cross-bilayer phospholipid transporters, comprising lipid flippases, floppases, and scramblases (Hankins et al., 2015; Ristovski et al., 2021).

Several methods have been developed to analyze the loss of phospholipid asymmetry in the plasma membrane of eukaryotic cells. These include chemical approaches using e.g., trinitrobenzene sulfonic acid or fluorescamine, which covalently react with amino groups of lipids and proteins (Marinetti et al., 1976; Pomorski et al., 2003). As the probes are membrane impermeant, only aminophospholipids exposed to the cell surface are modified and can then be detected by thin-layer chromatography or mass spectrometry. However, this approach is not suitable for live-cell imaging. More recent methods are based on fluorescently labeled lipid-binding proteins that can be added to the cells. One example is the PS-specific probe lactadherin, which binds to PS with a nanomolar affinity and without the need for cofactors (Waehrens et al., 2009). Another example is annexin V, a member of the annexin family of Ca^{2+} -dependent, non-covalent lipid-binding proteins. Annexin V binds negatively charged lipids with

Cite as: Baum, J. F. et al. (2023). Visualizing Loss of Plasma Membrane Lipid Asymmetry Using Annexin V Staining. Bio-protocol 13(14): e4754. DOI: 10.21769/BioProtoc.4754.

relatively high affinity and is used extensively for the detection of exofacial PS by flow cytometry or microscopy (Koopman et al., 1994; Vermes et al., 1995; Tait et al., 2004). A new generation of fluorescent probes is based on cyclic peptides that successfully mimic the function of lipid-binding proteins and benefit from their small size, ease of labeling, and cofactor-free PS recognition (Hanshaw et al., 2005; DiVittorio et al., 2006; Zheng et al., 2011).

In this protocol, we describe the use of fluorescently labeled lipid-binding protein sensors to detect the loss of lipid asymmetry in living cells by fluorescence microscopy, exemplified on mouse C2C12 wild-type myoblasts and corresponding knockout cells lacking the P4-ATPase flippase subunit CDC50A (also known as TMEM30A). Deletion of CDC50A results in loss of the aminophospholipid flippase activity and constitutive loss of plasma membrane lipid asymmetry (Grifell-Junyent et al., 2022). The approach is illustrated using commercially available annexin V conjugated to Alexa Fluor 568, but other fluorescently labeled lipid-binding proteins or peptide probes can also be used.

To validate the specificity and sensitivity of such lipid binding probes, we also describe here the use of giant unilamellar vesicles (GUVs) as simple model membrane systems. One of the major advantages of using GUVs as model membrane systems is their similarity in size to cells. This allows GUVs to be observed directly under the microscope, making them a convenient and accessible tool for lipid-binding studies. By preparing GUVs with defined lipid compositions, the specificity and sensitivity of lipid-binding probes can be evaluated and their accuracy and reproducibility in live cell experiments can be ensured (Weingärtner et al., 2012; Chandra and Datta, 2022). GUVs with defined lipid compositions can be prepared by various methods, including swelling, PVA or agarose swelling, and electroformation using indium tin oxide glass slides and droplet transfer methods (Angelova and Dimitrov, 1986; Weinberger et al., 2013; Bhatia et al., 2015; Shimane and Kuruma, 2022). In this study, we describe the swelling method due to its simplicity. For alternative preparation methods, the reader is referred to other bio-protocols (Parigoris et al., 2020; Mathiassen and Pomorski, 2022). Our protocol provides a reliable and efficient method for detecting loss of lipid asymmetry in living cells and can be adapted for use with a variety of lipid-binding proteins.

Materials and reagents

A. Mammalian cell culture

In this study, we used mouse myoblast cells (C2C12; cell number: ACC 565, DSMZ Braunschweig, Germany) and the corresponding knockout cells lacking CDC50A (Grifell-Junyent et al., 2022) that were cultured in growth medium (see Recipe 1). Optimal culture media and conditions may differ for other cell lines.

1. Basal cell culture medium for growth (e.g., high glucose DMEM, without pyruvate; Sigma-Aldrich, catalog number: D5796), store at 4 °C
2. Ethanol absolute ≥ 99.8% (VWR, catalog number: 20821.321)
3. Ethylene glycol-bis(2-aminoethylether)-N,N,N',N'-tetraacetic acid (EGTA) (e.g., Sigma-Aldrich, catalog number: E4378)
4. Fetal bovine serum (FBS), heat inactivated before use (e.g., Capricorn Scientific, catalog number: FBS-11A), store at -20 °C
5. Hanks' balanced salt solution, Ca²⁺ and Mg²⁺ free (HBSS) (e.g., Sigma-Aldrich, catalog number: H6648), store at 4 °C
6. 35 mm polymer bottom dishes (e.g., Ibidi, catalog number: 81156)
7. 1.5 mL microcentrifuge tubes (Sarstedt, catalog number: 72.690.001)
8. Penicillin-streptomycin, 100× solution (e.g., Sigma-Aldrich, catalog number: P4333), store at -20 °C
9. Pipette controller (e.g., accu-jet pro, Brand, catalog number: 263 00)
10. Polypropylene tubes, 15 mL capacity (e.g., Falcon tubes, Sarstedt, catalog numbers: 62.554.502 and 62.547.254)
11. Sterile serological pipettes (e.g., Serological pipettes of 5, 10, and 25 mL; Sarstedt, catalog numbers: 86.1253.001, 86.1254.001, and 86.1685.001)
12. Sterile culture vessels T-75 flasks (e.g., Sarstedt, catalog number: 83.3911)

13. Trypsin-EDTA solution (e.g., Sigma-Aldrich, catalog number: T3924), store at -20 °C
14. Trypan Blue solution, 0.4% (e.g., Thermo Fischer Scientific, catalog number: 15250061)
15. Growth medium (see Recipe 1)

B. For annexin V labeling

1. Annexin V conjugated to Alexa Fluor 568 (e.g., Roche, catalog number: A13202), store at 4 °C
2. 4',6-Diamidino-2-phenyl-indol-dihydrochlorid (DAPI) (e.g., Sigma-Aldrich, catalog number: D9542)
3. Dead cell staining reagents, e.g., SYTOX Blue (Thermo Scientific, catalog number: S34857)
4. Ice
5. Tyrode's balanced salt solution with Ca²⁺ (TBSS + Ca²⁺; see Recipe 2), store at 4 °C
6. Tyrode's balanced salt solution without Ca²⁺ (TBSS - Ca²⁺; see Recipe 3), store at 4 °C
7. DAPI stock solution (1 mg/mL) (see Recipe 4)

Note: This procedure has also been successfully performed using FITC-labeled lactadherin (e.g., Haematologic Technologies, catalog number: BLAC-FITC).

C. For the preparation of giant unilamellar vesicles (GUVs)

1. 1,2-dioleoyl-sn-glycero-3-phosphocholine (DOPC) (Avanti® Polar Lipids, catalog number: 850375)
2. 1,2-dioleoyl-sn-glycero-3-phosphoethanolamine (DOPE) (Avanti® Polar Lipids, catalog number: 850725)
3. 1,2-dioleoyl-sn-glycero-3-phospho-L-serine (sodium salt) (DOPS) (Avanti® Polar Lipids, catalog number: 840035)
4. Calcium chloride (CaCl₂) (Grüssing, catalog number: 10043-52-4)
5. Chloroform, ethanol-stabilized and certified for absence of HCl (Sigma-Aldrich, catalog number: 32211-M)
6. Detergent/soap
7. Ethanol, 70% (Sigma-Aldrich, catalog number: 64-17-5)
8. Glucose (Duchefa Biochemie, catalog number: G0802.5000)
9. HEPES (Carl Roth, catalog number: 7365-45-9)
10. Ice
11. Magnesium chloride hexahydrate (MgCl₂·6H₂O) (Sigma-Aldrich, catalog number: 7791-18-6)
12. Methanol ≥ 99.8% (VWR, catalog number: 67-56-1)
13. Potassium hydroxide (KOH) (Sigma-Aldrich, catalog number: 1310-58-3)
14. Potassium chloride (KCl) (Merck, catalog number: 7447-40-7)
15. Sodium chloride (NaCl) (Carl Roth, catalog number: 7647-14-5)
16. Sucrose (Duchefa Biochemie, catalog number: S0809.5000)
17. Lipid stock in chloroform (see Recipe 5)
18. Swelling buffer (320 mM sucrose) (see Recipe 6)
19. Binding buffer (see Recipe 7)

Note: Store or keep all reagents at room temperature, except indicated items. All buffers are prepared the day before and stored at 4 °C.

Equipment

A. General

1. Analytical balance (e.g., Sartorius Entris-I II, 220 g/0.1 mg; Buch Holm, catalog number: 4669128)
2. Computer with monitor (e.g., DELL U2415)
3. Confocal laser scanning microscope (e.g., Leica TCS SP8 confocal laser scanning microscope, Leitz, Wetzlar, Germany, equipped with a 63×/1.20 water objective)

4. Eppendorf Research® plus pipettes P20, P200, P1000 (Eppendorf, catalog numbers: 3123000039, 3123000055, 3123000063)
5. Eppendorf tube, 2 mL (Merck, catalog number: EP0030120094)
6. Freezers -20 °C and -80 °C
7. Magnetic stirrer (e.g., IKAMAG®, DREHZAHL ELECTRONIC, IKA, Staufen im Breisgau, Germany)
8. Magnets
9. pH meter (pH-Meter 761 Calimatic, Knick, Berlin, Germany)
10. Pipette tips 10, 200, 1,000 µL (Sarstedt, catalog numbers: 70.760.002, 70.3030.020, 70.3050.020)
11. Refrigerator (5 °C)
12. Water distillation system

B. For cell culture

1. Autoclave sterilizer (e.g., Systec VX-65, Systec, Linden, Germany)
2. Biological safety cabinet certified for handling biological materials (e.g., Herasafe KSP Class II Biological Safety Cabinets, Thermo Fisher Scientific)
3. Centrifuge with rotor for 15 and 50 mL polypropylene tubes (e.g., Eppendorf 5810 R; Wesseling, Germany)
4. Incubator with humidity and gas control to maintain 37 °C and 95% humidity in an atmosphere of 5% CO₂ in air (e.g., Binder, Tuttlingen, Germany)
5. Inverted phase contrast microscope equipped with a 10× objective (HI PLAN I 10×/0.22 PH1; Leica DMI1, Mannheim, Germany)
6. Neubauer counting chamber (improved dark lines, 0.1 mm) and cover glasses (20 mm × 26 mm × 0.4 mm)
7. Water bath (e.g., WPE45 Memmert, Schwabach, Germany) for mammalian cells and for NBD-lipid labeling (Julabo CORIO C-BT5, catalog number: 9011305)

C. For preparation of GUVs

1. Cover glass slides (26 mm × 76 mm, #1.5, Thermo Fisher Scientific, Life Technologies Corporation Eugene)
2. Flow cabinet to work with organic solvents
3. Glass beads, 3 mm (Merck, catalog number: 104015)
4. Glass desiccator Boro 3.3 with a socket in the lid, 20 cm, including stopcock (Brand, catalog number: 65238)
5. Glass pipettes (e.g., graduated pipettes BLAUBRAND® Type 3 Class AS, 10 mL, graduation: 10 mL; Carl Roth, catalog number: HXT8.1)
6. Glass slide (Thermo Scientific, microscope slides 76 mm × 26 mm, catalog number: MEZ 101026)
7. Glass vials (Rotilabo® screw neck ND8 vials, brown/white glass, 1.5 mL; Carl Roth, catalog number: KE30.1) with screw caps (without a borehole, without septum, PP, black, ND8; Carl Roth, catalog number: KE39.1)
8. Glass tubes (Carl Roth, catalog number: DURAN C208.1)
9. Hamilton 700 Series syringes 25, 100, 1,000 µL (Hamilton Company, Nevada, USA)
10. High vacuum grease (DOW CORNING, 65201 Wiesbaden, made in USA, Artwork Nr. 0315)
11. Ice bucket (e.g., Magic Touch 2™ ice bucket with lid; Sigma-Aldrich, catalog number: BAM168072002)
12. O-ring (28 mm × 1 mm, Nanion Technologies, München)
13. Parafilm (PARAFILM® M; Sigma-Aldrich, catalog number: P7793-1EA)
14. Rotavapor® R-100 Evaporator with I-100 Controller and V-100 vacuum pump (Flawil, Switzerland)
15. Scissors
16. Ultra-violet/ozone probe and surface decontamination unit (e.g., Novascan Technologies Inc., Boone, IA, USA)
17. Vortex mixer (e.g., Vortex Genie 2 Scientific Industries Inc., catalog number: SI-0236)
18. Vacuum Pump V-100 with Interface I-100 (Buchi, catalog numbers: 11593636 and 11593655D)
19. Wipes (Precision Wipes, KIMTECH Science, Kimberly-Clark® Professional, catalog number: 7552)

Cite as: Baum, J. F. et al. (2023). Visualizing Loss of Plasma Membrane Lipid Asymmetry Using Annexin V Staining. Bio-protocol 13(14): e4754. DOI: 10.21769/BioProtoc.4754.

Software

1. ImageJ (Wayne, Rasband, S., U. S. National Institutes of Health, Bethesda, Maryland, USA, <https://imagej.nih.gov/ij/index.html>, version v.153q)
2. Leica Application Suite AF (LAS AF, Leitz, Wetzlar, Germany)
3. Microsoft Excel (Microsoft Corporation, 2018)
4. PowerPoint (Microsoft Corporation, 2018)
5. OriginPro (OriginLab, 2023)

Procedure

The following procedure outlines four main steps: (A) preparation of mammalian cells, (B) cell counting, (C) annexin V staining of adherent cells, and (D) preparation of GUVs. The last step was originally applied to study the binding specificity of annexin V to different membrane lipid compositions (Weingärtner et al., 2012; Grifell-Junyent et al., 2022). We recommend this analysis before applying new probes in cell studies.

A. Preparation of mammalian cells

1. Grow adherent cells in sterile culture vessels (T-75 flask) in growth medium (see Recipe 1) in a tissue culture incubator (37 °C, 5% CO₂, 95% humidity) until they reach ~60%–70% confluence.
Caution: C2C12 cells will differentiate if grown too confluent and start to fuse. Differentiation and fusion are accompanied by transcriptional changes, which can lead to different results.
2. Aspirate and discard growth media with sterile serological pipette.
3. Wash cells twice with 5 mL of HBSS (Ca²⁺ and Mg²⁺ free, pre-warmed at 37 °C) using a sterile serological pipette.
4. Add 1.5 mL of trypsin-EDTA solution (pre-warmed at 37 °C) using a sterile serological pipette and incubate the T-75 flasks in a tissue culture incubator (37 °C, 5% CO₂, 95% humidity). Tilt the vessel back and forth a few times to make sure the thin layer of trypsin is evenly spread.
5. After 5 min, check for detachment by gently tilting vessel and/or observing under the microscope. If all cells have not detached in 5 min, incubate an additional 1–2 min and check again. Continue to incubate and check as necessary, only until cells are no longer attached to the plate surface.
Caution: Avoid prolonged incubation period with trypsin-EDTA solution.
6. Stop trypsinization by adding 7.5 mL of growth medium (pre-warmed at 37 °C, see Recipe 1) to the cell suspension.
7. Transfer the cell suspension into a 15 mL Falcon tube and set aside 100 µL in a 1.5 mL microcentrifuge tube for cell counting, e.g., using the hemocytometer (see section B).
8. Centrifuge cells in the 15 mL Falcon tube at 300× g for 5 min at room temperature and discard the supernatant to remove the trypsin-EDTA containing medium from the cells.
9. Add 10 mL of fresh growth medium (pre-warmed at 37 °C, see Recipe 1) to the cell pellet and re-suspend completely by gently pipetting up and down using a serological pipette.
Caution: Cells in suspension settle quickly. After counting, we recommend gently re-suspending the cell suspension approximately every 2–3 min when seeding multiple dishes.
10. After counting (see section B), seed 1.5 × 10⁴ cells per 35 mm polymer bottom dishes and add growth medium (pre-warmed at 37 °C, see Recipe 1) up to a final volume of 1 mL per dish.
Note: Prepare sufficient Petri dishes for control samples (see section C). We used a low cell number for seeding because C2C12 is a fast-growing cell line (doubling time: ~20 h) and this cell number guarantees that single cells are still present when the assay is performed the next day.
11. Keep the cells in a tissue culture incubator (37 °C, 5% CO₂, 95% humidity) overnight.

B. Cell counting (supplemental; if information on cell counting is not required, proceed to section C)

The purpose of this step is to quantify the cell concentration to resuspend the cells at the appropriate concentration for the assay. We routinely use the trypan blue hemocytometer assay. Alternative cell counting methods such as automatic cell counters may be used.

1. Prepare the hemocytometer by cleaning the chambers and coverslip with ethanol. Dry the hemocytometer by using lint-free tissue. Place the glass coverslip over the counting chambers.
Note: The correct placement is indicated by the appearance of the Newton rings.
2. Add 100 μ L of 0.4% trypan blue solution to 100 μ L of cell suspension (step A7) to obtain a 1:1 dilution using a P200 Eppendorf pipette.
3. Load the hemocytometer with 10 μ L of cell suspension per counting chamber with a P20 Eppendorf pipette and examine immediately under an inverted phase contrast microscope at low magnification (e.g., 5–10 \times magnification).
- Critical:** To ensure accurate results, it is important to avoid over- or underfilling the cell suspension chamber.
4. Count the number of viable (seen as bright cells) and non-viable cells (stained blue) in the large outer quadrants.
5. Calculate the percentage of viable cells: % viable cells = [1.00 - (number of blue cells ÷ number of total cells)] \times 100. Cell viability should be at least 95%.
6. Calculate the cell concentration based on the premise that each square accounts for a volume of 10 $^{-4}$ mL of cell suspension.
7. To obtain the total number of viable cells per milliliter of aliquot, multiply the total number of viable cells by 2 (the dilution factor for trypan blue) and the correction factor of 10 4 (volume of each square).

C. Annexin V staining of adherent cells

We suggest that at least four samples are prepared (Figure 1): i) a negative control without staining to determine background fluorescence, ii) a sample stained with DAPI only, iii) a sample to be stained with DAPI and annexin V in the presence of calcium, and iv) a sample to be stained with DAPI and annexin V in the absence of calcium.

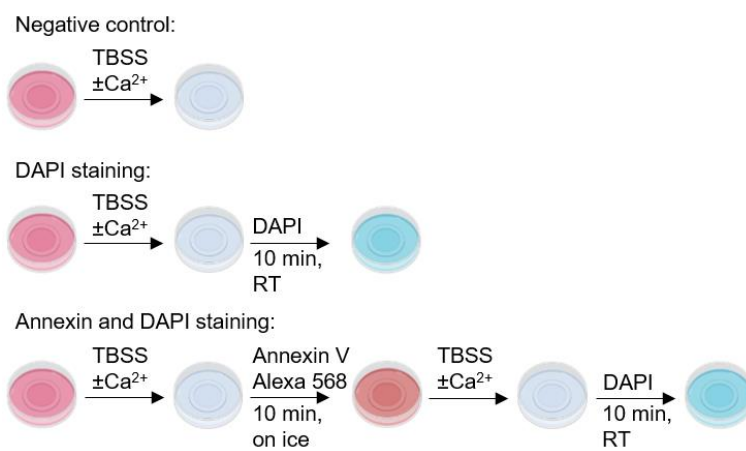


Figure 1. Schematic illustration of the annexin V binding assay. Preparation of a negative control without DAPI and annexin V staining, a control with DAPI-stained cells, and cells stained with DAPI and annexin V conjugated to Alexa Fluor 568 for 10 min on ice with TBSS with or without calcium, respectively. The negative control without staining is used to assess the level of background fluorescence in the sample. This is important because even in the absence of a fluorescent stain, there may still be some level of background fluorescence

Cite as: Baum, J. F. et al. (2023). Visualizing Loss of Plasma Membrane Lipid Asymmetry Using Annexin V Staining. Bio-protocol 13(14): e4754. DOI: 10.21769/BioProtoc.4754.

present due to autofluorescence or other sources. DAPI staining (at a final concentration of 10 µg/mL) is used for visualization of nuclei and cell counting. Non-specific binding of Ca²⁺-dependent annexin V is tested in the same assay by using TBSS without Ca²⁺.

1. Prior to the start of the assay, prepare TBSS with and without calcium (\pm Ca²⁺; see Recipes 2 and 3) and a DAPI stock solution (see Recipe 4).

Note: Annexin V requires the presence of Ca²⁺ to bind to PS. TBSS without Ca²⁺ is used as a negative control.

2. To prepare the cells for labeling, carefully aspirate and discard the growth medium using a P1000 Eppendorf pipette.

3. Wash cells twice with 1 mL of TBSS (\pm Ca²⁺; cooled on ice, see Recipes 2 and 3) using a P1000 Eppendorf pipette.

4. After washing, add 0.5 mL of TBSS (\pm Ca²⁺; cooled on ice, see Recipes 2 and 3) using a P1000 Eppendorf pipette.

5. Add 5 µL of the annexin V conjugated to Alexa Fluor 568 using a P20 Eppendorf pipette and incubate for 10 min on ice in the dark.

Note: Skip steps C5–C8 for the negative control (i); skip steps C5–C7 for the sample only stained with DAPI (ii).

6. Remove staining solution and wash the cells twice with 1 mL of TBSS (\pm Ca²⁺; cooled on ice, see Recipes 2 and 3) using a P1000 Eppendorf pipette.

7. After washing, add 0.5 mL of TBSS (\pm Ca²⁺; cooled on ice, see Recipes 2 and 3) using a P1000 Eppendorf pipette.

8. Add DAPI stock solution to a final concentration of 10 µg/mL (stock 1 mg/mL: add 5 µL using a P20 Eppendorf pipette). Incubate the cells at room temperature for 10 min in the dark.

Note: At the concentration used here, DAPI stains the nucleus of both live and dead cells and is used for the visualization of nuclei and cell counting. When using DAPI for dead cell staining, a final concentration of 0.1 µg/mL is recommended. Alternatively, other dead cell staining reagents such as SYTOX Blue can also be used.

9. Remove staining solution and wash cells twice with 1 mL of TBSS (\pm Ca²⁺; cooled on ice, see Recipes 2 and 3) using a P1000 Eppendorf pipette.

10. Add 1 mL of TBSS (\pm Ca²⁺; cooled on ice, see Recipes 2 and 3) using a P1000 Eppendorf pipette and image on the microscope.

D. Preparation of GUVs

1. Prepare the stock and working solutions of the lipids

- a. Clean the Hamilton syringes by flushing them ten times with chloroform:methanol (1:1, v:v).

Caution: Chloroform is a hazardous solvent. Conduct all work in a fume hood, while wearing proper protective clothing.

- b. To have a 5 mg/mL lipid film, transfer 500 µL of a 10 mg/mL DOPC stock solution (see Recipe 5) into a round bottom glass tube on ice using Hamilton syringes. For 5 mg/mL DOPC:DOPE or DOPE:DOPS lipid mix, add 9 mol DOPC and 1 mol DOPE or DOPS (lipid stocks, see Recipe 5). In this study, the lipid mixtures DOPC:DOPE and DOPC:DOPS will be named only DOPE and DOPS, respectively.

Caution: Avoid any use of plastic ware when handling organic solvents. For more complex or different lipid mixtures, the volume of used lipids needs to be adjusted.

- c. Evaporate the organic solvent at room temperature under reduced pressure in a rotary evaporator at 250 mbar for 2–4 h followed by evaporation at ~10 mbar for 15 min (see Figure 2A and 2B).

- d. Store the lipid film at -20 °C until use.

- e. Dissolve the lipid film in 1 mL of chloroform:methanol (1:1; v:v).

- f. Transfer into a glass vial with screw caps closed with parafilm and store it at -20 °C.

2. Cleaning of the glass slides

- a. Clean the glass slides with detergent, deionized water, and 70% ethanol.
 - b. Dry the slides with wipes.
 - c. Place glass slides in the UV/ozone cleaner.
 - d. Run the UV/ozone cleaner for 30 min.
- Caution:** The UV/ozone cleaner must be placed under a fume hood.
- e. Turn off the UV/ozone cleaner and wait at least 15 min before opening the chamber.
3. Preparation of GUVs
 - a. Glue the O-ring using vacuum grease onto the cleaned side of one of the glass slides to have a tight, closed chamber. Apply 35–40 drops of 1 μ L of lipid mix inside the O-ring under the fume hood (see Figure 2C).
 - b. Evaporate the solvent under vacuum for 30–60 min at 250 mbar in a desiccator.
 - c. Fill the O-ring with swelling buffer (see Recipe 6) and place the other glass slide on top with the cleaned side facing downwards.
 - d. Place the chamber in a dark room for 2–4 h at room temperature (see Figure 2D).
 - e. Carefully tap on each side of the chamber.
 - f. Transfer the GUVs to a 2 mL tube by removing the glass slide and O-ring.
 - g. Store the GUVs covered in aluminum foil at room temperature.

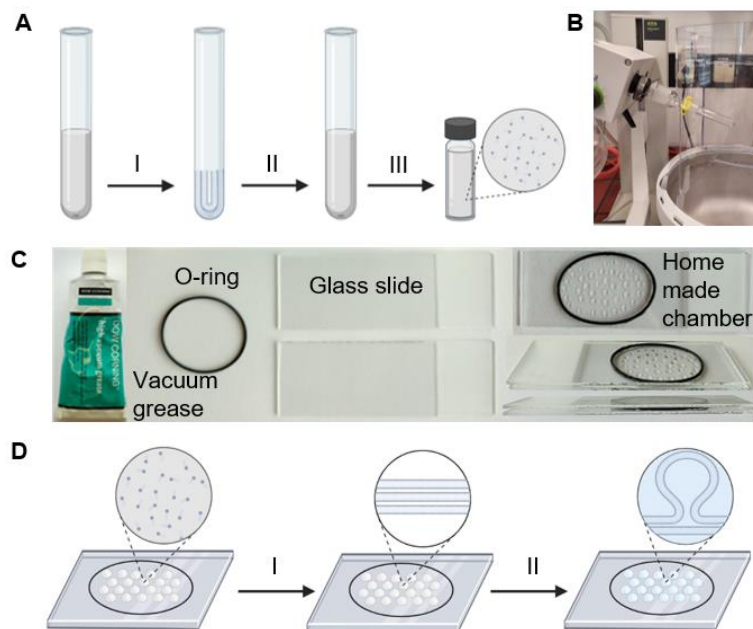


Figure 2. Generation of giant unilamellar vesicles (GUVs) from lipid mixtures. (A, B) Preparation of the lipid mixture. The desired volume and type of lipid is mixed in chloroform:methanol (1:1; v:v) in a glass tube and (I) the solvent is evaporated in rotary evaporator under the reduced pressure of 250 mbar for 2–4 h; (II) the resulting thin lipid film on the glass tube is dissolved in chloroform:methanol (1:1; v:v) and (III) stored in a glass vial with screw caps sealed with parafilm. (B) The glass tube containing the lipids in chloroform is connected to the rotary evaporator. (C) Equipment for a GUV formation of the home-made chamber. (D) Schematic workflow of GUV formation by the swelling method. The lipid mixture is applied to the cleaned glass slides and (I) dehydrated in a desiccator at 250 mbar for 30–60 min. The dried lipid film is then (II) rehydrated in a swelling buffer for 2–4 h, resulting in the formation of giant vesicles.

4. Annexin V staining of GUVs
 - a. Place 25 μ L of GUVs (with a cut tip) in 25 μ L of binding buffer (see Recipe 7) on a cover glass slide.

Note: As additional control, a GUV sample in buffer without Ca^{2+} can be prepared.

Cite as: Baum, J. F. et al. (2023). Visualizing Loss of Plasma Membrane Lipid Asymmetry Using Annexin V Staining. Bio-protocol 13(14): e4754. DOI: 10.21769/BioProtoc.4754.

- b. Place the cover glass slide under the microscope.
- c. Let the GUVs settle for approximately 5 min before imaging in a white light channel and an annexin V channel.

Data analysis

Data acquisition

Images are acquired at a Leica TCS SP8 confocal laser scanning microscope (Leitz, Wetzlar, Germany) equipped with a $63\times/1.20$ water objective. For detailed imaging settings, see Table 1. All images are acquired at the same resolution, magnification, and orientation. This allows direct comparison of images and saves time when arranging figures.

Table 1. Confocal microscope settings

Channel	Laser	Detector	Scan speed	Excitation, nm	Intensity, %	Emission, nm	Gain
Annexin V	White light laser, intensity at 85%	Hybrid Detector (HyD)	400 Hz	577	5	587–757	100
Bright light	White light laser, intensity at 85%	Photomultiplier tube (PMT)	400 Hz	trans channel	-	-	300

For analysis of the adherent cells

1. Export the raw image data in a format compatible with ImageJ (e.g., .tif) from the imaging system.
2. Open the ImageJ software and import the images of the blue fluorescence (DAPI) and the red fluorescence (Annexin V conjugated to Alexa Fluor 568).
3. Click on *Image* in the upper operation row of the interface and select in the color menu *Merge Channels*.
4. For C1 (red), the image showing the red fluorescence needs to be selected; for C3 (blue), the DAPI picture needs to be chosen. Press *Ok* to merge the two images.
5. Click on *Image* in the upper operation row of the interface and change the image type to RGB Color.
6. Save the images as a .tif or .jpg file by selecting the *File menu* in the upper operation row of the interface and press *Save As*. Representative images are shown in Figure 3.

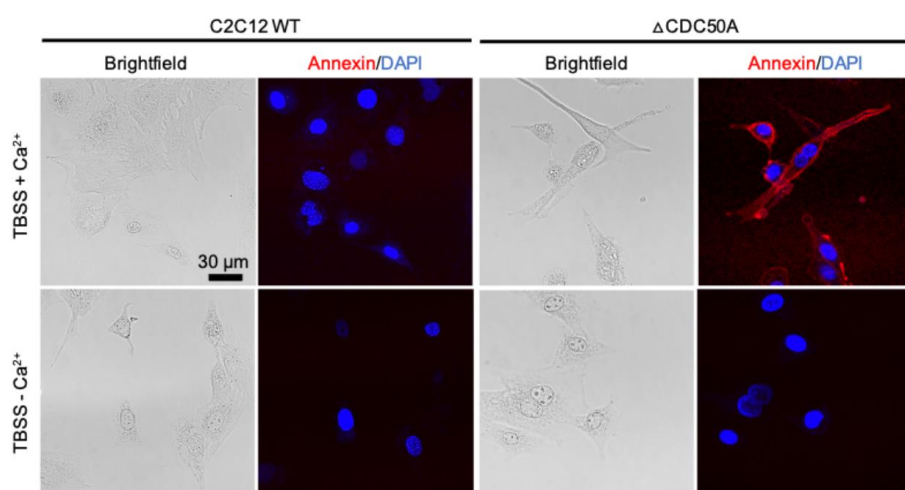


Figure 3. Representative confocal images of proliferating C2C12 wild-type and CDC50A knockout cells.

Cite as: Baum, J. F. et al. (2023). Visualizing Loss of Plasma Membrane Lipid Asymmetry Using Annexin V Staining. Bio-protocol 13(14): e4754. DOI: 10.21769/BioProtoc.4754.

Cells are stained with Alexa Fluor 568 conjugated annexin V (red) for 10 min in ice-cold TBSS with and without calcium. DAPI staining is used for visualization of nuclei. In contrast to C2C12 wild-type cells, CDC50A-deficient cells stained positive for annexin V, indicating increased surface exposure of aminophospholipids. Images are representative of three independent experiments. Scale bar: 30 μ m.

For analysis of GUVs

ImageJ is used to analyze the membrane fluorescence intensity of individual GUVs before and after annexin V treatment. Only unilamellar giant vesicles are used for analysis.

1. Open the images with ImageJ by importing the LIF-file.
2. Split the channels to have bright light and annexin channel separately and save as Tiff.
3. Tiff images can be assembled (see Figure 4).

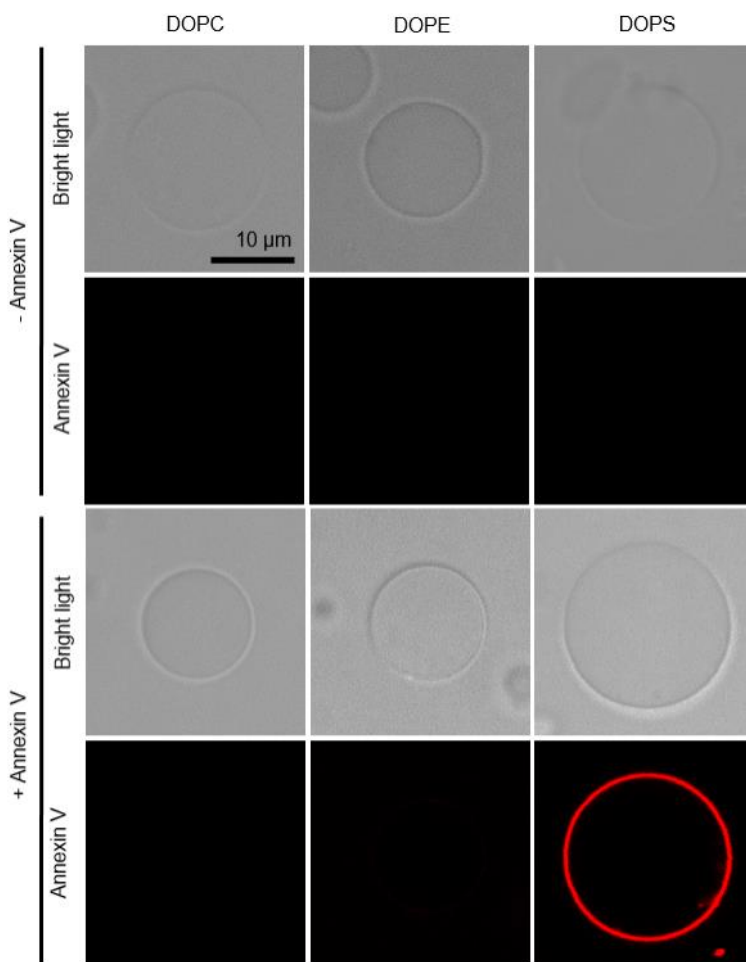


Figure 4. Imaging the binding of fluorescent annexin V on giant unilamellar vesicles (GUVs). Giant unilamellar vesicles are prepared from different lipids and incubated without (-) and with (+) annexin V in the presence of Ca^{2+} . Vesicles are observed in bright light and annexin channel. DOPC, PC (18:1/18:1) only; DOPE, PC (18:1/18:1)/PE (18:1/18:1), (9/1, mol/mol); DOPS, PC (18:1/18:1)/PS (18:1/18:1), (9/1, mol/mol). Data shown are from one experiment representative of two independent vesicle preparations. Scale bar: 10 μ m.

Extract signal intensities with ImageJ software

1. Continue with the annexin channel.
2. A region of interest (ROI) is placed around the GUV (ROI_{outer}) of interest to measure the annexin V fluorescence intensity of the membrane, by measuring the integrated density value per pixel.
3. The second ROI is placed within the GUV lumen (ROI_{inner}) (see Figure 5A).
4. The inner ROI is subtracted from the outer ROI to have the membrane density value per pixel of the annexin V fluorescent intensity (ΔI):

$$\Delta I = I(ROI_{outer}) - I(ROI_{inner})$$

5. Repeat the procedure for each GUV and save the data as an Excel (.xls) file.
6. The annexin V fluorescence intensities are plotted in form of a bar diagram using the OriginPro (see Figure 5B and Table 2).

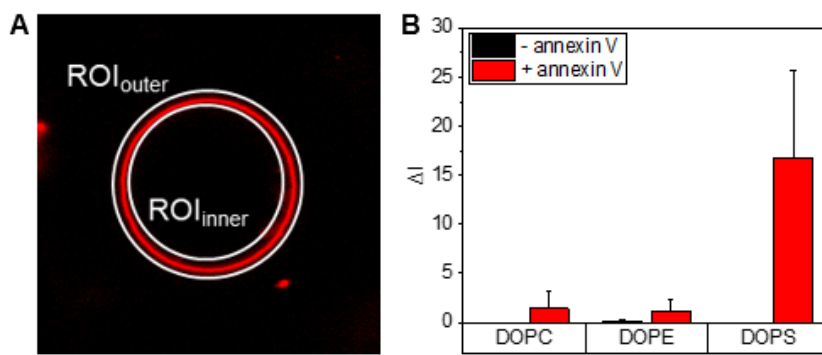


Figure 5. Fluorescence intensity analysis on giant unilamellar vesicles (GUVs). (A) A first region of interest (ROI) is placed around the GUV (ROI_{outer}), and a second ROI is placed within the GUV lumen (ROI_{inner}) of interest to measure the annexin V fluorescence intensity of the membrane, by measuring the integrated density value per pixel using the software ImageJ. (B) The mean annexin V fluorescence intensities for GUVs with the indicated lipid compositions are presented as averages, based on individual measurements of $n \leq 10$ GUVs. Error bars indicate standard deviations. Data are from one experiment representative of two independent vesicle preparations.

Table 2. The mean annexin V fluorescence intensities (ΔI) for giant unilamellar vesicles (GUVs) with the indicated lipid compositions. Data are from one experiment representative of two independent vesicle preparations. Data are plotted in Figure 5.

Lipids of GUVs	-Annexin V		+Annexin V	
	ΔI , average ($n = 10$)	s.d.	ΔI , average ($n = 13–15$)	s.d.
DOPC	0.001	0.001	1.430	1.814
DOPE	0.086	0.114	1.107	1.229
DOPS	0.001	0.002	16.732	8.934

Recipes

Buffers were prepared using double-distilled water (ddH₂O), which was obtained using an in-house water distillation system. Alternatively, all buffers are prepared using ultrapure water with purification sensitivity of 18 MΩ·cm⁻¹ at 25 °C.

1. Growth medium

Open a 500 mL flask of high-glucose DMEM medium
Add 100 mL of FBS (heat-inactivated)
Optional: add 5 mL of 100× penicillin-streptomycin solution
Prepare in sterile cabinet; store at 4 °C

2. TBSS buffer + Ca²⁺ (0.5 L)

136 mM NaCl (3.97 g)
2.6 mM KCl (96.9 mg)
1.8 mM CaCl₂ (132.3 mg)
1 mM MgCl₂·6H₂O (101.6 mg)
0.36 mM NaH₂PO₄·2H₂O (24.8 mg)
5.56 mM D-glucose (500.8 g)
5 mM HEPES (600 mg)

Adjust pH to 7.4 with 1 M NaOH. Complete volume to 0.5 L. Sterilize by filtering using a 0.22 µm filter. Store at 4 °C up to several months.

3. TBSS buffer - Ca²⁺ (0.5 L)

136 mM NaCl (3.97 g)
2.6 mM KCl (96.9 mg)
1 mM MgCl₂·6H₂O (101.6 mg)
0.36 mM NaH₂PO₄·2H₂O (24.8 mg)
5.56 mM D-glucose (500.8 g)
5 mM HEPES (600 mg)
100 µM EGTA (19 mg)

Adjust pH to 7.4 with 1 M NaOH. Complete volume to 0.5 L. Sterilize by filtering using a 0.22 µm filter. Store at 4 °C up to several months.

4. DAPI stock solution (1 mg/mL)

Dissolve DAPI in ultrapure water to 1 mg/mL. Stock solution is stable for several months and repeated use, if stored protected from light at -20 °C.

5. Lipid stocks in chloroform

Lipids are ordered in chloroform at a concentration of 25 mg/mL and stored at -20 °C until further use. For longer storage, aliquot 10 mg of lipids in glass vials with screw caps, evaporate the chloroform, and store the dried lipid at -20 °C. Before using it, dissolve the 10 mg of lipid in 1 mL of chloroform:methanol (1:1; v:v).

Critical: Some lipids may have limited or very poor solubility in chloroform:methanol (1:1; v:v) and require a mixture of chloroform:methanol:water.

6. Swelling buffer (320 mM)

Dissolve 5.48 g of sucrose to a final volume of 50 mL in deionized water. The buffer is filter-sterilized over a 0.2 µm Acrodisc® syringe filter and stored at 5 °C.

7. Binding buffer (100 mL)

10 mM HEPES-KOH pH 7.4 (238.31 mg)
150 mM NaCl (876.6 mg)
5 mM KCl (37.275 mg)
1 mM MgCl₂·6H₂O (20.33 mg)
1 mM CaCl₂ (11.098 mg)

Adjust pH to 7.4 with 1 M NaOH. Complete volume to 100 mL. Store at 4 °C up to several months.

Acknowledgments

We gratefully acknowledge Michelle Werner for technical assistance. This protocol was adapted from our previous work (Weingärtner et al., 2012; Grifell-Junyent et al., 2022; Herrera et al., 2022). The work was supported by the Lundbeckfonden (R221-2016-1005 to T.G.P.) and an instrument grant from the Deutsche Forschungsgemeinschaft (INST 213/886-1 FUGG to T.G.P.). HDU is a scholar of the Friedrich Ebert Foundation.

Competing interests

The authors declare that no competing interests exist.

References

- Angelova, M. I. and Dimitrov, D. S. (1986). [Liposome electroformation](#). *Faraday Discuss. Chem. Soc* 81: 303.
- Bhatia, T., Husen, P., Brewer, J., Bagatolli, L. A., Hansen, P. L., Ipsen, J. H. and Mouritsen, O. G. (2015). [Preparing giant unilamellar vesicles \(GUVs\) of complex lipid mixtures on demand: Mixing small unilamellar vesicles of compositionally heterogeneous mixtures](#). *Biochim Biophys Acta Biomembr* 1848(12): 3175-3180.
- Bevers, E. M. and Williamson, P. L. (2016). [Getting to the Outer Leaflet: Physiology of Phosphatidylserine Exposure at the Plasma Membrane](#). *Physiol. Rev.* 96(2): 605-645.
- Chandra, A. and Datta, A. (2022). [A Peptide-Based Fluorescent Sensor for Anionic Phospholipids](#). *ACS Omega* 7(12): 10347-10354.
- DiVittorio, K. M., Johnson, J. R., Johansson, E., Reynolds, A. J., Jolliffe, K. A. and Smith, B. D. (2006). [Synthetic peptides with selective affinity for apoptotic cells](#). *Org. Biomol. Chem.* 4(10): 1966.
- Ewers, H. and Helenius, A. (2011). [Lipid-Mediated Endocytosis](#). *Cold Spring Harbor Perspect. Biol.* 3(8): a004721-a004721.
- Grifell-Junyent, M., Baum, J. F., Välimets, S., Herrmann, A., Paulusma, C. C., López-Marqués, R. L. and Günther Pomorski, T. (2022). [CDC50A is required for aminophospholipid transport and cell fusion in mouse C2C12 myoblasts](#). *J. Cell Sci* 135(5): e258649.
- Hankins, H. M., Baldridge, R. D., Xu, P. and Graham, T. R. (2015). [Role of Flippases, Scramblases and Transfer Proteins in Phosphatidylserine Subcellular Distribution](#). *Traffic* 16(1): 35-47.
- Hanshaw, R. G., Lakshmi, C., Lambert, T. N., Johnson, J. R. and Smith, B. D. (2005). [Fluorescent Detection of Apoptotic Cells by Using Zinc Coordination Complexes with a Selective Affinity for Membrane Surfaces Enriched with Phosphatidylserine](#). *ChemBioChem* 6(12): 2214-2220.
- Herrera, S., Grifell-Junyent, M. and Pomorski, T. (2022). [NBD-lipid Uptake Assay for Mammalian Cell Lines](#). *Bio Protoc* 12(4): e4330.
- Jackson, S. P. (2011). [Arterial thrombosis—insidious, unpredictable and deadly](#). *Nat. Med* 17(11): 1423-1436.
- Koopman, G., Reutelingsperger, C. P., Kuijten, G. A., Keehnen, R. M., Pals, S. T. and van Oers, M. H. (1994). [Annexin V for flow cytometric detection of phosphatidylserine expression on B cells undergoing apoptosis](#). *Blood* 84(5): 1415-1420.
- Krahling, S., Callahan, M. K., Williamson, P. and Schlegel, R. A. (1999). [Exposure of phosphatidylserine is a general feature in the phagocytosis of apoptotic lymphocytes by macrophages](#). *Cell Death Differ.* 6(2): 183-189.
- Lentz, B. R. (2003). [Exposure of platelet membrane phosphatidylserine regulates blood coagulation](#). *Prog Lipid Res* 42(5): 423-438.
- Malhotra, R., Taylor, N. R. and Bird, M. I. (1996). [Anionic phospholipids bind to L-selectin \(but not E-selectin\) at a site distinct from the carbohydrate-binding site](#). *Biochem. J* 314(1): 297-303.
- Marinetti, G. and Love, R. (1976). [Differential reaction of cell membrane phospholipids and proteins with chemical probes](#). *Chem. Phys. Lipids* 16(4): 239-254.
- Mathiassen, P. P. M. and Pomorski, T. G. (2022). [A Fluorescence-based Assay for Measuring Phospholipid Scramblase Activity in Giant Unilamellar Vesicles](#). *Bio Protoc* 12(6): e4366.

Cite as: Baum, J. F. et al. (2023). Visualizing Loss of Plasma Membrane Lipid Asymmetry Using Annexin V Staining. *Bio-protocol* 13(14): e4754. DOI: 10.21769/BioProtoc.4754.

- Parigoris, E., Dunkelmann, D. L. and Silvan, U. (2020). [Generation of Giant Unilamellar Vesicles \(GUVs\) Using Polyacrylamide Gels](#). *Bio Protoc* 10(21): e3807.
- Pomorski, T., Lombardi, R., Riezman, H., Devaux, P. F., van Meer, G. and Holthuis, J. C. (2003). [Drs2p-related P-type ATPases Dnf1p and Dnf2p are required for phospholipid translocation across the yeast plasma membrane and serve a role in endocytosis](#). *Mol Biol Cell* 14(3): 1240-1254.
- Ristovski, M., Farhat, D., Bancud, S. E. M. and Lee, J. Y. (2021). [Lipid Transporters Beam Signals from Cell Membranes](#). *Membranes (Basel)* 11(8): 562.
- Schlegel, R. A., McEvoy, L. and Williamson, P. (1985). [Membrane phospholipid asymmetry and the adherence of loaded red blood cells](#). *Bibl Haematol* (51): 150-156.
- Sebastian, T. T., Baldridge, R. D., Xu, P. and Graham, T. R. (2012). [Phospholipid flippases: Building asymmetric membranes and transport vesicles](#). *Biochim. Biophys. Acta Mol. Cell Biol. Lipids* 1821(8): 1068-1077.
- Shimane, Y. and Kuruma, Y. (2022). [Rapid and Facile Preparation of Giant Vesicles by the Droplet Transfer Method for Artificial Cell Construction](#). *Front Bioeng Biotechnol* 10: 873854.
- Sprong, H., van der Sluijs, P. and van Meer, G. (2001). [How proteins move lipids and lipids move proteins](#). *Nat. Rev. Mol. Cell Biol.* 2(7): 504-513.
- Tait, J. F., Gibson, D. F. and Smith, C. (2004). [Measurement of the affinity and cooperativity of annexin V-membrane binding under conditions of low membrane occupancy](#). *Anal Biochem*. 329(1):112-119.
- van den Eijnde, S. M., van den Hoff, M. J., Reutelingsperger, C. P., van Heerde, W. L., Henfling, M. E., Vermeij-Keers, C., Schutte, B., Borgers, M. and Ramaekers, F. C. (2001) [Transient expression of phosphatidylserine at cell-cell contact areas is required for myotube formation](#). *J Cell Sci.* 114(Pt 20):3631-3642.
- van Meer, G., Voelker, D. R. and Feigenson, G. W. (2008). [Membrane lipids: where they are and how they behave](#). *Nat. Rev. Mol. Cell Biol.* 9(2): 112-124.
- van Meer, G. (2011). [Dynamic Transbilayer Lipid Asymmetry](#). *Cold Spring Harbor Perspect. Biol.* 3(5): a004671-a004671.
- Vermes, I., Haanen, C., Steffens-Nakken, H. and Reutelingsperger, C. (1995). [A novel assay for apoptosis. Flow cytometric detection of phosphatidylserine expression on early apoptotic cells using fluorescein labelled Annexin V](#). *J Immunol Methods* 184(1): 39-51.
- Waehrens, L. N., Heegaard, C. W., Gilbert, G. E. and Rasmussen, J. T. (2009) [Bovine lactadherin as a calcium-independent imaging agent of phosphatidylserine expressed on the surface of apoptotic HeLa cells](#). *J Histochem Cytochem.* 57(10):907-914.
- Wautier, M. P., Héron, E., Picot, J., Colin, Y., Hermine, O. and Wautier, J. L. (2011) [Red blood cell phosphatidylserine exposure is responsible for increased erythrocyte adhesion to endothelium in central retinal vein occlusion](#). *J Thromb Haemost.* 9(5):1049-1055.
- Weinberger, A., Tsai, F. C., Koenderink, G. H., Schmidt, T. F., Itri, R., Meier, W., Schmatko, T., Schroder, A. and Marques, C. (2013). [Gel-assisted formation of giant unilamellar vesicles](#). *Biophys J* 105(1): 154-164.
- Weingärtner, A., Kemmer, G., Müller, F. D., Zampieri, R. A., Gonzaga dos Santos, M., Schiller, J. and Pomorski, T. G. (2012). [Leishmania Promastigotes Lack Phosphatidylserine but Bind Annexin V upon Permeabilization or Miltefosine Treatment](#). *PLoS One* 7(8): e42070.
- Zheng, H., Wang, F., Wang, Q. and Gao, J. (2011). [Cofactor-free detection of phosphatidylserine with cyclic peptides mimicking lactadherin](#). *J Am Chem Soc* 133(39): 15280-15283.

Quantifying Single and Dual Channel Live Imaging Data: Kymograph Analysis of Organelle Motility in Neurons

Laura Digilio, Lloyd P. McMahon, Alois Duston, Chan Choo Yap*, and Bettina Winckler*

Department of Cell Biology, University of Virginia, 1340 Jefferson Park Avenue, Pinn Hall 3226, Charlottesville, VA 22908, USA

*For correspondence: BWinckler@virginia.edu; cxy5x@virginia.edu

Abstract

Live imaging is commonly used to study dynamic processes in cells. Many labs carrying out live imaging in neurons use kymographs as a tool. Kymographs display time-dependent microscope data (time-lapsed images) in two-dimensional representations showing position vs. time. Extraction of quantitative data from kymographs, often done manually, is time-consuming and not standardized across labs. We describe here our recent methodology for quantitatively analyzing single color kymographs. We discuss the challenges and solutions of reliably extracting quantifiable data from single-channel kymographs. When acquiring in two fluorescent channels, the challenge becomes analyzing two objects that may co-traffic together. One must carefully examine the kymographs from both channels and decide which tracks are the same or try to identify the coincident tracks from an overlay of the two channels. This process is laborious and time consuming. The difficulty in finding an available tool for such analysis has led us to create a program to do so, called KymoMerge. KymoMerge semi-automates the process of identifying co-located tracks in multi-channel kymographs and produces a co-localized output kymograph that can be analyzed further. We describe our analysis, caveats, and challenges of two-color imaging using KymoMerge.

Keywords: Kymograph, KymoMerge, Time-lapse imaging, Co-localization, FIJI, Dual-channel imaging, Neurons, Dendrites

This protocol was validated in: J Neurosci (2022), DOI: 10.1523/JNEUROSCI.2530-21.2022

Background

Time-lapse imaging using fluorescence microscopy is a useful tool for studying vesicle trafficking in neurons. Information about vesicle behaviors (such as speed, directionality, pause times, etc.) needs to be quantified in order to understand and compare how different vesicle populations behave under different conditions. Extracting quantitative information from live imaging data is time consuming and carried out differently by different labs. Kymographs are often used to easily display vesicle behavior over time in a figure but can also be used to quantify these behaviors. A kymograph shows the directionality on the x-axis and time along the y-axis. This technique has applications across a wide variety of studies: it is used in studying microtubule growth (Zwetsloot et al., 2018), kinetochore movement (Hertzler et al., 2020), lamellipodial advance or collapse (Menon et al., 2014), and, probably most commonly, vesicle movement in neurons (Maday and Holzbaur, 2016; Farías et al., 2017; Farfel-Becker et al., 2019). Neuronal processes are particularly amenable to the use of kymograph analysis because of their inherent linear morphology. The highly polarized structure of axons and dendrites provides built-in tracks along one axis where movement of a variety of biological structures can be followed. With fluorescent labeling, either from adding fluorescent tracers or by transfection with plasmids encoding fluorescent proteins, various processes and structures can be analyzed, such as trafficking of organelles (Wang et al., 2009; Yap et al., 2018) or cytoskeletal elements (Liang et al., 2020; Ganguly and Roy, 2022).

Kymographs contain a great deal of information about trafficking dynamics. Parameters available for analysis include the number of anterograde, retrograde, and stationary events, event speed, pause time, and event distance. Quantifying these parameters can be done manually or by several available software programs suitable for one-channel images. If these parameters are to be measured under the condition where two proteins are trafficking together, events must be identified that coincide in both channels. A review of the literature shows that current kymograph analysis is largely limited to tracking one channel at a time (Lasiecka et al., 2010; Chien et al., 2017; Boecker et al., 2020). The common method of creating kymographs from time-lapse fluorescent microscope data is done on one channel, producing one independent kymograph per marker with no direct connection between them, even though multiple channels can easily be acquired. To analyze two objects that co-traffic together, one has to carefully examine the kymographs from both channels and decide which tracks are the same, or one could try to identify the coincident tracks from an overlay of the two channels (see Lasiecka et al., 2014 as an example). Tracks can merge and diverge, and such events are not easy to identify when looking at two separate images, so marking them can be a challenge. The whole process is laborious and time consuming. Detailed information from two kymographs would only be useful if all the data of interest were in one image. Our lab has been studying the dynamics of a variety of endosomal compartments and their inter-relationship in neurons using more than one endosomal marker (Yap et al., 2008, 2017 and 2018). The difficulty in finding an available application for such analysis has led us to create a program to do so, called KymoMerge (McMahon et al., 2021). KymoMerge addresses the issues discussed by automating the process of identifying co-located tracks in multi-channel kymographs and producing an output that can be analyzed directly.

Software

1. FIJI open-source image analysis software (<https://imagej.net/software/fiji/downloads>)

Procedure

A. Live imaging

1. Live imaging was done as previously described (Yap et al., 2018). Brief procedure description:
 - a. Neuronal cultures are prepared from E18 rat hippocampi combining all embryos from one litter (as described in Lasiecka and Winckler, 2016). Other cultured neurons can also be used.

Cite as: Digilio, L. et al. (2023). Quantifying Single and Dual Channel Live Imaging Data: Kymograph Analysis of Organelle Motility in Neurons. Bio-protocol 13(10): e4675. DOI: 10.21769/BioProtoc.4675.

- b. Cells are plated on a 35 mm glass-bottomed microwell dish coated with poly-L-lysine. After 4 h, the plating medium is removed and replaced with serum-free medium supplemented with B27, and neurons are cultured for 7–10 days *in vitro* (DIV) for experimental use.
- c. Transfections are performed with Lipofectamine 2000 according to manufacturer's instructions.
- d. All live imaging is performed on a 37 °C heated stage in a chamber with 5% CO₂ on an inverted LSM880 confocal microscope using a 40× water objective (LD-C Apochromat 1.2W). Spinning disk confocal microscopes are also well suited for imaging cultured neurons live. Higher magnification objectives can also be used, as per the research question.
- e. Images are collected from single or dual channels using the bidirectional scan-frame mode with the lowest laser power that allows visualization of object of interest. Spinning disk confocal microscopy is also very well suited for imaging live organelle movements in cultured neurons. Images are captured at 1–2 frames per second, but faster moving organelles may require more frequent image acquisition. We routinely capture 400–500 frames (approximately 8 min) before photobleaching becomes substantial. If longer imaging times are desired, frame capture rates can be less frequent (one per 3 s, one per 10 s) with the caveat that very fast-moving events will be missed. A single focal plane is chosen for imaging such that the most organelles are in focus. The speed of most motile organelles precludes z-stack acquisition during live imaging for microscope in common use.
- f. Images are saved as TIFF files and opened in FIJI.

Note: We always carry out all control and experimental conditions for any experiment on the same cultures on the same day and image on the same day. This ensures that any differences in motility are not due to culture-to-culture variation, but due to the experimental manipulation. We have found this to be an important aspect of experimental design and rigor.

B. Single-channel kymograph production

1. Open the live imaging image file in FIJI and display the first frame of the live imaging file. Since the position of the dendrites do not change over the course of the live imaging, the first frame can be used for tracing.
2. Open the ROI manager (Analyze > Tools > ROI manager).
3. Using the segmented line tool in FIJI, trace the dendrite or axon starting at the soma and extend out to desired end point, and add this line to the ROI manager. Continue drawing, tracing the rest of the dendrites, and add them to the ROI manager (Figure 1). Dendrites with a lot of crisscrossing or bundling are omitted. Click Show All and Labels boxes to view all traces.
4. Highlight the trace in ROI manager and run the Multiple Kymograph Plugin in FIJI, which is included in its updated version. When prompted for the line width, enter the pixel width of the dendrite you wish to make a kymograph from. With our imaging conditions, typical values of line width are 3 pixels for axons and 5 pixels for dendrites. Once you enter line width, the kymograph will generate.
5. Save the kymograph of this dendrite as a TIFF file. Continue making kymographs (as in steps B3 and B4) from the remaining dendrites of the same cell. In our imaging conditions (40× objective), all dendrites of one neuron are captured simultaneously in the same live imaging (see example in Figure 1) and multiple kymographs can be obtained from one live imaging session.

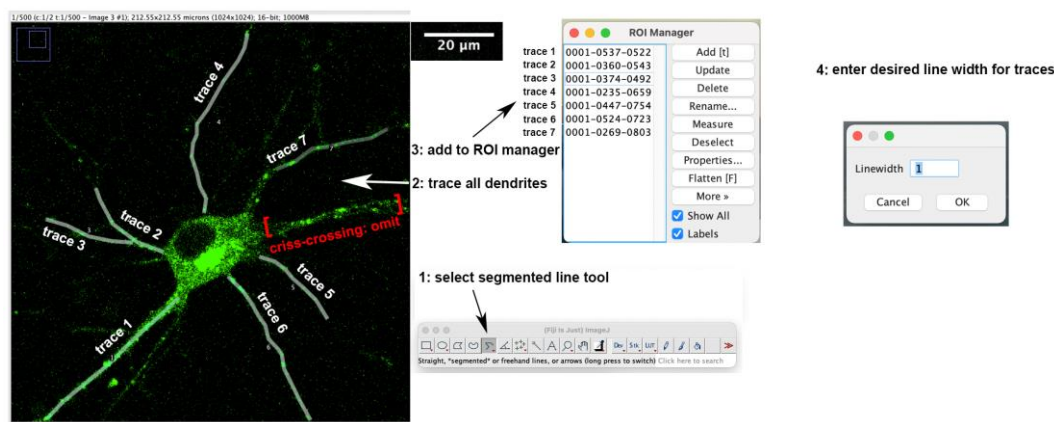


Figure 1. Tracing dendrites and adding to the ROI manager. Single plane image of the first time-lapse frame of a neuron transfected with GFP-RILP (Rab-interacting lysosomal protein) is shown. Dendrites are traced using the segmented line tool and added to the ROI manager. One trace is omitted because of crisscrossing dendrites.

6. Once you are finished making the kymographs from the cell, save the image with the traced ROI on top of it. To do this, click **Image > Overlay > From ROI Manager** and then save as TIFF file for reference. This will allow you to go back to each cell at any point in the future and see which dendrite each kymograph came from.

Note: Potential problem—if there is bleaching during the imaging, use the bleach correcting plugin for FIJI (Miura, 2020; <https://imagej.net/plugins/bleach-correction>). If one experiences microscope stage drift during the imaging, a drift correction plugin exists in FIJI (<https://imagej.net/plugins/manual-drift-correction>).

C. Kymograph analysis

Multiple software packages exist. We have used manual analysis (Lasiecka et al., 2010 and 2014) as well as Kymograph Clear/Kymograph Direct software (Barford et al., 2018). These are briefly described in the Note below. Other programs exist and will also work.

Most recently, we have used KymoButler (Yap et al., 2022), a web-based software (Jakobs et al., 2019) available to customize with machine learning for a fee. A free version is available, which outputs velocities, track duration, and distances. <https://www.wolframcloud.com/objects/deepmirror/Projects/KymoButler/KymoButlerForm>. KymoButler is also available through a plugin for FIJI https://github.com/fabricecordelieres/IJ-Plugin_KymoButler_for_ImageJ.

Analysis: KymoButler output can be customized to fit desired criteria for the questions of interest. For our purposes, KymoButler was customized to identify individual events and calculate data for each event, including speed, duration of movement or pausing, distance moved, or direction of movement. KymoButler also creates vesicle trajectories, which are comprised of multiple individual events. Data can be compiled for trajectories in addition to individual events. Creating trajectories from individual events can often not be accomplished for all vesicles for the entirety of the time-lapse imaging, but shorter unambiguous trajectories can usually be identified. In our experience, the trajectories created manually by a human user are almost identical to those created by KymoButler, since the same limitations exist for trajectory assignment by both (Figure 2).

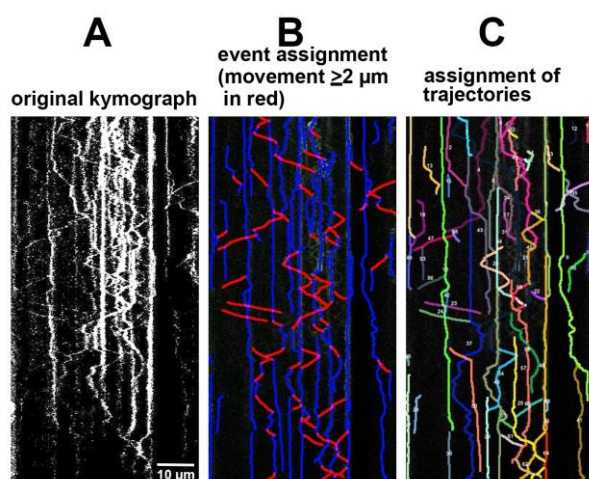


Figure 2. Software output for kymograph analysis. Original kymographs (A) are assigned events per user preference (for instance, defining motile events as $\geq 2 \mu\text{m}$ movements) (B) or trajectories (C). All events or trajectories identified by the software can be quantified in multiple ways, including speed, directionality, run lengths, or pause times.

We have found it useful to use trajectory data to determine the net motility of individual vesicles over a longer time of the whole live imaging experiment instead of individual events. Net retrograde/anterograde/stationary data can be obtained from these measurements. For our purposes, we distinguished stationary trajectories (zero net movement) from short ($< 2 \mu\text{m}$) and long ($> 2 \mu\text{m}$) net movements. These cutoffs can be chosen by the user for their own questions. The raw data includes a full readout of distances traveled and can be binned into *stationary* vs. *motile* as per the user's wishes. Since endosomes in dendrites pause and reverse direction a lot, we were more interested in the net behavior of vesicles and less interested in individual event measurements. For other questions, the user might be interested in individual event data. We create kymographs from all dendrites on any imaged cell for analysis (see Figure 1) and do not exclude dendrites unless they are not in focus or crisscrossing or bundling. We usually combine data from all the dendrites from one cell into one data point of motility data. So, the number of samples (n) for statistical purposes is usually one cell and not one dendrite or one vesicle. We find that imaging of ~20 cells (80–100 dendrites) gives good statistical power for endosome motility in dendrites. We recommend imaging at least 4–5 cells from 3–4 independent cultures and making kymographs from all dendrites for statistical analysis.

Note: We repeatedly trained the machine learning function of KymoButler on 20 kymographs for which ground truths had been established manually. Once the output from KymoButler closely matched the manual ground truth established by a human user, the same settings were used for all analyses. This initial training might need to be repeated for different types of fluorescent markers, because background haze might differ, and the same settings might not give satisfactory results. The event and trajectory assignments for each kymograph can be visually verified after KymoButler has finished to ensure accuracy.

Notes:

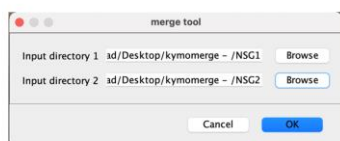
1. *Manual analysis:* Using the line tool in FIJI, manually trace all tracks on the kymograph and save them to the ROI manager as above. Using the known pixel size as determined from the objective and camera used, one can determine average velocities, retrograde and anterograde events, and pause events/times. This is laborious and time consuming, but the user has maximal control over the output. We usually validate software automation by comparing their output to manually established ground truth measurements for 10–20 kymographs.
2. *Kymograph Clear/Kymograph Direct:* open-source programs (Mangeol et al., 2016) available online for download and use with FIJI. These are sequential kymograph production and analysis programs that give user information regarding particle velocities, intensities, directionality, and run lengths.
<http://sites.google.com/site/kymographanalysis>.

D. Double-channel kymograph: preparation and analysis

For generating double-channel kymographs, we created a plugin for ImageJ FIJI, called KymoMerge (currently only functional when using a Mac; McMahon et al., 2021).

1. Install KymoMerge: download from <https://github.com/alduston/kymomerge>. To begin using the merge tool, open FIJI and open the KymoMerge.py script in the FIJI console. The program can be installed as a plugin or run from the console.
2. Input the directory folders for the kymographs from each channel (Figure 3A).

A input directory window (step D.2)



B image thresholding window (step D.3)

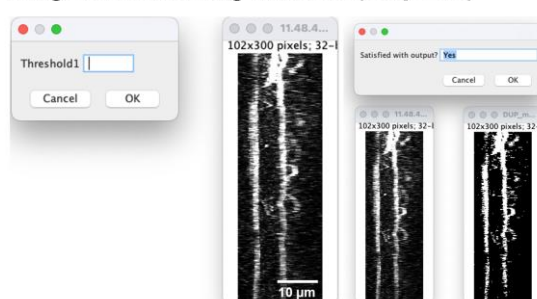


Figure 3. KymoMerge workflow. (A) Input directory window. This window will be used to choose the folders containing the kymographs from each channel. (B) Image thresholding window. This window will be used to input threshold values determined by the user for all images individually from each channel. Thresholding depends on the level of background fluorescence and the brightness of the signal. Each user needs to visually determine the optimal threshold value for their particular image.

The files from each input directory (individual kymograph files) should have identical naming. Input directory should be a directory containing a series of named .tif files, using the naming convention ‘filename’-‘i’.tif, where i is the given .tif files ‘index’ in the folder. For instance, given three files in ‘groupA’ directory, using ‘kymo’ as file name, the .tif files would be given “kymo-1.tif, kymo-2.tif, kymo-3.tif.”

Input directory 2 should be a directory containing a series of named .tif files, using the naming convention ‘filename’-‘i’.tif, where i is the given .tif files ‘index’ in the folder. This index and file name should correspond to the index of input directory 1. The algorithm will compare files with corresponding indexes. For instance, given three files in ‘groupB’ directory, using ‘kymo’ as the file name as before, the .tif files would be given “kymo-1.tif, kymo-2.tif, kymo-3.tif.”

3. Kymograph image thresholding

The dialog box and image on the left comes up and shows the original kymograph along with an input to set the threshold (Figure 3B). The contrast for the original image is automatically increased so the data are clearly visible. When a value is chosen for the threshold by the user (typically 10–100 depending on background fluorescence and brightness of signal), the binarized image appears and can be compared to the original, as shown with the dialog box and images on the right. At this point, the user can accept the

value by typing in Yes or choosing OK or try a new value by typing in No or choosing Cancel. Once a value is accepted, the next image opens. Once all images from the input folders are thresholded, they will be processed, and the output (individual binary images and merged image) will be available for further analysis as described above. Should the user want to quit the analysis at any point, simply type Quit into the dialog box.

Once the threshold is set, it is applied, and the image is converted to eight bits from the bit depth of the original image. This is then converted to a binary file and saved. Each pixel in the two channels is now set to a value of either 0 or 254.

Note: 8-bit images are used at this point because 16–32 bit formats interpolate locally to achieve greater color depth and make direct manipulation of individual pixel values more difficult.

The program then goes pixel by pixel between the two kymographs comparing values and creating a new image. If the values are both zero, or one is zero and the other is 254, the new image is set at zero at that pixel. If they are both 254 (positive signal in both channels), then the value is set at 254. The result is an image consisting only of those pixels where a positive signal is in both channels. This produces a kymograph containing tracks where the two proteins of interest are co-located, and the dynamics of the co-localized tracks can now be analyzed. The folder of co-located kymographs is saved in a new “output folder” in the folder containing the folder of original kymographs. The output folder contains the binarized kymographs from the input folders and the new, co-located kymograph. The program will open a file from the Group A directory of kymograph files (channel 1) for the user to threshold, followed by the corresponding file from the Group B directory (channel 2). This will continue until all the images are thresholded.

Notes

1. KymoMerge vs. manual kymograph analysis

Two sample data sets are used to test and validate the reliability and efficiency of the program. One consists of the neuronal membrane proteins NSG1-cherry and NSG2-GFP. NSG1 and NSG2 are members of a neuron-specific gene family of proteins. Both proteins are highly expressed in neurons and localized to a variety of endosomal compartments in dendrites (Yap et al., 2017). Our previous live imaging data showed that both proteins co-trafficked in neurons, and thus serve as a good example for analyzing the dynamics of two highly co-localized membrane cargos with low background noise signals (Figure 4A). The second data set contains NSG1-cherry with GFP-RAB7, a late endosome marker. RAB7 is a small GTPase involved in regulating transport to late endocytic compartments. We have previously shown that RAB7 co-trafficked and regulated the endocytic transport of NSG1 in neurons (Yap et al., 2017). Like other Rabs, RAB7 is constantly cycling between the activated form (GTP-bound) when it is recruited to membranes and inactivated form (GDP-bound) after hydrolysis and when it is cytosolic. This feature allows us to test the ability of our program in extracting membrane-bound signals from cytosolic high background signals (Figure 4C).

2. Visualizing co-localized tracks

In Figure 4, we give examples of typical output from KymoMerge. Figure 4A shows kymographs from the NSG1 and NSG2 data set with NSG1 in red and NSG2 in green, while Figure 4C shows example kymographs from the GFP-RAB7 and NSG1-mcherry data set. The top row shows the original 32-bit single-channel images followed by an overlay of the two channels. Below are the binary outputs from KymoMerge. Careful comparison of the original images in Figure 4A, C with the binary output of KymoMerge (Figure 4B and 4D) shows very similar tracks between the two. Due to the binary nature of the KymoMerge output, it does not show intensity differences as in the original files, but this is not a parameter that is usually of interest in kymograph analysis. Intensity differences are only used initially in determining background levels and true signal during the thresholding stage before the binary output is created. Comparison of the overlaid and merged files also shows similar characteristics.

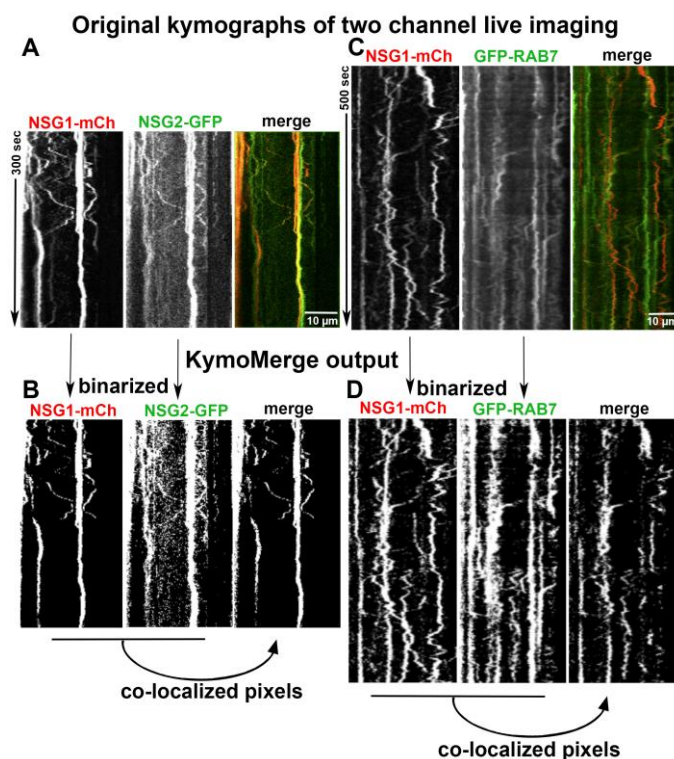


Figure 4. Comparison of original images vs. KymoMerge-generated images. Dual live imaging was carried out for two transmembrane proteins, NSG1-mCh and NSG2-GFP (A and B), and for NSG1-mCh with a cytosolic regulator GFP-RAB7 (C and D). The original kymographs for each channel and a merged kymograph are shown in (A) and (C). The binarized single-channel kymographs created by KymoMerge are shown in (B) and (D), together with the co-localized output kymograph. This final output of co-localized pixels can be used for further quantitative analysis.

One of the principal strengths of our approach is that any track seen in the merged binary data is a co-located track. In contrast, it can be difficult to discern coincident tracks in the original data.

3. Testing the robustness of KymoMerge

Our approach is useful only if the program produces results that are robust and reliable. We find that KymoMerge produces results comparable to those from a careful count done by hand, which is often how kymograph data is analyzed. For this purpose, we took the two data sets referenced in Figure 4A, B and 4C, D and independently counted anterograde and retrograde events ($\geq 2 \mu\text{m}$) manually, referencing either the original and overlayed data (as shown in Figure 4A and 4C) or using the merged binary output from KymoMerge (as shown in Figure 4B and 4D). The results in Figure 5A and 5B show that there was no statistical difference between the two methods (Mann-Whitney test).

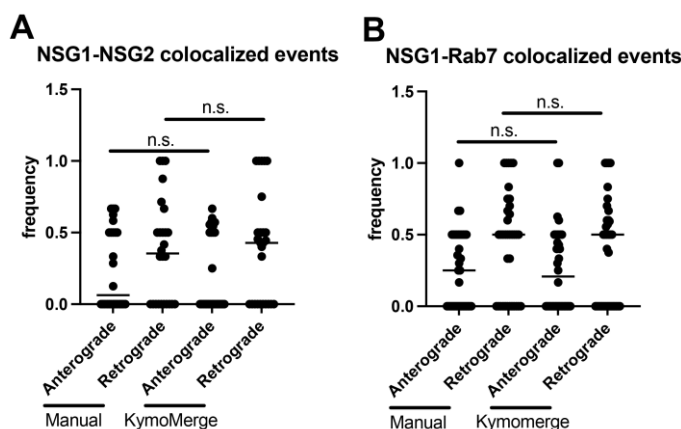


Figure 5. Comparison between manual counts of anterograde and retrograde events ($\geq 2 \mu\text{m}$) using original 32-bit images and KymoMerge created kymographs. (A) n = 26 dendrites from seven neurons in the NSG1-mCherry/NSG2-GFP data set. (B) n = 36 dendrites from seven neurons in the NSG1-mCherry/GFP-RAB7 data set. Statistical results from Mann-Whitney test between anterograde or retrograde pairs.

4. Caveats on binary thresholding

Thresholding of images is often necessary in image analysis, but it can also be somewhat subjective and, therefore, potentially problematic. With KymoMerge, thresholding requires attention particular to the process of creating binary images. There is a difficulty inherent to the process of creating the binary images: if one region is noisier than another, the noise can be of the same magnitude as the signal elsewhere. The result is that the set threshold will either eliminate actual signal if it is at a level suitable for the noisier regions, or potentially background will be left, creating false co-localized tracks. Careful thresholding with KymoMerge can produce an accurate and interpretable merged kymograph. For kymographs with areas of high background, it may be necessary to crop excessively noisy areas before analysis. Since these areas would generally be uninterpretable even with manual analysis, analyzable data are not being lost and the rest of the image will produce accurate results. It is important to understand that any data set is only a sampling of the system being studied. It is better to err on the side of excluding false positive co-localized tracks and analyze only the resulting tracks that are truly co-localized. Because KymoMerge allows for individual screening and thresholding of the individual channels before the merged images are created, any problematic kymographs can be identified by the user and properly processed. More examples are shown in McMahon et al. (2021), including direct comparisons of two different thresholds used on the same data sets.

Acknowledgments

This research was supported by NIH R01NS083378. The initial publication where this method is published: Yap et al. (2022).

Competing interests

No competing financial interests for this study.

Ethics

Neuronal cultures used for live imaging were prepared from E18 rat embryos as approved by the University of Virginia Animal Care and Use Committee. All experiments were performed in accordance with relevant guidelines and regulations (ACUC #3422).

References

- Barford, K., Keeler, A., McMahon, L., McDaniel, K., Yap, C. C., Deppmann, C. D. and Winckler, B. (2018). [Transcytosis of TrkA leads to diversification of dendritic signaling endosomes](#). *Sci Rep* 8(1): 4715.
- Boecker, C. A., Olenick, M. A., Gallagher, E. R., Ward, M. E., Holzbaur, E.L.F. (2020). [ToolBox: Live Imaging of intracellular organelle transport in induced pluripotent stem cell-derived neurons](#). *Traffic* 21: 138-155.
- Chien, A., Shih, S. M., Bower, R., Tritschler, D., Porter, M. E. and Yildiz, A. (2017). [Dynamics of the IFT machinery at the ciliary tip](#). *Elife* 6: e28606.
- Farías, G. G., Guardia, C. M., De Pace, R., Britt, D. J. and Bonifacino, J. S. (2017). [BORC/kinesin-1 ensemble drives polarized transport of lysosomes into the axon](#). *Proc Natl Acad Sci U S A* 114(14): E2955-E2964.
- Farfel-Becker, T., Roney, J. C., Cheng, X. T., Li, S., Cuddy, S. R. and Sheng, Z. H. (2019). [Neuronal Soma-Derived Degradative Lysosomes Are Continuously Delivered to Distal Axons to Maintain Local Degradation Capacity](#). *Cell Rep* 28(1): 51-64.
- Ganguly, A. and Roy, S. (2022). [Imaging Diversity in Slow Axonal Transport](#). *Methods Mol Biol*. 2431:163-179.
- Hertzler, J. I., Simonovitch, S. I., Albertson, R. M., Weiner, A. T., Nye, D. M. R. and Rolls, M. M. (2020). [Kinetochore proteins suppress neuronal microtubule dynamics and promote dendrite regeneration](#). *Mol Biol Cell* 31(19): 2125-2138.
- Jakobs, M. A., Dimitracopoulos, A. and Franze, K. (2019). [KymoButler, a deep learning software for automated kymograph analysis](#). *Elife* 8: e42288.
- Lasiecka, Z. M., Yap, C. C., Caplan, S. and Winckler, B. (2010). [Neuronal early endosomes require EHD1 for L1/NgCAM trafficking](#). *J Neurosci* 30(49): 16485-16497.
- Lasiecka, Z. M., Yap, C. C., Katz, J. and Winckler, B. (2014). [Maturational conversion of dendritic early endosomes and their roles in L1-mediated axon growth](#). *J Neurosci* 34:14633.
- Lasiecka, Z. M. and Winckler, B. (2016). [Studying endosomes in cultured neurons by live-cell imaging](#). In K. K. Pfister (Ed.), The Neuronal Cytoskeleton, Motor Proteins, and Organelle Trafficking in the Axon. Methods in Cell Biology 131:389-408.
- Liang, X., Kokes, M., Fetter, R. D., Sallee, M. D., Moore, A. W., Feldman, J. L. and Shen, K. (2020). [Growth cone-localized microtubule organizing center establishes microtubule orientation in dendrites](#). *Elife* 9: e56547.
- Maday, S. and Holzbaur, E. L. (2016). [Compartment-Specific Regulation of Autophagy in Primary Neurons](#). *J Neurosci* 36(22): 5933-5945.
- Mangeol, P., Prevo, B. and Peterman, E. J. (2016). [KymographClear and KymographDirect: two tools for the automated quantitative analysis of molecular and cellular dynamics using kymographs](#). *Mol Biol Cell* 27(12): 1948-1957.
- McMahon, L. P., Digilio, L., Duston, A., Yap, C. C. and Winckler, B. (2021). [KymoMerge: a new tool for analysis of multichannel kymographs](#). *BioRxiv* doi: <https://doi.org/10.1101/2021.11.29.470387>
- Menon, M., Askinazi, O. L. and Schafer, D. A. (2014). [Dynamin2 organizes lamellipodial actin networks to orchestrate lamellar actomyosin](#). *PLoS One* 9(4): e94330.
- Miura, K. (2020). [Bleach correction ImageJ plugin for compensating the photobleaching of time-lapse sequences](#). [version 1]. *F1000Res* 9: 1494.
- Wang, X. and Schwarz, T. L. (2009). [Chapter 18: Imaging Axonal Transport of Mitochondria](#). *Methods Enzymol* 457: 319-333.
- Yap, C. C., Wisco, D., Kujala, P., Lasiecka, Z. M., Cannon, J. T., Chang, M. C., Hirling, H., Klumperman, J. and Winckler, B. (2008). [The somatodendritic endosomal regulator NEEP21 facilitates axonal targeting of L1/NgCAM](#). *J Cell Biol* 180(4): 827-842.

Cite as: Digilio, L. et al. (2023). Quantifying Single and Dual Channel Live Imaging Data: Kymograph Analysis of Organelle Motility in Neurons. Bio-protocol 13(10): e4675. DOI: [10.21769/BioProtoc.4675](https://doi.org/10.21769/BioProtoc.4675).

- Yap, C. C., Digilio, L., McMahon, L. and Winckler, B. (2017). [The endosomal neuronal proteins Nsg1/NEEP21 and Nsg2/P19 are itinerant, not resident proteins of dendritic endosomes](#). *Sci Rep* 7(1): 10481.
- Yap, C. C., Digilio, L., McMahon, L. P., Garcia, A. D. R. and Winckler, B. (2018). [Degradation of dendritic cargos requires Rab7-dependent transport to somatic lysosomes](#). *J Cell Biol* 217(9): 3141-3159.
- Yap, C.C., Digilio, L., McMahon, L.P., Wang, T. Winckler, B. (2022). [Dynein Is Required for Rab7-Dependent Endosome Maturation, Retrograde Dendritic Transport, and Degradation](#). *J Neurosci* 42(22): 4415-4434.
- Zwetsloot, A. J., Tut, G. and Straube, A. (2018). [Measuring microtubule dynamics](#). *Essays Biochem* 62(6): 725-735.

Dual-Color Live Imaging of Adult Muscle Stem Cells in the Embryonic Tissues of *Drosophila melanogaster*

Monika Zmojdzian¹, Binoj Dhanarajan², Krzysztof Jagla¹, and Rajaguru Aradhy^{2,*}

¹GReD Institute - UMR CNRS 6293 / INSERM U1103 University of Clermont-Auvergne, Clermont-Ferrand, France

²School of Biotechnology, Amrita Vishwa Vidyapeetham, Kollam, Kerala, India

*For correspondence: rajagurua@am.amrita.edu

Abstract

Adult muscle stem cells (MuSCs) show remarkable capability in repairing injured tissues. Studying MuSCs in suitable model organisms, which show strong homology with vertebrate counterparts, helps in dissecting the mechanisms regulating their behavior. Additionally, ease of handling and access to technological tools make model organisms well suited for studying biological processes that are conserved across species. MuSCs quiescence, proliferation, and migration are regulated by various input of signals from the surrounding tissues that constitute the MuSCs niche. Observing MuSCs along with their niche in vivo through live imaging provides key information on how MuSCs behave in quiescent and activated states. *Drosophila melanogaster* is well known for its genetic tool arsenal and the similarity of its different biological processes with vertebrates. Hence, it is widely used to study different types of stem cells. Gained knowledge could then be extrapolated to the vertebrate/mammalian homologous systems to enhance our knowledge in stem cell fields. In this protocol, we discuss how to perform live cell imaging of *Drosophila* MuSCs, called adult muscle precursors (AMPs) at embryonic stages, using dual-color labelling to visualize both AMPs and the surrounding tissues. This dual-color fluorescent labelling enables the observation of in vivo behavior of two types of cells simultaneously and provides key information on their interactions. The originality of this protocol resides in its biological application to MuSCs and their niche.

Keywords: Muscle stem cells, *Drosophila*, Live imaging, Embryo, Time-lapse microscopy, Adult muscle precursors, GFP, mCherry, Peripheral nervous system, 3D image analysis

This protocol was validated in: eLife (2015), DOI: 10.7554/eLife.08497

Cite as: Zmojdzian, M. et al. (2023). Dual-Color Live Imaging of Adult Muscle Stem Cells in the Embryonic Tissues of *Drosophila melanogaster*. Bio-protocol 13(03): e4605. DOI: 10.21769/BioProtoc.4605.

Background

Drosophila's adult muscle precursors (AMPs) are quiescent muscle stem cells specified from the mesodermal lineages during embryonic stage 12 (Bate et al., 1991; Figeac et al., 2010; Aradhya et al., 2015). They form as sibling cells of muscle progenitor cells, giving rise to differentiated skeletal muscle tissue for larval locomotion. However, AMPs remain quiescent and non-differentiated during the embryonic and first parts of the larval life (Aradhya et al., 2015). The ability to maintain their quiescent nature makes AMPs an attractive model to study mechanisms regulating their dormant state, which could be homologous to those that control quiescence of mammalian muscle stem cells (MuSCs) that ensure repair of damaged muscle tissue (Sambasivan and Tajbakhsh, 2015). Through live cell imaging, using a gap-GFP transgene to mark cell membranes, we have previously demonstrated that AMPs display dynamic cellular processes during their quiescent state (Figeac et al., 2010; Aradhya et al., 2015). In contrast to the dot-like pattern of AMPs revealed by antibody staining against the nuclear protein Twist (Bate et al., 1991; Broadie and Bate, 1991; Sellin et al., 2009), our time-lapse live imaging allowed to observe that quiescent AMPs send both filopodia and cellular projections to the neighboring cells (Figeac et al., 2010). This new finding encouraged us to look deeper into the cellular behavior of AMPs through further generation of molecular and genetic tools for dual-color live imaging. Using these new transgenic *Drosophila* lines and in-depth observations through confocal imaging, we showed that AMPs interact with the embryonic muscles and the peripheral nervous system (Aradhya et al., 2015). We were able to visualize how filopodia projected by AMPs find the surrounding muscles, which in turn serve as their niche (Figure 1). These fine cellular structures would not have been discovered in fixed tissue due to the harsh nature of fixative agents. Hence, studying the cellular nature of a given cell type during development through live imaging provides a better resolution of the tissue morphogenesis. Dual-color live imaging allows documenting the dynamic behavior of two types of cells/tissues over time (Video 1). In this article, we describe the detailed protocol for performing dual-color time-lapse live imaging in *Drosophila* embryos using our previously generated molecular tools (Aradhya et al., 2015). The readers can apply this protocol to their own transgene combinations to label other cells of interest.

Though there are other methods to visualize multiple cell types with different colors in *Drosophila*, they require the construction of a fluorescent gene cassette combined with GAL4 drivers, each specific to the cells of interest or unable to label tissues that are different in origin. Additionally, the signal intensity and ability to observe fine cellular structures at embryonic stages are comparatively weaker in the method we have described in this protocol (Boulina et al., 2013, Hadjieconomou et al., 2011, Hampel et al., 2011). The strength of the genetic tool mentioned here lies in combining already known enhancer driver lines, which directly drive the expression of GFP cassette, instead of using a binary expression system such as UAS-GAL4 in the cells of interest. GFP cassette expression through binary systems tends to delay the temporal activity of a given enhancer. Also, restricting the expression of GFP cassette under the regulation of cell type-specific enhancers allows the manipulation of complementary cell types using other transgenes, such as RNA interference lines, against a specific gene by incorporating a separate binary expression system using a simple genetic cross.

Materials and Reagents

1. NuncTM ThermanoxTM coverslips (Fisher Scientific, catalog number: 174942)
2. Flystuff embryo collection cage-mini, fits 35 mm Petri dishes (Genesee Scientific, catalog number: 59-105)
3. FisherbrandTM dissecting needle wood (Fisher Scientific, catalog number: 13-820-024)
4. Double-sided tape (Scientific Industries, catalog number: SI1616)
5. NuncTM cell culture/Petri dishes (Fisher Scientific, catalog number: 12-565-90)
6. NuncTM square BioAssay dishes (Fisher Scientific, catalog number: 166508)
7. Flystuff mesh basket, small, 3/4 inch inside diameter (Genesee Scientific, catalog number: 46-101)
8. Flystuff Nitex nylon mesh 630 µm, 45 inch wide roll, 1 foot/unit (Genesee Scientific, catalog number: 57-101)
9. Dechorionation chamber, prepared by adding a suitable size of Flystuff nylon mesh to the Flystuff mesh basket
10. Agar powder (Fisher Scientific, catalog number: A10752.22)
11. Sucrose (crystalline/certified ACS) (Fisher Scientific, catalog number: S5-500)

Cite as: Zmojdzian, M. et al. (2023). Dual-Color Live Imaging of Adult Muscle Stem Cells in the Embryonic Tissues of *Drosophila melanogaster*. Bio-protocol 13(03): e4605. DOI: 10.21769/BioProtoc.4605.

12. Apple/grape juice (any commercial product available from local sources)
13. Yeast granules (any commercial product available from local sources)
14. Methyl 4-hydroxybenzoate, 99% (Fisher Scientific, catalog number: AAA1428930)
15. Sodium hypochlorite solution (commercial bleach), available chlorine 4% (Fisher Scientific, catalog number: Q27908)
16. N-heptane, certified AR for analysis (Fisher Scientific, catalog number: H/0160/15)
17. Halocarbon oil 27 (Sigma-Aldrich, catalog number: H8773)
18. Ultra-soft tissues (Kleenex)

Fly stocks

1. Duf-Gal4 (a gift from K. Vijayraghavan, NCBS, India)
 2. M6-GapGFP [lines were created as part of a previous study (Aradhya et al., 2015)]
 3. UAS-mCD8-mCherry (Bloomington Drosophila Stock Center, stock number: BL27391)
- Note: All stocks should be maintained at 25°C on standard Drosophila food medium.*

Equipment

1. *Drosophila* incubator (Percival, catalog number: DR-36VL)
2. P10 micropipette (Eppendorf, catalog number: 3123000020)
3. Stereo dissecting microscope (Olympus Stereo Microscope System, catalog number: SZX7)
4. Leica TCS SP5 confocal microscope

Software

1. Imaris (BitPlane), <https://imaris.oxinst.com/>
2. Fiji (ImageJ), <https://imagej.net/software/fiji/downloads>

Procedure

A. *Drosophila* cage setup, embryo collection, and dechorionation

1. Set up a cross between the M6-gapGFP, Duf-Gal4, and UAS-mCD8-mCherry transgenic flies with 40–60 flies in an embryo collection cage of suitable size (Figure 2A).
2. Prepare apple/grape juice agar medium using methyl 4-hydroxybenzoate according to standard protocols (Cold Spring Harb Protoc, 2011), pour it into 35 mm cell culture dishes, and allow the food medium to solidify at room temperature. The plates with medium can be stored at 4°C for up to two weeks (Figure 2A).
3. Add a layer of yeast paste to the center of the apple juice agar plate before setting up the cage to stimulate the egg production.
4. Allow the flies to mate and start laying eggs in the egg-laying cage for two days in a 25°C incubator with a 12:12 h light/dark cycle.
5. Once the flies are synchronized to the cage, the apple juice agar plates can be changed every 12 h to collect embryos with a developmental time point ranging from 0 to 12 h. Alternatively, collect the egg-laying plates by transferring flies to a new egg collection cage every 2 h and incubate separately in a 25°C *Drosophila* incubator to obtain age-synchronized embryos.

6. Wash the embryos from the plates with a fine brush into a dechorionation chamber; rinse with water repeatedly to remove any traces of yeast paste (Figure 2B–D).
7. Dechorionate embryos using 50% commercial bleach with continuous swirling of the dechorionation chamber for up to 2 min, until all embryos look like shiny rice granules. At this step, embryos can be observed under the dissection microscope to ensure proper removal of the chorion membrane (Figure 2E).
8. Thoroughly rinse the dechorionation chamber with distilled water to remove any traces of bleach; pat dry the embryos by placing the nylon mesh from the dechorionation chamber on a pile of Kleenex tissues for a few minutes (Figure 2F).
9. Dechorionated embryos are hygroscopic in nature and tend to stick to each other. After pat drying for 2–3 min, gently pick up the clusters of embryos with a fine brush or dissecting needle; place them on a rectangular block of apple juice agar cut from the square cell culture plates containing a uniform layer of apple/grape juice agar medium (Figure 2G–H).

B. Embryo alignment and picking onto a coverslip

10. Align the embryos in a linear fashion on the edge of the rectangular agar block. Maintain the orientation of the embryos in such a way that the dorsal side faces the edge of the agar block, and the lateral side faces up to visualize the abdominal AMPs (Figure 2I). For other specific tissues or cells, the embryos can be aligned accordingly so they can be visualized easily using an inverted microscope.
11. Place approximately 10 strips of double-sided tape (10×1 cm) in a 100 mL glass bottle and fill it with 90 mL of N-heptane. Allow the tape and heptane mixture to sit at room temperature for 12 h for proper extraction of the glue. The heptane/glue solution can be kept at 4 °C and used for several experiments.
12. Using a P10 micropipette, add a small volume of heptane/glue solution to the center of a rectangular coverslip in a thin line that covers the entire coverslip length (Figure 2J).
13. Allow the glue to semidry for 5 min in a sterile empty plastic box.
14. Gently press the side containing glue against the aligned embryos on the agar block; this way, the embryos are transferred to the coverslip in the same alignment of the agar block, with the lateral side facing towards the coverslip (Figure 2K). This side can be easily visualized with high magnification lenses, which require applying immersion oil to the coverslip.
15. Cover the embryos with a thin layer of halocarbon oil 27 to prevent them from desiccation (Figure 2L). Halocarbon oil allows embryos to exchange gases with the surrounding air, keeping them in healthy conditions for a long period.

C. Imaging the embryos with a confocal microscope using time-lapse series

16. Visualize the embryos using an inverted microscope, in which the objectives can touch the bottom side of the coverslip without disturbing the embryos (Figure 2M). Place the coverslips in the microscope in the same manner as glass slides using suitable holders.
17. Using the lower magnification eyepiece of a Leica SP5 confocal microscope with time series imaging, select suitable embryos with appropriate developmental stage and better visualization of muscle stem cells and surrounding tissues (Figure 2N).
18. Use the 40× oil immersion objective for enlargement of particular hemisegments of the embryo and better observation of the tissues of interest. Select Z-stacks based on the depth of tissue needed to be imaged (Figure 2O).
19. Using the Fiji (ImageJ) software, analyze the raw files from the confocal microscope and generate images with the Z-stack of the selected optical section.
20. Using Imaris (BitPlane) software, perform 3D reconstruction of both single time-point image and time-series live imaging.

Data analysis

1. For maximum intensity projection of the single time-point image, select the desired optical sections in ImageJ and export them as a Z-stack picture.
2. Similarly, use the Imaris software to generate a 3D rotating model of either a single time-point projection or images captured on a time-lapse series mode.

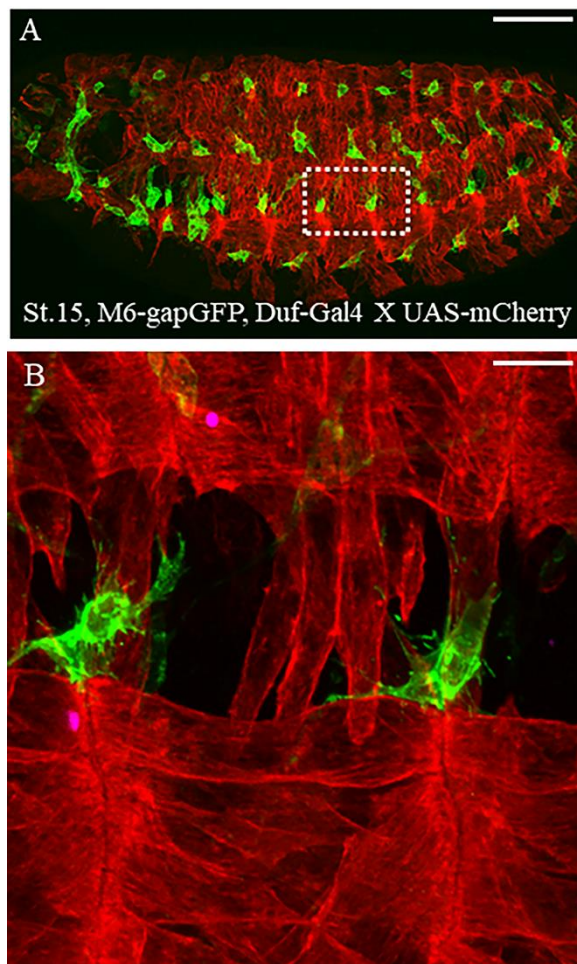
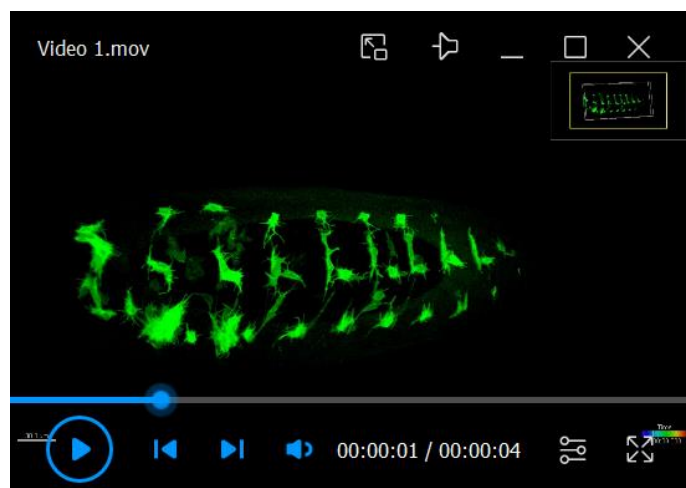


Figure 1. Dual-color live imaging of muscle stem cells and surrounding tissues. (A) Lateral view of stage 15 *Drosophila* M6-GapGFP; Duf-Gal4 X UAS-mCD8-mCherry embryos; AMPs expressing GFP are in green and the differentiated muscles expressing mCherry are in red. Scale bar: 100 μ m. (B) Two hemisegments around the lateral muscles and associated AMPs have been magnified to observe the ultrastructure of cytoplasmic extensions protruding from AMPs. Scale bar: 9 μ m.



Video 1. Time-lapse live imaging of M6-gapGFP embryos displaying dynamic behaviour of filopodia from the newly formed AMPs

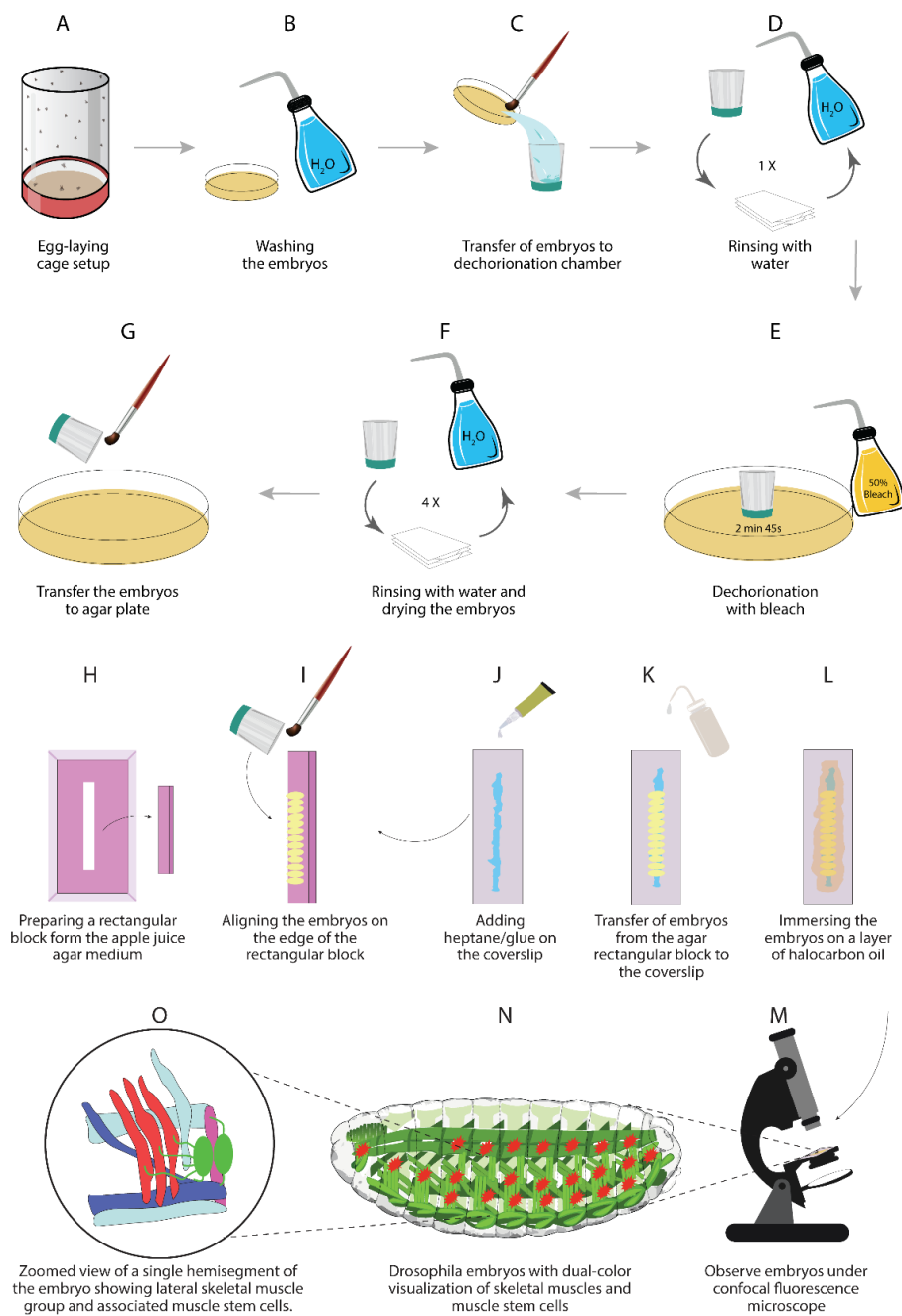


Figure 2. Illustrations of different steps described in this protocol

Acknowledgments

This protocol was adapted from the previously published paper (Aradhya et al., 2015). We thank Pierre Pouchin for helping in the image processing during the initial analysis. We also thank the Imaging platform at GReD institute, France for allowing us to use the Leica SP5 confocal microscope.

Competing interests

The authors declare no competing interests.

References

- Aradhya, R., Zmojdzian, M., Da Ponte, J. P. and Jagla, K. (2015). [Muscle niche-driven Insulin-Notch-Myc cascade reactivates dormant Adult Muscle Precursors in *Drosophila*](#). *Elife* 4: e08497.
- Bate, M., Rushton, E. and Currie, D. A. (1991). [Cells with persistent twist expression are the embryonic precursors of adult muscles in *Drosophila*](#). *Development* 113(1): 79-89.
- Boulina, M., Samarajeewa, H., Baker, J. D., Kim, M. D. and Chiba, A. (2013). [Live imaging of multicolor-labeled cells in *Drosophila*](#). *Development* 140(7): 1605-1613.
- Broadie, K. S. and Bate, M. (1991). [The development of adult muscles in *Drosophila*: ablation of identified muscle precursor cells](#). *Development* 113(1): 103-118.
- Cold Spring Harb Protoc. (2011). *Drosophila* apple juice-agar plates recipe. doi:10.1101/pdb.rec065672
- Figeac, N., Jagla, T., Aradhya, R., Da Ponte, J. P. and Jagla, K. (2010). [Drosophila adult muscle precursors form a network of interconnected cells and are specified by the rhomboid-triggered EGF pathway](#). *Development* 137(12): 1965-1973.
- Hadjieconomou, D., Rotkopf, S., Alexandre, C., Bell, D. M., Dickson, B. J. and Salecker, I. (2011). [Flybow: genetic multicolor cell labeling for neural circuit analysis in *Drosophila melanogaster*](#). *Nat Methods* 8(3): 260-266.
- Hampel, S., Chung, P., McKellar, C. E., Hall, D., Looger, L. L. and Simpson, J. H. (2011). [Drosophila Brainbow: a recombinase-based fluorescence labeling technique to subdivide neural expression patterns](#). *Nat Methods* 8(3): 253-259.
- Sambasivan, R. and Tajbakhsh, S. (2015). [Adult skeletal muscle stem cells](#). *Results Probl Cell Differ* 56: 191-213.
- Sellin, J., Drechsler, M., Nguyen, H. T. and Paululat, A. (2009). [Antagonistic function of Lmd and Zfh1 fine tunes cell fate decisions in the Twi and Tin positive mesoderm of *Drosophila melanogaster*](#). *Dev Biol* 326(2): 444-455.

Measuring Intracellular H₂O₂ in Intact Human Cells Using the Genetically Encoded Fluorescent Sensor HyPer7

Lianne J. H. C. Jacobs¹, Michaela N. Hoehne¹ and Jan Riemer^{1, 2, *}

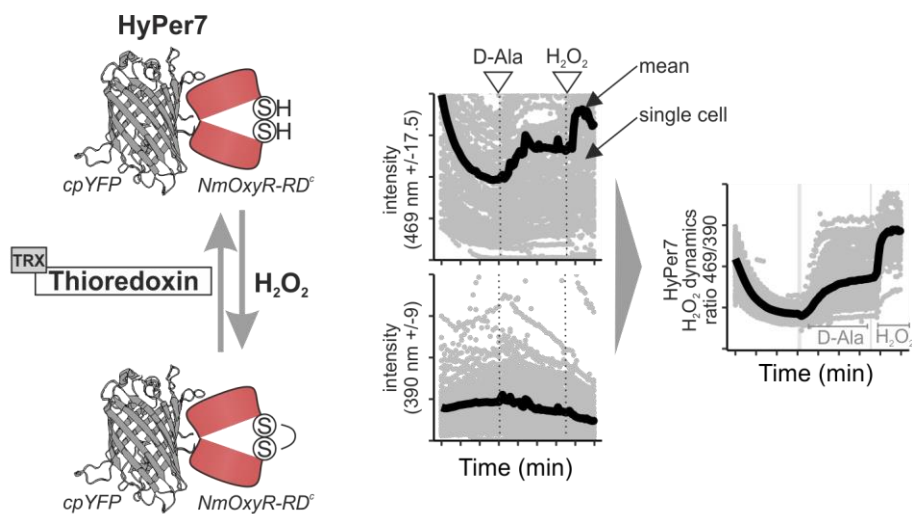
¹Institute of Biochemistry, Redox Biochemistry, University of Cologne, Zuelpicher Str. 47a/R. 3.49, 50674 Cologne, Germany

²Cologne Excellence Cluster on Cellular Stress Responses in Aging-Associated Diseases (CECAD), University of Cologne, 50931 Cologne, Germany

*For correspondence: jan.riemer@uni-koeln.de

[Abstract] Depending on its local concentration, hydrogen peroxide (H₂O₂) can serve as a cellular signaling molecule but can also cause damage to biomolecules. The levels of H₂O₂ are influenced by the activity of its generator sites, local antioxidative systems, and the metabolic state of the cell. To study and understand the role of H₂O₂ in cellular signaling, it is crucial to assess its dynamics with high spatiotemporal resolution. Measuring these subcellular H₂O₂ dynamics has been challenging. However, with the introduction of the super sensitive pH-independent genetically encoded fluorescent H₂O₂ sensor HyPer7, many limitations of previous measurement approaches could be overcome. Here, we describe a method to measure local H₂O₂ dynamics in intact human cells, utilizing the HyPer7 sensor in combination with a microscopic multi-mode microplate reader.

Graphical abstract:



Overview of HyPer7 sensor function and measurement results.

Keywords: H₂O₂ measurement, HyPer7, Real-time imaging, Subcellular resolution, pH-independent

[Background] Aerobic life comes at a price due to the formation of reactive oxygen species (ROS) as

Copyright © 2022 The Authors; exclusive licensee Bio-protocol LLC.

an unavoidable by-product of essential metabolic processes. ROS is a collective term for reactive chemical species containing oxygen, of which hydrogen peroxide (H_2O_2) is the most relevant member due to its long half-life and comparably high cellular concentration. H_2O_2 has both beneficial and deleterious effects on cells depending on its levels, flux, and the functional state of the cell (Sies and Jones, 2020). Consequently, cellular H_2O_2 levels are tightly controlled.

The subcellular dynamics of H_2O_2 are poorly understood in intact mammalian cells. To explore these dynamics, biosensors that are targetable, sensitive, specific, and reversible are required. Research previously relied on small chemical probes (mostly irreversible and therefore not measurements of dynamic fluxes of H_2O_2) or comparably insensitive genetically encoded sensors (reversible but insensitive) (Roma et al., 2018; Kalinovic et al., 2019; Liao et al., 2020; Plecita-Hlavata et al., 2020).

In recent years, more sensitive genetically encoded fluorescent H_2O_2 sensors were developed, including HyPer7 (Pak et al., 2020). HyPer7 consists of a circular permuted yellow fluorescent protein (cpYFP) that is integrated into the H_2O_2 -sensing regulatory domain of *Neisseria meningitidis* OxyR (Oxy-RD). OxyR is a natural H_2O_2 sensor and transcription factor. OxyR from different organisms have different sensitivities; the specific Oxy-RD domain from *N. meningitidis* renders HyPer7 particularly sensitive and allows measurement of close to baseline H_2O_2 levels in otherwise unperturbed mammalian tissue cell lines.

Oxy-RD contains two cysteine residues that react in a sensitive and highly specific manner with H_2O_2 and consequently form a disulfide bond. This disulfide bond in Oxy-RD puts a strain on the fused cpYFP, thus changing the cpYFP excitation spectrum. cpYFP has two excitation maxima at ca 400 nm and 499 nm, respectively, and emits at 516 nm. Changes in the sensor oxidation state result in ratiometric changes with decreases in the excitation maximum at 400 nm and increases at 499 nm upon Oxy-RD oxidation (Pak et al., 2020). Notably, targeted mutations in the cpYFP backbone result in pH insensitivity of HyPer7. This is a clear advantage compared with previous HyPer sensor variants (e.g., HyPer3) that were all pH sensitive in the physiological pH range and required laborious pH control experiments.

Sensors for different biomolecules can be combined with different treatments of cells, with different genetic backgrounds, or with genetic engineering tools. One such genetically encoded tool is D-amino acid oxidase (DAO), an enzyme that converts D-amino acids to the corresponding α -keto acid and generates as a by-product H_2O_2 (Matlashov et al., 2014). Since DAO can be targeted to different regions within a cell, it can be employed for the localized generation of H_2O_2 .

Here, we describe a protocol to measure local H_2O_2 dynamics in cytosol and mitochondria. Combining this method with genetically engineered tools, such as the DAO system or CRISPR-cas9-mediated gene editing, to specifically remove parts of the antioxidative system allows detailed investigations of subcellular H_2O_2 dynamics.

Materials and Reagents

A. Cultivation of HEK293 cells

1. 1.5 mL Eppendorf tube (Diagonal, catalog number: 02-023-0100)

2. Sterile filter pipette tips:
 - 10 µL (Greiner Bio-One, Sapphire, catalog number: 772353)
 - 100 µL (Greiner Bio-One, Sapphire, catalog number: 774353)
 - 1,250 µL (Greiner Bio-One, Sapphire, catalog number: 778353)
3. 96-well plate (µClear, Greiner Bio-One, catalog number: 655090)
4. 15 mL Falcon tube (VWR, catalog number: 734-0451)
5. LUNA reusable cell counting slide (Logos Biosystems, catalog number: L12011)
6. Autoclaved disposable glass Pasteur pipettes without cotton pad (VWR, catalog number: HECH40567001)
7. Sterile, individually packed serological pipettes:
 - 5 mL pipettes (Sarstedt, catalog number: 86.1253.001)
 - 10 mL pipettes (Sarstedt, catalog number: 86.1254.001)
8. 10% Fetal calf serum (FCS, Sigma-Aldrich, catalog number: F0804)
9. 1% Penicillin/streptomycin (P/S, Sigma-Aldrich, catalog number: P0781-100ML)
10. Dulbecco's Modified Eagle Medium high glucose (DMEM, Thermo Fisher, Gibco, catalog number: 41965062)
11. Reagent reservoir (VWR, catalog number: 613-1175)
12. Flp-In T-Rex HEK293 cells (Human embryonic kidney 293, Invitrogen, catalog number: R78007)
13. Poly-L-lysine (Sigma-Aldrich, catalog number: P4832-50mL)
14. Dulbecco's Phosphate Buffered Saline powder (DPBS, Sigma-Aldrich, catalog number: D5652)
15. 10× Trypsin-EDTA solution (Sigma-Aldrich, catalog number: T4174)
16. Trypan Blue (Logos Biosystems, catalog number: T13001)
17. DMEM medium-complete (Gibco, catalog number: 41965039) (see Recipes)
18. DPBS (see Recipes)
19. Trypsin-EDTA solution (see Recipes)

B. Transfection of HEK293 cells

1. Plasmids:
 - pCS2+HyPer7-NES [addgene: plasmid #136467 (Pak et al., 2020)]
 - pCS2+MLS-HyPer7 [addgene: plasmid #136470 (Pak et al., 2020)]
2. Polyethylenimine (PEI) (Polysciences, catalog number: 23966-1)
3. Polyethylenimine (PEI) 1 mg/mL (see Recipes)
4. Dulbecco's Modified Eagle Medium medium-pure (DMEM, Thermo Fisher, Gibco, catalog number: 41965062) (see Recipes)

C. Induced expression of DAO in HEK293 cells

1. Doxycycline (DOX) (AppliChem, catalog number: A2951,0005)

D. H₂O₂ measurement

1. D-Alanine (Sigma-Aldrich, catalog number: 338-69-2)
2. L-Alanin BioChemica (Applichem, catalog number: A3690,0100)
3. H₂O₂ (Sigma-Aldrich, catalog number: 216763-100ML)
4. Minimal media (see Recipes):
 NaCl (Roth, catalog number: 7647-14-5)
 KCl (Roth, catalog number: 7447-40-7)
 MgCl₂ (Roth, catalog number: 2189.2)
 CaCl₂ (Merck, catalog number: 23.891.000)
 HEPES (VWR, catalog number: 7365-45-9)
 Glucose (CIL, catalog number: 110187-42-3)
 10% Fetal calf serum (FCS, Sigma-Aldrich, catalog number: F0804)

Equipment

A. Cultivation of HEK293 cells

1. Laminar flow hood class II (ENVAIR eco)
2. CO₂ incubator (New Brunswick)
3. Vacuum pump (laboport)
4. Microscope (motic AE2000)
5. Multichannel pipette (VWR)
6. Cell counter – LUNA-II (Logos Biosystems, catalog number: L40002)

Equipped cell culture laboratory containing, e.g., a laminar flow hood class II (ENVAIR eco), a CO₂ incubator for cultivation of cells (with cultivation set at 37 °C and 5% CO₂), a vacuum pump for removal of medium using sterile glass Pasteur pipettes, a microscope, a cell counter, and a cooling centrifuge.

B. Transfection of HEK293 cells

In addition to A.

1. Vortex shaker

C. H₂O₂ measurement

1. Cytation 3 (Agilent, BioTek)
 CO₂ control
 Injection system (optional)
 390LED Rev H (Agilent, BioTek, catalog number: 1225009)
 roGFPsmall filterblock ex.390 em. 525 Rev D (Agilent, BioTek, catalog number: 1225108)
 465LED Rev I (Agilent, BioTek, catalog number: 1225001)
 GFP filterblock ex. 469 em. 525 Rev I (Agilent, BioTek, catalog number: 1225101)
2. Minimal media [HEPES buffer (HBSS) solution from (Poburko et al., 2011)] (see Recipes)

3. Complete minimal media [HEPES buffer (HBSS) solution from (Poburko et al., 2011)] (see Recipes)

Software

1. Redox Ratio Analysis (RRA) [Dr M.D. Fricker, <https://markfricker.org/77-2/software/redox-ratio-analysis/> (Fricker, 2016)]
2. R (<https://www.r-project.org/>)
3. Rstudio (<https://www.rstudio.com/>)

Procedure

An overview of the procedure is depicted in **Figure 1**.

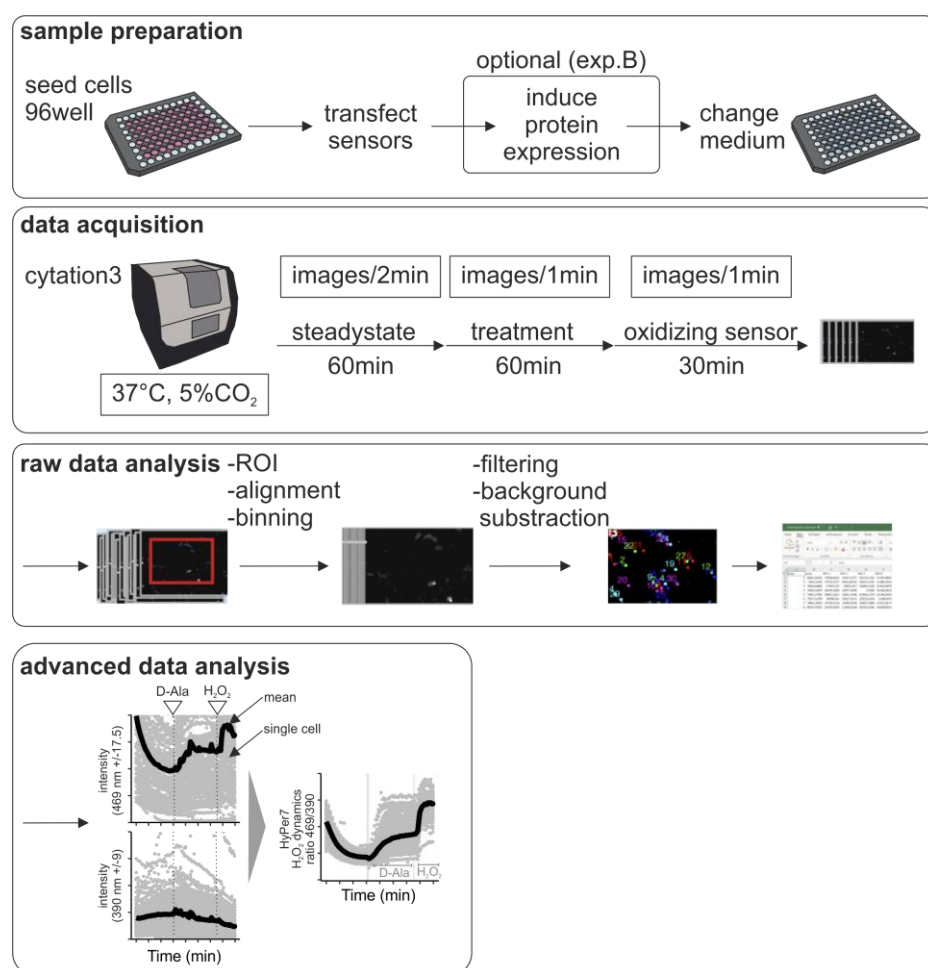


Figure 1. Schematic representation of the steps in the HyPer7 measurement protocol. Cells are seeded in 96-well plates. We describe two different experiments, one where the response upon addition of external bolus H₂O₂ is assessed (experiment A), and one where H₂O₂ is locally generated by DAO (optional experiment B). Data are acquired on a Cytation 3 automated multi-well microscope setup that

allows culturing cells at 37 °C in the presence of 5% CO₂. After data acquisition, data must be processed (raw data analysis) and then further analyzed for presentation.

A. Cultivation of HEK293 cells (day 1) (see **Note 1**)

Flp-In T-Rex HEK293 cells are cultured in high-glucose DMEM medium-complete containing FCS and a penicillin/streptomycin antibiotic mixture. HEK293 cells are cultured on 100 mm dishes in 10 mL of DMEM medium-complete until 90% confluence. For the described experiment, HEK293 cells are plated on a poly-L-lysine-coated 96-well plate in 100 µL of DMEM medium-complete.

1. Transfer a 96-well plate from the package together with the poly-L-lysine to a surface-sterilized laminar flow hood class II.
2. Take a 10 mL pipette, and dropwise add poly-L-lysine until the surface is fully covered. Let it sit at room temperature for 5 min.
3. Remove the poly-L-lysine carefully using a 1 mL pipette, as it can be reused up to approximately five times. Transfer the coated 96-well plate to an incubator at 37 °C and 5% CO₂ and let it dry for a minimum of 1 h.
4. Cultivate HEK293 cells on 100 mm dishes in 10 mL of DMEM medium-complete in an incubator at 37 °C and 5% CO₂ until they reach 90% confluence.
5. Transfer the sterile DMEM medium-complete, sterile DPBS, and sterile Trypsin-EDTA to a surface-sterilized laminar flow hood class II. Preheat all solutions to 37 °C.
6. Before seeding, transfer the coated 96-well plate to the laminar flow hood. Wash the plate three times carefully with preheated DPBS.
7. Transfer the dishes to the laminar flow hood.
8. Remove the media using an autoclaved disposable glass Pasteur pipette and a vacuum pump.
9. Wash the cells carefully by adding 5 mL of sterile DPBS at the edge of the dish using a serological pipette and a pipette boy.
10. Remove the DPBS using an autoclaved disposable glass Pasteur pipette and a vacuum pump.
11. Add 1 mL of sterile Trypsin-EDTA onto the cells using a 1 mL sterile filter pipette tip.
12. Incubate the dish at 37 °C and 5% CO₂ for 5 min until the cells detach. Flick the dish with the palm of your hand.
13. Transfer the dish back into the laminar flow hood, and add 4 mL of DMEM medium-complete using a 5 mL serological pipette.
14. Singularize the cells using a 5 mL serological pipette and a pipette boy.
15. Transfer the cell suspension to a 15 mL Falcon tube, and transfer 20 µL of this cell suspension to a 1.5 mL Eppendorf tube for counting.
16. Determine the concentration of cells using the small aliquot of cell suspension with a cell counter or hemocytometer using Trypan Blue.
17. Dilute the cell suspension so that they are at a concentration of 4,000 cells/100 µL. Of this solution, 100 µL needs to be seeded per well. Total volume depends on the number of wells needed. Try to avoid seeding the outer wells due to evaporation.

18. Seed the diluted cell suspension using a reservoir, sterile filter pipette tips, and a multichannel pipette.
19. Incubate the plate in an incubator at 37 °C and 5% CO₂.

B. Transfection of HEK293 cells (day 2) (see **Notes 2 and 3**)

The day after seeding, cells are transfected with the sensor of interest. If more wells are transfected with the same sensor, a transfection master mix is prepared in a 1.5 or 2 mL Eppendorf tube (dependent on the number of wells).

1. Transfer the sterile DMEM medium-pure and sterile DMEM medium-complete to a surface-sterilized laminar flow hood class II. Preheat all solutions to 37 °C.
2. Thaw the plasmid as well as the Polyethylenimine [PEI (1 mg/mL)].
3. Mix 0.05 µg/well of plasmid DNA with 10 µL/well of DMEM medium-pure and incubate at room temperature for 5 min.
4. After the incubation, add 0.15 µL/well of PEI (1 µg/mL final concentration), and vortex for 10 s. Incubate the transfection mix for 10 min at room temperature to ensure the formation of transfection complexes.
5. Transfer the seeded 96-well plate to the laminar flow hood.
6. Add 40 µL/well of DMEM medium-complete to the transfection solution.
7. Add 50 µL of plasmid transfection solution to each well.
8. Incubate the plate in an incubator at 37 °C and 5% CO₂.

C. Induce expression of DAO in HEK293 cells [day 3; only if inducible system is used (experiment B)] (see **Note 4**)

Induce the protein expression of the mitochondrial-targeted DAO (mtDAO), which was stably transfected using the Flp-In T-Rex system. DAO will generate H₂O₂ upon reacting with D-alanine. It does not react with L-alanine.

1. Transfer the sterile DMEM medium-complete to a surface-sterilized laminar flow hood class II. Preheat all solutions to 37 °C.
2. Thaw the doxycycline (DOX).
3. Prepare 1 mL of DMEM medium-complete with DOX 1:100 diluted (from 1 mg/mL stock, final concentration 10 µg/mL) using sterile filter pipette tips.
4. Transfer the 96-well plate to the laminar flow hood.
5. Transfer the prepared DOX solution to a reservoir.
6. Add 10 µL of this solution to each well of the 96-well plate using sterile filter pipette tips and a multichannel pipette.
7. Incubate the plate in an incubator at 37 °C and 5% CO₂.

D. H₂O₂ measurement (day 4) (see **Note 5**)

Measure the response of the HyPer7 to the addition of bolus H₂O₂ (experiment A), or if the DAO is

expressed by treating with D-alanine or L-alanine (experiment B).

1. Check the filters before starting up the Cytation 3. HyPer7 is measured at excitation levels of 390 nm (± 9) and 469 nm (± 17.5).
2. Preheat the Cytation 3 to 37 °C with 5% CO₂, and set up the measuring protocol accordingly.
Experiment A: 60 min steady-state (acquire a picture every 2 to 3 min); injection/addition by hand of 30 μ L of H₂O₂ (range for the initial experiment of 2.5–20 μ M of H₂O₂ final concentration); 60 min measurement (acquire a picture every 1 to 1.5 min); injection/addition by hand of 20 μ M of H₂O₂ (to fully oxidize the HyPer7 sensor); and 30 min measurement (acquire a picture every 1 to 1.5 min).
Experiment B: 60 min steady-state (acquire a picture every 2 to 3 min); injection/addition by hand of 30 μ L of D/L-alanine (range for the initial experiment of 1–8 mM D-alanine final concentration); 60 min measurement (acquire a picture every 1 to 1.5 min); injection/addition by hand of 20 μ M H₂O₂ (to fully oxidize the HyPer7 sensor); and 30 min measurement (acquire a picture every 1 to 1.5 min).
3. Prepare the H₂O₂ (experiment A) and D-alanine and L-alanine (experiment B) dilutions in minimal media (without 10% FCS). Consider that further dilution will take place, due to the already present 50 μ L of complete minimal media (with 10% FCS) in each well.
4. Prime the injection system with the H₂O₂, D-alanine, or L-alanine dilution.
5. Transfer the 96-well plate to a working bench, and add distilled water (dH₂O) to all the empty outer wells to prevent the evaporation of media.
6. Remove the media of the wells that will be measured. Do not remove media from wells that will be measured at a later point during the day. With these Cytation 3 settings, it is possible to measure up to 18 wells in the same measurement.
7. Add 50 μ L of complete minimal media (with 10% FCS) to each well.
8. Place the 96-well plate in the Cytation 3, and start setting the beacons for each well.
9. After setting the beacons and saving the settings, start the measurement.
10. Add between 10–30 μ L of treatment solution. Do not add less volume to ensure that the solutions will properly mix.

Data analysis

In this protocol, we describe the use of the ratiometric sensor HyPer7. Using two excitation peaks at approximately 405 and 488 nm, the redox state of the sensor and thus indirectly the levels of H₂O₂ in its surroundings can be assessed. Forming the ratio of the intensities at these peaks reduces errors that result from differences in sensor concentrations (Pak et al., 2020). Data can be analyzed using standard software like excel. For the waste amount of single cell data, we employ a semi-automatized software package, the RRA (redox ratio analysis) program (Fricker, 2016). The data exported from this program are further analyzed using R.

1. As the first step of the analysis, we use the RRA program to extract the fluorescence intensities for

both channels and each single cell. For this, load the images into RRA, and stack all images of one well. As the 469 nm channel is much brighter, make sure to first select this one and afterwards the 390 nm channel (roGFPsmall); it will improve the alignment.

2. Select a region of interest (ROI) and align the images. This is necessary to ensure that the cells are at the exact same spot over time and their signal can be extracted properly.
3. To remove background noise, continue the “advanced ratio analysis” mode, and filter the background.
4. Afterwards, select every cell present in the ROI, and export the data as an excel file.
5. As the second step, we perform downstream analysis in R. Load the excel file into R, where you will clean the data and remove potential outliers, such as floating dead cells. These outliers are easily identified as ROIs having ratio values of + 6000 as well as $\times 10^x$.
6. Merge the data of the replicates, and calculate the mean of all the single cells measured.
7. Represent each cell individually as points, together with the calculated mean as a line using ggplot2. This way, we can see the heterogeneity of the individual cell responses, as well as the cell population mean.
8. Export the graphs.

Notes

1. Cell seeding: Cells are seeded at a low density to ensure the measurement on a single-cell basis with a 70% confluence. It is important to score how fast different cell lines used in this experiment grow to adjust the seeding of cells on day 1. Cell density often has effects on the handling of the applied treatment by the cells (e.g., a higher number of cells might more rapidly remove H₂O₂ from the medium compared to a lower number). If the cells are too dense on the day of the measurement, this can cause the presence of more floating cells during your measurement and thus hamper proper automated data analysis. For the same reason, we also advise precoating the 96-well plate with poly-L lysine to increase cell attachment. When comparing multiple experiments, it is important to seed the same number of cells, transfect at the same time, and perform the experiment in a similar manner.
2. Transfection: We always perform measurements 48 h after transfection. This time can be varied as the transiently transfected sensor often is detectable for up to 5 days. A high transfection efficiency is important for the subsequent single-cell measurements.
3. The imaging parameters used in this protocol (390 and 469 nm) are not the most optimal. The maxima of the sensor excitation peaks are at 405 and 488 nm; however, the commercially available filters used are the best fitting ones for the Cyvation setup that we are using.
4. Sensor targeting to different compartments: Biosensors can be genetically targeted to different (sub-)compartments including cytosol (equipment with a nuclear export signal), mitochondrial matrix and intermembrane space (IMS), outer mitochondrial membrane and plasma membrane, and nucleus. For each localization, sensor measurements must be established from scratch. For

example, “small” compartments like the IMS might harbor only a small number of sensor molecules, thus giving rise to only small fluorescence signals (especially of the 405 nm channel). Moreover, the mechanisms of sensor reversibility often rely on the presence of enzymes. In the case of HyPer7, the sensor is oxidized by H₂O₂ directly but requires reduction by the thioredoxin system. Thus, if this system is not present in sufficient amounts in the compartment of choice, results might be affected. Conversely, biosensor expression might also affect its local surroundings. For HyPer7, it has to be considered that it scavenges H₂O₂ when it “detects” H₂O₂, and thus it might interfere with redox signaling.

5. Inducible expression systems: Instead of transient transfections, inducible expression systems might be used. We often combine the transient expression of biosensors with the inducible stable expression of genetic engineering tools like the mtDAO system. It is important to carefully titrate expression levels of these genetic tools (using different expression times and DOX amounts) and confirm (like for the biosensors) their correct localization. To confirm functionality of the engineering tool, it is advisable to directly assess its function. In the case of mtDAO, cotransfection with HyPer7 to the mitochondrial matrix and addition of D-alanine could serve as control.
6. Measurements:
 - a. Minimal medium: We often observe a strong interference of colored medium (e.g., medium containing phenol red) with the measurements. To ensure no interference, we use minimal medium. This medium can also be easily adapted to additional needs of the experimental regime, such as incubation of cells with different nutrient sources or depletion of cells from those nutrients.
 - b. Sensors: For a multiplexing/multiparameter measurement approach, it would be highly interesting to combine different biosensors within the very same cell. This would also help to explore the strong heterogeneity between cells that is observed in single-cell measurements. It is, however, important to consider that biosensors with similar fluorescence spectrum features cannot be combined.
 - c. Steady-state measurements: Like with most H₂O₂ sensors, assessing the steady state of HyPer7 can require a long time. The sensor is initially more oxidized due to the contact of the cells with oxygenated medium. The loss of oxygen from the medium reduces HyPer7. A steady signal is often reached after 40 min. This steady-state signal often corresponds to almost fully reduced HyPer7 indicating that experiments are most often performed to assess oxidizing insults.
 - d. Heterogeneity in sensor responses: When assessing single cells, we observe a strong heterogeneity in biosensor responses between cells. On the one hand, this necessitates the presentation of results on the level of single cells and the performance of the experiment with many cells to indicate a reliable mean for the experiment. It also indicates that multiparameter experiments should best be done with different sensors within the same cell to identify correlations.

Recipes

1. Dulbecco's Modified Eagle Medium (DMEM) medium-complete
Add 10% fetal calf serum (FCS) and 1% penicillin/streptomycin (P/S) to a fresh bottle of high glucose DMEM.
Store at 4 °C and prewarm to 37 °C before use.
2. Dulbecco's Modified Eagle Medium (DMEM) medium-pure
No fetal calf serum (FCS) and no penicillin/streptomycin (P/S) are added. Store at 4 °C and prewarm to 37 °C before use.
3. Dulbecco's Phosphate Buffered Saline (DPBS)
 - a. Dissolve one bottle of DPBS powder in double-distilled water (ddH₂O) according to the manufacturer's description.
 - b. Sterilize by autoclaving.
 - c. Store at 4 °C and prewarm to 37 °C before use.
4. Trypsin-EDTA solution
 - a. Dilute 10× Trypsin-EDTA solution 1:10 with sterile PBS.
 - b. Store at 4 °C and prewarm to 37 °C before use.
 - c. Aliquots can be kept frozen at -20 °C.
5. Polyethylenimine (PEI) 1 mg/mL
 - a. Dissolve PEI in ddH₂O.
 - b. While stirring, add HCl to increase the pH to 7.0.
 - c. Sterile filter the solution.
 - d. Store in small aliquots at -20 °C for short-term storage; for long-term storage store at -80 °C.
6. Minimal media [HEPES buffer (HBSS) solution from Poburko et al. (2011)]
 - a. 140 mM NaCl, 5 mM KCl, 1 mM MgCl₂, 2 mM CaCl₂, 20 mM HEPES and 10 mM glucose in distilled water.
 - b. Store at 4 °C.
7. Complete minimal media [HEPES buffer (HBSS) solution from Poburko et al. (2011)]
 - a. 140 mM NaCl, 5 mM KCl, 1 mM MgCl₂, 2 mM CaCl₂, 20 mM HEPES and 10 mM glucose in distilled water.
 - b. Add 10% FCS; aliquots can be kept frozen at -20 °C.
 - c. Preheat an aliquot of the Minimal media to 37 °C.

Acknowledgments

The Deutsche Forschungsgemeinschaft (DFG) funds research in the Laboratory of JR (RI2150/2-2 – project number 251546152, RI2150/5-1 – project number 435235019, CRC1218 / TP B02 – project number 269925409, and RTG2550/1 – project number 411422114). The protocol was used in the following original research paper (Hoehne et al., 2022).

Competing interests

The authors declare that they have no competing interests.

References

1. Fricker, M. D. (2016). [Quantitative Redox Imaging Software](#). *Antioxid Redox Signal* 24(13): 752-762.
2. Hoehne, M. N., Jacobs, L., Lapacz, K. J., Calabrese, G., Murschall, L. M., Marker, T., Kaul, H., Trifunovic, A., Morgan, B., Fricker, M., et al. (2022). [Spatial and temporal control of mitochondrial H₂O₂ release in intact human cells](#). *EMBO J* 41(7): e109169.
3. Kalinovic, S., Oelze, M., Kroller-Schon, S., Steven, S., Vujacic-Mirski, K., Kvandova, M., Schmal, I., Al Zuabi, A., Munzel, T. and Daiber, A. (2019). [Comparison of Mitochondrial Superoxide Detection Ex Vivo/In Vivo by mitoSOX HPLC Method with Classical Assays in Three Different Animal Models of Oxidative Stress](#). *Antioxidants (Basel)* 8(11).
4. Liao, P. C., Franco-Iborra, S., Yang, Y. and Pon, L. A. (2020). [Live cell imaging of mitochondrial redox state in mammalian cells and yeast](#). *Methods Cell Biol* 155: 295-319.
5. Matlashov, M. E., Belousov, V. V. and Enikolopov, G. (2014). [How much H₂O₂ is produced by recombinant D-amino acid oxidase in mammalian cells?](#) *Antioxid Redox Signal* 20(7): 1039-1044.
6. Pak, V. V., Ezerina, D., Lyublinskaya, O. G., Pedre, B., Tyurin-Kuzmin, P. A., Mishina, N. M., Thauvin, M., Young, D., Wahni, K., Martinez Gache, S. A., et al. (2020). [Ultrasensitive Genetically Encoded Indicator for Hydrogen Peroxide Identifies Roles for the Oxidant in Cell Migration and Mitochondrial Function](#). *Cell Metab* 31(3): 642-653 e646.
7. Plecita-Hlavata, L., Engstova, H., Holendova, B., Tauber, J., Spacek, T., Petraskova, L., Kren, V., Spackova, J., Gotvaldova, K., Jezek, J., et al. (2020). [Mitochondrial Superoxide Production Decreases on Glucose-Stimulated Insulin Secretion in Pancreatic beta Cells Due to Decreasing Mitochondrial Matrix NADH/NAD⁺ Ratio](#). *Antioxid Redox Signal* 33(12): 789-815.
8. Poburko, D., Santo-Domingo, J. and Demaurex, N. (2011). [Dynamic regulation of the mitochondrial proton gradient during cytosolic calcium elevations](#). *J Biol Chem* 286(13): 11672-11684.
9. Roma, L. P., Deponte, M., Riemer, J. and Morgan, B. (2018). [Mechanisms and Applications of Redox-Sensitive Green Fluorescent Protein-Based Hydrogen Peroxide Probes](#). *Antioxid Redox Signal* 29(6): 552-568.
10. Sies, H. and Jones, D. P. (2020). [Reactive oxygen species \(ROS\) as pleiotropic physiological signalling agents](#). *Nat Rev Mol Cell Biol* 21(7): 363-383.

Visualization, Quantification, and Modeling of Endogenous RNA Polymerase II Phosphorylation at a Single-copy Gene in Living Cells

Linda S. Forero-Quintero^{1,*}, William Raymond², Brian Munsky^{1,2} and Timothy J. Stasevich^{3,4}

¹Department of Chemical and Biological Engineering, Colorado State University, Fort Collins, CO 80523, USA

²School of Biomedical Engineering, Colorado State University, Fort Collins, CO 80523, USA

³Department of Biochemistry and Molecular Biology, Colorado State University, Fort Collins, CO 80523, USA

⁴Cell Biology Center and World Research Hub Initiative, Tokyo Institute of Technology, Yokohama, Kanagawa 226-8503, Japan

*For correspondence: Linda.Forero_Quintero@colostate.edu

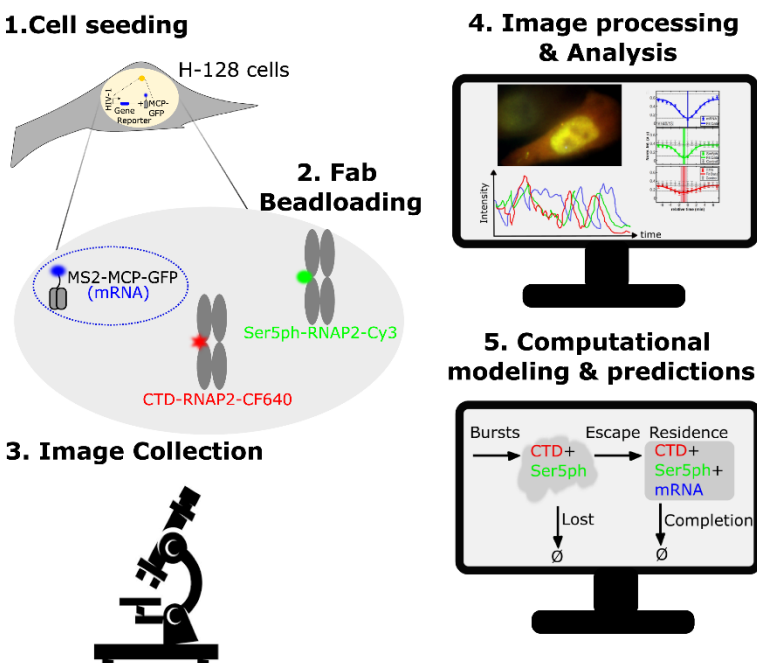
Abstract

In eukaryotic cells, RNA Polymerase II (RNAP2) is the enzyme in charge of transcribing mRNA from DNA. RNAP2 possesses an extended carboxy-terminal domain (CTD) that gets dynamically phosphorylated as RNAP2 progresses through the transcription cycle, therefore regulating each step of transcription from recruitment to termination. Although RNAP2 residue-specific phosphorylation has been characterized in fixed cells by immunoprecipitation-based assays, or in live cells by using tandem gene arrays, these assays can mask heterogeneity and limit temporal and spatial resolution. Our protocol employs multi-colored complementary fluorescent antibody-based (Fab) probes to specifically detect the CTD of the RNAP2 (CTD-RNAP2), and its phosphorylated form at the serine 5 residue (Ser5ph-RNAP2) at a single-copy HIV-1 reporter gene. Together with high-resolution fluorescence microscopy, single-molecule tracking analysis, and rigorous computational modeling, our system allows us to visualize, quantify, and predict endogenous RNAP2 phosphorylation dynamics and mRNA synthesis at a single-copy gene, in living cells, and throughout the transcription cycle.

Keywords: Transcription, RNA Polymerase II phosphorylation, Single-copy gene, Fluorescence microscopy, Fluorescent antibody-based probes, Transcription clusters, Computational modelling

This protocol was validated in: Nat Commun (2021), DOI: 10.1038/s41467-021-23417-0

Graphical abstract:



Schematic of the steps for visualizing, quantifying, and predicting RNAP2 phosphorylation at a single-copy gene.

Background

Interest in the phosphorylation status of the CTD increased due to recent studies showing its correlation with RNAP2 clustering (Cissé *et al.*, 2013; Cho *et al.*, 2016; Boehning *et al.*, 2018; Pancholi *et al.*, 2021). These findings suggest that RNAP2 clusters form around gene promoters, and early in the transcription cycle, they are enriched in unphosphorylated-RNAP2 and Ser5ph-RNAP2 (Nagashima *et al.*, 2019). RNAP2 phosphorylation distribution along the 1D genome has been extensively studied using immunoprecipitation-based assays (Heidemann *et al.*, 2013; Harlen and Churchman, 2017). However, these techniques are performed using fixed cells and require averaging over a population of cells, limiting temporal resolution and masking heterogeneity (Coulon *et al.*, 2013). Recent advances in fluorescent microscopy and single-molecule tracking (Tokunaga *et al.*, 2008; Chen *et al.*, 2014; Li *et al.*, 2019) have overcome these limitations. Now, it is possible to monitor single RNAP2 dynamics at different locations throughout the genome (Cissé *et al.*, 2013; Steurer *et al.*, 2018) and specific single-copy genes (Cho *et al.*, 2016; Li *et al.*, 2019) pre-marked with MS2 (Tantale *et al.*, 2016; Pichon *et al.*, 2018) or PP7 (Larson *et al.*, 2011; Coulon *et al.*, 2014) RNA stem-loops. When transcribed, MS2 and PP7 tags form hairpin-like secondary structures, which are then bound by their fluorescence-labeled coating proteins, MCP and PCP, respectively. Unfortunately, previous protocols use permanent fluorescent fusion tags to track RNAP2, which cannot distinguish between the crucial RNAP2 phosphorylation states that control transcription.

Fluorescent antibody-based (Fab) probes can detect post-translational modifications to RNAP2 by binding and lighting up specific modifications to the CTD of RNAP2 *in vivo* (Hayashi-Takanaka *et al.*, 2009; Stasevich *et al.*, 2014; Kimura *et al.*, 2015; Lyon and Stasevich, 2017). However, freely diffusing and unbound Fab probes lead to a high background; hence, this technique was previously limited to large tandem gene arrays (Stasevich *et al.*, 2014) that include multiple copies of the same gene to enhance the signal-to-noise ratio. However, using such a protocol averages over many gene copies, and masks heterogeneity from one gene copy to another. Recently, our lab developed a protocol to measure and predict the spatiotemporal dynamics of RNAP2 phosphorylation and mRNA production throughout the transcription cycle of a single-copy gene. This protocol, which we describe here,

Cite as: Forero-Quintero, L. S. *et al.* (2022). Visualization, Quantification, and Modeling of Endogenous RNA Polymerase II Phosphorylation at a Single-copy Gene in Living Cells. Bio-protocol 12(15): e4482. DOI: 10.21769/BioProtoc.4482.

combines multicolor single-molecule microscopy, complementary Fabs, and rigorous computational modeling (Forero-Quintero *et al.*, 2021). For our system (Forero-Quintero *et al.*, 2021), we utilized an established HeLa cell line (H-128) expressing a single-copy reporter gene controlled by an HIV-1 promoter, comprising an MS2-tag and its MS2 coating protein tagged with GFP (MCP, blue) (Tantale *et al.*, 2016). Our reporter gene is predominantly active due to persistent stimulation by Tat, leading to a bright MCP-GFP signal, that indicates the location of the transcription site within the nucleus, allowing us to observe fluctuations in mRNA synthesis in real-time (Figure 1a). Our loaded Fabs recognize the CTD of RNAP2 (CTD-RNAP2, conjugated with CF640, red) without or with residue-specific phosphorylation, and specific phosphorylation at the Serine 5 within the CTD of RNAP2 (Ser5ph-RNAP2, conjugated with Cy3, green). This combination of imaging probes makes it possible to observe RNAP2 regions enriched or depleted with Ser5ph within the nucleus (Figure 1a, b). Fab binding and unbinding from their targets occurs rapidly, making it a valuable tool to monitor temporal changes in the phosphorylation status of RNAP2 (Hayashi-Takanaka *et al.*, 2011; Stasevich *et al.*, 2014; Kimura *et al.*, 2015). At the HIV-1 reporter transcription site, we typically observe both Fabs present, but on occasion, the Ser5ph-RNAP2 signal becomes dim or absent despite the presence of CTD-RNAP2 and mRNA signals. Furthermore, all signals occasionally reduce to background levels, evidencing correlated fluctuations of the signals, which are caused by natural bursts and pauses in the transcriptional activity of the reporter gene (Figure 1b). By combining these multicolor elements, we can distinguish three distinct steps of the transcription cycle at the HIV-1 reporter gene: (1) RNAP2 recruitment (marked by Fab targeting CTD-RNAP2), (2) initiation (marked by Fab targeting CTD-RNAP2 and Fab targeting Ser5ph-RNAP2), and (3) elongation (marked by both Fabs and MCP binding to mRNA) (Figure 1a). To add a quantitative interpretation to these observations, we explored many possibilities and identified a simple computational model that matches all data. The optimal model that fits all data, but which avoided overfitting, consists of five basic rate parameters that describe four reactions: (1) the recruitment of RNAP2 in geometrically distributed bursts of average size (β) and frequency (ω), (2) the departure of unsuccessful or lost RNAP2 (k_{ab}), (3) promoter escape of RNAP2 (k_{esc}), and (4) a combined rate of transcription completion and RNAP2 release (k_c). Our simple mechanistic mathematical model allows us to estimate each of the above rates with excellent precision, as well as to predict the number of unphosphorylated and/or phosphorylated RNAP2 at each state throughout the transcription cycle at the HIV-1 reporter gene, and to simulate additional experimental features, such as RNAP2 positional densities or response to different transcriptional inhibition mechanisms.

Our integrated technique possesses several advantages: (1) Fab binds endogenous RNAP2, so all RNAP2 present in the cell at a given time has a high probability to be labeled; (2) The fluorescence of the Fabs is naturally amplified by the 52 heptad repeats contained in the CTD of RNAP2; (3) Fab continually binds and unbinds RNAP2, reducing the loss of fluorescence due to photobleaching; (4) Our technology can be employed to measure the RNAP2 dynamics and phosphorylation status at other single-copy genes, provided the location of the gene can be identified without (Gu *et al.*, 2018) or with labeling techniques [e.g., using MS2 or PP7 tags (Larson *et al.*, 2011; Coulon *et al.*, 2014; Tantale *et al.*, 2016; Pichon *et al.*, 2018), or other labeling systems such as ROLEX (Ochiai *et al.*, 2015), ANCHOR (Mariamé *et al.*, 2018), DNA FISH (Takei *et al.*, 2017) or CasFISH (Deng *et al.*, 2015)]; and (5) our modeling approach directly considers the temporal and statistical fluctuations of individual transcription sites, and applies information criteria to identify the simplest model that matches all experimental data.

In this protocol, we describe step-by-step how to fragment and fluorescently label antibodies targeting the CTD of RNAP2, how we put them into human cells using bead-loading (McNeil and Warder, 1987; Hayashi-Takanaka *et al.*, 2009; Stasevich *et al.*, 2014; Cialek *et al.*, 2021), the imaging conditions we employed and how to tune them to get a good signal-to-noise ratio based on the experimental needs, how to quantify signal intensities at the transcription site from 3D imaging movies, and how to infer an appropriate mathematical model to reproduce these data without overfitting.

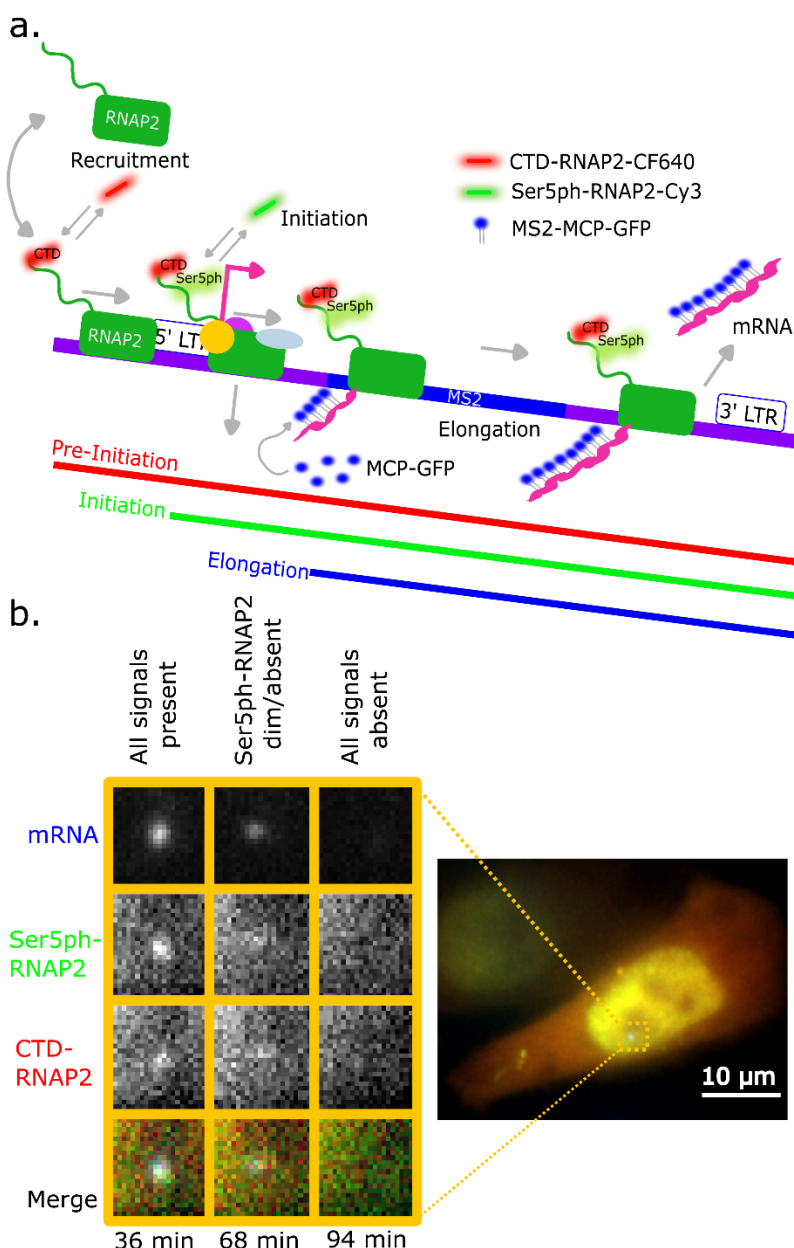


Figure 1. Schematic of our multicolor system to visualize RNAP2 phosphorylation at the transcription site of a reporter gene.

A. The reporter gene contains a 128x MS2 insert (blue) that, when transcribed, produces stem-loops which are then recognized and bound by MCP genetically fused to GFP, thus lighting up the location of the gene within the nucleus, as well as the synthesis of nascent and mature mRNAs. Our Fabs are capable of identifying the CTD of RNAP2, as well as its phosphorylation at serine 5, which were fluorescently labeled with CF640 (red) and Cy3 (green), respectively. By combining these three elements, it is possible to visualize the recruitment (by CTD-RNAP2-CF640), initiation (by Ser5ph-RNAP2-Cy3), and elongation (by MS2-MCP-GFP) steps at the transcription site of a reporter gene. **B.** Crops from an example cell displaying, from top to bottom, the mRNA, Ser5ph-RNAP2, CTD-RNAP2, and merge signals, at three characteristic time points, in which (left) all three signals are present, (middle) mRNA and CTD-RNAP2 are present, but Ser5ph-RNAP2 is dim or absent, and (right) all signals are absent. These data demonstrate transcription fluctuations and the occurrence of multiple transcription cycles (example cell image adapted from Forero-Quintero *et al.*, 2021).

Materials and Reagents

A. CTD-RNAP2 & Ser5ph-RNAP2 Fab generation and dye-conjugation

1. 15 mL conical collection tubes (Fisher Scientific, catalog number: 14-959-49D)
2. 500 mL Steritop Threaded Bottle Top Filter, 0.22 μ m, Polyethersulfone (PES), Sterile, 33 mm fitting, (Millipore Sigma, catalog number: SCGPS05RE)
3. Amicon Ultracel-4 (10 kDa-cutoff) centrifugal filter unit with cellulose membrane, 4 mL sample volume (Millipore Sigma, catalog number: UFC801024)
4. Amicon Ultracel-10 (10 kDa-cutoff) 0.5 centrifugal filter unit (Fisher Scientific, catalog number: UFC501024)
5. 0.6 mL and 1.7 mL low retention microcentrifuge tubes (Thomas Scientific, catalog numbers: 1149J99 and 1149K01, respectively)
6. PD-mini G-25 desalting column (VWR, GE Healthcare, catalog number: 95055-984)
7. Rack/stand for filtering using 15 mL conical tubes (we use the rack provided with the NucleoBond Xtra Midi Kit, from Macherey-Nagel, catalog number: 740420.50)
8. Pierce Mouse IgG1 Fab and F(ab')2 Preparation Kit (Thermo Fisher Scientific, catalog number: PI44980), store at 4 °C
9. Anti-CTD-RNAP2 and anti-Ser5ph-RNAP2 monoclonal antibodies used were kindly provided by Dr. Hiroshi Kimura, but now they are commercially available (Cosmo Bio USA, catalog numbers: MABI 0601 and MABI 0603, respectively), store at 4 °C
10. Sodium Azide (Millipore Sigma, catalog Number: 71289-5G), store at RT
11. Phosphate-buffered saline (10× PBS) (Fisher Scientific, catalog number: BP661-10), store at RT
12. Sodium Bicarbonate (NaHCO₃) (Millipore Sigma, catalog number: S5761-500G), store at RT, and 4 °C when in solution
13. Dimethyl sulfoxide (DMSO) (Millipore Sigma, catalog number: D8418), stored at RT
14. Cy3 N-hydroxysuccinimide ester mono-reactive dye pack (VWR, catalog number: 95017-373), store at -20 °C
15. CF640R Succinimidyl Ester (Biotium, catalog number: 92108), store at -20 °C
16. Sodium Bicarbonate (NaHCO₃) (Millipore Sigma, catalog number: S5761-500G), store at RT, and 4 °C when in solution
17. 1× PBS (see Recipes)

B. H-128 cell culture

1. 100 mm tissue culture dishes (VWR, CELLSTAR, catalog number: 82050-546)
2. Serological pipettes Polystyrene 10 mL (VWR, catalog number: 82050-482 (CS))
3. 1 L glass graduated cylinder (Chemistry stock room CSU)
4. HeLa Flp-in H9 cells (H-128) (Kindly provided by Dr. Edouard Bertrand (Tantale *et al.*, 2016), store at -80 °C, and maintain at 37 °C in culture)
5. Dulbecco's modified Eagle medium (DMEM), high glucose, no glutamine (Thermo Fisher Scientific, catalog number: 11960-044), store at 4 °C
6. L-glutamine (L-glut) (200 mM)-100× (Thermo Fisher Scientific, catalog number: 25030081), store at -20 °C
7. Penicillin Streptomycin (P/S) (10,000 U/mL) (Thermo Fisher Scientific, catalog number: 15140122), store at -20 °C
8. Fetal Bovine Serum (FBS), 100% US Origin (Atlas Biologicals, catalog number: F-0050-A), store at -20 °C
9. Hygromycin B (Gold Biotechnology, catalog number: H-270-1), store at -20 °C
10. Trypsin-EDTA (0.05%), phenol red (Thermo Fisher Scientific, catalog number: 25300062, store at -20 °C for long term, and at 4 °C when in regular use)

11. DMEM to maintain H-128 cells (see Recipes)
12. DMEM to image H-128 cells (see Recipes)
13. Transcription Inhibitors recipes (see Recipes)

C. Loading CTD-RNAP2-CF640 & Ser5ph-RNAP2-Cy3 Fabs into living H-128 cells

1. Glass bottom dishes (35 mm, 14 mm glass) (MatTek Corporation, catalog number: P35G-1.5-14-C).
2. Dye-conjugated Fabs “CTD-RNAP2-CF640 & Ser5ph-RNAP2-Cy3” (see details in Materials & Procedure sections A), store at 4 °C
3. Custom-made bead-loader with 106 µm glass beads [see details in our bead-loading protocol (Cialek *et al.*, 2021)].
4. DMEM medium-high glucose, no glutamine, phenol red-free (Thermo Fisher Scientific, catalog number: 31053-028), store at 4 °C

D. Imaging

1. Triptolide, Tripterygium wilfordii (Millipore Sigma, catalog number: 645900), store at -20 °C
2. Flavopiridol, Alvincidib (Selleck Chemicals, catalog number: S1230), store at -20 °C
3. THZ1 2HCl, CDK7 Inhibitor (Selleck Chemicals, catalog number: S7549), store at -20 °C

Note: The inhibitors above were reconstituted in DMSO before storage.

Equipment

1. Rocker/rotator (Thermo Fisher Scientific, model: HulaMixer PRS-5/12, catalog number: 15920D)
2. Arduino Uno-R3 (SparkFun Electronics, catalog number: DEV-11021), and mini rotor (SparkFun Electronics, Servo-Generic Sub-Micro Size, catalog number: ROB-09065)
3. Tissue culture CO₂ Incubator for cells (Heraeus, model: Heracell 150)
4. Tabletop centrifuge (Beckman Coulter, model: Microfuge 20)
5. Tabletop centrifuge capable of cooling (Thermo Fisher Scientific, model: Accusping Micro 17R, and/or Sorvall Legend XFR with F14 6x250LE)
6. UV-vis Spectrophotometer (Thermo Fisher Scientific, model: NanoDrop OneC, Catalog number: ND-ONE-W)
7. Biological safety cabinet (Nuair, model: Class II type A/B3, NU-425-400)
8. TC20 Automated Cell Counter (Bio-Rad, catalog number: 145-0102)
9. Pure water filtration (Thermo Fisher Scientific, model: Barnstead NANOpure II)
10. Digital water bath (Fisher Scientific, model: ISOTEMP 210)
11. Fluorescence microscope with highly inclined illumination and a stage top incubator (we employed our custom-made microscope (Forero-Quintero *et al.*, 2021))
12. Laptop or desktop computer with Mathworks Matlab

Software

1. Preprocess the images with Fiji ImageJ (Schindelin *et al.*, 2012) (<https://fiji.sc/>)
2. Analyze the preprocessed images using custom-made code written in Wolfram Mathematica 11.1.1 (<https://www.wolfram.com/mathematica/>), and available at https://github.com/MunskyGroup/Forero_2020/tree/master/Bioprotocol_Codes.
3. Model identification scripts and model-exploration Graphical User Interface (GUI) were created using MATLAB R2019b (<https://www.mathworks.com/products/matlab.html>), and are available at https://github.com/MunskyGroup/Forero_2020/tree/master/Bioprotocol_Codes.

Procedure

A. CTD-RNAP2 & Ser5ph-RNAP2 antibodies fragmentation & dye-conjugation (see Figure 2 for visualization of the major steps in this preparation)

1. Use the Pierce Mouse IgG1 Fab and F(ab')2 Preparation Kit to fragment the Fabs.
 - a. Follow the instructions from the manufacturer available at: https://assets.fishersci.com/TFS-Assets/LSG/manuals/MAN0011653_Pierce_Mouse_IgG1_Fab_Fab2_Prep_UG.pdf.
 - b. From the manufacturer's protocol above, we used the following conditions for the CTD-RNAP2 and/or Ser5ph-RNAP2 antibodies fragmentation process, which resulted in good quality/concentrated Fabs.
 - i. Begin with the IgG sample preparation. Repeat the centrifugation step of the Zeba Spin Desalting Column [this column is included in the Pierce Mouse IgG1 Fab and F(ab')2 Preparation Kit, see details above in step A.1.a.] with 1 mL of Digestion buffer four times.
 - ii. Add 0.5 mL of CTD-RNAP2 or Ser5ph-RNAP2 full-length antibody in 1× PBS at the maximum concentration recommended by the manufacturer (4 mg).

Important notes:

- (1) *The preparation of the CTD-RNAP2 and Ser5ph-RNAP2 Fabs should be done on separate days, since the kit only provides a single NAb protein column. This column can be reused up to ten times for different antibodies, as long as it is properly regenerated after each use.*
 - (2) *We used highly concentrated CTD-RNAP2 & Ser5ph-RNAP2 antibodies, but if you are purchasing commercial antibodies (usually provided at 1 mg/mL), you should concentrate the antibodies to a higher concentration before generating and purifying Fabs (see details on how to concentrate antibodies at Koch et al., 2021).*
 - iii. After equilibrating the immobilized Ficin in a spin column tube, add the IgG sample obtained in the step above (A.1.b.ii.), and incubate the digestion reaction for four hours (or five hours for better digestion) in constant mixing of the resin at 37 °C.
Note: The manufacturer recommends an end-over-end mixer or tabletop rocker, but sometimes these do not fit in a 37 °C incubator. To be able to keep the resin constantly mixing during the incubation, we used a mini rotor and programmed it to rotate 360° using an Arduino, and place it into our 37 °C tissue culture incubator.
 - iv. Place the NAb Protein A Column to equilibrate at RT for approximately 30 min before finishing the digestion incubation. Then, perform the purification process as indicated by the manufacturer. This process involves a couple of washing and elution steps, in which the antibody can be lost. Thus, we recommend keeping the flow-throughs resulting from the washing and elution steps separately.
 - v. Measure the concentrations of the Fab, as well as the flow-throughs using the absorbance at 280 nm. We use a nanodrop, but any other spectrophotometer or a BCA protein assay would work.
Note: The Fabs generated with this protocol produce 50 kDa Fab, which corresponds to a third of the full-length antibody. Thus, if the starting mass of the antibody is 4 mg, it will produce 2.67 mg Fab. However, during digestion and purification processes, some of the antibodies are lost, resulting in 1–2 mg Fab mass. In many cases mass of Fab above 0.8 mg after digestion and purification could still result in good quality Fab (enough to concentrate, label, and later on, visualize transcriptional processes).
 - vi. Do not forget to regenerate the NAb protein A column after finishing the purification step to be able to reuse it. Place the column back at 4 °C in 1× PBS with 0.02% sodium azide).
2. Fabs concentration.
 - a. Add the Fab and the flow-through Fab from washes 1 and 2 up to 3 mL into the Amicon Ultracel-4 centrifugal filter unit with a cellulose membrane, and centrifuge at 7,500 × g and 4 °C for 20 min.
Note: Mixing the Fab and flow-through Fab from washes 1 and 2 after the purification process helps to increase the concentration of Fab, if the concentration measured after the purification was between

0.8 and 1.5 mg/mL.

- b. Add the 1 mL left to the filter unit and wash the 15 mL conical tube that contained the Fab using 2 mL of 1× PBS to complete 3 mL in the filter unit. Centrifuge one more time at 7,500 × g and 4 °C for 20 min.
 - c. Retrieve the solution retained by the filter unit. This is the concentrated Fab.
 - d. Measure the concentration of the concentrated Fab in the Nanodrop.
 - e. Another way to concentrate Fab is by using an Amicon Ultracel-10 filter 0.5 centrifugal unit:
 - i. Mix the Fab and the flow-through Fab from washes, and spin down 0.5 mL at a time, at 12,000 × g and 4 °C for 5 min, until all the volume (~3 mL) flows through.
 - ii. Some volume containing the Fab will remain in the filter unit, add the adequate amount of 1x PBS up to 0.5 mL, centrifuge at 12,000 × g and 4 °C for 5 min. Repeat this step once.
 - iii. Repeat step (A.2.e.ii.) one more time, but now for 20 min.
 - iv. Carefully, flip the filter unit into a 1.7-mL low binding tube, and centrifuge at 300 × g and 4 °C for 1 min.
 - v. Add 30 µL of 1× PBS to wash the filter unit, and centrifuge once again as in step (A.2.E.iv.).
 - vi. Measure the concentration using a nanodrop.
 - f. Purified unconjugated Fab can be stored at 4 °C until use. It can last up to a year or two without degrading, if properly stored.
3. Fabs dye-conjugation.
 - a. Get purified and concentrated Fab protein.
 - b. Use one low-binding tube per protein.
 - c. In one 0.6-mL low-binding tube, mix: 10 µL of 1 M NaHCO₃ (for better results, prepare fresh) with 100 µg of the purified Fab protein, and add 1× PBS to make a total volume of 100 µL.

Note: e.g., if the purified Fab protein concentration is 1.8 mg/mL, 100 µg corresponds to 55.5 µL. Thus, the mixture will consist of 55.5 µL of purified Fab protein, 10 µL of 1 M NaHCO₃, and 34.5 µL of 1× PBS, for a total volume of 100 µL.
 - d. Add the correct amount of dye. Use 2 µL of 1 µM CF640, and 2.66 µL of 1 µM Cy3 (*both dyes were previously diluted in DMSO*). After adding the dyes to the respective mixtures (CF640 to CTD-RNAP2, and Cy3 to Ser5ph-RNAP2), pipette up and down, and tap the tube to distribute the mixture evenly. Then, incubate at RT and protected from light for 2 h, while constantly rotating the mixture in a rotator.
 - e. Purify dye-conjugated Fabs using a G-25 mini trap desalting column (*use one per conjugated Fab protein*).
 - i. Discard the buffer in the mini trap column and replace it with 1× PBS (repeat this step three times for equilibration).
 - ii. After equilibrating the column, take the incubated mixture (containing the labeled Fab), and add it to the top of the mini trap column (*make sure it is centered and straight*). Add 450 µL of 1× PBS for circulation (*add it from above, do not touch the sides of the mini trap column*).

Note: The Fab protein conjugated with the dye is heavier than the unconjugated one; thus, it would pass through the mini trap column faster. You will be able to see two separate strips forming. The lower one contains your conjugated Fab.
 - iii. If the desired band is close to the bottom of the mini trap column, add 50 µL of 1× PBS; if further from the bottom, add up to 100 µL of 1× PBS. This will help to bring down the conjugated Fab.

Note: Keep a close look at the mini trap column, since you want to make sure you catch the conjugated Fab.
 - iv. Start cooling down the centrifuge to 4 °C.
 - v. Get one 1.7-mL low-binding tube for each conjugated Fab, place it underneath the respective mini trap column, and add 500 µL of 1× PBS.

Note: Watch carefully, since this step will bring down all the conjugated Fab drop by drop.
 - vi. Add the conjugated Fab resulting from the step above (A.3.e.v.) to the top of the Amicon Ultracel-10 (10 kDa-cutoff) 0.5 centrifugal filter unit (this filter allows proteins smaller than 10 kDa). Centrifuge at 12,000 × g and 4 °C for 5 min, and discard the flow-through.

- Note:** Align the filter perpendicularly to the centrifuge, so the protein is not centrifuged directly into the filter.
- vii. Add 500 µL of 1× PBS from the top of the filter, centrifuge one more time at 12,000 × g and 4 °C for 5 min, and discard the flow-through.
 - viii. Repeat the step above (A.3.e.vii.), but now centrifuge for 10 min.
Note: If your flow-through is colored, it means the filter may be defective. The flow-through should be clear, meaning your conjugated Fab remains in the filter, and the flow-through is disposable.
 - ix. Take the filter containing the conjugated Fab, and tightly place it in a 1.7-mL low-binding tube on top of it, and flip it. Centrifuge at 300 × g and RT for 2 min.
4. Measure the concentration and absorbance spectrum for each protein to calculate the degree of labeling.
- a. Use a nanodrop or other spectrophotometer that measures the absorbance spectrum. Choose IgG as sample type, and the corresponding dye (CF640 or Cy3). Ideally, you should get a concentration higher than 1 mg/mL for your protein, and a 1.2 for the ratio of the absorbances.
 - b. Calculate the degree of labeling (DOL) of the Fab using the following equation:
- $$DOL = \frac{\varepsilon_{IgG}}{\varepsilon_{dye}} \times \frac{1}{\left(\frac{A_{fab}}{A_{dye}}\right)^{-1} - CF}$$
- Where ε_{IgG} and ε_{dye} are the extinction coefficients of the Fab protein (IgG) at 280 nm ($83,000 \text{ M}^{-1}\text{cm}^{-1}$) and the dyes ($150,000 \text{ M}^{-1}\text{cm}^{-1}$ for Cy3, and $105,000 \text{ M}^{-1}\text{cm}^{-1}$ for CF640, respectively). These numbers are provided by the manufacturer. A_{Fab} and A_{Dye} are the absorbances determined at 280 nm for the IgG protein, and for the dyes at 550 nm for Cy3 and 650 nm for CF640, and CF is the correction factor for the dye at 280 nm (0.08, and 0.37 for Cy3, and CF640, respectively, provided by the manufacturer). Store the labeled Fabs at 4 °C for up to a year or so.
- Note:** In our study (Forero-Quintero et al., 2021), Fabs with a DOL between 0.75 and 1 were used successfully for live-imaging experiments.

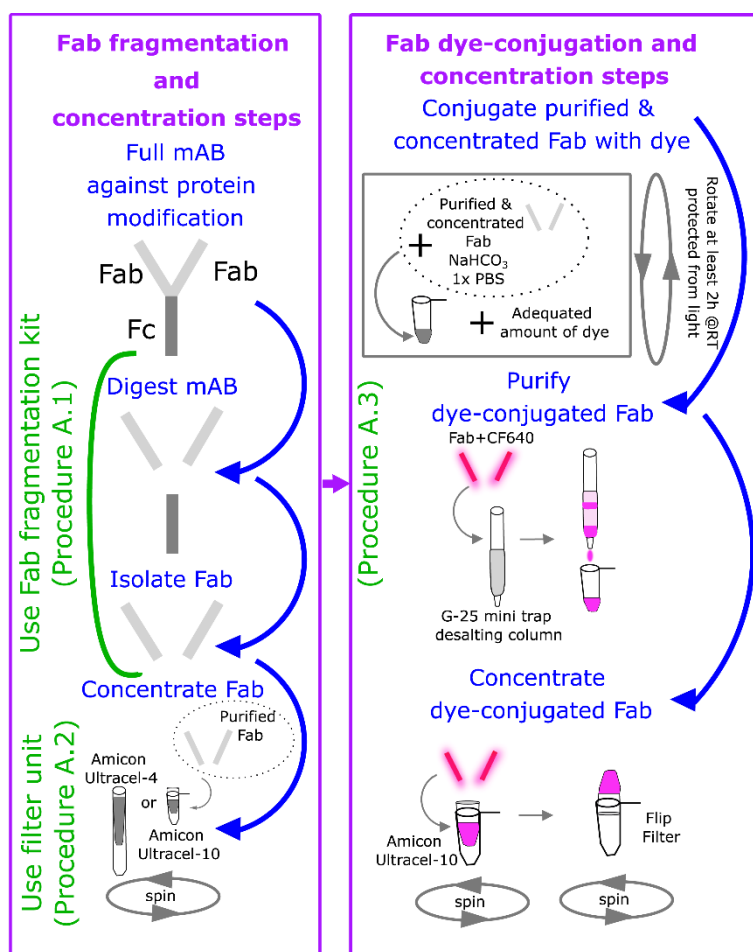


Figure 2. Major steps in fragmenting, labeling, and concentrating antibodies.

(Left), Digest the full monoclonal antibody (mAB) against the desired protein modification, and then isolate Fab by using the Pierce Mouse IgG1 Fab and F(ab')2 Preparation Kit to fragment the Fabs (Procedure A.1). Concentrate the isolated Fab using either an Amicon Ultracel-4 or -10 filter unit, as described in procedure A.2. (Right), Conjugate the purified and concentrated Fab with the desired fluorescent dye by assembling a reaction containing purified Fab, NaHCO₃, PBS, and the dye. Purify and concentrate the dye-conjugated Fab, as described in procedure A.3.

B. H-128 cell culture

1. Prepare DMEM to maintain H-128 cells (see details in the Recipes section).
2. Cells are maintained to a confluence not greater than 95% in supplemented DMEM medium (see Recipe 2 below) at 37 °C, 5% CO₂ incubator.
Note: The cells were passed a maximum of 25 times before bringing up a new batch of cells. Splitting of the cells was performed twice a week at most, to avoid stressing the cells due to the trypsinization procedure.
3. The day before performing an imaging experiment, plate the cells into MatTek dishes as follows:
 - a. Warm up the 0.05% trypsin stock, and supplemented DMEM to maintain H-128 cells.
 - b. Transfer the 100-mm dish from the incubator to the tissue culture hood.
 - c. Remove all the medium.
 - d. Wash the cells with 5 mL of 1× PBS three times.
 - e. Add 4 mL of 0.05% trypsin to cover the surface of the 100-mm dish. Let it stand at RT for approximately 40 s, and remove the trypsin with an aspirator. A thin layer will remain.

Cite as: Forero-Quintero, L. S. et al. (2022). Visualization, Quantification, and Modeling of Endogenous RNA Polymerase II Phosphorylation at a Single-copy Gene in Living Cells. Bio-protocol 12(15): e4482. DOI: 10.21769/BioProtoc.4482.

- f. Place the cells back in the incubator for 5 min. After incubation, tap the bottom and the edges of the dish, to detach and singularize the cells from the bottom of the dish.
- g. Observe the cells using a light microscope, to confirm the cells are detached and singularized.
- h. Add 10 mL of supplemented DMEM medium to the dish. Using a 10-mL serological pipette, pipette the cells in the suspension up and down, placing the tip of the pipette against an edge of the dish, to break up cell clusters or groups of cells that did not singularize when tapping the cells. To make sure all the cells at the bottom of the dish are in the suspension, tilt the dish, and let the mixture of cells and media run from different angles in the dish while pipetting up and down.
- i. Take a volume of 10 μ L of the suspension, and count the cells using a cell counter.
- j. Considering the number of cells measured, plate enough cells on the glass bottom region of the MatTek to reach a final concentration of 1.5×10^5 cells/mL. Let the resuspended cells stand on the glass region for a few seconds, before adding the supplemented DMEM medium. Approximately 0.8 mL of cells in suspension (3×10^5 cells/mL) and 1.2 mL of supplemented DMEM medium are required to maintain H-128 cells. This ratio results in good confluence of cells, to bead-load conjugated Fabs by bead-loading.
- k. Place the cells in the MatTek chambers back in the 37 °C, 5% CO₂ incubator, and let them sit for at least 24 h before any further procedure is done.

C. Loading CTD-RNAP2-CF640 & Ser5ph-RNAP2-Cy3 Fabs into living H-128 cells

1. Build your own bead loader consisting of 106 μ m glass beads, a 100 μ m nylon mesh [Spectramesh Woven Filters Polypropylene Opening: 105- μ m (Spectrum Labs, catalog number: 148496)], and a MatTek dish with the glass bottom part removed [see Cialek *et al.* (2021) and Koch *et al.* (2021) for details on the construction].
2. On your bench, place a 0.6-mL low-binding tube, and mix:
 - a. ~0.75 μ g of CTD-RNAP2-CF640 protein Fab (~1 μ L of the conjugated Fab obtained in procedure step A).
 - b. ~0.5 μ g of Ser5ph-RNAP2-Cy3 protein Fab (~1 μ L of the conjugated Fab obtained in procedure step A).
 - c. Add 1× PBS to a total volume of 4 μ L.
Note: Spin down the tubes containing the conjugated Fabs, and mix well by pipetting up and down before taking the volumes out for the mixture. Depending on the concentration of the conjugated Fabs, you can use up to 10 μ L of the mixture described above, as long as the concentrations are maintained.
 - d. Mix well by pipetting up and down, but avoid creating bubbles in the mixture. Spin down.
3. Start warming 50-mL aliquots of the DMEM medium to image H-128 cells (see Recipe 3, below), without (DMEM⁻) and with (DMEM⁺) supplementation.
Note: This DMEM is red phenol-free, to facilitate imaging.
4. Place the following items in the cell culture hood, and perform the following steps in there:
 - a. A custom-made bead loader [to see a detailed explanation of the bead loader construction and procedure, see our recent publication (Cialek *et al.*, 2021)].
 - b. The mixture of conjugated Fabs (described above).
 - c. A 15-mL conical tube per chamber to be bead-loaded.
 - d. A MatTek chamber with H-128 cells (plated at least 24 h before).
5. Load the 4 μ L of conjugated Fab in the pipette tip, and set it aside. Remove all the medium (including the remnants around the rim in the glass bottom region, to ensure cells are not scrapped with the pipette tip) from the MatTek chamber, and place it aside in a 15-mL conical tube.
Note: It is important to remove all medium, especially around the glass region, since even the smallest remnant might (1) affect the concentration of conjugated Fabs added, and (2) the beads might float on that medium, and therefore not come in direct contact with the cells.
6. Add the 4 μ L mixture of conjugated Fabs directly on top of the cells, right on the center of the glass bottom area.
7. Immediately after, place the custom-made bead loader on top of the MatTek chamber and gently sprinkle

- the glass beads on top of cells, by taping both chambers against the bench once.
8. Set aside the custom-made bead loader.
 9. Tap the MatTek chamber against the bench 7–10 times, using enough strength for the glass beads to exert force against the cell membranes and let the Fabs in, but gently enough so the cells do not peel off the glass.

Notes:

(1) *Similar to electroporation, the bead loading technique induces tiny tears in the cell membranes by a mechanical force, which allows the diffusion of conjugated Fabs into the cells through these tiny tears. This technique does not affect cell viability, and cells recover within hours post-procedure.*

(2) *Some cell types are more susceptible than others to peeling, especially if they do not attach directly to the glass and require some pre-treatment of the glass, like laminin, or polylysine, in which case bead loading might work, but the strength of tapping must be experimentally determined.*

10. Gently pour the medium removed in step (C.5.) back into cells through a side of the chamber, not directly on top of the cells, ensuring not to disturb the cells.

11. Place the cells back in the incubator at 37 °C, 5% CO₂, and let the cells recover for at least 1 h.

12. Bring the cells back to the hood and remove the medium. Wash out the glass beads by adding 1 mL of DMEM⁻ at a time and pouring the solution into a liquid waste container. Repeat this as many times as needed, until most of the glass beads are gone. Use a light microscope to visually confirm relatively few beads remain.

Note: *Tilting the MatTek chamber will help to bring down the beads, to the rim of the cover glass portion, where they can be aspirated with a pipette tip.*

13. Remove the last addition of DMEM⁻ and add 2 mL of DMEM⁺. Place the cells back in the incubator at 37 °C, 5% CO₂. Let them fully recover for another 4 h before beginning imaging.

Note: *In our experience, we observe cells recover fully and display active transcription sites co-localizing with RNAP2 5 h post-bead loading. To see a detailed explanation of the bead loading protocol and its applications, see our recent publication (Cialek et al., 2021).*

D. Imaging

Imaging can be performed on a microscope equipped with 488, 561, and 637 nm lasers with appropriate filters, a stage top incubator to maintain the cells at 37 °C, 5% CO₂, and sensitive EM-CCD cameras. We recommend using a widefield fluorescence microscope with highly inclined illumination (HILO) (Tokunaga et al., 2008) for better visualization of active and inactive transcription sites above the background.

1. Place the cells onto the stage-top incubator (37 °C, 5% CO₂).
2. Define the imaging conditions based on the activation rate (measured or expected) of the gene studied.
 - a. Set up the imaging experiment to cover the entire nucleus of the cells. For H-128 (HeLa) cells, 13 z-stacks with 0.5 μm spacing are enough.

Notes:

(1) *Capturing the whole volume of the nucleus is important to study transcription dynamics more precisely, and to guarantee that when the transcription sites disappear, this is not caused by it going out of the recorded region, but instead due to inactivation periods.*

(2) *The Z range we use covers from top to bottom HeLa, U-2 OS, HEK293, RPE1, and fibroblast cells.*

- b. Set up the temporal intervals according to the activation rate of the gene of interest and/or the type of event you desire to observe.

i. To visualize transcription fluctuations, you can set up your imaging experiment on the scale of minutes, depending on your gene of interest. The transcription site of our HIV-1 reporter gene exhibits fluctuations within the minute range. Thus, we did a short live-cell imaging set, in which each cell was imaged every minute, for 30 min. In this type of experiment, we were able to observe that mRNA, CTD-RNAP2, and Ser5ph-RNAP2 transcription fluctuations were nicely correlated; however, we were not able to observe multiple transcription cycles (multiple active and inactive periods) in a single cell record.

ii. To visualize multiple transcriptional active and inactive periods of a gene, you should set up your

imaging experiment in the order of hours, and depending on the total length of the measurement, set the scan of each cell every 1 or few minute(s) apart. You can also reduce the laser power if your movie lasts for several hours. Altering these two conditions would help to prevent photobleaching of the fluorescent probes and cell damage over the course of a movie. In our system, we recorded cells for a longer period of time; each cell was imaged every 1 min for 200-time points (~3 h 20 min), covering the entire cell (a representative recording is shown in Video 1). In our HIV-1 reporter gene, the mRNA signal rarely disappeared completely, however, longer movies allowed us to visualize these rare events in some of our cells. In some cases, the mRNA, Ser5ph-RNAP2, and CTD-RNAP2 signals turned on and off up to four times in a single movie, with RNAP2 signals appearing slightly earlier than the mRNA, indicating bursts of transcription and multiple complete transcription cycles.

- iii. To determine short time delays between signals, you should set up your experiment to a faster imaging rate. In our system, we observed a time delay between the CTD-RNAP2 and Ser5ph-RNAP2 signals at the HIV-1 transcription site. We expected serine 5 phosphorylation of the CTD tail of RNAP2 to occur in the order of seconds; therefore, we were not able to resolve the time lag between our RNAP2 signals using our 1-min rate movies. Thus, we imaged faster, 1 frame every 150 ms, for a total of 10,000-time points (150 s) in a single plane. Note that faster imaging is limited to a single plane, which is not problematic in this case, since transcription sites do not move much between z planes in the order of seconds.
3. Add triptolide to test for active transcription.
 - a. Set up your imaging experiment to capture the entire cell (13 z-stacks with 0.5 μm spacing), scanning each cell every 1 min for 35 min.
 - b. Acquire five time points.
 - c. After the first five time points, add triptolide at a final concentration of 5 μM directly to the top of the chamber.

Notes:

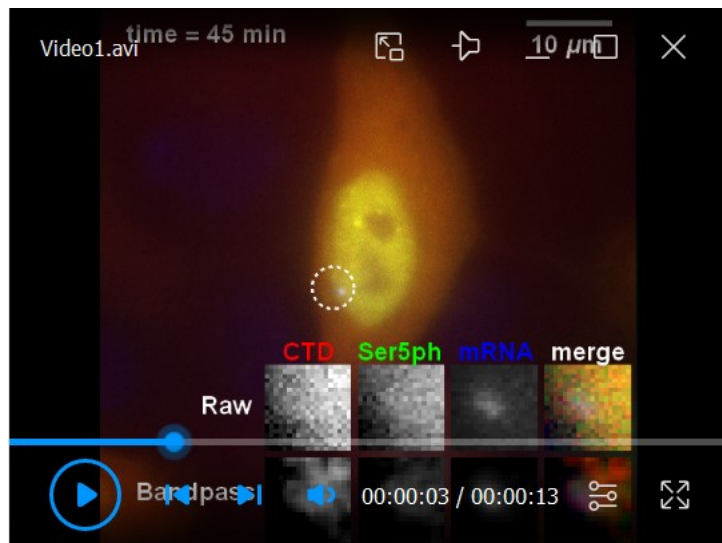
(1) For drug experiments, we usually withdraw 1 mL of the DMEM⁺ medium from the MatTek chamber before mounting it onto the microscope incubator and keep it at 37 °C. A few seconds before adding the stimuli to the cells, add triptolide to the reserved DMEM⁺, mix well, and add the mixture to cells.

(2) When adding the mixture to cells, make sure not to touch the chamber; otherwise, your field of view will go out of focus and be changed.

- d. Continue to image the cells for 30 time points (30 min) after adding triptolide.

Note: Active transcription sites together with RNAP2 Fab signals disappear within 5–10 min upon addition of triptolide at the transcription site of our HIV-1 reporter gene. Degradation of mature mRNAs occurs in the order of hours. Triptolide experiments are good to determine whether nuclear spots of the right size and brightness are active transcription sites.
4. Add THZ1 and flavopiridol to inhibit later steps in the transcription cycle (initiation, and elongation, respectively).
 - a. Set up your imaging experiment to capture the entire cell (13 z-stacks with 0.5- μm spacing), scanning each cell every 1 min for 35 or 55 min, for flavopiridol and THZ1, respectively.

Note: It takes 20–25 min for THZ1 to completely inhibit transcription initiation, and therefore mRNA synthesis. For this reason, we imaged for an extended time, so we could visualize complete transcriptional initiation inhibition at the transcription site of our HIV-1 reporter gene.
 - b. Acquire five time points.
 - c. After the first five time points, add THZ1 at a final concentration of 15 μM or flavopiridol at a final concentration of 1 μM directly to the top of the chamber, as described above.
 - d. Continue to image the cells for 55 time points (55 min) after adding THZ1, and for 30 time points (30 min) after adding flavopiridol.



Video 1. Representative 3-color movie from a long-time imaging course after processing.

Maximum projection of a 13 z-stack three-color movie, representing an exemplary H-128 cell. The dashed white circle shows the transcription site of the HIV-1 reporter, in which the mRNA, CTD-RNAP2, and Ser5ph-RNAP2 signals are co-localized. The images were acquired every 1 min for a total of 200 min. The field of view is 512 by 512 pixels = $66.56\text{ }\mu\text{m} \times 66.56\text{ }\mu\text{m}$. Scale bar, 10 μm .

E. Data analysis

1. Image processing and signal quantification:

- Correct the 3D images for photobleaching and laser fluctuation in each z-stack, by dividing the movie by the mean intensity of the whole cell or the nucleus in each channel to create a new corrected 3D movie. We used a script in Mathematica to perform this task. The code is available at https://github.com/MunskyGroup/Forero_2020/tree/master/Bioprotocol_Codes, saved as “BleachCorrectionZ_bioprotocol”.

Note: A max of the max image is required to construct a mask in this step (create a maximum projection through z, and then a maximum projection of the z-maximum projection in time). Creating the maximum projections is straight-forward using Fiji ImageJ max-projection (see Figure 3 for further details).

- Using Fiji ImageJ, preprocess the corrected 3D movie from step E.1.a. (see Figure 3 for further explanation in how to create the following files), and:
 - Subtract the background intensity from each channel.
 - Create a 2D maximum projection through z.
 - Create a maximum projection in time of the 2D maximum projection in z (from step E.1.b.ii).
 - Save the 3D image sequences in a folder named with the cell number.

Image Pre-processing Pipeline

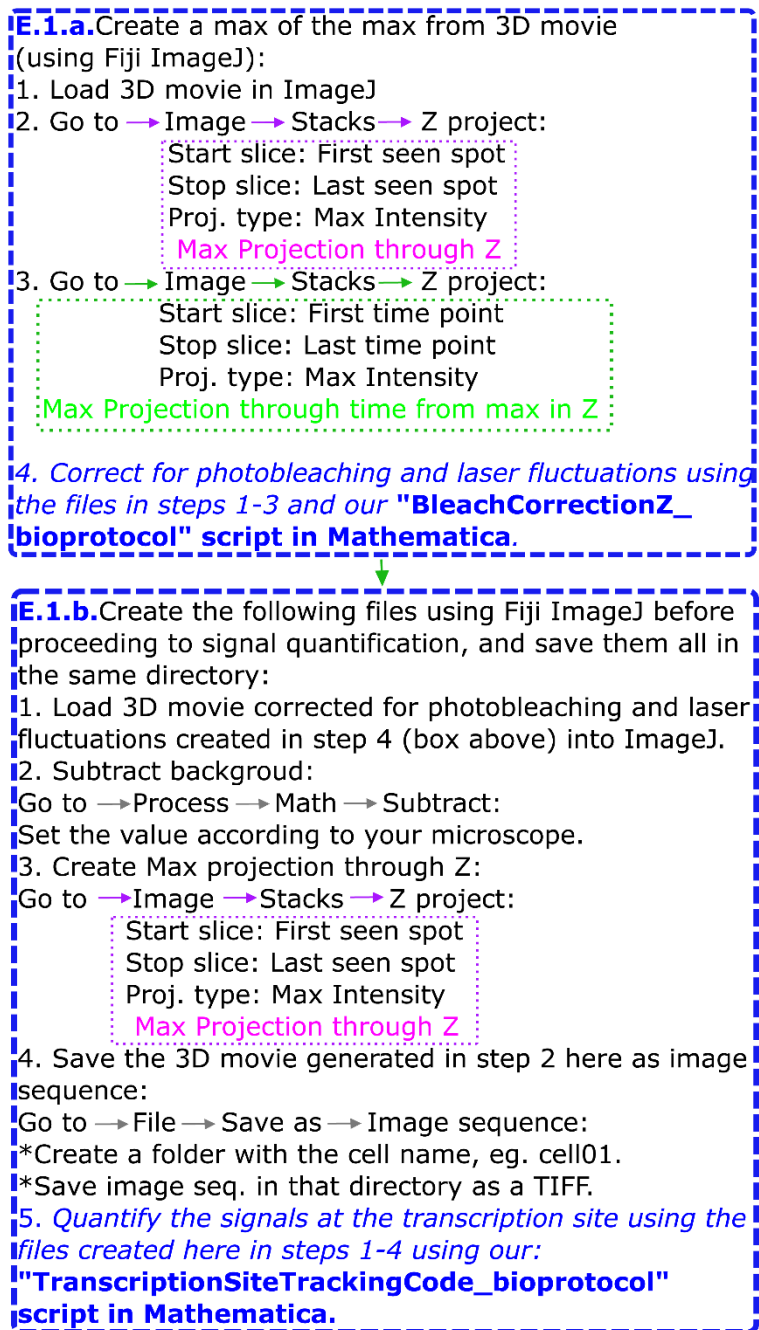


Figure 3. Image pre-processing pipeline.

The flow chart displays how to pre-process a 3D movie to generate the files needed to quantify the intensity signals at the transcription site, using our custom-made script in Mathematica.

Note: We performed the tasks described in the following steps (E.1.c–E.1.l) using a custom code written in Mathematica, saved as “TranscriptionSiteTrackingCode_Bioprotocol” and available on Github at https://github.com/MunskyGroup/Forero_2020/tree/master/Bioprotocol_Codes.

- Create a mask delineating the nucleus of the cell.

Note: Use the maximum projection in time of the 2D maximum projection in z (“max of the max image”).

- d. Optional: If the signal-to-noise ratio is poor, it is a good idea to create a running average projection over time (using a few frames, ~3).
- e. Select the thresholds in each channel to visualize spots at the transcription site, and a bandpass filter to highlight just the transcription site in the mRNA channel.
- f. Binarize the image generated in step E.1.e.
- g. Track the transcription site over time. You can use the Trackmate (Tinevez *et al.*, 2017) plugin in Fiji, or create your own tracking routine. We tracked transcription sites over time by using the ComponentMeasurements-IntensityCentroid built-in Mathematica routine, together with our click and track function, which allowed us to find the XY coordinates through time.
- h. Create two masks for each time point: one marking the transcription site (TS) and one marking the background (BG).
- i. Using the 3D image sequences (folder created in step E.1.b.iv.), determine the Z coordinate or z-stack at which the transcription site in XY has its maximum (“best z”).

Note: If the transcription site disappears due to transcription inactivation or inhibition, the Z or Zs where there is no signal remaining are replaced by the Z coordinate of the last visible position.

- j. Calculate a new 2D maximum projection from the XYZ coordinates considering the “best z” in step E.1.i. at each time point.
- k. Calculate the mean intensity values over time for the transcription site and background, using the TS and BG masks created as described in step E.1.h.

Note: We calculated the raw and normalized intensity vectors per channel using a moving average of three points to display the raw intensity as a function of time, and we calculated the normalized intensity by dividing the raw intensity by the average 95% intensity from all transcription sites.

- l. To display the transcription sites over time, generate cropped images of the 3-time point moving average trims from the “best z” in each channel. Center each trim with the intensity centroid of the transcription site in the mRNA channel. We displayed CTD-RNAP2, Ser5ph-RNAP2, mRNA, and a merge.

Notes:

(1) Our Mathematica script “TranscriptionSiteTrackingCode_Bioprotocol” can be tested using the original raw movie (without processing except for the photobleaching and laser fluctuations correction) corresponding to Video 1. The movie is saved as “SupFig3a_PBC_Cell14_woProj_ExemplaryCell.tif”, and available at <https://doi.org/10.6084/m9.figshare.14187011> [repository created for our original publication (Forero-Quintero *et al.*, 2021) from which this protocol is derived]. We also provided an image of beads saved as “Beads02.tif” in the same repository, to correct for camera offset.

(2) We calculated the raw mean intensity for each channel at the transcription site over time, including background subtraction for each cell, without running average, and saved a file collecting all the data for all cells analyzed as “Raw_Intensities_Analysis-BLC_W_BG_WO_RunAve_Date.XLS”. This file was then used in step E.2.

- m. Biophysical parameters that can be extracted from the data analyzed in the steps above:
 - i. XYZ transcription site position through time without generalized maximum projections in Z [see Sup. Figure 3d in the original paper (Forero-Quintero *et al.*, 2021), from which this protocol is derived].
 - ii. Transcription dynamics throughout the transcription cycle (by CTD-RNAP2, Ser5ph-RNAP2, mRNA intensity signals at the transcription site, Figure 4).

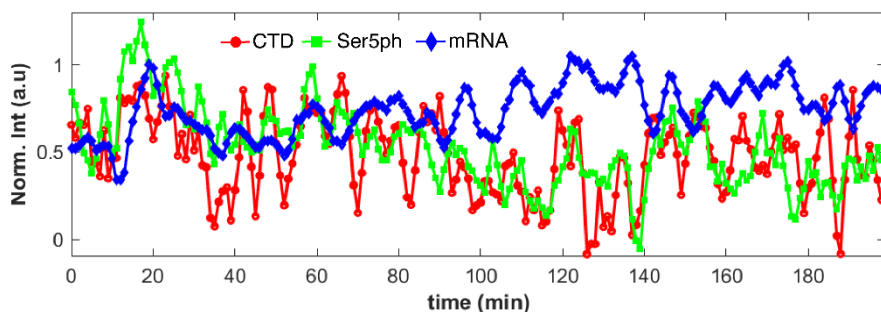


Figure 4. Representative data after signal quantification.

Normalized signal intensities over time for the exemplary 3D movie shown in Video 1. The signals co-localize at the transcription site, and represent CTD-RNAP2 (red circles), Ser5ph-RNAP2 (green squares), and mRNA (blue diamonds). Figure adapted from Forero-Quintero *et al.* (2021).

- iii. Analysis of minima signals when transcription is inactive [see Figure 2d in the original paper (Forero-Quintero *et al.*, 2021)].
- iv. Analysis of transcription site spatial organization through time and the transcription cycle [see Figure 2e–h, Sup. Figure 3h, and Sup. Figure 4 in the original paper (Forero-Quintero *et al.*, 2021)].
- Note:** Our “TranscriptionSiteTrackingCode_Bioprotocol” includes a Distance Analysis tab that can be adjusted for this quantification according to your purpose.
- v. Quantification of the number of mRNAs per transcription site [see Figure 3d in the original paper (Forero-Quintero *et al.*, 2021)].
- vi. Probability distributions for CTD-RNAP2, Ser5ph-RNAP2 intensity signals, and mRNA counts at the transcription site [see Figure 3d in the original paper (Forero-Quintero *et al.*, 2021)].
- vii. Auto- and cross-correlations at the transcription site for CTD-RNAP2, Ser5ph-RNAP2, and mRNA signals [see Figure 3a–b in the original paper (Forero-Quintero *et al.*, 2021)].
- viii. Transcription response upon transcriptional inhibition at different steps in the transcription cycle [see Figure 4 in the original paper (Forero-Quintero *et al.*, 2021)].
- n. Please refer to our original paper (Forero-Quintero *et al.*, 2021) for details on criteria for data inclusion/exclusion, details on the number of replicates in each experiment, and statistical tests.

2. Quantitative model of transcription

- a. Download Forero2020/Bioprotocol_Codes/ from: https://github.com/MunskyGroup/Forero_2020/tree/master/Bioprotocol_Codes.
- b. Load trajectory data from XLS file (named as “Raw_Intensities_Analysis-BLC_W_BG_WO_RunAve_Date.XLS” in our example) and normalize intensities and correlations (Section 1 in “ComputationalProtocol.m”).
 - i. Intensity data should be formatted such that it contains one column for each channel and (number of time points) × (number of cells) rows, where each subsequent cell is appended vertically. For example, 3 channels with 20 cells of 200-min trajectories should have a shape of 4000 rows × 3 columns.
 - ii. Change intensity normalization options if desired: Default settings are minimum 0, and maximum 1.5, normalization to the 95th percentile of each intensity trajectory.
 - iii. Change correlation lengths and normalization options: Default settings linearly interpolate to find the zero-lag autocorrelation $G(\tau = 0)$ and then average over all cells to find $\overline{G}(\tau = 0)$ for each signal. This provides an estimate of the variance after removal of shot noise. Cross-correlations are computed separately for each cell, and then divided by the average correlation at zero lag time. By default, correlations are calculated for

- delays of -10 to +10 min for cross-correlations, and for 0 to 30 min for auto-correlations.
- c. Define the model (Section 2 in “ComputationalProtocol.m”).
 - i. Specify the number of states.
 - ii. Specify the number and initial guess for parameters and noise.
 - iii. Specify stoichiometry matrix, S, and affine linear propensity functions $W = W1*x + W0$.
 - iv. Specify intensity transformation matrix, c.
 - v. Additional details on formulating bursting models are found in Methods. Alternative models are described in Forero-Quintero *et al.* (2021, Sup. Figure 6).
 - d. Solve the model to compute steady state means, variances, auto-, and cross- correlations at specified time points (Section 3 in “ComputationalProtocol.m”).
 - i. Details for solution methods are provided in Forero-Quintero *et al.* (2021), Section 9, Methods, “A quantitative model of transcription.”
 - ii. Calculate log-likelihood of the data given the model (Section 4 in “ComputationalProtocol.m”).
 - iii. Provide measured mean expression values (‘DataMeans’) for each channel, standard error of the mean for the molecules quantified (‘DataSEMs’), and the number of transcription sites (‘Nmolecules’) for each species. These values can be left as zero (0) in the code for channels that are not quantified. In our original paper (Forero-Quintero *et al.*, 2021), we determined the number of nascent mRNAs at the transcription site (‘Ntranscripts’) by counting mature mRNAs and comparing their average intensity to the transcription site intensity for the reporter gene.
 - iv. Specify which parameters are fixed “par_fixed” and which are allowed to change “par_changed” as needed for parameter searching.
 - e. Conduct parameter search to identify maximum likelihood estimate (MLE) (Section 5 in “ComputationalProtocol.m”).

We recommend using 20 or more iterative combinations of genetic algorithm (GA) and fminsearch analyses with multiple initial guesses and then select the best fit over these iterations.
 - f. Calculate Bayes Information Criterion (BIC) or Akaike Information Criterion (AIC) for model selection (Section 6 in “ComputationalProtocol.m”).
 - i. Specify the number of free parameters ($k=5$ in our example).
 - ii. If using BIC, specify an estimated number of degrees of freedom in the data. We recommend a conservative estimate as (*e.g.*, $n=8$). If using AIC, it is not necessary to estimate the number of degrees of freedom.
 - g. Run Metropolis Hastings search for parameter uncertainty quantification (Section 7 in “ComputationalProtocol.m”).

We recommend settings of 5,000 samples over 50 segments with a thinning rate of 20 for at least 20 chains (10 million total samples). For a proposal function, we recommend an N-dimensional Gaussian with variances selected to be 3%–5% of each parameter.
 - h. Plot correlation fit (Section 8 in “ComputationalProtocol.m”).
 - i. Additional Analyses (Sections 9–12 in “ComputationalProtocol.m”).
 - i. Sample model intensities.
 - ii. Compare model and data intensity histograms.
 - iii. Predict ChIP from the model.
 - iv. Predict perturbation analyses.

Recipes

1. 1× PBS

- a. Bring into the cell culture hood:
 - i. 10× PBS [add the whole content of PBS powder concentrate to 1 L of ultrapure water from a Milli Q, and mix properly. Make sure the pH is ~7.4, and then filter the solution using a Steritop Threaded Bottle Top Filter (0.22 μ m)].

- ii. Four autoclaved bottles (500 mL).
 - iii. 900 mL of ultrapure water from a Nanopure.
 - iv. Parafilm.
 - v. Steritop Threaded Bottle Top Filter (for 500 mL).
- b. Add 100 mL of 10× PBS to 900 mL of ultrapure water from a Milli Q in a 1-L graduated cylinder, cover with parafilm, and mix it properly. Open a new Steritop Threaded Bottle Top Filter, and place it in the first bottle, add 500 mL of the solution, turn on the vacuum, and plug the hose.
Note: To make good use of the filter, make 3 L of 1× PBS at a time.
 - c. Store at RT until use. It lasts several months on the shelf.

2. DMEM to maintain H-128 cells

- a. Thaw 50 mL of FBS, 5 mL of P/S, and 5 mL of L-glut. Add them to 500 mL of DMEM, high glucose, no glutamine, with red phenol, and mix well. Store at 4°C until use.
- b. Make a 50-mL aliquot of the supplemented medium described above and add 150 µL of hygromycin (previously diluted in ultrapure water from Milli-Q, at a concentration of 50 mg/mL) to obtain a final concentration of 150 µg/mL of hygromycin in the medium.

Note: Hygromycin is necessary to maintain the expression of the HIV-1 reporter in the H-128 stable cell line. When the medium is supplemented with hygromycin, use it within two weeks and store at 4 °C when not in use.

3. DMEM to image H-128 cells

Follow the same instructions as above (Recipe 2), but now use DMEM, high glucose, no glutamine, without red phenol.

Note: A clear medium is necessary to guarantee crisp fluorescent images. Store at 4 °C. It is stable for several weeks when properly stored.

4. Transcription Inhibitors

- a. Add 555 µL of DMSO to the whole content of Triptolide (TPL, 1 mg), and mix well, to obtain a stock concentration of 5 mM.
- b. Add 6.2214 mL of DMSO to the whole content of Flavopiridol (Flav, 5 mg), and mix well, to obtain a stock concentration of 2 mM.
- c. Add 3.9125 mL of DMSO to the whole content of THZ1 (5 mg), and mix well, to obtain a stock concentration of 2 mM.

Note: Store all the inhibitor stocks at -20 °C when not in use.

Acknowledgments

We thank all the members of the Stasevich and Munsky labs for their support and helpful discussion and suggestions. T.J.S was supported by the NIH (grant no. R35GM119728) and the NSF (grant no. MCB-1845761). L.S.F.Q., B.M., and W.R. were supported by the NIH (grant no. R35GM124747), and L.S.F.Q. was also supported by the W.M. Keck Foundation. This protocol was derived from the work published in Forero-Quintero *et al.* (2021).

Competing interests

The authors declare no competing interests.

References

- Boehning, M., Dugast-Darzacq, C., Rankovic, M., Hansen, A. S., Yu, T., Marie-Nelly, H., McSwiggen, D. T., Kokic, G., Dailey, G. M., Cramer, P., et al. (2018). [RNA polymerase II clustering through carboxy-terminal domain phase separation](#). *Nat Struct Mol Biol* 25(9): 833-840.
- Chen, B. C., Legant, W. R., Wang, K., Shao, L., Milkie, D. E., Davidson, M. W., Janetopoulos, C., Wu, X. S., Hammer, J. A., 3rd, Liu, Z., et al. (2014). [Lattice light-sheet microscopy: imaging molecules to embryos at high spatiotemporal resolution](#). *Science* 346(6208): 1257998.
- Cho, W. K., Jayanth, N., English, B. P., Inoue, T., Andrews, J. O., Conway, W., Grimm, J. B., Spille, J. H., Lavis, L. D., Lionnet, T., et al. (2016). [RNA Polymerase II cluster dynamics predict mRNA output in living cells](#). *Elife* 5: e13617.
- Cialek, C. A., Galindo, G., Koch, A. L., Saxton, M. N. and Stasevich, T. J. (2021). [Bead Loading Proteins and Nucleic Acids into Adherent Human Cells](#). *J Vis Exp* (172).
- Cissé, II, Izeddin, I., Causse, S. Z., Boudarene, L., Senecal, A., Muresan, L., Dugast-Darzacq, C., Hajj, B., Dahan, M. and Darzacq, X. (2013). [Real-time dynamics of RNA polymerase II clustering in live human cells](#). *Science* 341(6146): 664-667.
- Coulon, A., Chow, C. C., Singer, R. H. and Larson, D. R. (2013). [Eukaryotic transcriptional dynamics: from single molecules to cell populations](#). *Nat Rev Genet* 14(8): 572-584.
- Coulon, A., Ferguson, M. L., de Turris, V., Palangat, M., Chow, C. C. and Larson, D. R. (2014). [Kinetic competition during the transcription cycle results in stochastic RNA processing](#). *Elife* 3: e03939.
- Deng, W., Shi, X., Tjian, R., Lionnet, T. and Singer, R. H. (2015). [CASFISH: CRISPR/Cas9-mediated in situ labeling of genomic loci in fixed cells](#). *Proc Natl Acad Sci U S A* 112(38): 11870-11875.
- Forero-Quintero, L. S., Raymond, W., Handa, T., Saxton, M. N., Morisaki, T., Kimura, H., Bertrand, E., Munsky, B. and Stasevich, T. J. (2021). [Live-cell imaging reveals the spatiotemporal organization of endogenous RNA polymerase II phosphorylation at a single gene](#). *Nat Commun* 12(1): 3158.
- Gu, B., Swigut, T., Spenceley, A., Bauer, M. R., Chung, M., Meyer, T. and Wysocka, J. (2018). [Transcription-coupled changes in nuclear mobility of mammalian cis-regulatory elements](#). *Science* 359(6379): 1050-1055.
- Harlen, K. M. and Churchman, L. S. (2017). [The code and beyond: transcription regulation by the RNA polymerase II carboxy-terminal domain](#). *Nat Rev Mol Cell Biol* 18(4): 263-273.
- Hayashi-Takanaka, Y., Yamagata, K., Wakayama, T., Stasevich, T. J., Kainuma, T., Tsurimoto, T., Tachibana, M., Shinkai, Y., Kurumizaka, H., Nozaki, N., et al. (2011). [Tracking epigenetic histone modifications in single cells using Fab-based live endogenous modification labeling](#). *Nucleic Acids Res* 39(15): 6475-6488.
- Hayashi-Takanaka, Y., Yamagata, K., Nozaki, N. and Kimura, H. (2009). [Visualizing histone modifications in living cells: spatiotemporal dynamics of H3 phosphorylation during interphase](#). *J Cell Biol* 187(6): 781-790.
- Heidemann, M., Hintermair, C., Voss, K. and Eick, D. (2013). [Dynamic phosphorylation patterns of RNA polymerase II CTD during transcription](#). *Biochim Biophys Acta* 1829(1): 55-62.
- Kimura, H., Hayashi-Takanaka, Y., Stasevich, T. J. and Sato, Y. (2015). [Visualizing posttranslational and epigenetic modifications of endogenous proteins in vivo](#). *Histochem Cell Biol* 144(2): 101-109.
- Koch, A. L., Morisaki, T. and Stasevich, T. J. (2021). [A Multi-color Bicistronic Biosensor to Compare the Translation Dynamics of Different Open Reading Frames at Single-molecule Resolution in Live Cells](#). *Bio-protocol* 11(14): e4096.
- Larson, D. R., Zenklusen, D., Wu, B., Chao, J. A. and Singer, R. H. (2011). [Real-time observation of transcription initiation and elongation on an endogenous yeast gene](#). *Science* 332(6028): 475-478.
- Li, J., Dong, A., Saydamanova, K., Chang, H., Wang, G., Ochiai, H., Yamamoto, T. and Pertsinidis, A. (2019). [Single-Molecule Nanoscopy Elucidates RNA Polymerase II Transcription at Single Genes in Live Cells](#). *Cell* 178(2): 491-506 e428.
- Lyon, K. and Stasevich, T. J. (2017). [Imaging Translational and Post-Translational Gene Regulatory Dynamics in Living Cells with Antibody-Based Probes](#). *Trends Genet* 33(5): 322-335.
- Mariamé, B., Kappler-Gratias, S., Kappler, M., Balor, S., Gallardo, F. and Bystricky, K. (2018). [Real-time visualization and quantification of human Cytomegalovirus replication in living cells using the ANCHOR DNA labeling technology](#). *J Virol* 92(18), e00571-18.
- McNeil, P. L. and Warder, E. (1987). [Glass beads load macromolecules into living cells](#). *J Cell Sci* 88 (Pt 5): 669-

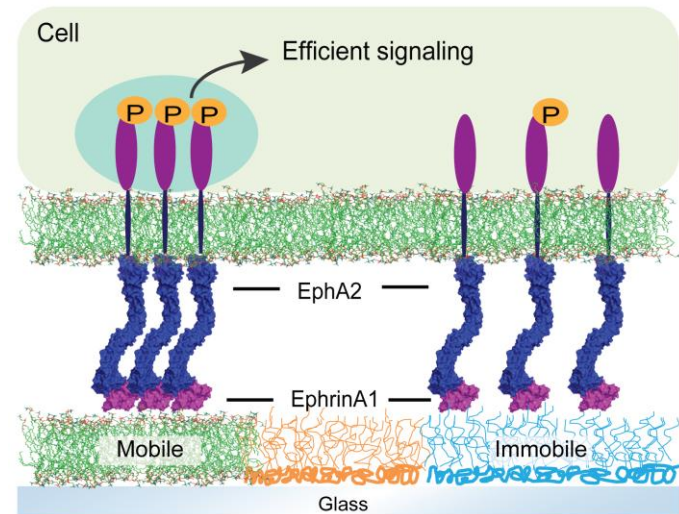
Cite as: Forero-Quintero, L. S. et al. (2022). Visualization, Quantification, and Modeling of Endogenous RNA Polymerase II Phosphorylation at a Single-copy Gene in Living Cells. *Bio-protocol* 12(15): e4482. DOI: 10.21769/BioProtoc.4482.

678.

- Nagashima, R., Hibino, K., Ashwin, S. S., Babokhov, M., Fujishiro, S., Imai, R., Nozaki, T., Tamura, S., Tani, T., Kimura, H., et al. (2019). [Single nucleosome imaging reveals loose genome chromatin networks via active RNA polymerase II](#). *J Cell Biol* 218(5): 1511-1530.
- Ochiai, H., Sugawara, T. and Yamamoto, T. (2015). [Simultaneous live imaging of the transcription and nuclear position of specific genes](#). *Nucleic Acids Res* 43(19): e127.
- Pancholi, A., Klingberg, T., Zhang, W., Prizak, R., Mamontova, I., Noa, A., Sobucki, M., Kobitski, A. Y., Nienhaus, G. U., Zaburdaev, V., et al. (2021). [RNA polymerase II clusters form in line with surface condensation on regulatory chromatin](#). *Mol Syst Biol* 17(9): e10272.
- Pichon, X., Lagha, M., Mueller, F. and Bertrand, E. (2018). [A Growing Toolbox to Image Gene Expression in Single Cells: Sensitive Approaches for Demanding Challenges](#). *Mol Cell* 71(3): 468-480.
- Schindelin, J., Arganda-Carreras, I., Frise, E., Kaynig, V., Longair, M., Pietzsch, T., Preibisch, S., Rueden, C., Saalfeld, S., Schmid, B., et al. (2012). [Fiji: an open-source platform for biological-image analysis](#). *Nature Methods* 9(7): 676-682.
- Stasevich, T. J., Hayashi-Takanaka, Y., Sato, Y., Maehara, K., Ohkawa, Y., Sakata-Sogawa, K., Tokunaga, M., Nagase, T., Nozaki, N., McNally, J. G., et al. (2014). [Regulation of RNA polymerase II activation by histone acetylation in single living cells](#). *Nature* 516(7530): 272-275.
- Steurer, B., Janssens, R. C., Geverts, B., Geijer, M. E., Wienholz, F., Theil, A. F., Chang, J., Dealy, S., Pothof, J., van Cappellen, W. A., et al. (2018). [Live-cell analysis of endogenous GFP-RPB1 uncovers rapid turnover of initiating and promoter-paused RNA Polymerase II](#). *PNAS* 115(19), E4368–E4376.
- Takei, Y., Shah, S., Harvey, S., Qi, L. S. and Cai, L. (2017). [Multiplexed Dynamic Imaging of Genomic Loci by Combined CRISPR Imaging and DNA Sequential FISH](#). *Biophys J* 112(9): 1773-1776.
- Tantale, K., Mueller, F., Kozulic-Pirher, A., Lesne, A., Victor, J.-M., Robert, M.-C., Capozi, S., Chouaib, R., Bäcker, V., Mateos-Langerak, J., et al. (2016). [A single-molecule view of transcription reveals convoys of RNA polymerases and multi-scale bursting](#). *Nature Communications* 7(1): 12248.
- Tinevez, J. Y., Perry, N., Schindelin, J., Hoopes, G. M., Reynolds, G. D., Laplantine, E., Bednarek, S. Y., Shorte, S. L. and Eliceiri, K. W. (2017). [TrackMate: An open and extensible platform for single-particle tracking](#). *Methods* 115: 80-90.
- Tokunaga, M., Imamoto, N. and Sakata-Sogawa, K. (2008). [Highly inclined thin illumination enables clear single-molecule imaging in cells](#). *Nat Methods* 5(2): 159-161.

Patterned Substrate of Mobile and Immobile Ligands to Probe EphA2 Receptor ClusteringZhongwen Chen^{1, \$,*}, Kabir H. Biswas², and Jay T. Groves³¹Multiscale Research Institute of Complex Systems, Fudan University, Shanghai, China²College of Health and Life Sciences, Hamad Bin Khalifa University, Doha, Qatar³Department of Chemistry, University of California, Berkeley, California, USA^{\$}Current address: Interdisciplinary Research Center on Biology and Chemistry, Shanghai Institute of Organic Chemistry, Chinese Academy of Sciences, Shanghai, China*For correspondence: chenzw@sioc.ac.cn

[Abstract] A multitude of membrane-localized receptors are utilized by cells to integrate both biochemical and physical signals from their microenvironment. The clustering of membrane receptors is widely presumed to have functional consequences for subsequent signal transduction. However, it is experimentally challenging to selectively manipulate receptor clustering without altering other biochemical aspects of the cellular system. Here, we describe a method to fabricate multicomponent, ligand-functionalized microarrays, for spatially segregated and simultaneous monitoring of receptor activation and signaling in individual living cells. While existing micropatterning techniques allow for the display of fixed ligands, this protocol uniquely allows for functionalization of both mobile membrane corrals and immobile polymers with selective ligands, as well as microscopic monitoring of cognate receptor activation at the cell membrane interface. This protocol has been developed to study the effects of clustering on EphA2 signaling transduction. It is potentially applicable to multiple cell signaling systems, or microbe/host interactions.

Graphical abstract:

A side-by-side comparison of clustered or non-clustered EphA2 receptor signaling in a single cell.

Keywords: Supported lipid bilayer, Micropatterning, EphA2 receptor, Receptor clustering, Signaling transduction

[Background] Cells engage membrane-localized receptors to sense various signals present in their local environment, and respond to these signals appropriately to survive, organize, and proliferate. The signals presented to the cells include both soluble ligands, as well as ligands that are present in the extracellular matrix (ECM), or displayed on the membranes of other cells (also referred to as juxtacrine signaling systems). Membrane receptor interactions of the latter types of ligands enable sensing of the spatial organization of receptor-ligand complexes at the cell-cell interface, and ECM rigidity (Groves and Kuriyan, 2010; Manz and Groves, 2010). A number of these signaling systems have been reconstituted on synthetic supported lipid bilayers in a hybrid format, wherein a live cell interacts with the supported lipid bilayer, recapitulating many of the features of individual receptor types (Biswas and Groves, 2019). These include both reconstitution of the individual receptor signaling system, or a combination of two different receptor signaling systems, to recapitulate the cellular exposure to multiple signals simultaneously, and ensuing signaling crosstalk between the receptors (Chen *et al.*, 2018).

Assembly of cell surface receptors into clusters or organized arrays is a common feature of cell membranes, and has long been implicated as an important factor for modulating signaling activity. However, it is not straightforward to deconvolve the contribution of receptor clustering on signaling itself. A major reason for this is that chemical perturbation of assemblies, such as those achieved with pharmacological agents or mutations (Davis *et al.*, 1994; Seiradake *et al.*, 2013; Bugaj *et al.*, 2013, 2015; Schaupp *et al.*, 2014; Wu *et al.*, 2015; Su *et al.*, 2016), are likely to produce side effects on the cell, other than modulating molecular assembly. Therefore, we seek to modulate spatial organization of receptors by controlling ligand mobility, instead of perturbing intracellular components. In the current protocol, we developed a technique wherein a ligand of interest is displayed in both mobile and immobile configurations, and spatially juxtaposed on length scales small enough to enable a side-by-side comparison within an individual living cell. The immobile ligands are displayed on a functionalized poly L-Lysine-poly ethylene glycol [PLL-(g)-PEG] scaffold, while the mobile ligands are displayed on supported lipid membranes, which allow cluster formation. This method has been applied to the study of EphA2 receptor signaling (Chen *et al.*, 2021), and is potentially applicable to other cell signaling systems or microbe/host interactions (Wong *et al.*, 2021).

Materials and Reagents

1. Round bottom flask (25 mL)
2. Glass coverslips (Thorlabs, catalog number: CG15XH)
3. PLL(20)-g[3.5]-PEG(2)/PEG(3.4)-biotin(50%) (Susos, <https://susos.com/shop/pll20-g3-5-peg2peg3-4-biotin50-2/>)
4. PLL(20)-g[3.5]-PEG(3.4)-NTA (Susos, <https://susos.com/shop/pll20-g3-5-peg3-4-nta-2/>)
5. PLL(20)-g[3.5]-PEG(2) (Susos, <https://susos.com/shop/pll20-g3-5-peg2/>)

6. 18:1 (Δ 9-Cis) PC (DOPC) (Avanti, catalog number: 850375)
7. 18:1 DGS-NTA(Ni) (Avanti, catalog number: 790404)
8. NeutrAvidin (ThermoFisher, catalog number: 22831)
9. RGD-biotin (Vivitide, catalog number: PCI-3697-PI)
10. Tris (ThermoFisher, catalog number: 15504020)
11. NaCl
12. KCl
13. CaCl₂
14. MgCl₂
15. D-glucose
16. EphrinA1 protein (purified in the Groves' lab, plasmid available upon request)
17. Alexa Fluor™ 680 dye (ThermoFisher, catalog number: A37574)
18. Chromium-quartz photomask

We use a 5-inch photomask that was fabricated in the Mechanobiology Institute Core facility, at the National University of Singapore. The photomask can also be purchased from other manufacturing companies.
19. TBS buffer (see Recipes)
20. Imaging buffer (see Recipes)

Equipment

1. Imaging chamber (ThermoFisher, Attofluor™ cell imaging chamber, catalog number: A7816)
2. Water bath
3. UVO cleaner (Jelight Company INC, hbUVO Cleaner, model 342)
4. Rotary evaporator (with a standard dry ice condenser, and equipped with a vacuum pump,
<https://www.asynt.com/product/ika-dry-ice-rotary-evaporator-range/>, or
<https://www.coleparmer.co.uk/i/buchi-23012c000-rotary-evaporator-dry-ice-condenser-220v/2301220>)
5. Tip sonicator (<https://www.sonicator.com/collections/sonicators/products/q125-sonicator>)

Procedure

This technique requires preparation of (A) small unilamellar vesicles (SUVs), (B) micropatterned polymer surface on a glass substrate, and (C) assembly of membrane arrays on the micropatterned substrate and protein functionalization (Figure 1). The SUVs can be prepared in advance and stored at 4°C for up to 2 weeks. Steps (B) and (C) take 2–3 days, depending on the flexible incubation times.

Briefly, PLL-(g)-PEG scaffold polymers are first coated on a glass coverslip, followed by selective deep UV etching with a photomask and lipid vesicle deposition, to generate regions of immobile polymers and

mobile lipid membranes. The ephrinA1 ligands are then functionalized to the substrate in mobile and immobile configurations, to probe EphA2 receptor clustering in cells.

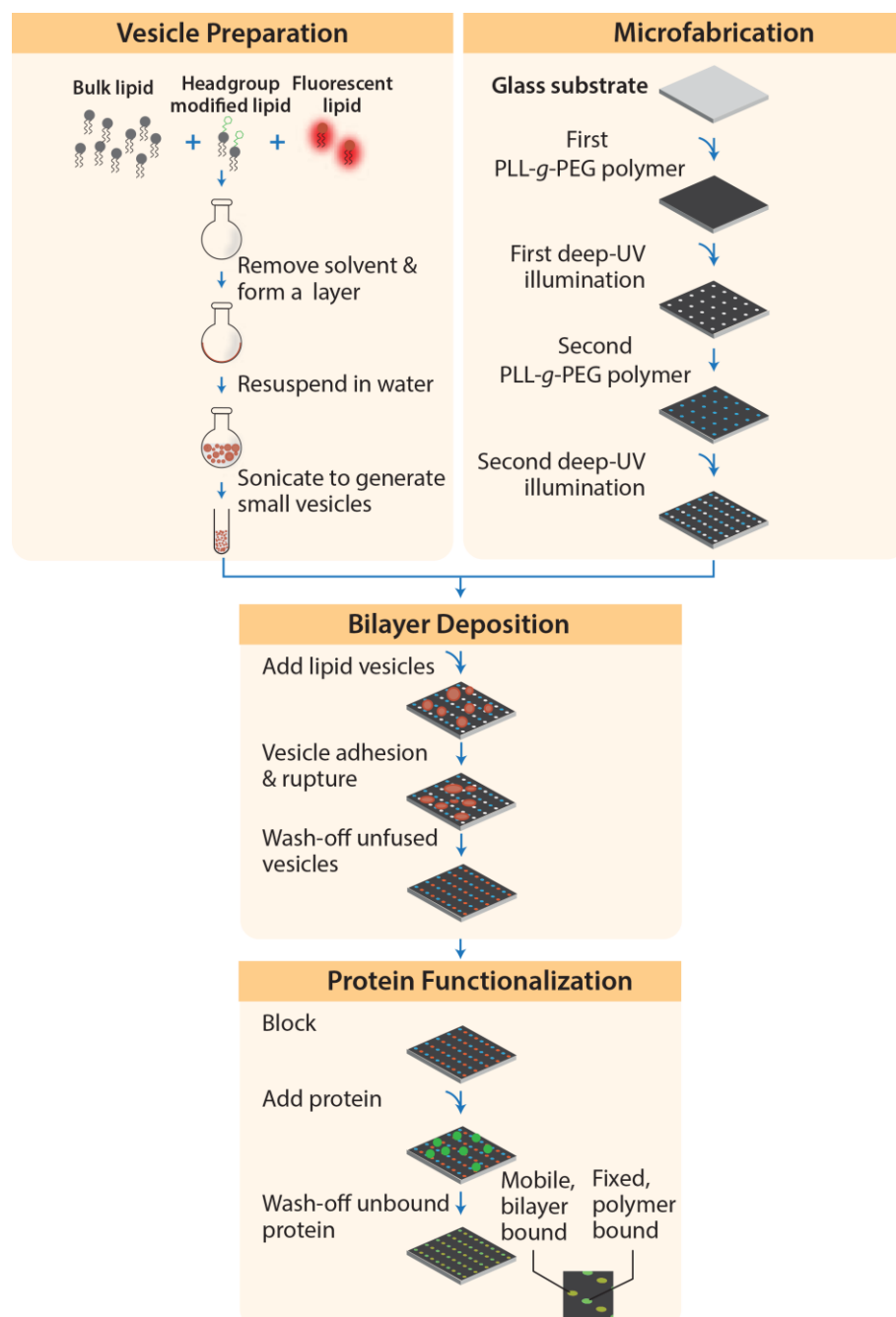


Figure 1. Procedures to Fabricate Micropatterned Substrate of Mobile and Immobile Ligands.

A. Vesicle preparation

For this step, the audiences can refer to a more detailed protocol (Lin *et al.*, 2009).

1. Prepare lipid films, by mixing required amounts of various lipid molecules [96% DOPC + 4% DGS-NTA(Ni), with a total mass of 2 mg], which are dissolved in chloroform in a round bottom flask, followed by evaporation of chloroform using a rotary evaporator under vacuum pumping

and 50°C water bath, leading to the formation of a thin lipid film in the flask. During this procedure, slowly lower the round bottom flask to the water bath, to avoid chloroform boiling.

2. Resuspend the lipid film in 2 mL of deionized water by pipetting, allowing the formation of large and often multilamellar vesicles (1 mg/mL).
3. Sonicate the vesicle suspensions in ice using a probe tip sonicator, to generate SUVs. Typically, use a program of '10 s on, and 5 s off' for 8–10 cycles for sonication. Transfer the SUV suspension to a fresh tube, and centrifuge at 20,000 × g and 4°C for 2 h, to remove any debris. Transfer the supernatant to a fresh tube, and store at 4°C until further use. The SUVs can be stored for up to 2 weeks, to form a good lipid bilayer.

B. Microfabrication

Micropatterned surfaces are prepared on glass substrates, using the deep ultraviolet (UV) etching method.

1. Clean glass coverslips by sonication in a 1:1 mixture of isopropanol and water for 15–30 min, followed by overnight (or longer) incubation in 50% H₂SO₄ solution. Before usage, take the coverslips out of H₂SO₄, rinse with water, and expose the glass coverslips to UV light in an enclosed UVO cleaner for 10 min. Rinse with water, and dry by N₂ jet.
2. Incubate the glass coverslips with PLL(20)-g[3.5]-PEG(2)/PEG(3.4)-biotin(50%) at a concentration of 0.1 mg/mL at room temperature for 2 h, or overnight. To reduce the usage of reagents, drop ~30 μL of the incubating solution in parafilm, and lay the glass coverslips on top of it.
3. Rinse the substrates with water to remove excess polymer, and dry by N₂ jet.
4. Drop ~1.5 μL of water on the micropatterned area (1 cm × 1 cm square) of a chromium-quartz photomask, and lay the polymer-coated glass substrate on its top, to ensure close contact. Expose the substrates to deep UV light for 9–12 min in a UVO cleaner. The UV light-exposed polymer will be degraded. Rinse the substrates with excess water to remove any degraded polymer.
5. Incubate the same glass substrates with PLL(20)-g[3.5]-PEG(3.4)-NTA at a concentration of 0.1 mg/mL at room temperature for 2 h, and repeat the deep UV etching and washing procedures. After the second etching, the glass substrates should be used for lipid bilayer deposition immediately.

C. Bilayer deposition and protein functionalization

1. Before usage, mix SUVs with TBS buffer in 1:1 ratio.
2. Incubate the micropatterned substrates with SUV solution for 5 min, to allow the self-assembly of lipid bilayers in regions of the substrates that were UV etched in the previous step.
3. Rinse the substrates with excess TBS buffer, and assemble the glass coverslips into a cell culture imaging chamber, under the aqueous environment.

4. Block the substrates with bovine serum albumin (BSA) solution (0.05–0.1 mg/mL in TBS buffer) at room temperature for 2h, or at 4°C overnight.
5. Wash the substrates with TBS buffer, and incubate with NeutrAvidin (1.5 µg/mL) for 15 min, to bind surface biotin groups.
6. Wash excess NeutrAvidin with TBS buffer, and incubate with ephrinA1-His 10 (purified ephrinA1 protein with a 10-histidine tail in the C-terminus, labeled with Alexa Fluor™ 680), and RGD-biotin, for an additional 60–90 min. The ephrinA1-His 10 will bind to both DGS-NTA(Ni) lipids on mobile regions, and PLL(20)-g[3.5]-PEG(3.4)-NTA polymers on immobile regions, while RGD-biotin will bind to NeutrAvidin. The RGD peptides can bind integrins at the cell membrane, to allow cell spreading, during which cells dynamically interact with multiple ephrinA1-functionalized mobile or immobile regions.
7. Remove unbound proteins by washing with imaging buffer.
8. Check fluorescence intensity of mobile and immobile ephrinA1 under a microscope.
9. The substrates are ready for use in a live cell experiment. Prepare cells in the imaging buffer, and seed a low density of cells into the substrate chamber at 37°C for live imaging. The cellular EphA2 receptors will form clusters only after binding with mobile ephrinA1 (Figure 2).

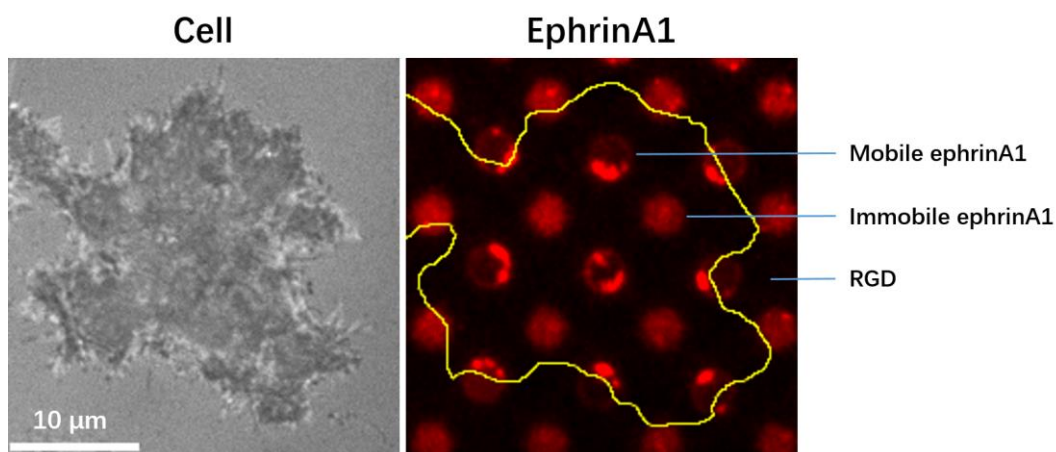


Figure 2. Images of a cell spreading on the micropatterned substrate. Left: The RIC (reflective interference contrast) image showing the cell surface that is adhered to the substrate; Right: The fluorescent image of micropatterned ephrinA1, with the yellow line marking the contour of the cell.

Data analysis

The substrates were observed under a standard fluorescence microscope to compare the fluorescence intensity of mobile and immobile ephrinA1 regions. The mobility of ephrinA1 on lipid bilayers was checked by fluorescence recovery after photobleaching (FRAP).

Notes

© Copyright Chen et al.

This article is distributed under the terms of the [Creative Commons Attribution License](#) (CC BY 4.0).

1. The mobile and immobile regions are aligned randomly in two independent UV-etch steps. Usually, the two regions are overlapped in some of the areas, but it is easy to find non-overlapped regions in a centimeter-sized substrate.
2. The mobile and immobile ephrinA1 intensity may not be the same. Titrate PLL(20)-g[3.5]-PEG(3.4)-NTA with non-reactive PLL(20)-g[3.5]-PEG(2), to modify surface ephrinA1 intensity on immobile regions, or change the lipids molar ratio of DOPC and DGS-NTA(Ni), to modify ephrinA1 intensity on mobile regions.

Recipes

1. TBS buffer
25 mM Tris
150 mM NaCl
3 mM KCl
2. Imaging buffer
25 mM Tris
140 mM NaCl
3 mM KCl
2 mM CaCl₂
1 mM MgCl₂
5.5 mM D-glucose

Acknowledgments

This work was supported by the National Institutes of Health, National Cancer Institute Physical Sciences in Oncology Network Project 1-U01CA202241, and Shanghai Pujiang Program (20PJ1400800). This protocol is derived from published papers (Chen *et al.*, 2018, 2021).

Competing interests

The authors declare no conflicts of interest or competing interests.

References

1. Biswas, K. H. and Groves, J. T. (2019). [Hybrid Live Cell-Supported Membrane Interfaces for Signaling Studies](#). *Annu Rev Biophys* 48: 537-562.
2. Bugaj, L. J., Choksi, A. T., Mesuda, C. K., Kane, R. S. and Schaffer, D. V. (2013). [Optogenetic protein clustering and signaling activation in mammalian cells](#). *Nat Methods* 10(3): 249-252.

3. Bugaj, L. J., Spelke, D. P., Mesuda, C. K., Varedi, M., Kane, R. S. and Schaffer, D. V. (2015). [Regulation of endogenous transmembrane receptors through optogenetic Cry2 clustering](#). *Nat Commun* 6: 6898.
4. Chen, Z., Oh, D., Biswas, K. H., Yu, C. H., Zaidel-Bar, R. and Groves, J. T. (2018). [Spatially modulated ephrinA1:EphA2 signaling increases local contractility and global focal adhesion dynamics to promote cell motility](#). *Proc Natl Acad Sci U S A* 115(25): E5696-E5705.
5. Chen, Z., Oh, D., Biswas, K. H., Zaidel-Bar, R. and Groves, J. T. (2021). [Probing the effect of clustering on EphA2 receptor signaling efficiency by subcellular control of ligand-receptor mobility](#). *Elife* 10: e67379.
6. Davis, S., Gale, N. W., Aldrich, T. H., Maisonpierre, P. C., Lhotak, V., Pawson, T., Goldfarb, M. and Yancopoulos, G. D. (1994). [Ligands for EPH-related receptor tyrosine kinases that require membrane attachment or clustering for activity](#). *Science* 266(5186): 816-819.
7. Groves, J. T. and Kuriyan, J. (2010). [Molecular mechanisms in signal transduction at the membrane](#). *Nat Struct Mol Biol* 17(6): 659-665.
8. Lin, W. C., Yu, C. H., Triffo, S. and Groves, J. T. (2010). [Supported membrane formation, characterization, functionalization, and patterning for application in biological science and technology](#). *Curr Protoc Chem Biol* 2(4): 235-269.
9. Manz, B. N. and Groves, J. T. (2010). [Spatial organization and signal transduction at intercellular junctions](#). *Nat Rev Mol Cell Biol* 11(5): 342-352.
10. Schaupp, A., Sabet, O., Dudanova, I., Ponserre, M., Bastiaens, P. and Klein, R. (2014). [The composition of EphB2 clusters determines the strength in the cellular repulsion response](#). *J Cell Biol* 204(3): 409-422.
11. Seiradake, E., Schaupp, A., del Toro Ruiz, D., Kaufmann, R., Mitakidis, N., Harlos, K., Aricescu, A. R., Klein, R. and Jones, E. Y. (2013). [Structurally encoded intraclass differences in EphA clusters drive distinct cell responses](#). *Nat Struct Mol Biol* 20(8): 958-964.
12. Su, X., Ditlev, J. A., Hui, E., Xing, W., Banjade, S., Okrut, J., King, D. S., Taunton, J., Rosen, M. K. and Vale, R. D. (2016). [Phase separation of signaling molecules promotes T cell receptor signal transduction](#). *Science* 352(6285): 595-599.
13. Wong, J. J., Chen, Z., Chung, J. K., Groves, J. T. and Jardetzky, T. S. (2021). [EphrinB2 clustering by Nipah virus G is required to activate and trap F intermediates at supported lipid bilayer-cell interfaces](#). *Sci Adv* 7(5): eabe1235.
14. Wu, Y., Kanchanawong, P. and Zaidel-Bar, R. (2015). [Actin-delimited adhesion-independent clustering of E-cadherin forms the nanoscale building blocks of adherens junctions](#). *Dev Cell* 32(2): 139-154.

CRISPR/Cas9 Gene Editing of HeLa Cells to Tag Proteins with mNeonGreen

Sachin Surve* and Alexander Sorkin

Department of Cell Biology, University of Pittsburgh School of Medicine, Pittsburgh, PA, USA

*For correspondence: svs23@pitt.edu

[Abstract] Subcellular localization dynamics of proteins involved in signal transduction processes is crucial in determining the signaling outcome. However, there is very limited information about the localization of endogenous signaling proteins in living cells. For example, biochemical mechanisms underlying the signaling pathway from epidermal growth factor (EGF) receptor (EGFR) to RAS-RAF and ERK1/2/MAPK are well understood, whereas the operational domains of this pathway in the cell remain poorly characterized. Tagging of endogenous components of signaling pathways with fluorescent proteins allows more accurate characterization of their intracellular dynamics at their native expression levels controlled by endogenous regulatory mechanisms, thus avoiding possible tainting effects of overexpression and mistargeting. In this study, we describe methodological approaches to label components of the EGFR-RAS-MAPK pathway, such as Grb2, KRAS, and NRAS, with the fluorescent protein mNeonGreen (mNG) using CRISPR/Cas9 gene-editing, as well as generation of homozygous single-cell clones of the edited target protein.

Keywords: mNeonGreen, EGF receptor, KRAS, NRAS, CRISPR-Cas9

[Background] The epidermal growth factor (EGF) receptor (EGFR) is activated by EGF or other ligands at the cell surface, which triggers the RAS-RAF-MAPK/ERK1/2 signaling pathway involved in cell proliferation, differentiation, survival, and motility (Karnoub and Weinberg, 2008). Activated EGFR is endocytosed and accumulated in early endosomes, where it is either recycled back to the plasma membrane or targeted for lysosomal degradation. Whether active EGFR continues to signal through the RAS-ERK1/2 axis from endosomes to sustain ERK1/2 activation remains controversial and is under debate in the literature (reviewed in von Zastrow and Sorkin, 2021). Evidence for the endosomal signaling to ERK1/2 is based on the detection of components of the ERK1/2 pathway in endosomes in cells stimulated with EGF (Pol *et al.*, 1998; Howe *et al.*, 2001; Jiang and Sorkin, 2002; Lu *et al.*, 2009; Schmick *et al.*, 2014). However, these observations were made either with overexpressed recombinant proteins or with chemically fixed cells or by subcellular fractionation, approaches that may not correctly report subcellular localization of endogenous proteins. We initially studied the spatio-temporal dynamics of the endogenous tagged EGFR and components of the ERK1/2 pathway by fluorescently tagging these proteins using gene editing techniques utilizing zinc finger nucleases (ZFN) and transcription activator-like effector nucleases (TALEN) (Pinilla-Macua *et al.*, 2017, 2016). Subsequently, we switched to using the CRISPR-Cas9 system (Surve *et al.*, 2019; Surve *et al.*, 2021) for gene-editing. We selected for these studies a subvariant of HeLa cells that we consistently used in the laboratory because they

express EGFR at levels similar to those in many mammalian cells *in vivo*, and because we have rigorously characterized the EGFR endocytic trafficking system in these cells.

CRISPR-Cas9 has proven to be versatile and efficient method of gene editing compared to ZFNs and TALEN, and is widely used for gene knockouts, gene activation, gene inhibition, and knock-ins. The fascinating discovery and evolution of CRISPR technology is beyond scope of this article, and excellent reviews on this topic can be found elsewhere. We used this technology to tag KRAS, NRAS, and Grb2. Generally, there are two main components of CRISPR-Cas9 technology: i) Cas9—a RNA guided endonuclease, ii) a short non-coding guide RNA consisting of a target complementary CRISPR RNA (crRNA) and a trans-activating crRNA (tracrRNA) that shuttles Cas9 to a specific site. These components are delivered inside the cells via plasmids or via direct delivery of an *in vitro* generated complex of purified Cas9 and purified sgRNA (Ran *et al.*, 2013). Following the delivery, gRNA through Watson-Crick base pairing binds to its target DNA sequence, and Cas9 makes a double stranded break (DSB) near the PAM site of gRNA. The DSB is either repaired by the error prone non-homologous end joining (NHEJ) mechanism or by precise homology dependent repair (HDR) mechanism. In case of gene tagging, an additional component is provided in the form of a repair template, *i.e.*, a donor DNA containing sequences of a fluorescent protein or small tags such as His, HA, or MYC, which through HDR allows the insertion of the tag of interest. HDR mechanism of repair is inherently inefficient, resulting in lower yields of clones of cells with the in-frame incorporated tag compared to generation of knockout clones, which generally involves NHEJ. The protocol here describes the variations (Table 1) in the approach by which gene tagging (knock-in) can be achieved in transformed cell lines like HeLa.

Materials and Reagents

1. CellTrics 50 µm sterile Disposable Filters (Sysmex, catalog number: 04-004-2327)
2. 96-well plate (Ibidi, 15 µ-Plate 96 Well Black)
3. 12-well cell culture plate (Corning, catalog number: 3513)
4. 25 or 75 cm² cell culture flasks (Corning, catalog number: 430639 or 430641U)
5. 15 mL tube conical base (Sarstedt, catalog number: 62.554.205)
6. DNA oligonucleotide primers from IDT
7. GeneArt Precision gRNA Synthesis kit (Invitrogen, catalog number: A29377)
8. Tracr Fragment + T7 Primer Mix (contains the universal PCR amplification primers and the 80-nt constant region of the crRNA/tracrRNA) (Invitrogen, catalog number: A29377)
9. Phusion™ High-Fidelity PCR Master Mix (2×) (Invitrogen, catalog number: A29377)
10. Nuclease free water
11. dNTP mix (10 mM each of dATP, dGTP, dCTP, dTTP) (NEB, catalog number: N0447)
12. 5× TranscriptAid™ Reaction Buffer (Invitrogen, catalog number: A29377)
13. TranscriptAid™ Enzyme Mix (Invitrogen, catalog number: A29377)
14. DNase I (Invitrogen, catalog number: A29377)
15. Single stranded DNA (ssDNA) oligos from IDT

16. NEBuilder® HiFi DNA Assembly Master Mix (NEB, catalog number: E2621)
17. pSpCas9(BB)-2A-Puro (PX459) plasmid (Addgene plasmid # 62988)
18. BbsI (NEB, catalog number: R0539)
19. NEB Buffer 2 (NEB, catalog number: B7002S)
20. NEB® 5- α Competent *E. coli* (High Efficiency) (NEB, catalog number: C2987)
21. Ampicillin Agar plates and Kanamycin Agar plates
22. NEB buffer 2.1 (NEB, catalog number: B7202)
23. QIAquick PCR Purification Kit (Qiagen, catalog number: 28104)
24. Synthetic double stranded donor DNAs from IDT
25. Phusion High-Fidelity DNA Polymerase (NEB, catalog number: M0530)
26. Phusion GC buffer 5× (NEB, catalog number: B0519)
27. Zero Blunt™ TOPO™ PCR Cloning Kit (Invitrogen, catalog number: 45-1245)
28. EcoRI-HF (NEB, catalog number: R3101)
29. CutSmart Buffer 10× (NEB, catalog number: B6004)
30. QIAquick Gel Extraction Kit (Qiagen, catalog number: 28704)
31. XbaI (NEB, catalog number: R0145)
32. Easy-Fusion Halo plasmid (Addgene plasmid # 112850)
33. EcoRI-HF (NEB, catalog number: R3101)
34. Aval (NEB, catalog number: R0152)
35. HincII (NEB, catalog number: R0103)
36. DMEM (Gibco, catalog number: 11965-092) with 10% FBS (Invitrogen, catalog number: 16140071)
37. DPBS (without Ca²⁺ or Mg²⁺) (Gibco, catalog number: 14190-144)
38. Trypsin (Gibco, catalog number: 25200-056)
39. Neon Transfection System (Invitrogen, catalog number: MPK5000)
40. Neon Transfection System 10 μ L Kit (Invitrogen, catalog number: MPK1025)
41. Buffer R
42. Puromycin (Sigma-Aldrich, catalog number: P8833)
43. Platinum Cas 9 (Invitrogen, catalog number: A36498)
44. BD FACSAria III sorter fitted with 488 100 mW Trigon laser and 100 μ m nozzle (BD Biosciences)
45. Nocodazole (Sigma-Aldrich, catalog number: M1404)
46. Lipofectamine 3000 (Invitrogen, catalog number: L3000001)
47. OptiMEM (Invitrogen, catalog number: 31985062)
48. Recombinant KRAS rabbit monoclonal antibody (Thermo Fisher Scientific, catalog number: 703345)
49. Cell Sorting buffer (see Recipes)
50. TGH buffer (see Recipes)

Software

1. <https://www.benchling.com/>. Benchling is a cloud-based informatics platform that is free to academic

researchers. It provides design tools for DNA, oligonucleotides, and amino acids.

2. <https://portals.broadinstitute.org/gppx/crispick/>. The website is hosted by the Genetic Perturbation Platform of the Broad institute, MA, USA.
3. <http://chopchop.cbu.uib.no/>. CHOPCHOP is a web-based tool, designed by the Valen group at the University of Bergen, Norway. The website is for non-profit and academic use only.
4. <https://nebuilder.neb.com>. The Web tool can be used to design primers for HiFi DNA assembly or Gibson assembly.

Procedure

Experimental Design

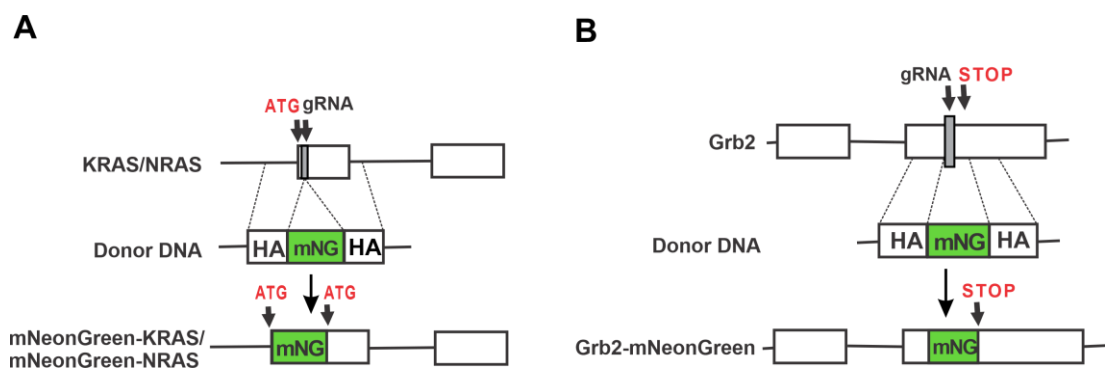


Figure 1. Schematics of insertion of mNG in KRAS, NRAS, and Grb2.

mNG sequence was inserted at amino terminus of *KRAS* and *NRAS* genes (A) and at carboxy terminus of *Grb2* gene (B). Donor DNAs were generated for all three genes with homology arms ranging from 500 to 1,000 bp. ATG, Start codon; STOP, Stop codon; HA, Homology Arm; mNG, mNeongreen; gRNA-guide RNA; empty boxes represent exons of *KRAS*, *NRAS* and *Grb2*.

Table 1. Sources of the components used to tag the genes

	<i>KRAS</i>	<i>NRAS</i>	<i>Grb2</i>
Cas9	Commercial purified enzyme	Commercial purified enzyme	Plasmid -PX459
gRNA	<i>In vitro</i> transcribed	<i>In vitro</i> transcribed	Cloned in Plasmid- PX459
Donor	Synthetic gene fragment	Synthetic gene fragment	Homology arms and mNG fragments cloned in a plasmid
Delivery method	Electroporation	Electroporation	Transfection via Lipofectamine

A. Generation of gRNAs for KRAS, NRAS, and Grb2

1. *In-vitro* Synthesis of gRNAs for tagging *KRAS* and *NRAS*
 - a. Identification of the target gRNA

We used amino termini of both *KRAS* and *NRAS* genes to tag with mNeonGreen fluorescent protein sequence because all RAS proteins are processed at their carboxy termini (Figure 1). Several guide RNA design tools are available online. We routinely use Benchling, Broad Institute GPP (now CRISPRick), and CHOPCHOP, among others, to design target gRNAs. Using these tools, two targets for both *KRAS* and *NRAS* were identified, which were very close to the Start codons of both the genes. Order two complementary primers for each target (Table 2).

Table 2. Primers for in vitro translation of gRNAs

Primer	Sequence 5'---3'	
Kras_1F	TAATACGACTCACTATAGGAATATAAAGTTGTGGTAGT	Target 1
Kras_1R	TTCTAGCTCTAAAACACTACCACAAGTTATATTTC	Target 1
Kras_2F	TAATACGACTCACTATAGAATGACTGAATATAAACTTG	Target 2
Kras_2R	TTCTAGCTCTAAAACCAAGTTATTCAGTCATT	Target 2
Nras_1F	TAATACGACTCACTATAGGACTGAGTACAAACTGGTGG	Target 1
Nras_1R	TTCTAGCTCTAAAACCCACCAGTTGTACTCAGTC	Target 1
Nras_2F	TAATACGACTCACTATAGAATGACTGAGTACAAACTGG	Target 2
Nras_2R	TTCTAGCTCTAAAACCCAGTTGTACTCAGTCATT	Target 2

- i. Dilute target primers to a stock solution 100 µM in 1× TE buffer.
 - ii. Prepare a mixture of target primers of 10 µM stock solution by adding 10 µL each of the 100 µM forward and reverse target primer to 80 µL of nuclease-free water.
 - iii. Prepare the 0.3 µM target primer mix working solution by diluting 3 µL of the 10 µM target primer mix stock solution in 97 µL of nuclease-free water.
- b. Assembly of the gRNA DNA templates

This step generates the DNA template required for the *in vitro* transcription of the gRNAs. Thaw the reagents from GeneArt Precision gRNA synthesis kit on ice. Mix and centrifuge contents of all the vials. Set up the following PCR assembly reaction in a 25-µL volume, adding the reaction components in the order given (Table 3).

Table 3. Components to make gRNA DNA template

Phusion™ High-Fidelity PCR Master Mix (2×)	12.5 µL
Tracr Fragment + T7 Primer Mix	1 µL
0.3 µM Target F/R oligonucleotide mix	1 µL
Nuclease free water	10.5 µL

Since the PCR product is expected to be very short (120 bp), perform a two-step assembly PCR using following parameters (Table 4).

Table 4. PCR parameters to generate gRNA DNA template

Cycle Step	Temperature	Time	Cycles
Initial denaturation	98°C	10 s	1×
Denaturation	98°C	5 s	32×
Annealing	55°C	15 s	32×
Final extension	72°C	1 min	1×
Hold	4°C	Hold	1×

c. *In vitro* transcription (IVT) of gRNAs

Use the gRNA DNA template generated in step A.1.b for *in vitro* transcription of gRNAs. Set up the reaction as follows in the order given (Table 5).

Table 5. Components of IVT reaction

NTP mix (100 mM each of ATP, GTP, CTP, UTP)	8 µL
gRNA DNA template (from PCR assembly)	6 µL
5× TranscriptAid™ Reaction Buffer	4 µL
TranscriptAid™ Enzyme Mix	2 µL

Mix the contents thoroughly and centrifuge. Carry out the IVT reaction for 3 h at 37°C.

d. Removal of the DNA template by DNase I digestion

It is helpful to remove DNA from IVT reaction so that it does not interfere with the subsequent applications of the RNA transcript.

- i. Incubate the IVT reaction mix with 1 µL of DNase I (1 U/µL) immediately after the IVT reaction and incubate at 37°C for 15 min.

e. Purification of gRNAs using the columns and the buffers supplied in the kit

- i. Dilute the IVT reaction to 200 µL with nuclease-free water and add 100 µL of Binding Buffer. Mix by pipetting.
- ii. Add 300 µL of ethanol (>96%) and mix by pipetting.
- iii. Transfer the mixture to the GeneJET™ RNA Purification Micro Column (preassembled with a collection tube) and centrifuge for 30–60 s at 14,000 × g. Discard the flow-through
- iv. Wash the bound RNA with 700 µL Wash Buffer 1 and Wash Buffer 2.
- v. Centrifuge the empty purification column for an additional 60 s at 14,000 × g to completely remove any residual Wash Buffer.
- vi. Transfer the purification column to a clean 1.5-mL Collection Tube.

vii. Add 10 μ L of nuclease-free water to the center of the purification column filter, and centrifuge for 60 s at 14,000 $\times g$ to elute the RNA.

viii. Store eluted gRNA at -20°C until use. For prolonged storage, store the gRNA at -80°C.

Note: Follow all the necessary precautions while working with RNA to avoid its degradation or contamination and refer to the manufacturer's instructions for detailed guidelines for generating gRNAs.

2. Cloning of gRNAs for tagging Grb2

a. Identification of the target gRNA

Grb2 was tagged with mNG at its carboxy terminal. Cloning of Grb2 gRNAs was performed using NEBuilder HiFi DNA assembly mix which allows assembly of a linear plasmid and a single stranded DNA fragment, just as multiple DNA fragments assembly. Similar to RAS proteins, two target gRNAs for Grb2 were identified using Benchling and Broad Institute GPP (now CRISPRick). The following target gRNA sequence oligos were ordered as ssDNA from IDT (Table 6). Underlined sequences represent the actual target gRNA sequence flanked by overlapping sequences around BbsI restriction enzyme cut site from PX459.

Table 6. ssDNA oligos for Grb2 gRNA

grb2-RNA_T1	ATCTTGAAAGGACGAAACACC <u>GGTTAGACGTTCCGGTTC</u> ACGGGTTTAGAGCT AGAAAATAGCAAGTT
grb2- gRNA_T2	ATCTTGAAAGGACG AAACACC <u>GGGCTTAG</u> ACGTTCCGGTT <u>CACGGTTAGAGCTAGAAAATAGCAAGTT</u>

b. Digestion of PX459 with BbsI

Linearize PX459 plasmid by digestion with BbsI at 37°C for 4 h (Table 7). Purify the digested plasmid using QIAquick PCR purification kit.

Table 7. PX459 digestion set up

PX459 Plasmid (500 ng/ μ L)	10 μ L
10× Buffer 2.1	2 μ L
BbsI (10 U/ μ L)	1 μ L
ddH ₂ O	7 μ L

c. Ligation of ssDNA into digested PX459

Centrifuge ssDNA oligo pellet and resuspend it in 1× TE to a final concentration of 100 μ M, which is further diluted to a working stock of 0.4 μ M in NEB Buffer 2. Set up the ligation reaction of linearized PX459 and ssDNA oligos in the order given below (Table 8).

Table 8. HiFi DNA assembly set up

Linear PX459 plasmid (50 ng)	1 µL
0.4 µM ssDNA stock	5 µL
ddH ₂ O	4 µL
NEBuilder® HiFi DNA Assembly Master Mix	10 µL

Incubate assembly reaction at 50°C for 1 h and transform 2 µL of the reaction mix into NEB 5-α Competent *E. coli* cells. Select the ampicillin resistant colonies by plating transformed *E. coli* cells onto Ampicillin agar plates.

d. Screening and confirmation of the positive clones

Select a few colonies from the ampicillin plates for plasmid isolation. Confirm the positive clones containing gRNA sequences by Sanger sequencing.

B. Generation of donor DNAs for tagging *KRAS*, *NRAS*, and *Grb2*

1. Cloning of donor DNA for tagging KRAS and NRAS

Donor DNAs with mNG sequence flanked by 5' and 3' homology arms of approximately 500 b each were obtained from IDT as gene fragments. The fragments were amplified using primers and cloned into pCRBluntII-TOPO plasmid using TOPO PCR cloning kit.

a. Amplification of the donor DNAs

Centrifuge vials containing gene fragments to collect the precipitate in 50 µL 1× TE. Amplify the synthetic DNA using Phusion polymerase (Tables 10 and 11) and primers mentioned below (Table 9).

Table 9. Primers for amplification of KRAS and NRAS synthetic donor DNA

Primers	5'-----3'
KRas_5HAF	AGGTGGGGTCCACTAGGAA
KRas_3HAR	CATATGATGTCACAATACCAAGAAC
NRas_5HAF	CAGAGGCAGTGGAGCTTG
NRas_3HAR	ACAATCAGACAGTCTCGCTACTAT

Table 10. PCR set up for amplification of KRAS and NRAS synthetic donor DNA

	KRAS donor DNA	NRAS Donor DNA
Donor gene fragment	5 µL	5 µL
Phusion GC Buffer 5×	10 µL	10 µL
10mM dNTP	1 µL	1 µL
5HAF	2.5 µL	2.5 µL
3HAR	2.5 µL	2.5 µL
Phusion Polymerase	1 µL	1 µL
Nuclease free water	28 µL	28 µL

Table 11. PCR parameters for amplification of KRAS and NRAS synthetic donor DNA

Cycle Step	Temperature		Time	Cycles
	KRAS donor	NRAS donor		
Initial denaturation	98°C	98°C	1 min	1×
Denaturation	98°C	98°C	15 s	30×
Annealing	61.6°C	64.7°C	15 s	30×
Extension	72°C	72°C	1 min	30×
Final extension	72°C	72°C	10 min	1×
Hold	4°C	4°C	Hold	1×

Perform gel purification of 1.68 kb of PCR products from KRAS and NRAS amplified donor DNAs.

- b. Ligation of amplified donor DNAs and pCRBluntII-TOPO plasmid

Set up ligation reaction of gel eluted KRAS and NRAS donor DNAs and pCRII-Blunt-TOPO plasmid in a 6 µL volume as follows (Table 12).

Table 12. Donor DNA and pCRBluntII-TOPO ligation set up

	KRAS Donor	NRAS Donor
Gel eluted fragment	2 µL	2 µL
Salt Solution	1 µL	1 µL
Nuclease free water	2 µL	2 µL
pCR-II-Blunt-TOPO	1 µL	1 µL

Incubate the ligation reaction at room temperature for 5 min. Transform 1–2 µL of the ligation mixture into competent *E. coli* and plate on kanamycin containing plates for selection.

- c. Screening and confirmation of donor DNAs

Select few colonies from kanamycin plates and grow them to isolate plasmid. Confirm the positive clones by EcoRI digestion and by Sanger sequencing to make sure there are no changes in the donor sequence.

d. Digestion and gel elution of donor DNA sequences from positive clones

The fragments are inserted in pCRII-Blunt-TOPO in such a way that EcoRI sites lie at the ends of the insert, allowing recovery of the insert by EcoRI digestion. Digest the positive clones containing donor sequences with EcoRI as follows (Table 13).

Table 13. Digestion of pCR-II-Blunt-TOPO-Donor plasmid

	KRAS	NRAS
pCR-II-Blunt-TOPO-Donor (1 µg/µL)	20 µL	20 µL
CutSmart buffer 10×	5 µL	5 µL
EcoRI-HF (10 U/µL)	3 µL	3 µL
Nuclease free water	22 µL	22 µL

Carry out the digestion for 3 h at 72°C. Gel elute the 1.68 kb bands from both the samples. Store the eluted donor fragments at -20°C.

Note: The donor PCR fragments were cloned to facilitate the confirmation of correct donor sequence using Sanger sequencing and to avoid repeated amplification. Purified PCR fragments can be used directly as donor DNAs, thus reducing the time of cloning.

2. Cloning of donor DNA for tagging *Grb2*

To clone donor DNA for *Grb2* gene editing, 5' and 3' homology arms (HA) were amplified from HeLa genomic DNA using primers designed by the NEbuilder algorithm (NEB), whereas KRAS donor DNA was used as a template to amplify mNG ORF. The primers add overlapping sequences to the resulting PCR fragments and these fragments are then assembled with Easy-Fusion Halo plasmid using NEBuilder® HiFi DNA Assembly Master Mix (Table 14).

Table 14. Component Fragments for HiFi DNA assembly

Name	Length (bp)	Produced by
5HA fragment	793	PCR
3HA fragment	743	PCR
mNG fragment	755	PCR
EasyFusion halo plasmid as backbone vector	2,927	Restriction Digestion

a. Amplification of homology arms (HA) and mNG ORF

Design primers with overlapping sequences using NEBuilder algorithm (Table 15). Amplify all three fragments required for the construction of the donor DNA as follows (Tables 16, 17, and 18).

Table 15. Primers for amplification of Grb2 homology arms and mNG ORF

Primer	5' 3'
Grb2-5HA_f	TATCGATAAGCTT GATATCGAGAGGCAGTGTGAGCCAG
Grb2-5HA_r	CTCCTCCTAAGACGTTCCGGTTACCGGG
Grb2-Neon_f	CCGGAACGTCTTAGGAGGAGGAGGATCAG
Grb2-Neon_r	TTGACTCTTACTTGTACAGCTCGTCCATG
Grb2-3HA_f	GCTGTACAAGTAAGAGTCAGAAAGCAATTATTTAAAG
Grb2-3HA_r	CCACCGCGGTGGCGGCCGCTTCTGAACCTCTGACCTTG

Table 16. PCR set up for amplification of Grb2 HAs

	5HA Fragment	3HA Fragment
HeLa genomic DNA (100 ng/µL)	3 µL	3 µL
Phusion GC Buffer 5×	10 µL	10 µL
10 mM dNTP	1 µL	1 µL
Grb2-5/3HA_f	2.5 µL	2.5 µL
Grb2-5/3HA_r	2.5 µL	2.5 µL
Phusion Polymerase	1 µL	1 µL
Nuclease free water	30 µL	30 µL

Table 17. PCR set up for amplification of mNG ORF

	mNG Fragment
mNG-KRAS donor (100 ng/µL)	3 µL
Phusion GC Buffer 5×	10 µL
10mM dNTP	1 µL
Grb2-Neon_f	2.5 µL
Grb2-Neon_r	2.5 µL
Phusion Polymerase	1 µL
Nuclease free water	30 µL

Table 18. PCR parameters for amplification of Grb2 HAs and mNG ORF

Cycle Step	Temperature			Time	Cycles
	5HA	3HA	mNG		
Initial denaturation	98°C	98°C	98°C	1 min	1×
Denaturation	98°C	98°C	98°C	15 s	30×
Annealing	64.4°C	60°C	59.6°C	15 s	30×
Extension	72°C	72°C	72°C	25 s	30×
Final extension	72°C	72°C	72°C	10 min	1×
Hold	4°C	4°C	4°C	Hold	1×

Gel elute the PCR products using QIAquick Gel Extraction Kit and estimate the DNA concentration of the eluted fragments.

b. Restriction enzyme digestion of EasyFusion-Halo plasmid.

Digest EasyFusion-Halo plasmid with EcoRI and XbaI to remove the Halo insert at 37°C for 4 h (Table 19).

Table 19. Digestion of EasyFusion-Halo plasmid to remove Halo insert

EasyFusion-Halo (5 µg)	10 µL
CutSmart buffer 10×	2 µL
EcoRI	2 µL
XbaI	2 µL
Nuclease free water	2 µL

Gel elute the 2.9 kb fragment of the digested plasmid using QIAquick Gel Extraction Kit and estimate the DNA concentration of the eluted fragment.

c. HiFi DNA assembly ligation reaction

Mix all four fragments required for the generation of Grb2 donor DNA to a final volume of 10 µL. Thaw HiFi DNA assembly mix on ice and vortex thoroughly. Add equal volume of HiFi DNA assembly master mix to the fragments (Table 20).

Table 20. Ligation set up for the generation of Grb2 donor DNA

0.1 pmol of 5HA	50 ng	0.8 µL
0.1 pmol of mNG	50 ng	0.9 µL
0.1 pmol of 3HA	50ng	1.1 µL
0.1 pmol of digested vector	185 ng	2 µL
HIFI DNA assembly master mix		10 µL
Nuclease free water		5.2 µL

Carry out the ligation reaction at 50°C for 1 h. Transform 2 µL of the reaction mix into competent *E. coli*. Screen several colonies for positive clones containing all three fragments (5HA-mNG-3HA) using restriction enzyme digestion and Sanger sequencing.

C. Delivery of gRNAs and Donor DNAs in HeLa cells

1. Electroporation of RNP complex to tag KRAS and NRAS
 - a. Grow HeLa cells in DMEM with 10% FBS to 90% confluence in a 75 cm² flask. Treat the cells with 100 ng/mL Nocodazole for 12 h.
 - b. On the day of the electroporation, thaw and store buffer R, KRAS and NRAS specific *in vitro* transcribed gRNA, and donor DNAs on ice. Dilute gRNAs and donor DNA to appropriate concentrations in nuclease free water.
 - c. Wash away Nocodazole with 1× DPBS. Split the cells with Trypsin and inactivate it by the addition of FBS containing DMEM. Centrifuge the single cell suspension at 300 × g for 5 min. Resuspend the pellet in 10 mL of DMEM with 10% FBS. Perform cell counting using hemocytometer.
 - d. Prepare RNP mixture as follows (Table 21), one for each gene-editing reaction in a 1.5 mL microcentrifuge tube.

Table 21. Components of RNP mixture for electroporation

Buffer R	1 µL
Platinum Cas9 (1 µg)	0.5 µL (1 µg)
gRNA (500 ng)	2 µL

- e. Incubate RNP complex at room temperature for 20 min.
- f. While the RNP is incubating, prepare electroporation set up and keep cells ready for the electroporation by centrifuging them at 300 × g for 5 min. Aspirate DPBS and resuspend the cell pellet to a final cell density of 8 × 10⁷ cells/ml in buffer R.
- g. Add 3 mL of Electrolytic buffer (Buffer E) into the Neon Pipette station.
- h. Add 5 µL of cells (final 4 × 10⁵ cells) and 1 µg of respective donor DNA fragments to the RNP mixture. Make sure the volume of the final mixture is 10 µL. Aspirate the final mix in

- Neon Tip using Neon Pipette without incorporating air bubbles and electroporate at pulse voltage of 1,005 V, pulse width of 35 ms for 2 pulses.
- i. Transfer the electroporated cells in a 12-well plate containing prewarmed DMEM with 10% FBS without antibiotics and continue incubating the plate at 37°C in a CO₂ incubator.

 2. Transfection of gRNA and donor to tag *Grb2*
 - a. Grow HeLa cells in DMEM with 10% FBS to 90% confluence in 12-well plates. Treat the cells with 100 ng/mL Nocodazole for 12 h.
 - b. On the day of the transfections, dilute PX459-Grb2-gRNAs and Grb2-mNG donor DNA plasmids to appropriate concentrations in nuclease free water.
 - c. Wash away Nocodazole with 1× DPBS. Add 1 mL of fresh FBS containing DMEM.
 - d. Prepare DNA-lipid mixture as follows (Table 22), in a 1.5 mL microcentrifuge tube in the order given.

Table 22. Components of transfection mixture to tag Grb2

	Tube 1
OptiMEM	50 µL
PX459-Grb2-gRNA (250 ng)	0.5 µL
Grb2-mNG donor (750 ng)	1 µL
P3000 reagent	2 µL
	Tube 2
OptiMEM	50 µL
Lipofectamine 3000 Reagent	1.5 µL

- e. Add contents from Tube 1 to Tube 2. Incubate the mixture at RT for 10 min.
- f. Add plasmid-lipid mixture to the cells dropwise.
- g. Next day after the transfection, treat transfected cells with 2 µg/mL of puromycin for 48 h to enrich transfected cells by killing un-transfected cells.
- h. Remove puromycin containing DMEM, wash the cells with DPBS twice and allow the cells to recover. Split the surviving cells and expand them for flow sorting analysis.

D. Flow Sorting of mNG positive cells

1. Expand tagged HeLa cells in DMEM with 10% FBS in 25 or 75 cm² flasks.
2. On the day of sorting, split the cells using Trypsin and inactivate it with FBS containing DMEM. Centrifuge the cells and wash once with PBS. Resuspend the final pellet in Cell sorting buffer.
3. Pass the cell suspension through disposable filters to get rid of cell aggregates just before the sorting. Use positive (parental HeLa cells transiently or stably expressing mNG) and negative (parental untagged HeLa cells) controls to calibrate the sorting instrument.

4. Collect single sorted cells in 96-well plate or in a 15 mL conical tube as a pooled population with prewarmed DMEM with 10% FBS and antibiotics to prevent contamination.

E. Confirmation of positive clones

1. Freeze at least one vial of single cell clones as a backup before using them for confirmation.
2. Clones can be confirmed by Western blot analysis using protein-specific antibody or mNG antibody. The correct fusion protein should have an apparent molecular mass ~25 kD larger than the parental protein. It is also important to sequence the region around the site of mNG sequence insertion to make sure there are no unwanted insertions or deletions during homology repair.

Note: Head-to-head comparison of efficiency of different delivery methods was not performed. In all the cases, the yield of mNG positive cells as determined during flow sorting was 0.1% to 0.5%. Since we were interested in single cell colonies for screening, one 96 well plate of single sorted cells was sufficient to screen them. It should be noted that flow sorting could inadvertently result in clones expressing higher yields of fusion protein.

Data analysis

1. Characterization of the tagged cell line clones

Select several colonies arising from flow sorted population. Process the colonies for DNA isolation for Sanger sequencing and for making lysates for Western blot analysis. To generate PCR products for Sanger sequencing, design primers that can amplify the region beyond the homology arms. The sequencing should reveal the correctly inserted mNG sequence as well as linkers and start/stop codons. Western blot should reveal the correct molecular weight of the fusion protein. For example, a screen of HeLa/mNG-KRAS clones using Western blot is shown in Figure 2. The colonies were lysed in TGH buffer, and the lysates were electrophoresed and transferred onto nitrocellulose membrane. We detected two homozygous clones in 24 colonies screened. Load lysates from parental cell line as control for the WT untagged protein. It is essential to make sure that off target changes occurring during Cas9 mediated gene editing do not affect the cells in such a way that they are unfit for the study. Since our focus is to study EGFR-RAS-MAPK pathway, we chose the clones that exhibited similar ERK1/2 phosphorylation kinetics in HeLa parental and tagged KRAS and NRAS cells in presence of EGF (Surve *et al.*, 2021).

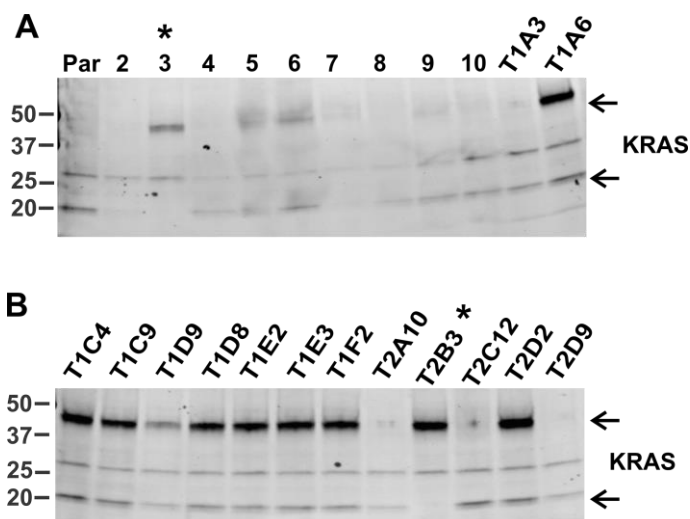


Figure 2. Screening of HeLa/mNG-KRAS single cell clones.

The single cell colonies were obtained either from a 10-cm plate where transfected cells were diluted or from a flow cytometer sorted population in a 96 well plate. First screening was done by checking cell fluorescence using a confocal microscope. Second screening was performed by probing lysates of parental (Par) HeLa and single-cell clones of HeLa/mNG-KRAS cells using Western blotting (WB) with KRAS antibodies to determine the zygosity of the clones expressing mNG-KRAS. Clones from 2 to 10 (in **A**) were obtained from 10 cm plate, whereas remaining clones were obtained via flow sorting. Clone names starting with T1 are from Target 1 gRNA, whereas those with T2 are the results of Target 2 gRNA transfection. Top arrow in **A** and **B** indicate mNG-KRAS fusion protein, whereas lower arrow indicates untagged KRAS protein. Clones with asterisk are homozygous clones as they are missing a band corresponding to the untagged native KRAS.

2. Examples of localization of endogenous tagged KRAS, NRAS and Grb2

After the screening and confirmation of the tagged cell lines, we imaged living tagged cell lines with spinning disc confocal microscope (Figure 3).

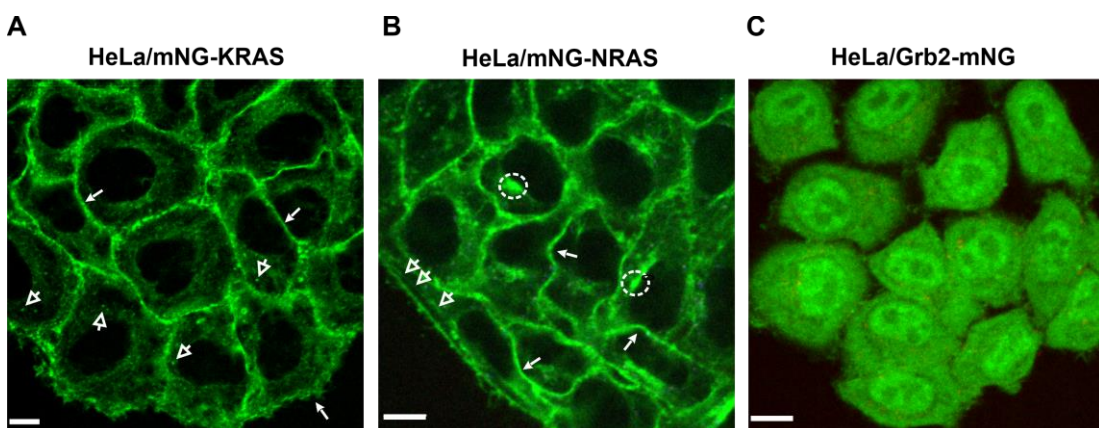


Figure 3. Localization of endogenous tagged KRAS, NRAS, and Grb2 with mNG in HeLa

cells.

Live cell imaging was performed using a spinning disc confocal microscope through 488 nm (green; mNG) channel. Single confocal sections are shown. **A.** mNG-KRAS localized mostly at the plasma membrane (closed arrows), and a small proportion also localized in vesicles (open arrows). **B.** Majority of mNG-NRAS localized at the plasma membrane. mNG-NRAS was also in the juxta-nuclear region (dotted circle) and tubular shaped structures (open arrows). **C.** Grb2-mNG localized to cytoplasm and nucleus.

Recipes

1. Cell Sorting buffer
 - 1× PBS (Ca/Mg++ free)
 - 2% heat-inactivated FBS
 - 1 mM EDTA
2. TGH buffer
 - 1% Triton X-100
 - 10% glycerol
 - 50 mM HEPES
 - 2 mM EGTA
 - Phosphatase and protease inhibitors

Acknowledgments

Authors thank Drs Feng Zhang, Broad Institute, Cambridge, MA, and Janet Rossant, Peter Gilgan Centre for Research and Learning, The Hospital for Sick Children, Toronto, ON, Canada, for plasmids. This study was supported by NIH grants CA089151 and GM124186. S. Surve was also supported by the fellowship from National Cancer Center. This protocol was adapted from Surve *et al.* (2021).

Competing interests

The authors declare no competing financial interests.

References

1. Howe, C. L., Valletta, J. S., Rusnak, A. S. and Mobley, W. C. (2001). [NGF signaling from clathrin-coated vesicles: evidence that signaling endosomes serve as a platform for the Ras-MAPK pathway](#). *Neuron* 32(5): 801-814.
2. Jiang, X. and Sorkin, A. (2002). [Coordinated traffic of Grb2 and Ras during epidermal growth factor receptor endocytosis visualized in living cells](#). *Mol Biol Cell* 13(5): 1522-1535.

3. Karnoub, A. E. and Weinberg, R. A. (2008). [Ras oncogenes: split personalities.](#) *Nat Rev Mol Cell Biol* 9(7): 517-531.
4. Lu, A., Tebar, F., Alvarez-Moya, B., Lopez-Alcala, C., Calvo, M., Enrich, C., Agell, N., Nakamura, T., Matsuda, M. and Bachs, O. (2009). [A clathrin-dependent pathway leads to KRas signaling on late endosomes en route to lysosomes.](#) *J Cell Biol* 184(6): 863-879.
5. Pinilla-Macua, I., Grassart, A., Duvvuri, U., Watkins, S. C. and Sorkin, A. (2017). [EGF receptor signaling, phosphorylation, ubiquitylation and endocytosis in tumors *in vivo*.](#) *Elife* 6: e31993.
6. Pinilla-Macua, I., Watkins, S. C. and Sorkin, A. (2016). [Endocytosis separates EGF receptors from endogenous fluorescently labeled HRas and diminishes receptor signaling to MAP kinases in endosomes.](#) *Proc Natl Acad Sci U S A* 113(8): 2122-2127.
7. Pol, A., Calvo, M. and Enrich, C. (1998). [Isolated endosomes from quiescent rat liver contain the signal transduction machinery. Differential distribution of activated Raf-1 and Mek in the endocytic compartment.](#) *FEBS Lett* 441(1): 34-38.
8. Ran, F. A., Hsu, P. D., Wright, J., Agarwala, V., Scott, D. A. and Zhang, F. (2013). [Genome engineering using the CRISPR-Cas9 system.](#) *Nat Protoc* 8(11): 2281-2308.
9. Schmick, M., Vartak, N., Papke, B., Kovacevic, M., Truxius, D. C., Rossmannek, L. and Bastiaens, P. I. H. (2014). [KRas localizes to the plasma membrane by spatial cycles of solubilization, trapping and vesicular transport.](#) *Cell* 157(2): 459-471.
10. Surve, S., Watkins, S. C. and Sorkin, A. (2021). [EGFR-RAS-MAPK signaling is confined to the plasma membrane and associated endorecycling protrusions.](#) *J Cell Biol* 220(11).
11. Surve, S. V., Myers, P. J., Clayton, S. A., Watkins, S. C., Lazzara, M. J. and Sorkin, A. (2019). [Localization dynamics of endogenous fluorescently labeled RAF1 in EGF-stimulated cells.](#) *Mol Biol Cell* 30(4): 506-523.
12. von Zastrow, M. and Sorkin, A. (2021). [Mechanisms for Regulating and Organizing Receptor Signaling by Endocytosis.](#) *Annu Rev Biochem* 90: 709-737.

Single Molecule Tracking Nanoscopy Extended to Two Colors with MTT2col for the Analysis of Cell-Cell Interactions in Leukemia

Loriane Maillot¹, Magali Irla² and Arnauld Sérgé^{1,*}

¹Aix Marseille Univ, CNRS, INSERM, LAI, Turing Center for Living Systems, France

²Aix Marseille Univ, CNRS, INSERM, CIML, France

*For correspondence: arnauld.serge@univ-amu.fr

Abstract

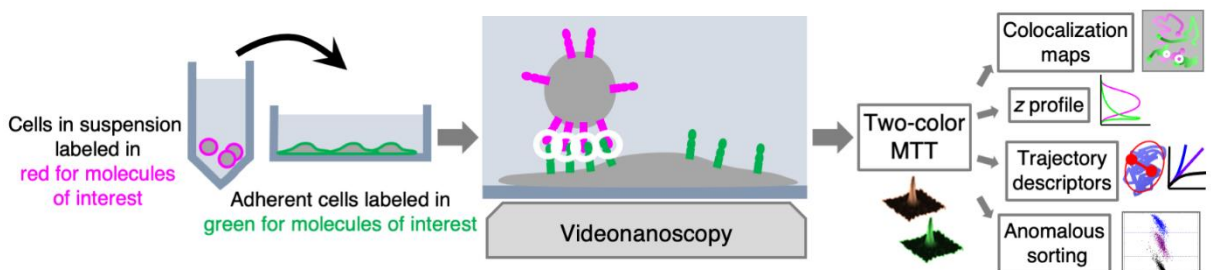
Single molecule tracking (SMT) is a powerful technique to study molecular dynamics, and is particularly adapted to monitor the motion and interactions of cell membrane components. Assessing interactions among two molecular populations is classically performed by several approaches, including dual-color videomicroscopy, which allows monitoring of interactions through colocalization events. Other techniques, such as fluorescence recovery after photobleaching (FRAP), Förster resonance energy transfer (FRET), and fluorescence correlation spectroscopy (FCS), are also utilized to measure molecular dynamics.

We developed MTT2col, a set of algorithmic tools extending multi-target tracing (MTT) to dual-color acquisition (<https://github.com/arnauldserge1/MTT2col>). In this protocol, we used MTT2col to monitor adhesion molecules at the contact between leukemic stem cells and stromal cells, a process involved in cancer resistance to chemotherapy and in relapse. Our dual-color single molecule protocol includes the following steps: (i) labeling molecules of interest with fluorescent probes, (ii) video-acquisition, (iii) analyses using our MTT2col in-house software, to obtain positions and trajectories, followed by (iv) detailed analyses of colocalization, distribution, and dynamic motion modes, according to the issues addressed. MTT2col is a robust and efficient SMT algorithm. Both MTT and MTT2col are open-source software that can be adapted and further developed for specific analyses.

Keywords: Nanoscopy, Single molecule tracking, Super-resolution, Dual-color analyses, Molecular interactions, Membrane dynamics

This protocol was validated in: J Cell Sci (2021), DOI: 10.1242/jcs.258736

Graphical abstract:



Background

Single molecule tracking (SMT) is a powerful approach to investigate molecular dynamics in live cells, at the plasma membrane, in the cytosol, or in the nucleus (Figure 1A). Noteworthy, determining the position of a single fluorescent molecule at sub-resolution accuracy can be achieved using a two-dimensional (2D) Gaussian fit, provided there is a sufficient signal-to-noise ratio. We typically achieve ~40 nm lateral accuracy for living cell images (Sergé *et al.*, 2008). Labeling and monitoring two molecular species by dual-color SMT allows for the comparison of their dynamic state and kinetic interactions *in situ*. Single molecule labeling can be done classically with fluorescently coupled antibodies (either primary alone, or primary and secondary), Fab fragments, and nanobodies, or by fluorescent proteins, such as GFP and its variants (in other colors or photoactivatable for instance). Additionally, protein tags such as HaloTag, SnapTag, and ClipTag, with their bright and stable fluorescent ligands, may also be utilized (Figure 1B). Each approach has its advantages and limitations, notably in terms of stoichiometry, steric hindrance, brilliance, and photostability (Achimovich, Ai and Gahlmann, 2019; Jacquemet *et al.*, 2020; Lemon and McDole, 2020; Petazzi, Aji and Chiantia, 2020). There are already several SMT algorithms available, each of which vary in performance due to critical issues, such as signal-to-noise ratio and probe density (Manzo and Garcia-Parajo, 2015).

Alternative microscopy approaches for monitoring molecular dynamics (classically for one, and eventually for two populations) include fluorescence recovery after photobleaching (FRAP), fluorescence correlation spectroscopy (FCS), and Förster resonance energy transfer (FRET), as well as the more recently introduced super-resolution SMT methods (Owen *et al.*, 2009; Sergé, 2016). Super-resolution SMT methods comprise single-particle tracking by photo-activation localization microscopy (sptPALM) (Manley *et al.*, 2008), points accumulation for imaging in nanoscale topography (PAINT) (Sharonov and Hochstrasser, 2006), and minimal photon fluxes (MINFLUX) nanoscopy (Balzarotti *et al.*, 2017).

Of note, concerning temporal limits, FRAP and FCS are more sensitive to fast motions (*i.e.*, above ~0.1 $\mu\text{m}^2/\text{s}$, providing a higher contribution to the measurement), while SPT is more sensitive to slow motions (leading to more efficient reconnections). Furthermore, concerning spatial limits, SMT can reach nanometer accuracy, FRET is efficient only for distances around 10 nm, and both can document entire cell(s) within the microscope field of view, while FRAP and FCS provide local measurements, inherently applied over distances larger than the diffraction limit. Other non-dynamic approaches to assess molecular interactions at the cell or tissue level, *in vivo* or *in vitro*, include immunostaining or coimmunoprecipitation. A key advantage of single molecule techniques, as opposed to ensemble-average measurements, is that they provide access to the distribution of descriptors, hence to the dynamic of each molecule.

All these techniques may be applied to different space and time domains, with various advantages and limitations (De Los Santos *et al.*, 2015; Li and Vaughan, 2018). For instance, SMT approaches such as MTT2col cover a broad range of space and time, as can be addressed both at the global and local level. Globally, SMT is spatially limited to the field of view of the imaging system: microscope and camera. Images have a width of 512 pixels, with 160-nm pixels and 100 \times objective, leading to 82- μm width. Temporally, the limit is only the biology (and the storage capacity, often not limiting). We consider that cells should be kept no more than one hour in the microscope. However, some experimental conditions may need shorter or longer time periods: for instance, endo/exocytosis and Cite as: Maillot, L. et al. (2022). Single Molecule Tracking Nanoscopy Extended to Two Colors with MTT2col for the Analysis of Cell-Cell Interactions in Leukemia. Bio-protocol 12(08): e4390. DOI: 10.21769/BioProtoc.4390.

protein synthesis occur on minute and hour time-scales, respectively. For each video, we arbitrarily set the length to typically 100–500 frames at 100-ms exposure, hence 10–50 s. This can be readily adjusted to the kinetics of the biological system being measured. Locally, space and time resolution limits are linked, essentially by the equation of diffusion $MSD = 4Dt$. The acquisition time is usually set at its lowest value, as imposed by the fastest video rate of the camera, typically in the 10-ms range. For a diffusion coefficient ranging from 10^{-3} to $1 \mu\text{m}^2/\text{s}$, this leads to 50–500 nm.

MTT2col may be tuned using several parameters, including probability of false alarm (PFA) detection for different signal-to-noise ratios, spatiotemporal search windows, probability parameters for the reconnection statistical laws, target size, and cutoffs for discarding short and slow trajectories. Each parameter may be adjusted by visual inspection of the results obtained with the default values. For instance:

- For too many/not enough detections, PFA should be increased/decreased to become more/less stringent.
- Similarly, if trajectories are connecting too many/not enough targets, spatiotemporal search windows and probability parameters for reconnection should be adjusted accordingly. In particular, the spatiotemporal search window should match the spatiotemporal resolution limits [see supplementary Figure 6B in Gorshkova *et al.* (2021)]. Cutoffs relate to statistical laws describing the past statistics and recombination probabilities. Thus, they should be of general scope [see Sergé *et al.* (2008) for a description of these parameters]. Given the robustness of MTT, the default values are often satisfactory.
- For a single molecule, the target size is equal to the diffraction limit. Hence, the physical value is almost constant over the visible spectrum, *i.e.*, 200–300 nm. It was converted into pixels with a pixel size of 160 nm in the original version. If the pixel size substantially varies, then the value of the target size should be modified accordingly.
- Cutoffs for discarding short and slow trajectories are defined according to the distribution of trajectory length and diffusion coefficient. Irrelevant values (too short and/or too slow) are determined by comparing experimental results and negative controls for non-specific staining for length and immobile dyes for diffusion, see supplementary Figure 6B of Gorshkova *et al.* (2021). Nevertheless, raw data are saved as *dat* files and these cutoffs can be reconsidered *a posteriori*.

However, the algorithm is ultimately robust regarding these values, which are often kept at their original level or easily adjusted.

Finally, the main parameter to optimize is the input diffusion coefficient, which has to correspond to the measured molecules and can be readily identified by testing a range of values [as described in the paragraph *Material and Methods/SMT determination of the input diffusion coefficient for MTT*, associated to the supplementary Figure 6A of Gorshkova *et al.* (2021)]. MTT2col is an open-source software, hence the code may be freely adapted to given conditions and/or completed by supplementary analyses tailored for further measurements.

Dual-color SMT can be applied to a broad range of interacting molecules, such as ligands and receptors, or associated proteins like scaffolds, cell adhesion molecule partners, enzymes and cognate substrates, as well as DNA sequences and associated binding regulatory elements. Tracking can also be performed at other scales, for other target types, namely cells, animals (*i.e.*, fishes or birds), or vehicles (*i.e.*, cars or planes). The core of the MTT algorithm has been extensively downloaded to be used by the scientific community, leading to numerous publications. Notably, MTT has been adapted for use in various contexts, *i.e.*, cell tracking, allowing monitoring in space and time of the fluorescence level associated with the intracellular calcium concentration of a population of T cells (Salles *et al.*, 2013).

Importantly, efficient tracking can be achieved provided there is a sufficient signal-to-noise ratio. MTT has good performances down to about 20 dB [as illustrated in Figure 4 from Sergé *et al.* (2008)]. Of note, noise may be reduced by cultivating cells in a medium without phenol red. Choosing fluorochromes with emission spectra in the red or even infrared can also be helpful to discriminate from autofluorescence (mostly in the green and yellow part of the visible spectrum), hence reducing signal-to-noise ratio. Furthermore, the signal intensity of a single molecule is expected to remain constant until photoblinking or photobleaching, except if photoblinking occurs on timescales shorter than the acquisition time, leading to a lower intensity. Observing stepwise variations instead of gradual decays provides a signature of single molecule measurements. As a supplementary analysis (not implemented in MTT2col), successive stepwise variations in intensity are expected to be due to variations in stoichiometry, for monomers, dimers, trimers, and so on (Schmidt, 1996). To perform these measurements, the intensity of the laser illuminating the sample must be carefully set, by measuring the laser power at the exit of the objective.

The junctional adhesion molecule (JAM) C has been previously reported to be highly expressed in a subset of leukemic stem cells (De Grandis *et al.*, 2017). Thus, JAM-C provides a signature for leukemic initiating cells, potentially leading to relapse after therapy, hence constituting a potential therapeutic target. Thus, we analyzed the dynamics of JAM-B and JAM-C at contacts between leukemic and stromal cells. The MTT2col protocol was initially developed for tracking JAM-B on MS5 stromal cells, and JAM-C on KG1 leukemia cells (Gorshkova *et al.*, 2021). However, it can be readily applied to any other molecules of interest, for instance implicated in cell-cell contacts.

Materials and Reagents

1. Micropipette tips (Thermo Fisher Scientific, catalog numbers: 11752584 [10 µL]; 10731194 [20 µL]; 16641953 [100 µL]; 11782584 [200 µL]; 11749855 [1,000 µL])
2. 1.5 mL tubes (Eppendorf, Dutscher, catalog number: 033305)
3. µ-Slide 8 Well Glass Bottom (Ibidi cells in focus, catalog number: 80827)
4. Trypan blue (Thermo Fisher Scientific, Invitrogen™, catalog number: T10282)
5. Rabbit serum (Thermo Fisher Scientific, Gibco™, catalog number: 16120099)
6. Cell lines
 - a. MS5 (DSMZ ACC 441)
 - b. KG1 (ATCC CCL-246)
7. IMDM (Thermo Fisher Scientific, Gibco™, catalog number: 12440053)
8. HBSS, with calcium and magnesium, no phenol red (Thermo Fisher Scientific, Gibco™, catalog number: 14025092)
9. L-glutamine (Thermo Fisher Scientific, Gibco™ 25030149, catalog number: 15430614)
10. Penicillin and streptomycin (Thermo Fisher Scientific, Gibco™, catalog numbers: 15140122 and 15140148)
11. β-mercaptoethanol (PanReac AppliChem, catalog number: A1108)
12. HEPES (Thermo Fisher Scientific, Gibco™, catalog number: 15630080)
13. Fetal bovine serum (Thermo Fisher Scientific, Gibco™, catalog number: 10270106)
14. Sodium pyruvate (Thermo Fisher Scientific, Gibco™, catalog number: 11360070)
15. Antibodies:
 - a. Anti-JAM-B: in-house rabbit polyclonal antibody, clone 829
 - b. Anti-JAM-C, blocking: mouse IgG (R&D, catalog number: MAB1189, clone 208206)
 - c. Anti-JAM-C, non-blocking: in-house rat IgG, clone 19H36
 - d. Alexa Fluor 488 conjugated anti-rabbit-IgG (Thermo Fisher Scientific, catalog number: A-11008)
 - e. Alexa Fluor 594 conjugated anti-mouse or anti-rat IgG (Thermo Fisher Scientific, catalog number: A-11001 or A-11006)
 - f. Quantum-dot 655 conjugated anti-mouse IgG (Thermo Fisher Scientific, catalog number: Q-11021MP)
 - g. Quantum-dot 655 conjugated anti-rat IgG (Thermo Fisher Scientific, catalog number: Q-11621MP)
16. Culture medium for MS5 cells (see Recipes)
17. Culture medium for KG1 cells (see Recipes)

Equipment

1. Micropipettes 20, 100 and 1000 (Eppendorf, Thermo Fisher Scientific, catalog number: 05-403-152, model: Research)
2. Centrifuge (Eppendorf, Thermo Fisher Scientific, catalog number: 5805 000.010)
3. CO₂ incubator Forma Scientific 3548 (Labexchange, Forma Scientific, catalog number: B00032422)
4. 4°C refrigerator
5. -80°C freezer
6. Hemocytometer (Ozyme, C-Chip, catalog number: DHC-M01)

Cite as: Maillot, L. et al. (2022). Single Molecule Tracking Nanoscopy Extended to Two Colors with MTT2col for the Analysis of Cell-Cell Interactions in Leukemia. Bio-protocol 12(08): e4390. DOI: 10.21769/BioProtoc.4390.

7. Axio Observer Z1 inverted microscope (Zeiss), with thermostated incubator at 37°C
8. Yokogawa spinning disk device
9. 491- and 561-nm lasers (ILas2 or Cobolt Calypso 1358, 100 mW)
10. 100× α Plan Neofluar NA 1.45 oil-immersion objective (Zeiss) or equivalent, with high NA
11. Filter cubes n°15 and 44 (Zeiss), with 120-W metal halide lamp (X-cite) for visual inspection
12. 405/488/568/647 nm Yokogawa quadriband dichroic beamsplitter (Semrock, catalog number: Di01-T405/488/568/647-13x15x0.5)
13. BS 573 dichroic beamsplitter (Semrock, catalog number: FF573-Di01-25x36), between the two cameras
14. 525/50 nm (green channel) and 641/75 nm (red channel) emission filters (Semrock, catalog numbers: FF03-525/50-25 and FF02-641/75-25)
15. Two Evolve 512 EMCCD cameras (Photometrics) or equivalent, such as the Prime 95B sCMOS camera (Photometrics)

Software

1. Metamorph software (Version 7.4.8, Molecular Devices)
2. MTT2col set of MATLAB functions and scripts, using the Image Processing Toolbox with Statistics and Machine Learning Toolbox (any version) (The Mathworks)

Procedure

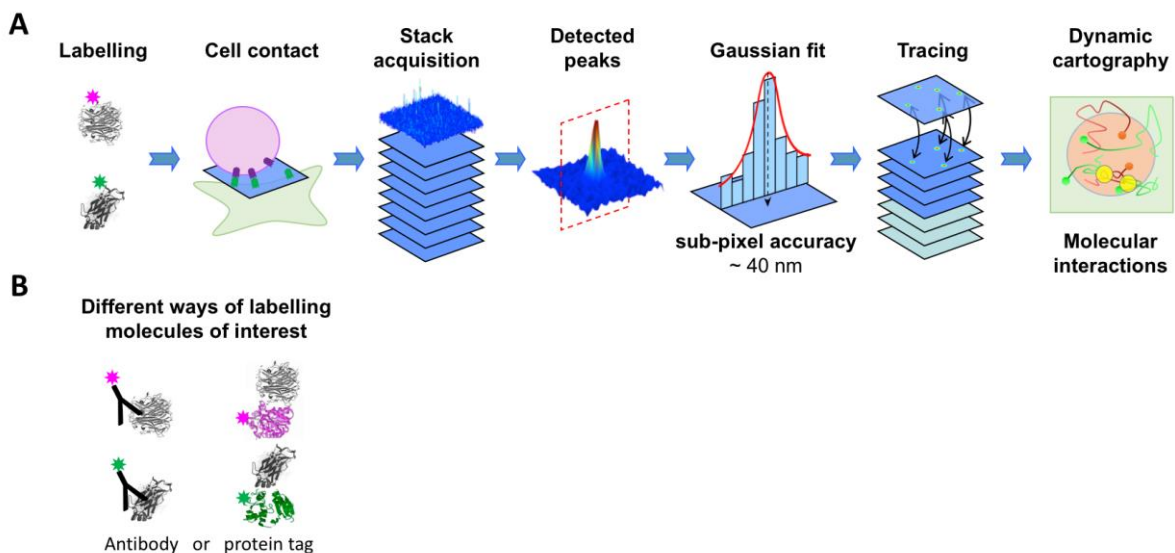


Figure 1. Overview of the experiment.

(A) Steps of the experimental procedure: preparation, acquisition, and data analysis. (B) Of note, labeling molecules of interest can be performed by a broad range of strategies.

A. Cell preparation 24 h or 48 h before videonanoscopy

1. Pass MS5 cells (adherent): spread in a 1-cm² area Ibidi glass-bottom well at 30,000 cells in a 300- μ L culture volume overnight. This cell density allows reaching about 50% confluence (about 50,000 cells) the day of the experiment, according to DSMZ guidelines. Of note, glass-bottom wells may need specific treatment, such as extracellular matrix coating, for proper adhesion of some cell lines.

Cite as: Maillot, L. et al. (2022). Single Molecule Tracking Nanoscopy Extended to Two Colors with MTT2col for the Analysis of Cell-Cell Interactions in Leukemia. Bio-protocol 12(08): e4390. DOI: 10.21769/BioProtoc.4390.

2. Pass KG1 cells (in suspension) at the appropriate culture density, between 100,000 and 1,000,000 cells/mL, according to ATCC guidelines.
3. Incubate the cultures in a 37°C 5% CO₂ air humidified incubator.
If using other types of chamber, they must have a glass bottom to allow fluorescence imaging, and cell numbers should be adjusted to the area.

B. Immunofluorescence staining of MS5 cells (Figure 1)

1. Dilute the primary and secondary antibodies in 100 µL of fresh cell culture medium, according to the determined optimal concentration. The optimal antibody concentration gives the best staining with minimum background. It is determined by using a series of dilutions in a titration experiment: 10 nM for anti-JAM-B 829 and for Alexa Fluor 488 conjugated anti-rabbit antibodies (or equivalent, such as quantum-dot conjugated antibodies) in IMDM supplemented with serum, which is necessary to saturate and limit non-specific binding.
2. Aspirate the culture medium from the well of the live cells to be stained and add 100 µL of the medium containing the diluted antibody directly to the well.
3. Incubate the cells at room temperature for 10 min.
4. Aspirate the supernatant and gently wash the cells twice with HBSS with 1% HEPES (or fresh culture medium—to limit autofluorescence, use culture medium without phenol red).

C. Immunofluorescence staining of KG1 cells

1. Dilute the primary antibody, blocking or not, and secondary antibody in 100 µL of fresh cell culture medium, according to the determined optimal concentration: 10 nM for anti-JAM-C (blocking: mouse RnD 208206, non-blocking: homemade rat 19H36), and for Alexa Fluor 594 conjugated anti-mouse (or equivalent, such as quantum-dot conjugated antibodies) in supplemented IMDM.
2. Determine the total number of cells and percent of cell viability using a hemocytometer: mix 0.4% trypan blue with the cell suspension, in a 1:1 proportion (or in other proportions, using the appropriate dilution factor for your calculations). Thoroughly mix the two solutions and pipette 20 µL of this mix into one hemocytometer chamber. Place the hemocytometer under the microscope. Count the unstained (live) and stained (dead) cells (according to the datasheet of the hemocytometer used). Multiply the total number of live cells by two (or by the appropriate dilution factor, if using a different dilution for trypan blue).
3. Pipette the appropriate volume to have either 50,000 cells (low density: as many as MS5 cells to image one KG1 cell per field of view, allowing cell by cell measurement) or 500,000 cells (high density: 10 times more than MS5 cells, to image several KG1 cells per field of view, enabling more statistics per video).
4. Transfer the cells to a 1.5-mL Eppendorf tube.
5. Briefly centrifuge at 88 × g for 3 min.
6. Resuspend in 1 mL of medium and saturate with 10% rabbit serum, in a 5% CO₂ incubator at 37°C for 60 min.
7. Briefly centrifuge at 88 × g for 3 min.
8. Resuspend in 100 µL of medium containing the diluted antibodies (see step 1).
9. Incubate the cells at room temperature for 10 min.
10. Briefly centrifuge at 88 × g for 3 min, aspirate the supernatant, and gently wash the cells twice with 1 mL of HBSS with 1% HEPES (or fresh culture medium without phenol red). Resuspend the cell pellet in 200 µL of HBSS with 1% HEPES.
11. Remove the supernatant from the MS5 cells, and add the 200 µL of KG1 cell suspension.
12. Examine the cells using a spinning disc fluorescence microscope with a thermostated incubator set to 37°C, and appropriate filters (see Equipment, items 7 to 15). Cells should be imaged immediately after staining, to limit endocytosis (Figure 2).

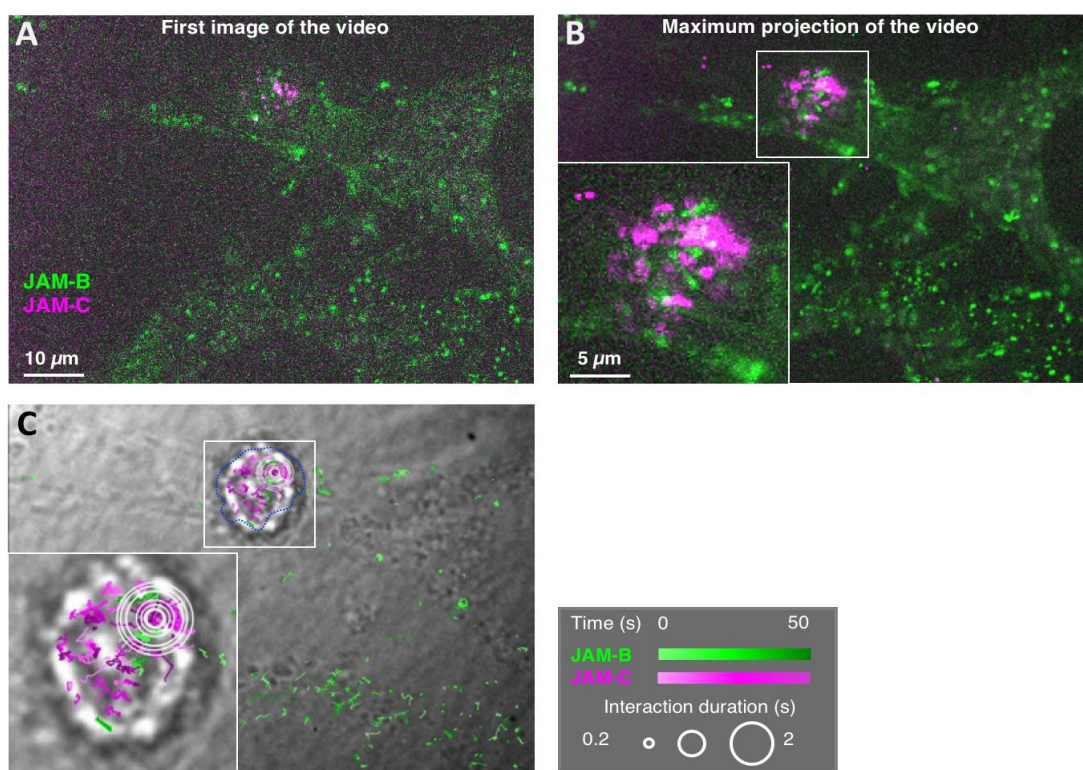


Figure 2. Representative videonanoscopy acquisition and MTT2col trajectory maps.

(A) First image of a videonanoscopy acquisition, with the two colors combined into an RGB image. JAM-B staining on MS5 cells is in the green channel, and JAM-C staining on the KG1 cell is in the magenta channel. (B) Maximum projection of the video. (C) JAM-B and JAM-C single molecule trajectories are represented by green and magenta gradients, respectively, according to time, and superimposed on the transmission image of the cells (right). Inserts show magnifications of the framed areas around a leukemic KG1 cell. Spatiotemporal colocalizations are denoted by white circles, with a size proportional to duration. Several concentric circles correspond to successive colocalization events at nearby locations.

Representative videos can be seen from the supplementary data of the related article (Gorshkova *et al.*, 2021).

D. Performing acquisitions on a confocal microscope

1. Create a folder, usually named with the date and a brief description of the experiment.
2. Select a field of view with KG1 cells on top of spread MS5 cells.
3. First, acquire a brightfield image that allows for further checking of cellular aspects and spatial limitations (as used, in combination with all trajectories, in Figure 2C).
4. Save this image using the same name as the video (time-stack), in a subfolder named “trans”. With this convention, the algorithm can automatically find the matching brightfield image for each stack.
5. Next, acquire one (or several) video (time-stack), typically at a 36-ms or 100-ms rate. Save the video file in the folder created for the experiment, as either *tif* or *stk* file format. For each video, 300 frames were usually acquired (see Figure 2A for an example). Video rate and length may be adapted for a given experiment. For instance, an experiment may require faster video rate or longer trajectories.
6. Last, optionally, acquire a z-stack ranging over the entire height of both MS5 and KG1 cells (typically more than 10 μm). Save the z-stack in a subfolder named ‘z’.
7. Repeat steps 2–5 as many times as needed. Cells should be kept less than an hour in HBSS with 1% HEPES.

Data analysis

A. Running MTT2col (Figure 1) (Gorshkova *et al.*, 2021)

1. Start Matlab (or Octave, alternatively, at least for MTT).
2. Within the Matlab environment, navigate to the folder containing the data to be analyzed (either on a local drive or on the network). Evaluating a given dataset with Matlab or Octave essentially requires selecting the path to the directory containing the video files.
3. Then, type the command MTT_2_colors in Matlab, which first displays a graphic interface listing all the parameters used, then runs the fully automated analysis (Figure 3).
4. Of note, when analyzing a mix of one- and two-color datasets, the supplementary Matlab function MTT_1_or_2_colors can determine if the data correspond to one color (square images, such as 512×512 pixels), two colors (double square, meaning that the width is double the height, such as 1024×512 pixels) or any other possibility. The function automatically runs the analysis for one or two colors if it can be determined without ambiguity. Otherwise the file is skipped.



Figure 3. MTT2col graphical user interface.

The graphical user interface (GUI) lists all input parameters for molecule detection and estimation, trajectory reconnection, and further analyses, with their default values (as defined in the Matlab functions MTT23_dialog_box MTTparams_def and MTT_param).

B. Overview of the MTT2col algorithm (Sergé *et al.*, 2008; Rouger *et al.*, 2012)

1. Inputs for each field of view

The program expects to run the analysis using the following files and subfolders in the local path:

- Dual-color time-stacks (i.e. left: green / right: magenta)
- Dual-color 'DIC' image (transmitted light, in a subfolder named '**'dic'**', optional but used for registration)
- Dual-color z-stacks (in a subfolder named '**'z'**', optional)

2. Analysis

The main function of the MTT2col algorithm is called MTT_2_colors. Below is a list of the main Matlab functions and sub-functions in MTT2col. Key steps are in bold, variables are in purple, and comments are in green. This fully automated procedure allows to build trajectories from dual-color video acquisitions (Figure 2), and to extract several descriptors (Figure 4), as explained in the main text. See the original articles (Sergé *et al.*, 2008; Rouger *et al.*, 2012; Gorshkova *et al.*, 2021) for an extensive description of the algorithmic processes and input/output parameters.

```
MTT_2_colors % MTT dedicated to 2 colors
    MTT23i % with method = 'coloc' by default
    MTT23_dialog_box, MTTparams_def, MTT_param % User interface
        listing input parameters
    detect_reconnex_23 % trajectories (Sergé et al., 2008; Rouger et
        al., 2012)
    sort_traces % select long & fast enough trajectories
    ct4_by_file, ct5_by_file % histograms of peak & trajectory
        descriptors such as number, length, diffusion coefficient
    fit_directed_by_file % sort trajectories for D & γ
    cartobyf % maps for all files
    reg_2_colors % compute registration from DIC images, save
        mean_tform.mat
    traj_xy_coloc % map with colocalizations, registering magenta
        trajectories
        coloc3 % compute distance from green to magenta SM
    merge_colors % magenta/green stacks & max. projection
    detect_cell_contact % statistics at cell contact only
    cd(zdir) % analyze z-stack data
    MTT23i % run MTT on z-stack
    gradient_z2 % z profile of z-stack
    merge_colors % for z-stack
```

3. Outputs

MTT2col generates several files for each video (time-stack or z-stack), placed in different folders:

- '**output23**': this folder contains the raw data, as a matrix of trajectory parameters. Each column corresponds to a trajectory, and lines correspond to parameters: frame number, x and y position, signal, radius, offset, blink, and noise. Each set of 8 lines corresponds to a given frame. Thus, the matrix has as many columns as trajectories, and 8 times more lines than frames in the video. The *dat* file contains all trajectories, and the *mat* file is filtered for trajectories with length and diffusion coefficient above the thresholds defined in the list of input parameters. See code from *detect_reconnex_23* for more details (Sergé *et al.*, 2008).

- '`ct4_by_file`', '`ct5_by_file`': these folders contain histograms of peak & trajectory descriptors (ct4) and trajectory shape (ct5), as `png` images for each file and for all files pulled together, as well as a text file containing a table of the mean value for each parameter and file.
- '`carto`': this folder contains a map, *i.e.*, an image of the trajectories superimposed over the image of the cells, as saved in the '`dic`' folder (or the first frame of the video otherwise). The color code corresponds to the method selected in the input parameters: colocalization (for 2 colors), linearity (SCI), intensity, time, relative or absolute confinement level, or speed.

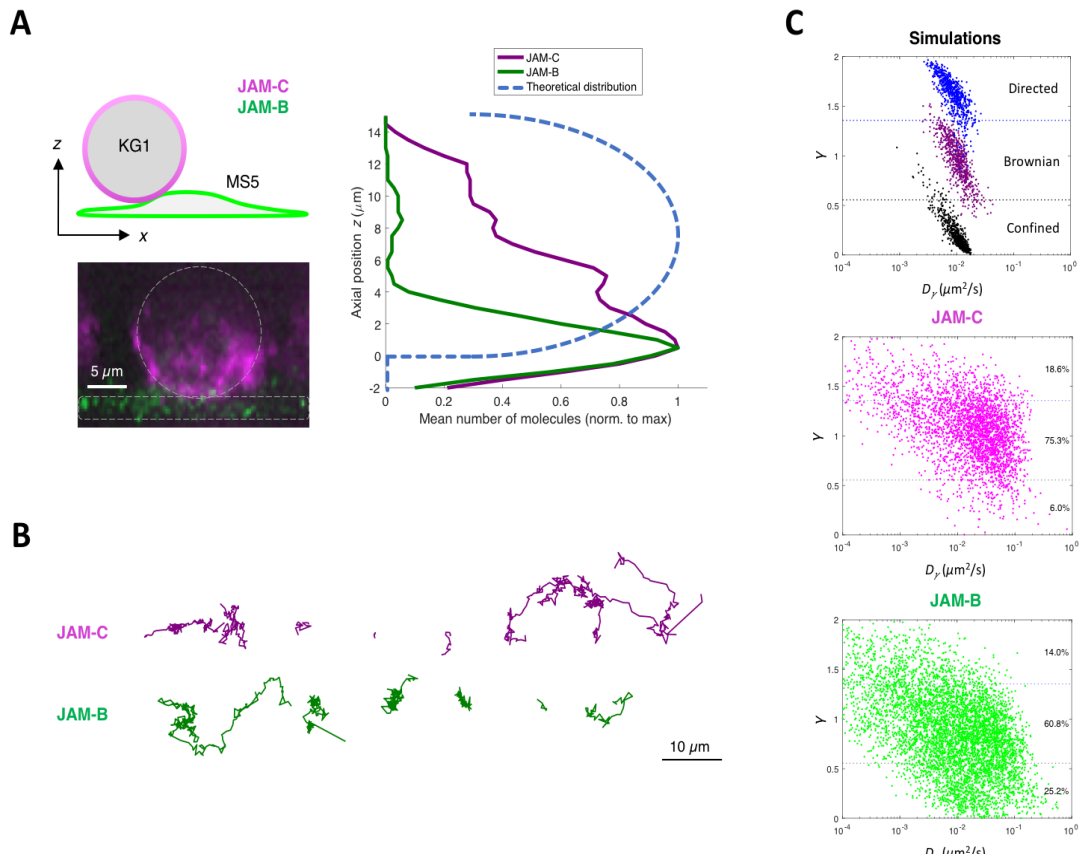


Figure 4. Representative results from MTT2col.

(A) Diagram of localization (top left), lateral view of a z-stack with each cell delimited by a white dotted line (bottom left), and z-profile of JAM axial positions, with the expected theoretical distribution for a uniform repartition on a sphere (right). (B) Representative trajectories, illustrating the variety of either Brownian, linear, or confined motions. (C) Dot plot of the anomalous exponent γ vs. the anomalous diffusion coefficient D_γ , which was computed from the mean squared displacement of each trajectory for simulations (top), JAM-C (middle), and JAM-B (bottom).

C. Data and code availability

The source code for both MTT and MTT2col is available for download as open-source software on GitHub at <https://github.com/arnauldserge1/MTT2col>.

The data that support the findings of this study are accessible for academic and non-profit research, upon reasonable request to the corresponding author, A.S. (arnauld.serge@univ-amu.fr).

Notes

Cite as: Maillot, L. et al. (2022). Single Molecule Tracking Nanoscopy Extended to Two Colors with MTT2col for the Analysis of Cell-Cell Interactions in Leukemia. Bio-protocol 12(08): e4390. DOI: 10.21769/BioProtoc.4390.

1. The signal-to-noise ratio of the fluorescence images may be enhanced by:
 - Increasing laser power, but avoiding photobleaching and photodamage.
 - Using bright (as well as stable) dyes: high cross section and quantum yield.
 - Increasing the acquisition time, but this is limited by the dynamics of the molecules: displacement (increasing with time, according to $r^2 = 4Dt$ for Brownian motion) should remain smaller than the pixel size to generate diffraction limited signals.
 - Increase the gain, while avoiding saturation, when using an EMCCD camera.
2. The pixel size in the images is determined by the pixel size of the camera, divided by the magnifications of the objective and the tube lens (optovar) and multiplied by the binning. We use a camera with a pixel size of 16 μm , a 100 \times lens, no optovar, and no binning, resulting in a pixel size of 160 nm in the images. Ideally, according to the Shannon-Nyquist theorem, the pixel size should be equal to (or less than) half the diffraction limit, *i.e.*, $0.3\lambda/\text{NA}$ (λ : fluorescence emission wavelength, NA: numerical aperture of the lens).
 - Too large a size leads to under-sampling of the single molecule signal (*i.e.*, the point-spread function of the microscope, with a size set by diffraction).
 - Too small a size dilutes the signal over neighboring pixels, leading to a weaker signal (lower number of collected photons per pixel).
3. Scientific cameras may generate 8, 12, 14, 16, or 32-bit images (as well as 24, 36, or 48-bit for color cameras, which is not appropriate here). MTT is intended for 16-bit images by default. It might be used for other formats, but with careful checking of the results.
4. A typical experiment generates about tens of videos, with about hundreds of molecules per frame, and hundreds of frames per video. There is thus a large variability in the total size of data to analyze. Similarly, computer processing capability can change over at least an order of magnitude. Of note, computing time scales linearly with the number of videos, as well as the number and size of frames, but exponentially with the density of targets (labeled molecules), which leads to the increasing computation of connectivity possibilities, when molecules are getting close to each other. Running MTT2col analysis on a standard computer (*e.g.*, 6–8 cores, 3–3.5 GHz processor, and 16–32 Gb RAM) for a few tens of video files typically takes a few hours (*e.g.*, 0.5–6 h). Therefore, an experiment performed during one day can be analyzed overnight, with results available the next day.
5. Statistical tests can be automatically performed using an appropriate Matlab script.

Recipes

1. Culture medium for MS5 cells

Iscove's Modified Dulbecco's Medium (IMDM)
10% Fetal Calf Serum
1% HEPES, essential amino acids
1% sodium pyruvate
25 μM β -mercaptoethanol
1% L-glutamine

2. Culture medium for KG1 cells

Iscove's Modified Dulbecco's Medium (IMDM)
10% Fetal Calf Serum
1% L-glutamine

Acknowledgments

We thank Jessica Chevallier (TAGC, CIML, LAI, Aix-Marseille Univ) for critical reading of the manuscript. We Cite as: Maillot, L. et al. (2022). Single Molecule Tracking Nanoscopy Extended to Two Colors with MTT2col for the Analysis of Cell-Cell Interactions in Leukemia. Bio-protocol 12(08): e4390. DOI: 10.21769/BioProtoc.4390.

thank Martine Biarnes-Pelicot (LAI, Aix-Marseille Univ) for providing technical help for cell culture. We thank Dr. Dalia El Arawi and Dr. Laurent Limozin (LAI, Aix-Marseille Univ) for providing technical help for the microscopy setup. We thank Rémi Torro and Dr. Pierre-Henri Puech (LAI, Aix-Marseille Univ) for providing technical help for Github. We also thank the microscopy, cytometry, and statistics research facilities at CRCM, as well as Thi Tien Nguyen for the cell culture facility at LAI, for excellent technical support.

This work was supported by the Fondation ARC pour la Recherche sur le Cancer (PJA 20131200238 to A.S.), the Institute Marseille Imaging, and institutional grants from INSERM and Aix-Marseille Univ. L.M. was supported by grants from the GdR Imabio (Bourse Accueil Master Interdisciplinaire) and from the Ligue contre le Cancer (IP/SC/SK - 17250). This protocol was originally developed in Gorshkova *et al.* J Cell Sci. 2021.

Competing interests

We declare no competing interest.

References

- Achimovich, A. M., Ai, H. and Gahlmann, A. (2019). [Enabling technologies in super-resolution fluorescence microscopy: reporters, labeling, and methods of measurement](#). *Curr Opin Struct Biol* 58: 224-232.
- Balzarotti, F., Eilers, Y., Gwosch, K. C., Gynna, A. H., Westphal, V., Stefani, F. D., Elf, J. and Hell, S. W. (2017). [Nanometer resolution imaging and tracking of fluorescent molecules with minimal photon fluxes](#). *Science* 355(6325): 606-612.
- De Grandis, M., Bardin, F., Fauriat, C., Zemmour, C., El-Kaoutari, A., Serge, A., Granjeaud, S., Pouyet, L., Montersino, C., Chretien, A. S., *et al.* (2017). [JAM-C Identifies Src Family Kinase-Activated Leukemia-Initiating Cells and Predicts Poor Prognosis in Acute Myeloid Leukemia](#). *Cancer Res* 77(23): 6627-6640.
- Gorshkova, O., Cappai, J., Maillot, L. and Serge, A. (2021). [Analyzing normal and disrupted leukemic stem cell adhesion to bone marrow stromal cells by single-molecule tracking nanoscopy](#). *J Cell Sci* 134(18): jcs258736.
- Jacquemet, G., Carisey, A. F., Hamidi, H., Henriques, R. and Leterrier, C. (2020). [The cell biologist's guide to super-resolution microscopy](#). *J Cell Sci* 133(11): jcs240713.
- Lemon, W. C. and McDole, K. (2020). [Live-cell imaging in the era of too many microscopes](#). *Curr Opin Cell Biol* 66: 34-42.
- Li, H. and Vaughan, J. C. (2018). [Switchable Fluorophores for Single-Molecule Localization Microscopy](#). *Chem Rev* 118(18): 9412-9454.
- De Los Santos, C., Chang, C. W., Mycek, M. A. and Cardullo, R. A. (2015). [FRAP, FLIM, and FRET: Detection and analysis of cellular dynamics on a molecular scale using fluorescence microscopy](#). *Mol Reprod Dev* 82(7-8): 587-604.
- Manley, S., Gillette, J. M., Patterson, G. H., Shroff, H., Hess, H. F., Betzig, E. and Lippincott-Schwartz, J. (2008). [High-density mapping of single-molecule trajectories with photoactivated localization microscopy](#). *Nat Methods* 5(2): 155-157.
- Manzo, C. and Garcia-Parajo, M. F. (2015). [A review of progress in single particle tracking: from methods to biophysical insights](#). *Rep Prog Phys* 78(12): 124601.
- Owen, D. M., Williamson, D., Rentero, C. and Gaus, K. (2009). [Quantitative Microscopy: Protein Dynamics and Membrane Organisation](#). *Traffic* 10: 962-971.
- Petazzi, R. A., Aji, A. K. and Chiantia, S. (2020). [Fluorescence microscopy methods for the study of protein oligomerization](#). *Prog Mol Biol Transl Sci* 169: 1-41.
- Rouger, V., Bertaux, N., Trombik, T., Mailfert, S., Billaudeau, C., Marguet, D. and Serge, A. (2012). [Mapping molecular diffusion in the plasma membrane by Multiple-Target Tracing \(MTT\)](#). *J Vis Exp* (63): e3599.
- Salles, A., Billaudeau, C., Serge, A., Bernard, A. M., Phelipot, M. C., Bertaux, N., Fallet, M., Grenot, P., Marguet, D., He, H. T., *et al.* (2013). [Barcoding T cell calcium response diversity with methods for automated and accurate analysis of cell signals \(MAAACS\)](#). *PLoS Comput Biol* 9(9): e1003245.
- Schmidt, T., Schütz, G. J., Gruber, H. J. and Schindler, H. (1996). [Local Stoichiometries Determined by Counting](#)

Cite as: Maillot, L. *et al.* (2022). Single Molecule Tracking Nanoscopy Extended to Two Colors with MTT2col for the Analysis of Cell-Cell Interactions in Leukemia. Bio-protocol 12(08): e4390. DOI: 10.21769/BioProtoc.4390.

- [Individual Molecules.](#) *Analytical Chemistry* 68(24): 4397-4401.
- Sergé, A., Bertaux, N., Rigneault, H. and Marguet, D. (2008). [Dynamic multiple-target tracing to probe spatiotemporal cartography of cell membranes.](#) *Nat Methods* 5(8): 687-694.
- Sergé, A. (2016). [The Molecular Architecture of Cell Adhesion: Dynamic Remodeling Revealed by Videonanoscopy.](#) *Front Cell Dev Biol* 4: 36.
- Sharonov, A. and Hochstrasser, R. M. (2006). [Wide-field subdiffraction imaging by accumulated binding of diffusing probes.](#) *Proc Natl Acad Sci U S A* 103(50): 18911-18916.

Activation of Mitochondrial Ca²⁺ Oscillation and Mitophagy Induction by Femtosecond Laser Photostimulation

Xiaoying Tian and Hao He*

School of Biomedical Engineering, Shanghai Jiao Tong University, Shanghai, China

*For correspondence: haohe@sjtu.edu.cn

[Abstract] Ultra-precise stimulation solely to individual mitochondria, without any influence to the whole cell, is quite difficult by traditional biochemical reagents. In mitophagy research, the mitochondria and even the whole cell usually suffer irreversible and great damage caused by treatment with potent chemicals. In this protocol, we present the technical procedures of our developed noninvasive **ultra-precise laser stimulation (UPLaS)** technology, which introduces precise stimulation to individual mitochondria, to excite mitochondrial Ca²⁺ (mitoCa²⁺) oscillations, with little perturbation to mitochondrial membrane potential (MMP), or mitochondrial reactive oxygen species (mitoROS). The mitoCa²⁺ oscillation by UPLaS was able to initiate the PINK1/Parkin pathway for mitophagy. This protocol has good potential to benefit researches on mitophagy and mitochondrial diseases.

Graphic abstract:

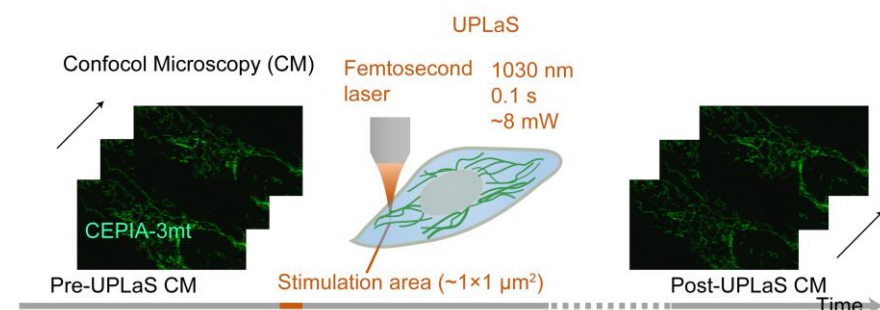


Figure 1. Flowchart of the UPLaS technology.

The femtosecond laser (1030 nm, 1 MHz, 220 fs) can stimulate individual mitochondria ($1 \mu\text{m}^2$) for a short period (0.1 s), whereas confocal microscopy (CM) provides continuous cell imaging to monitor molecular dynamics in real time, before and after UPLaS.

Keywords: Ultra-precise laser stimulation, Femtosecond laser, Confocal microscope, Ca²⁺, Mitophagy, PINK1, Parkin

[Background] Precise stimulation of individual mitochondria, without perturbation to the whole cell or damage to mitochondria, is of great significance to mitochondrial research (Russell *et al.*, 2020). Moreover, the isolated modulation of mitochondrial membrane potential (MMP), mitochondrial reactive oxygen species (mitoROS), or mitochondrial Ca²⁺ (mitoCa²⁺), without perturbation to the other two, might

provide more insights into mitochondria function. Mitophagy is abnormal in Parkinson's disease (PD) (Liu, J. et al., 2019; Ge et al., 2020). The mechanism of mitophagy and its dysregulation is essential to the better understanding of PD. In previous works, where PINK1/Parkin mediated mitophagy has been studied (Jin and Youle, 2013; Lazarou et al., 2015; Pickrell and Youle, 2015; Chung et al., 2020), carbonyl cyanide m-chlorophenyl hydrazine (CCCP) was extensively used to depolarize mitochondria and trigger mitophagy. However, the completely depolarization of MMP and significant high-level mitoROS are irreversible, and prevent further investigation of the mechanism of action of mitochondria.

Femtosecond laser has advanced biological researches by providing efficient multiphoton excitation, while maintaining good biological safety (Smith et al., 2005, 2008; Iwanaga, et al., 2006; Liu, X. et al., 2009; Zhao et al., 2009; Wang et al., 2014). Specifically, a transient tightly-focused femtosecond laser irradiation to a localized subcellular structure has been demonstrated to be a highly efficient optical method to directly induce molecular signaling events in single cells (He et al., 2012; Wang et al., 2014, 2018; Cheng et al., 2021). In this protocol, we present a noninvasive **ultra-precise laser stimulation** (UPLaS) technology to individual mitochondria that excites mitoCa²⁺ oscillations, with little perturbation to MMP or mitoROS. This UPLaS technology is achieved by coupling a femtosecond laser to a confocal microscope, to provide single target cells with a short flash photostimulation. The mitoCa²⁺ oscillation induced by UPLaS initiates the PINK1/Parkin pathway for mitophagy.

The UPLaS technology provides a noninvasive method for simultaneous photostimulation and confocal microscopy of subcellular organelles at a resolution of 628.3 nm. This method is highly flexible, as it can be demonstrated on any two-photon microscope system, and any subcellular organelle can be stimulated by this system.

Materials and Reagents

A. Hela cell culture

1. P100 mm Petri dish (Corning, catalog number: 3262)
2. 35 mm Glass Bottom Cell Culture Dish (Nest, catalog number: 801002)
3. μ-Dish 35 mm, high Grid-500 Glass Bottom (IBidi, catalog number: 81168)
4. Hela cells (National Collection of Authenticated Cell Cultures, Manufacturer, Brand, catalog number: TCHu187)
5. DMEM (Hyclone, catalog number: SH30243.01)
6. Fetal Bovine Serum (FBS; Gibco, catalog number: 10099141)
7. Penicillin/Streptomycin (Gibco, catalog number: 10378016)
8. Phosphate-buffered saline (PBS; Hyclone, catalog number: SH30256.01)
9. 0.25% Trypsin-EDTA (Gibco, catalog number: 25200056)
10. Hela culture medium (see Recipes)

B. SH-SY5Y cell culture

1. SH-SY5Y cells (COBIOER BIOSCIENCES, catalog number: CBP60913)

2. MEM, no glutamine (Gibco, catalog number: 11090081)
3. Ham's F-12 Nutrient Mix (Gibco, catalog number: 11765054)
4. GlutaMAX™ (Gibco, catalog number: 35050061)
5. Sodium Pyruvate (Gibco, catalog number: 11360070)
6. MEM NEAA (Gibco, catalog number: 11140050)
7. SH-SY5Y culture medium (see Recipes)

C. Cell Transfection and loading

1. CEPIA-3mt (Addgene, Plasmid #58219)
2. Parkin-mCherry (Addgene, Plasmid #23956)
3. LC3-GFP (Addgene, Plasmid #11546)
4. jetPRIME (Polyplus, catalog number: 101000046)
5. MitoTracker™ Green (Invitrogen, catalog number: M7514)
6. MitoTracker™ Red CMXRos (Invitrogen, catalog number: M7512)
7. Tetramethylrhodamine, Methyl Ester, Perchlorate (TMRM) (Invitrogen, catalog number: T668)
8. MitoSOX™ Red Mitochondrial Superoxide Indicator (Invitrogen, catalog number: M36008)
9. Dimethyl sulfoxide (DMSO,Sigma-Aldrich, catalog number: D9170)

D. Immunofluorescence

1. 4% Paraformaldehyde Fix Solution (Beyotime, catalog number: P0099)
2. Triton X-100 (Sigma-Aldrich, catalog number: 9036-19-5)
3. NON-Fat Powdered Milk (Sangon Biotech, catalog number: A600669-0250)
4. Tween-20 (Sigma-Aldrich, catalog number: P1379)
5. anti-PINK1 antibody (Abcam, catalog number: ab216144)
6. antibody anti-Rabbit IgG H&L (Sigma, catalog number: AP307P)
7. Antifade Mounting Medium (Beyotime, catalog number: P0126)

Equipment

1. Femtosecond-laser (MenloSystems, Type: BlueCut OEM Seed, Serial No: 111; Type: BlueCut Amp, Serial No: 116; 1030 nm, 1 MHz, 220 fs)
2. Confocal microscope (Olympus, model: FV1200)
3. Laser power meter (COHERENT, Item #: 1098297, Model: FIELDMATE, Serial #: 0763K14R)

Software

1. FV1200 (Olympus)
2. ImageJ
3. GraphPad Prism 7

4. Adobe Illustrator CC 2017

Procedure

A. Cell culture and transfection

1. Hela cell passage
 - a. Hela cells were cultured in DMEM supplemented with 10% FBS and 1% Penicillin/Streptomycin (hitherto referred to as DMEM10).
 - b. Remove the DMEM10 culture medium from the 100 mm Petri cell culture dish when cell density reaches approximately 80%.
 - c. Wash the Petri dish three times with 1.5 mL of PBS. Remove the PBS.
 - d. Slowly add 1 mL of trypsin, and place the dish back into the incubator at 37°C for 1 min.
 - e. Remove the trypsin. Add 2–3 mL of DMEM10 culture medium. Pipette the medium several times to help the cells detach. Transfer the medium containing cells to a 15 mL tube.
 - f. Seed ~25,000 cells into a 35 mm glass bottom Petri dish, and add DMEM10 culture medium up to 1.5 mL.
 - g. Place the dish containing cells back in the incubator. Incubate the cells at 37°C for 24 h before transfection, staining, or UPLaS experiments.
2. Cell transfection
 - a. Dilute 1 µg of DNA (CEPIA-3mt, Parkin-mCherry, or LC3-GFP) in 200 µL of jetPRIME buffer.
 - b. Vortex for 10 s and spin down.
 - c. Add 2 µL of jetPRIME reagent (DNA/jetPRIME ratio 1:2).
 - d. Vortex for 1 s, spin down, and incubate at room temperature (RT) for 10 min.
 - e. Add the transfection mix to the cells cultured in 2 mL of DMEM10 culture medium in a 35 mm Petri dish.
 - f. Replace DMEM10 culture medium with 2 mL of fresh DMEM10 culture medium 4 h after transfection.
 - g. Check transfection efficiency 24–48 h after transfection. Normally, select several fields of view (FOV) by fluorescence microscopy, the transfection is ideal when 60–80% of cells have been transfected successfully.

Note: According to the actual transfection efficiency and cell density, 1–3 µg of DNA can be added, while maintaining the DNA/jetPRIME ratio previously used. The culture and transfection procedures for SH-SY5Y cells are the same as that of Hela cells. The SH-SY5Y full serum culture medium (MEM/F12-10 culture medium) contains 43.5 mL of MEM, 43.5 mL of Ham's F-12 Nutrient Mix, 10 mL of FBS, 1 mL of GlutaMAX, 1 mL of Sodium Pyruvate, 1 mL of MEM NEAA, and 1 mL of (1×) Penicillin/Streptomycin. The culture medium for SH-SY5Y cells in all culture and transfection steps is MEM/F12-10.

B. Setting up the UPLaS system

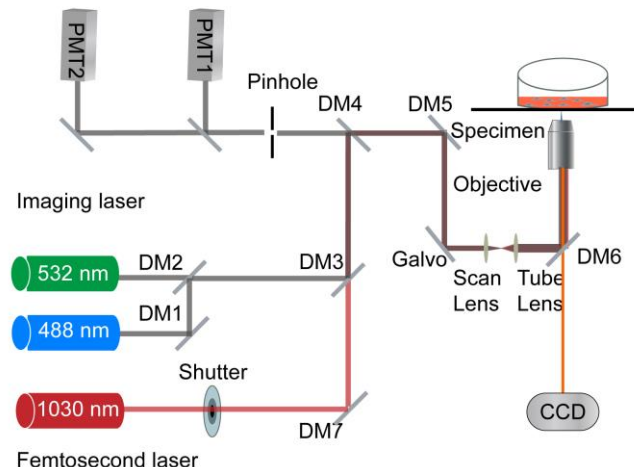
This UPLaS system consists of a commercial confocal microscope and a femtosecond laser. In Figure 2, a fiber femtosecond laser (1,030 nm, 1 MHz, 220 fs, 1 W) is incorporated into the excitation path of a confocal system.

1. Turn on the confocal microscope.
2. Fix the Galvo to the center of the FOV.
3. Turn on the femtosecond laser.

Note: Please set the femtosecond laser power at a low level (~50 mW, tested between Shutter and RM3 by a laser power meter) for the process of adjusting the optical path.

4. Use the reflective mirrors (RM1 and RM2, shown in Figure 2B) to direct the femtosecond laser beam through a mechanical shutter. Open the shutter.

A



B

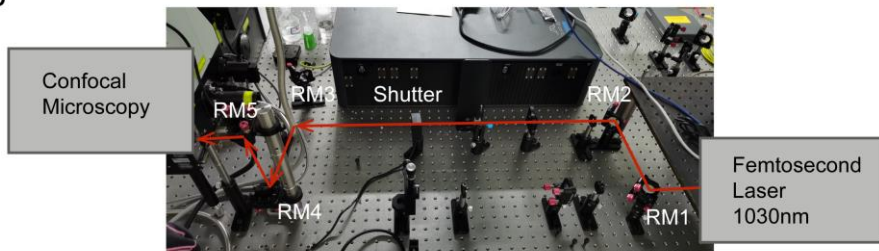


Figure 2. The photostimulation scheme established on a femtosecond laser coupling into a confocal microscope.

(A) Optical paths of (B) the UPLaS system. The femtosecond laser is aligned into the microscope scanning system through RM4 and RM5, to form a UPLaS system. A CCD camera is used to provide a bright-field image to align the optical path. DM = dichroic mirror, RM = reflective mirror. The wavelength of confocal scanning laser is 488 nm/532 nm, and the typical collection wavelength interval of fluorescence is <560 nm/560–625 nm/> 625 nm. The fiber femtosecond laser (1,030 nm, 120 fs, 50 MHz, 1 W) can be replaced by a Ti = Sapphire laser (810 nm, 80 MHz, 65 fs, 1 W), or other commercial femtosecond laser oscillators.

5. Steer RM4 and RM5 to make the femtosecond laser beam coincide with the scanning laser beam.
6. Measure the transmission efficiency of the objective of the femtosecond laser.

Note: It will use the power at specimen to illustrate the related experiment procedures below.

7. Turn off the shutter, femtosecond laser, and confocal microscope until experiments start.

Notes:

- a. *The shutter is synchronized with the confocal scanning process. It opens at the pre-designed time which is set through the confocal imaging controlling software. The stimulation area can be pre-assigned manually in the confocal imaging controlling software to any form like line, polygon, or circle. Thus, the sample is only stimulated by the femtosecond laser when the confocal scanning process enters a given imaging frame. Along with femtosecond laser stimulation, confocal microscopy provides continuous cell imaging to monitor molecular dynamics in real time.*
- b. *It can be replaced by a Ti: Sapphire laser or other commercial femtosecond oscillators in the NIR range. The laser power and some other photostimulation parameters need to be tuned because the optical parameters (pulse width, wavelength, and repetition rate) vary a lot in different femtosecond lasers, which thus induce different multiphoton excitation efficiencies. Especially if the wavelength is changed, the power needs to be adjusted carefully. Our experience is that, if the wavelength reaches 800 nm, the power needs to be reduced a lot. If the wavelength is as short as 700 nm, the cells will be extremely sensitive, and this is not recommended.*

C. Activation of mitoCa²⁺ oscillation by UPLaS

1. Transfecting cells with fluorescent Ca²⁺ indicated protein
 - a. Prepare Hela cells transfected with CEPIA-3mt, as described in step A.

Note: For a 35 mm glass Petri dish, 1 µg of plasmid CEPIA-3mt is enough. The amount of plasmid can be adjusted according to the actual transfection efficacy and cell density, as mentioned in step A.2.g.
 - b. Replace the medium 4 h after transfection, and incubate for 24 h before UPLaS experiments.
2. Activation of Ca²⁺ oscillation by UPLaS.
 - a. Turn on the femtosecond laser 30 min before the start of the experiment, to stabilize the laser energy output and ensure the shutter is closed.
 - b. Turn on the laser-scanning confocal microscope and open the microscope software. Set the excitation laser at 473 nm. Set the power level of the 473 nm laser at 0.1 mW. Set the image size to 512 × 512 pixels. Set the interval time of each pixel as 2 µs. Set the total imaging frames at approximately 100, to provide ~3 min of continuous microscopy for any individual experiment.
 - c. Take out the Petri dish containing cells transfected with CEPIA-3mt from the incubator, and place the cells into the 37°C incubator mounted over the microscope stage.

- d. Select the target cell, and acquire fluorescent images of CEPIA-3mt with the 473 nm laser, as shown in Figure 1.
- e. Select the target mitochondria and define the parameters of stimulation.
 - i. Set a stimulation point ($1 \times 1 \mu\text{m}^2$) in a submicron region, in a single mitochondrial tubular structure
 - ii. Set the total stimulation time at 0.1 s. Synchronize the shutter of femtosecond laser with the confocal scanning according to the predefined photostimulation area, which is only open when the laser scanning drops in the stimulation frame, and closes immediately when it goes out.
 - iii. Set the power of the femtosecond laser to 8 mW (1,030 nm) at the sample.
- f. Set the scanning and stimulation time sequence.
- g. Scan the targeted cells during Pre-UPLaS CM and Post-UPLaS CM with a 473 nm laser. Stimulate the cells during UPLaS with the femtosecond laser.
- h. Click on the XY-T button to start the continuous microscopy imaging progress.
- i. Wait until the imaging process is finished and save the imaging data.
- j. Turn off the femtosecond laser and confocal microscope after the experiment.

D. Detecting the change in MMP and mitoROS

1. Detecting MMP change in cells stimulated by UPLaS
 - a. Prepare Hela cells following step A.1.
 - b. Dissolve 5 mg of TMRM into 200 μL of DMSO, to a stock concentration of 50 mM.
 - c. Dissolve 1 μL of TMRM into 1 mL of DMSO to 50 μM .
 - d. Prepare the TMRM staining solution: dilute 1 μL of TMRM (50 μM) in 1mL of DMEM10 culture medium, to a final concentration of 50 nM.
 - e. Incubate the cells in the TMRM staining solution at 37°C for 20 min.
 - f. Replace the TMRM staining solution with 2 mL of DMEM10 culture medium.
 - g. Use the UPLaS system to stimulate a single mitochondria and detect the change in MMP, following step C.2.

Note: In step C.2, excite the fluorescence of TMRM with the 543 nm laser.

2. Detecting mitoROS change in cells stimulated by UPLaS
 - a. Prepare Hela cells following step A.1.
 - b. Dissolve 50 μg of MitoSOX in 6.6 μL of DMSO, to a stock concentration of 10 mM.
 - c. Prepare the MitoSOX staining solution: dilute 1 μL of MitoSOX (10 mM) into 1 mL of DMEM10 culture medium, to a final concentration of 10 μM .
 - d. Incubate the cells in the MitoSOX staining solution at 37°C for 20 min.
 - e. Replace the MitoSOX staining solution with 2 mL of DMEM10 culture medium.
 - f. Use the UPLaS system to stimulate a single mitochondria, and detect the change in mitoROS following step C.2.

Note: In step C.2, excite the fluorescence of MitoSOX with the 543 nm laser.

E. Detecting the recruitment of Parkin

1. Transfecting cells with fluorescent Parkin indicated protein
 - a. Seed ~25,000 cells into a 35 mm glass bottom Petri dish with grids, and transfect cells with Parkin-mCherry, as described in step A.

Note: For a 35 mm Petri dish, 1 µg of plasmid DNA Parkin-mCherry is enough. The amount of plasmid can be adjusted according to the actual transfection efficacy and cell density as mentioned in step A.2.g.

 - b. Replace the DMEM10 culture medium with 2 mL of fresh DMEM10 culture medium 4 h after transfection, and incubate for 24 h before UPLaS experiments.
2. Loading cells with MitoTracker
 - a. Prepare Hela cells transfected with Parkin-mCherry, following step E.1.
 - b. Dissolve 50 µg of MitoTracker Green in 74.4 µL of DMSO, to a stock concentration of 1 mM.
 - c. Dissolve 1 µL of MitoTracker Green (1 mM) in 10 µL of DMSO, to 100 µM.
 - d. Prepare the MitoTracker Green staining solution: dilute 1 µL of MitoTracker Green (100 µM) into 1 mL of DMEM10 culture medium, to a final concentration of 100 nM.
 - e. Incubate the cells in the MitoTracker Green staining solution at 37°C for 20 min.
 - f. Replace the MitoTracker Green staining solution with 2 mL of DMEM10 culture medium.
3. Detecting the recruitment of Parkin to the mitochondria induced by UPLaS
 - a. Use the UPLaS system to stimulate a single mitochondria tubular structure, and acquire fluorescent images of Parkin-mCherry and MitoTracker Green, following step C.2.

Note: In step C.2, excite the fluorescence of Parkin-mcherry with the 543 nm laser and MitoTracker Green with the 473 nm laser. Set the total imaging frames at 2, to acquire an image of Parkin distribution before UPLaS.

 - b. Place the cells back into the incubator.
 - c. After 30 min, put the dish with grids on the microscope stage. Locate the selected grid and the cell that was stimulated by the femtosecond laser.
 - d. Start single frame confocal scanning. Locate the mitochondrion which is stimulated by the femtosecond laser. Save the Parkin distribution fluorescent picture of photostimulation for further data analysis.
 - e. Place the cells back into the incubator again, and repeat steps E.3.c and d, after 1 h, and 2 h of stimulation.
 - f. Turn off the femtosecond laser and confocal microscope after the experiment.

F. Detecting the change in PINK

1. Cell Preparation and Stimulation
 - a. Prepare Hela cells seeded into a 35 mm glass bottom Petri dish with grids, as describe in step A.1.
 - b. Dissolve 50 µg of MitoTracker Red in 94 µL of DMSO, to a stock concentration of 1 mM.
 - c. Dissolve 1 µL of MitoTracker Red (1 mM) in 10 µL of DMSO, to 100 µM.

- d. Prepare the MitoTracker Red staining solution: dilute 1 µL MitoTracker Red (100 µM) in 1 mL of DMEM10 culture medium, to a final concentration of 100 nM.
 - e. Incubate the cells in the MitoTracker Red staining solution at 37°C for 20 min.
 - f. Replace the MitoTracker Red staining solution with 2 mL of DMEM10 culture medium.
 - g. Use the UPLaS system to stimulate an individual mitochondrion, as described in step E.3.
Note: In step E.3, excite the fluorescence of MitoTracker Red with the 543 nm laser.
 - h. Place the dish back in the incubator. Incubate the cells for 5 min, 30 min, and 1 h before immunofluorescence (IF) microscopy.
2. Immunofluorescence (IF) microscopy of PINK1 in cells with UPLaS
 - a. Wash: Take the dish containing cells with photostimulation treatment in step F.1 out of the incubator. Remove DMEM10 culture medium. Wash the cells with PBS three times. Remove PBS.
 - b. Fix: Add 1 mL of 4% paraformaldehyde (PFA) at 4°C into the dish. Fix the cells with 4% PFA for 10 min. Remove the PFA. Wash the cells with PBS twice for 5 min each time. Remove PBS.
 - c. Permeabilise: Incubate the cells in 1 mL of 0.1% Triton X-100 in PBS at RT for 15 min. Remove the Triton X-100 buffer. Wash the cells with PBS twice for 5 min each time. Remove PBS.
 - d. Block: Incubate the cells in 1 mL of 1% non-fat powdered milk in PBS at RT for 30 min. Remove the blocking buffer.
 - e. Primary antibody incubation: Dilute anti-PINK antibody in PBS with 0.1% Tween-20 (1:500). Incubate the cells in primary antibody buffer at 4°C for 12 h. Remove the primary antibody incubation buffer.
 - f. Secondary antibody incubation: Dilute the secondary antibody, anti-Rabbit IgG H&L, in PBS with 1% Tween-20 (1:10,000). Incubate the cells in the secondary antibody buffer at RT for 2 h. Remove the secondary antibody incubation buffer.
 - g. Wash the cells with PBS. Remove PBS.
 - h. Sealing: add the antifade mounting medium into the Petri dish to maintain the fluorescence.
 - i. Place the treated dish on the microscope stage. Locate the selected grid and the cell which was treated with the femtosecond laser.
 - j. Start single frame confocal scanning. Excite the fluorescence of Anti-PINK with the 473 nm laser, and excite the fluorescence of MitoTracker Red with the 543 nm laser.
 - k. Save the fluorescent images of stimulated cells for further data analysis.

G. Detecting the change in mitophagy

1. Transfecting cells with fluorescent autophagosomes indicated protein
 - a. Prepare HeLa cells seeded into a 35 mm glass bottom Petri dish with grids and transfect cells with LC3-GFP as described in step A.
Note: For a 35 mm Petri dish, 1 µg of DNA plasmid LC3-GFP is enough. The amount of

plasmid can be adjusted according to the actual transfection efficacy and cell density as mentioned in step A.2.g.

- b. Replace the DMEM10 culture medium with 2 mL of fresh DMEM10 culture medium 4 h after transfection, and incubate for 24 h before UPLaS experiments.
2. Loading cells with MitoTracker Red
 - a. Prepare HeLa cells transfected with LC3-GFP, following step E.1.
 - b. Dissolve 50 µg of MitoTracker Red in 94 µL of DMSO, to a stock concentration of 1 mM.
 - c. Dissolve 1 µL of MitoTracker Red (1 mM) in 10 µL of DMSO, to 100 µM.
 - d. Prepare the MitoTracker Red staining solution: dilute 1 µL of MitoTracker Red (100 µM) in 1 mL of DMEM10 culture medium, to a final concentration of 100 nM.
 - e. Incubate the cells in the MitoTracker Red staining solution at 37°C for 20 min.
 - f. Replace the MitoTracker Red staining solution with 2 mL of DMEM10 culture medium.
3. Detecting the formation of autophagosomes induced by UPLaS
 - a. Carry out UPLaS experiment on cells transfected with LC3-GFP and loaded with MitoTracker Red, as described in step C.2.
Note: In step C.2, excite the fluorescence of MitoTracker Red with the 543 nm laser and LC3-GFP with the 473 nm laser.
 - b. Place the cells back into the incubator.
 - c. After 30 min, place the dish on the microscope stage. Locate the selected grid and the cell which was stimulated by the femtosecond laser.
 - d. Start single frame confocal scanning. Locate the mitochondrion which was stimulated by the femtosecond laser. Save the LC3-GFP distribution fluorescent images of photostimulation cell for further data analysis.

Data analysis

A. The steps of processing fluorescence images

1. Acquire fluorescence images according to confocal microscope software FV1200 (Olympus).
 - a. Choose File > Open.
 - b. Select an experiment file and click on Open.
 - c. Choose File > Export > File type: TIFF.
 - c. Choose a destination folder and click on Save, as shown in Figure 3.

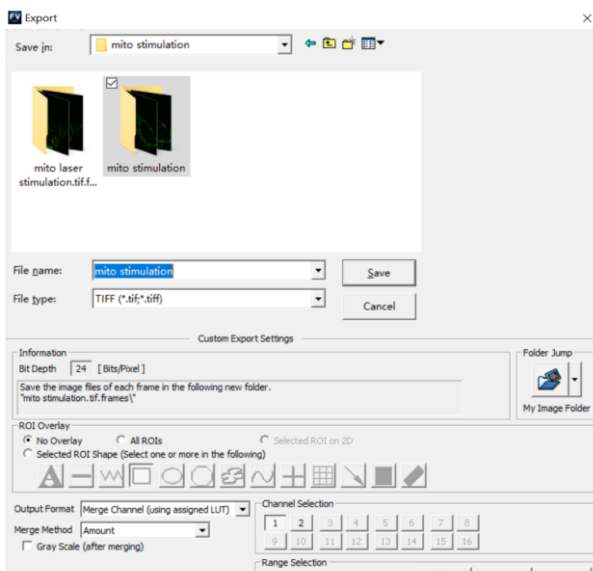


Figure 3. Exporting an experiment file as TIFF image series.

2. Acquire fluorescence intensity by ImageJ software.
 - a. Drag your file folder into ImageJ. Select Convert to RGB and Use Virtual Stack. Click on Yes, as shown in Figure 4A. All images in this folder are shown as a stack (Figure 4B).
 - b. Click on the ‘polygon’ button (Figure 4C). To create a polygon selection, click repeatedly with the mouse to create line segments. When finished, click in the small box at the starting point (or double click), and ImageJ will automatically draw the last segment (Figure 4D). The points that define a polygon selection can be moved, and modifier keys can be used to delete or add new vertices to the polygon.
 - c. Choose Image > Stacks > Measure Stack (Figure 4E), to display the mean value of all images in this stack (Figure 4F).
3. Copy the mean values of all images from ImageJ and the time sequence recorded by FV1200 to GraphPad Prism 7. Plot the charts using GraphPad Prism 7.

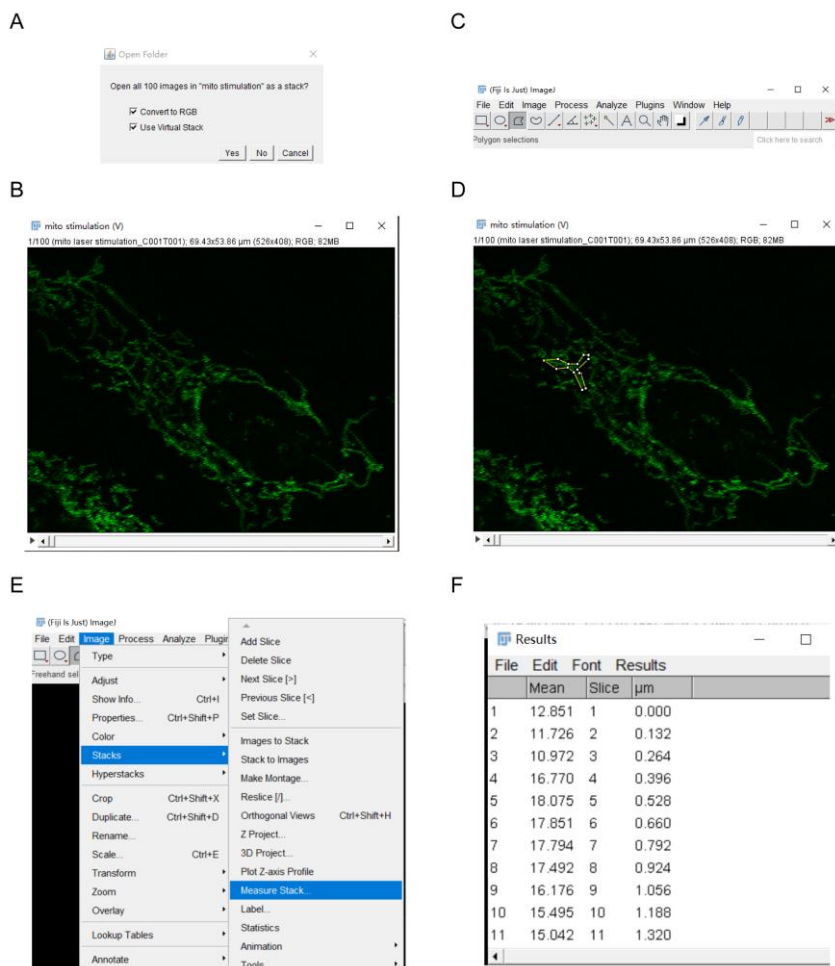


Figure 4. The workflow of acquiring fluorescence intensity using ImageJ software.

B. Representative data

As shown in Figures 1 and 2, we established a noninvasive **ultra-precise laser stimulation** (UPLaS) technology by aligning a femtosecond laser into the optical path of a confocal microscope. This UPLaS method enables spatiotemporal-specific stimulations to target individual mitochondria. As shown in Figure 5, the UPLaS evoked localized mitoCa^{2+} oscillations in a single mitochondrial tubular structure, with transient, moderate, and fast-recovered MMP depolarization, while the mitoROS increased there, without any perturbation to its neighbors.

The time-lapse dynamics of Parkin-mCherry indicate the most significant Parkin recruitment to the stimulated mitochondria was presented 1 h after UPLaS. Then, we measured the colocalization of PINK1 [visualized by immunofluorescence (IF) microscopy] and mitochondria (indicated by MitoTracker Red). The IF microscopy of PINK1 was performed at 5, 30, and 60 min after UPLaS. The level of PINK1 on the stimulated mitochondria was higher 1 h after UPLaS. Ultimately, the mitochondria treated with UPLaS all presented consistent coincidence with autophagosomes. The detailed analysis can be found at <https://doi.org/10.1038/s41419-021-03913-3>.

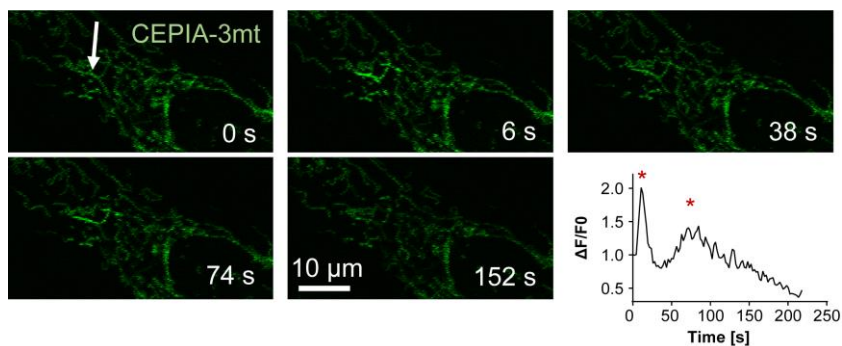


Figure 5. UPLaS excites mitoCa²⁺ oscillations in the target mitochondria.

The individual mitochondrion stimulated by UPLaS. The responses of mitoCa²⁺ to UPLaS (at t = 5 s) are indicated by CEPIA-3mt. The white arrow points at the single mitochondria tubular structure stimulated by the femtosecond laser.

C. Each independent experiment should be executed with at least three experimental repeats.

Notes

1. In our experiment, we align the femtosecond laser into the confocal microscope. The function of two-photon microscope can realize the UPLaS technology completely.
2. We conducted the same UPLaS experiments on Hela cells and SH-SY5Y cells. The culture and transfection processes were all the same as that of Hela cells.
3. Turn off the femtosecond laser and confocal microscope after the experiment.
4. Keep the power of visible lasers (473 nm and 543 nm) as low as possible when using TMRM.

Recipes

1. Hela culture medium (DMEM10 culture medium)
500 mL of DMEM
10 mL of (1×) Penicillin/Streptomycin
50 mL of Fetal Bovine Serum
2. SH-SY5Y culture medium (MEM/F12-10 culture medium)
43.5 mL of MEM, no glutamine
43.5 mL of Ham's F-12 Nutrient Mix
10 mL of FBS
1 mL of GlutaMAX
1 mL of Sodium Pyruvate
1 mL of MEM NEAA
1 mL of (1×) Penicillin/Streptomycin

Acknowledgments

This work was supported by the National Natural Science Foundation of China (NSFC 92054105, 62022056 and 61975118), Science & Technology Commission Shanghai Municipality 18QA1402300, and Innovation Research Plan supported by Shanghai Municipal Education Commission ZXWF082101 to H.H.

Original research paper Yu *et al.* (2021): Mitochondrial Ca²⁺ oscillation induces mitophagy initiation through the PINK1-Parkin pathway. <https://doi.org/10.1038/s41419-021-03913-3>.

Competing interests

The authors declare no competing financial interests.

Ethics

This study was approved by the Ethic Committee of the School of Biomedical Engineering at Shanghai Jiao Tong University.

References

1. Cheng, P., Tian, X., Tang, W., Cheng, J., Bao, J., Wang, H., Zheng, S., Wang, Y., Wei, X., Chen, T., *et al.* (2021). [Direct control of store-operated calcium channels by ultrafast laser](#). *Cell Res* 31(7): 758-772.
2. Chung, E., Choi, Y., Park, J., Nah, W., Park, J., Jung, Y., Lee, J., Lee, H., Park, S. and Hwang, S. (2020). [Intracellular delivery of Parkin rescues neurons from accumulation of damaged mitochondria and pathological α-synuclein](#). *Sci Adv* 6(18): eaba1193.
3. Ge, P., Dawson, V. L. and Dawson, T. M. (2020). [PINK1 and Parkin mitochondrial quality control: a source of regional vulnerability in Parkinson's disease](#). *Mol Neurodegener* 15(1): 20.
4. He, H., Li, S., Wang, S., Hu, M., Cao, Y. and Wang, C. (2012). [Manipulation of cellular light from green fluorescent protein by a femtosecond laser](#). *Nat Photonics* 6(10): 651-656.
5. Iwanaga, S., Smith, N., Fujita, K. and Kawata, S. (2006). [Slow Ca²⁺ wave stimulation using low repetition rate femtosecond pulsed irradiation](#). *Opt Express* 14(2): 717-725.
6. Jin, S. M. and Youle, R. J. (2013). [The accumulation of misfolded proteins in the mitochondrial matrix is sensed by PINK1 to induce PARK2/Parkin-mediated mitophagy of polarized mitochondria](#). *Autophagy* 9(11): 1750-1757.
7. Lazarou, M., Sliter, D. A., Kane, L. A., Sarraf, S. A., Wang, C., Burman, J. L., Sideris, D. P., Fogel, A. I. and Youle, R. J. (2015). [The ubiquitin kinase PINK1 recruits autophagy receptors to induce mitophagy](#). *Nature* 524(7565): 309-314.

8. Liu, J., Liu, W., Li, R. and Yang, H. (2019). [Mitophagy in Parkinson's disease: from pathogenesis to treatment](#). *Cells* 8(7): 712.
9. Liu, X., Lv, X., Zeng, S., Zhou, W. and Luo, Q. (2009). [Noncontact and nondestructive identification of neural circuits with a femtosecond laser](#). *Appl Phys Lett* 94(6): 061113.
10. Pickrell, A. M. and Youle, R. J. (2015). [The roles of PINK1, parkin, and mitochondrial fidelity in Parkinson's disease](#). *Neuron* 85(2): 257-273.
11. Russell, O. M., Gorman, G. S., Lightowers, R. N. and Turnbull, D. M. (2020). [Mitochondrial diseases: hope for the future](#). *Cell* 181(1): 168-188.
12. Smith, N. I., Iwanaga, S., Beppu, T., Fujita, K., Nakamura, O. and Kawata, S. (2005). [Femtosecond laser-induced calcium release in neural-type cells](#). In: Nanobiophotonics and Biomedical Applications II, International Society for Optics and Photonics. Proc SPIE 5705, <https://doi.org/10.1117/12.596923>.
13. Smith, N. I., Kumamoto, Y., Iwanaga, S., Ando, J., Fujita, K. and Kawata, S. (2008). [A femtosecond laser pacemaker for heart muscle cells](#). *Opt Express* 16(12): 8604-8616.
14. Wang, S., Liu, Y., Zhang, D., Chen, S. c., Kong, S. K., Hu, M., Cao, Y. and He, H. (2018). [Photoactivation of Extracellular-Signal-Regulated Kinase Signaling in Target Cells by Femtosecond Laser](#). *Laser Photonics Rev* 12(7): 1700137.
15. Wang, Y., He, H., Li, S., Liu, D., Lan, B., Hu, M., Cao, Y. and Wang, C. (2014). [All-optical regulation of gene expression in targeted cells](#). *Sci Rep* 4: 5346.
16. Yu, Z., Wang, H., Tang, W., Wang, S., Tian, X., Zhu, Y. and He, H. (2021). [Mitochondrial Ca²⁺ oscillation induces mitophagy initiation through the PINK1-Parkin pathway](#). *Cell Death Dis* 12(7): 632.
17. Zhao, Y., Zhang, Y., Liu, X., Lv, X., Zhou, W., Luo, Q. and Zeng, S. (2009). [Photostimulation of astrocytes with femtosecond laser pulses](#). *Opt Express* 17(3): 1291-1298.

High-speed Atomic Force Microscopy Observation of Internal Structure Movements in Living *Mycoplasma*

Kohei Kobayashi^{1, #}, Noriyuki Kodera^{2, #} and Makoto Miyata^{1, 3, *}

¹Graduate School of Science, Osaka City University, 3-3-138 Sugimoto, Sumiyoshi-ku, Osaka 558-8585, Japan

²Nano Life Science Institute (WPI-NanoLSI), Kanazawa University, Kakuma-machi, Kanazawa, Ishikawa 920-1192, Japan

³The OCU Advanced Research Institute for Natural Science and Technology (OCARINA), Osaka City University, 3-3-138 Sugimoto, Sumiyoshi-ku, Osaka 558-8585, Japan

*For correspondence: miyata@osaka-cu.ac.jp

#Contributed equally to this work

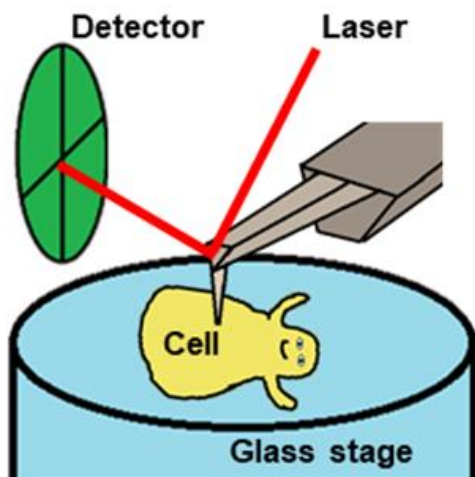
Abstract

Dozens of *Mycoplasma* species belonging to the class *Mollicutes* bind to solid surfaces through the organelle formed at a cell pole and glide in its direction by a unique mechanism. In *Mycoplasma mobile*, the fastest gliding species in *Mycoplasma*, the force for gliding is generated by ATP hydrolysis on an internal structure. However, the spatial and temporal behaviors of the internal structures in living cells were unclear. High-speed atomic force microscopy (HS-AFM) is a powerful method to monitor the dynamic behaviors of biomolecules and cells that can be captured while maintaining their active state in aqueous solution. In this protocol, we describe a method to detect their movements using HS-AFM. This protocol should be useful for the studies of many kinds of microorganisms.

Keywords: AFM, Probing, Pathogenic bacteria, ATPase, Class *Mollicutes*, Internal structure

This protocol was validated in: mBio (2021), DOI:10.1128/mBio.00040-21

Graphic abstract:



Scanning *Mycoplasma* cell

Background

Class *Mollicutes*, a small group of bacteria featuring a single-layered cell membrane, has as many as three unique motility mechanisms different from other organisms. Recently, the isolated internal structure of *M. mobile* was shown to hydrolyze ATP with conformational changes, suggesting that the internal structure functions as a force generator for gliding (Miyata and Hamaguchi, 2016; Nishikawa *et al.*, 2019). However, the spatial and temporal behaviors and movements of internal motors in living cells have not been examined.

High-speed atomic force microscopy (HS-AFM) is a powerful method to monitor the dynamic behaviors of biomolecules and cells that can be captured while maintaining their active state in aqueous solution (Ando, 2018). In recent years, this approach has been dramatically improved, and the behaviors of more and more proteins have been elucidated (Kodera *et al.*, 2010 and 2021; Ando, 2018; Kodera and Ando, 2020). In addition, HS-AFM has been applied to understanding the structures in the cell wall surface (Yamashita *et al.*, 2012) and below the cell membrane (Zhang *et al.*, 2017).

Here, we provide a protocol detailing how to detect the movements of the internal structure in a living *M. mobile* cell, based on our recent study (Kobayashi *et al.*, 2021).

Materials and Reagents

1. 1.5 mL microtube (Greiner Bio-One, catalog number: 616201)
2. Glass substrate stage for HS-AFM (custom-made glass rod with 2 mm in diameter and 2 mm in height, Japan Cell)
3. Cantilever (Olympus, BLAC10DS-A2)
4. #3000 sand paper (Riken Corundum, Precision Polishing Film Sheet #3000, catalog number: 3-9013-06)
5. 100 mL beaker
6. Kimwipes (Nippon Paper Crecia, catalog number: 62015)
7. Filter paper for liquid replacement on glass stage (ADVANTEC, catalog number: 01531090) (Cut into triangles as shown in Figure 2)
8. 25 cm² tissue culture flask (AS ONE, catalog number: 2-8589-01)
9. Micro pipette tip (Greiner Bio-One, catalog numbers: 740290 and 739285)
10. Acetone (FUJIFILM Wako Pure Chemical Corporation, catalog number: 012-00343)

Cite as: Kobayashi, K. *et al.* (2022). High-speed Atomic Force Microscopy Observation of Internal Structure Movements in Living Mycoplasma. Bio-protocol 12(05): e4344. DOI: 10.21769/BioProtoc.4344.

11. Potassium hydroxide (KOH) (Nacalai Tesque, catalog number: 28616-45)
12. Ethanol (FUJIFILM Wako Pure Chemical Corporation, catalog number: 057-00456)
13. Fluorosurf (FluoroTechnology, catalog number: FG-3020C-20)
14. Colorless nail polish (Shiseido, MAQuillAGE (Top base coat))
15. Deionized water
16. 3-aminopropyltriethoxymethylsilane (APTES) (Shin-Etsu Chemical, catalog number: KBE-903)
17. Glutaraldehyde (Sigma-Aldrich, catalog number: G5882)
18. Heart infusion broth (BD, catalog number: 238400)
19. Yeast extract (BD, catalog number: 212750)
20. 10 N NaOH (Nacalai Tesque, catalog number: 31511-05)
21. Horse serum (Thermo Fisher Scientific, GibcoTM, catalog number: 16050122)
22. Amphotericin B (Sigma-Aldrich, catalog number: A2942)
23. Ampicillin Na (Nacalai Tesque, catalog number: 02739-32)
24. di-Sodium hydrogenphosphate (Nacalai Tesque, catalog number: 31801-05)
25. Sodium dihydrogenphosphate dihydrate (FUJIFILM Wako Pure Chemical Corporation, catalog number: 192-02815)
26. NaCl (Nacalai Tesque, catalog number: 31320-05)
27. Glucose (Nacalai Tesque, catalog number: 16806-25)
28. Phosphate-buffered saline containing glucose (PBS/G) (see Recipes)
29. Aluotto medium (see Recipes)

Biological materials

1. A mutant strain (*gli521*[P476R]) isolated from *M. mobile* 163K strain (ATCC, catalog number: 43663) (Uenoyama and Miyata, 2005)

Equipment

1. Micro pipette (Gilson, catalog numbers: F123600, F123601, and F123602)
2. Centrifuge (Sigma Laborzentrifugen, model: Sigma 1-14)
3. 25°C incubator (Tokyo Rikakikai, model: LTI-400E)
4. Heater (TAITEC CORPORATION, CTU-Neo)
5. Magnetic stirrer (AS ONE, model: CT-1AT)
6. HS-AFM (An apparatus with the same performance is commercially available from Research Institute of Biomolecule Metrology Co., Ltd., model: SS-NEX)
7. Autoclave (TOMY SEIKO, model: LSX-700)

Procedure

A. Cell preparation

1. Inoculate 1 mL of frozen *M. mobile* stock into 10 mL of Aluotto medium in a 25 cm² tissue culture flask and statically cultivate it at 25°C for a few days, to reach an optical density at 600 nm of 0.06–0.08.
2. Collect 2 mL of cultured cells by centrifugation at 12,000 × g and room temperature (RT) for 4 min, discard the supernatant, resuspend the cell pellet in 400 µL of PBS/G, and centrifuge it again at 12,000 × g and RT for 4 min (Note 1).
3. Repeat this process twice.
4. Resuspend the cells in 100 µL of PBS/G to 20-fold density of the original culture.

B. Glass stage treatment

Cite as: Kobayashi, K. et al. (2022). High-speed Atomic Force Microscopy Observation of Internal Structure Movements in Living Mycoplasma. Bio-protocol 12(05): e4344. DOI: 10.21769/BioProtoc.4344.

1. Lightly press the substrate surface against the #3000 sandpaper and scrub 200 times back and forth to scratch the surface (The rough surface provides a more stable observation. This step is optional). Note that this process should not be applied to the other side.
2. Put the glass stage into the 1.5 mL microtube filled with acetone and shake it to remove glass debris. (Optional: as mentioned above)
3. To prepare saturated KOH-ethanol solution, add 10 g of KOH into 50 mL of ethanol, stir using a magnetic stirrer for 5 min, and transfer the supernatant of the saturated KOH-ethanol solution into a new beaker.
4. Put several glass stages into the prepared saturated KOH-ethanol solution.
5. Leave for 15 min to hydrophilize the glass surface.
6. Discard the solution, add some deionized water, and shake the beaker gently.
7. Repeat this process ten times to remove the chemicals.
8. Move the glass stages onto Kimwipes and remove the water.
9. Keep the glass stages with some slant in a heater, for 20 min at 40–45°C to dry.

C. Cell immobilization on the glass surface

1. Treat the sides of the glass stage with Fluorosurf for hydrophobization.

Note: If not treated, the liquid placed on the substrate surface will spill over to the sides.

2. Fix the glass stage onto the Z-piezo of the HS-AFM scanner with nail polish (Figure 1).

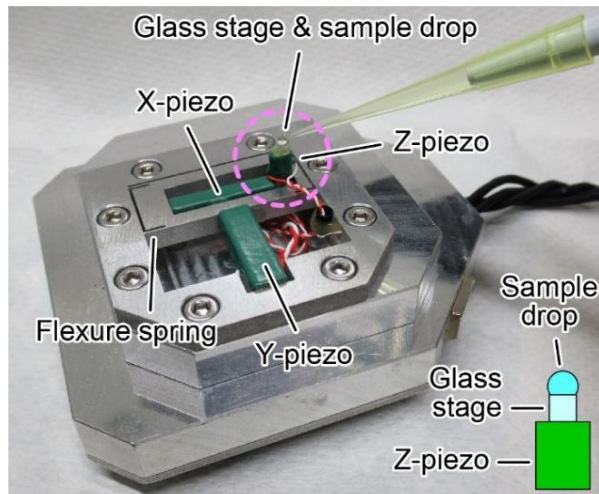


Figure 1. HS-AFM scanner with glass stage and sample drop.

Piezoelectric elements are used to drive each axis in the XYZ directions. Z piezo, glass stage, and sample solution are seen in a pink dashed circle, as illustrated in the lower right. The glass stage is fixed onto the Z-piezo using nail polish.

3. Just before use, dilute 1 μL of APTES with 999 μL of water.
4. For silanization on the glass stage surface, load 5 μL of APTES solution onto the treated glass substrate immediately after the dilution and leave it for 10 min.
5. Rinse the substrate surface with 20 μL of water dropwise. Repeat this four times (Figure 2).
6. Replace the water on the glass substrate with 0.1% glutaraldehyde solution and leave for 5 min.
7. Rinse the substrate surface with 20 μL of water dropwise. Repeat this four times.
8. Replace the glutaraldehyde solution on the substrate with PBS/G.

9. Replace the PBS/G on the substrate to cell suspension and leave for 10 min at 25–28°C.
10. Rinse the substrate surface with 20 µL of PBS/G dropwise. Repeat this four times.

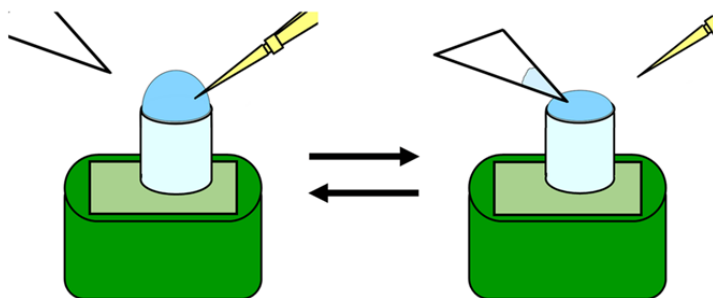


Figure 2. Procedure for liquid replacement on the glass stage.

D. Observation by HS-AFM

1. Set the HS-AFM scanner equipped with the glass stage and sample solution upside down to the HS-AFM mechanical unit and start imaging (Figure 3).

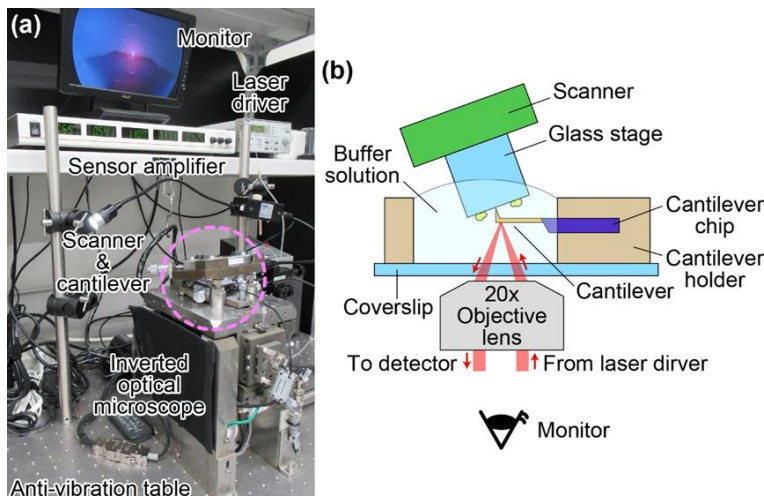


Figure 3. HS-AFM.

(a) Picture showing the mechanical parts and some of the electrical devices of HS-AFM. The AFM unit (scanner and cantilever) is mounted on an inverted optical microscope which is placed on an anti-vibration table. (b) Schematic of experimental setup. Cantilever and *M. mobile* cells are not in scale. The optical view around the cantilever and the glass substrate can be observed through the monitor.

2. Set the cantilever's free oscillation amplitude (A_0) and set-point amplitude (A_{sp}) at ~2.5 nm and ~0.8 × A_0 , respectively. Under these conditions, the average tapping force $\langle F \rangle$ can be approximated as ~40 pN using the following equation:

$$\langle F \rangle = \frac{k_c}{2Q_c} \sqrt{A_0^2 - A_{sp}^2}$$

where k_c and Q_c are the spring constant and the quality factor of the cantilever, respectively. The nominal values of k_c and Q_c in liquid are ~0.08 N/m and 1.5, respectively. The detail conditions were described previously (Uchihashi *et al.*, 2012).

3. For searching cells (Figure 4a), scan the sample at 150×150 pixels with an imaging rate of 1,000 ms per frame in an area of $3,000 \times 3,000 \text{ nm}^2$.
(<https://journals.asm.org/doi/10.1128/mBio.00040-21#movS1>).
4. To observe particle structure like Figure 4b, scan the cell surface with an imaging rate of 330 or 200 ms per frame in an area of $200 \times 200 \text{ nm}^2$, with 100×100 pixels.
(<https://journals.asm.org/doi/10.1128/mBio.00040-21#movS3>).
5. Other details are common with general observation of samples in solution using HS-AFM (Uchihashi *et al.*, 2012).

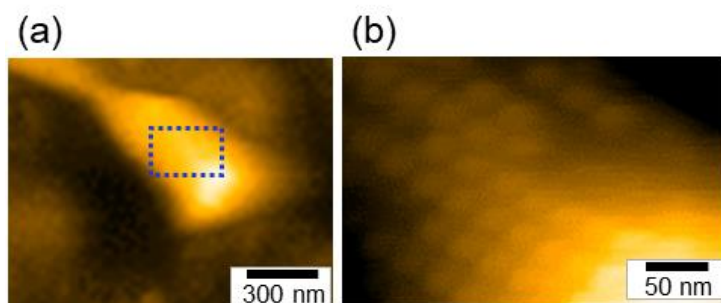


Figure 4. Representative images taken by HS-AFM.

(a) Whole cell image (b) Particle structure image [Magnified image of the boxed area of the panel (a)]. This figure was modified a previous paper (Kobayashi *et al.*, 2021).

Data analysis

All procedures were published in our previous paper (Kobayashi *et al.*, 2021, (Kobayashi et al., 2021, <https://journals.asm.org/doi/10.1128/mBio.00040-21>). Briefly, videos were processed by three steps (i) to (iii) and analyzed for particle movements. (i) The image contrast was improved by a bandpass filter. (ii) Image drifts were corrected by a plugin for ImageJ, “align slices in stack” (Tseng *et al.*, 2012). (iii) Image noises were reduced by averaging three consecutive slices. Then, each particle image was cropped, binarized, and traced for the mass center. All analyses were performed with ImageJ version 1.52A.

Notes

1. Suspension of cell pellet
More than 100 up-and-down movements with the pipette are recommended to separate cells completely.
2. Heat treatment of horse serum
For *M. mobile* growth and gliding, the horse serum should be inactivated by heat treatment at 56°C for 30 min.

Troubleshooting

1. Unable to obtain even a flat substrate image.
Cells or other suspended particles may be sticking to the cantilever. To shake them off, keep the cantilever away from the substrate surface, set the cantilever's amplitude at free oscillation for 1 min, and try imaging again. If

- this is not improved after several attempts, remove the scanner and wash the cantilever, using a pipetting water stream in the chamber.
2. No cells are found on the field.
Small molecules, including amino groups, may be bound to the glass stage and block cell binding. Prepare the cell suspension and the glass stage again carefully. For the cell preparation, increase the number of pipetting times to remove small molecules. Note that too many washes may also reduce cell number. Check the cell conditions by optical density at 600 nm and an optical microscope, because old cultures tend to include particles other than cells.
 3. Cells easily detach from the substrate during observation.
The glass stage with a rough surface may be helpful [refer to Glass stage treatment option (Procedure B)].
 4. The cell images look strange.
The cells may have dried out. Replace the cell suspension and the glass stage. Place a wet tissue at the edge, to humidify the area around the chamber.
 5. The particle structures are not found on the cells.
This may be caused by damage on the cantilever tip. Replace the cantilever.

Recipes

1. Aluotto medium

1% heart infusion broth
0.56% yeast extract
0.035% 10 N NaOH

Note: Dissolve the above three reagents as a mixture, autoclave, cool to lower than 37°C, and add below three reagents in clean bench.

10% horse serum (Note 2)
0.025% amphotericin B
0.005% ampicillin Na

2. Phosphate-buffered saline containing glucose (PBS/G)

75 mM sodium phosphate (pH 7.3)
68 mM NaCl
20mM Glucose
Sterilize by using filtering or autoclaving

Acknowledgments

This work was supported by Grants-in-Aid for Scientific Research (B) and (A) (MEXT KAKENHI, Grant Numbers JP24390107, JP17H01544), and JST CREST (Grant Number JPMJCR19S5) to MM.

This protocol was adapted from a previously published paper (Kobayashi *et al.*, 2021).

Competing interests

There are no conflicts of interest or competing interests.

References

- Ando, T. (2018). [High-speed atomic force microscopy and its future prospects](#). *Biophys Rev* 10(2): 285-292.
- Kobayashi, K., Kodera, N., Kasai, T., Tahara, Y. O., Toyonaga, T., Mizutani, M., Fujiwara, I., Ando, T. and Miyata, M. (2021). [Movements of *Mycoplasma mobile* gliding machinery detected by high-speed atomic force microscopy](#). *mBio* 12(3): e0004021.
- Kodera, N. and Ando, T. (2020). [High-speed atomic force microscopy to study myosin motility](#). *Adv Exp Med Biol* 1239: 127-152.
- Kodera, N., Noshiro, D., Dora, S. K., Mori, T., Habchi, J., Blocquel, D., Gruet, A., Dosnon, M., Salladini, E., Bignon, C., et al. (2021). [Structural and dynamics analysis of intrinsically disordered proteins by high-speed atomic force microscopy](#). *Nat Nanotechnol* 16(2): 181-189.
- Kodera, N., Yamamoto, D., Ishikawa, R. and Ando, T. (2010). [Video imaging of walking myosin V by high-speed atomic force microscopy](#). *Nature* 468(7320): 72-76.
- Miyata, M. and Hamaguchi, T. (2016). [Prospects for the gliding mechanism of *Mycoplasma mobile*](#). *Curr Opin Microbiol* 29: 15-21.
- Nishikawa, M. S., Nakane, D., Toyonaga, T., Kawamoto, A., Kato, T., Namba, K. and Miyata, M. (2019). [Refined mechanism of *Mycoplasma mobile* gliding based on structure, atpase activity, and sialic acid binding of machinery](#). *mBio* 10(6): e02846-19.
- Tseng, Q., Duchemin-Pelletier, E., Deshiere, A., Balland, M., Guillou, H., Filhol, O. and Thery, M. (2012). [Spatial organization of the extracellular matrix regulates cell-cell junction positioning](#). *Proc Natl Acad Sci USA* 109(5): 1506-1511.
- Uchihashi, T., Kodera, N. and Ando, T. (2012). [Guide to video recording of structure dynamics and dynamic processes of proteins by high-speed atomic force microscopy](#). *Nat Protoc* 7(6): 1193-1206.
- Uenoyama, A. and Miyata, M. (2005). [Gliding ghosts of *Mycoplasma mobile*](#). *Proc Natl Acad Sci U S A* 102(36): 12754-12758.
- Yamashita, H., Taoka, A., Uchihashi, T., Asano, T., Ando, T. and Fukumori, Y. (2012). [Single-molecule imaging on living bacterial cell surface by high-speed AFM](#). *J Mol Biol* 422(2): 300-309.
- Zhang, Y., Yoshida, A., Sakai, N., Uekusa, Y., Kumeta, M. and Yoshimura, S. H. (2017). [In vivo dynamics of the cortical actin network revealed by fast-scanning atomic force microscopy](#). *Microscopy (Oxf)* 66(4): 272-282.

Laser Microirradiation and Real-time Recruitment Assays Using an Engineered Biosensor

Carolina dos Santos Passos, Robert E. Cohen* and Tingting Yao*

Department of Biochemistry and Molecular Biology, Colorado State University, Fort Collins, CO, USA

*For correspondence: bob.cohen@colostate.edu; tingting.yao@colostate.edu

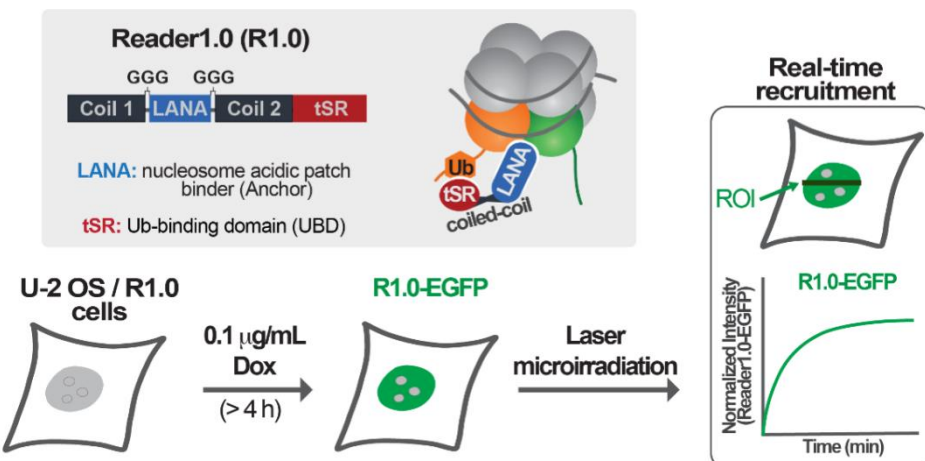
Abstract

Double-strand breaks (DSBs) are lesions in DNA that, if not properly repaired, can cause genomic instability, oncogenesis, and cell death. Multiple chromatin posttranslational modifications (PTMs) play a role in the DNA damage response to DSBs. Among these, RNF168-mediated ubiquitination of lysines 13 or 15 at the N-terminal tail of histone H2A (H2AK13/15Ub) is essential for the recruitment of effectors of both the non-homologous end joining (NHEJ) and the homologous recombination (HR) repair pathways. Thus, tools and techniques to track the spatiotemporal dynamics of H2AK13/15 ubiquitination at DNA DSBs are important to facilitate studies of DNA repair. Previous work from other groups used the minimal focus-forming region (FFR) of the NHEJ effector 53BP1 to detect H2AK15Ub generated upon damage induced by gamma or laser irradiation in live cells. However, 53BP1-FFR only binds nucleosomes modified with both H2AK15Ub and dimethylation of lysine 20 on histone H4 (H4K20me2); thus, 53BP1-FFR does not recognize H2AK13Ub-nucleosomes or nucleosomes that contain H2AK15Ub but lack methylation of H4K20 (H4K20me0). To overcome this limitation, we developed an avidity-based sensor that binds H2AK13/15Ub without dependence on the methylation status of histone H4K20. This sensor, called Reader1.0, detects DNA damage-associated H2AK13/15Ub in live cells with high sensitivity and selectivity. Here, we present a protocol to detect the formation of H2AK13/15Ub at laser-induced DSBs using Reader1.0 as a live-cell reporter for this histone PTM.

Keywords: RNF168-mediated ubiquitination, H2AK13/15Ub, DNA damage repair, DSB, Laser microirradiation, Live-cell sensor

This protocol was validated in: J Cell Biol (2021), DOI:10.1083/jcb.201911130

Graphic abstract:



Background

DNA double-strand breaks (DSBs) are a threat to genome integrity and stability. DSBs can be generated in response to external agents (*e.g.*, irradiation, radiomimetic chemicals) or formed as byproducts of normal cell metabolism (*e.g.*, oxidative stress, DNA replication errors). To deal with DSBs, eukaryotic cells use complex repair machinery equipped with protein effectors responsible for detecting, signaling, and promoting the repair of these lesions. Defects in DNA DSB repair can lead to mutations or chromosomal aberrations and, ultimately, contribute to the onset of cancer and neurodegenerative diseases (Jackson and Bartek, 2009; Ciccia and Elledge, 2010; Polo and Jackson, 2011).

In response to DNA DSBs, the serine/threonine kinase ataxia-telangiectasia mutated (ATM) is activated and promotes the phosphorylation of various proteins in chromatin surrounding the damage sites. These phosphorylation substrates include histone variant H2AX in vertebrates. Phosphorylated H2AX (γ H2AX) leads to the sequential recruitment of mediator of DNA damage checkpoint protein 1 (MDC1) and the E3 ubiquitin ligases RNF8 and RNF168. RNF168 specifically ubiquitinates lysines 13 or 15 at the N-terminal tail of histone H2A (H2AK13/15Ub) (Mattioli *et al.*, 2012), which in turn can recruit effectors of non-homologous end joining (NHEJ) or homologous recombination (HR)-mediated repair (Mattioli and Penengo, 2021). The NHEJ repair factor 53BP1 is recruited by nucleosomes containing both H4K20me2 and H2AK15Ub (Fradet-Turcotte *et al.*, 2013; Wilson *et al.*, 2016; Hu *et al.*, 2017). In contrast, the BRCA1/BARD1 complex promotes the HR pathway and is recruited by nucleosomes modified with H2AK13Ub or H2AK15Ub, only if H4K20 is not methylated (H4K20Me0) (Becker *et al.*, 2021; Hu *et al.*, 2021). The minimal focus-forming region (FFR) of 53BP1 has been previously shown to localize to DSBs induced by gamma or laser irradiation, and thereby report local increases in H2AK15Ub at DNA lesions (Fradet-Turcotte *et al.*, 2013; dos Santos Passos *et al.*, 2021). However, structural and biochemical studies have demonstrated that 53BP1 binding to the nucleosomes requires both H2AK15Ub and H4K20Me2 modifications. The H4K20Me2 modifications are enriched in the G1 and early S-phases of the cell cycle (Fradet-Turcotte *et al.*, 2013; Wilson *et al.*, 2016; Hu *et al.*, 2017; Michelena *et al.*, 2021).

In recent work, we developed and validated an avidity-based sensor to detect H2AK13/15Ub-nucleosomes. This sensor, which we call Reader1.0, can bind nucleosomes containing either H2AK13Ub or H2AK15Ub *in vitro*, and it localizes to sites of RNF168-mediated ubiquitination in mammalian cells. In addition, Reader1.0 binding to H2AK13/15Ub-nucleosomes does not depend on the methylation status of histone H4K20; *i.e.*, Reader1.0 recognizes H2AK13/15Ub-nucleosomes containing either H4K20me0 or H4K20me2. When fused to fluorescent proteins and expressed at tightly-controlled levels, Reader1.0 can be used to monitor the dynamics of H2AK13/15Ub in live cells over long time intervals without causing significant perturbation of cell growth rate or DNA repair kinetics (dos Santos Passos *et al.*, 2021).

Cite as: dos Santos Passos, C. *et al.* (2022). Laser Microirradiation and Real-time Recruitment Assays Using an Engineered Biosensor. Bio-protocol 12(05): e4337. DOI: 10.21769/BioProtoc.4337.

The protocol presented here describes how to measure the recruitment of readers of RNF168-dependent H2AK13/15 ubiquitination to DNA DSBs. To rapidly generate local high concentrations of H2AK13/15Ub, laser microirradiation was used to induce DNA damage in the nuclei of U-2 OS cells. The main advantages of this method are the abilities to target defined nuclear volumes and to generate similar amounts of DNA damage in different nuclei within a cell population (Bekker-Jensen *et al.*, 2006; Lukas *et al.*, 2003). By co-expressing mCherry-53BP1-FFR and Reader1.0-EGFP, we demonstrated that our designed sensor Reader1.0 and 53BP1-FFR both redistribute to laser-induced DNA lesions with similar kinetics. In sum, this protocol describes the detection of H2AK13/15Ub at DNA DSBs in live cells by fluorescence confocal microscopy.

Materials and Reagents

1. 60 mm tissue culture dishes (Genesse Scientific, catalog number: 26-260)
2. 35-mm glass-bottom dishes (MatTek, catalog number: P35G-1.5-14-C)
3. Phosphate buffered saline (PBS; Corning, catalog number: 21-040-CV)
4. TrypLE™ express enzyme (Gibco, catalog number: 12604021)
5. Dulbecco's modified Eagle's medium (DMEM; Corning, catalog number: 15-013-CV)
6. FluoroBrite™ DMEM (Gibco, catalog number: A1896701)
7. Opti-MEM™ reduced serum medium (Gibco, catalog number: 11058021)
8. Penicillin-Streptomycin 100× solution (10,000 U/mL; HyClone, catalog number: SV30010)
9. L-Glutamine 200 mM solution (HyClone, catalog number: SH30034.01)
10. Fetal bovine serum (FBS; Sigma-Aldrich, catalog number: F0926)
11. Lipofectamine™ 3000 transfection reagent (ThermoFisher, catalog number: L3000015)
12. Dimethyl sulfoxide (DMSO, Fisher Scientific, catalog number: BP231-100)
13. Doxycycline (Dox) hydrochloride (Fisher Scientific, catalog number: BP2653-1)
14. U-2 OS cells stably expressing Reader1.0-EGFP under the control of a Dox-inducible promoter (dos Santos Passos *et al.*, 2021)
15. Plasmid mCherry-BP1-2 pLPC-Puro (Addgene, plasmid number: 12259)
16. Growth medium (see Recipes)
17. Live-cell medium (see Recipes)

Equipment

1. CO₂ incubator (Thermo Fisher Scientific, model: Heracell VIOS 160i)
2. Bead bath 37°C incubator (Lab Armor, model: 74300-706)
3. Vortex mixer (Fisher Scientific, model: Genie 2, catalog number: 12-812)
4. Confocal laser scanning microscope (Carl-Zeiss, model: LSM 880) operated with Zen Black 2.3 software (v.14.0.9.201) and equipped with a Plan-Apochromat 63×/1.40 oil-immersion objective
5. Stage Incubator for Live-Cell Imaging (PECON, PM 2000 RBT)

Software

1. Zen Black 2.3 software (v.14.0.9.201; Carl-Zeiss)
2. Zen Blue 2.3 software (v.2.3.69.1000; Carl-Zeiss)

Procedure

A. Cell preparation

For this protocol, we used U-2 OS cells stably expressing the H2AK13/15Ub sensor Reader1.0-EGFP under the control of a doxycycline (Dox)-inducible promoter (dos Santos Passos *et al.*, 2021). Stable cell lines and plasmids encoding Reader1.0-EGFP for transient or stable expression in mammalian cells are available from the corresponding author (T.Y.; tingting.yao@colostate.edu) and will be deposited with Addgene.org.

1. Procedure for 35 mm glass bottom dish:
 - a. Day 1 – Seed cells for transfection:
 - i. Seed 3×10^5 cells per dish in 2 mL of growth medium to obtain approximately 70% confluence the next day.
 - ii. Incubate for 16–24 h at 37°C in a 5% CO₂ incubator.
 - b. Day 2 – Transfect cells with mCherry-BP1-2 pLPC-Puro (mCherry-53BP1-FFR):
 - i. Prepare the DNA-Lipofectamine 3000 complex as follows: dilute 0.5 µg plasmid DNA in 125 µL of Opti-MEM I, then add 1 µL of P3000 reagent B and mix well (Tube A). In a separate tube, add 1 µL of Lipofectamine 3000 reagent A in 125 µL of Opti-MEM I and mix well (Tube B). Add the diluted DNA from Tube A to the diluted Lipofectamine 3000 reagent in Tube B, mix gently, and incubate at room temperature for 15 min.
 - ii. Add DNA-Lipofectamine 3000 complex to cells in a dropwise fashion.
 - iii. Incubate for 16–20 h at 37°C in a 5% CO₂ incubator.
 - c. Day 3 – Induce Reader1.0-EGFP expression with 0.1 µg/mL Dox:
 - i. Aspirate to remove the medium and rinse with 2 mL of PBS.
 - ii. Add 2 mL of live-cell medium supplemented with 0.1 µg/mL Dox.
 - iii. Incubate for 4 h at 37°C in a 5% CO₂ incubator.
 - iv. Perform laser microirradiation and real-time recruitment as in ‘B’.

B. Laser microirradiation and real-time recruitment

Note 1: Experiments require a confocal laser scanning microscope equipped with 405, 488, and 561 laser lines for fluorescence excitation and a stage incubator to maintain 37°C and a humidified 5% CO₂ atmosphere. The experiments described here were conducted using a Zeiss LSM 880 inverted microscope.

Note 2: Previous experience with confocal laser scanning microscopy is required to execute this protocol.

Note 3: The LSM 880 microscope is a laser hazard class 3B instrument. Users must take care to not expose themselves to the radiation and, in particular, never look into the laser beam. Only personnel

1. Turn on the microscope and set the temperature of the stage incubator to 37°C and the CO₂ concentration to 5%.
2. Wait for the temperature and CO₂ concentration to stabilize (approximately 15 min) and then transfer the 35 mm glass-bottom culture dish to the stage incubator of the microscope.
3. Acquire pre-microirradiation images of cells co-expressing mCherry-53BP1-FFR and Reader1.0-EGFP according to the parameters below and save the images as .czi files:
 - a. mCherry-53BP1-FFR was excited at 561 nm and the fluorescence emission was collected using the 488/543/633 main dichroic beam splitter (MBS) and the Gallium Arsenide Phosphide (GaAsP) photomultiplier (PMT) detector (Figure 1).
 - b. Reader1.0-EGFP was excited at 488 nm and the fluorescence emission was collected using the 488/543/633 MBS and the GaAsP PMT detector (Figure 2).

Note: The 405 MBS for invisible light should be selected considering that the 405 nm diode laser will be used to microirradiate the cells to generate local DNA damage. Note 3: The LSM 880 microscope is a laser hazard class 3B instrument. Users must take care to not expose themselves to the radiation and, in particular, never look into the laser beam. Only personnel instructed on laser safety should be allowed to operate the system.

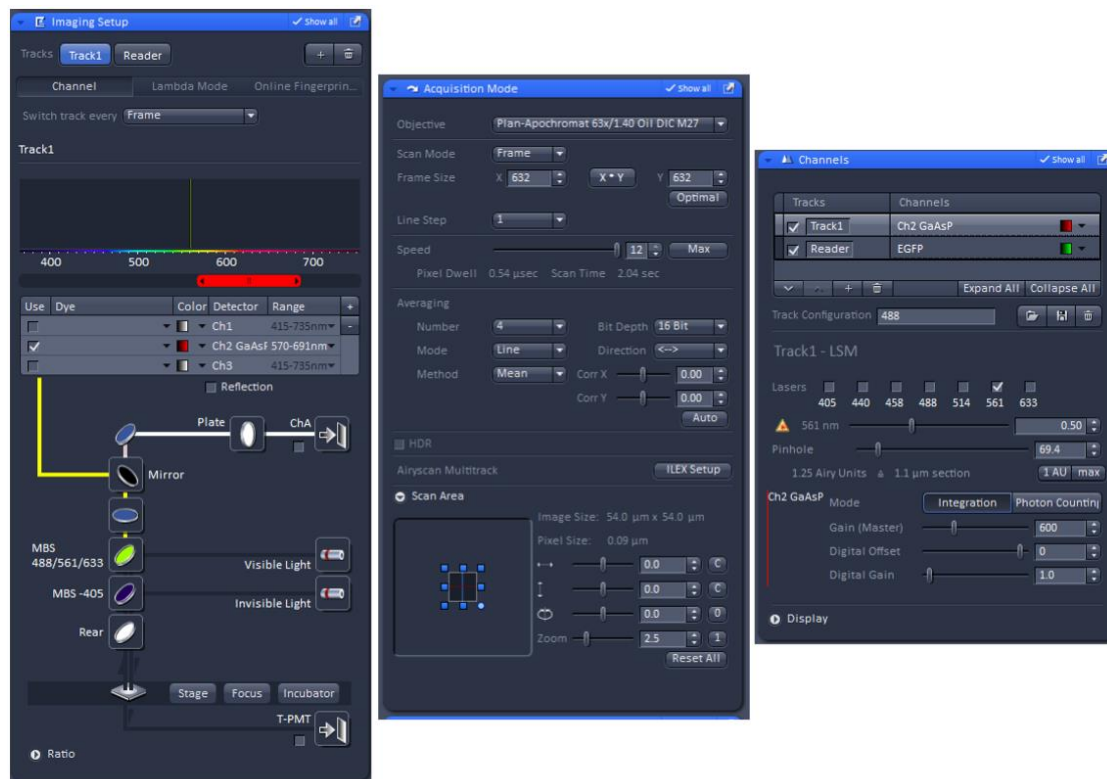


Figure 1. Zen Black software setting for mCherry-53BP1-FFR imaging.

Note: The 'Imaging Setup', 'Acquisition Mode', and 'Channels' tabs will automatically open when Zen Black is started.

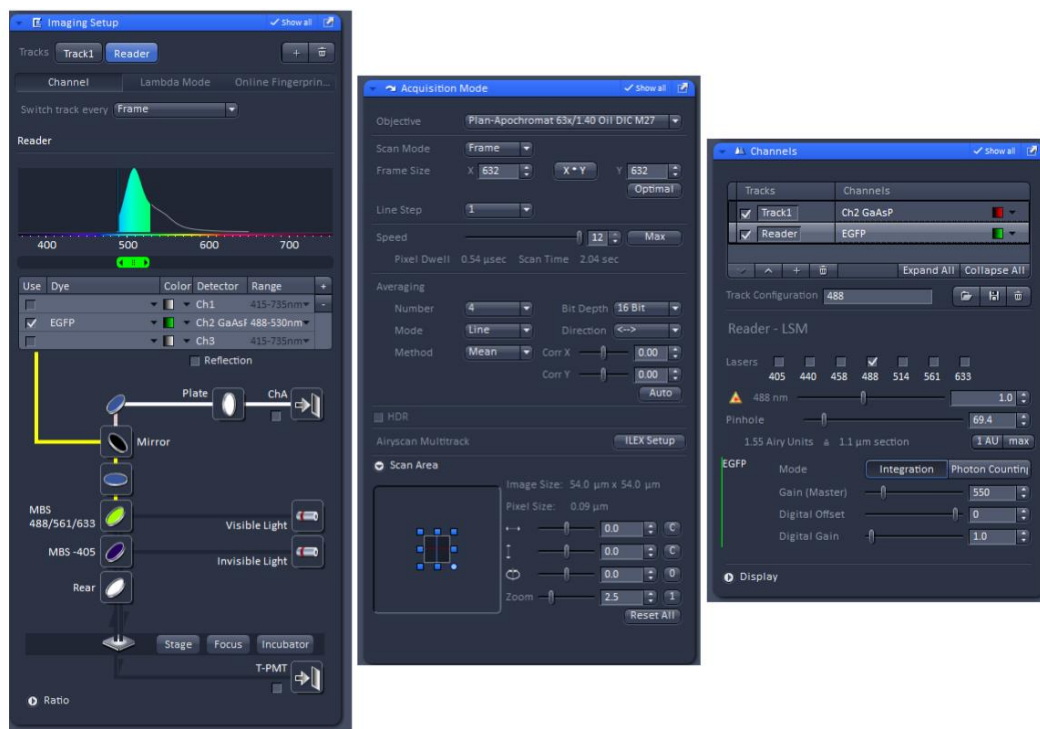


Figure 2. Zen Black software setting for Reader1.0-EGFP imaging.

4. Configure the microscope for the microirradiation experiment:
 - a. In the ‘Acquisition’ tab, check the boxes ‘Time Series’, ‘Bleaching’, and ‘Regions’ (Figure 3A).
 - b. Expand the ‘Bleaching’ tool tab and set up the conditions for laser microirradiation according to Figure 3B.

Note: It may be necessary to test different laser intensities in ‘Excitation of Bleach’ in order to efficiently induce DNA damage.

- c. Expand the ‘Time Series’ tool tab and define the number ‘Cycles’ (number of frames to be acquired) and the time ‘Interval’ between cycles (Figure 3C).
- d. Expand the ‘Regions’ tool tab to define the Region of Interest (ROI) in the nucleus that will be microirradiated with the 405 nm laser (Figure 3D).

Note: In this example, the ROI for laser microirradiation was a rectangle 300 × 5 pixels (L × W). Considering that the scanner is configured to move along the y-axis, to generate a uniform amount of damage, only the width (W = 5 pixels) of the irradiated ROI needs to be kept constant. The length (L) of the rectangle may be adjusted within the confines of the area of the nucleus.

- e. After verifying the settings, go to the ‘Acquisition’ tab and hit the ‘Start Experiment’ button (Figure 3A).

Note: Make sure to select both the 488 nm and the 561 nm tracks for image acquisition.

- f. The real-time recruitment of mCherry-53BP1-FFR and Reader1.0-EGFP to the irradiated tracks can be monitored in the ‘Mean ROI’ view tab in Zen Black (Figure 4).

Cite as: dos Santos Passos, C. et al. (2022). Laser Microirradiation and Real-time Recruitment Assays Using an Engineered Biosensor. Bio-protocol 12(05): e4337. DOI: 10.21769/BioProtoc.4337.

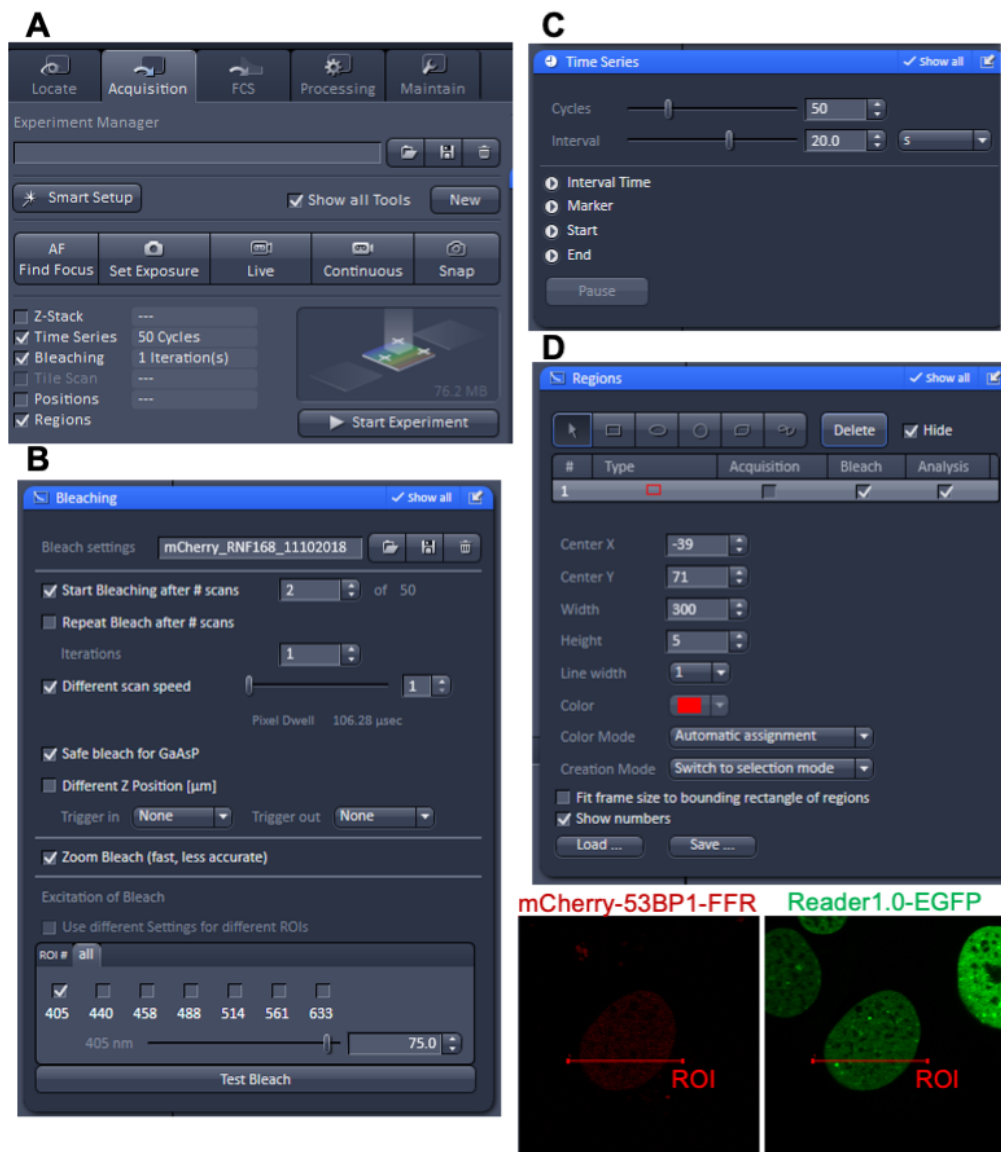


Figure 3. Zen Black software settings for laser microirradiation and real-time recruitment.

(A) ‘Acquisition’ tab. (B) ‘Bleaching’ tool tab. (C) ‘Time Series’ tool tab. (D) ‘Regions’ tool tab and example depicting the Region of Interest (ROI) that will be microirradiated.

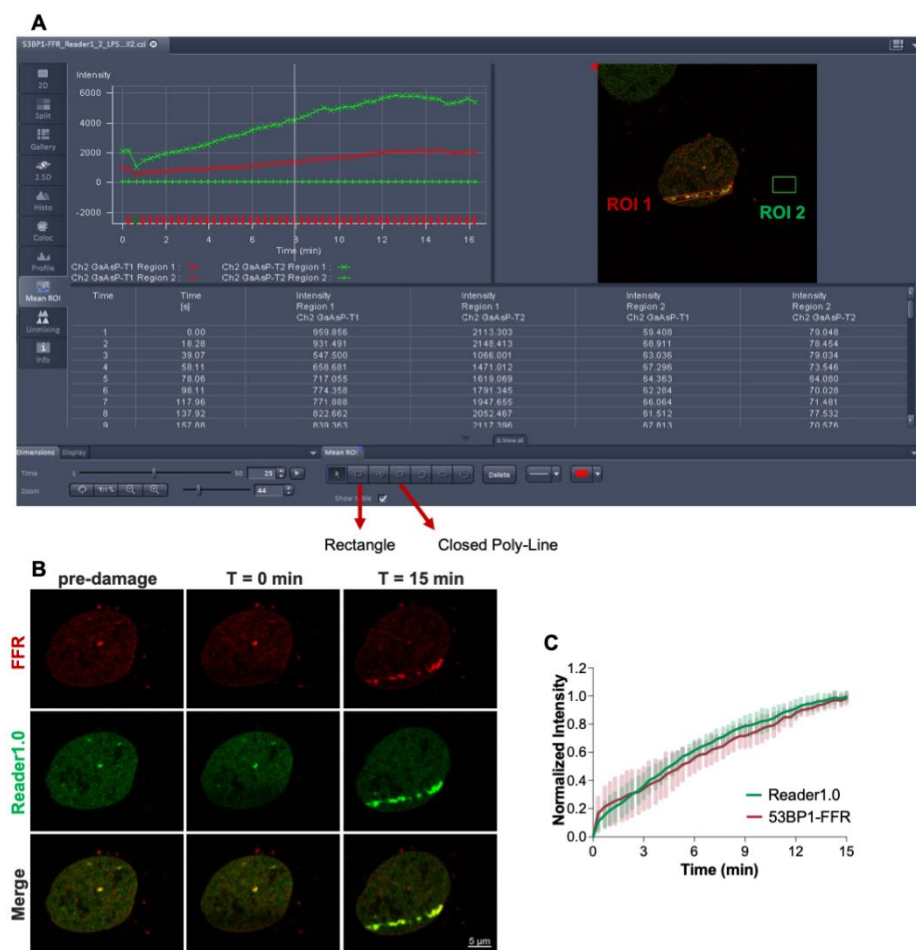


Figure 4. Laser microirradiation and real-time recruitment of mCherry-53BP1-FFR and Reader1.0-EGFP to DSBs.

(A) U-2 OS cells co-expressing mCherry-53BP1-FFR and Reader1.0-EGFP were microirradiated using the 405 nm laser and fluorescence redistribution to the laser-induced DSBs were extracted from background-corrected individual frames (ROI 1: DSB track; ROI 2: background). (B) Representative images of the irradiated cell at the indicated time points. (C) Reader1.0-eGFP and mCherry-53BP1-FFR showed similar rates of recruitment to DNA lesions ($n = 12$).

Data analysis

Recruitment analysis

Note: Figure 4A shows an example of raw data acquired for one cell and opened in the ‘Mean ROI’ view tab of Zen Black. Figure 4B shows representative images of the cell shown in 4A at selected times: Pre-irradiation, $T = 0$ min (time zero after irradiation) and $T = 15$ min (15 min after irradiation). These images were extracted and processed using the Zen Blue software. Figure 4C shows the processed data plotted using Excel.

1. Open the .czi files in Zen Black and go to the ‘Mean ROI’ view tab.
2. Go to the frame #25 and define a Region of Interest (ROI 1) encompassing the micro-irradiated track where the accumulation of mCherry-53BP1-FFR (561 nm track) and Reader1.0-EGFP (488 nm track) is visible (Figure 4A).

Cite as: dos Santos Passos, C. et al. (2022). Laser Microirradiation and Real-time Recruitment Assays Using an Engineered Biosensor. Bio-protocol 12(05): e4337. DOI: 10.21769/BioProtoc.4337.

3. Draw a rectangle outside the nucleus (ROI 2) for background subtraction (Figure 4A).

Notes:

- The 'Mean ROI' view tab in the Zen Black software allows the operator to define ROIs with different shapes. In the example shown in Figure 4A, ROI 1 was drawn using the 'Closed Poly-Line' option and ROI 2 using the 'Rectangle' option.
- Considering that cells can move over the time of image acquisition, the region of interest (ROI 1) for analysis may need to be redefined. Here, ROI 1 was defined as a closed poly-line encompassing the fluorescent protein accumulating at the laser track in frame #25; frame #25 was chosen because it corresponds to a time point (7.3 min after irradiation) in which there is noticeable accumulation of both Reader1.0 and 53BP1-FFR.

4. Save the data table in .xlsx format.

Note: The data table will contain columns for time interval(s) and mean fluorescence intensities within ROI 1 and ROI 2 for the 561 and 488 nm excitation tracks.

5. After background subtraction (ROI 1-ROI 2), calculate the local increases in mCherry-53BP1-FFR and Reader1.0-EGFP fluorescence at the laser-induced DNA lesions as follows:
 - Fold Increase = I_t/I_{pre} , where I_t denotes the fluorescence intensity at the damaged region at time t, and I_{pre} denotes the fluorescence intensity before microirradiation (dos Santos Passos *et al.*, 2021).
 - Normalized intensity = $(I_t - I_{pre})/(I_{last} - I_{pre})$, where I_t denotes the fluorescence intensity at the damaged region at time t, I_{pre} denotes the fluorescence intensity before microirradiation, and I_{last} denotes the fluorescence intensity at the lesion in the last time point (Figure 4C).

Note 1: Typically, $N \geq 6$ cells should be analyzed per tested condition. If the goal of the experiment is to compare different experimental groups (e.g., transfections with siRNAs to deplete DNA repair effectors), the number of cells analyzed should be sufficient to detect significant differences when they exist. In this case, the sample size should be determined taking into account the standard deviations of the measurements and the amplitudes of the differences (i.e., differences between control and tested conditions).

*Note 2: When we analyzed U-2 OS cells stably expressing Reader1.0 and transfected with siCtrl or siRNF168, we determined that $N = 6$ cells was sufficient to detect differences in Reader1.0 recruitment to DSBs in cells depleted of RNF168 (dos Santos Passos *et al.*, 2021).*

*Note 3: Reader1.0 competes with endogenous DNA repair machinery (53BP1 or BARD1) for binding to RNF168-mediated ubiquitinated nucleosomes. High Reader1.0 expression inhibits the recruitment of 53BP1-FFR to laser-induced DSBs (dos Santos Passos *et al.*, 2021). This observation highlights the importance of expressing the sensor at low but detectable levels. In this protocol, stable expression of Reader1.0 under the control of a Dox-inducible promoter allows sensor levels that can effectively report H2AK13/15Ub under the tested conditions without causing perturbation to DNA repair.*

By performing competition experiments between Reader1.0 and 53BP1-FFR, we determined that optimal expression levels of Reader1.0 can be achieved by treating U-2 OS/Reader1.0-EGFP cells with 0.1 μ g/mL Dox for 4–12 h before live-cell imaging or, alternatively, with 0.01 μ g/mL Dox for 24–48 h before imaging. An alternative approach is to do transient transfection to express Reader1.0; here, the subset of cells expressing Reader1.0 at low levels can be identified microscopically and used for experiments.

The dynamics of sensor binding to DNA damage sites can be determined by Fluorescence Recovery After Photobleaching (FRAP) measurements. Titrating the levels of Reader1.0 expression can be used to deconvolute FRAP half-lives (FRAP $t_{1/2}$) into kinetic parameters (k_{on} and k_{off}). For quantitative analysis of FRAP experiments, we recommend readers to refer to the review by McNally (2008).

Recipes

1. Growth medium

(DMEM supplemented with 10% FBS, 1% Penicillin-Streptomycin, and 2 mM L-Glutamine)
440 mL of DMEM
50 mL of FBS
5 mL of 100× Penicillin-Streptomycin solution
5 mL of L-Glutamine 200 mM solution

2. Live-cell medium

(FluorBrite™ DMEM supplemented with 10% FBS, 1% Penicillin-Streptomycin, and 2 mM L-Glutamine)
44 mL of FluorBrite™ DMEM
5 mL of FBS
0.5 mL of 100× Penicillin-Streptomycin solution
0.5 mL of L-Glutamine 200 mM solution

Note: Growth medium and Live-Cell medium should be stored at 4°C and warmed up to 37°C before use. For storage time, see manufacturer's instructions.

3. 1 mg/mL Dox solution

1 mg Doxycycline hydrochloride
1 mL of DMSO

Note: 1 mg/mL Dox solution should be separated into 1 mL aliquots and stored at -20°C for up to 12 months.

Acknowledgments

This research was supported by National Institutes of Health grants R21ES029150 to R.E. Cohen and T. Yao, R01GM115997 to R.E. Cohen, and R01GM098401 to T. Yao. This protocol describes methodology used in the research paper (DOI: 10.1083/jcb.201911130) by dos Santos Passos *et al.* (2021).

Competing interests

The authors declare no competing financial interests.

References

- Becker, J. R., Clifford, G., Bonnet, C., Groth, A., Wilson, M. D., Chapman, J. R. (2021). [BARD1 reads H2A lysine 15 ubiquitination to direct homologous recombination](#). *Nature* 596: 433-437.
- Bekker-Jensen, S., Lukas, C., Kitagawa, R., Melander, F., Kastan, M. B., Bartek, J., Lukas, J. (2006). [Spatial organization of the mammalian genome surveillance machinery in response to DNA strand breaks](#). *J Cell Biol* 173: 195-206.
- dos Santos Passos, C., Choi, Y.-S., Snow, C. D., Yao, T., Cohen, R. E. (2021). [Design of genetically encoded sensors to detect nucleosome ubiquitination in live cells](#). *J Cell Biol* 220: e201911130.

Cite as: dos Santos Passos, C. et al. (2022). Laser Microirradiation and Real-time Recruitment Assays Using an Engineered Biosensor. Bio-protocol 12(05): e4337. DOI: 10.21769/BioProtoc.4337.

- Ciccia, A. and Elledge, S. J. (2010). [The DNA damage response: making it safe to play with knives](#). *Mol Cell* 40: 179-204.
- Fradet-Turcotte, A., Canny, M. D., Escribano-Diaz, C., Orthwein, A., Leung, C. C., Huang, H., Landry, M. C., Kitevski-LeBlanc, J., Noordermeer, S. M., Sicheri, F., Durocher, D. (2013). [53BP1 is a reader of the DNA-damage-induced H2A Lys 15 ubiquitin mark](#). *Nature* 499: 50-54.
- Hu, Q., Botuyan, M. V., Cui, G., Zhao, D., Mer, G. (2017). [Mechanisms of ubiquitin-nucleosome recognition and regulation of 53BP1 chromatin recruitment by RNF168/169 and RAD18](#). *Mol Cell* 66: 473-487.
- Hu, Q., Botuyan, M. V., Zhao, D., Cui, G., Mer, E., Mer, G. (2021). [Mechanisms of BRCA1-BARD1 nucleosome recognition and ubiquitylation](#). *Nature* 596:438-443.
- Jackson, S. P. and Bartek J. (2009). [The DNA-damage response in human biology and disease](#). *Nature* 461: 1071-1078.
- Lukas, C., Falck, J., Bartkova, J., Bartek, J., and Lukas, J. (2003). [Distinct spatiotemporal dynamics of mammalian checkpoint regulators induced by DNA damage](#). *Nat Cell Biol* 5: 255-260.
- Mattioli, F. and Penengo, L. (2021). [Histone ubiquitination: an integrative signaling platform in genome stability](#). *Trends Genet* 37: 566-581.
- Mattioli, F., Vissers, J. H., van Dijk, W. J., Ikpa, P., Citterio, E., Vermeulen, W., Marteijn, J. A., and Sixma, T. K. (2012). [RNF168 ubiquitinates K13-15 on H2A/H2AX to drive DNA damage signaling](#). *Cell* 150: 1182-1195.
- McNally, J. G. (2008). [Quantitative FRAP in analysis of molecular binding dynamics in vivo](#). *Methods Cell Biol* 85:329-51.
- Michelena, J., Pellegrino, S., Spegg, V., Altmeyer, M. (2021). [Replicated chromatin curtails 53BP1 recruitment in BRCA1-proficient and BRCA1-deficient cells](#). *Life Sci Alliance* 4: e202101023.
- Polo, S. E. and Jackson, S. P. (2011). [Dynamics of DNA damage response proteins at DNA breaks: a focus on protein modifications](#). *Genes Dev* 25: 409-433.
- Wilson, M. D., Benlekbir, S., Fradet-Turcotte, A., Sherker, A., Julien, J. P., McEwan, A., Noordermeer, S. M., Sicheri, F., Rubinstein, J. L., Durocher, D. (2016). [The structural basis of modified nucleosome recognition by 53BP1](#). *Nature* 536: 100-103.

Spherical Invasion Assay: A Novel Method to Measure Invasion of Cancer Cells

Stephen D. Richbart^{1, #}, Justin C. Merritt^{1, #}, Emily G. Moles¹, Kathleen C. Brown¹, Adeoluwa A. Adeluola¹, Paul T. Finch², Joshua A. Hess², Maria T. Tirona³, Sarah L. Miles¹, Monica A. Valentovic¹, and Piyali Dasgupta^{1, *}

¹Department of Biomedical Sciences, Joan C. Edwards School of Medicine, Marshall University, Huntington, WV, 25755, USA

²Department of Oncology, Edwards Cancer Center, Joan C. Edwards School of Medicine, Marshall University, 1400 Hal Greer Boulevard, Huntington, West Virginia, WV 25755, USA

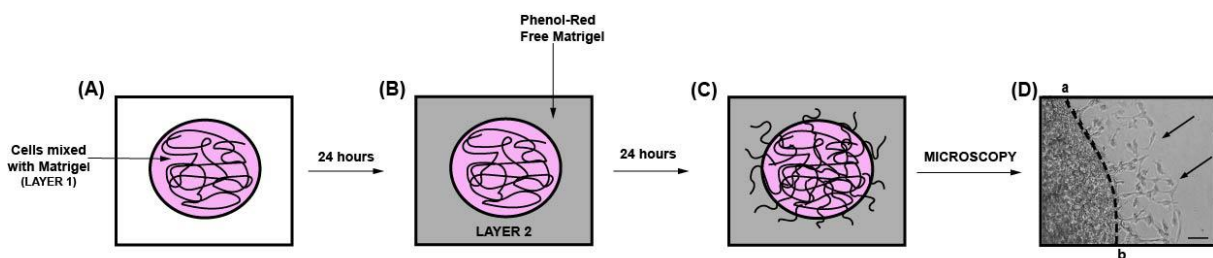
³Department of Hematology-Oncology, Edwards Cancer Center, Joan C. Edwards School of Medicine, Marshall University, 1400 Hal Greer Boulevard, Huntington, West Virginia, WV 25755, USA

#Contributed equally to this work

*For correspondence: dasgupta@marshall.edu

[Abstract] The invasion of tumor cells into the neighboring blood vessels and lymph nodes is a vital step for distant metastasis. Traditionally, the invasive activity of growth factors (or the anti-invasive activity of drugs) is measured with the Boyden chamber assay. However, this assay has a few disadvantages like poor physiological relevance of transwell inserts and an inability to control chemokine gradients. The Boyden chamber assay is one of the most prevalent methods to measure the invasion of cancer cells. It would be advantageous to develop another assay that could validate the results of the Boyden chamber assay. With this in mind, our laboratory developed the spherical invasion assay (SIA) to measure the pro-invasive activity of human cancer cells. The SIA also circumvents some of the drawbacks of the Boyden chamber assay. The present manuscript measures the anti-invasive activity of the Src kinase inhibitor PP2 in A549 human non-small cell lung carcinoma (NSCLC) cells using the SIA. The SIA protocol is comprised of two steps. In the first step, A549 human NSCLC cells (treated or not with PP2) were mixed with Matrigel and seeded in the middle of an eight-well chamber slide. After 24 h, a second layer of Matrigel was overlaid over the first layer. Over the course of the next 24 h, the A549 cells invade from the primary to the secondary Matrigel layers. Subsequently, the cells are visualized by phase-contrast microscopy and the images obtained are quantified using ImageJ to calculate the anti-invasive activity of PP2 in A549 cells. The results of the SIA correlate well with Boyden chamber assays. The SIA may be adapted for multiple experimental designs, such as drug screening (to combat invasion and metastasis), measuring the pro-invasive activity of growth factors, and elucidating the signaling pathways underlying the pro-invasive/anti-invasive activity of biological modifiers.

Graphic abstract:

**Diagrammatic illustration of the spherical invasion assay (Hurley et al., 2017).**

A. The first layer is comprised of human cancer cells mixed in a 1:1 suspension with Phenol Red containing Matrigel (represented as LAYER 1 in the figure). After 24 h, the cancer cells grow and extend up to the boundary of this first layer. B. A second layer of 1:1 solution Phenol Red-free Matrigel, in Phenol Red-free RPMI (represented as LAYER 2 in the figure) is added on top of the first Matrigel spot. The cells are incubated for 24 h at 37°C. C. Over these 24 h, the cancer cells invade from the primary layer into the secondary Matrigel layer. The chamber slides are observed by phase-contrast microscopy. D. A representative photograph of the images obtained by the SIA is shown. The black arrow indicates the cancer cells invading into the second layer of Matrigel. The dotted line represents the interface between the two layers. The distance to which the cells have traveled (into the secondary Matrigel layer) is measured at ten sites (for each photograph) in a randomized double-blind fashion by three independent observers, using NIH ImageJ Version 1.47. This process is repeated for three separate photographic fields per sample.

Keywords: Spherical, Invasion, Matrigel, NSCLC, PP2, Microscopy

[Background] Tumor invasion refers to the process by which cancer cells penetrate the basement membrane into surrounding stroma, neighboring blood vessels, and lymph nodes (Stuelten et al., 2018; Baghban et al., 2020). Tumor invasion is an essential step for metastasis of human cancers (Baghban et al., 2020). Amongst the many steps of metastasis, the process of tumor invasion has been targeted by many therapeutic agents to suppress the distant spread of tumors (Gandalovicova et al., 2017). The Boyden chamber assay is the benchmark technique for measuring the invasion of cancer cells (Guy et al., 2017). This assay involves the movement of a single-cell suspension through a microscopic mesh (8 micrometers in pore size) coated with an extracellular matrix. However, this assay suffers from several caveats. The physiological relevance of transwell inserts (to recapitulate invasion *in vivo*) is poor. The pore size of the membrane highly influences the number of cells that invade (Guy et al., 2017). In the Boyden chamber assay, a chemokine is added to the lower basolateral chamber to facilitate the invasion of tumor cells through the transwell membrane; however, it is very difficult to control the concentration of the chemokine gradient, and this may produce aberrant results (Guy et al., 2017). The Boyden chamber is one of the prevalent methods to measure tumor cell invasion. The “wound-healing assay” measures the migration (NOT THE INVASION) of human cancer cells. There are subtle differences between a “migration assay” and an “invasion assay” (Justus et al., 2014; Pijuan et al., 2019). In the migration assay, the movement of cells across a vacant area (like a scratch or wound) is measured. A

second method to measure “cell migration” is to quantify the movement of cancer cells across a transwell filter (pore size of 8 μm) from the apical chamber to the basolateral chamber. Taken together, the migration assay measures the chemotactic capability of cells to travel toward a chemo-attractant or mixture of chemo-attractants (as observed with the use of conditioned medium). The invasion assay measures both cell chemotaxis and the invasion of cells through the layer of extracellular matrix proteins, a process that is commonly found in cancer metastasis. In the “invasion assay”, the transwell filters are coated with a thin layer of basement membrane (usually Matrigel). The first event in the “invasion assay” is that the cancer cells in the apical chamber secrete matrix metalloproteases to degrade basement membrane proteins, producing a gap in the basement membrane. Subsequently, the cancer cells travel through this gap in the basement membrane and pass through the transwell filter (pore size of 8 μm), to arrive at the basolateral chamber of the transwell filter. The process through which cancer cells degrade the basement membrane to penetrate the transwell insert is a unique feature of the “invasion assay”, which is not present in “migration assays”. The invasion assay faithfully recapitulates the process of “tumor invasion” during metastasis, where the neoplastic cells degrade the basement membrane to launch themselves into circulation in the neighboring blood vessel/lymph node. It would be useful to have a second invasion assay that could validate the results obtained with the Boyden chamber assay. All these considerations led us to develop a novel method of measuring tumor invasion namely the spherical invasion assay (SIA) in our laboratory. The SIA measures the invasion of human cancer cells as they migrate from the primary Matrigel layer, over the interface, and travel into a secondary Matrigel layer. The SIA mirrors the actual process of invasion under physiological conditions (Hurley *et al.*, 2017). The cells that grow in extracellular matrix (ECM) retain biological characteristics of tumors, such as responsiveness to diffusion gradient of oxygen, nutrients, and pH. The growth of the cells inside the ECM allows for complex cell-cell and cell-matrix interaction. The SIA can be adapted to organoids, spheroids (Gunti *et al.*, 2021), retinal angiogenic sprouts (Stitt *et al.*, 2005), tumor stem cells (Atashzar *et al.*, 2020), neurospheres (da Silva Siqueira *et al.*, 2021), and cells grown on polymeric scaffolds (Stratton *et al.*, 2016). In such cases, it is important to remember that the conditions for culturing normal cells are very different from cancer cells. In addition, normal cells should be used at a low passage number, so that they do not become senescent. For example, if the SIA is performed with retinal endothelial cells, then the assay should be performed between passages 3-6 (Stitt *et al.*, 2005). Furthermore, these invading cells can be characterized by confocal laser microscopy and transmission electron microscopy. Most importantly, the results of the SIA correlate with the data obtained in the Boyden chamber assay, so the SIA can be used to confirm the results obtained in Boyden chamber assays (Hurley *et al.*, 2017). The present protocol examines the effect of the Src Kinase inhibitor PP2 (Hanke *et al.*, 1996) (at a concentration of 10 μM) on the invasion of A549 human NSCLC cells. We hope that the SIA will be a useful tool for researchers working in the field of tumor microenvironment biology and cancer metastasis.

Materials and Reagents

1. Fisherbrand High Precision Sterile Scalpel Blade (Fisher, catalog number: 12-000-161)
2. Nunc™ EasYFlask™ T-75 Cell Culture Flasks (Fisher, catalog number: 12-565-349)
Tissue culture dishes (diameter 100 mm) may also be used (Nunc™ EasYDish™ Dishes; Fisher catalog number: 12-600-003).
3. Ice cold 1.5 mL microfuge tubes (Fisher, catalog number: 05-408-129)
4. 5 mL microfuge tubes (Eppendorf, catalog number: 0030119401)
5. Sterile 15 mL centrifuge tube (Thermo Scientific Nunc, Fisher, catalog number: 12-565-268)
6. Sterile 50 mL centrifuge tubes (ThermoScientific Nunc, Fisher, catalog number: 12-565-270)
7. Thermo Scientific Nunc Lab-Tek eight well Permanox plastic Chamber Slide System (Fisher, catalog number: 12-565-22)
8. A549 human NSCLC cells (ATCC, catalog number: CCL-185)
9. F-12K Medium (Kaighn's Modification of Ham's F-12 Medium; ATCC; catalog number: 30-2004).
Store at 4°C
10. Roswell Park Memorial Institute (RPMI)-1640 medium with phenol-red (ATCC, catalog number: 30-2001). Store at 4°C
11. Roswell Park Memorial Institute (RPMI)-1640 medium without Phenol Red (Fisher, catalog number: 30-404-014). Store at 4°C
12. Fetal bovine serum (FBS) (ATCC, catalog number: 30-2020)
Long-term storage for FBS is -20°C. In our laboratory, FBS is aliquoted into 50 mL centrifuge tubes and stored at -20°C. The FBS aliquot is stored at 4°C for immediate use.
13. Trypsin-EDTA (0.25% Trypsin, 0.53 mM EDTA, ATCC, catalog number: 30-2101)
Long-term storage for Trypsin-EDTA is stored at -20°C. However, Trypsin-EDTA is aliquoted and stored at 4°C for immediate use.
14. Dulbecco's Phosphate buffered saline (PBS) without calcium and magnesium (Corning, Fisher, catalog number: 21-031-CM). Store at 4°C.
15. Matrigel membrane matrix (Fisher, catalog number: CB-40234)
Matrigel is a liquid at 4°C and it solidifies at 37°C. Matrigel is aliquoted and stored at -70°C for long-term storage. Before the experiment, Matrigel is kept overnight at 4°C for thawing. Matrigel is kept on ice throughout the experiment.
16. Phenol red-free Matrigel membrane matrix (Fisher, catalog number: CB-40234C)
17. PP2 (A potent and selective inhibitor of the Src family tyrosine kinases) was obtained from Enzo Biosciences (catalog number, 50-201-0681)
PP2 is a powder and is stored at -20°C. The PP2 is dissolved in DMSO (Corning DMSO, Fisher MT-25950CQC) at a final concentration of 10 mM. This stock solution of PP2 solution is aliquoted into microfuge tubes and stored at -20°C. Just before the SIA, the PP2 is thawed and diluted to the desired concentration using serum-free RPMI. After use, the remainder of the diluted PP2 solution (at a concentration of 10 µM) is discarded.

18. 10 mM PP2 (see Recipes)
19. 200 µM PP2 (see Recipes)

Equipment

1. NU-540 (LabGard® ES NU-540 Class II, Type A2) Laminar-Flow Biosafety Cabinet (NuAire, Plymouth, MN)
2. Cell culture incubator maintained at 37°C and 5% CO₂ (Heracell VIOS 150i cell culture incubator, Thermo Scientific, Waltham, MA)
3. Leica DM IL LED Inverted Phase Contrast Microscope with a camera (Leica Microsystems, Welzlar, Germany)
4. Corning Cell Counting Chamber (Fisher, catalog number: 07-200-988)
5. Labnet Hermle Z306 Universal Benchtop Centrifuge; 120V (Labnet International, Cary, NC)

Software

1. LAS Image Capture Software (Leica Microsystems)
2. Adobe Photoshop 2021 (Adobe Inc. for Windows)
3. Adobe Illustrator 2021 (Adobe Inc. for Windows)
4. NIH ImageJ Version 1.47 (National Institutes of Health, Bethesda)
5. GraphPad Prism Version 8

Procedure

- A. Culture of A549 cells in RPMI supplemented with 10% FBS
 1. The human NSCLC cell line A549 was authenticated by the ATCC Cell Authentication Service (ATCC, Manassas, VA).
 2. A549 cells were grown to 70-80% confluence in a F12K medium mixture containing 2 mM glutamine, 100 units/mL penicillin, 50 µg/mL streptomycin, and 10% FBS in a humidified environment at 37°C (in the presence of 5% CO₂) in a cell culture incubator.
- B. Working with Matrigel
 1. The Matrigel is aliquoted in ice-cold microfuge tubes and stored at -70°C.
 2. Before starting the experiment, the required amount of Matrigel is thawed overnight at 4°C. The Matrigel is always kept on ice.
 3. Matrigel is a liquid at 4°C and it solidifies at 37°C. So all plasticware and reagents have to be kept ice cold while handling the Matrigel.
 4. The thawed Matrigel is a thick viscous liquid. Therefore, the pipette tips should be trimmed at the tip (to increase the diameter of the tip) to transport the Matrigel in/out of microfuge tubes.

The tips are trimmed by using a sterile scalpel blade. All microfuge tubes and pipette tips are kept ice cold while handling the Matrigel. In our laboratory, we use ice-cold RPMI as a cooling media. All the pipette tips are dipped into the ice-cooled media to chill them down before using them to handle Matrigel.

C. Spherical Invasion Assay

Day 1

1. Before starting the experiment, draw the schema of the assay as shown in **Figure 1**. The assay will be set up in an eight-well chamber slide. The yellow region of the side of the chamber slide is used to lift it up and transport it around.

Control	Control	PP2, 10µM	PP2, 10µM	

Figure 1. Schema of an example spherical invasion assay in an eight well chamber slide.

2. A549 human NSCLC cells were grown to approximately 70-80% confluence in T-75 tissue culture flasks in F-12K supplemented with 10% FBS.
3. Wash cells once with DPBS and trypsinize them from the flask using 0.25% Trypsin-EDTA.
4. Add 1 mL of FBS to inactivate the Trypsin. Aspirate cells by pipetting up and down gently, and collect them in a 15 mL/50 mL sterile centrifuge tube.
5. Gently spin down the cells at $800 \times g$ for 5 min. Aspirate the media and resuspend the cells in RPMI (containing phenol red)/ 20% FBS.
6. Count the cells using the Corning cell counting chamber. Adjust the concentration of the cells to 50×10^6 cells/mL in RPMI (containing phenol red) containing 20% FBS. This tube is identified as TUBE A.
7. The PP2 was diluted to a concentration of 200 µM in serum-free RPMI (containing phenol red). This stock is always prepared at 20 \times concentration, where x is the final concentration of the drug in the SIA. The final concentration of PP2 to be used for the SIA is 10 µM. Therefore, the PP2 stock was 200 µM.
8. In a separate microfuge tube, mix the cells (from TUBE A) with PP2 (at a concentration of 200 µM) at a ratio of 10:1 (v/v). This dilutes the PP2 to a concentration of PP2 = 20 µM. For example, you may add 45 µL of cell suspension (from TUBE A) to 5 µL of the PP2. Therefore, the new concentration of PP2 = 20 µM. We will call this TUBE B.
9. Keep a few microfuge tubes on ice to chill them down. Mix the cells with Matrigel at a ratio of 1:1 in an ice-cold microfuge tube. As mentioned in Step 6, the cells are resuspended in RPMI (containing phenol red)/20% FBS. Once the cells are mixed (at a ratio of 1:1) in Matrigel, the final concentration of the media comes down to RPMI (containing phenol red)/10% FBS. For

example, mix 15 µL of Matrigel with 15 µL of cell suspension (taken from TUBE B). Mix the cells with the Matrigel by flicking the tube, making the final PP2 concentration in the tube 10 µM. This tube is referred to as TUBE C.

10. Similarly, 15 µL of untreated control A549 cells were mixed with 15 µL of Matrigel in a separate microfuge tube. This tube is referred to as TUBE D.
11. Take a chamber slide out of the packet. Keep the chamber slide in a dish over a piece of tissue paper. If you keep it directly on the surface of the head, the bottom of the chamber slide tends to stick to the floor of the hood, and it is hard to lift the chamber slide.
12. Take 6 µL of the cell suspension from TUBE C and plate it as a drop in the center of the chamber slide. Each sample is assayed in duplicate. A similar process is followed for TUBE D. The chamber slide is incubated at 37°C for one hour in a cell culture incubator. **Figure 2** is a schematic representation of the chamber slide with the drop in the middle of the well.

Control	Control	PP2, 10µM	PP2, 10µM	

Figure 2. Schema of the first step of the spherical invasion assay in an eight well chamber slide.

The cells are mixed with phenol red-containing Matrigel (as a 1:1 suspension) and plated as a drop in the middle of each well of the chamber slide. This drop is represented as a pink circle in the figure above.

13. After 1 h, add 250 µL of RPMI (containing phenol red) with 10% FBS to each well. Leave the chamber slide at 37°C for 24 h in a cell culture incubator.
14. Thaw a vial of phenol red-free Matrigel overnight at 4°C. If the assay is set up like shown in the schematic diagram above, then we will need 125 µL of phenol red-free Matrigel per well of the chamber slide.

Day 2

1. Dilute the phenol red-free Matrigel with an equal volume of phenol red-free RPMI containing 20% FBS. Keep this solution on ice.
2. Look at the chamber slide under a phase-contrast microscope. The cells are located inside the drop.
3. Aspirate the medium from the chamber slide. Use a pipette to gently remove the medium without disturbing the drop at the center of the chamber slide.
4. Overlay 250 µL of the 1:1 solution of phenol red-free Matrigel (diluted with phenol-red free RPMI supplemented with 20% FBS) over the drop. The schematic diagram of the chamber slide is provided below (**Figure 3**). The pink color drop represents the primary layer of Matrigel and the

light grey region around the pink drop represents the phenol red-free Matrigel. The chamber slide is incubated at 37°C for 1 h in a cell culture incubator. After 1 h, add 250 µL of RPMI (containing phenol red) with 10% FBS to each well. Leave the chamber slide at 37°C for 24 h in a cell culture incubator.

We have performed the SIA by adding drugs (in this case PP2) to the secondary layer of Matrigel. However, we have observed that the presence/absence of the drug in the secondary Matrigel layer does not make a substantial difference in the outcome of the assay. Therefore, we do not add the drugs to the secondary layer of Matrigel.

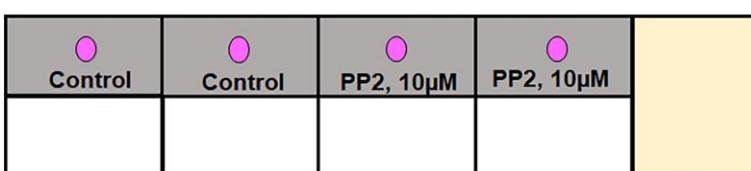


Figure 3. Schema of the second step of the spherical invasion assay in an eight-well chamber slide.

The first step involves mixing the cells with phenol red-containing Matrigel (as a 1:1) suspension and plating them as a drop in the middle of each well of the chamber slide (shown as the pink circle in the figure above). In the second step, phenol red-free Matrigel is mixed with phenol red-free RPMI (at a 1:1 volume by volume ratio) and overlaid over the first layer (as shown by the grey region in the figure above).

Day 3

1. Observe the chamber slide under a phase-contrast microscope. The cells are clearly seen invading out radially from the primary Matrigel layer in to the secondary Matrigel layer. The first layer contains a high concentration of A549 cells mixed with phenol-red containing Matrigel. The second layer is made up of phenol-red-free Matrigel and contains no cells. Therefore, the migration of cells from the primary layer to the secondary layer is very clear and distinct. Another factor that helps to make the interface very clear is the fact that two different colored Matrigels are used for creating the primary and secondary layers. The first layer is comprised of A549 cells mixed with phenol-red containing Matrigel. Under a phase-contrast microscope, this layer is red-black in appearance (Figure 4). The second layer is created by using phenol red-free Matrigel and is light pink in color. The interface is always very clear and defined. Photograph three independent fields for each sample.

Processing the images using adobe illustrator and ImageJ.

1. **Figure 4** shows the representative images obtained from the SIA. The images are photographed at 20× magnification (scale bar = 1 mm). The black arrows indicate the A549 cells which have invaded from the primary to the secondary Matrigel layers.

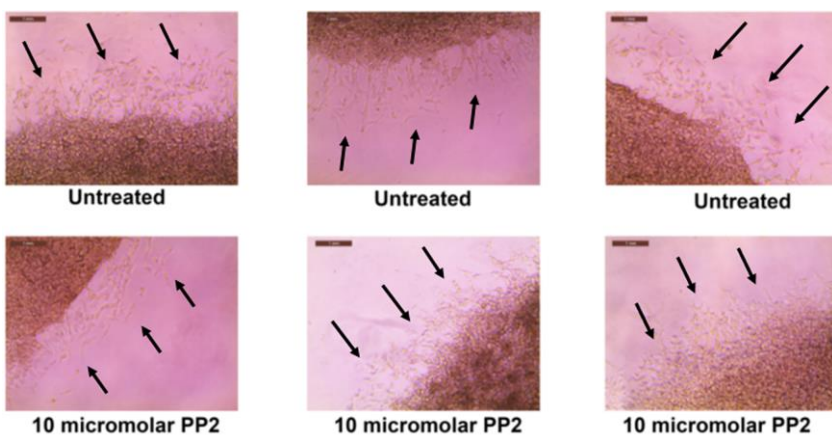


Figure 4. Representative images obtained after performing the SIA, as described in Section C.

2. Open the images in ADOBE ILLUSTRATOR. Using the pen curvature tool, draw a dotted line across the interface the two layers (**Figure 5**).

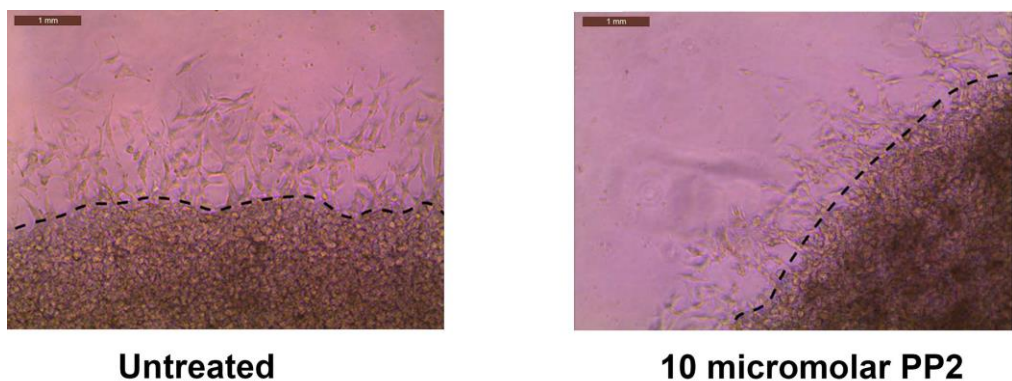


Figure 5. Adobe Illustrator is used to process the images obtained in Figure 4.

A dotted line is drawn across the interface of the two layers.

3. Export the images to ADOBE PHOTOSHOP and save them in jpeg format.
4. Open the jpeg files in ImageJ. Using the line tool, draw a set of ten lines tracing the distance that the A549 cells have invaded into the secondary Matrigel layer (**Figure 6**). After drawing each line, press CTRL-M to obtain the length of the line drawn.

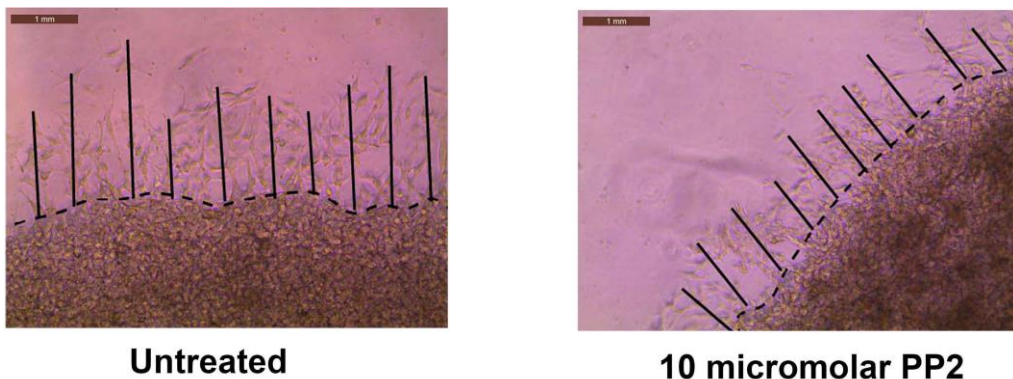


Figure 6. The image files obtained in Figure 5 are opened via ImageJ.

With the help of the line tool, a set of ten lines tracing the distance that the A549 cells have invaded into the secondary Matrigel layer are drawn.

5. Open GraphPad Prism. Using the numbers obtained by the ImageJ program, create a column graph (**Figure 7**). Values represented by the symbol * are statistically different relative to control ($P < 0.05$).

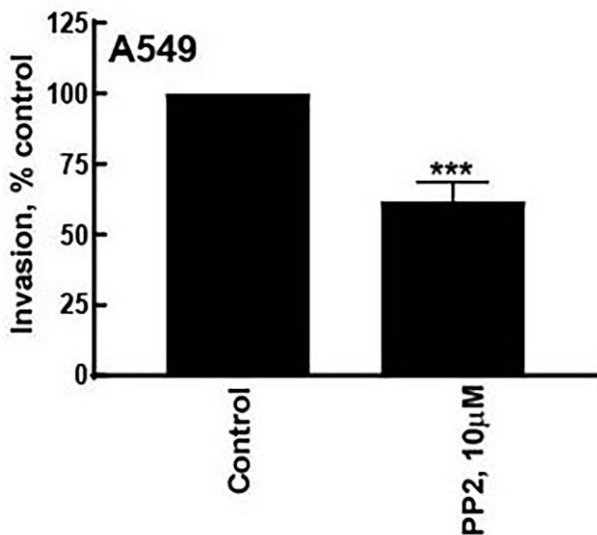


Figure 7. After quantifying the microscopy images by the ImageJ program, the data is graphed using GraphPad Prism.

Values represented by the symbol * are statistically significantly different from control ($P \leq 0.05$).

Data analysis

Each sample was tested in duplicate in the SIA. The entire assay was repeated six independent times. The assay was quantified using phase-contrast microscopy. Three representative images (at 20 \times magnification) were captured for each sample. These images were quantified by ImageJ by three independent observers in a randomized double-blind manner. The data were graphed using

GraphPad Prism (Version 8). All data were plotted as mean \pm standard deviation (SD). The data were analyzed by performing an analysis of variance (ANOVA) followed by the Tukey *posthoc* test. All analyses were completed using a 95% confidence interval. Data were considered significant when $P < 0.05$. The protocol of the SIA has been published in Cell Adhesion and Migration. The link to the paper is provided below:

Hurley, J. D., Akers, A. T., Friedman, J. R., Nolan, N. A., Brown, K. C., Dasgupta, P. (2017). [Non-pungent long chain capsaicin-analogs arvanil and olvanil display better anti-invasive activity than capsaicin in human small cell lung cancers.](#) *Cell Adh Migr* 11(1): 80-97.

Discussion

The SIA is a novel method to measure the invasive ability of cells, growth factors, cytokines, and steroids. It can also be used to quantify the invasion-inhibitory activity of anti-metastatic drugs. A very important factor to remember in this assay is to use relevant concentrations of the drug. For example, if a very high concentration of the anti-cancer drug is used, it will kill the cells and that will also abrogate the invasion of cells into the secondary Matrigel layer. Therefore, the drugs should be used at concentrations where they do not impact the viability of cells. If the drug does not affect the viability of cells and yet it shows reduced invasion into the secondary layer, then it may be conjectured that the drug has anti-invasive activity. The results of the SIA should be confirmed by the Boyden chamber invasion assay and, based on the combined results of these two assays, we can decide whether a candidate drug displays anti-invasive activity. It is also vital to include relevant controls for the SIA. The distance invaded by the cells (in the secondary Matrigel layer) is not an absolute number; it varies upon the nature of the cell line, culture conditions, lot-lot variations in Matrigel, and the time-scale of the assay. It is essential to compare the invasion of a test sample to the control to determine if there is an effect of the process of invasion. For example, the absolute distance invaded by PP2-treated cells may vary from cell line to cell line, but it will always be lower than the pro-invasive activity of untreated cells. In our laboratory, we perform the SIA over 48 h. However, the SIA can be performed at shorter time points than 48 h. We have observed that it takes about 12-18 h for the cells to migrate from the primary layer to the secondary layer. Keeping this fact in mind, the time-frame of the assay can be adjusted accordingly.

The SIA can be performed using growth-factor-reduced Matrigel. This enables the researcher to control pro-invasive growth factors, chemokine gradients, and endogenous anti-invasive factors present in the secondary layer. This process allows the creation of specific chemokine gradients and defined tumor microenvironments in the experiment. An important question involves the use of positive and negative controls in the SIA. The process of invasion is not limited to cancer; it occurs during many normal physiological processes like wound-healing, menstruation, tissue remodeling, development, embryogenesis, and immune responses. Given the appropriate cellular signal, all cells have the ability to invade into the surrounding stroma, therefore it is not possible to identify a cell line that will not show any invasion in the SIA. It is generally observed that cancer cells display

higher invasiveness compared to normal cells. With this in mind, a good positive control for the SIA is to use known pro-invasive or anti-invasive drugs, depending on the nature of the experiment.

Recipes

1. 10 mM PP2

Molecular weight of PP2=301.78

Weigh 6 mg of PP2 in a sterile 5 mL microfuge tube. In the laminar flow hood, dissolve the PP2 in 2 mL of DMSO (Corning DMSO, Fisher MT-25950CQC). Vortex briefly to obtain 10 mM PP2. This stock solution of PP2 solution is aliquoted (as 50 µL aliquots) into microfuge tubes and stored at -20°C.

2. 200 µM PP2

Thaw out one aliquot of PP2. Add 20 µL of PP2 in 1 mL of serum-free RPMI. Vortex vigorously.

Now the concentration of PP2 is 200 µM. Use this PP2 solution as described in Section C, Step 7. Discard the remaining solution.

Acknowledgments

We acknowledge Dr. S. Chellappan and his laboratory for their continuous support. SDR is a recipient of NSF-SURE and WV-NASA Space Consortium undergraduate fellowships respectively. PD and MAV are supported by a National Institutes of Health R15 Academic Research Enhancement Award (Grants 1R15CA161491-02 and 2R15CA161491-03). MAV is also supported by NIH R15AI15197-01 and R15HL145573-01. This work was supported in part by the West Virginia IDeA Network of Biomedical Research Excellence (WV-INBRE) grant (NIH grant P20GM103434; PI: Dr. G. Rankin), the National Institute of General Medical Sciences of the National Institutes of Health under the award number P30GM122733. The protocol of SIA was based on the research papers of Evensen *et al.* (2013), and Stitt *et al.* (2005). The paper by Evensen *et al.* (2013) described a high throughput invasion assay to screen novel anti-cancer drugs. The published report by Stitt *et al.* (2005) outlines the protocol for the Matrigel Duplex assay.

Competing interests

The authors declare no competing interests.

References

1. Atashzar, M. R., Baharlou, R., Karami, J., Abdollahi, H., Rezaei, R., Pourramezan, F. and Zoljalali Moghaddam, S. H. (2020). [Cancer stem cells: A review from origin to therapeutic implications](#). *J Cell Physiol* 235(2): 790-803.

2. Baghban, R., Roshangar, L., Jahanban-Esfahlan, R., Seidi, K., Ebrahimi-Kalan, A., Jaymand, M., Kolahian, S., Javaheri, T. and Zare, P. (2020). [Tumor microenvironment complexity and therapeutic implications at a glance](#). *Cell Commun Signal* 18(1): 59.
3. da Silva Siqueira, L., Majolo, F., da Silva, A. P. B., da Costa, J. C. and Marinowic, D. R. (2021). [Neurospheres: a potential *in vitro* model for the study of central nervous system disorders](#). *Mol Biol Rep* 48(4): 3649-3663.
4. Evensen, N. A., Li, J., Yang, J., Yu, X., Sampson, N. S., Zucker, S. and Cao, J. (2013). [Development of a high-throughput three-dimensional invasion assay for anti-cancer drug discovery](#). *PLoS One* 8(12): e82811.
5. Gandalovicova, A., Rosel, D., Fernandes, M., Vesely, P., Heneberg, P., Cermak, V., Petruzelka, L., Kumar, S., Sanz-Moreno, V. and Brabek, J. (2017). [Migrastatics-Anti-metastatic and Anti-invasion Drugs: Promises and Challenges](#). *Trends Cancer* 3(6): 391-406.
6. Guy, J. B., Espenel, S., Vallard, A., Battiston-Montagne, P., Wozny, A. S., Ardail, D., Alphonse, G., Rancoule, C., Rodriguez-Lafrasse, C. and Magne, N. (2017). [Evaluation of the Cell Invasion and Migration Process: A Comparison of the Video Microscope-based Scratch Wound Assay and the Boyden Chamber Assay](#). *J Vis Exp*(129): 56337.
7. Gunti, S., Hoke, A. T. K., Vu, K. P. and London, N. R., Jr. (2021). [Organoid and Spheroid Tumor Models: Techniques and Applications](#). *Cancers (Basel)* 13(4).
8. Hanke, J. H., Gardner, J. P., Dow, R. L., Changelian, P. S., Brissette, W. H., Weringer, E. J., Pollok, B. A. and Connelly, P. A. (1996). [Discovery of a novel, potent, and Src family-selective tyrosine kinase inhibitor. Study of Lck- and FynT-dependent T cell activation](#). *J Biol Chem* 271(2): 695-701.
9. Hurley, J. D., Akers, A. T., Friedman, J. R., Nolan, N. A., Brown, K. C. and Dasgupta, P. (2017). [Non-pungent long chain capsaicin-analogs arvanil and olvanil display better anti-invasive activity than capsaicin in human small cell lung cancers](#). *Cell Adh Migr* 11(1): 80-97.
10. Justus, C. R., Leffler, N., Ruiz-Echevarria, M. and Yang, L. V. (2014). [In vitro cell migration and invasion assays](#). *J Vis Exp* (88): 51046.
11. Pijuan, J., Barceló, C., Moreno, D. F., Maiques, O., Sisó, P., Martí, R. M., Macià, A. and Panosa, A. (2019). [In vitro Cell Migration, Invasion, and Adhesion Assays: From Cell Imaging to Data Analysis](#). *Front Cell Dev Biol* 7(107). doi: 10.3389/fcell.2019.00107. eCollection 2019.
12. Stitt, A. W., McGoldrick, C., Rice-McCaldin, A., McCance, D. R., Glenn, J. V., Hsu, D. K., Liu, F. T., Thorpe, S. R. and Gardiner, T. A. (2005). [Impaired retinal angiogenesis in diabetes: role of advanced glycation end products and galectin-3](#). *Diabetes* 54(3): 785-794.
13. Stratton, S., Shelke, N. B., Hoshino, K., Rudraiah, S. and Kumbar, S. G. (2016). [Bioactive polymeric scaffolds for tissue engineering](#). *Bioact Mater* 1(2): 93-108.
14. Stuelten, C. H., Parent, C. A. and Montell, D. J. (2018). [Cell motility in cancer invasion and metastasis: insights from simple model organisms](#). *Nat Rev Cancer* 18(5): 296-312.

An Alternative Technique for Monitoring the Live Interaction of Monocytes and Tumor Cells with Nanoparticles in the Mouse Lung

Fernanda Ramos-Gomes^{1,*}, Nathalia Ferreira¹, Frauke Alves^{1,2} and M. Andrea Markus^{1,*}

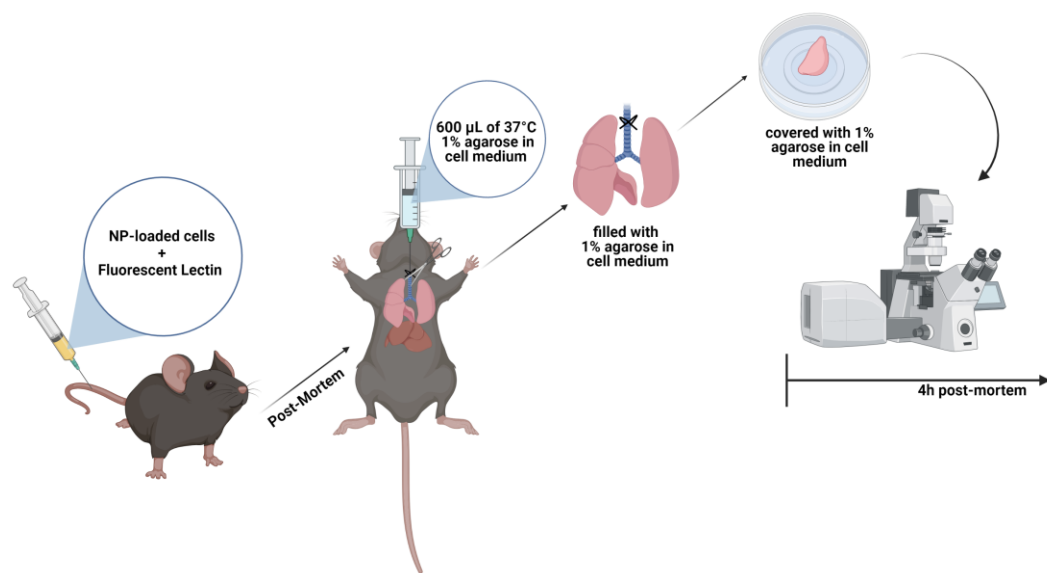
¹Translational Molecular Imaging, Max-Planck-Institute for Multidisciplinary Sciences, Göttingen, Germany

²Clinic of Hematology and Medical Oncology/Institute of Diagnostic and Interventional Radiology, University Medical Center Göttingen, Germany

*For correspondence: markus@mpinat.mpg.de; ramos@mpinat.mpg.de

[Abstract] Nanomaterials are increasingly used for the diagnosis and treatment of cancer, including lung cancer. For the clinical translation of nano-based theranostics, it is vital to detect and monitor their accumulation in the tumor, as well as their interaction with tumor, immune cells, and the tumor microenvironment (TME). While high resolution microscopy of fixed tumor specimens can provide some of this information from individual thin slices, it cannot capture cellular events over time and lacks 3D information of the tumor tissue. On the other hand, *in vivo* optical procedures either fall short of providing the necessary cellular resolution, as in the case of epifluorescence optical imaging, or are very demanding, as for instance intravital lung microscopy. We describe an alternative approach to investigate nanoparticle-cell interactions in entire mouse lung lobes, by longitudinal live cell confocal microscopy at nanometer resolution. By filling the lung *ex vivo* with 1% agarose, we were able to stabilize the lung lobes and visualize the interaction of fluorescent cells and nanoparticles for at least 4 hours post mortem. This high resolution *ex vivo* live cell imaging approach is an easy 4D tool for assessing several dynamic processes in tumor tissue, such as the traffic of cells, shedding of extracellular vesicles (EVs), and the accumulation of nanoparticles in tumor tissue.

Graphic abstract:



Schematic of the workflow for live cell imaging in the mouse lung.

Keywords: Live cell imaging, Cell dynamics, Nanoparticles, Fluorescence microscopy, TME

[Background] The advancement of the nanotechnology field has enabled the exploitation of nanoparticle (NP)-based cancer therapies (Jain and Stylianopoulos, 2010; Shi *et al.*, 2017). Compared to the standard chemotherapeutic approach, NPs confer several advantages as they improve drug solubility and stability, prolong drug half-lives in plasma, minimize off-target effects, and concentrate drugs at the target site (Mudshinge *et al.*, 2011). Combining all these characteristics, some NPs have been successfully approved by the FDA or are currently in clinical trials (Dinndorf *et al.*, 2007; Ediriwickrema and Saltzman, 2015). Despite these achievements, several details have to be considered in novel nanoparticle formulations, as most NP-based drugs have failed to improve patient outcomes. One of the most important is the relation of NPs with the tumor microenvironment (TME), which includes tumor cells, immune cells, and blood vessels (Blank *et al.*, 2017).

Traditionally, the characterization of the cellular uptake and interaction of NPs in the TME has been evaluated by 2D tissue sections. Despite the nanoscale resolution, immunohistochemistry and histology fail to demonstrate the complex organization of biological specimens and only provide static snapshots of events. With the development of new volumetric microscopy techniques, the understanding of cell-cell interactions in intact samples has become clearer. Furthermore, in comparison with other live-cell or *in vivo* technologies, confocal microscopy enables real-time imaging from general tissue architecture at nanoscale resolution (Ramos-Gomes *et al.*, 2020).

Recently, we published a protocol for live high-resolution imaging of the interaction between monocytes and tumor cells with nanoparticles in the mouse lung (Ramos-Gomes *et al.*, 2020). Here, we were able to demonstrate the dynamics between tumor and immune cells, the reaction of the

macrophages/monocytes towards NPs, and characterize the NP deposition in the tumor. This approach opens new avenues to dynamically understand how nanotherapies are going to affect the TME and reach target sites.

Materials and Reagents

1. 6-well plates
2. 20 G blunt cannula with the tips cut-off (BD Microlance 3, catalog number: 301300)
3. 1 mL syringe (BD Plastipak, catalog number: 303172)
4. U100 Insulin syringe (Braun, catalog number: 9151125)
5. Uncoated Ibidi 35 mm cell culture dishes (ibidi GmbH, catalog number: 80131)
6. Cotton sowing thread (not too thin; Wenco, catalog number: 140720)
7. Surgical disposable scalpel (Braun, catalog number: 5518075)
8. Kimtech paper (Kimtech Science, catalog number: 05511)
9. 25 mm round cover slips, 170 µm thick (Menzel-Gläser; VWR, catalog number: 631-1346)
10. Fluorescent-Labeled Lectin (Isolectin B4 from Bandeiraea simplicifolia, Sigma GmbH)
11. 1× Phosphate buffered saline (PBS, Gibco, catalog number: 14190-144)
12. Isoflurane (Forene, abbvie)
13. 70% ethanol (Honeywell, catalog number: 32205-2.5L-GL)
14. 1% agarose (BioFroxx, catalog number: 16500-500) in DMEM without phenol red (Gibco, catalog number: 31053-028) (see Recipes)

Cells

For visualization, tumor cells need to be fluorescent or preloaded with fluorescent NPs. Here, we use:

1. LLC-red fluorescence protein (RFP) lung tumor cells
2. human A549-mCherry lung tumor cells, which were prelabeled with fluorescent Atto488-Barium-NPs

Animals

1. Fluorescent reporter mouse for visualizing immune cells or tumor cells. Here we use C57BL/6-Tg(CD68-EGFP)1Drg/J transgenic mouse (The Jackson Laboratory, Stock No: 026827)
2. NMRI-Foxn1nu mice (Charles River Laboratories Inc, Strain code: 639)

Equipment

1. Surgical Wagner scissors (F.S.T., catalog number: 14068-12)
2. Tissue forceps (F.S.T., catalog number: 11021-12)
3. Standard pattern forceps (F.S.T., catalog number: 11000-14)

4. Water bath at 40°C (Memmert GmbH)
5. Isoflurane Vaporizer (VetEquip, catalog number: 911104)
6. Confocal/superresolution laser-scanning microscope system equipped with a tunable laser (470-670 nm) and GaAsP-PMT/Spectral detectors (Carl Zeiss, model: LSM880 equipped with Airyscan detection mode)
7. Microwave (Sharp)

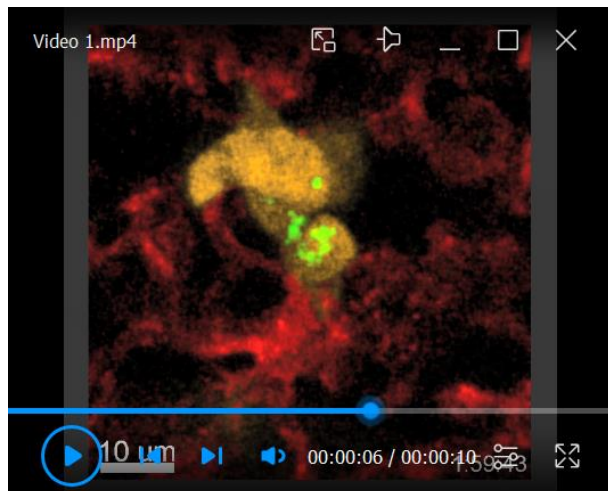
Software

1. Zen Black (Carl Zeiss)
2. Imaris (<https://imaris.oxinst.com>) (Bitplane, version 9.1.2)
3. Fiji (freeware; <https://fiji.sc/>)

Procedure

Two scenarios are described, to evaluate:

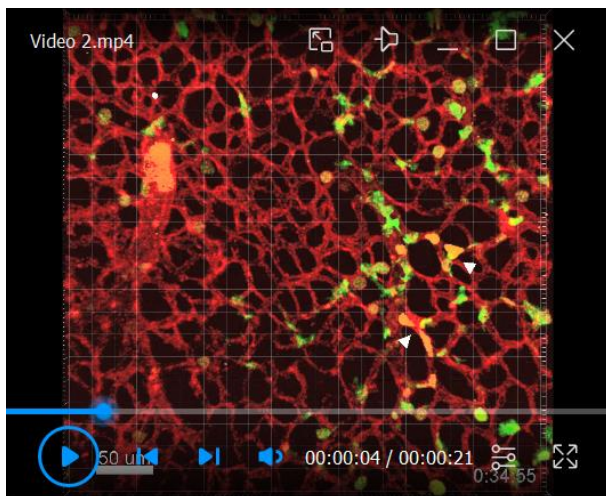
- A. The interaction between tumor cells, which were prelabeled with fluorescent NPs. As an example, we used human A549-mCherry lung tumor cells, which were prelabeled with Atto488-NPs, by incubating 3×10^5 adherent A549-mCherry cells with 25 mg/mL Atto488-NPs, in 6-well plates overnight at 37°C, 5% CO₂. We used the Atto488-NP-loaded cells in a NMRI-Fox1nu/nu mouse (Video 1).



Video 1. Exchange of green fluorescent nanoparticles between two A549-mCherry lung tumor cells active in the mouse lung [from Ramos-Gomes *et al.* (2020)].

- B. The interaction of fluorescent tumor cells with macrophages. As an example, we used mouse LLC-red fluorescence protein (RFP) lung tumor cells, in a C57BL/6-Tg(CD68-EGFP)1Drg/J (The Jackson Laboratory) transgenic mouse (Video 2).

There are no limitations regarding age and sex of the mice for these two described scenarios. However, age and sex of the mice may play a role for other settings or experiments, and thus may be dependent on the individual questions to be answered, cell lines to be used, or transgenic mice chosen.



Video 2. Interaction of LLC-RFP lung tumor cells with CD68-EGFP⁺ macrophages/monocytes in the mouse lung [from Ramos-Gomes et al. (2020)].

For visualization of blood vessels, fluorescent lectin (e.g., Alexa-647-lectin) is injected together with either tumor cells, or NP-loaded tumor cells.

1. Prepare a fresh solution of 1% agarose in phenol red free DMEM and keep in a 40°C water bath.
2. *In vivo* injection of tumor cells, NPs, and lectin
 - a. Anaesthetize the mouse with a consistent flow of 2% isoflurane in 1 L/min oxygen.
 - b. Into an U100 insulin syringe, take up 1×10^6 tumor cells, or NP-loaded 1×10^6 tumor cells, and 100 µg of lectin in the appropriate volume of PBS, depending on the weight of the mouse (maximum 5mL/kg body weight).
 - c. Place the mouse on a 37°C heat pad lying on its side, with the tail hanging over the edge, so that one of the lateral caudal veins is easily visible.
 - d. Warm up the tail of the mouse by soaking it in 37°C warm water for 1-2 min, to dilate the blood vessels.
 - e. The needle is placed on the surface almost parallel to the vein and carefully inserted into the vein. Once the needle tip is under the skin, it is important to pull back the syringe slightly during insertion, to confirm the blood will flow back, and then slowly inject the mixture without moving the needle tip.
 - f. Wait for 5 min, before sacrificing the animal with an overdose of anaesthesia.
3. Lung preparation
 - a. Immediately following sacrifice, fix the mouse with needles onto the surgical board, and clean the thoracic area with 70% ethanol.

- b. Open the chest cavity with surgical scissors and expose the lung and trachea.
- c. Place two 10 cm cotton threads underneath the trachea (Figure 1), by carefully sliding some standard pattern forceps underneath the trachea and pulling the threads through.
- d. Make a small incision at the very top of the trachea using surgical scissors.
- e. Insert the bland canula about 5 mm into the trachea.



Figure 1. Visualization of the cotton threads position below the trachea.

- f. Fix the canula to the trachea with the top cotton thread, by making a double knot.
- g. Load 600 μ L of warm 1% agarose in a 1 mL syringe, immediately insert it into the canula, and slowly inject the agarose into the lung, to prevent premature polymerisation of the agarose (Figure 2).



Figure 2. Image of the process for filling the lung with 1% agarose.

- h. Tighten the lower cotton thread with a knot below the canula, to seal the lung.
- i. Remove the canula carefully by cutting off the first thread.

- j. Dissect the lung from the chest cavity by carefully cutting all dorsal attachments with scissors, removing the esophagus, trachea, heart, and lungs *en bloc*. The esophagus is the dorsal landmark through the cervical region. The thoracic aorta is removed with the heart/lungs.
- k. Place the lung on a dry surface and remove the heart with a scalpel (Figure 3).



Figure 3. Appearance of the dissected lung filled with 1% agarose injection.

- i. Isolate individual lung lobes by cutting them off at the bronchial branches with a scalpel. Briefly rinse them in PBS to remove any blood.
- m. Dry the lung lobes on Kimtech paper.
- n. Choose individual lung lobes for imaging and place them with the flattest surface on an Ibidi 35 mm cell culture dish.
- o. Cover the entire lung lobe with 500-800 µL of 37°C warm 1% agarose, so that the lung lobe is just covered with agarose, ensuring the lung lobe does not float, and remains firmly on the bottom of the Ibidi dish.
- p. Place a cover slip on top of the agarose-sealed lung to prevent drying out of the lung (Figure 4).

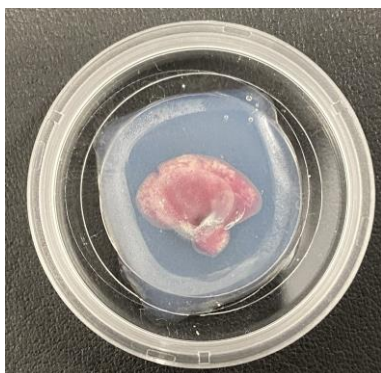


Figure 4. Arrangement of the lung lobe sample inside the Ibidi chamber.

- q. Immediately proceed to imaging.
4. Live image acquisition with Zeiss LSM880

- a. Set-up of the Zeiss LSM880 environmental system: Turn on the microscopy environmental incubator at least 4h before image acquisition to minimize focal drift: 37°C and 5% CO₂.
- b. Image acquisition
 - i. Place the sample-containing Ibidi chamber on the microscope stage (Figure 5).

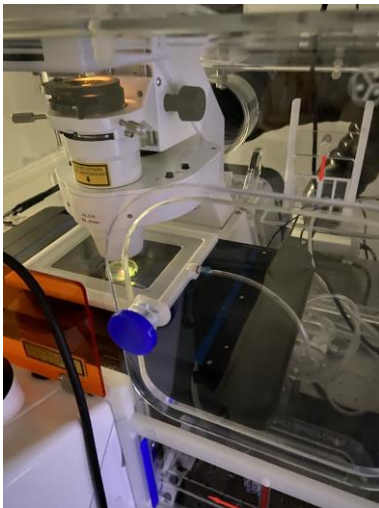


Figure 5. Placement of the sample in the environmental chamber of the microscope.

- ii. Perform a reflection of the cover slip using any of the available lasers and the 20× air objective.
- iii. Set the outer coverslip reflection as the zero μm position.
- iv. Set-up the appropriate lasers and filters according to the chosen combination of fluorophores. In our examples, we used the following: GFP-labeled monocytes of CD68-EGFP mouse lungs and Atto488-labeled NPs are excited with the Argon laser at 488 nm, LL2-RFP and A549-mCherry tumor cells are excited with the 561 nm laser, and Lectin-Alexa647 is excited with the 633 nm laser. The light path is divided with a beam splitter 488/561/633, and detected with GaAsP-PMT detectors. For high resolution imaging, we use 1024 × 1024 pixels with a 20x objective, and a field of view of 400 μm² or less in case of zoomed images. For an accurate quantification of fluorescent signals, we suggest a bit depth of at least 12, with the pinhole set to 1 airy unit, although these settings should be adjusted to the particular sample and experimental goal. Collect z slices of 10-12 μm range (step-size of 1-2 μm) of 3-color images at time intervals of 4 min (e.g., this time is suitable for monocyte dynamics observation).
- v. Raw data sets (z slice 3-color images at each timepoint) are exported as czi files.

Data analysis

Several software and freeware programs are available for image analysis. We recommend the Fiji distribution of the ImageJ software and Imaris (Bitplane, version 9.1.2). We commonly adjust the

maximum gray-value display range and time series for the desired time interval. Background noise can also be reduced by applying a median filter. Finally, if the data is captured as a z-stack, part of or the entire stack can be displayed as a 2D image, by applying a maximum intensity projection. Maximum projections are suitable for display, but not for quantification.

Examples of final time-lapse videos acquired by these procedures can be seen in Videos 1 and 2. Video 1 shows the exchange of green fluorescent nanoparticles between two A549-mCherry lung tumor cells active in the lung, that appear yellow. The exchange of nanomaterial took place over 3 h. Video 2 shows the interaction of LLC-lung tumor cells (yellow) with macrophages/monocytes of a transgenic C57BL/6-Tg(CD68-EGFP)1Drg/J mouse, that appear green fluorescent (arrows). The surveillance of the tumor cells by the macrophages/monocytes can be observed within the blood vessels, that are fluorescing in red. The lung tissue shows minimal movement and high focus stability over a period of 3 h 20 min.

Recipes

1. 1% agarose in DMEM without phenol red
 - a. Mix 1 g of agarose powder in 100 mL of DMEM without phenol red in a microwavable flask.
 - b. Microwave the solution for 1-3 min until the agarose is completely dissolved (do not overboil, as the excessive evaporation can alter the final agarose concentration).
 - c. Keep at 40°C until use.

Acknowledgments

This project has received funding from the European Union's Horizon 2020 research and innovation program under the Marie Skłodowska-Curie grant agreement No. 861190 (PAVE) and from the BMBF (VDI) funded projects THERAKON (No. 13GW0218A) and ELICIT (No. 13N14346).

This protocol has been adapted from Ramos-Gomes *et al.* (2020).

Competing interests

The authors declare that the research was conducted in the absence of any commercial or financial relationships that could be construed as a potential conflict of interest.

Ethics

The animal study was reviewed and approved by Nds. Landesamt für Verbraucherschutz und Lebensmittelsicherheit.

All the animals *in-vivo* experiments were performed in accordance with European Directive (2010/63/EU).

References

1. Blank, F., Fytianos, K., Seydoux, E., Rodriguez-Lorenzo, L., Petri-Fink, A., von Garnier, C. and Rothen-Rutishauser, B. (2017). [Interaction of biomedical nanoparticles with the pulmonary immune system](#). *J Nanobiotechnology* 15(1): 6.
2. Dinndorf, P. A., Gootenberg, J., Cohen, M. H., Keegan, P. and Pazdur, R. (2007). [FDA drug approval summary: pegaspargase \(oncaspar\) for the first-line treatment of children with acute lymphoblastic leukemia \(ALL\)](#). *Oncologist* 12(8): 991-998.
3. Ediriwickrema, A. and Saltzman, W. M. (2015). [Nanotherapy for Cancer: Targeting and Multifunctionality in the Future of Cancer Therapies](#). *ACS Biomater Sci Eng* 1(2): 64-78.
4. Jain, R. K. and Stylianopoulos, T. (2010). [Delivering nanomedicine to solid tumors](#). *Nat Rev Clin Oncol* 7(11): 653-664.
5. Mudshinge, S. R., Deore, A. B., Patil, S. and Bhalgat, C. M. (2011). [Nanoparticles: Emerging carriers for drug delivery](#). *Saudi Pharm J* 19(3): 129-141.
6. Ramos-Gomes, F., Ferreira, N., Kraupner, A., Alves, F. and Markus, M. A. (2020). [Ex vivo Live Cell Imaging of Nanoparticle-Cell Interactions in the Mouse Lung](#). *Front Bioeng Biotechnol* 8: 588922.
7. Shi, J., Kantoff, P. W., Wooster, R. and Farokhzad, O. C. (2017). [Cancer nanomedicine: progress, challenges and opportunities](#). *Nat Rev Cancer* 17(1): 20-37.

A Multi-color Bicistronic Biosensor to Compare the Translation Dynamics of Different Open Reading Frames at Single-molecule Resolution in Live Cells

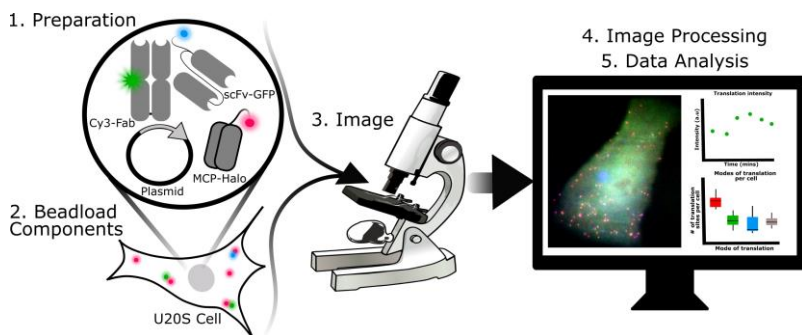
Amanda L. Koch¹, Tatsuya Morisaki¹ and Timothy J. Stasevich^{1, 2, *}

¹Department of Biochemistry and Molecular Biology, Colorado State University, Fort Collins, CO 80523, USA; ²Cell Biology Center and World Research Hub Initiative, Tokyo Institute of Technology, Yokohama, Kanagawa 226-8503, Japan

*For correspondence: Tim.Stasevich@colostate.edu

[Abstract] Here, we describe how to image and quantitate the translation dynamics of a bicistronic biosensor that we recently created to fairly compare cap-dependent and IRES-mediated translation at single-molecule resolution in live human cells. This technique employs a pair of complementary intrabodies loaded into living cells that co-translationally bind complementary epitopes in the two separate ORFs of the bicistronic biosensor. This causes the biosensor to fluoresce in different colors depending on which ORF/epitopes are translated. Using the biosensor together with high-resolution fluorescence microscopy and single-molecule tracking analysis allows for the quantitative comparison of translation dynamics between the two ORFs at a resolution of tens-of-nanometers in space and sub-seconds in time, which is not possible with more traditional GFP or luciferase reporters. Since both ORFs are on the same biosensor, they experience the same microenvironment, allowing a fair comparison of their relative translational activities. In this protocol, we describe how to get this assay up and running in cultured human cells so that translation dynamics can be studied under both normal and stressful cellular conditions. We also provide a number of useful tips and notes to help express components at appropriate levels inside cells for optimal live cell imaging.

Graphical abstract:



Steps required for 3-color single-molecule translation imaging and analysis.

Keywords: Translation, Single-molecule, Fluorescence microscopy, Non-canonical initiation, Viral translation, Internal ribosomal entry site

[Background] Recently, it has become possible to measure the translation dynamics of single mRNA molecules in live cells (Morisaki *et al.*, 2016; Pichon *et al.*, 2016; Wang *et al.*, 2016; Wu *et al.*, 2016; Yan *et al.*, 2016). This technology allows for the quantitation of the heterogeneity of translation dynamics among mRNA (Morisaki and Stasevich, 2018). To image and quantitate single mRNA translation dynamics, fluorescent intrabodies such as Fab (Hayashi-Takanaka *et al.*, 2011), scFv (Tanenbaum *et al.*, 2014; Zhao *et al.*, 2019), or nanobodies (Boersma *et al.*, 2019) are required. These intrabodies bind and label repeated epitopes inserted at the N-terminus of a protein of interest. As the protein of interest is translated, the repeated epitopes emerge from the ribosome and are bound within seconds by the fluorescent intrabodies (Morisaki and Stasevich, 2018; Cialek *et al.*, 2020). This strategy amplifies fluorescence within the translation sites at two levels: firstly, multiple fluorescent intrabodies can bind the repeated epitopes within a single nascent peptide chain at the same time; and secondly, multiple ribosomes can translate the mRNA in polysomes to produce multiple nascent peptide chains within a single translation site. These two levels of amplification produce bright fluorescent puncta that can be detected with single-molecule precision above the background using a sensitive fluorescence microscope. As ribosomes initiate, elongate, and terminate translation, the fluorescence intensity at individual translation sites fluctuates up or down, yielding insight into translation dynamics.

Over the last few years, complementary intrabodies and epitopes have been developed that make it possible to image translation in multiple colors at the same time. For example, our lab has developed anti-FLAG and anti-HA Fab that bind the classic FLAG and HA epitopes (Morisaki *et al.*, 2016). More recently, we developed a genetically encodable scFv version of the anti-HA Fab that we call the anti-HA frankenbody (Zhao *et al.*, 2019). Likewise, the Tanenbaum lab has developed the SunTag (SunTag epitopes + anti-SunTag scFv-GFP) and MoonTag (MoonTag epitopes + anti-MoonTag nanobody) systems (Tanenbaum *et al.*, 2014; Boersma *et al.*, 2019). Used together, these complementary imaging tools make it possible to compare the dynamics of different open reading frames (ORFs) at the single-molecule level within live cells.

Here, we describe how to use a 3-color bicistronic biosensor that we recently developed to compare translation kinetics at internal ribosomal entry sites (IRES) versus at the canonical 5' cap (Figure 1a) (Koch *et al.*, 2020). The biosensor encodes an MS2 tag to mark and track individual mRNA molecules (red) (Coulon *et al.*, 2013; Pichon *et al.*, 2020). When these mRNAs are expressed in cells, they light up in different colors depending on the nature of translation initiation. If translation is initiated at the cap, then FLAG epitopes are translated and bound by anti-FLAG Fab conjugated with Cy3 (green). If translation is initiated at the IRES, then SunTag epitopes are translated and bound by anti-SunTag scFv fused to eGFP (blue). This produces a variety of colorful puncta in cells that mark individual mRNA and their translation status (Figure 1a and 1c).

This basic imaging biosensor is unique because it enables quantitative comparisons between the translation dynamics of two ORFs at a spatial resolution on the tens-of-nanometers scale and temporal resolution on the sub-seconds scale. This is not possible with more traditional bulk assays that lack single-molecule resolution, including traditional luciferase and GFP reporters as well as bulk assays like western blotting. The biosensor is also versatile because a different IRES sequence can easily be

inserted to study the translational dynamics of that IRES in diverse cell types and cellular conditions (Bornes Stéphanie *et al.*, 2007; Firth and Brierley, 2012). Further, our 3-color assay can be extended to compare ORF translation dynamics on two separate mRNAs (Figure 1b). This can be achieved by simply splitting the bicistronic biosensor into two monocistronic biosensors, each encoding a probe/epitope pair and an MS2 tag. This setup is not only beneficial for comparing the translation dynamics of two different ORFs but also for fairly comparing different endogenous 5' or 3' UTRs or viral elements within single cells.

In this protocol, we focus mainly on the wet lab skills needed to express our biosensor in live human cells. In particular, since our biosensor fluoresces in three colors, multiple components need to be expressed within cells at appropriate levels. Here, we advocate the use of beadloading (McNeil and Warder, 1987; Hayashi-Takanaka *et al.*, 2011) to achieve this with high efficiency and minimal effort. We describe how the various probes – including the MS2 coat protein used to label mRNA with an MS2 tag, Fab to label FLAG-tagged epitopes, and SunTag scFv to label SunTag epitopes – can be purified and loaded together in a single, simple step (Cialek *et al.*, 2021; Morisaki *et al.*, 2016; Koch *et al.*, 2020). We find this approach to be very convenient, enabling the fine-tuning of probe levels, rapid testing, and combinatorial experimentation. Finally, we describe the basics of our imaging and analyses, including a specific test to verify translation, useful conditions for stressing cells while under the microscope, and basic codes to quantitate translation site intensities and distributions.

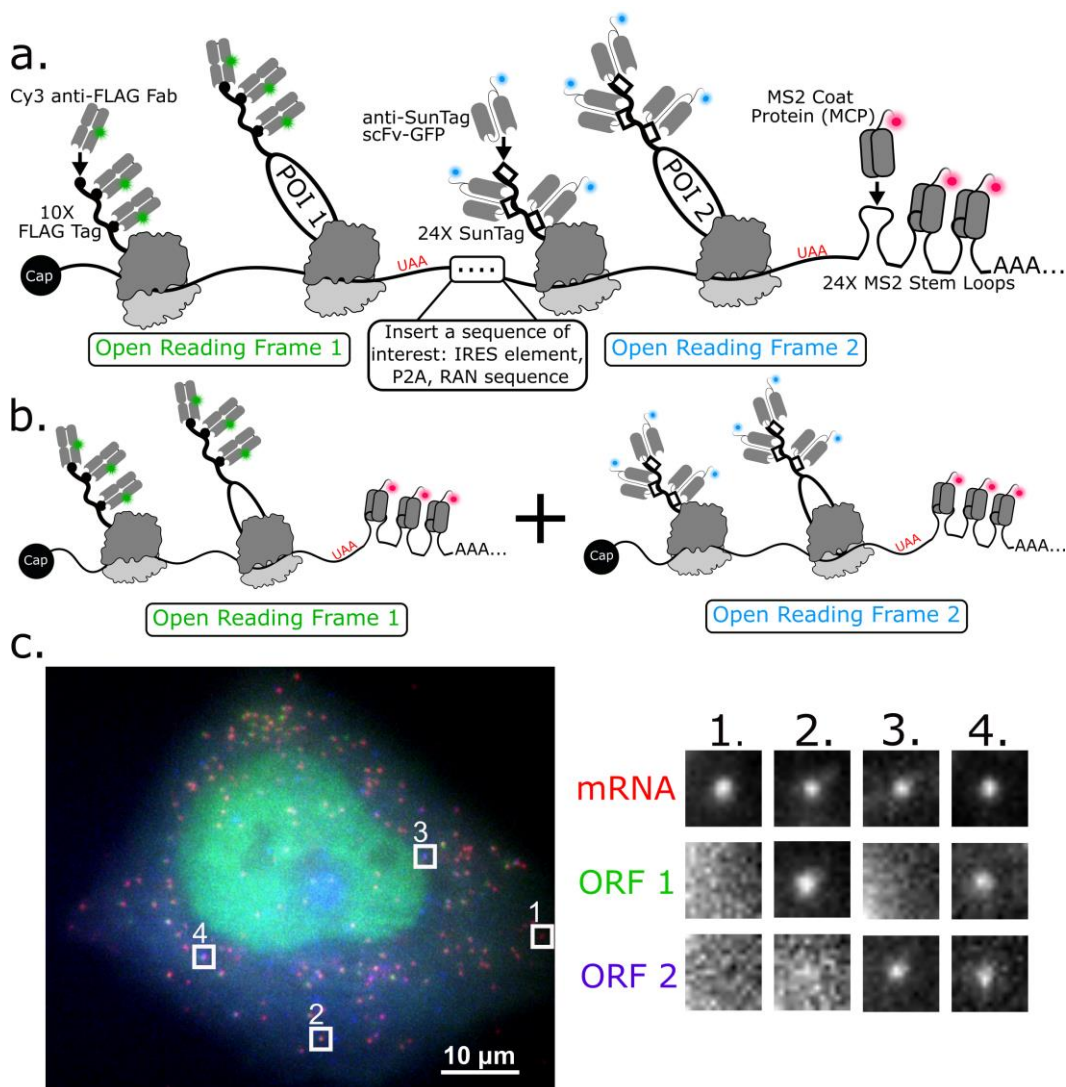


Figure 1. 3-color imaging of the translation of a single bicistronic or pair of monocistronic biosensors in live cells. a) Schematic illustrating a bicistronic 3-color single-molecule translation reporter. b) Schematic illustrating a 2-mRNA single-molecule translation reporter system. c) A 3-color bicistronic reporter (representative cell). Crops showing all types of translation are on the right panel.

Materials and Reagents

A. Anti-FLAG Fab generation and dye-conjugation

1. Pierce Fab preparation kit (Thermo Fisher Scientific, catalog number: 44985)
2. 0.6 ml or 1.7 ml low retention tubes (Thomas Scientific, catalog numbers: 1149K01 and 1159M35PK, respectively)
3. PD-mini G-25 desalting column (GE Healthcare, catalog number: 95055-984)
4. Amicon Ultracel-50 (50 kDa-cutoff) 15-ml centrifugal filter unit (Millipore Sigma, catalog number: UFC9050)

5. Amicon Ultracel-10 (10 kDa-cutoff) 15-ml centrifugal filter unit (Millipore Sigma, catalog number: UFC9010)
6. Amicon Ultracel-10 (10 kDa-cutoff) 0.5-ml centrifugal filter unit (Millipore Sigma, catalog number: UFC5010)
7. FLAG antibodies (FujiFilm Wako Pure Chemical Corporation, catalog number: 012-22384 (Anti-DYKDDDDK mouse monoclonal IgG2b antibodies))
8. Cy3 N-hydroxysuccinimide ester mono-reactive dye pack (VWR, catalog number: 95017-373 PK)
9. Dimethyl sulfoxide (DMSO) (Millipore Sigma, catalog number: D8418)
10. Sodium bicarbonate (NaHCO_3) (Millipore Sigma, catalog number: S5761-500G)
11. Phosphate-buffered saline (PBS) (Thermo Fisher Scientific, catalog number: AM9625)

B. Halo-MCP and anti-SunTag scFv-GFP purification

1. BL21 *E. coli* (DE3) pLysS competent cells (Novagen, EMD millipore, catalog number: 69451-3)
2. 2× YT growth media (Research Products International, catalog number: X15600-5000.0)
3. Ampicillin (sodium) USP grade (GoldBio, catalog number: A-301-100)
4. Chloramphenicol USP grade (GoldBio, catalog number: C-105-100)
5. Isopropyl- β -D-thiogalactoside (IPTG) (GoldBio, catalog number: I2481C100)
6. Phosphate-buffered saline (PBS) pH 7.4
7. Sodium chloride (NaCl) ACS grade
8. Protease inhibitor cocktail tablets (Pierce™ EDTA-free Protease Inhibitor Mini Tablets, Thermo Scientific, catalog number: A32955)
9. 4-(2-aminoethyl) benzenesulfonyl fluoride hydrochloride (AEBSF serine protease inhibitor) (GoldBio, catalog number: A-540-10)
10. Imidazole ACS reagent, \geq 99% titration (Sigma-Aldrich)
11. Amicon Ultracel-30 (30 kDa-cutoff) 15-ml centrifugal filter unit (EMD Millipore, catalog number: UFC903024)
12. HEPES-based buffer (see Recipes)
13. HisTrap buffer A (see Recipes)
14. HisTrap buffer B (see Recipes)
15. Superdex buffer (see Recipes)

C. U-2 OS cell culture

1. U-2 OS cells (ATCC, catalog number: ATCC HTB-96)
2. DMEM (+/-), high glucose, no glutamine (See Recipes for DMEM (+) media) (Thermo Fisher Scientific, catalog number: 11960069)
3. Fetal bovine serum (Atlas Biologics, catalog number: F-0050-A)
4. Penicillin-streptomycin (Thermo Fisher Scientific, catalog number: 15140-122)
5. L-glutamine, 200 mM (100×) (Thermo Fisher Scientific, catalog number: 25030081)

6. Trypsin (Thermo Fisher Scientific, catalog number: 25300062)
 7. 100-mm cell culture dishes (VWR, catalog number: 82050-916)
- D. Beadloading and staining Halo-MCP with JF646 ligand
1. 106- μ m glass beads (Millipore Sigma, catalog number: G4649)
 2. Spectramesh Woven Filters Polypropylene Opening: 105- μ m (Spectrum Labs, catalog number: 148496)
 3. Plasmid DNA of interest
 4. Cy3 anti-FLAG Fab (prepared as described in Step B8)
 5. Purified anti-SunTag scFv-GFP (prepared as described in Step C19)
 6. Purified Halo-MCP (prepared as described in Step C19)
 7. Phenol-free DMEM (Thermo Fisher Scientific, catalog number: 31053036)
 8. Janelia Fluor 646 HaloTag ligands (Promega, catalog number: GA1120)
 9. 0.6-ml low retention tubes (Thomas Scientific, catalog number: 1149K01)
 10. Phosphate-buffered saline (Thermo Fisher Scientific, catalog number: AM9625)

E. Imaging

1. Glass-bottomed dishes, 35-mm, #1.5, 14-mm glass, uncoated (MatTek Corporation, catalog number: P35G-1.5-14-C)
2. Opti-MEM, Reduced Serum Medium (Thermo Fisher Scientific, catalog number: 31985070)
3. Puromycin (Thermo Fisher Scientific, catalog number: A1113803)
4. Harringtonine (Cayman Chemical Company, catalog number: 26833-85-2)
5. Sodium arsenite (NaAs) (Millipore Sigma, catalog number: S7400-100G)
6. Dithiothreitol (DTT) (Thermo Fisher, catalog number: R0861)

Equipment

1. UV-Vis spectrophotometer (Thermo Fisher Scientific, model: NanoDrop OneC)
2. Table top centrifuge (Beckman Coulter, model: Microfuge 20)
3. Cooled centrifuge (Thermo Fisher Scientific, model: Sorvall Legend XFR with F14 6x250LE)
4. Sonicator
5. HisTrap HP, 5-ml (Cytiva, formerly GE Healthcare catalog number: 17524801)
6. HiLoad 16/600 Superdex 200 pg column (Cytiva catalog number 28989335)
7. Fluorescence microscope (capable of thin sectioning; confocal, light-sheet, and HILO microscopes recommended) with a stage-top incubator

Software

1. Software for single-molecule tracking, e.g., TrackMate (Tinevez *et al.*, 2017) or our custom Mathematica code found at:

https://github.com/Colorado-State-University-Stasevich-Lab/mRNA_Tracking_BioProtocol

Procedure

A. Concentrating anti-FLAG antibody and preparing anti-FLAG Fabs

General comment: 5 mg anti-FLAG antibodies are shipped at a concentration of ~0.4-0.6 mg/ml. In this step, 4 mg antibody is concentrated to 4-8 mg/ml to create the Fab. Note: the Ultracel-50 filter allows anything smaller than 50 kDa to pass through. Full-length antibody is ~150 kDa and thus does not pass through, but Fab does. Therefore, this filter is not suitable for concentrating Fab in Procedure B below.

1. Cool centrifuge to 4°C.
2. Pipette 4 mg anti-FLAG AB from the shipping container into an Ultracel-50 centrifugal filter unit (up to 15 ml sample volume). Add 1× PBS to fill the filter unit to 15 ml.
3. Centrifuge at 5,000 × g for 10-20 min at 4°C.
 - a. Discard flowthrough and add 1× PBS to fill the filter unit to 15 ml.
 - b. Repeat 4× to fully replace the buffer to 1× PBS and sufficiently concentrate the antibodies.
4. After centrifugation, around 0.5-1 ml antibody should remain at the top of the Ultracell chamber. Transfer this to a low retention tube.
5. After transfer, wash the sides of the Ultracel-50 filter by pipetting 50 µl 1× PBS. Pipette up and down a few times and let the PBS wash over the filter surface so that all residual antibody is washed to the bottom of the filter unit, where it can be easily pipetted and added to the concentrated antibody in the low retention tube (from step above).
6. Measure the concentration using a NanoDrop.
The final concentration should be around 4-8 mg/ml.
7. Use the Pierce Fab preparation kit to generate the Fab following the manufacturer's instructions.
Tip: We recommend performing Fab preparation just once with 4 mg concentrated anti-FLAG antibody (keeping 1 mg full-length antibody as a backup). This is not only cost- and time-effective, but in our hands also leads to a minimal amount of antibody loss during the Fab preparation process.
 - a. The Pierce Fab preparation kit instructions can be found at:
https://assets.fishersci.com/TFS-Assets/LSG/manuals/MAN0011651_Pierce_Fab_Prep_UG.pdf.
 - b. Note that two Fabs are generated for each antibody, with each Fab roughly 50 kDa (or one-third of the full-length antibody). Thus, 4 mg antibody starting material will produce 2.67 mg

Fab. Generally, we lose some antibody material in the process of making the Fab, so we typically end up with 1.5-2 mg Fab.

8. Concentrate the anti-FLAG Fab using a 15-ml Ultracel-10 centrifugal filter unit as in Procedure A above.

Notes:

- a. *Do not accidentally use the Ultracel-50 centrifugal filter unit! The Ultracel-10 will allow everything less than 10 kDa to pass through. Thus, Fab, which is ~50 kDa, will not pass through and will become concentrated at the top of the filter unit.*
- b. *You can also use 0.5-ml Ultracel-10 centrifugal filter units for this step; however, this will require more time since only 0.5 ml can be concentrated at a time.*

9. Measure the concentration using a NanoDrop.

The final concentration should ideally be around 2 mg/ml, such that 0.5 ml will be 1 mg Fab.

10. Store the concentrated anti-FLAG Fab at 4°C.

Tip: We find that both anti-FLAG full-length antibody and Fab can be stored in a standard 4°C refrigerator for years without degrading. Repeated freeze-thaw cycles will be detrimental to Fab function and are therefore not recommended.

B. Anti-FLAG Fab dye-conjugation (Cy3 anti-FLAG Fab)

General comment: The starting component is purified anti-FLAG Fab prepared in Procedure A.

1. Take a vial from a 5 pack of Cy3 mono-reactive NHS Ester.

- a. Dissolve the Cy3-NHS Ester reagent in a vial in 100 µl DMSO and store at -20°C.

2. Pipette 100 µg purified Fab (~50 µl) from Step A into a low retention tube.

3. Add sterilized 1× PBS to reach a total volume of 90 µl.

4. Add 10 µl 1 M sodium bicarbonate to reach a total volume of 100 µl.

Tip: It is recommended to prepare fresh 1 M sodium bicarbonate before the reaction.

5. Add the correct amount of dye (this amount is found empirically, see Hayashi-Takanaka et al., 2014).

- a. For Cy3 diluted in 100 µl DMSO, add 1.33 µl.

- b. Tap the tube lightly to evenly distribute.

6. Place the tube in a light-proof bag and attach to a rotator or any equipment that can rotate the tube effectively.

7. Incubate for 1 hour at room temperature while rotating.

8. Purify Cy3 anti-FLAG Fab with a G-25 minitrap.

- a. Cool the centrifuge to 4°C.

- b. Discard the buffer from the G-25 minitrap and equilibrate by allowing 500 µl 1× PBS to fully run through by gravity flow.

Notes:

- i. *Repeat three times to fully equilibrate.*

- ii. *Be careful not to let the G-25 minitrap column dry out.*

- c. Briefly spin down the tube holding the incubated Fab to remove conjugated Fab from the lid and sides.
- d. Pipette all 100 μl incubated Fab onto the top of the G-25 minitrap.
Note: Make sure the column is straight and pipette the mixture directly into the center.
- e. Pipette 450 μl 1 \times PBS on top of the column for circulation.
Note: You can pipette an additional 50-100 μl to force the conjugated Fab (lower pinkish band) to move closer to the bottom of the column.
- f. When the conjugated Fab band is close to the bottom of the column, obtain a new low retention tube to capture the conjugated Fab.
- g. Pipette 500 μl 1 \times PBS into the center of the column. The lower Fab band will flow out and should be captured in the low retention tube.
Note: The solution containing the conjugated Fab will appear pinkish.
- h. Concentrate the captured conjugated Fab protein by transferring it to an Ultra-10 0.5-ml centrifugal filter unit.
- i. Align the filter perpendicular to the centrifuge.
- j. Centrifuge at 12,000 $\times g$ for 5 min.
- k. Discard the flowthrough and add up to 500 μl 1 \times PBS to the filter.
 - i. Usually, the flowthrough is clear, indicating that most of the dye is conjugated to the Fab.
- l. Centrifuge at 4°C, 12,000 $\times g$ for 5 min.
- m. Discard the flowthrough.
- n. Add 500 μl 1 \times PBS.
- o. Centrifuge at 12,000 $\times g$ for 10 min.
- p. Pipette out the conjugated Fab that remains at the top of the Amicon Ultra filter and transfer to a new 0.6-ml low retention tube (Typically this volume is around 50 μl).
- q. After transfer, wash the sides of the Ultracel-10 0.5-ml filter by pipetting 20-30 μl 1 \times PBS. Pipette up and down a few times and let the PBS wash over the filter surface so that all residual conjugated Fab is washed to the bottom of the filter unit, where it can be easily pipetted and added to the concentrated conjugated Fab in the 0.6-ml low retention tube (from step above).
- r. Measure the concentration and absorbance spectrum with a NanoDrop.
 - i. Firstly, choose Protein and Labels; then choose the sample type as IgG and the appropriate Cy3 dye. The measured concentration should be close to 1 mg/ml with an absorbance ratio of ~1-2.
 - ii. Calculate the degree of labeling:

$$DOL = \frac{\varepsilon_{Fab}}{\varepsilon_{dye}} \times \frac{1}{A_{280}/A_{dye} - CF}$$

where ϵ_{Fab} is the extinction coefficient of Fab ($70,000 \text{ M}^{-1}\text{cm}^{-1}$), ϵ_{dye} is the extinction coefficient of the dye used for conjugation ($150,000 \text{ M}^{-1}\text{cm}^{-1}$ for Cy3), A_{280} and A_{dye} are the measured absorbances of dye-conjugated Fab fragments at 280 nm and at the peak of the emission spectrum of the dye (570 nm for Cy3), respectively, and CF is the correction factor of the dye (the ratio of the absorbances of the dye alone at 280 nm to at the peak; 0.08 for Cy3).

Ideally, the DOL should be close to 1, corresponding to ~1 dye per Fab. If the DOL is too low, the entire process can be repeated.

- s. For working stocks, dilute Cy3 anti-FLAG Fab to a concentration of 0.5 mg/ml in 1× PBS.

Note: Store at 4°C.

- C. Purification of MCP fused to HaloTag (Halo-MCP) and anti-SunTag scFv fused to eGFP (anti-SunTag scFv-GFP)
 1. Transform *E. coli* BL21 (DE3) pLysS competent cells with the expression plasmid (pHis-Halo-2MCP or pHis-scFv-GFP – plasmids are available upon request).
 2. Grow and shake transformed cells at 37°C in 2× YT broth containing 100 mg/L ampicillin and 25 mg/L chloramphenicol until the cells reach OD600.
 3. Lower the temperature to 30°C (Halo-MCP) or 18°C (anti-SunTag scFv-GFP) when this density is reached.
 - a. Add 0.4 mM IPTG.
 - b. Incubate for 3 or 16 h for Halo-MCP or anti-SunTag scFv-GFP, respectively.
 4. Cool the centrifuge to 4°C.
 5. Pellet the cells by centrifugation at $2,041 \times g$ for 30 min at 4°C.
 6. Resuspend the pellet in HisTrap buffer A (20 ml per 1 L culture) and add protease inhibitor cocktail (manufacturer's suggestion).
 7. Lyse the cells by sonication at 50% output; 30 s on and 90 s off.
 8. Pellet the lysate by centrifugation at $30,186 \times g$, 4°C for 30 min.
 9. Connect two HisTrap HP 5-ml columns in series and pre-equilibrate columns with HisTrap buffer A.
 10. Load the supernatant onto the columns.
 11. Wash columns with 5 column volumes (CV, 50 ml) of HisTrap buffer A.
 12. Elute with 10 CV (100 ml) of a linear gradient of 0-500 mM imidazole (HisTrap buffer B).
 13. Concentrate the purified protein (Halo-MCP or anti-SunTag scFv-GFP) fraction using an Amicon Ultracel-30 (30 kDa-cutoff) 15-ml centrifugal filter unit to a final volume of approximately 2 ml.
 14. Equilibrate a HiLoad 16/600 Superdex 200 pg column with Superdex buffer.
 15. Load concentrated sample onto the equilibrated HiLoad 16/600 Superdex 200 pg column.
 16. Check the purity of the fractions by 15% SDS-PAGE. Concentrate the fractions containing purified protein using an Amicon Ultracel-30 15-ml centrifugal filter unit.

17. Determine the protein concentration using a NanoDrop.
18. Aliquot into small volumes, flash freeze with liquid nitrogen, and store at -80°C.
19. For working stocks, dilute purified Halo-MCP to a concentration of 0.13 mg/ml in 1× PBS and anti-SunTag scFv-GFP to 0.5 mg/ml in 1× PBS.

Store at 4°C.

Tip: Try to make a small working stock volume of 10-20 µl. Diluted purified protein lasts for ~2 months at 4°C.

D. Preparing glass beads by acid washing

Note: Be careful not to inhale the glass beads; they are toxic to the lungs.

1. Sterilize 5 ml glass beads in 25 ml 2 M NaOH for 2 h in a 50-ml conical tube with gentle mixing, preferably using a rotator.
2. Decant the NaOH, retaining as many beads as possible. If the beads are in suspension, they can be briefly spun in a centrifuge.
3. Wash the beads thoroughly with cell culture grade water until the pH is neutral (use a pH test strip on the eluate). Decant the wash water each time, as before.
4. Rinse the beads thoroughly with 100% ethanol 2-3 times. Decant the ethanol each time, as before.
5. Sprinkle the beads into a sterile container (such as a 100-mm Petri dish) and allow to air dry in a biosafety cabinet overnight.

Note: When the beads are completely dry, they will look sandy, i.e., they will not clump or flake when the container is tapped.

6. UV-sterilize the beads for 30 min, if possible.
7. Store in a desiccator to keep the beads dry.

E. U-2 OS cell culture

1. Make DMEM (+). See recipe below.
Store at 4°C.
2. Maintain U-2 OS cells at a confluence no greater than 90%.
3. The day before imaging, split cells into MatTek chambers as follows:
 - a. Warm up the Trypsin and DMEM (+).
 - b. Remove the cells from the 37°C, 5% CO₂ incubator.
 - c. Remove all media.
 - d. Wash 2-3 times with 1× PBS.
 - e. Add enough Trypsin to cover the bottom of the dish.
 - f. Incubate at room temperature for 30 s.
 - g. Aspirate or pipette out the Trypsin. This will leave a thin layer on top that is sufficient for cell detachment. Tilt the dish back and forth a few times to make sure the thin layer of Trypsin is evenly spread.

- h. Wait 1-5 min for the cells to detach. This can be facilitated by shaking/tapping the dish or placing the dish in the incubator at 37°C briefly.
 - i. Add DMEM (+) (10 ml for a 100-mm dish).
 - j. Tilt the dish at a 45° angle.
 - k. To ensure that most cells are removed, pipette the media at the top of the dish so that it runs down and washes the cells toward the bottom, where they can be pipetted. Repeated pipetting can also help to remove cell clumps.
 - l. Transfer the cells and media into a 15-ml conical tube. This is optional but will help to prevent cells from re-adhering to the dish if there is some time before plating onto MatTek chambers.
 - m. Plate cells onto MatTek chambers at 75% confluence (approximately 9.0×10^5 cells).
4. 1-2 hours before beadloading, change media from DMEM (+) to Opti-MEM supplemented with 10% FBS (v/v):
- a. Wash the cells twice with 1× PBS.
 - b. Add Opti-MEM + 10% FBS (v/v).
 - c. Incubate at 37°C.

Note: This step is optional. Cells can be left in DMEM (+) before beadloading. Our lab has empirically found that cells in OPTI-MEM + FBS are more likely to express the plasmid of interest and are generally healthier.

F. Beadloading

Note: Applying the glass beads to the top of the cells can be achieved in multiple ways. We recommend using a hand-made beadloader that will effectively sprinkle an evenly distributed monolayer of beads across the cells. See also Cialek et al. (2021).

1. Create a custom beadloader (Figure 2).
 - a. Remove the glass bottom from a MatTek chamber.
 - b. Place a ~100-µm nylon mesh over the hole. Secure with tape.
 - c. Add the glass beads.
 - d. Cover the top with a MatTek lid. Secure with parafilm.
 - e. Cover the bottom of the dish (side with the mesh) with another MatTek lid.
 - f. Store in a desiccator upside down to keep the beads dry and within the chamber.

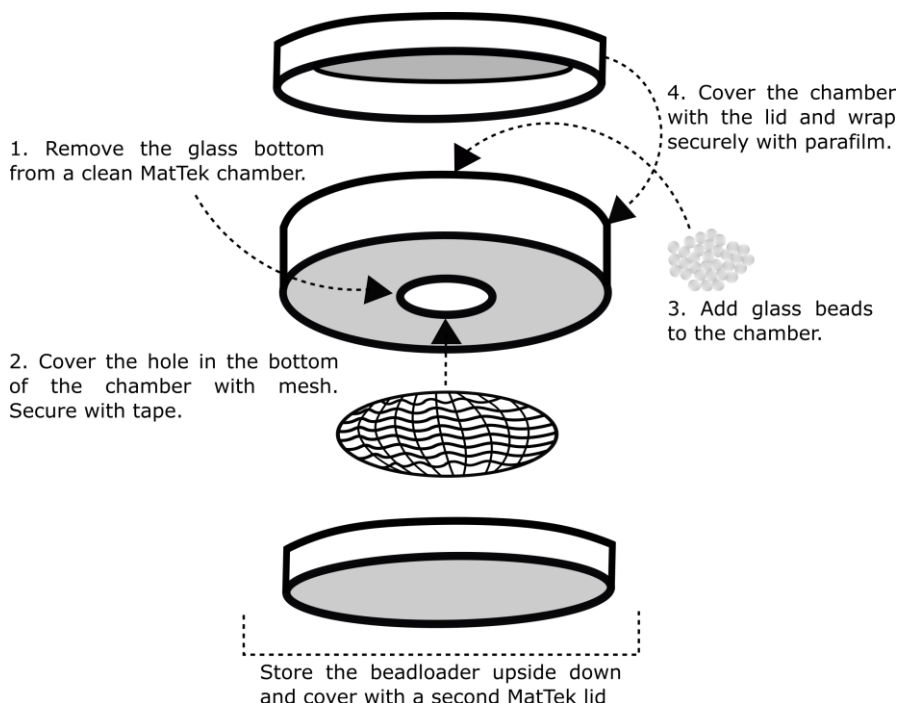


Figure 2. Steps depicting how to make a custom beadloader

2. On the bench, add the following to a low retention 0.6-ml tube:
 - a. ~0.5 µg Cy3 anti-FLAG Fab (~1 µl working stock prepared in Step B8).
 - b. ~0.5 µg anti-SunTag scFv-GFP (~1 µl working stock prepared in Step C19).
 - c. ~0.13 µg purified Halo-MCP (~1 µl working stock prepared in Step C19).
 - d. 750 ng plasmid DNA of interest.
 - e. 1× PBS to a total volume of 4 µl.
 3. Mix well by pipetting and flicking the tube; do not vortex.
 4. Spin down rapidly.
 5. Take the MatTek chamber containing the cells out of the incubator and into a sterile hood.
 6. Remove the medium (Opti-MEM + FBS) and place in a 15-ml conical tube.
- Tip: Make sure to remove all medium to avoid diluting the sample solution, especially from the coverslip area that can retain some medium because of its concave shape. If medium is left on the coverslip, glass beads sprinkled on top in step 8 below will sometimes float and not actually contact the cells. Be careful not to allow cells to dry out by proceeding through the following steps promptly.*
7. Add the 4 µl solution to the top of the cells.
 8. Sprinkle glass beads onto the cells by gently tapping the homemade beadloader against the chamber.

Tips:

- a. *The beadloader helps to sprinkle the beads in a uniform fashion, so that it is easy to obtain a monolayer across the entire coverslip. However, this can be achieved without a beadloader by simply pipetting the beads using a 1,000-µl pipette tip and briefly shaking the*

tip over the cells to sprinkle the beads on top. While this method works, sometimes the beads will fall in clumps on the cells, which tends to cause the cells to peel more readily.

- b. *The easiest cells to beadload are adherent, such as U-2 OS, HeLa, RPE1, or fibroblast cells. Other cells that easily detach (for example, HEK293 cells) are more difficult to beadload because they tend to peel. In this case, we recommend polylysine to facilitate adherence to coverslips and prevent peeling after beadloading.*
- c. *If the cells are too confluent, they can peel in one massive layer after beadloading. The ideal confluence is 70-90%.*
9. Remove the beadloader.
10. Tap the chamber against the hood bench 5-12 times.
Note: This action causes the glass beads to roll over and bang against the cells. Similar to the action of electroporation, the rolling beads induce tiny tears in the cell membranes. Purified protein/DNA pipetted on top of the cells can then diffuse through these tiny tears (whilst the beads are much too large to enter). Although these tears do physically damage cells, we find the the cells recover pretty quickly. In our experience, in 2-3 h, cells are fine, display no stress granules, and are ready for imaging.
11. Tip the chamber at a 45° angle.
12. Pour the Opti-MEM + FBS medium that was removed in step 5 back onto the cells.
Tip: When pouring medium back onto cells, be careful not to disturb the cells too much. We recommend pouring the medium into the corner of the MatTek chamber and allow it to gently wash over the coverslip. By tipping the chamber, this step also helps the beads to float off to the edge, where they can easily be removed using a pipette or aspirator.
13. Incubate at 37°C, 5% CO₂ for 1 h.
14. During the incubation time, warm phenol-free (white) DMEM +/- media to 37°C.

G. Staining Halo-MCP with Janelia Fluor 646 HaloTag ligands (JF646-Halo ligand)

1. Dissolve the JF646-Halo ligand to a concentration of 10 mM in DMSO as the stock solution. Dilute the stock solution to a concentration of 0.2 mM in DMSO as the working stock.
 - a. Store at -20°C.
 - b. Make aliquots of 10-15 µl to avoid excessive freeze-thaw cycles.
2. Remove an aliquot of JF646-Halo ligand from -20°C.
3. Bring the JF646-Halo ligand and warmed white DMEM (+/-) medium into the hood.
4. Prepare a 1:1,000 dilution of the JF646-Halo ligand in white DMEM (+) medium.
 - a. The final volume of the dilution should be sufficient to cover the surface of the cells.
 - b. For 35-mm MatTek chambers, 500 µl is sufficient.
5. Remove cells from the incubator and bring them into the hood.
6. Tilt the chamber at a 45° angle.
7. Remove all medium.
8. Wash cells gently with white DMEM (-) until most of the beads have been removed.

9. Add the JF646-Halo ligand dilution to the top of the cells.
10. Incubate at 37°C, 5% CO₂ for 20 min.
11. Wash cells twice with white DMEM (-) medium.
12. Add 2 ml white DMEM (+) to the cells.
13. Cells can be imaged immediately after washing.
14. Keep cells at 37°C, 5% CO₂ until ready to image.

H. Imaging [Video 1 - Example of a 3-color movie]

Note: Imaging can be performed on any microscope equipped with ~488, ~563, and ~647 nm lasers, appropriate filters, a stage-top incubator, and sensitive EMCCD or sCMOS cameras. We recommend using a HILO microscope (Tokunaga et al., 2008), a light-sheet microscope, or a confocal microscope to reduce the background signal. TIRF microscopy can be used to examine translation sites near the coverslip. Widefield can also be used, but signal-to-noise for single RNA translation sites will be somewhat diminished because there is no sectioning.

Tip: Autofluorescence can look like translating spots because it fluoresces over a wide range of wavelengths and therefore appears in multiple channels simultaneously. Thus, it is important to add puromycin to confirm that the spots are translation sites.

1. Place cells onto a stage-top incubator (37°C, 5% CO₂)
2. Add puromycin to test for active translation
 - a. Set up your imaging experiment to capture the entire cell with a 1-min interval between each volume capture for 15 total timepoints.

Notes:

- i. The interval between each volume capture can be decreased to more precisely measure the dynamics of translation shut-off in a single cell.
- ii. Volume indicates the z-stacks needed to image the entire cell from top to bottom. For our purpose, we image 13 z-stacks, where each stack is 0.5 μm. The stack number and size can be adjusted to fit specific needs.
- b. Acquire five timepoints.
- c. After the first five timepoints, add puromycin at a final concentration of 50-100 μg/ml directly to the top of cells.

Note: Avoid touching the chamber directly, as this could move the chamber and change your imaging field.

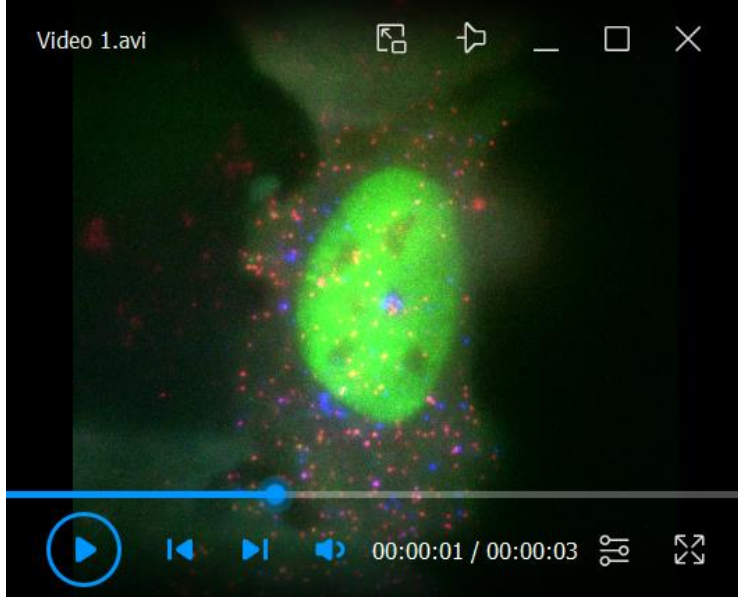
- d. Continue imaging cells for 10 min (10 frames). If translation sites are real, they will disappear quickly, typically within a minute or two.

Note: As an initial test for cell stressors and Harringtonine-induced ribosomal run-off assays, we recommend conducting imaging experiments with a larger interval (3-5 min) for several hours. After determining the time of response, intervals and imaging time can be adjusted accordingly. The following describes the imaging conditions in U-2 OS cells that we found fruitful for stressors and Harringtonine experiments.

3. Add Harringtonine to test for ribosomal run-off times
 - a. Set up your imaging experiment to capture the entire cell with a 1-min interval between each volume capture for 50 total timepoints.
 - b. Acquire five timepoints.
 - c. After the first five timepoints, add Harringtonine at a final concentration of 3-5 µg/ml directly to the top of cells.

Note: Avoid touching the chamber directly, as this could move the chamber and change your imaging field.
 - d. Continue imaging cells for the remaining 45 frames (45 min).
4. Adding stressors such as sodium arsenite (NaAs) and dithiothreitol (DTT)
 - a. Set up your imaging experiment to capture the entire cell with intervals of 3 min for NaAs and 2 min for DTT between each volume capture for 35 total timepoints.
 - b. Acquire five timepoints.
 - c. After the first five timepoints, add NaAs or DTT at a final concentration of 0.5 mM or 0.75 mM, respectively.

Note: Avoid touching the chamber directly, as this could move the chamber and change your imaging field.
 - d. Continue imaging cells for the remaining 30 frames.



Video 1. Representative movie of a cell after the image pre-processing step (Step I1). The movie was acquired at one frame per 6 s. The field of view is 512 pixels × 512 pixels = 66.56 µm × 66.56 µm.

- I. Data analysis (Figure 3)
 1. Preprocessing movies (Video 1)
 - a. Create maximum intensity projection through z.

- b. Subtract the background intensity from each channel.

Note: Background levels were determined by measuring the inherent noise of the cameras used. This can be achieved by taking images with the camera shutters closed and then calculating the average pixel intensity of those images.

- c. Make a mask that contains the entire cell. This masking step will avoid including any molecules from adjacent cells.
- d. Create a running average projection over time (using a few frames). This is necessary if the signal-to-noise ratio is poor.

Note: We use the ImageJ software for Steps 1a-1b and Mathematica for Steps 1c-1d.

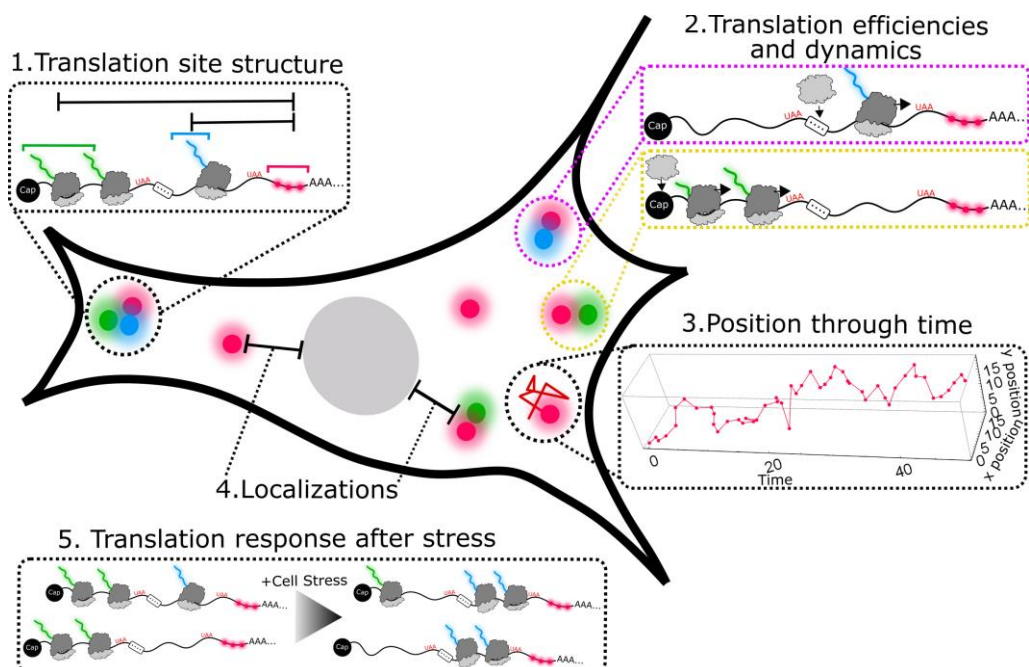


Figure 3. Schematic illustration of example biophysical parameters that analysis of the acquired data can provide

2. Track mRNAs. Any single-molecule tracking package can be used. We recommend TrackMate for its ease of use (Tinevez et al., 2017). We also have custom Mathematica code available on Github at:

https://github.com/Colorado-State-University-Stasevich-Lab/mRNA_Tracking_BioProtocol

- a. Detect mRNA molecules in each time frame.
 - i. Apply a difference-of-Gaussian filter to enhance the signals of single molecules.
 - ii. Set a threshold to binarize the image such that all mRNAs are recognized.
 - iii. Detect objects and their intensity centroids.
 - iv. Filter objects out that are either too large or too small. This will exclude aggregations and noise, respectively.
 - v. If analyzing Harringtonine or stress experiments, skip to Step 15.
- b. Link detected mRNAs over time.

- i. A nearest-neighbor tracking algorithm can be used. We allow a maximum mRNA jump size of 5 pixels (650 nm) between subsequent frames (assuming <10 sec intervals).
 - ii. Hand-curate tracks to merge tracks that are split accidentally because of dimmer mRNA signals for a few frames and/or to omit tracks that are indistinguishable among other mRNAs due to dense environments.
3. Categorize mRNA into four different types of translation status (no translation, translation of ORF 1, translation of ORF 2, and translation of ORF 1 and ORF 2 simultaneously).
 - a. Make crops in all channels by centering around tracked mRNAs.

In the case that multiple cameras are used, a correction factor must be applied to adjust for potential camera misalignment. For this, a calculated transformation function is applied to other channels based on the centroid position of the tracked mRNA signals. The transformation function can be determined by imaging fixed beads that fluoresce in all channels simultaneously (for example, TetraSpeck Microspheres, 0.1 μ m, Thermo Fisher Scientific, T7279).
 - b. Average the cropped images for each track in all channels.
 - c. Detect signals in the other channels (*i.e.*, non-mRNA channels) and categorize into four groups based on the presence or absence of signals in the other channels.
 - d. Hand-curate the categorization. This is a check to ensure that the generated categorization was correct.
 - e. Use these results to analyze the population of different mRNAs within cells.
 4. Fit a 2D Gaussian to the cropped data; this will calculate intensities in all channels and super-resolve the localization of mRNAs.
 - a. Use these results to analyze ribosome density and mean square displacement.
 5. Stress and Harringtonine analysis
 - a. Use detected RNA molecules found in Step I2a.

Note: Linking tracks over time is not possible when using a large time interval between each frame. Since Harringtonine and stress-induced ribosomal run-offs can take tens of mins to an hour, we typically image infrequently (once per minute or longer) so individual translation sites cannot all be tracked (although there usually are a few that can be tracked by chance because they are relatively immobile). The analysis below therefore does not require the tracking of individual translation sites.
 - b. Make crops in all channels by centering around detected mRNA signals.
 - c. Detect signals in other channels and categorize into four groups based on the presence or absence of signals in the other (non-mRNA) channels.
 - d. Fit a 2D Gaussian to the cropped data; this will calculate the intensities in all channels.
 - e. Combine the translation site intensity data from all cells and all experiments.
 - f. Plot as intensity or translation site number over time.

Recipes

1. 1 M HEPES buffer

25 mM HEPES pH 7.9

12.5 mM MgCl₂

100 mM KCl

0.1 mM EDTA

0.01% NP40

10% glycerol

1 mM DTT

2. HisTrap buffer A

1× PBS pH 7.4

300 mM NaCl

0.2 mM AEBSF

5 mM b-mercaptoethanol

3. HisTrap buffer B

1× PBS pH 7.4

300 mM NaCl

500 mM immidazole

0.2 mM AEBSF

5 mM b-mercaptoethanol

4. Superdex buffer

25 mM HEPES pH 7.9

12.5 mM MgCl₂

100 mM KCl

0.1 mM EDTA

0.01% NP40

10% glycerol

1 mM DTT

5. DMEM (+) media (for phenol-free as well)

To 500 ml DMEM, add 50 ml FBS, 5 ml Pen/strep, 5 ml L-Glu

Acknowledgments

We sincerely thank Dr. Hataichanok (Mam) Scherman for the protocol to purify Halo-MCP and anti-SunTag scFv-GFP. We thank Dr. Luke Lavis for kindly providing the JF646-labeled HaloTag ligand. We thank all members of the Stasevich lab for their support and helpful discussion. TJS, ALK, and TM were supported by the NIH (grant no. R35GM119728). TJS was also supported by the NSF (grant no. MCB-1845761). This protocol was derived from the work published in Koch *et al.* (2020).

The beadloading protocol was first described in Hayashi-Takanaka *et al.* (2011) and the single-molecule translation imaging assay was first described in Morisaki *et al.* (2016).

Competing interests

The authors declare no competing interests.

Ethics

No human and/or animal subjects are used in this protocol.

References

1. Boersma, S., Khuperkar, D., Verhagen, B. M. P., Sonneveld, S., Grimm, J. B., Lavis, L. D. and Tanenbaum, M. E. (2019). [Multi-Color Single-Molecule Imaging Uncovers Extensive Heterogeneity in mRNA Decoding](#). *Cell* 178: 458-472.e19.
2. Bornes Stéphanie, Prado-Lourenco Leonel, Bastide Amandine, Zanibellato Catherine, Iacovoni Jason S., Lacazette Eric, Prats Anne-Catherine, Touriol Christian, and Prats Hervé (2007). [Translational Induction of VEGF Internal Ribosome Entry Site Elements During the Early Response to Ischemic Stress](#). *Circ Res* 100: 305-308.
3. Cialek, C. A., Koch, A. L., Galindo, G., and Stasevich, T. J. (2020). [Lighting up single-mRNA translation dynamics in living cells](#). *Curr Opin Genet Dev* 61: 75-82.
4. Cialek, C. A., Galindo, G., Koch, A. L., Saxton, M. N. and Stasevich, T. J. (2021). [Bead Loading Proteins and Nucleic Acids into Adherent Human Cells](#). *J Vis Exp* e62559.
5. Coulon, A., Chow, C. C., Singer, R. H., and Larson, D. R. (2013). [Eukaryotic transcriptional dynamics: from single molecules to cell populations](#). *Nat Rev Genet* 14(8): 572-584.
6. Firth, A. E. and Brierley, I. (2012). [Non-canonical translation in RNA viruses](#). *J Gen Viro* 93: 1385-1409.
7. Hayashi-Takanaka, Y., Stasevich, T.J., Kurumizaka, H., Nozaki, N. and Kimura, H. (2014). [Evaluation of chemical fluorescent dyes as a protein conjugation partner for live cell imaging](#). *PloS One* 9: e106271.
8. Hayashi-Takanaka, Y., Yamagata, K., Wakayama, T., Stasevich, T.J., Kainuma, T., Tsurimoto, T., Tachibana, M., Shinkai, Y., Kurumizaka, H., Nozaki, N., *et al.* (2011). [Tracking epigenetic histone modifications in single cells using Fab-based live endogenous modification labeling](#). *Nucleic Acids Res* 39(15): 6475-6488.
9. Koch, A., Aguilera, L., Morisaki, T., Munsky, B. and Stasevich, T. J. (2020). [Quantifying the dynamics of IRES and cap translation with single-molecule resolution in live cells](#). *Nat Struct Mol Biol* 27: 1095-1104.
10. McNeil, P. L., and Warder, E. (1987). [Glass beads load macromolecules into living cells](#). *J Cell*

Sci 88 (Pt 5): 669-678.

11. Morisaki, T. and Stasevich, T. J. (2018). [Quantifying Single mRNA Translation Kinetics in Living Cells](#). *Cold Spring Harb Perspect Biol* 10(11): a032078.
12. Morisaki, T., Lyon, K., DeLuca, K. F., DeLuca, J. G., English, B. P., Zhang, Z., Lavis, L.D., Grimm, J. B., Viswanathan, S., Looger, L. L., et al. (2016). [Real-time quantification of single RNA translation dynamics in living cells](#). *Science* 352(6292): 1425-1429.
13. Pichon, X., Bastide, A., Safieddine, A., Chouaib, R., Samacoits, A., Basyuk, E., Peter, M., Mueller, F. and Bertrand, E. (2016). [Visualization of single endogenous polysomes reveals the dynamics of translation in live human cells](#). *J Cell Biol* 214(6): 769-781.
14. Pichon, X., Robert, M.-C., Bertrand, E., Singer, R.H., and Tutucci, E. (2020). [New Generations of MS2 Variants and MCP Fusions to Detect Single mRNAs in Living Eukaryotic Cells](#). *Methods Mol Biol* 2166: 121-144.
15. Tanenbaum, M. E., Gilbert, L. A., Qi, L. S., Weissman, J. S. and Vale, R. D. (2014). [A Protein-Tagging System for Signal Amplification in Gene Expression and Fluorescence Imaging](#). *Cell* 159(3): 635-646.
16. Tinevez, J. Y., Perry, N., Schindelin, J., Hoopes, G. M., Reynolds, G. D., Laplantine, E., Bednarek, S. Y., Shorte, S. L. and Eliceiri, K. W. (2017). [TrackMate: An open and extensible platform for single-particle tracking](#). *Methods* 115: 80-90.
17. Tokunaga, M., Imamoto, N., and Sakata-Sogawa, K. (2008). [Highly inclined thin illumination enables clear single-molecule imaging in cells](#). *Nat Methods* 5: 159-161.
18. Wang, C., Han, B., Zhou, R. and Zhuang, X. (2016). [Real-Time Imaging of Translation on Single mRNA Transcripts in Live Cells](#). *Cell* 165(4): 990-1001.
19. Wu, B., Eliscovich, C., Yoon, Y. J. and Singer, R. H. (2016). [Translation dynamics of single mRNAs in live cells and neurons](#). *Science* 352(6292): 1430-1435.
20. Yan, X., Hoek, T. A., Vale, R. D. and Tanenbaum, M. E. (2016). [Dynamics of Translation of Single mRNA Molecules In Vivo](#). *Cell* 165(4): 976-989.
21. Zhao, N., Kamijo, K., Fox, P. D., Oda, H., Morisaki, T., Sato, Y., Kimura, H. and Stasevich, T. J. (2019). [A genetically encoded probe for imaging nascent and mature HA-tagged proteins in vivo](#). *Nat Commun* 10(1): 2947.

Monitoring Changes in the Oxidizing Milieu in the Endoplasmic Reticulum of Mammalian Cells Using HyPerER

Julia Birk¹, Beata Lizak², Christian Appenzeller-Herzog^{1,3} and Alex Odermatt^{1,*}

¹Division of Molecular and Systems Toxicology, Department of Pharmaceutical Sciences, University of Basel, Basel, Switzerland; ²Department of Molecular Biology, Semmelweis University, Budapest, Hungary; ³University Medical Library, University of Basel, Basel, Switzerland

*For correspondence: alex.odermatt@unibas.ch

[Abstract] The production of reactive oxygen species (ROS) and endoplasmic reticulum (ER) stress are tightly linked. The generation of ROS can be both the cause and a consequence of ER stress pathways, and an increasing number of human diseases are characterized by tissue atrophy in response to ER stress and oxidative injury. For the assessment of modulators of ER luminal ROS generation and for mechanistic studies, methods to monitor changes in ER reduction-oxidation (redox) states in a time-resolved and organelle-specific manner are needed. This has been greatly facilitated by the development of genetically encoded fluorescent probes, which can be targeted to different subcellular locations by specific amino acid extensions. One of these probes is the yellow fluorescent protein-based redox biosensor, HyPer. Here, we provide a protocol for the time-resolved monitoring of the oxidizing milieu in the ER of adherent mammalian cells using the ratiometric sensor, HyPerER, which is specifically targeted to the ER lumen.

Keywords: Endoplasmic reticulum, Hydrogen peroxide, HyPer, Redox, Oxidative stress, Fluorescence microscopy

[Background] The endoplasmic reticulum (ER) plays key roles in essential functions including protein folding and maturation in the secretory pathway, lipid metabolism, hormone synthesis, and detoxification of reactive metabolites (Bock and Kohle, 2009; Chen and Cubillos-Ruiz, 2020; Erdbrugger and Frohlich, 2020; Morishita and Arvan, 2020). Research on the ER has attracted increasing interest in recent years, mainly due to the discovery of the unfolded protein response (UPR) signaling pathway, which is triggered by diverse forms of protein folding stress in the ER. The physical contact sites of the ER with other cell organelles and their involvement in cellular communication networks establish the ER as a multifaceted regulator of cell signaling. The relationship between ER stress and oxidative injury has been extensively investigated; however, the origin of ER stress-induced ROS production remains unclear (Appenzeller-Herzog, 2011), and tools to detect xenobiotics that enhance ROS in the ER are limited.

To understand the mechanisms of oxidative insults, specific tools are required to quantitate and describe ER redox conditions. Genetically encoded sensors to quantitate the oxidative status of the many redox couples present in the ER have proven useful. Changes in the amount of H₂O₂ in the cytoplasm can be monitored using the fluorescent probe, HyPer (Belousov *et al.*, 2006). The HyPer sensor was constructed by inserting a circularly permuted yellow fluorescent protein (YFP) into the

regulatory domain of the bacterial H₂O₂-sensing protein, OxyR. Importantly, HyPer was shown to selectively detect H₂O₂ over superoxide, peroxinitrite, nitric oxide, and oxidized glutathione in the cytosol. Upon oxidation of the cysteine corresponding to Cys199 of OxyR, the sensor protein HyPer undergoes a conformational change. HyPer has two excitation peaks at 420 nm and 500 nm, and one emission peak at 516 nm. Upon transition from the reduced to the oxidized state, the peak at 420 nm decreases and the peak at 500 nm increases, thus allowing ratiometric measurement of H₂O₂.

Here, we describe a detailed protocol for the real-time imaging and monitoring of the oxidizing milieu in the ER using the HyPerER sensor, which is targeted specifically to the ER lumen (Enyedi *et al.*, 2010; Malinowski *et al.*, 2011) by the addition of an N-terminal ER-targeting sequence and a C-terminal ER-retrieval signal (KDEL). It must be noted that the ER-targeted HyPerER, unlike cytosolic HyPer, is not specific for H₂O₂ but rather reflects the oxidative milieu within the ER (Mehmeti *et al.*, 2012). The approach can be used in different cellular systems with basic understanding of live cell imaging and fluorescence microscopy (an example is shown in Figure 1), whereby data analysis is dependent on the available software. A limitation of the original HyPer sensors is their sensitivity to pH changes. To overcome this limitation, a very recent study introduced a new generation HyPer probe, HyPer7, which is pH-resistant yet remains ultra-sensitive to changes in H₂O₂ (Pak *et al.*, 2020). Monitoring H₂O₂ specifically in the ER remains challenging, and most of the probes available to date have not been used in this very special cellular compartment.

Materials and Reagents

A. Materials

1. Pipette tips
2. Glass-bottomed dishes (such as MatTek, catalog number: P35G-1.5-20-C; IBIDI μ-Dish 35 mm, high Glass Bottom, catalog number: 81158; Sarstedt lumox dish 35, catalog number: 94.6077.331; Nunc Glass Bottom Dishes, catalog number: 150680)
3. 1.5-ml tubes
4. 50-ml conical centrifugation tubes

B. Reagents

1. HeLa cells (ATCC, catalog number: CCL-2)
2. Dulbecco's Modified Eagle's Medium (DMEM) – high glucose (Sigma-Aldrich, catalog number: D5796)
3. Fetal bovine serum, FBS (South America) (Biowest, catalog number: S1810)
4. Penicillin/streptomycin 100× (BioConcept-Amimed, catalog number: 4-01F00-H)
5. Trypsin-EDTA solution 10× (Sigma-Aldrich, catalog number: T4174-100ML)
6. OptiMEM-I (Gibco, catalog number: 51985026)
7. FuGENE HD (Promega, catalog number: E2311)
8. HEPES (PanReac AppliChem, catalog number: A1069)

9. $\text{CaCl}_2 \cdot 2\text{H}_2\text{O}$ (Merck, catalog number: 1.02382.0500)
10. KCl (Merck, catalog number: 1.04936.1000)
11. $\text{MgCl}_2 \cdot 6\text{H}_2\text{O}$ (Fluka, catalog number: 63064)
12. NaCl (PanReac AppliChem, catalog number: A2942)
13. DTT (PanReac AppliChem, catalog number: A1101)
14. H_2O_2 solution (Sigma-Aldrich, catalog number: 95321)
15. pCMV/myc/ER/GFP HyPerER (Enyedi et al., 2010) (Kind gift from Dr. Miklos Geiszt, Semmelweis University, Budapest, Hungary)
16. Stimulants and inhibitors (experiment-dependent), e.g., thapsigargin (EMD Millipore, catalog number: 586005)
17. HEPES Imaging Buffer (1 L) (see Recipes)

Equipment

1. Pipettes
2. Casy cell counter (Omni Life Science) or hemocytometer
3. Heat block for 50-ml conical tubes
4. Inverted microscope; we use an Olympus Fluoview3000 laser scanning microscope
5. 60 \times Objective UPLSAPO60XS2 Universal Plan Super Apochromat silicone immersion objective N.A. 1.3 (N5203000)
6. For excitation, we use an Olympus FVL-LAS405-LX50 Laser 405 nm and FVL-LAS488-LS20 Laser 488 nm (somewhat below the excitation peaks at 420 nm and 500 nm, respectively)
Note: Monitoring of HyPer probes does not require confocality! A fluorescence microscope with suitable filter sets for excitation and emission is sufficient.
Excitation maximum of HyPer: 500 nm
Emission maximum of HyPer: 516 nm
7. Climate control unit; we use the Olympus CellVivo incubator system for IX83 (E0439957)
Note: Live cell experiments should be performed under optimal environmental conditions; the minimal requirement is a temperature controller to maintain the optimal temperature of 37°C; for long-term experiments, e.g., longer than 30 min, an additional CO₂ supply will be needed.

Software

1. FV300 (Olympus)
2. Excel (Microsoft)

Procedure

A. Cell culture and seeding

Cells should be cultured in their corresponding growth medium until they reach a confluence of around 70%.

1. Wash the cells with 10 ml 1× PBS.
2. Detach the cells with 2 ml pre-warmed (37°C) 1× trypsin (0.5 g/L) at room temperature for 4 min and resuspend in 8 ml complete growth medium.
3. Determine the number of cells in the suspension using a Casy cell counter or hemocytometer.
4. Seed 30,000 cells in 400 µl complete growth medium to the center well of a Matek glass-bottomed dish.

Cell density may depend on the cell type and transfection method used.

5. Place the dish in a humidified cell culture incubator (37°C, 5% CO₂) and incubate overnight.

B. Transfection

1. Mix 25 µl Opti-MEM medium with 0.5 µg HyPerER plasmid and 1.5 µl Fugene® HD solution (according to the manufacturer's protocol).
2. Incubate the mixture for 15 min at room temperature and add dropwise to the cells.
3. Add 2.6 ml complete growth medium approximately 6 h after transfection.
4. Incubate the cells at 37°C for 24-48 h.

Note: The optimal transfection conditions, e.g., cell density, DNA amount, and DNA:Fugene® HD ratio, will require optimization depending on the cell line of choice.

C. Imaging

Imaging is performed on an Olympus Fluoview 3000 laser-scanning microscope with a temperature- and CO₂-controlling unit. Samples are excited sequentially using the 405 nm and 488 nm lasers. Emission is recorded in a window from 500 to 600 nm.

Note: There is only one emission window for both excitation wavelengths!

1. Take out the cell culture dish from the incubator and remove culture medium with a pipette.
2. Carefully wash the dish twice with 1 ml pre-warmed HEPES Imaging Buffer.
3. Add 1 ml HEPES Imaging Buffer and place the dish on the microscope stage.
4. Search for a field of view that contains several healthy-looking cells with sufficient YFP fluorescence signal.
5. Optimize the voltage of the photomultiplier tube to obtain good image quality (signal-to-noise) for both channels.
6. Measure the baseline oxidative status of HyPerER in the cells every 20 s for at least 5 min, then carefully add stimulating substances, such as thapsigargin (final concentration 1 µM), at double working concentration in 1 ml HEPES Imaging Buffer with a pipette and record until the signal stabilizes (or according to the stimulation protocol). Make sure to complete the addition within the 20-s time window between two image acquisitions. The speed of the acquisition and the total imaging time should be optimized to achieve proper temporal resolution but also to avoid photobleaching.

Conclude each measurement by the addition of a single dose of saturating H₂O₂ (100 μM final concentration in 1 ml HEPES Imaging Buffer) as a positive control, carefully applied with a pipette. An example in HeLa cells is shown in Figure 1.

Data analysis

Analysis using the FV3000 software:

1. Define the regions of interest (ROI) in your sample and select a suitable area to place a background ROI.
2. Measure the raw emission intensity within these ROIs.
3. Export the raw intensity values from the software as .csv files.
4. Open the .csv files in Microsoft Excel. You will obtain two emission intensity values, determined at 516 nm, for each time point measured for every ROI, one for excitation at 488 nm and one for excitation at 405 nm. Perform the following calculation:
Subtract the intensity values of the background ROI obtained at 405-nm excitation from the target ROI measured at 405 nm.
Subtract the intensity values of the background ROI obtained at 488-nm excitation from the target ROI measured at 488 nm.

Calculate the fluorescence ratio using the following formula (for an example, see Figure 1):

$$\text{Ratio} = \frac{\text{Fluorescence Intensity}_{488\text{ nm}} - \text{Background}_{488\text{ nm}}}{\text{Fluorescence Intensity}_{405\text{ nm}} - \text{Background}_{405\text{ nm}}}$$

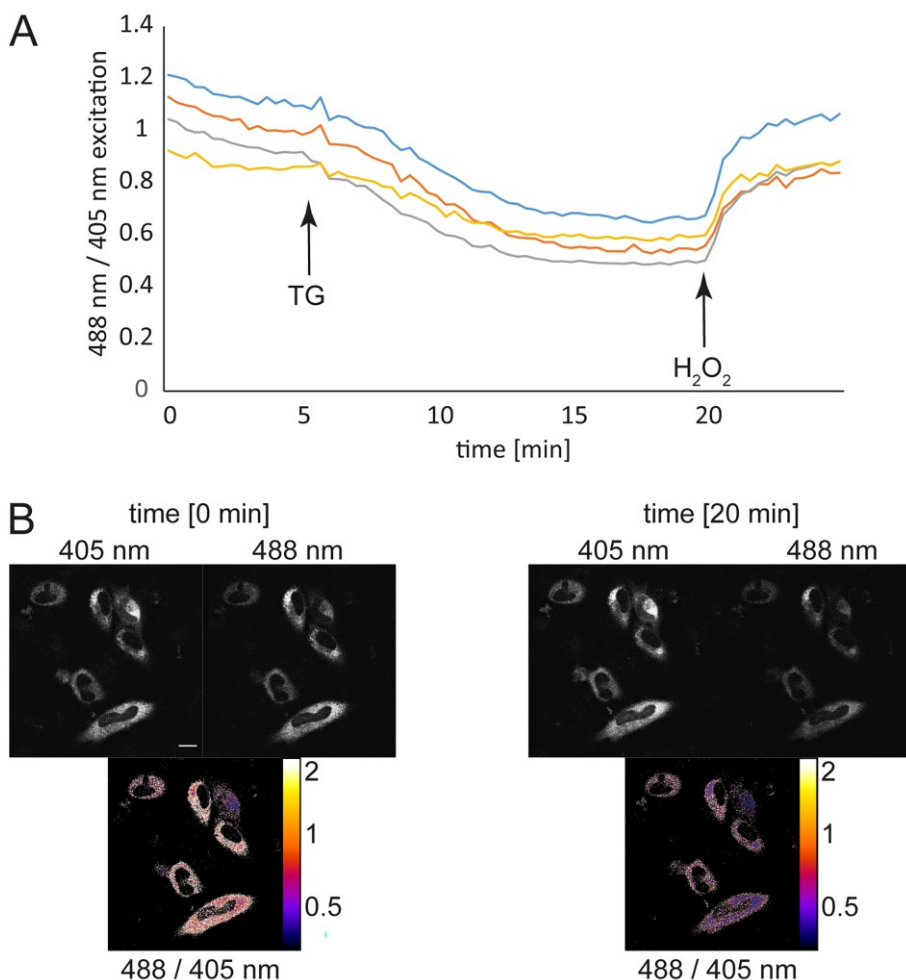


Figure 1. Real-time monitoring of ER redox changes. HeLa cells were transfected with the HyPerER sensor using Fugene® HD. At 48 h post-transfection, the cells were prepared for imaging. Fluorescence ratio changes were monitored over time. A. Each trace corresponds to the data recorded from one cell. The cells were treated with 1 μ M thapsigargin (TG), which reduces the ER environment by facilitating the influx of reduced glutathione (Lizak *et al.*, 2020), followed by the application of 100 μ M H_2O_2 , which leads to re-oxidation. B. Exemplary fluorescence pictures in the 405-nm or 488-nm channel and the corresponding ratiometric images. Scale bar = 10 μ m. The pseudocolored images represent the ratio R, obtained by dividing the values measured at 488-nm excitation and 516-nm emission after background subtraction by the values measured at 405-nm excitation and 516-nm emission. A darker color indicates a lower ratio and hence less H_2O_2 ; a lighter color represents a higher ratio and hence more H_2O_2 .

Recipes

1. HEPES Imaging Buffer (1 L)
1 M HEPES solution (sterile-filtered) 20 ml; final concentration 20 mM

1 M KCl solution (sterile-filtered) 5 ml; final concentration 5 mM
1 M CaCl₂ solution (sterile-filtered) 1.8 ml; final concentration 1.8 mM
1 M MgCl₂ solution (sterile-filtered) 1 ml; final concentration 1 mM
1 M NaCl solution (sterile-filtered) 130 ml; final concentration 130 mM
Fill to 1 L with ddH₂O and adjust pH to 7.4

Acknowledgments

This protocol was adapted from Lizak *et al.* (2020). Funding by the Swiss National Science Foundation (SNSF, 31003A-179400) and the University of Basel is gratefully acknowledged.

Competing interests

The authors declare that this research was conducted in the absence of any commercial or financial relationships that could be construed as a potential conflict of interest.

References

1. Appenzeller-Herzog, C. (2011). [Glutathione- and non-glutathione-based oxidant control in the endoplasmic reticulum](#). *J Cell Sci* 124(Pt 6): 847-855.
2. Belousov, V. V., Fradkov, A. F., Lukyanov, K. A., Staroverov, D. B., Shakhbazov, K. S., Terskikh, A. V. and Lukyanov, S. (2006). [Genetically encoded fluorescent indicator for intracellular hydrogen peroxide](#). *Nat Methods* 3(4): 281-286.
3. Bock, K. W. and Kohle, C. (2009). [Topological aspects of oligomeric UDP-glucuronosyltransferases in endoplasmic reticulum membranes: advances and open questions](#). *Biochem Pharmacol* 77(9): 1458-1465.
4. Chen, X. and Cubillos-Ruiz, J. R. (2021). [Endoplasmic reticulum stress signals in the tumour and its microenvironment](#). *Nat Rev Cancer* 21(2): 71-88.
5. Enyedi, B., Varnai, P. and Geiszt, M. (2010). [Redox state of the endoplasmic reticulum is controlled by Ero1L-alpha and intraluminal calcium](#). *Antioxid Redox Signal* 13(6): 721-729.
6. Erdbrugger, P. and Frohlich, F. (2020). [The role of very long chain fatty acids in yeast physiology and human diseases](#). *Biol Chem* 402(1): 25-38.
7. Lizak, B., Birk, J., Zana, M., Kosztyi, G., Kratschmar, D. V., Odermatt, A., Zimmermann, R., Geiszt, M., Appenzeller-Herzog, C. and Banhegyi, G. (2020). [Ca²⁺ mobilization-dependent reduction of the endoplasmic reticulum lumen is due to influx of cytosolic glutathione](#). *BMC Biol* 18(1): 19.
8. Malinowski, M., Zhou, Y., Belousov, V. V., Hatfield, D. L. and Gladyshev, V. N. (2011). [Hydrogen peroxide probes directed to different cellular compartments](#). *PLoS One* 6(1): e14564.

9. Mehmeti, I., Lortz, S. and Lenzen, S. (2012). [The H₂O₂-sensitive HyPer protein targeted to the endoplasmic reticulum as a mirror of the oxidizing thiol-disulfide milieu](#). *Free Radic Biol Med* 53(7): 1451-1458.
10. Morishita, Y. and Arvan, P. (2020). [Lessons from animal models of endocrine disorders caused by defects of protein folding in the secretory pathway](#). *Mol Cell Endocrinol* 499: 110613.
11. Pak, V. V., Ezerina, D., Lyublinskaya, O. G., Pedre, B., Tyurin-Kuzmin, P. A., Mishina, N. M., Thauvin, M., Young, D., Wahni, K., Martinez Gache, S. A., Demidovich, A. D., Ermakova, Y. G., Maslova, Y. D., Shokhina, A. G., Eroglu, E., Bilan, D. S., Bogeski, I., Michel, T., Vriz, S., Messens, J. and Belousov, V. V. (2020). [Ultrasensitive Genetically Encoded Indicator for Hydrogen Peroxide Identifies Roles for the Oxidant in Cell Migration and Mitochondrial Function](#). *Cell Metab* 31(3): 642-653 e646.

Building a Total Internal Reflection Microscope (TIRF) with Active Stabilization (Feedback SMLM)

Simao Coelho^{1, 2, 3, #, *}, Jongho Baek^{1, 2, \$, #}, J. Justin Gooding^{4, 5} and Katharina Gaus^{1, 2, *}

¹EMBL Australia Node in Single Molecule Science, School of Medical Sciences, University of New South Wales, Sydney, Australia; ²ARC Centre of Excellence in Advanced Molecular Imaging, University of New South Wales, Sydney, Australia; ³Structural Biology Program, Memorial Sloan Kettering Cancer Center, New York, USA; ⁴School of Chemistry and Australian Centre of NanoMedicine, University of New South Wales, Sydney, Australia; ⁵ARC Centre of Excellence in Convergent Bio-Nano Science and Technology, University of New South Wales, Sydney, Australia; ^{\$}Current address: NetTargets, National Nanofab Center, KAIST, Daejeon, Republic of Korea

*For correspondence: k.gaus@unsw.edu.au; s.pereiracoelho@unsw.edu.au

#Contributed equally to this work

[Abstract] The data quality of high-resolution imaging can be markedly improved with active stabilization, which is based on feedback loops within the microscope that maintain the sample in the same location throughout the experiment. The purpose is to provide a highly accurate focus lock, therefore eliminating drift and improving localization precision. Here, we describe a step-by-step protocol for building a total internal reflection microscope combined with the feedback loops necessary for sample and detection stabilization, which we routinely use in single-molecule localization microscopy (SMLM). The performance of the final microscope with feedback loops, called feedback SMLM, has previously been described. We demonstrate how to build a replica of our system and include a list of the necessary optical components, tips, and an alignment strategy.

Keywords: TIRF microscopy, Drift correction, Active stabilization, Single-molecule imaging, Localization microscopy, Biophysics

[Background] Optical microscopy is routinely used to image the spatial and temporal coordinates of individual molecules. Of the many different techniques, total internal reflection fluorescence (TIRF) microscopy is extensively used to image cells seeded onto glass coverslips. Excitation under TIRF is achieved by adjusting the laser incidence angle to a value greater than the critical angle (Axelrod, 2001; Fish, 2009). This creates an evanescent field in the specimen medium immediately adjacent to the glass-water interface, restricting the depth of the illumination to ~200 nm. As only the contact area between the glass and the cell is imaged, TIRF has an excellent signal-to-noise ratio; however, mechanical movement of the sample in 3D reduces the precision of experiments. For conditions of low-photon emission, such as single-molecule imaging, drift reduces the localization precision and therefore decreases the overall quality of the data. Here, we provide a step-by-step protocol showing how to build the feedback SMLM (Coelho *et al.*, 2020a), thereby facilitating user development and/or integration. The protocol incorporates a TIRF microscope and active stabilization to eliminate drift (Coelho *et al.*, 2020b).

Active stabilization is compatible with multiple types of single-molecule acquisition methods, including TIRF (Fish, 2009; Kim *et al.*, 2020), highly inclined and laminated optical sheets (Tokunaga *et al.*, 2008), stochastic optical reconstruction microscopy (STORM), photo-activated localization microscopy (PALM), DNA points accumulation in nanoscale topography (DNA-PAINT), in 3D (*e.g.*, 3D-STORM (Huang *et al.*, 2008), double-helix-PSF (Pavani *et al.*, 2009), saddle-point PSF (Shechtman *et al.*, 2014), 4-PI (Shtengel *et al.*, 2009), fixed- and live-cell imaging (Shroff *et al.*, 2008), waveguides (Diekmann *et al.*, 2017), light-sheet approaches (Gao *et al.*, 2014; Huang *et al.*, 2016; Baek *et al.*, 2017), fluorescence resonance energy transfer (Aoki *et al.*, 2009; Poland *et al.*, 2014 and 2015) and lifetime imaging (Krstajić *et al.*, 2013; Suhling *et al.*, 2015 and 2017), adaptive optics (Coelho *et al.*, 2013 and 2020c; Burke *et al.*, 2015), and point-detection schemes (Eggeling *et al.*, 2009). It can be further incorporated into high-content screening (Boutros *et al.*, 2015; Gustavsson *et al.*, 2018), multiplexed acquisitions (Jungmann *et al.*, 2014) and/or automatic acquisition, as well as non-fluorescence imaging methods that require focus-locking with high precision, such as atomic force microscopy (Giessibl *et al.*, 2003; Schmidt *et al.*, 2018).

Equipment

Illumination

1. White LED (Mightex, catalog number: BSLCS-4000-03-22)
2. Infrared LED (Mightex, catalog number: BLS-LCS-4000-03-22)
3. LED control box (Mightex, catalog number: BLS-SA02-US)
4. Lasers (Vortran Stradus, catalog numbers: 405-100 [405 nm]; 488-150 [488 nm]); 637-180 [637 nm])

Optical components

1. Bandpass filter (Semrock, catalog number: FF01-842/56-25)
2. Dichroic beamsplitter (Semrock, catalog number: FF801-Di02-25x36 and Chroma, catalog number: ZT488/640rpc)
3. Emission filter (Semrock, catalog number: Em01- R405/488/635-25)
4. Dichroic mirrors (Chroma, catalog number: ZT442rdc and ZT594rdc)
5. Aspheric condenser lens (Thorlabs, catalog number: ACL25416U-B)
6. Infrared achromatic doublets lens (Thorlabs, catalog number: AC254-200-B-ML)
7. Visible achromatic doublets lens (Thorlabs, catalog numbers: AC254-300-A-ML, AC254-200-A-ML, AC254-30-A-ML, AC254-50-A-ML)
8. Polarization-maintaining fiber (Thorlabs, catalog number: P3-405BPM-FC-2)
9. Elliptical mirror (Thorlabs, catalog number: BBE1-E03)
10. Oil-immersion objective, 100× Apo SR TIRF objective, numerical aperture (NA) = 1.49, working distance (WD) = 0.12 (Nikon)

Mechanical components

1. Fiber port (Thorlabs, catalog number: PAF2-A7A)
2. Optical post (Thorlabs, catalog numbers: TR75/M and TR50/M)
3. Optical post spacers (Thorlabs, catalog numbers: RS4/M, RS5/M and RS10/M)
4. Pedestal post holder (Thorlabs, catalog number: PH100E/M and PH50E/M)
5. Cage assembly rod (Thorlabs, catalog number: ER025 and ER4-P4)
6. Cage XY translator (Thorlabs, catalog number: CXY1)
7. Elliptical mirror mount (Thorlabs, catalog number: KCB1E/M)
8. Mirror mounts (Polaris-K25S4/M)
9. Piezoelectric mirror (Thorlabs, catalog number: Polaris-K1S3P)
10. Threaded standard cage plates (Thorlabs, catalog number: CP33/M)
11. Clamping forks (Thorlabs, catalog number: CF125C/M-P5)
12. M6 cap screw and hardware kit (Thorlabs, catalog number: HW-KIT2/M)
13. Cage alignment plate (Thorlabs, catalog number: CPA1)
14. Adapter C-Mount to SM1 (Thorlabs, catalog number: SM1A39 and SM1A9)
15. Lens tubes (Thorlabs, catalog number: SM1)
16. Actively stabilized optical table (Newport, catalog number: M-ST-46-8)
17. Smart table controller (Newport, catalog number: ST-300)
18. Microscope frame (Mad City Labs, catalog number: RM21-M)
19. Cage-compatible rectangular filter holder (Thorlabs, catalog number: FFM1)
20. Support bracket (Custom designed, CAD: <https://github.com/spcoelho/Active-Stabilization.git>)
21. Cage cube (Thorlabs, catalog number: C6W)
22. Blank cover plate (Thorlabs, catalog number: B1C/M)
23. Kinematic cage cube platform (Thorlabs, catalog number: B4C/M)
24. XYZ translation stage with standard micrometers (Thorlabs, catalog number: PT3/M)
25. Right-angle kinematic elliptical mirror mount (Thorlabs, catalog number: KCB1E/M)
26. Camera baseplate (Manta, 1/4-20 Tripod Adapter)
27. Translation stage (Newport, catalog number: M-423-MIC)
28. Threaded frosted glass alignment disk (Thorlabs, catalog number: DG10-1500-H1-MD)

Cameras

1. CMOS camera (Allied Vision, Manta Camera)
2. EMCCD (Andor, catalog number: 897)

Software

1. Active Stabilization Software and Custom Bracket: <https://github.com/spcoelho/Active-Stabilization.git>
2. NicoLase: <https://github.com/PRNicovich/NicoLase>

Resources

1. How to Align a Laser: <https://www.youtube.com/watch?v=qzxILY6nOmA&t=311s>
2. Coupling a Laser into a Fiber: <https://www.youtube.com/watch?v=kQvhbJbDG0M>
3. Collimating a Laser Beam: <https://www.youtube.com/watch?v=Z7Q17-ctQVQ>
4. TIRF Microscopy: <https://www.youtube.com/watch?v=egmJlaIDR48&t=1039s>

Procedure

A. TIRF Assembly

The TIRF microscope that we describe is built on a Mad City Labs RM21 body. This microscope frame is convenient as it allows for easy access to the optical components within the frame, facilitating alignment. The RM21 frame is particularly stable, and the rectangular geometry permits simple addition of support brackets.

1. The first step is to place the microscope body on the optical table. Figure 1 is a top-down view of a CAD design showing the location of the microscope frame in relation to the rest of the optical components. We suggest placing the body close to the center of the optical table. This then enables enclosing of the microscope in the final stages.

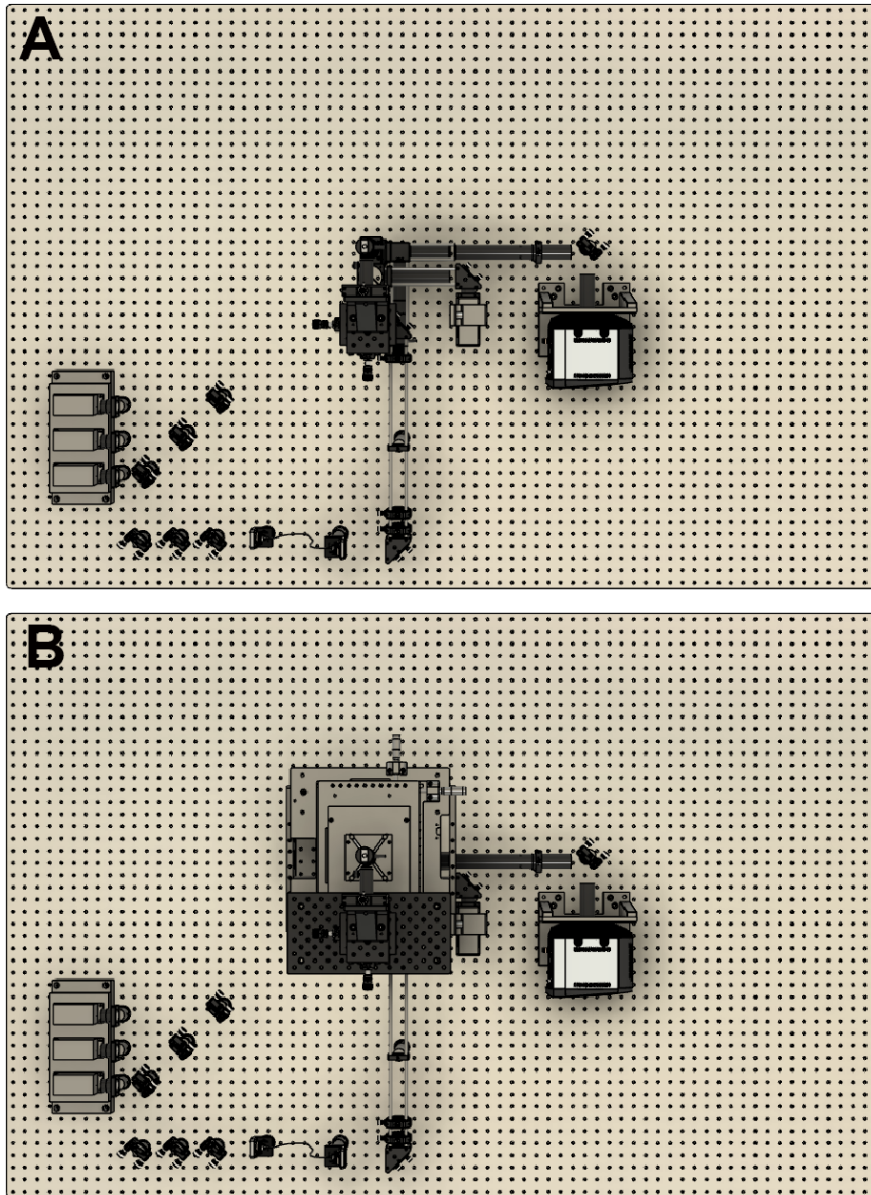


Figure 1. CAD design showing a top-down view of the optical assembly. A. Without the microscope frame. B. With the microscope frame.

2. Next, lasers are placed onto a heat sink at the appropriate height. Currently, we use Vortran lasers (detailed in the components section) that can be purchased with clean-up filters to minimize extra components. Compact and simple designs have been previously described, for example by Nicovich *et al.* (2017). Links in the paper provide good guidelines on assembling the lasers (including designs) and useful resources including triggering and timing. Figure 2 below shows a close-up of the design that we implemented. Three lasers (405 nm, 488 nm, and 640 nm) are placed onto a heat sink, filtered using laser filters, and combined into a single line using dichroics. In practice, more lasers can be combined if necessary (e.g., 561 nm) by expanding the design. The lasers are then aligned into a fiber. Once installed, we expect ~70% coupling efficiency.

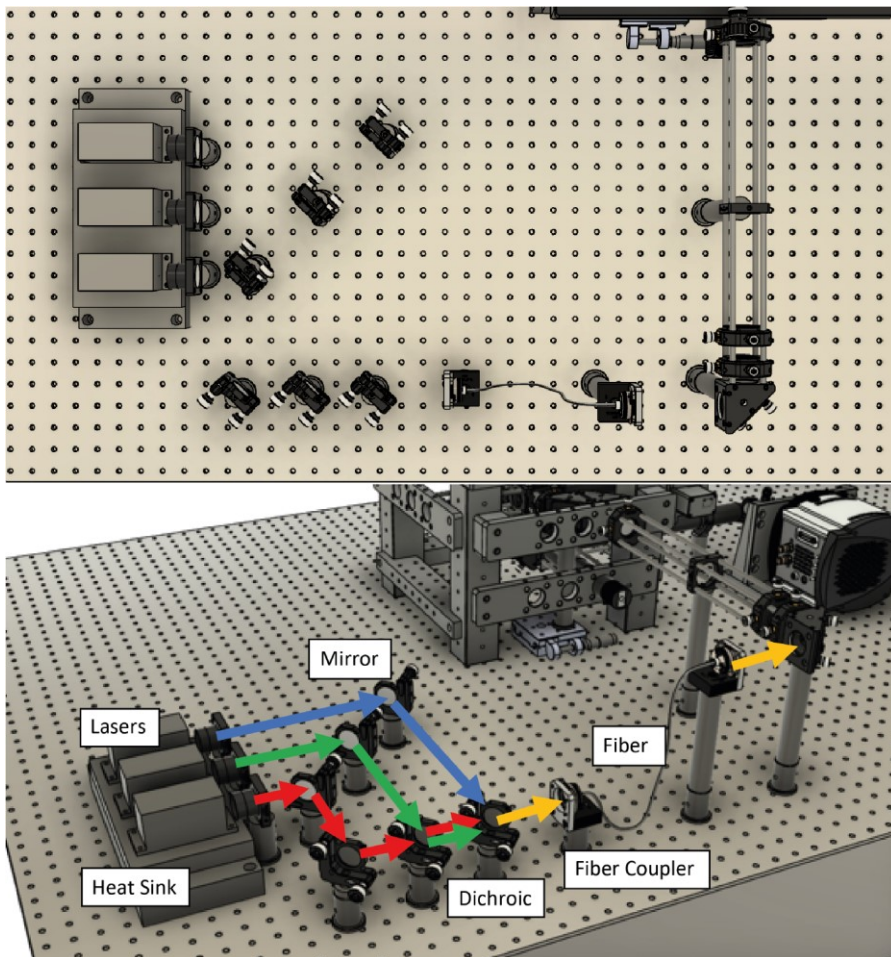


Figure 2. Laser assembly and fiber coupling. Three lasers (405 nm, 488 nm, and 640 nm) are placed onto a heat sink, combined using dichroics, and coupled to a laser fiber.

3. Place the output of the optical fiber at the intended height of the expansion optics. Ensure that the laser output is straight and travels parallel to the table without deviating.
4. Set up the laser expansion cage assembly (cage rods, $\times 2$ right-angle mirror mounts, and $\times 3$ cage XY translation mounts) attached to a custom RM21 bracket frame (<https://github.com/spcoelho/Active-Stabilization-Design>) and place at the required height. We recommend using steel pedestals to ensure greater stability. Figure 3 illustrates the assembly.

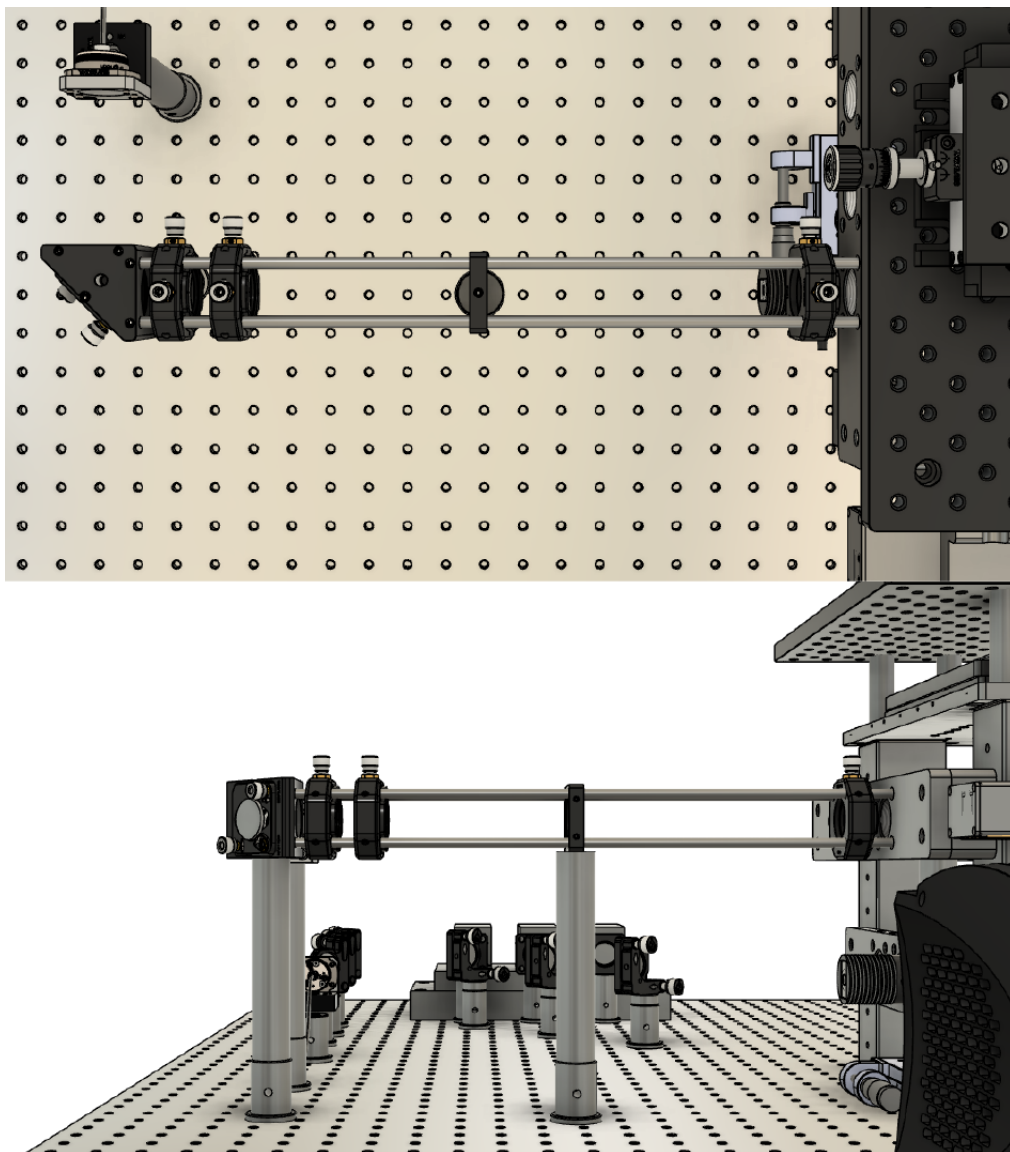


Figure 3. Assembly of the laser expansion

5. Align the laser so that it is centered throughout the cage assembly.
6. Place the lenses to provide ~10-fold expansion of the laser (e.g., 30 mm and 300 mm). Ensure that these are placed at the correct distance from each other using a Shearing Interferometer.
7. Assemble the mirror and tube lens (200 mm focal length) on top of the translation stage. The translation stage moves the lens and mirror assembly together. Ensure that the reflected beam is straight and parallel to the optical table. Place the mirror/lens centered within the frame of the microscope.
8. Take the dichroic holders ($\times 2$) and attach to each other. Place below the position of the imaging objective at the height of the laser.
9. Attach the dichroics, via cage rods, to the microscope frame using the RM21 bracket (<https://github.com/spcoelho/Active-Stabilization-Design>) (Figure 4, left hand side and Figure 5).

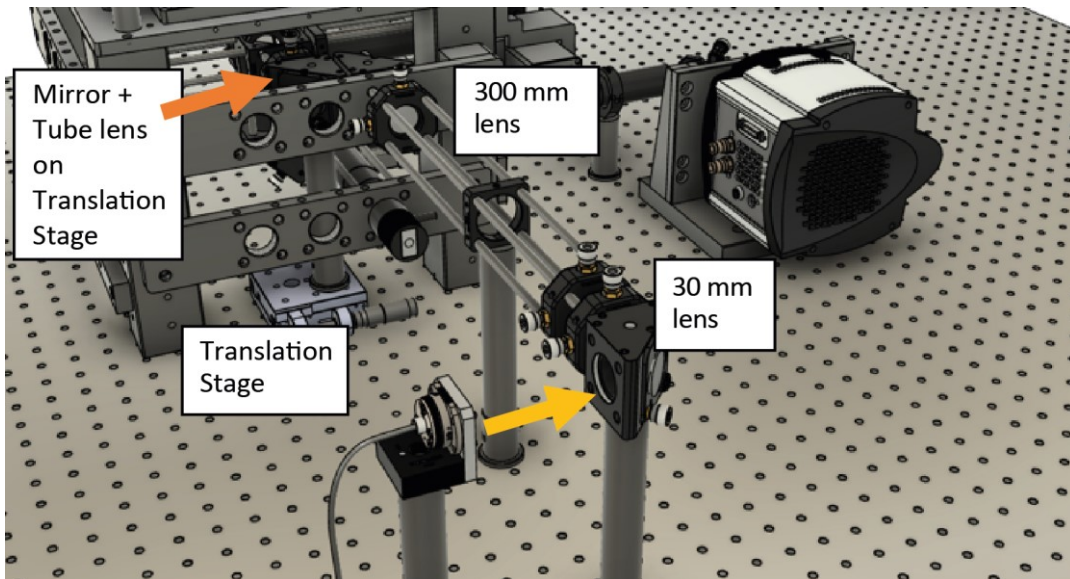


Figure 4. Mirror and tube lens are on top of a translation stage located within the microscope frame shown within the final assembly

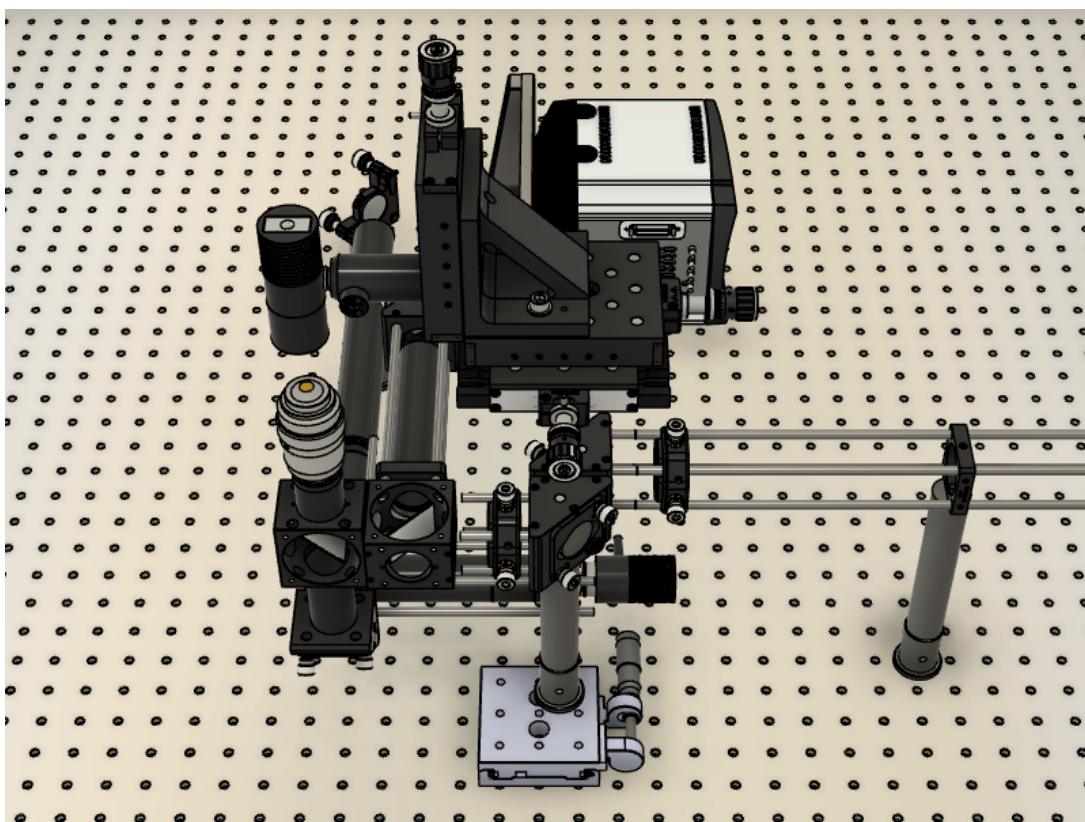


Figure 5. Internal components without the microscope body frame

10. Place the dichroics within their holders. One dichroic is used to reflect the laser toward the sample/objective; the second dichroic is used to separate the infrared light for active stabilization. For more details on how to assemble and configure, please refer to Coelho *et al.* (2020b).

11. Align the laser so that it is centered onto the back of the imaging objective. A simple method consists of replacing the objective for a Frosted Glass Alignment Disk and observing the position of the laser.
12. To ensure that the tube lens is at the correct distance from the back of the objective, the laser output should be as small as possible after exiting the objective. While observing the laser profile at a large distance (e.g., ceiling), adjust the position of the tube lens to ensure that a Gaussian beam with minimal diameter exits the objective. Misalignments can lead to a distorted beam profile (e.g., astigmatic).

B. Assemble the Infrared Camera/LED Path

1. Assemble the cage system (cage rods, right angle mirror mount, and 200 mm infrared lens) and attach it to the dichroic cube (Figure 6).
2. Secure to the microscope frame using an RM21 bracket (<https://github.com/spcoelho/Active-Stabilization-Design>).
3. Attach the infrared camera using an SM1 adapter and connect to a PC.
4. Assemble the infrared LED, place on the XYZ translation stage, and align onto the infrared camera [for more details, see Coelho *et al.* (2020b)].
5. Turn on the infrared LED and check that the illumination is centered and uniform on the infrared camera.
6. Place polystyrene beads on the glass coverslip and record their diffraction rings.

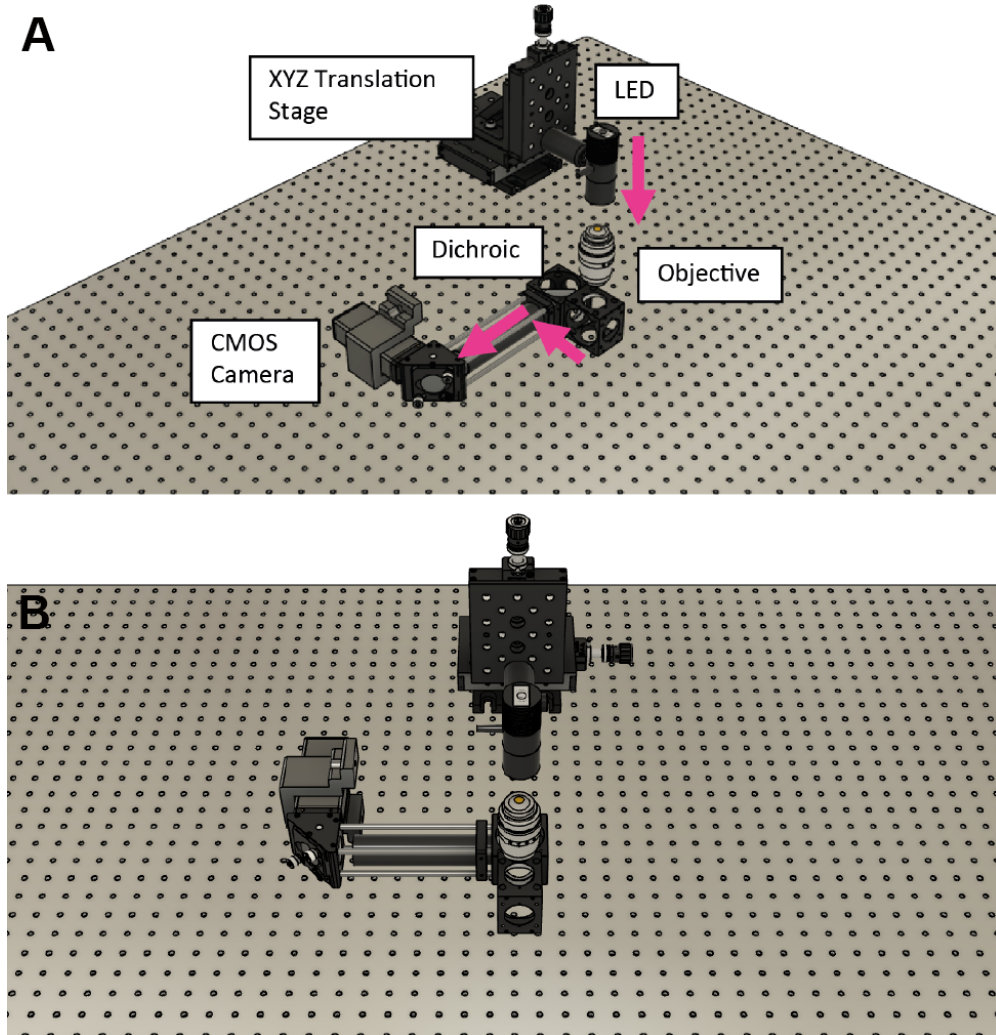


Figure 6. Assembly of the cage system to secure the infrared camera. The components are shown in relation to the infrared LED without the brackets/microscope frame. A. Front view. B. 45° view.

C. Detection (Emission camera and camera stabilization path)

This section describes how to introduce an optical feedback loop for the emission path (Figure 7). This allows to correct for movement in the detection path, facilitating high stability for prolonged acquisitions.

1. Emission Camera

- To direct the fluorescence from the sample toward the camera, attach a right-angle mirror mount to tubing and connect it to the bottom of the laser dichroic holder (Figure 7).

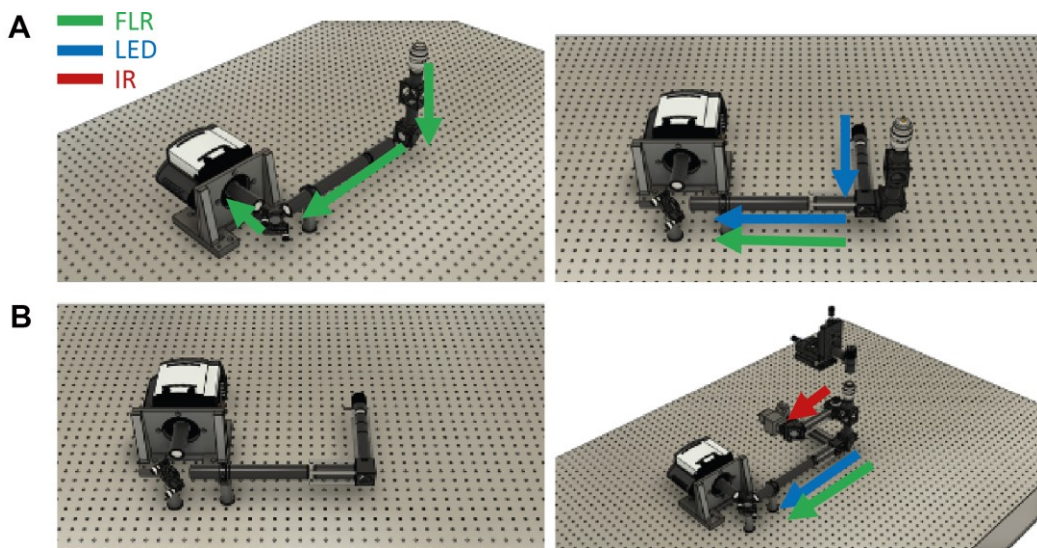


Figure 7. Assembly of the fluorescence emission path. A. Left: Without the white LED. Right: With the white LED. B. Left: Only the camera stabilization path. Right: Detection assembly in relation to the infrared detection.

- b. Adjust the length of the tube to match the predicted height of the fluorescent camera.
 - c. Within the tube, insert the emission filter (Em01-R405/488/635-25; Semrock). This removes the laser light and/or infrared LED.
 - d. Attach the tube lens (e.g., 400 mm focal length).
For the white LED: Attach the cage cube to the free side of the right-angle mirror mount.
Note: If extra distance between the camera and the tube lens is required, add a pair of relay lenses (e.g., 2 × 50 mm).
 - e. Secure the assembly to the RM21 microscope frame using cage rods and/or SM1 tubing.
 - f. Attach the camera to an optical table at the correct distance away from the lens.
 - g. Place a mirror (or piezo-electric mirror) in front of the camera.
 - h. Adjust the focal length of the tube lens. A simple way to get the correct distance is to flip the laser dichroic so that it reflects toward the camera. Using a very low laser power and multiple neutral density filters, focus the laser onto the camera. To get the correct distance, also remove the laser filter and last lens in the laser excitation path (TIRF lens mounted on the translation stage).
 - i. Place a uniform fluorescent sample (fluorescent molecules in solution or fluorescent marker) and check the emission onto the camera.
 - j. Center the emission onto the camera using the elliptical mirror underneath the objective lens. The emission should be uniform across the recorded field-of-view.
2. Camera Stabilization
 - a. Attach the white LED to the microscope frame (Figures 4 and 7B left).
 - b. Assemble the cage/tube system containing a pinhole (diameter = 50 μm) and lens (e.g., f = 400 mm).

- c. Center the pinhole and adjust the position of the lens to ensure a bright Gaussian spot focused on the camera.
- d. Position the white LED spot on the edge of the imaging field-of-view (Figure 8).

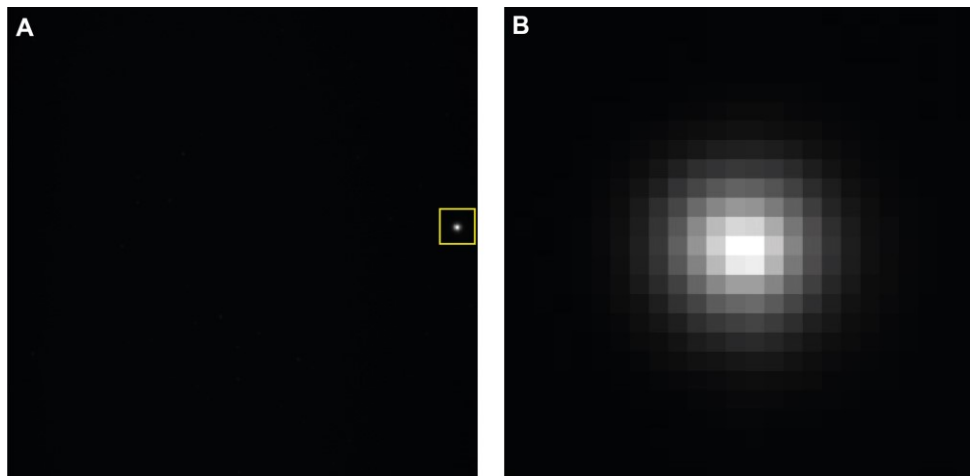


Figure 8. Camera stabilization. A. Full camera image showing LED projection toward the edge chip. B. Zoomed in region highlighted in the yellow square.

Acknowledgments

We are thankful for support from the Australia Research Council (CE140100011 to K.G., FL150100060 and CE140100036 to J.J.G.) and the National Health and Medical Research Council of Australia (APP1059278 to K.G.). This protocol is based on previous work, mainly from Coelho *et al.* (2020a).

Competing interests

The authors declare no competing financial interests.

References

1. Axelrod, D. (2001). [Total Internal Reflection Fluorescence Microscopy in Cell Biology](#). *Traffic* 2(11): 764-774.
2. Aoki, K. and Matsuda, M. (2009). [Visualization of small GTPase activity with fluorescence resonance energy transfer-based biosensors](#). *Nat Protoc* 4(11): 1623.
3. Baek, J., Loua, J., Coelhoa, S., Lim, D., Seidlitz S., Nicovich, P. R., Gaus, K. (2017). [Imaging galectin-3 dependent endocytosis with lattice light-sheet microscopy](#). *International Conference on Biophotonics V 10340: SPIE*.
4. Boutros, M., Heigwer, F. and Laufer, C. (2015). [Microscopy-Based High-Content Screening](#). *Cell* 163(6): 1314-1325.

5. Burke, D., Patton, B., Huang, F., Bewersdorf, J. and Booth M.J. (2015). [Adaptive optics correction of specimen-induced aberrations in single-molecule switching microscopy](#). *Optica* 2(2): 177-185.
6. Coelho, S., Baek, J., Graus, M.S., Halstead, J.M., Nicovich, P.R., Feher, K., Gandhi, H., Gooding, J.J. and Gaus, K. (2020a). [Ultraprecise single-molecule localization microscopy enables in situ distance measurements in intact cells](#). *Sci Adv* 6(16): eaay8271.
7. Coelho, S., Baek, J., Walsh, J., Gooding, J.J. and Gaus, K. (2020b). [3D active stabilization for single-molecule imaging](#). *Nat Protoc* 16(1): 497-515.
8. Coelho, S., Poland, S., Krstajic, N., Li, D., Monypenny, J., Walker, R., Tyndall, D., Ng, T., Henderson, R. and Ameer-Beg, S. (2013). [Multifocal multiphoton microscopy with adaptive optical correction](#). *Progress in Biomedical Optics and Imaging - Proceedings of SPIE* 8588: 17. 2013: SPIE.
9. Coelho, S., Coelho, S., Poland, S.P., Devauges, V. and Ameer-Beg, S.M. (2020c). [Adaptive optics for a time-resolved Förster resonance energy transfer \(FRET\) and fluorescence lifetime imaging microscopy \(FLIM\) in vivo](#). *Opt Lett* 45(10): 2732-2735.
10. Diekmann, R., Helle, Ø.I., Øie C.I., McCourt, P., Huser, T.R., Schüttelpelz, M. and Ahluwalia, B. S. (2017). [Chip-based wide field-of-view nanoscopy](#). *Nat Photon* 11(5): 322-328.
11. Eggeling, C., Ringemann, C., Medda, R., Schwarzmann, G., Sandhoff, K., Polyakova, S., Belov, V.N., Hein, B., von Middendorff, C., Schönle, A. and Hell, S.W. (2009). [Direct observation of the nanoscale dynamics of membrane lipids in a living cell](#). *Nature* 457(7233): 1159-1162.
12. Fish, K. N. (2009). [Total internal reflection fluorescence \(TIRF\) microscopy](#). *Curr Protoc Cytom* Chapter 12: Unit12.18.
13. Gao, L., Shao, L., Chen, B.C. and Betzig, E. (2014). [3D live fluorescence imaging of cellular dynamics using Bessel beam plane illumination microscopy](#). *Nat Protoc* 9(5): 1083-1101.
14. Giessibl, F.J., [Advances in atomic force microscopy](#). (2003). *Rev Mod Phys* 75(3): 949.
15. Gustavsson, A.K., Petrov, P.N., Lee, M.Y., Shechtman, Y. and Moerner, W.E. (2018). [3D single-molecule super-resolution microscopy with a tilted light sheet](#). *Nat Commun* 9(1): 1-8.
16. Huang, B., Wang, W., Bates, M. and Zhuang, X. (2008). [Three-Dimensional Super-Resolution Imaging by Stochastic Optical Reconstruction Microscopy](#). *Science* 319(5864): 810-813.
17. Huang, F., Sirinakis, G., Allgeyer, E.S., Schroeder, L.K., Duim, W.C., Kromann, E.B., Phan, T., Rivera-Molina, F.E., Myers, J.R., Irnov, I., Lessard, M., Zhang, Y., Handel, M.A., Jacobs-Wagner, C., Lusk, C.P., Rothman, J.E., Toomre, D., Booth, M.J. and Bewersdorf, J. (2016). [Ultra-High Resolution 3D Imaging of Whole Cells](#). *Cell* 166(4): 1028-1040.
18. Kim, J., Park, B.W., Baek, J., Yun, J.S., Kwon, H.W., Seidel, J., Min, H., Coelho, S., Lim, S., Huang, S., Gaus, K., Green, M.A., Shin, T.J., Ho-Baillie, A.W.Y., Kim, M.G. and Seok, S.I. (2020). [Unveiling the relationship between the perovskite precursor solution and the resulting device performance](#). *J Am Chem Soc* 142(13): 6251-6260.

19. Krstajić, N., Poland, S., Tyndall, D., Walker, R., Coelho, S., Li, D.D.U., Richardson, J., Ameer-Beg, S. and Henderson, R. (2013). [Improving TCSPC data acquisition from CMOS SPAD arrays in European Conference on Biomedical Optics](#). *Optical Society of America* paper: 879709.
20. Jungmann, R., Avendaño, M.S., Woehrstein, J.B., Dai, M., Shih, W.M. and Yin, P. (2014). [Multiplexed 3D cellular super-resolution imaging with DNA-PAINT and Exchange-PAINT](#). *Nat Methods* 11(3): 313-318.
21. Nicovich, P.R., Walsh, J., Böcking, T. and Gaus, K. (2017). [NicoLase-an open-source diode laser combiner, fiber launch, and sequencing controller for fluorescence microscopy](#). *PLoS One* 12(3): e0173879.
22. Pavani, S.R., Thompson, M.A., Biteen, J.S., Lord, S.J., Liu, N., Twieg, R.J., Piestun, R. and Moerner, W.E. (2009) [Three-dimensional, single-molecule fluorescence imaging beyond the diffraction limit by using a double-helix point spread function](#). *Proc Natl Acad Sci U S A* 106(9): 2995-2999.
23. Poland, S.P., Krstajić, N., Monypenny, J., Coelho, S., Tyndall, D., Walker, R.J., Devauges, V., Richardson, J., Dutton, N., Barber, P., Li, D.D., Suhling, K., Ng, T., Henderson, R.K. and Ameer-Beg, S.M. (2015). [A high speed multifocal multiphoton fluorescence lifetime imaging microscope for live-cell FRET imaging](#). *Biomed Opt Express* 6(2): 277-296.
24. Poland, S.P., Krstajić, N., Coelho, S., Tyndall, D., Walker, R.J., Devauges, V., Morton, P.E., Nicholas, N.S., Richardson, J., Li, D.D., Suhling, K., Wells, C.M., Parsons, M., Henderson, R.K. and Ameer-Beg, S.M. (2014). [Time-resolved multifocal multiphoton microscope for high speed FRET imaging in vivo](#). *Opt Lett* 39(20): 6013-6016.
25. Suhling, K., Hirvonen, L.M., Levitt, J.A., Chung, P.H., Tregidgo, C., Marois, A.L., Rusakov, D.A., Zheng, K., Ameer-Beg, S., Poland, S., Coelho, S., Henderson, R. and Nikola Krstajic. (2015) [Fluorescence lifetime imaging \(FLIM\): Basic concepts and some recent developments](#). *MedPhoton* 27: 3-40.
26. Suhling, K., et al. (2017). Fluorescence lifetime imaging. In: *Handbook of Photonics for Biomedical Engineering*. Springer: 353-405.
27. Suhling, K., Hirvonen, L. M., Levitt, J.A., Chung, P.H., Tregido, C., Marois, A., Rusakov, D.A., Zheng, K., Ameer-Beg, S., Poland, S., Coelho, S. and Dimble, R. (2015). [Fluorescence lifetime imaging \(Flim\): Basic concepts and recent applications, in Advanced Time-Correlated Single Photon Counting Applications](#). *Springer Series in Chemical Physics* 111:119-188.
28. Schmidt, P.D., Reichert, B.H., Lajoie, J.G. and Sivasankar, S. (2018). [Method for high frequency tracking and sub-nm sample stabilization in single molecule fluorescence microscopy](#). *Sci Rep* 8(1): 13912.
29. Shechtman, Y., Sahl, S.J., Backer, A.S. and Moerner, W.E. (2014). [Optimal point spread function design for 3D imaging](#). *Phys Rev Lett* 113(13): 133902.
30. Shtengel, G., Galbraith, J.A., Galbraith, C.G., Lippincott-Schwartz, J., Gillette, J.M., Manley, S., Sougrat, R., Waterman, C.M., Kanchanawong, P., Davidson, M.W., Fetter, R.D. and Hess, H.F.

- (2009). [Interferometric fluorescent super-resolution microscopy resolves 3D cellular ultrastructure](#). *Proc Natl Acad Sci U S A* 106(9): 3125-3130.
31. Shroff, H., Galbraith, C.G., Galbraith, J.A. and Betzig, E. (2008). [Live-cell photoactivated localization microscopy of nanoscale adhesion dynamics](#). *Nat Methods* 5(5): 417.
32. Tokunaga, M., Imamoto, N. and Sakata-Sogawa, K. (2008). [Highly inclined thin illumination enables clear single-molecule imaging in cells](#). *Nat Methods* 5(2): 159-161.

Retention Using Selective Hooks (RUSH) Cargo Sorting Assay for Live-cell Vesicle Tracking in the Secretory Pathway Using HeLa Cells

Mehrshad Pakdel^{1, #}, Natalia Pacheco-Fernandez^{1, #, \$} and Julia von Blume^{2, *}

¹Department of Molecular Medicine, Max-Planck Institute of Biochemistry, Martinsried, Germany;

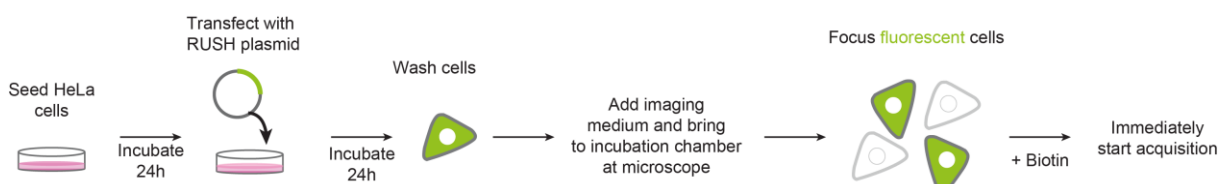
²Department of Cell Biology, Yale University, New Haven (CN), USA; ^{\$}Current address: Department of Structural Cell Biology, Max Planck Institute of Biochemistry, Martinsried, Germany

*For correspondence: julia.vonblume@yale.edu

#Contributed equally to this work

[Abstract] More than 30% of the total amount of proteins synthesized in mammalian cells follow the secretory pathway in order to mature and be properly sorted to their final destinations. Among several methodologies that describe live-cell monitoring of vesicles, the Retention Using Selective Hooks (RUSH) system is a powerful one that allows to visualize cargo trafficking under physiological conditions. The present protocol describes a method to use the RUSH system in live-cell microscopy and a subsequent quantitative analysis of cargo vesicles to dissect protein trafficking. In brief, HeLa cells are transiently transfected with an MMP2-RUSH construct and vesicle trafficking is evaluated by wide-field microscopy, recording videos in 1-min time frames for 45 min. We also present a quantitative approach that can be used to identify kinetics of uncharacterized protein cargo, as well as to evaluate with more detail processes such as ER-to-Golgi vesicle trafficking.

Graphic abstract:



Live-cell RUSH: a tool to monitor real-time protein trafficking in the secretory pathway

Keywords: Protein trafficking, RUSH, Cargo sorting, Confocal microscopy, Vesicle trafficking

[Background] More than 30% of the total amount of proteins synthesized in mammalian cells follow the secretory pathway (Pfeffer, 2010; Boncompain and Weigel, 2018). Through this pathway, proteins mature by trafficking from the ER and along the different Golgi stacks until they reach the *trans*-Golgi network (TGN), where they are finally sorted and packed into vesicles that will be delivered to other organelles within the cell, or to the extracellular milieu (Glick and Luini, 2011; Pantazopoulou and Glick, 2019).

In the recent years, several reports in the literature document advance in the live-cell monitoring of

vesicles that follow the secretory pathway (Stephens and Perez, 2013). One of the most helpful tools is the Retention Using Selective Hooks (RUSH) system, a methodology that enables the synchronized monitoring of fluorescent vesicles in a living cell upon biotin addition (Boncompain *et al.*, 2012). In this system, cells are either transiently transfected or stably express a two-part protein complex consisting of a protein of interest (POI) tagged with a fluorophore and bound to a streptavidin binding peptide (SBP), and streptavidin bound to a retention signal (known as the “hook”, e.g., a KDEL sequence for retention in the ER; Figure 1). Given the higher affinity of streptavidin to biotin, once the latter is added to the cell culture media, the SBP-POI complex is released to the next compartment and the trafficking can be followed either live by wide-field microscopy or monitored at different fixed time points by confocal microscopy (Boncompain *et al.*, 2012).

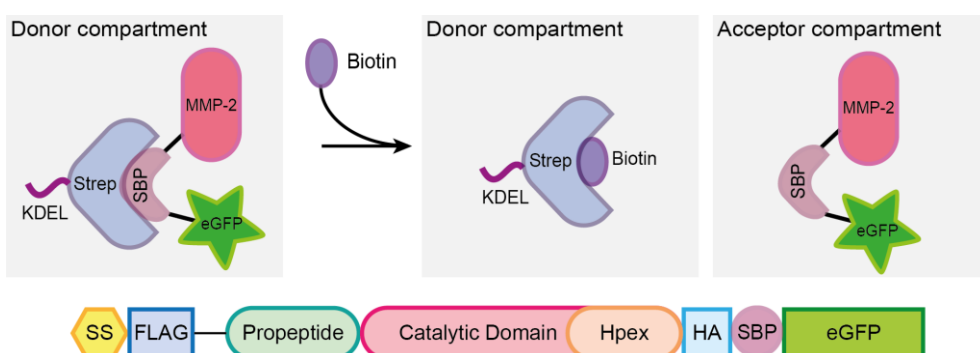


Figure 1. Scheme representing the RUSH system. A protein complex containing the protein of interest (here matrix metalloprotease 2, MMP2), a streptavidin binding peptide (SBP) and a fluorescent protein (eGFP) is bound via SBP to streptavidin (Strep), which is linked to a KDEL sequence for the retention of the complex in the donor compartment (in this example, the ER). Once biotin is added to the media, it binds to streptavidin, enabling the MMP2-SBP-eGFP protein complex to travel to the acceptor compartment (the Golgi apparatus in the secretory pathway). Figure taken from Pacheco-Fernandez *et al.* (2020) and adapted from Boncompain *et al.* (2012).

One of the main advantages of using the RUSH system is that it enables to carefully dissect the trafficking kinetics of soluble and membrane proteins that follow the secretory pathway under physiological conditions (Boncompain *et al.*, 2012). Some other techniques developed in recent years have also enabled the characterization of vesicle trafficking through the secretory pathway. Among others, super-resolution confocal live imaging (Kurokawa *et al.*, 2019); synchronization of cargo-retention and release by polymerization/depolymerization (Cancino *et al.*, 2013) and a light-triggered protein secretion system (Chen *et al.*, 2013). However, such techniques require either a more complex set up, the use of more sensitive equipment, or the aggregation of the protein of interest previous to its synchronized trafficking, which may lead to cargo trafficking through different pathways than those followed by the unaggregated protein (Boncompain and Perez, 2013).

Based on the original RUSH methodology developed by Boncompain *et al.* (2012), here we present a protocol that provides in addition a quantitative analysis, which aims to better dissect intra-Golgi

trafficking by counting the number of cargo vesicles in 1-minute time video frames during a defined period of time, in order to assess post-Golgi cargo sorting kinetics (Deng *et al.*, 2018). Furthermore, the ImageJ macro developed for such analysis is also optimized for dissecting the ER-to-Golgi cargo trafficking kinetics using Golgi compaction (ratio between Golgi:ER fluorescent signal per minute) as a measure (Pacheco-Fernandez *et al.*, 2020).

Materials and Reagents

1. 35 mm µ-dish, High Glass Bottom (ibidi, catalog number: 81158)
2. Polyethylenimine (PEI), linear, MW 25000, transfection grade (PEI 25K™; Polysciences, catalog number: 23966-1)
3. 60-70% confluent HeLa cells

For this analysis, cells were obtained from Cell Lines Service. We used these cells because they are easy to transfect, have a good size for vesicle visualization and are easy to handle, however, other cell lines can also be used (see Note 1).
4. 1× Dulbecco's Phosphate Buffered Saline (DPBS), no calcium, no magnesium (Life Technologies, Gibco, catalog number: 14190144). Storage temperature: 4 °C
5. pIRESneo3-Str-KDEL-MMP2-SBP-EGFP vector. Storage temperature: -20 °C

Important note: This plasmid was generated by replacing the ST (ST6GAL1) sequence by the MMP2 one (our protein of interest) in the Addgene plasmid number 65264 (Str-KDEL_ST-SBP-EGFP).
6. Opti-MEM® reduced serum media (Life Technologies, Gibco, catalog number: 31985070). Storage temperature: 4 °C
7. 500 mM d-biotin (Merck, SUPELCO, catalog number: 47868). Storage temperature: 4 °C
8. Dulbecco's Modified Eagles Medium, high glucose, GlutaMAX™, sodium pyruvate (DMEM, Life Technologies, Gibco, catalog number: 10569010). Storage temperature: 4 °C
9. Heat inactivated Fetal Bovine Serum (FBS; Life Technologies, Gibco, catalog number: 16000044). Storage temperature: -20 °C
10. Penicillin/Streptomycin (P/S; Life Technologies, Gibco, catalog number: 15140122). Storage temperature: -20 °C
11. DMEM, high glucose, HEPES, no phenol red (Life Technologies, Gibco, catalog number: 21063029). Storage temperature: 4 °C
12. PEI solution at 1 mg/ml (see Recipes)
13. DMEM complete medium (see Recipes)

Equipment

1. Magnetic stirrer
2. Laminar flow hood

3. Cell incubator set at 37 °C, 5% CO₂
4. Water bath set at 37 °C
5. Microscope:
 - a. DeltaVision Elite System based on:
 - i. Olympus IX-71 inverted microscope (Olympus Corporation)
 - ii. Olympus 60×/1.42 PLAPON oil objective (Olympus Corporation)
 - b. PCO pco.edge sCMOS 5.5 microscope camera
 - c. 7-colour InsightSSI module laser
 - d. DAPI-FITC-TRITC-Cy5 and/or CFP-YFP-mCherry filters
 - e. Live-cell imaging incubation chamber set up at 37 °C. Optional: 5% CO₂ and humidity.

Software

1. SoftWoRx 5.5 software (GE Healthcare, <https://cdn.cytilifesciences.com/dmm3bwsv3/AssetStream.aspx?mediaformatid=10061&destinationid=10016&assetid=17238>)
2. Fiji (Schindelin *et al.*, 2012, <https://fiji.sc>)

Procedure

A. Cell culture and plasmid transfection

1. All steps involving cell culture must be performed in a laminar flow hood
2. Seed 3 × 10⁴ HeLa cells in an ibidi 35 mm µ-dish using 2 ml DMEM complete medium. Prepare at least 3-5 dishes per experiment.
3. Incubate the cells at 37 °C, 5% CO₂ for 24 h.
4. Set up PEI transfection reaction (Per dish/well: 200 µl OptiMEM + 2 µg RUSH construct, e.g., pIREneo3-SS-Str-KDEL-MMP2-SBP-EGFP + 15 µl 50 mM PEI solution).
5. Vortex the transfection reaction and incubate it at room temperature for 20 min.
6. Add dropwise to the cells and incubate at 37 °C, 5% CO₂ for 24 h.

B. Live-cell imaging

1. Set up the incubation chamber for live-cell imaging. Pre-heat the chamber for at least 2 h before starting the experiment.
2. Remove medium from cells and wash once with 1× DPBS.
3. Add 1 ml DMEM high glucose, HEPES, no phenol red.
4. Bring the cells to the incubation chamber and focus fluorescent cells on multiple fields of views. Adjust exposure time to 50 % of maximum fluorescent intensity as the signal will increase while cargo is compacted at the Golgi. Figure 2 depicts an example of a field of view at time 0.

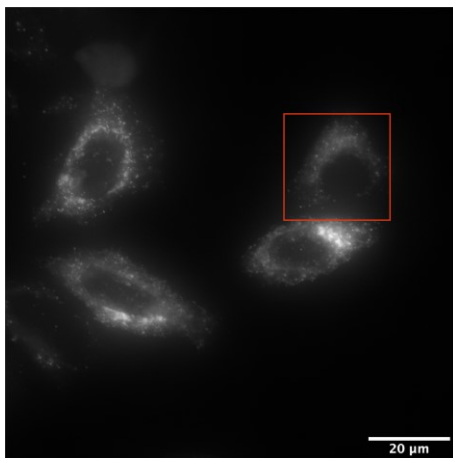
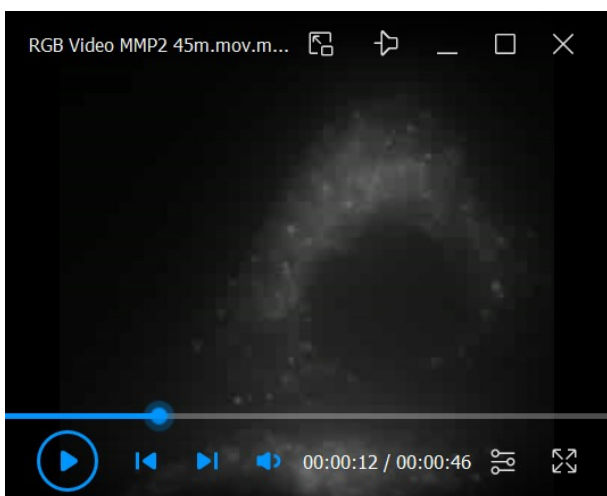


Figure 2. HeLa cells transiently expressing an MMP2-RUSH construct. Wide-field deconvoluted microscopy image of a selected field of view for the recording of MMP2 vesicle trafficking. The image corresponds to the first time frame of the video (t=0). The red square highlights the cell showed in Video 1. Scale bar: 20 μ m.



Video 1. Live-cell microscopy of MMP2eGFP trafficking. The video depicts the cell highlighted in Figure 1 with a red square. It nicely shows the Golgi compaction after 20 min of biotin incubation and the budding of vesicles from the Golgi at 35 min after biotin addition.

5. Optional: Acquire Z-stacks at 0.35 μ m step sizes to image multiple planes.
 6. Add 1 ml DMEM high glucose, HEPES, no phenol red supplemented with 80 μ M Biotin to the dish on top of the cells to reach a final biotin concentration of 40 μ M (1:1 dilution).
 7. Immediately start acquisition at 1 min time frames for 45 min.
 8. Repeat the procedure using a new dish every time until at least 10-15 cells are imaged
- C. Imaging analysis
1. Live-cell
 - a. Deconvolute the image sequences using the softWoRx software. It is also possible to

perform image deconvolution during the data analysis using Fiji (see plugins Deconvolve 3D and Deconvolution Lab).

- b. Save files as *.dv. Video 1 shows the sequence of 45 1-min time frames for MMP2 RUSH in HeLa cells.

Data analysis

1. Open the image sequence files in Fiji. If every image was saved as a single file, open a group of corresponding files and use the tool “Images to Stack” to group them as a sequence. If the image was saved as a sequence you will see the following window popping up when opening the file (Figure 3):

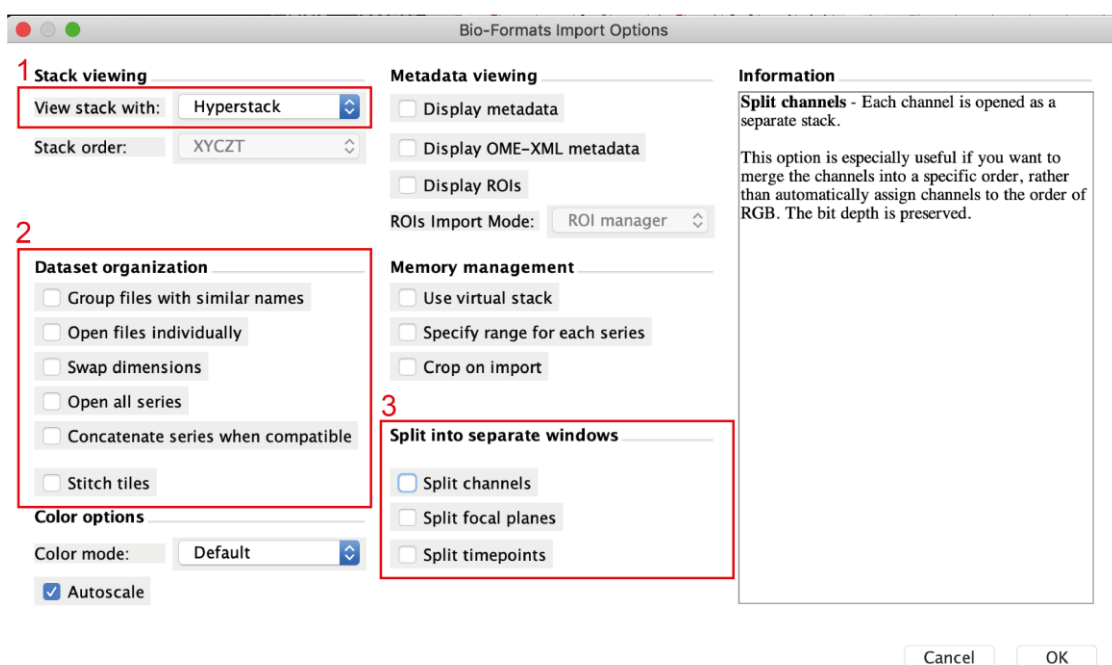


Figure 3. Import image window in Fiji

2. To open the file correctly, make sure that you select Hyperstack in the view stack menu (no.1), not to import the files individually (*i.e.*, no selection in no.2) and not to split time points nor channels (no.3). The macro used for analysis already integrates the splitting channels function.
3. Optional: Stack the Z frames by clicking in Image menu > Stack > Z-project (Figure 4A). In this menu make sure that the projection type selected is “Max Intensity” (arrow, Figure 4B).

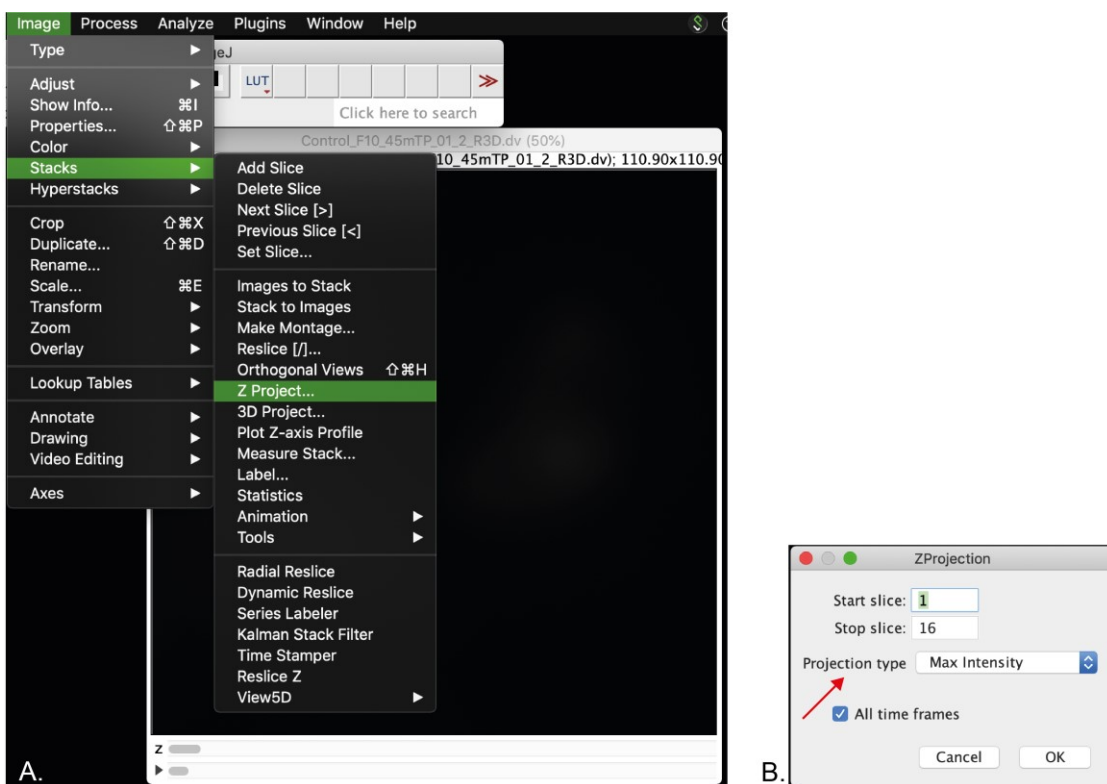


Figure 4. Screenshot of the Z-projection menu. A. Selection of Z-stack. B. Z-stack menu. Arrow indicates the projection type that should be selected.

4. A file (MAX_ "name of your original file") will be generated. Save it in the location where the processed image will be saved.
5. Depending on the number of cells imaged per file, you can crop the full field of view to single cells if required. For this purpose:
 - a. Select the rectangle tool (red arrow, Figure 5A). Selecting the free hand tool is also useful.
 - b. Duplicate the selection by clicking on the Image menu > Duplicate (Figure 5B).
 - c. Save the duplicated image and close the original one. The macro will not run with 2 images open.

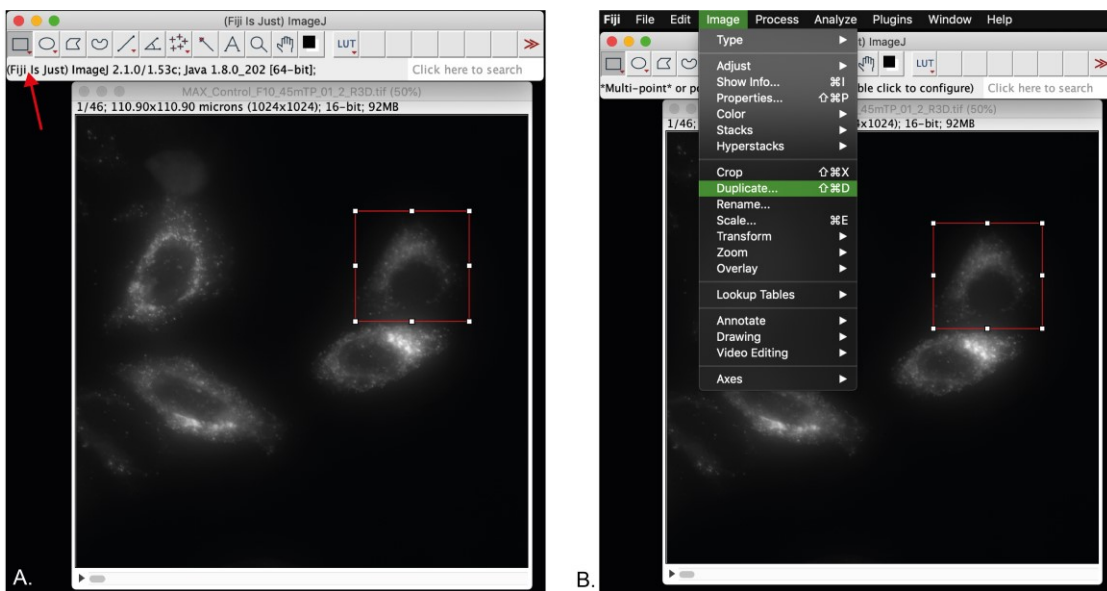


Figure 5. Selection of a single cell for analysis. A. Selection of a single cell using the rectangle tool (red arrow). B. Duplication of the selected cell for further processing.

6. Open in Fiji our custom-made ImageJ macro for “Live-cell vesicle analysis” available at https://github.com/MehrshadPakdel/RUSH-Vesicle-Analysis/blob/master/Live-Cell_Vesicle_Analysis_V2.ijm (Figure 6).

```

31     setSlices();
32     run("Auto Threshold", "method=Minimum white");
33   }
34   for (n=26; n<=nSlices; n++) {
35     setSlice(n);
36     run("Auto Threshold", "method=Moments white");
37   }
38   for (n=1; n<=nSlices; n++) {
39     setSlice(n);
40     run("Analyze Particles...", "size=4~40 pixel show=Outlines display exclude");
41     print(nResults);
42     run("Clear Results");
43     selectWindow("Drawing of dupImage");
44     run("Close");
45   }
46   selectWindow("dupImage");
47   run("Analyze Particles...", "size=4~40 pixel show=Outlines display exclude stack");
48   splitDir= dir + "/Results_" + originalImage + "/";
49   File.makeDirectory(splitDir);
50   list = getList("image.titles");
51   selectWindow(list[0]);
52   saveAs("tiff", splitDir + "Binary_" + originalImage);
53   selectWindow(list[1]);
54   saveAs("tiff", splitDir + "Particles_" + originalImage);
55   selectWindow("Log");
56   saveAs("text", splitDir + "Log_" + originalImage);
57   selectWindow("Results");
58   run("Close");

```

The image shows a screenshot of the ImageJ macro editor window titled "Macro.ijm.ijm". The code is a Java script for ImageJ, specifically for live-cell vesicle analysis. It includes loops for slicing, thresholding, and analyzing particles, followed by saving binary and particle images, and a log file. The code is annotated with green arrows pointing to specific lines: one arrow points to the "Binary_" saveAs line, and another points to the "Log_" saveAs line. At the bottom of the window, there are buttons for "Run", "Batch", "Kill", "persistent", "Show Errors", "Clear", and a timestamp: "Started Macro.ijm.ijm at Wed Sep 23 20:24:40 CEST 2020".

Figure 6. Window showing the macro for life cell analysis

7. You can adjust in the macro the Auto Threshold methods for optimized ER signals and Golgi signals according to signal intensity and trafficking rate of your cargo of interest.
8. Run the macro. Vesicles will be quantified for all frames and result files will be generated and saved automatically in a new results folder, located in the original file directory (see step 4). Figure 7 illustrates the final result, showing the binary file for every frame (Binary_filename, Figure 7A), together with the particle analyzer window (Particle_filename, Figure 7B) and the count of vesicles (log window, Figure 7C). These values can be copied to an excel spreadsheet for single cell quantification or comparison with other cell lines. For further possible analyses please see Deng *et al.* (2018) and Pacheco-Fernandez *et al.* (2020).
9. Importantly, not all the cells show cargo trafficking. We observed that in a small percentage of cells, the cargo never left the ER upon biotin addition. These cells should be excluded of the analysis.
10. Statistical analysis can compare between time points, different treatments, different cell lines, etc. For this purpose, compare the average number of vesicles from at least 15 cells using a non-parametric *t*-test, unless the data follows a normal distribution. If is the case, perform a one-sample *t*-test.

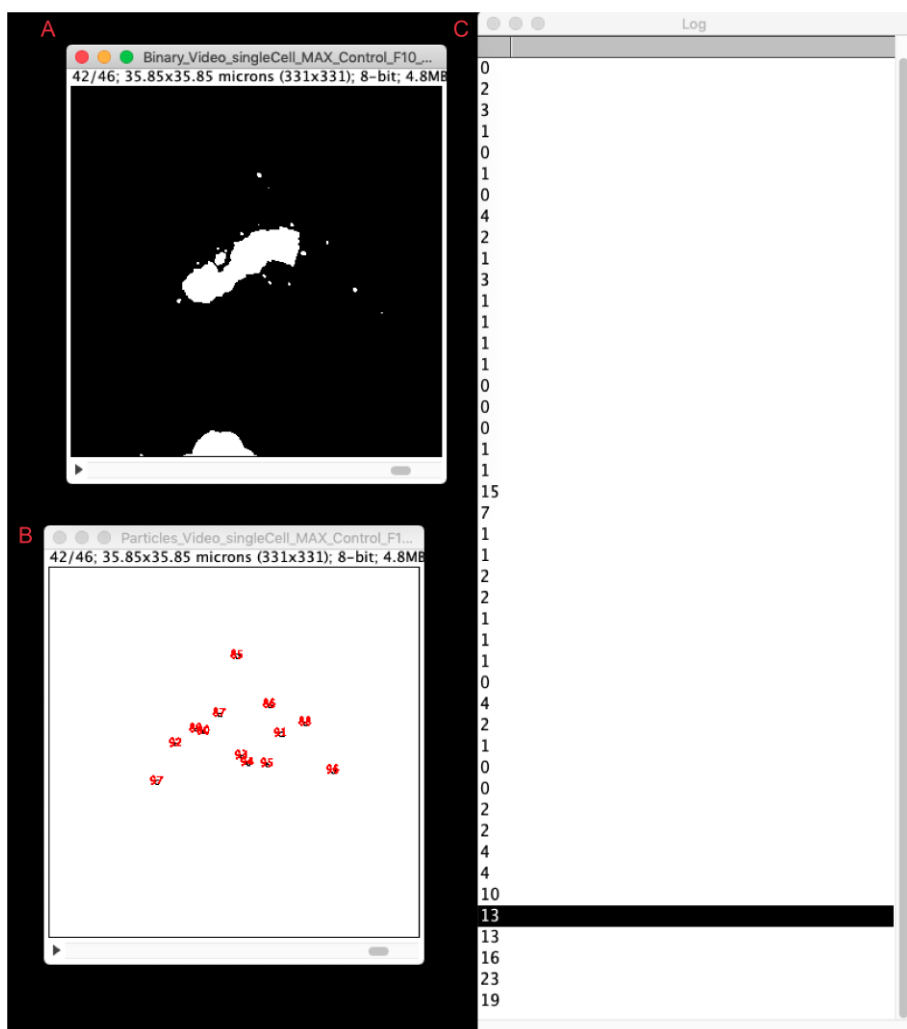


Figure 7. Results from the vesicle quantification analysis. The figure shows a screenshot of the vesicle quantitative analysis using the live-cell RUSH vesicle analysis macro. Window (A) depicts the Binary image generated for each time frame; window (B) the particle (*i.e.*, vesicle) identification; and window (C) the quantification of vesicles per time frame. Highlighted is the number of vesicles for the depicted time frame (42/46).

Notes

1. The system works also well with other cell lines, however, the PEI transfection protocol might not be suitable and other transfection reagents or methods should be first established. In our experience, the RUSH system works well also in HEK and MDA-MB-231 cells, although, for the MDA-MB-231 cells, transfection was only successful using Lipofectamine 2000.
2. The set up for confocal microscopy can also be done in 35-mm dishes. We recommend counting at least 15 cells for a valid statistical analysis.

Recipes

1. PEI solution
 - a. Dissolve 50 mg of Polyethylenimine in 40 ml of distilled water
 - b. Mix well the solution with a magnetic stirrer on a slightly warmed plate
 - c. Adjust pH to 7.4
 - d. Complete volume up to 50 ml
 - e. Aliquot in 500 μ l and store at -20 °C
2. DMEM complete medium
Prepare 500 ml of DMEM medium by adding FBS and P/S to a final concentration of 10% and 1%, respectively

Acknowledgments

This protocol was previously documented in the publications (Deng *et al.*, 2018) and (Pacheco-Fernandez *et al.*, 2020). This work was supported by grants from the Deutscher Akademischer Austauschdienst (DAAD), Deutsche Forschungsgemeinschaft (DFG), National Institutes of Health (NIH), the Perspective Program (Boehringer Ingelheim Fonds) and the Max Planck Institute of Biochemistry.

Competing interests

The authors declare no competing financial interests.

References

1. Boncompain, G., Divoux, S., Gareil, N., de Forges, H., Lescure, A., Latreche, L., Mercanti, V., Jollivet, F., Raposo, G. and Perez, F. (2012). [Synchronization of secretory protein traffic in populations of cells](#). *Nat Methods* 9(5): 493-498.
2. Boncompain, G. and Perez, F. (2013). [Fluorescence-based analysis of trafficking in mammalian cells](#). *Methods Cell Biol* 118: 179-194.
3. Boncompain, G. and Weigel, A. V. (2018). [Transport and sorting in the Golgi complex: multiple mechanisms sort diverse cargo](#). *Curr Opin Cell Biol* 50: 94-101.
4. Cancino, J., Capalbo, A. and Luini, A. (2013). [Golgi-dependent signaling: self-coordination of membrane trafficking](#). *Methods Cell Biol* 118: 359-382.
5. Chen, D., Gibson, E. S. and Kennedy, M. J. (2013). [A light-triggered protein secretion system](#). *J Cell Biol* 201(4): 631-640.
6. Deng, Y., Pakdel, M., Blank, B., Sundberg, E. L., Burd, C. G. and von Blume, J. (2018). [Activity of the SPCA1 Calcium Pump Couples Sphingomyelin Synthesis to Sorting of Secretory Proteins](#)

- [in the Trans-Golgi Network.](#) *Dev Cell* 47(4): 464-478 e468.
7. Glick, B. S. and Luini, A. (2011). [Models for Golgi traffic: a critical assessment.](#) *Cold Spring Harb Perspect Biol* 3(11): a005215.
 8. Kurokawa, K., Osakada, H., Kojidani, T., Waga, M., Suda, Y., Asakawa, H., Haraguchi, T. and Nakano, A. (2019). [Visualization of secretory cargo transport within the Golgi apparatus.](#) *J Cell Biol* 218(5): 1602-1618.
 9. Pacheco-Fernandez, N., Pakdel, M., Blank, B., Sanchez-Gonzalez, I., Weber, K., Tran, M. L., Hecht, T. K., Gautsch, R., Beck, G., Perez, F., Haussner, A., Linder, S. and von Blume, J. (2020). [Nucleobindin-1 regulates ECM degradation by promoting intra-Golgi trafficking of MMPs.](#) *J Cell Biol* 219(8).
 10. Pantazopoulou, A. and Glick, B. S. (2019). [A Kinetic View of Membrane Traffic Pathways Can Transcend the Classical View of Golgi Compartments.](#) *Front Cell Dev Biol* 7: 153.
 11. Pfeffer, S. R. (2010). [How the Golgi works: a cisternal progenitor model.](#) *Proc Natl Acad Sci U S A* 107(46): 19614-19618.
 12. Schindelin, J., Arganda-Carreras, I., Frise, E., Kaynig, V., Longair, M., Pietzsch, T., Preibisch, S., Rueden, C., Saalfeld, S., Schmid, B., Tinevez, J. Y., White, D. J., Hartenstein, V., Eliceiri, K., Tomancak, P. and Cardona, A. (2012). [Fiji: an open-source platform for biological-image analysis.](#) *Nat Methods* 9(7): 676-682.
 13. Stephens, D. and Perez, F. (2013). Preface. In: Perez, F. and Stephens, D. (Eds.). *Methods for Analysis of Golgi Complex Function* (Vol. 118, pp. xix–xx). Academic Press.

Generation and Implementation of Reporter BHK-21 Cells for Live Imaging of Flavivirus Infection

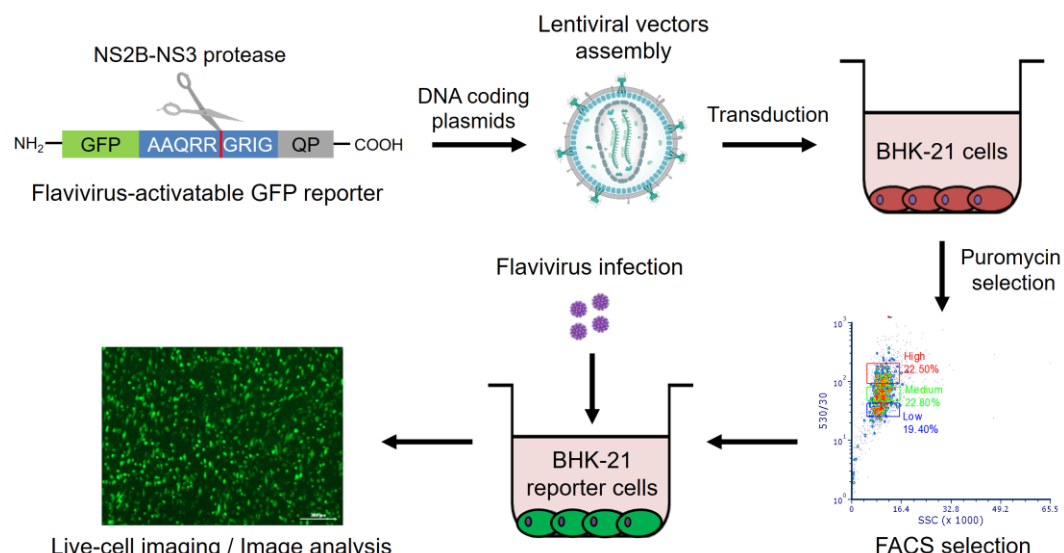
Jorge L. Arias-Arias and Rodrigo Mora-Rodríguez*

Centro de Investigación en Enfermedades Tropicales, Facultad de Microbiología, Universidad de Costa Rica, San José, 11501-2060, Costa Rica

*For correspondence: rodrigo.morarodriguez@ucr.ac.cr

[Abstract] The genus *Flavivirus* within the family Flaviviridae includes many viral species of medical importance, such as yellow fever virus (YFV), Zika virus (ZIKV), and dengue virus (DENV), among others. Presently, the identification of flavivirus-infected cells is based on either the immunolabeling of viral proteins, the application of recombinant reporter replicons and viral genomes, or the use of cell-based molecular reporters of the flaviviral protease NS2B-NS3 activity. Among the latter, our flavivirus-activatable GFP and mNeptune reporters contain a quenching peptide (QP) joined to the fluorescent protein by a linker consisting of a cleavage site for the flavivirus NS2B-NS3 proteases (AAQRRRGRIG). When the viral protease cleaves the linker, the quenching peptide is removed, and the fluorescent protein adopts a conformation promoting fluorescence. Here we provide a detailed protocol for the generation, selection and implementation of stable BHK-21 cells expressing our flavivirus genetically-encoded molecular reporters, suitable to monitor the viral infection by live-cell imaging. We also describe the image analysis procedures and provide the required software pipelines. Our reporter cells allow the implementation of single-cell infection kinetics as well as plaque assays for both reference and native strains of flaviviruses by live-cell imaging.

Graphic abstract:



Workflow for the generation and implementation of reporter BHK-21 cells for live imaging of flavivirus infection.

Keywords: Flavivirus, Fluorescence, NS2B-NS3, Protease, Live-cell imaging, Reporter cells, Plaque assay, Image analysis

[Background] Flaviviruses represent an emerging and re-emerging global threat that cause diseases both in animals and humans, including many medically relevant viruses like yellow fever virus (YFV), West Nile virus (WNV), Japanese encephalitis virus (JEV), dengue virus (DENV), and Zika virus (ZIKV), among others (Gould and Solomon, 2008). At present, the detection of flavivirus-infected cells is based on either the antibody labeling of viral proteins (Balsitis *et al.*, 2008), the use of recombinant reporter replicons and viral genomes (Li *et al.*, 2013; Schmid *et al.*, 2015; Xie *et al.*, 2016; Tamura *et al.*, 2017; Kümmerer, 2018), or the application of genetically-encoded molecular reporters of the flavivirus NS2B-NS3 proteolytic activity (Medin *et al.*, 2015; Hsieh *et al.*, 2017; McFadden *et al.*, 2018). Immunolabeling implies both fixation and permeabilization which hamper their implementation for studies in living cells. Reporter replicons and viral genomes are suitable for live-cell imaging assays, but they are restricted to particular molecular clones mainly derived from reference strains and thus, not applicable when working with clinical isolates or native viral strains. In this context, cell-based molecular reporters of the flaviviral proteases constitute a favorable alternative for the study of native flavivirus strains by live-cell imaging. Based on our recently published flavivirus-activatable GFP (FlaviA-GFP) and flavivirus-activatable mNeptune (FlaviA-mNeptune) reporters (Arias-Arias *et al.*, 2020), here we describe in detail a protocol for the generation, selection, and implementation of stably-transduced reporter BHK-21 cells for live imaging of flavivirus infection in single cells and viral plaques. Furthermore, we provide a rationale for a software-based image analysis approach to demonstrate the capabilities of this reporter cell line for single-cell and viral-plaque tracking. In addition, we include the optimized CellProfiler analysis pipelines for studies employing this or other cell-based reporters. Our approach represents the first fluorescence activatable cell-based reporter system for monitoring the kinetics of infection by both reference and native strains of flaviviruses like DENV, ZIKV, and YFV using live-cell imaging.

Materials and Reagents

1. Cell culture flasks, 75 cm² (Greiner Bio-One, CELLSTAR®, catalog number: 658175)
2. Cell culture dishes, 100/20 mm (Greiner Bio-One, CELLSTAR®, catalog number: 664160)
3. 2 ml reaction tubes (Greiner Bio-One, catalog number: 623201)
4. 3 ml sterile syringes (Ultident Scientific, catalog number: BD-309657)
5. Syringe filters 0.2 µm hydrophilic polyethersulfone, 32 mm diameter (Pall, Acrodisc®, catalog number: 4652)
6. 10 ml sterile syringes (Ultident Scientific, catalog number: BD-302995)
7. Syringe filters 0.45 µm hydrophilic cellulose acetate, 28 mm diameter (Sartorius, Minisart®, catalog number: 16555)

8. 15 ml conical tubes (Greiner Bio-One, CELLSTAR®, catalog number: 188271)
9. 0.5 ml reaction tubes (Greiner Bio-One, catalog number: 667201)
10. Hexadimethrine bromide (Merck, Sigma-Aldrich, catalog number: H9268)
11. 48-well cell culture plates (Greiner Bio-One, CELLSTAR®, catalog number: 677180)
12. 1.5 ml reaction tubes (Greiner Bio-One, catalog number: 616201)
13. 12-well cell culture plates (Greiner Bio-One, CELLSTAR®, catalog number: 665180)
14. 1.5 ml light protection reaction tubes (Greiner Bio-One, catalog number: 616283)
15. Cell culture flasks, 25 cm² (Greiner Bio-One, CELLSTAR®, catalog number: 690175)
16. 6-well cell culture plates (Greiner Bio-One, CELLSTAR®, catalog number: 657160)
17. 96-well black cell culture plates (Greiner Bio-One, μCLEAR®, catalog number: 655096)
18. 24-well cell culture plates (Greiner Bio-One, CELLSTAR®, catalog number: 662160)
19. HEK 293T cells (ATCC, catalog number: CRL-3216)
20. Plasmids:
 - pLenti-FlaviA-GFP-puro (a gift from Jorge L. Arias-Arias, Addgene plasmid #140088)
 - pLenti-CMV-FlaviA-mNeptune-puro (a gift from Jorge L. Arias-Arias, Addgene plasmid #140091)
 - pMD2.G (a gift from Didier Trono, Addgene plasmid #12259)
 - psPAX2 (a gift from Didier Trono, Addgene plasmid #12260)
21. LB agar plates with 100 µg/ml ampicillin (Merck, Sigma-Aldrich, catalog number: L5667)
22. LB broth (Miller) (Merck, Sigma-Aldrich, catalog number: L2542)
23. 100 mg/ml ampicillin solution (Merck, Sigma-Aldrich, catalog number: A5354)
24. NucleoSpin plasmid mini kit (Macherey-Nagel, catalog number: 740588.50)
25. DMEM, high glucose, GlutaMAX™, pyruvate (Thermo Fisher Scientific, Gibco, catalog number: 10569044)
26. Antibiotic-antimycotic 100× (Thermo Fisher Scientific, Gibco, catalog number: 15240062)
27. Fetal bovine serum (FBS) qualified, heat inactivated (Thermo Fisher Scientific, Gibco, catalog number: 10438-026)
28. Polyethylenimine (PEI), linear, MW 25000, transfection grade (Polysciences, PEI 25K™, catalog number: 23966-1)
29. UltraPure™ DNase/RNase-free distilled water (Thermo Fisher Scientific, Invitrogen, catalog number: 10977015)
30. Hydrochloric acid, 36.5-38.0%, BioReagent (Merck, Sigma-Aldrich, catalog number: H1758)
31. BHK-21 [C-13] (ATCC, catalog number: CCL-10)
32. MEM, GlutaMAX™ supplement (Thermo Fisher Scientific, Gibco, catalog number: 41090101).
33. Sodium pyruvate, 100 mM (Thermo Fisher Scientific, Gibco, catalog number: 11360070).
34. PBS, pH 7.4 (Thermo Fisher Scientific, Gibco, catalog number: 10010023).
35. TrypLE™ express enzyme (1×), no phenol red (Thermo Fisher Scientific, Gibco, catalog number: 12604013)
36. Puromycin dihydrochloride from *Streptomyces alboniger* (Merck, Sigma-Aldrich, catalog number: P8833)

37. Clinical isolate DENV-2/CR/13538/2007 (Instituto Costarricense de Investigación y Enseñanza en Nutrición y Salud, Cartago, Costa Rica) (Soto-Garita *et al.*, 2016)
38. Vaccine strain YFV/US/17D/1937 (Sanofi Pasteur, YF-VAX®)
39. FluoroBrite™ DMEM (Thermo Fisher Scientific, Gibco, catalog number: A1896701)
40. GlutaMAX™ supplement (Thermo Fisher Scientific, Gibco, catalog number: 35050061)
41. Minimum essential medium eagle AutoMod™ (Merck, Sigma-Aldrich, catalog number: M0769)
42. Carboxymethylcellulose sodium salt (Merck, Sigma-Aldrich, catalog number: C4888)
43. Sodium bicarbonate (Merck, Sigma-Aldrich, catalog number: S5761)
44. Complete DMEM (see Recipes)
45. PEI solution (1 mg/ml) (see Recipes)
46. Polybrene solution (10 mg/ml) (see Recipes)
47. Complete MEM (see Recipes)
48. PBS 1% FBS (see Recipes)
49. Puromycin solution (10 mg/ml) (see Recipes)
50. FluoroBrite™ DMEM 2% FBS (see Recipes)
51. Plaque media 2% FBS (see Recipes)

Equipment

1. Biological safety cabinet (ESCO, Labculture® Class II, Type A2, catalog number: LA2-3A2-E)
2. CO₂ incubator (Thermo Scientific, model: Forma Series II, catalog number: 3110)
3. 4 °C refrigerator (Thermo Scientific, Value Lab, catalog number: 20LREETSA)
4. -20 °C freezer (Thermo Scientific, Value Lab, catalog number: 20LFEETSA)
5. -80 °C freezer (Sanyo, VIP series, catalog number: MDF-U32V)
6. Water bath (PolyScience, catalog number: WBE20A12E)
7. Centrifuge (Eppendorf, model: 5810)
8. Microcentrifuge (Eppendorf, model: 5418)
9. Pipettes (Thermo Scientific, Finnpipette™ F2 GLP Kit, catalog number: 4700880)
10. Pipet filler (Thermo Scientific, S1, catalog number: 9511)
11. Hemocytometer (Boeco, Neubauer improved, catalog number: BOE 13)
12. Shaking incubator (Shel Lab, catalog number: SSI3)
13. ThermoMixer® C block (Eppendorf, catalog number: 5382000015)
14. Vortex mixer (Thermo Scientific, MaxiMix™, catalog number: M16715Q)
15. Ultraviolet crosslinker (UVP, CL-100, catalog number: UVP95017401)
16. NanoDrop™ 2000 spectrophotometer (Thermo Scientific, catalog number: ND-2000)
17. Steam sterilizer (Yamato, catalog number: SQ510)
18. Water purification system (Merck, Milli-Q advantage A10)
19. Inverted microscope (Nikon, Eclipse, catalog number: TS100)
20. Flow cytometer (BD Biosciences, BD Accuri™ C6)

21. Cell sorter (BD Biosciences, BD FACSJazz™)
22. Automated fluorescence microscope (Biotek, Lionheart FX) with:
 - CO₂ gas controller (Biotek, catalog number: 1210012)
 - Humidity chamber (Biotek, catalog number: 1450006)
 - 4× objective (Biotek, catalog number: 1220519)
 - 20× objective (Biotek, catalog number: 1220517)
 - GFP filter cube (Biotek, catalog number: 1225101)
 - 465 nm LED cube (Biotek, catalog number: 1225001)
 - Cy5 filter cube (Biotek, catalog number: 1225105)
 - 623 nm LED cube (Biotek, catalog number: 1225005)

Software

1. Gen5 Image+ (Biotek, <https://www.biotek.com>)
2. CellProfiler 4.0 (Broad Institute, <https://cellprofiler.org/releases>)

Procedure

A. Lentiviral vectors assembly and titration

Assembly

1. Prepare plasmid stocks following standard molecular biology procedures (<https://www.jove.com/v/5062/plasmid-purification>) and the protocol provided by the manufacturer of the NucleoSpin plasmid mini kit (Macherey-Nagel).
2. Manually seed 6,000,000 HEK 293T cells in 100/20 mm cell culture dishes with 8 ml of DMEM 10% FBS (Recipe 1) and incubate overnight at 37 °C and 5% CO₂ to reach 70-80% confluency. For a detailed procedure of seeding cells please refer to the bio-protocol paper by Freppel *et al.*, 2018 (reference 3).
3. Using a pipette, replace the medium by removing and discarding all the DMEM 10% FBS in the dishes (~8 ml) and adding 4 ml of fresh DMEM 2% FBS (Recipe 1).
4. Prepare the transfection mix as follows:
Suspension A: 45 µl PEI 1 mg/ml (Recipe 2) + 955 µl unsupplemented DMEM (without FBS and antibiotic-antimycotic).
Suspension B: 6 µg pLenti-FlaviA-GFP-puro or pLenti-CMV-FlaviA-mNeptune-puro + 6 µg pMD2.G + 6 µg psPAX2 and bring to 1,000 µl with unsupplemented DMEM.
Mix suspensions A with B and incubate for 15 min at room temperature.
5. Add the 2 ml transfection mix to the cells (dropwise) and incubate overnight at 37 °C and 5% CO₂.
6. Replace the medium with 6 ml of fresh DMEM 2% FBS and incubate for 48 h at 37 °C and 5% CO₂.

7. Harvest culture supernatants and filter them (0.45- μ m pore size) to eliminate cells and debris. Use filters with low protein adherence, like cellulose acetate or polyethersulfone (PES). Do not use nitrocellulose filters as they could bind the lentiviral particles.
8. Prepare 500 μ l aliquots and store at -80 °C.

Titration

1. As described above, seed 50,000 BHK-21 cells per well in a 48-well cell culture plate with 500 μ l/well of MEM 2% FBS (Recipe 4) and incubate overnight at 37 °C and 5% CO₂. Prepare extra wells to be used as control cells.
2. Thaw in a water bath (37 °C) one of the lentiviral 500 μ l stock aliquots and add polybrene (Recipe 3) at a final concentration of 5 μ g/ml.
3. Prepare 10-fold serial dilutions (10⁻¹-10⁻⁶) of the lentiviral stock in 1.5 ml reaction tubes. Start mixing 50 μ l of the lentiviral particles in 450 μ l of DMEM 2% FBS + 5 μ g/ml polybrene (10⁻¹). Vortex the tube for 5 s and mix 50 μ l of the 10⁻¹ lentiviral dilution in 450 μ l of DMEM 2% FBS + 5 μ g/ml polybrene (10⁻²). Repeat this procedure for the other dilutions (10⁻³-10⁻⁶) and incubate for 15 min at room temperature. Change the tip between dilutions to avoid cross-contamination. For a detailed and graphical explanation of 10-fold serial dilutions preparation please refer to the bio-protocol paper by Freppel *et al.*, 2018 (reference 3).
4. Replace the medium of the cells with 150 μ l/well of undiluted lentiviral stock and each serial dilution thereof. Add 150 μ l/well of DMEM 2% FBS + 5 μ g/ml polybrene to the control cells. To avoid cross contamination, make the inoculation of the samples in order, starting with the control, following with the serial dilutions (from higher to lower dilution), and ending with the undiluted lentiviral stock.
5. Centrifuge at 300 \times g for 2 h at 25 °C for viral adsorption.
6. Replace the inoculum with 500 μ l/well of DMEM 2% FBS and incubate for 48 h at 37 °C and 5% CO₂.
7. Discard the medium, wash the cells once with 100 μ l/well of PBS, add 100 μ l/well of TrypLE™ express (no phenol red), incubate for 5 min at 37 °C, and resuspend the cells with 400 μ l/well of PBS 1% FBS (Recipe 5).
8. Based on the basal background of the reporter proteins and by comparison with the non-transduced control cells (Figure 1), determine by flow cytometry the percentage of GFP+ (488 nm laser - 530/30 nm filter) or mNeptune+ (640 nm laser - 675/25 nm filter) cells present in the samples infected with different dilutions of the lentiviral seed. For a detailed procedure about flow cytometry of fluorescent proteins please refer to the protocol by Hawley *et al.*, 2004 (reference 5).
9. Using the data of the higher dilution with detectable transduced cells, calculate the biological titer in transducing units per milliliter (TU/ml), applying the following formula:

$$\text{TU/ml} = (P \times N / 100 \times V) \times 1/DF$$

where P = % GFP+ or mNeptune+ cells, N = number of cells at transduction = 50,000, V = volume of inoculum per well = 0.15 ml, and DF = dilution factor = 1 (undiluted), 10^{-1} (diluted 1/10), 10^{-2} (diluted 1/100), and so on (Tiscornia *et al.*, 2006).

B. Reporter cell lines production and selection

Production

1. As described above, seed 100,000 BHK-21 cells per well in a 12-well cell culture plate with 1 ml/well of MEM 2% FBS and incubate overnight at 37 °C and 5% CO₂. Prepare an extra well for the control cells.
2. Thaw in a water bath (37 °C) one of the 500 µl stock aliquots of lentiviral particles carrying genetic constructs codifying for either the FlaviA-GFP or the FlaviA-mNeptune reporters and add polybrene at a final concentration of 5 µg/ml.
3. Based on the previously calculated biological titer in TU/ml, prepare 500 µl/well of lentiviral inoculum at a multiplicity of infection (MOI) of 1 (1 TU per cell). As 100,000 cells per well were plated in maintenance medium (MEM 2% FBS), 100,000 TU must be diluted in MEM 2% FBS + 5 µg/ml polybrene to a final volume of 500 µl. Incubate for 15 min at room temperature.
4. Replace the medium of the cells with the 500 µl/well of lentiviral inoculum. Add 500 µl/well of MEM 2% FBS + 5 µg/ml polybrene to the control cells.
5. Centrifuge at 300 × g for 2 h at 25 °C for viral adsorption.
6. Replace the inoculum with 1 ml/well of MEM 2% FBS and incubate for 48 h at 37 °C and 5% CO₂.
7. Based on the basal background of the reporter proteins, monitor the effectiveness of the transduction by fluorescence microscopy in the green/GFP (FlaviA-GFP) and far-red/Cy5 (FlaviA-mNeptune) channels.

Selection

1. For the antibiotic selection of transduced cells, replace the medium with 750 µl/well of MEM 10% FBS containing 8 µg/ml of puromycin (Recipe 6) and incubate overnight at 37 °C and 5% CO₂. Apply the same treatment to the control cells.
2. Replace the medium of both transduced and control cells with 1 ml/well of MEM 10% FBS containing 4 µg/ml of puromycin. Incubate at 37 °C and 5% CO₂ until 100% mortality of the control cells is evidenced by light microscopy (commonly 24-48 h).
3. Replace the medium of the selected cells with 1 ml/well of MEM 10% FBS + 0.5 µg/ml puromycin and incubate at 37 °C and 5% CO₂ until reaching confluence of 80-90%.
4. Passage the selected cells to 25 cm² culture flasks with 5 ml of MEM 10% FBS + 0.5 µg/ml puromycin and incubate at 37 °C and 5% CO₂ until reaching a confluence of 80-90% (<https://www.jove.com/v/5052/passaging-cells>).

5. For the FACS selection, discard the medium, wash the cells once with 1 ml of PBS, add 500 μ l of TrypLETM express (no phenol red), incubate for 5 min at 37 °C, and resuspend the cells with 1 ml of PBS 1% FBS.
6. Count the cells with a hemocytometer (<https://www.jove.com/v/5048/using-a-hemacytometer-to-count-cells>) and prepare 2 ml of cell suspensions at 1,000,000 cells/ml in PBS 1% FBS.
7. Aspirate the cell suspensions into the cell sorter. For the FlaviA-GFP reporter isolate at least two cell subpopulations with different but homogeneous levels of the reporter's basal background using the FL1 detector (488 nm laser - 530/30 nm filter) (Figure 1). Apply the same procedure to the FlaviA-mNeptune reporter but using the FL4 detector (640 nm laser - 675/25 nm filter).

Note: The basal background of the FlaviA-GFP and FlaviA-mNeptune reporters make them sensitive to the levels of cellular expression: If the expression is too high the background will mask the signal produced upon activation of the reporters. If the expression is too low there will not be enough reporter's signal over the background.

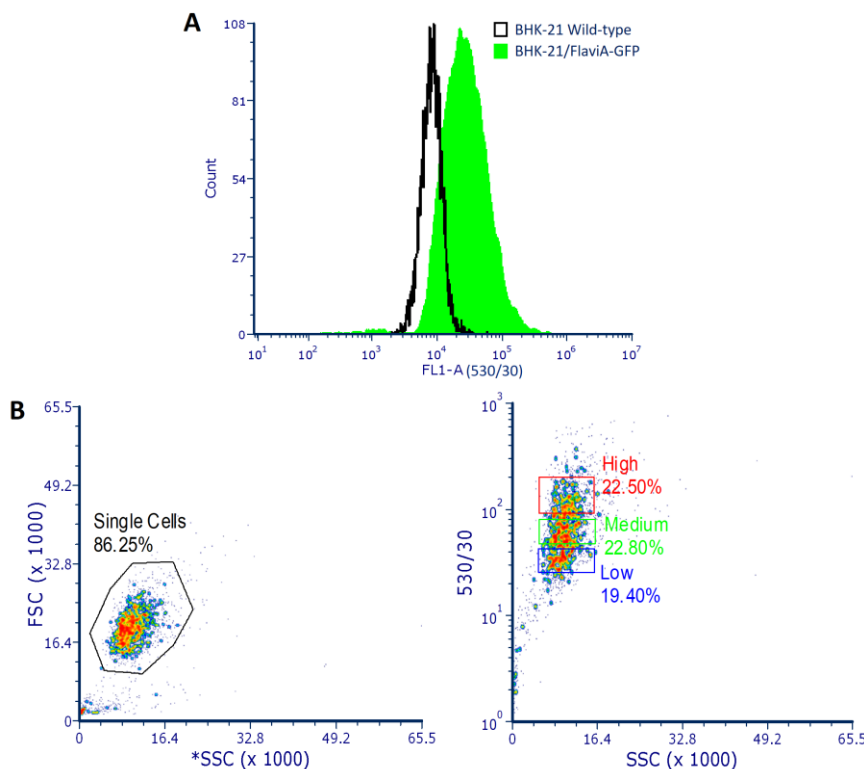


Figure 1. FACS analysis of BHK-21/FlaviA-GFP stable cells. A. Histogram showing the difference in the green fluorescence (FL1 detector- 530/30 nm filter) between wild-type and reporter BHK-21 cells due to the basal background of the FlaviA-GFP reporter proteins. B. Scatter plots showing the heterogeneity in the population of stable BHK-21 cells with different levels of expression of the FlaviA-GFP reporter. For the selection of the best reporter cells

(highest signal-to-noise ratio), at least two cell subpopulations with different (low, medium or high) but homogeneous levels of the reporter's basal background must be isolated and tested by live-cell imaging upon flavivirus infection.

8. Seed the isolated cell subpopulations in different wells of a 48-well cell culture plate with 1 ml/well of MEM 10% FBS + 0.5 µg/ml puromycin and incubate at 37 °C and 5% CO₂ until reaching a confluence of 80-90%.
9. Passage the selected cells to a 6-well cell culture plate with 3 ml of MEM 10% FBS + 0.5 µg/ml puromycin and incubate at 37 °C and 5% CO₂ until reaching a confluence of 80-90%.
10. Test the different isolated cell subpopulations by a live-cell imaging flavivirus infection kinetics according to the protocol described in Procedure C.

Note: The best reporter cells will be those with the highest signal-to-noise ratio upon flavivirus infection. The fluorescence signal-to-noise ratio is calculated by dividing the signal of the reporter cells treated with infectious virus by the noise given by the reporter cells treated with UV-inactivated virus at the same post-inoculation time.

C. Infection kinetics in reporter cells by live-cell imaging

1. Prepare and titer the flaviviral seed of your choice (e.g., DENV, ZIKV, or YFV) according to standard virological methodologies (Medina *et al.*, 2012; Freppel *et al.*, 2018). For viral inactivation, place 200 µl/well of the flaviviral seed in a 24-well cell culture plate, remove the lid and apply 5 cycles of UV light (254 nm) exposure at an energy of 400,000 µJ/cm² into an ultraviolet crosslinker. Between cycles, shake the plate for 5 s using your hands.
2. As described above, seed 15,000 BHK-21/FlaviA-GFP stable cells per well in a µClear black 96-well plate with 100 µl/well of MEM 2% FBS and incubate overnight at 37 °C and 5% CO₂.
3. Based on the calculated titer of the flaviviral seed in plaque forming units (PFU)/ml, prepare 50 µl/well of inoculum at a low MOI (between 0.1 and 0.25). As 15,000 cells per well were plated in maintenance medium, between 1,500 and 3,750 PFUs must be diluted in MEM 2% FBS to a final volume of 50 µl/well. Multiply for the total number of wells to be inoculated and prepare a single inoculum suspension. Likewise, prepare the UV-inactivated inoculum suspension.
4. Replace the medium of the cells with 50 µl/well of either the infectious or the UV-inactivated flaviviral inoculum and incubate for 2 h at 37 °C and 5% CO₂ for viral adsorption. Using your hands, shake the plate for 5 s every 15 min.
5. Replace the inoculum with 150 µl/well of FluoroBrite™ DMEM 2% FBS (Recipe 7) and incubate for the desired time of your kinetics (e.g., 120 h) at 37 °C and 5% CO₂ into the automated fluorescence microscope. Add 200 µl/well of PBS to the surrounding wells to avoid desiccation.
6. Using your microscope's software (e.g., Gen5 Image+), program the image acquisition with the 4× or the 20× objective in the green/GFP channel at the desired post-infection times (Figure 2A).

Note: The acquisition parameters (excitation intensity, exposure time, and camera gain) of the

images are variable according to the particular reporter cell subpopulation isolated by FACS. Always include an extra well of control cells for the adjustment of the acquisition parameters as the overexposure to the excitation light may harm the cells of the experimental conditions. Our recommendation is to set those parameters to a level where the background signal of the reporter proteins is just perceptible in the first images of the kinetics, in order to increase the dynamic range of the reporter's fluorescence upon activation by flaviviral proteases.

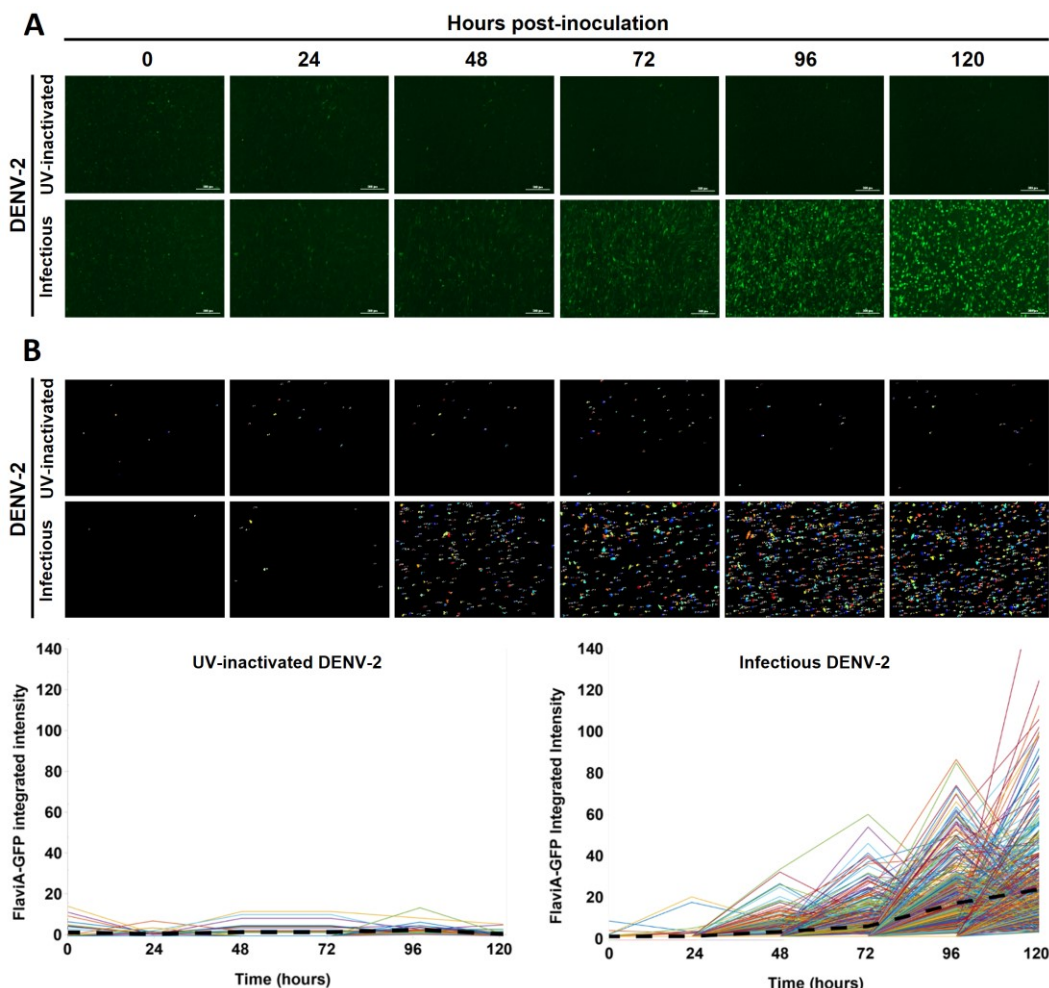


Figure 2. DENV-2 infection kinetics in reporter BHK-21 cells by live-cell imaging. A. Stable BHK-21 cells expressing the FlaviA-GFP reporter were inoculated with either infectious or UV-inactivated DENV-2 13538 at a low MOI of 0.1 and captured by live-cell imaging at the specified time periods. Magnification of 40×, scale bar = 100 μm. B. The image analysis of the infection kinetics with the software CellProfiler 4.0 allowed the tracking of single cells over time based on the reported fluorescence (each colored line in the graphs corresponds to an individual cell). The black dashed lines represent the mean values of cell fluorescence.

D. Kinetic plaque assay in reporter cells by live-cell imaging

- As described above, seed 25,000 BHK-21/FlaviA-mNeptune stable cells per well in a μClear

black 96-well plate with 100 µl/well of MEM 10% FBS and incubate overnight at 37 °C and 5% CO₂.

2. Prepare 10-fold serial dilutions (10⁻¹-10⁻⁶) of the flaviviral seed in 1.5 ml reaction tubes. Start mixing 50 µl of the flaviviral seed in 450 µl of MEM 2% FBS (10⁻¹). Vortex the tube for 5 s and mix 50 µl of the 10⁻¹ flaviviral dilution in 450 µl of MEM 2% FBS (10⁻²). Repeat this procedure for the other dilutions (10⁻³-10⁻⁶). Change the tip between dilutions to avoid cross-contamination. For a detailed and graphical explanation of 10-fold serial dilutions preparation please refer to the bio-protocol paper by Freppel *et al.*, 2018 (reference 3).
3. Replace the medium of the cells with 50 µl/well of each serial dilution of the flaviviral seed. Inoculate a control well with 50 µl of UV-inactivated flaviviral seed. Incubate for 2 h at 37 °C and 5% CO₂ for viral adsorption. Using your hands, shake the plate for 5 s every 15 min.
4. Replace the inoculum with 150 µl/well of plaque media 2% FBS (Recipe 8) and incubate for 120 h at 37 °C and 5% CO₂ into the automated fluorescence microscope. Add 200 µl/well of PBS to the surrounding wells to avoid desiccation.
5. Using your microscope's software (e.g., Gen5 Image+), program the image acquisition (a montage of the whole well) with the 4× objective in the far-red/Cy5 channel at the desired post-infection times (Figure 3A).

Note: The acquisition parameters (excitation intensity, exposure time, and camera gain) of the images are variable according to the particular reporter cell suppopulation isolated by FACS. Always include an extra well of control cells for the adjustment of the acquisition parameters, as the overexposure to the excitation light may harm the cells of the experimental conditions. Our recommendation is to set those parameters to a level where the background signal of the reporter proteins is just perceptible in the first images of the kinetics, in order to increase the dynamic range of the reporter's fluorescence upon activation by flaviviral proteases.

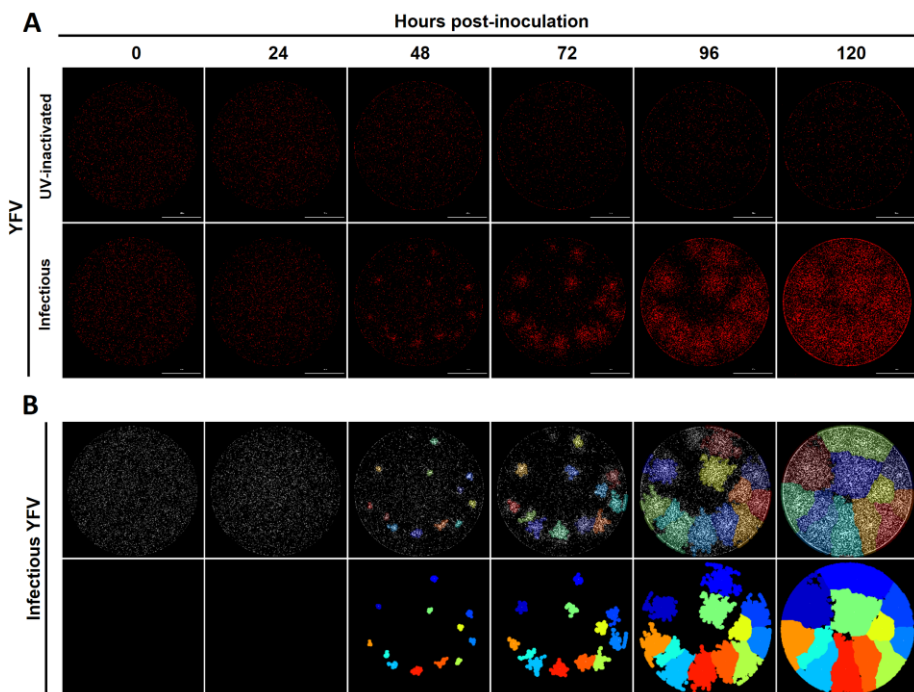
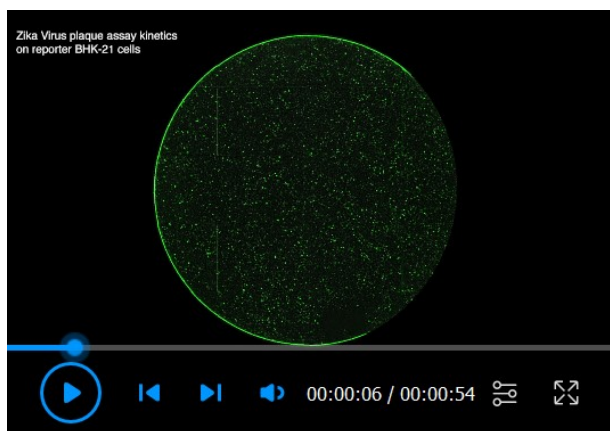


Figure 3. YFV kinetic plaque assay in reporter BHK-21 cells by live-cell imaging. A. Stable BHK-21 cells expressing the FlaviA-mNeptune reporter were inoculated with decimal dilutions (10^{-1} - 10^{-6}) of either infectious or UV-inactivated YFV 17D. After addition of plaque media 2% FBS, entire wells of the plate were captured by live-cell imaging at the specified time periods. Magnification of 40 \times , scale bar = 1,000 μ m. B. The image analysis of the kinetic plaque assay with the software CellProfiler 4.0 allowed the identification of single viral plaques (upper panel) and the tracking of those plaques over time (lower panel). For a deeper exemplification of the results obtained with our kinetic plaque assay please watch the live-cell imaging video (Video 1).



Video 1. ZIKV plaque assay kinetics on reporter BHK-21 cells

Data analysis

A. Infection kinetics in reporter cells

Single cell tracking of infected cells based on its fluorescence (Figure 2B) was performed using our CellProfiler pipeline for single cell analysis (“SingleCellsTracking.cppproj”, Figure 4). To perform this analysis just drag and drop the images in the *Images* module and press *Analyze Images*. In order to modify the pipeline for your cells and conditions, go to *Start Test Mode*, adjust the parameters described in the modules (one by one) and press *Step* to see the output of the modifications applied to a particular module. Once all the modifications are ready, press *Exit Test Mode* and go to *Analyze Images*. The modules contained in the single cell analysis pipeline are the following:

1. *Images*: Simply drag and drop the image files of a time series in the *Images* module. Make sure that the name of all the files in the dataset do include the name of the channel where the fluorescence was measured (e.g., GFP) and the increasing consecutive numbers for time-lapse microscopy images (e.g., GFP_72h).
2. *NamesAndTypes*: Select the rule criteria with an expression contained in the name of all the files in the dataset, in this case, indicating the channel of the fluorescence (e.g., GFP). For each file of the dataset it creates an image called “Sensor”.

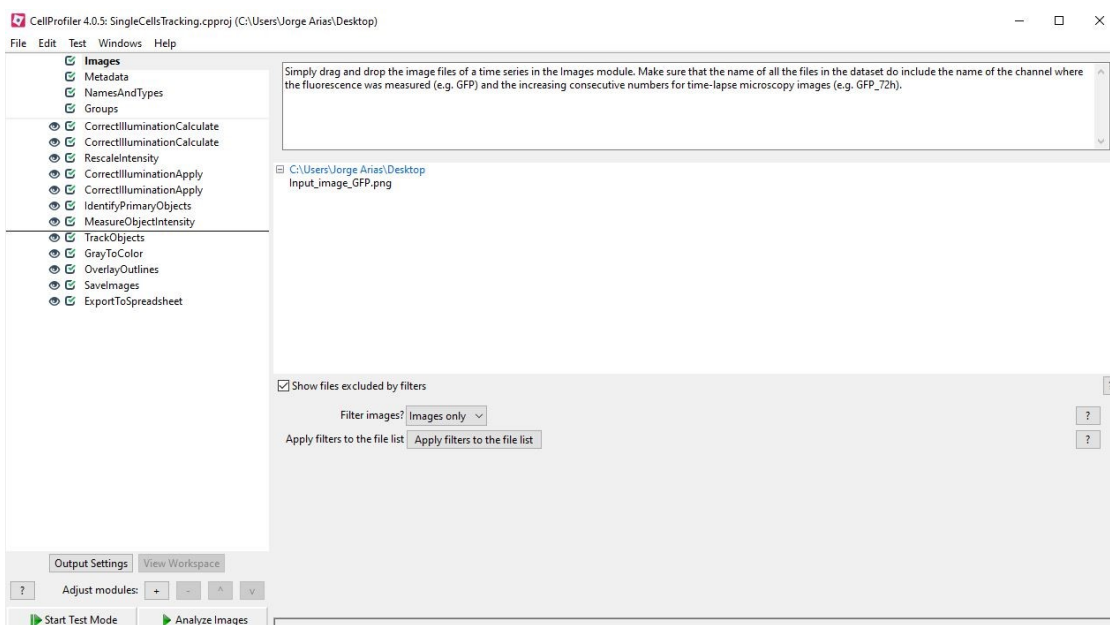


Figure 4. CellProfiler image analysis pipeline for single cell tracking of flavivirus infected BHK-21/FlaviA-GFP reporter cells

3. *CorrectIlluminationCalculate (Illumination function calculation: Regular)*: From the “Sensor” image, this module calculates a regular illumination correction function and creates an image with enhanced contrast, named “IllumSensor”.
4. *CorrectIlluminationCalculate (Illumination function calculation: Background)*: From the “Sensor”

image, this module calculates a background-based illumination function called “IllumSensorbackground”.

5. *RescaleIntensity*: Converts the output image of the regular illumination function (“IllumSensor”) to an image with rescaled intensity (“RescaleSensor”).
6. *CorrectIlluminationApply*: This module applies the “IllumSensorbackground” correction function to the “RescaleSensor” image and generates an enhanced image named “CorrSensor”.
7. *CorrectIlluminationApply*: This second module of correction works on the original “Sensor” image, applies the “IllumSensorbackground” correction function but keeping the original intensity values and generates an output image called “mSensor”.
8. *IdentifyPrimaryObjects*: This module works with the enhanced image “CorrSensor” to identify the objects *Cells*. You may modify the *Typical diameter* to obtain the correct cell segmentation with other cell lines or parameters.
9. *MeasureObjectIntensity*: Measures the intensities of the identified objects *Cells* but on the image with the original intensity values only corrected by illumination (“mSensor”).
10. *TrackObjects*: This module tracks cells over the time-lapse microscopy and generates an output image called “TrackedCells”.
11. *GraytoColor*, *OverlayOutlines*, *SaveImages*: These modules create and save color images with the outlines of the primary objects identification for documentation and validation of the cell segmentation by the researcher’s eye and criteria.
12. *ExportToSpreadsheet*: Saves the selected measurements to an excel spreadsheet (e.g., Integrated intensity).

Note: Together with this protocol we supply the Zip file “[SingleCellsTracking pipeline and dataset](#)” which contains the applied pipeline (“SingleCellsTracking.cpproj”) and an example dataset composed of a single input image to run the pipeline (“Input_image_GFP”) and two output files to corroborate the expected results (“Output_image_GFP” and “Infected_Cells”).

B. Kinetic plaque assay in reporter cells

The identification and tracking of viral plaques were performed using two different pipelines programmed in CellProfiler. For single-plaque recognition use our “PlaqueIdentification.cpproj” pipeline (Figure 5) to generate images such as those depicted in the upper panel of Figure 3B. To track the plaques over a time series and determine the cell counts for every recognized plaque, first apply the “PlaqueIdentification.cpproj” pipeline to generate an image with the identified plaques and then use that image and the “PlaqueTracking.cpproj” pipeline (Figure 6) to obtain tracking images such as those showed in the lower panel of Figure 3B. Depending on the cell type and/or density, some modifications to several parameters may be done for an optimal plaque identification using the option *Start Test Mode* and running each module step by step. The modules of the above mentioned pipelines are the following:

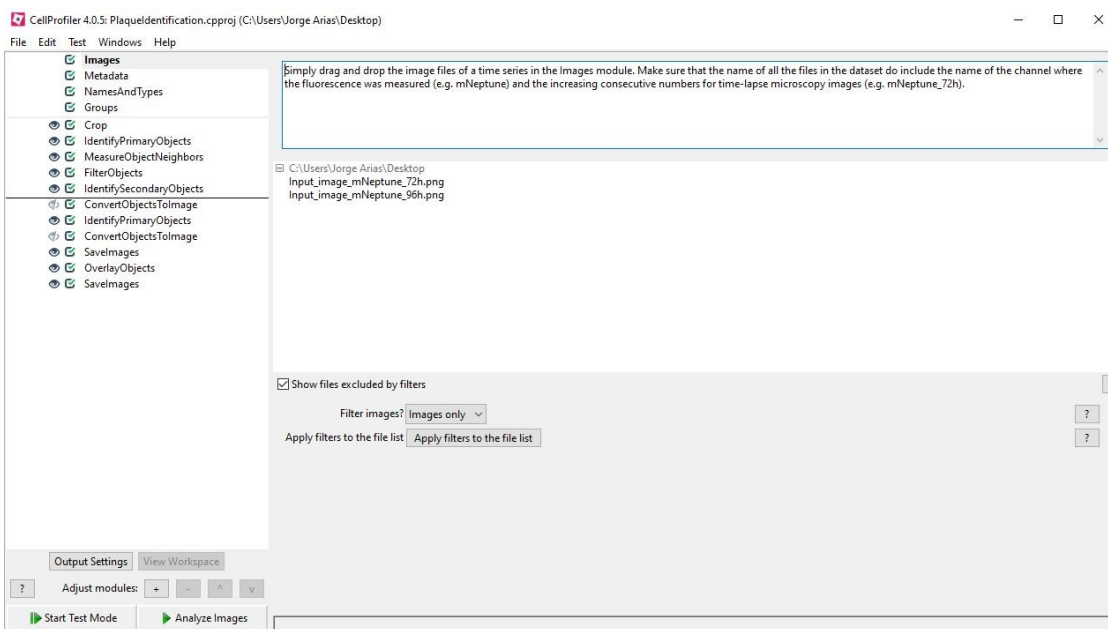


Figure 5. CellProfiler image analysis pipeline for flaviviral plaques identification in BHK-21/mNeptune reporter cells

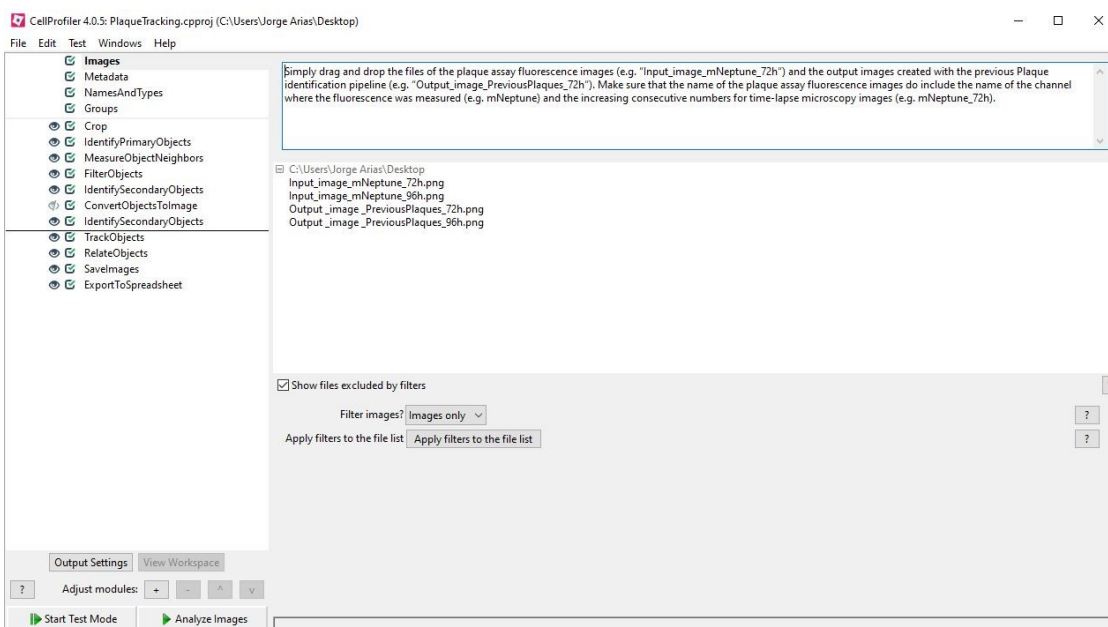


Figure 6. CellProfiler image analysis pipeline for flaviviral plaques tracking in BHK-21/mNeptune reporter cells

Plaque identification pipeline

1. *Images*: Simply drag and drop the image files of a time series in the *Images* module. Make sure that the name of all the files in the dataset do include the name of the channel where the fluorescence was measured (e.g. mNeptune) and the increasing consecutive numbers for time-lapse microscopy images (e.g. mNeptune_72h).

fluorescence was measured (e.g., mNeptune) and the increasing consecutive numbers for time-lapse microscopy images (e.g., mNeptune_72h).

2. *NamesAndTypes*: Select the rule criteria with an expression contained in the name of all the files in the dataset, in this case, indicating the channel of the fluorescence (e.g., mNeptune). For each file of the dataset it creates an image called “Sensor”.
3. *Crop*: This is an optional module in case you need to remove part of the image (e.g., distance bars). It generates an output image named “CropSensor”.
4. *IdentifyPrimaryObjects*: This module identifies the individual objects *Nuclei* from the “CropSensor” image. You may need to change the *Typical diameter of objects* or the *Threshold strategy* and its parameters to obtain an optimal identification of your cells.
5. *MeasureObjectNeighbors*: Measures the number of neighbors for each *Nuclei* object within a specified *Neighbor distance*. You may need to modify this parameter to obtain a good optimal range of neighbor numbers to differentiate the plaque-belonging cells from the surrounding cells. This module creates an image called “ObjectNeighborCount”.
6. *FilterObjects*: This module sets a threshold to identify plaque-belonging *Nuclei* objects using the range of number of neighbors calculated in the previous module. You may need to set this *Minimum value* according to the range of neighbors for an optimal identification of plaque belonging *Nuclei* objects. It generates the output objects *FilteredNuclei*.
7. *IdentifySecondaryObjects*: Extends the above *FilteredNuclei* by a determined number of pixels to fill the gaps between the plaque-belonging cells in the “CropSensor” image. You may need to modify the *Number of pixels by which to expand the primary objects* in order to fill most of the gaps. This module identifies the output objects *Cells*.
8. *ConvertObjectstolImage*: The expanded *Cells* objects constitute the basis to create a new image named “CellImage”.
9. *IdentifyPrimaryObjects*: Uses the previous “CellImage” to identify the new *Plaque* objects. You may need to modify the range of *Typical diameter of objects* to obtain the correct plaque identification with images from different post-infection times, as shown in the colored frame *Plaque*, within the visual output generated by this module. In such an instance images must be analyzed one by one, like in the case of our example dataset.
10. *ConvertObjectstolImage*: Converts the *Plaque* objects to an image called “PlaqueImage”.
11. *SaveImages*: Uses the “PlaqueImage” to create and save an image called “Output_image_PrevousPlaques”, that constitutes one of the input images for the plaque tracking with the pipeline “PlaqueTracking.cpproj”.
12. *OverlayObjects*: This module fuses the “CropSensor” image with the *Plaque* objects to make a composite image named “OverlayImage”.
13. *SaveImages*: Creates an image called “Output_image_OverlayPlaques” based on the “OverlayImage”.

Note: Together with this protocol we supply the Zip file “[PlaqueIdentification tracking pipeline and dataset](#)” which contains the applied pipeline (“PlaqueIdentification.cpproj”) and an example

dataset composed of two input images to run the pipeline and practice the required adjustments (“Input_image_mNeptune_72h” and “Input_image_mNeptune_96h”) and four output files to corroborate the expected results (“Output_image_PreviousPlaques_72h”, “Output_image_PreviousPlaques_96h”, “Output_image_OverlayPlaques_72h”, and “Output_image_OverlayPlaques_96h”).

Plaque tracking pipeline

1. *Images*: Simply drag and drop the files of the plaque assay fluorescence images (e.g., “Input_image_mNeptune_72h”) and the output images created with the previous *Plaque identification pipeline* (e.g., “Output_image_PreviousPlaques_72h”). Make sure that the name of the plaque assay fluorescence images do include the name of the channel where the fluorescence was measured (e.g., mNeptune) and the increasing consecutive numbers for time-lapse microscopy images (e.g., mNeptune_72h).
2. *NamesAndTypes*: Select the rule criteria with an expression contained in the name of all the plaque assay fluorescence images, in this case, indicating the channel of the fluorescence (e.g., mNeptune). For each fluorescence image it creates an image called “Sensor”.
3. The modules 3-8 are the same as those described in the *Plaque identification pipeline*.
4. *IdentifySecondaryObjects*: This module identifies the new *Plaque* objects in the “CellImage” as secondary objects around the previously identified *PreviousPlaques* primary objects.
5. *TrackObjects*: This module tracks the plaques over time using an overlap criteria across the time-resolved images and creates an output image named “TrackedPlaques”. You may adjust the *Maximum distance to consider matches* for an optimal plaque tracking.
6. *SaveImages*: Saves the “Tracked_Plques” image for your validation and final results.
7. *RelateObjects*: This module correlates the new *Plaque* objects with the previously identified *Nuclei* objects.
8. *ExporttoSpreadSheet*: This module exports to an excel spreadsheet the data of the number of cells (*Nuclei* objects) that compose every recognized plaque in all the analyzed images.

Note: Together with this protocol we supply the Zip file “[PlaqueIdentification tracking pipeline and dataset](#)” which contains the applied pipeline (“PlaqueTracking.cppproj”) and an example dataset composed of four input images to run the pipeline (“Input_image_mNeptune_72h”, “Input_image_mNeptune_96h”, “Output_image_Previous_Plques_72h”, and “Output_image_PreviousPlaques_96h”) and three output files to corroborate the expected results (“Tracked_Plques_72h”, “Tracked_Plques_96h” and “Viral_Plque”).

Recipes

1. Complete DMEM
500 ml DMEM (Gibco)
5 ml Antibiotic-antimycotic 100×

- 5 ml (for 2%) or 50 ml (for 10%) of FBS
Homogenize by hand rotation (20 times, gently to avoid formation of foam)
Store at 4 °C. Stable for 4 months
2. PEI solution (1 mg/ml)
1 mg of PEI powder
1 ml of HCl 0.2 M in distilled water
Heat and shake at 60 °C, 600 rpm in a ThermoMixer® block
Sterilize by filtration (0.2 µm pore size)
Prepare 45 µl aliquots into 2 ml reaction tubes and store at -80° C. Stable for 4 months
3. Polybrene solution (10 mg/ml)
10.6 mg of hexadimethrine bromide powder
Dissolve in 1 ml of distilled water
Sterilize by filtration (0.2 µm pore size)
Prepare 50 µl single use aliquots into 0.5 ml reaction tubes and store at -20 °C. Stable for 1 year
4. Complete MEM
500 ml MEM (Gibco)
5 ml Sodium pyruvate 100 mM
5 ml Antibiotic-antimycotic 100×
5 ml (for 2%) or 50 ml (for 10%) of FBS
Homogenize by hand rotation (20 times, gently to avoid formation of foam)
Store at 4 °C. Stable for 4 months
5. PBS 1% FBS
45 ml PBS, pH 7.4
5 ml complete MEM 10% FBS
Store at 4 °C. Stable for 4 months
6. Puromycin solution (10 mg/ml)
10 mg of puromycin
Dissolve in 1 ml of distilled water
Sterilize by filtration (0.2 µm pore size)
Prepare 20 µl single use aliquots into 1.5 ml light protection reaction tubes and store at -20 °C.
Stable for 2 years
7. FluoroBrite™ DMEM 2% FBS
500 ml FluoroBrite™ DMEM (Gibco)
5 ml GlutaMAX™ supplement
5 ml Sodium pyruvate 100 mM
5 ml Antibiotic-antimycotic 100×
5 ml of FBS
Homogenize by hand rotation (20 times, gently to avoid formation of foam)

- Store at 4 °C. Stable for 4 months
8. Plaque media 2% FBS
 - 9.4 g MEM (Sigma)
 - 900 ml Milli-Q water
 - Adjust pH to 4.0
 - 10 g Carboxymethylcellulose sodium salt
 - Autoclave (121 °C at 100 kPa for 15 min)
 - 30 ml 7.5% sodium bicarbonate solution in Milli-Q water (sterilized by filtration – 0.2 µm pore size)
 - 10 ml GlutaMAX™ supplement
 - 10 ml Sodium pyruvate 100mM
 - 10 ml Antibiotic-antimycotic 100×
 - 20 ml of FBS
 - Homogenize by hand rotation (20 times, gently to avoid formation of foam)
 - Store at 4 °C. Stable for 4 months

Acknowledgments

We want to thank Dr. Jeanne A. Hardy from the Department of Chemistry, University of Massachusetts, for her kindness and scientific advice during our outstanding collaboration. We also want to acknowledge our funding sources at Universidad de Costa Rica (project VI-803-B9-505) and International Centre for Genetic Engineering and Biotechnology (Grant CRP/CRI18-02).

Competing interests

The authors declare that they do not have any conflicts of interests.

References

1. Arias-Arias, J. L., MacPherson, D. J., Hill, M. E., Hardy, J. A. and Mora-Rodriguez, R. (2020). [A fluorescence-activatable reporter of flavivirus NS2B-NS3 protease activity enables live imaging of infection in single cells and viral plaques](#). *J Biol Chem* 295(8): 2212-2226.
2. Balsitis, S. J., Coloma, J., Castro, G., Alava, A., Flores, D., McKerrow, J. H., Beatty, P. R. and Harris, E. (2009). [Tropism of dengue virus in mice and humans defined by viral nonstructural protein 3-specific immunostaining](#). *Am J Trop Med Hyg* 80(3): 416-424.
3. Freppel, W., Mazeaud, C. and Chatel-Chaix, L. (2018). [Production, titration and imaging of Zika virus in mammalian cells](#). *Bio-protocol* 8(24): e3115.
4. Gould, E. A. and Solomon, T. (2008). [Pathogenic flaviviruses](#). *Lancet* 371(9611): 500-509.
5. Hawley, T. S., Herbert, D. J., Eaker, S. S. and Hawley, R. G. (2004). [Multiparameter flow cytometry of fluorescent protein reporters](#). *Methods Mol Biol* 263: 219-237.

6. Hsieh, M. S., Chen, M. Y., Hsieh, C. H., Pan, C. H., Yu, G. Y. and Chen, H. W. (2017). [Detection and quantification of dengue virus using a novel biosensor system based on dengue NS3 protease activity.](#) *PLoS One* 12(11): e0188170.
7. Kümmeler, B. M. (2018). [Establishment and application of flavivirus replicons.](#) *Adv Exp Med Biol* 1062: 165-173.
8. Li, S. H., Li, X. F., Zhao, H., Deng, Y. Q., Yu, X. D., Zhu, S. Y., Jiang, T., Ye, Q., Qin, E. D. and Qin, C. F. (2013). [Development and characterization of the replicon system of Japanese encephalitis live vaccine virus SA14-14-2.](#) *Virol J* 10: 64.
9. McFadden, M. J., Mitchell-Dick, A., Vazquez, C., Roder, A. E., Labagnara, K. F., McMahon, J. J., Silver, D. L. and Horner, S. M. (2018). [A Fluorescent Cell-Based System for Imaging Zika Virus Infection in Real-Time.](#) *Viruses* 10(2).
10. Medin, C. L., Valois, S., Patkar, C. G. and Rothman, A. L. (2015). [A plasmid-based reporter system for live cell imaging of dengue virus infected cells.](#) *J Virol Methods* 211: 55-62.
11. Medina, F., Medina, J. F., Colon, C., Vergne, E., Santiago, G. A. and Munoz-Jordan, J. L. (2012). [Dengue virus: isolation, propagation, quantification, and storage.](#) *Curr Protoc Microbiol* Chapter 15: Unit 15D 12.
12. Schmid, B., Rinas, M., Ruggieri, A., Acosta, E. G., Bartenschlager, M., Reuter, A., Fischl, W., Harder, N., Bergeest, J. P., Flossdorf, M., Rohr, K., Höfer, T. and Bartenschlager, R. (2015). [Live cell analysis and mathematical modeling identify determinants of attenuation of dengue virus 2'-o-methylation mutant.](#) *PLoS Pathog* 11(12): e1005345.
13. Soto-Garita, C., Somogyi, T., Vicente-Santos, A. and Corrales-Aguilar, E. (2016). [Molecular Characterization of Two Major Dengue Outbreaks in Costa Rica.](#) *Am J Trop Med Hyg* 95(1): 201-205.
14. Tamura, T., Fukuhara, T., Uchida, T., Ono, C., Mori, H., Sato, A., Fauzyah, Y., Okamoto, T., Kurosu, T., Setoh, Y. X., Imamura, M., Tautz, N., Sakoda, Y., Khromykh, A. A., Chayama, K. and Matsuura, Y. (2018). [Characterization of recombinant flaviviridae viruses possessing a small reporter tag.](#) *J Virol* 92(2).
15. Tiscornia, G., Singer, O. and Verma, I. M. (2006). [Production and purification of lentiviral vectors.](#) *Nat Protoc* 1(1): 241-245.
16. Xie, X., Zou, J., Shan, C., Yang, Y., Kum, D. B., Dallmeier, K., Neyts, J. and Shi, P. Y. (2016). [Zika virus replicons for drug discovery.](#) *EBioMedicine* 12: 156-160.

Carboxyfluorescein Dye Uptake to Measure Connexin-mediated Hemichannel Activity in Cultured Cells

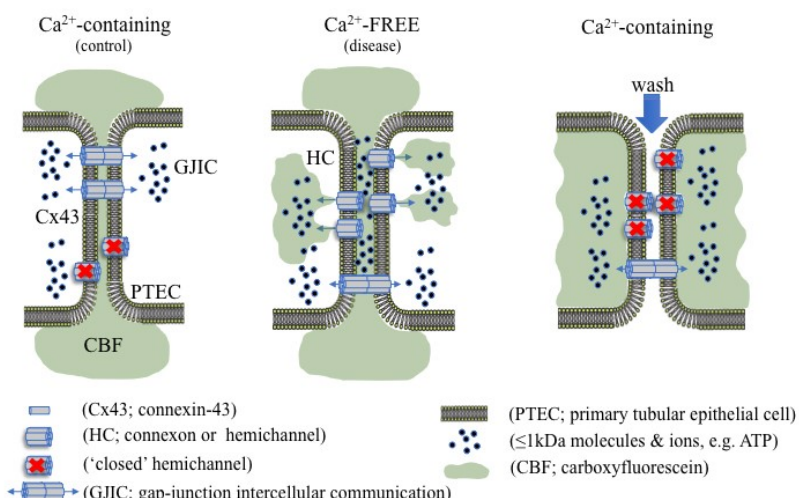
Joe A. Potter, Gareth W. Price, Chelsy L. Cliff, Bethany M. Williams,
Claire E. Hills and Paul E. Squires*

Joseph Banks Laboratories, School of Life Sciences, University of Lincoln, Lincoln, United Kingdom

*For correspondence: psquires@lincoln.ac.uk

[Abstract] Connexins are membrane bound proteins that facilitate direct and local paracrine mediated cell-to-cell communication through their ability to oligomerise into hexameric hemichannels. When neighbouring channels align, they form gap-junctions that provide a direct route for information transfer between cells. In contrast to intact gap junctions, which typically open under physiological conditions, undocked hemichannels have a low open probability and mainly open in response to injury. Hemichannels permit the release of small molecules and ions (approximately 1kDa) into the local intercellular environment, and excessive expression/activity has been linked to a number of disease conditions. Carboxyfluorescein dye uptake measures functional expression of hemichannels, where increased hemichannel activity/function reflects increased loading. The technique relies on the uptake of a membrane-impermeable fluorescent tracer through open hemichannels, and can be used to compare channel activity between cell monolayers cultured under different conditions, e.g. control versus disease. Other techniques, such as biotinylation and electrophysiology can measure cell surface expression and hemichannel open probability respectively, however, carboxyfluorescein uptake provides a simple, rapid and cost-effective method to determine hemichannel activity *in vitro* in multiple cell types.

Graphic abstract:



Using dye uptake to measure hemichannel activity

Copyright © 2021 The Authors; exclusive licensee Bio-protocol LLC.

Keywords: Connexin, Hemichannels, Carboxyfluorescein, Dye uptake

[Background] Connexins (Cx) are integral transmembrane proteins that oligomerise into connexons at the cell surface. Connexons dock with similar hexameric protein complexes on adjacent cells to form a bidirectional conduit for gap junction intercellular communication (GJIC; Bosco *et al.*, 2011). Gap junctions play an important role in synchronizing cellular activity and allow for the direct exchange of small ions, metabolites and secondary messengers, crucial for cellular function, survival and tissue homeostasis (Spray and Hanani, 2019). Under normal conditions, undocked connexons, known as hemichannels, remain mostly closed; however, in a pathophysiological context hemichannel-mediated intercellular communication can predominate, permitting the release of 1-2 kDa molecules, including adenosine triphosphate (ATP) into the extracellular milieu (Solini *et al.*, 2015; Hills *et al.*, 2018; Taruno, 2018; Siamantouras *et al.*, 2019). Altered hemichannel activity has previously been linked to inflammation, fibrosis and the progression of various disease states (Roy *et al.*, 2017; Hills *et al.*, 2018; Cea *et al.*, 2020; Sáez *et al.*, 2020). Consequently, quantitative characterisation of hemichannel activity can inform on the onset and progression of disease, *e.g.*, chronic kidney disease (CKD), along with highlighting potential targets for therapeutic intervention (Price *et al.*, 2020).

Depending on the constituent connexin isoform, several factors are known to open hemichannels, including temperature, pH, enteric pathogenic infections and low extracellular calcium ($[Ca^{2+}]_e$) (Trexler *et al.*, 1999; Ceelen *et al.*, 2011; Lopez *et al.*, 2016; Pinto *et al.*, 2017). Whilst various methods can determine expression and localisation of connexin hemichannel subunits at the cell surface, *e.g.*, biotinylation combined with immunoblot analysis and immunocytochemistry respectively, these do not provide a measure for functional changes in connexin-mediated cell communication. In recent years, a range of different methods have been used to evaluate the functional implications of altered hemichannel activity and/or function (Johnson *et al.*, 2016). One of these techniques involves electrophysiological characterisation using whole-cell patch clamp recordings. Although dual whole-cell voltage recordings offer a highly attractive method to attain vast amounts of information on hemichannel permeability selectivity, opening/closing kinetics, open probability latency and presence of subconductance states, it is not without its drawbacks (Brokamp *et al.*, 2012). Not only is this technique highly complex, the membrane potential needed to gate hemichannels is cell-type specific, a difficult hurdle to overcome (Veenstra, 2001). Quantification of hemichannel-permeable molecules into the local extracellular environment (*e.g.*, ATP release) via luminescence based assays is much simpler, yet provides minimal, indirect information with regards to hemichannel activity and would benefit from the use of potentially costly general or local connexin inhibitors (Musil and Goodenough, 1991; Brokamp *et al.*, 2012; Sáez and Green, 2018; Price *et al.*, 2020). Although these techniques provide excellent methodological approaches for identifying cell-surface connexin expression and hemichannel open probability, it is the use of simpler hemichannel-permeable, membrane impermeant dye uptake studies that are routinely used (Johnson *et al.*, 2016). Dye uptake studies make use of controlled parameters and utilise altered $[Ca^{2+}]_e$ to gate hemichannels, providing a simple, efficient and reliable procedure. Several fluorescent tracers, including Lucifer Yellow, ethidium bromide, 4',6-diamidino-2-phenylindole

(DAPI), propidium iodide (PI), and 5(6)-carboxyfluorescein can be used to quantify hemichannel activity, with the extent of dye uptake proportional to the number of active cell-surface hemichannels (Lopez *et al.*, 2016). Unfortunately, the majority of these tracers are hazardous and carcinogenic and require careful handling; however, this step-by-step protocol utilises the non-hazardous, 376 Da polyanionic fluorescent probe, 5(6)-carboxyfluorescein, to quantitatively measure hemichannel activity in proximal tubular epithelial cells *in vitro*.

Materials and Reagents

1. 50 ml Falcon tubes
2. Fluorodish, 35 mm (World Precision Instruments, catalog number: FD35-100)
3. Pasteur pipette, 4 ml (Sigma-Aldrich, catalog number: BR747770)
4. Clonal human kidney proximal tubule (HK-2) epithelial cell line (American Type Culture Collection, catalog number: CRL-2190)
5. Dulbecco's Modified Eagle Medium/Ham's F-12 (Fisher Scientific, catalog number: 31331093)
6. Dulbecco's Modified Eagle Medium (Fisher Scientific, catalog number: 11966025)
7. Ham's F-12 (Fisher Scientific, catalog number: 31-765-035)
8. Penicillin (100 IU/ml)-streptomycin (100 µg/ml) (Sigma-Aldrich, catalog number: P4458-100mL)
9. Epidermal growth factor (5 ng/ml) (Sigma-Aldrich, catalog number: E9644-.5mg)
10. Transforming Growth Factor-beta1 (TGF-β1), stored at -20 °C (Sigma-Aldrich, catalog number: T1654)
11. Foetal calf serum (Fisher Scientific, catalog number: 10500064)
12. Sodium chloride (NaCl) (Fisher scientific, catalog number: S/3160/65)
13. Potassium chloride (KCl) (Sigma-Aldrich, catalog number: P3911)
14. Magnesium sulphate heptahydrate ($MgSO_4 \cdot 7H_2O$) (Sigma-Aldrich, catalog number: 230391)
15. Sodium phosphate dibasic dihydrate ($Na_2HPO_4 \cdot 2H_2O$) (Sigma-Aldrich, catalog number: 71643)
16. Potassium dihydrogen phosphate (KH_2PO_4) (Sigma-Aldrich, catalog number: 1.04873)
17. Sodium bicarbonate ($NaHCO_3$) (Sigma-Aldrich, catalog number: S5761)
18. HEPES (4-(2-hydroxyethyl)-1-piperazineethanesulfonic acid) (Sigma-Aldrich, catalog number: H3375)
19. Calcium chloride dihydrate ($CaCl_2 \cdot 2H_2O$) (Sigma-Aldrich, catalog number: 223506)
20. D-glucose ($C_6H_{12}O_6$) (Sigma-Aldrich, catalog number: G8270)
21. Sodium hydroxide (NaOH) (Sigma-Aldrich, catalog number: S8045)
22. Hydrochloric acid (HCl) (Sigma-Aldrich, catalog number: 320331)
23. EGTA (ethylene glycol-bis(β-aminoethyl ether)-N,N,N',N'-tetraacetic acid) (Sigma-Aldrich, catalog number: E3889)
24. Cell culture
 - a. Growth culture medium, stored at 4 °C (see Recipes)
 - b. Low (5 mM) glucose medium, stored at 4 °C (see Recipes)

- c. Low (5 mM) glucose serum free medium, stored at 4 °C (see Recipes)
- 25. 5(6)-Carboxyfluorescein, stored at RT (Sigma-Aldrich, catalog number: 21879) (see Recipes)
- 26. 1× Calcium-containing balanced salt solution, stored at 4 °C (see Recipes)
- 27. 1× Calcium-free balanced salt solution, stored at 4 °C (see Recipes)

Equipment

- 1. Small, unstirred, heated water bath (37 °C) (Grant instruments Ltd, catalog number: 600142003)
- 2. Clifton 14 L, heated water bath (37 °C) (Nickel-electro Ltd, catalog number: NE1-14)
- 3. Humidified incubator: 37 °C, pH 7.4, 5% CO₂ (CO₂ incubator, Panasonic, catalog number: MCO-170AICD)
- 4. Linus photonics metafluor imaging workbench (Technical Manufacturing Corporation, catalog number: 63-530)
- 5. Photometrics CoolSNAP HQ CCD monochrome camera with power supply (Roper Scientific, catalog number: A01C881022)
- 6. Zeiss Axiovert 200 research inverted fluorescence microscope with heated stage (Carl Zeiss Ltd, catalog number: B40-080)
- 7. Zeiss XBO 75 microscope lamp housing with EBX 75 isolated power supply (Carl Zeiss Ltd, catalog number: B40-065)
- 8. Lambda 10-2 optical filter changer (Sutter Instrument, catalog number: LB10-2)
- 9. Tempcontrol 37 (Carl Zeiss Ltd, catalog number: 37-2)
- 10. Dell precision PC (Dell, catalog number: T3500)
- 11. Liyama prolite PC monitor (liyama, catalog number: E2472HD)
- 12. Sonomatic sonicator (Jencon scientific Ltd, catalog number: E0375)

Software

- 1. Metamorph v7.7.5.0 software (available from <https://www.moleculardevices.com/products/cellular-imaging-systems/acquisition-and-analysis-software/metamorph-microscopy#gref>) (Meta imaging series by Molecular Devices Inc)
- 2. Fiji (ImageJ) v2.1.0 software (available from <https://fiji.sc/>) (ImageJ studio Ltd)

Procedure

A. Tissue culture

- 1. Maintain HK-2 cells (passages 18-30) in DMEM/F-12-containing FCS, EGF and penicillin-streptomycin growth media, which has a high basal glucose concentration (17.5 mM) to encourage cell growth.

2. Seed HK-2 cells on sterile 35 mm fluorodishes at a seeding density of 1×10^4 in 2 ml DMEM/F-12-containing FCS, EGF and penicillin-streptomycin growth media (see Note 1).
3. Prior to treatment, culture HK-2 cells in low (5 mM) glucose DMEM/F-12-containing FCS, EGF and penicillin-streptomycin medium for a period of 48 h, followed by an overnight incubation in serum free low (5 mM) glucose DMEM/F-12-containing EGF and penicillin-streptomycin medium to negate any pre-stimulatory effects from the high (17.5 mM) glucose.
4. After overnight incubation in serum free low (5 mM) glucose DMEM/F-12-containing EGF and penicillin-streptomycin media, treat HK-2 cells with a desired stimulus (e.g., TGF- β 1, 10 ng/ml) against control HK-2 cells in serum free low (5 mM) glucose DMEM/F-12-containing EGF and penicillin-streptomycin media for 48 h with a final confluence of 80%.

B. Balanced salt solutions and 5(6)-carboxyfluorescein preparation

1. Prepare 1 L 1× calcium-containing and 1 L 1× calcium-free balanced salt solution (see Recipes) and keep warm at 37 °C in the small water bath.
2. Prepare two adequate carboxyfluorescein solutions (200 μ M) in 50 ml Falcon tubes (see Note 2). One in 50 ml 1× calcium-containing balanced salt solution and one in 50 ml 1× calcium-free balanced salt solution (see Note 3). Sonicate both solutions at 44 kHz for 10-20 min (37 °C) until the carboxyfluorescein powder has fully dissolved. Leave the solutions at 37 °C in the water bath and use as needed.

C. Initial rig preparation

As seen in Figure 1, and in this order:

1. Switch on EBX 75 isolated lamp.
2. Switch on tempcontrol 37, adjust the setpoint to 37 °C (real). Allow 20-30 min for the heated stage to reach the desired temperature.
3. Switch on the CoolSNAP HQ CCD monochrome camera.
4. Switch on Lambda 10-2 optical filter change, ensure light emission at 510 nm on the Axiovert 200 inverted microscope (see Note 4).
5. Remove cover and switch on microscope.
6. Switch on PC, load Metamorph and press 'acquire' from the acquire tab at the top of the screen.

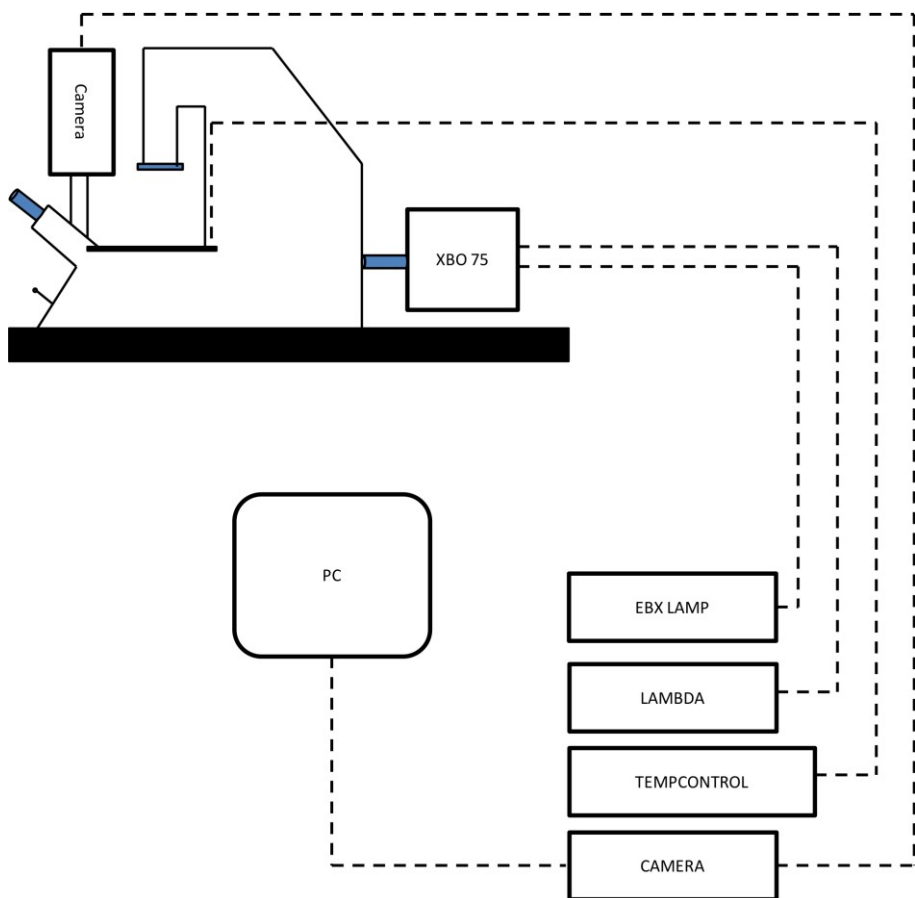


Figure 1. Axiovert inverted fluorescent microscope rig. A schematic of the inverted fluorescent microscope setup for carboxyfluorescein dye uptake assessment. Mounted on an anti-vibration Metafluor imaging workbench, the inverted fluorescent microscope has an XBO 75 microscope lamp connected to an EBX 75 isolated housing unit, along with a Lambda 10-2 optical filter changer. A heated stage is also fitted and controlled by a tempcontrol 37 unit. Located at the front of the microscope, a coolSNAP HQ CCD monochrome camera is mounted, linked to a power supply and subsequently connected to a PC for image visualisation.

D. Carboxyfluorescein dye uptake

1. Remove one fluorodish from the humidified incubator and aspirate the media using a Pasteur pipette into a waste pot.
2. To permit hemichannel dye uptake, incubate cells in 2 ml 1× calcium-free carboxyfluorescein solution at 37 °C in a humidified incubator for 10 min (see Note 5).
3. To close the hemichannels, using a Pasteur pipette, remove the 1× calcium-free carboxyfluorescein solution and replace with 2 ml 1× calcium-containing carboxyfluorescein solution at 37 °C in a humidified incubator for 5 min.
4. To remove any residual carboxyfluorescein dye which may interfere with imaging, wash cells carefully using 20 ml pre-warmed 1× calcium-containing balanced salt solution leaving 1-2 ml of 1× calcium-containing balanced salt solution in the fluorodish (see Note 6).

E. Image capture

1. Ensure image capture is completed in a dark environment. To standardise image capture, cells producing the brightest signal (TGF- β 1 treated cells) are measured first and exposure opening time is fixed for comparison between treatments.
2. To fix the exposure time, initially place the cells on the microscope heated stage, turn on the fluorescence (emitted light captured at 510 nm) and set the slider switch to the lens (eye symbol) on the microscope (see Note 7).
3. Locate a cell population producing a bright image, switch the microscope slider to the camera (camera symbol), and using the acquire window in Metamorph, press ‘F2: Show Live’ to visualise cells on the PC screen. Adjust the focus of the image and press ‘AutoExpose’ (Figure 2) (see Note 8).
4. Once the exposure time is set, to reduce photobleaching, set the slider switch back to the lens and efficiently move the fluorodish to locate another isolated cell population for image capture. After this time, set the slider switch to the camera and in Metamorph, press ‘F2: Show Live’, adjust the focus of the image and finally press the ‘Acquire’ button to capture the image (Figure 2) (see Note 9).

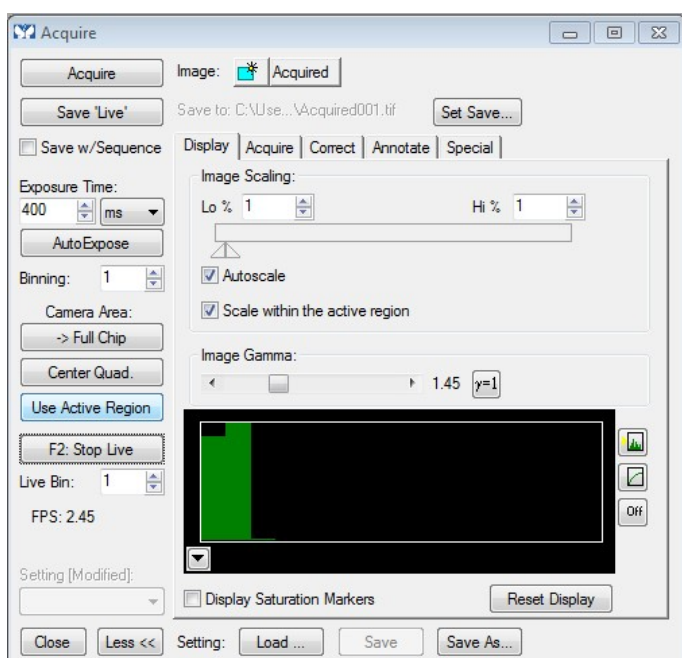


Figure 2. A representation of the ‘Acquire’ tab in Metamorph V.7.7.5.0. A screenshot of the ‘Acquire’ window to understand the different functions is shown. In order to visualise the cell image on the PC screen, ‘F2: Show Live’/‘F2: Stop Live’ should be pressed, followed by either the ‘AutoExpose’ button or the ‘Acquire’ button to capture the live image.

5. Repeat the process until 10-15 images are captured (see Note 10).
6. To save the images in Metamorph, go to:
 - a. File (located top left of the screen).

- b. Setup Sequential File Names...
 - c. Set the ‘Base Name’ as the condition (*i.e.*, TGF- β 1).
 - d. Set the Image Number starting from 1.
 - e. Set the number width to 1.
 - f. Set the ‘Save As Type’ to ‘Metamorph TIFF’.
 - g. Set ‘If image already exists’ to ‘Skip to end of sequence’.
 - h. ‘Select Directory’ saves the files to a designated folder.
 - i. On the PC keyboard, use the ‘Control+U’ shortcut to complete this for each image.
7. Turn off the fluorescence, discard the fluorodish and repeat from Section D (do not alter the exposure time for the remainder of the experiment).

Data analysis

The images are analysed using Fiji, an imaging processing software based on ImageJ. First, the images are batch converted into JPG files and enhanced. Each image is then individually processed to acquire cell intensity values which are averaged and statistically tested.

A. Image Preparation

1. Images are batch processed using a set of instructions called a macro, which achieve the following:
 - a. TIFF files are lossless (or uncompressed) images which are often difficult to handle, and so we batch convert them to JPG.
 - b. Fiji defaults to a grayscale colour lookup table, so this is changed to green.
 - c. The images often require enhancement (contrast *etc.*).
2. In the toolbar, click ‘Process’, ‘Batch’, and then ‘Macro’. A box will appear (Figure 3)
3. Click ‘Input’ and select the folder of input images.
4. Create a new folder for the processed images, click ‘Output’, and select this new folder.
5. Under the ‘Output format’ list, select ‘JPEG’.
6. In the big textbox in the centre of the window, type in the following (see Note 11):

```
run("Green");  
run("Enhance Local Contrast (CLAHE)", "blocksize=127 histogram=256  
maximum=3 mask=*None*");
```
7. Click ‘Process’ to start the batch conversion.

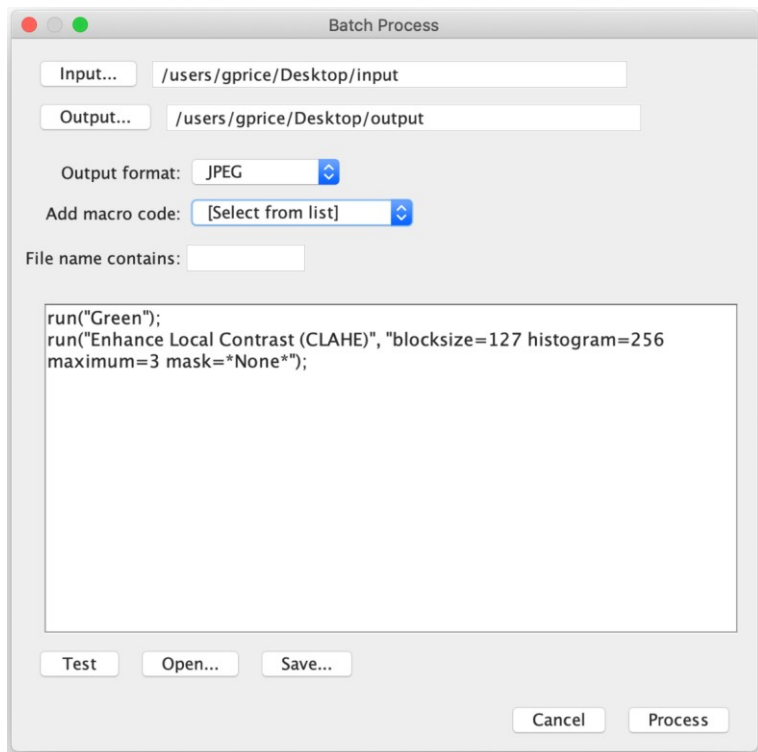


Figure 3. The Batch Process window. The ‘Batch Process’ window allows the use of a macro to apply changes to all images in the input folder, converting them to a JPEG, and saving in an output folder. Here, the colour lookup table is changed to “Green”, and local contrast is enhanced using default settings.

B. Image analysis

1. Open an image (from the output folder selected above) by clicking ‘File’, ‘Open’. Multiple images can be opened simultaneously.
2. In the toolbar, click ‘Analyze’, ‘Tools’, and ‘ROI Manager’. A box will appear (Figure 4A).
3. From the main Fiji program, select an oval selection tool (Figure 4B).
4. Draw regions of interest (ROI), around each cell in the image. Each time you draw an ROI, click ‘Add [t]’ on the ROI Manager (or press ‘t’ on your keyboard). Ticking ‘Show All’ helps to identify already selected cells.
5. After all cells have been selected (Figure 4C), draw a final ROI in a background area where cells are not present. Add this ROI to the ROI Manager.
6. In the toolbar, click ‘Analyze’, and ‘Set Measurements’. A box will appear (Figure 4D). Untick all except for Integrated Density.
7. In the ROI Manager, click ‘Measure’. A results box will appear with the intensity values for each ROI (Figure 4E). Copy this to Excel and subtract the last value (the background ROI).

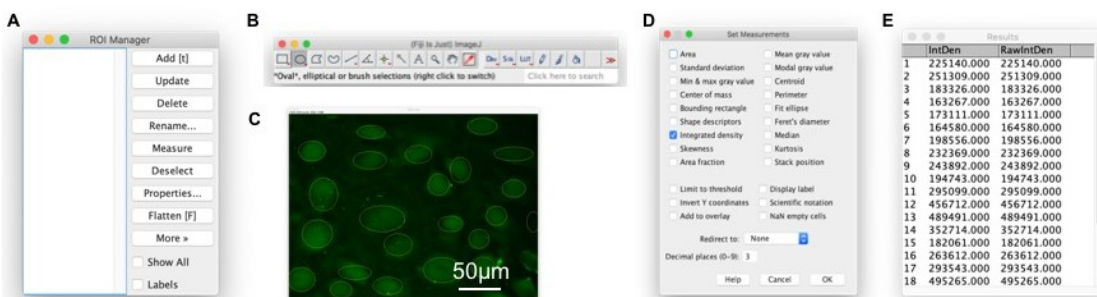


Figure 4. Adding regions of interest allows the measurement of fluorescence intensity. A. The Region of Interest (ROI) manager, which keeps track of all ROI added to the image. Once a selection is drawn on the image, click ‘Add [t]’ to add the ROI to the manager. B. An oval selection tool is selected. C. ROI around each cell have been drawn and added to the ROI Manager. A ROI of the background has also been added (right hand side) which will be subtracted from each cell. D. Select ‘Integrated density’ from the list of measurements. E. Once ‘Measure’ in Figure 4A has been clicked, a box of raw intensities will appear for further analysis.

- Average the values, omitting any clearly anomalous intensities, and repeat this section for all images and treatments. Between each image, select all ROI in the ROI Manager and click ‘Delete’.
- Once all images have been analysed, an ANOVA/t-Test can be used to determine statistical significance, with typical results represented in Figure 5.

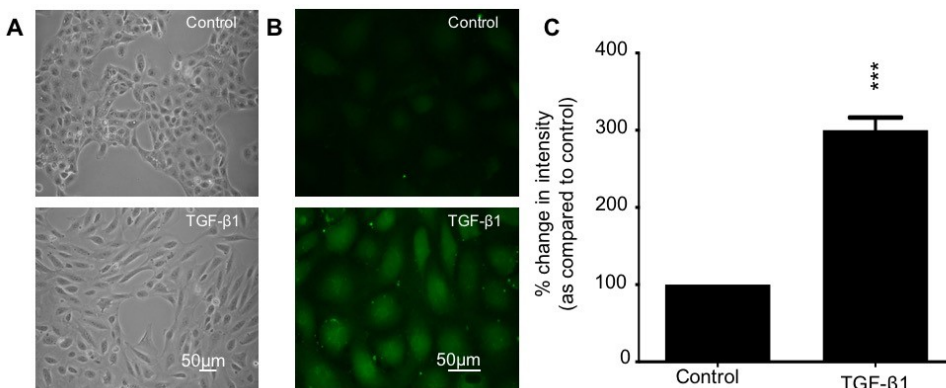


Figure 5. Example result using phase contrast microscopy and fluorescent images of control vs TGFβ1-treated HK-2 cells. Representative images of HK-2 cells treated with TGF-β1 as compared to control both under phase contrast (magnification $\times 20$) and fluorescence (magnification $\times 63$) microscopy. A. TGF-β1 (10 ng/ml) stimulates a shift in HK-2 cell morphology from a classic cobblestone appearance (upper panel) to a more elongated fibroblast-like phenotype (lower panel). B. Under fluorescence microscopy, HK-2 cells exposed to TGF-β1 exhibit increased dye uptake, as compared to control; C. TGF-β1 (10 ng/ml) treated cells demonstrate a 300% increase in dye uptake compared to control cells. Data is presented as

mean \pm SEM with intensity expressed as a percentage change compared to low glucose control and representative of multiple cell recordings from 3 separate experiments. (***, $P < 0.001$).

Notes

1. This seeding density is optimised for HK-2 cells for a 48-h treatment and may differ for other cell lines/treatment periods.
2. Carboxyfluorescein concentration (200 μ M), incubation durations and washes have been optimised for HK-2 cells. For other cell lines these parameters may vary and will have to be optimised.
3. Aliquot 50 ml of each balanced salt solution prior to adding 5(6)-carboxyfluorescein. Carefully weigh out 3.95 mg 5(6)-carboxyfluorescein and gently tip this into the balanced salt solution with the aid of a Pasteur pipette to ensure all 5(6)-carboxyfluorescein is mixed.
4. If the fluorescent light does not emit from the microscope, try pressing 'local' on the Lambda 10-2 optical filter changer. If this does not work, press 'reset' and ensure 'shutter A - ON' and 'shutter B - ON' are displayed on the Lambda unit.
5. A small number of hemichannels may be open without the removal of $[Ca^{2+}]_e$.
6. Leaving 1 ml 1 \times calcium-containing solution in the fluorodish will encourage permanent hemichannel closure, whilst preventing cell shrinkage and ultimate cell death.
7. To ensure captured light is emitted at 510 nm, on the inverted microscope, make sure 'Fs 09' is open.
8. TGF- β 1 treated HK-2 cells give an exposure time of ~200-400 ms.
9. In the process of image capture, prevent any unwanted noise/vibrations to preserve image quality ahead of data analysis.
10. During the localisation of a cell population, a high background may be present. Increase image quality/reduce background noise by further washing cells with 20 ml 1 \times calcium-containing balanced salt solution.
11. Refer to online documentation for other available commands. Using the 'Plugins', 'Macros', 'Recorder' functions can also be useful to map changes made to an image to the macro equivalent.

Recipes

1. Growth culture medium

500 ml Dulbecco's Modified Eagle Medium/Ham's F-12 nutrient mixture + Glutamine (2 mM)
(DMEM/F-12)

50 ml foetal calf serum (10% wt/vol)

10 ml Penicillin (100 IU/ml)-streptomycin (100 μ g/ml)

1 μ l epidermal growth factor (5 ng/ml)

Stored at 4 °C, pre-warm to 37 °C prior to use

2. Low (5 mM) glucose medium (1:1 ratio)
 - a. 500 ml DMEM (50 ml foetal calf serum (10% wt/vol), 10 ml penicillin (100 IU/ml)-streptomycin (100 µg/ml) and 1 µl epidermal growth factor (5 ng/ml)
 - b. 500 ml F-12 + GlutaMAX (10 mM glucose) (50 ml foetal calf serum (10% wt/vol), 10 ml penicillin (100 IU/ml)-streptomycin (100 µg/ml) and 1 µl epidermal growth factor (5 ng/ml)

On the day, mix each medium in a 1:1 ratio to a desired volume in a sterilised atmosphere.

Stored at 4 °C, pre-warm to 37 °C prior to use.

3. Low (5 mM) glucose serum free medium (1:1 ratio)
 - a. 500 ml DMEM (10 ml penicillin (100 IU/ml)-streptomycin (100 µg/ml) and 1 µl epidermal growth factor (5 ng/ml))
 - b. 500 ml F-12 + GlutaMAX (10 mM glucose) [10 ml penicillin (100 IU/ml)-streptomycin (100 µg/ml) and 1 µl epidermal growth factor (5 ng/ml)]

On the day, mix each medium in a 1:1 ratio to a desired volume in a sterilised atmosphere.

Stored at 4 °C, pre-warm to 37 °C prior to use.

4. 5(6)-Carboxyfluorescein (200 µM)

3.95 mg 5(6)-carboxyfluorescein

Add 50 ml of 1× calcium-containing balanced salt solution or 1× calcium-free balanced salt solution. Sonicate at 44 kHz for 10-20 min at 37 °C until completely dissolved.

5. 1× Calcium-containing balanced salt solution (1 L, pH 7.4)

8.0 g of Sodium chloride (NaCl, 137 mM)

0.4 g of Potassium chloride (KCl, 5.36 mM)

0.2 g of Magnesium sulphate heptahydrate ($MgSO_4 \cdot 7H_2O$, 0.81 mM)

0.06 g of Sodium phosphate dibasic dihydrate ($Na_2HPO_4 \cdot 2H_2O$, 0.34 mM)

0.06 g of Potassium dihydrogen phosphate (KH_2PO_4 , 0.44 mM)

0.35 g of Sodium bicarbonate ($NaHCO_3$, 4.17 mM)

2.38 g of HEPES (4-(2-hydroxyethyl)-1-piperazineethanesulfonic acid, 10 mM)

0.19 g of Calcium chloride dihydrate ($CaCl_2 \cdot 2H_2O$, 1.26 mM)

0.36 g of D-glucose ($C_6H_{12}O_6$, 2.02 mM)

Make up to 1 L using dH₂O and adjust pH to 7.4 using 1M sodium hydroxide (NaOH) or hydrochloric acid (HCl). Store at 4 °C until needed and heat at 37 °C.

This can be made up as a 10× stock without the addition of calcium chloride dihydrate and glucose and kept in the fridge for long term. On the day of use, make up 1 L by diluting the 10× stock 1:10 with dH₂O, add 0.19 g calcium chloride dihydrate and 0.36 g of D-glucose to the 1 L 1× balanced salt solution and pre-warm to 37 °C prior to use.

6. 1× Calcium-free balanced salt solution (1 L, pH 7.4)

8.64 g of Sodium chloride (NaCl, 137mM)

0.4 g of Potassium chloride (KCl, 5.36mM)

0.2 g of Magnesium sulphate heptahydrate ($MgSO_4 \cdot 7H_2O$, 0.81mM)

0.06 g of Sodium phosphate dibasic dihydrate ($\text{Na}_2\text{HPO}_4 \cdot 2\text{H}_2\text{O}$, 0.34 mM)
0.06 g of Potassium dihydrogen phosphate (KH_2PO_4 , 0.44 mM)
0.35 g of Sodium bicarbonate (NaHCO_3 , 4.17 mM)
2.38 g of HEPES (4-(2-hydroxyethyl)-1-piperazineethanesulfonic acid, 10 mM)
0.36 g of D-glucose ($\text{C}_6\text{H}_{12}\text{O}_6$, 2.02 mM)
0.038 g EGTA (ethylene glycol-bis(β -aminoethyl ether)-N,N,N',N'-tetraacetic acid, 100 μM)
Make up to 1 L using ddH₂O and adjust pH to 7.4 using 1 M sodium hydroxide (NaOH) or hydrochloric acid (HCl). Store at 4 °C until needed and heat at 37 °C.
This can be made up as a 10× stock without the addition of EGTA and glucose and kept in the fridge for long term. On the day of use, make up 1 L by dilute the 10× stock 1:10 with ddH₂O, add 0.038 g EGTA and 0.36 g of D-glucose to the 1 L 1× balanced salt solution and pre-warm to 37 °C prior to use.

Acknowledgments

CEH and PES would like to acknowledge the generous support of Diabetes UK (16/0005427 16/005544 and 18/0005919).

Competing interests

The authors declare that they have no competing interests.

References

1. Bosco, D., Haefliger, J. A. and Meda, P. (2011). [Connexins: key mediators of endocrine function](#). *Physiol Rev* 91(4): 1393-1445.
2. Brokamp, C., Todd, J., Montemagno, C. and Wendell, D. (2012). [Electrophysiology of single and aggregate Cx43 hemichannels](#). *PLoS One* 7(10): e47775.
3. Cea, L. A., Fernandez, G., Arias-Bravo, G., Castillo-Ruiz, M., Escamilla, R., Branes, M. C. and Saez, J. C. (2020). [Blockade of Hemichannels Normalizes the Differentiation Fate of Myoblasts and Features of Skeletal Muscles from Dysferlin-Deficient Mice](#). *Int J Mol Sci* 21(17): 6025.
4. Ceelen, L., Haesebrouck, F., Vanhaecke, T., Rogiers, V. and Vinken, M. (2011). [Modulation of connexin signaling by bacterial pathogens and their toxins](#). *Cell Mol Life Sci* 68(18): 3047-3064.
5. Hills, C., Price, G. W., Wall, M. J., Kaufmann, T. J., Chi-Wai Tang, S., Yiu, W. H. and Squires, P. E. (2018). [Transforming Growth Factor Beta 1 Drives a Switch in Connexin Mediated Cell-to-Cell Communication in Tubular Cells of the Diabetic Kidney](#). *Cell Physiol Biochem* 45(6): 2369-2388.
6. Johnson, R. G., Le, H. C., Evenson, K., Loberg, S. W., Myslajek, T. M., Prabhu, A., Manley, A. M., O'Shea, C., Grunenwald, H., Haddican, M., Fitzgerald, P. M., Robinson, T., Cisterna, B. A.,

- Saez, J. C., Liu, T. F., Laird, D. W. and Sheridan, J. D. (2016). [Connexin Hemichannels: Methods for Dye Uptake and Leakage](#). *J Membr Biol* 249(6): 713-741.
7. Lopez, W., Ramachandran, J., Alsamarah, A., Luo, Y., Harris, A. L. and Contreras, J. E. (2016). [Mechanism of gating by calcium in connexin hemichannels](#). *Proc Natl Acad Sci U S A* 113(49): E7986-E7995.
8. Musil, L. S. and Goodenough, D. A. (1991). [Biochemical analysis of connexin43 intracellular transport, phosphorylation, and assembly into gap junctional plaques](#). *J Cell Biol* 115(5): 1357-1374.
9. Pinto, B. I., Pupo, A., Garcia, I. E., Mena-Ulecia, K., Martinez, A. D., Latorre, R. and Gonzalez, C. (2017). [Calcium binding and voltage gating in Cx46 hemichannels](#). *Sci Rep* 7(1): 15851.
10. Price, G. W., Chadjichristos, C. E., Kavvadas, P., Tang, S. C. W., Yiu, W. H., Green, C. R., Potter, J. A., Siamantouras, E., Squires, P. E. and Hills, C. E. (2020). [Blocking Connexin-43 mediated hemichannel activity protects against early tubular injury in experimental chronic kidney disease](#). *Cell Commun Signal* 18(1): 79.
11. Roy, S., Jiang, J. X., Li, A. F. and Kim, D. (2017). [Connexin channel and its role in diabetic retinopathy](#). *Prog Retin Eye Res* 61: 35-59.
12. Sáez, J. C., Contreras-Duarte, S., Labra, V. C., Santibanez, C. A., Mellado, L. A., Inostroza, C. A., Alvear, T. F., Retamal, M. A., Velarde, V. and Orellana, J. A. (2020). [Interferon-γ and high glucose-induced opening of Cx43 hemichannels causes endothelial cell dysfunction and damage](#). *Biochim Biophys Acta Mol Cell Res* 1867(8): 118720.
13. Sáez, J. C. and Green, C. (2018). [Involvement of Connexin Hemichannels in the Inflammatory Response of Chronic Diseases](#). *Int J Mol Sci* 19(9): 2469.
14. Siamantouras, E., Price, G. W., Potter, J. A., Hills, C. E. and Squires, P. E. (2019). [Purinergic receptor \(P2X7\) activation reduces cell-cell adhesion between tubular epithelial cells of the proximal kidney](#). *Nanomedicine* 22: 102108.
15. Solini, A., Usuelli, V. and Fiorina, P. (2015). [The dark side of extracellular ATP in kidney diseases](#). *J Am Soc Nephrol* 26(5): 1007-1016.
16. Spray, D. C. and Hanani, M. (2019). [Gap junctions, pannexins and pain](#). *Neurosci Lett* 695: 46-52.
17. Taruno, A. (2018). [ATP Release Channels](#). *Int J Mol Sci* 19(3): 808.
18. Trexler, E. B., Bukauskas, F. F., Bennett, M. V., Bargiello, T. A. and Verselis, V. K. (1999). [Rapid and direct effects of pH on connexins revealed by the connexin46 hemichannel preparation](#). *J Gen Physiol* 113(5): 721-742.
19. Veenstra, R. D. (2001). [Voltage clamp limitations of dual whole-cell gap junction current and voltage records. I. Conductance measurements](#). *Biophys J* 80(5): 2231-2247.

Imaging of Human Cancer Cells in 3D Collagen Matrices

Karin Pfisterer^{1, 2, *}, Brooke Lumicisi¹ and Maddy Parsons^{1, *}

¹Randall Centre for Cell and Molecular Biophysics, King's College London, Guy's Campus, London, UK;

²Department of Dermatology, Medical University of Vienna, Vienna, Austria

*For correspondence: maddy.parsons@kcl.ac.uk; karin.pfisterer@meduniwien.ac.at

[Abstract] Research on cell migration and interactions with the extracellular matrix (ECM) was mostly focused on 2D surfaces in the past. Many recent studies have highlighted differences in migratory behaviour of cells on 2D surfaces compared to complex cell migration modes in 3D environments. When embedded in 3D matrices, cells constantly sense the physicochemical, topological and mechanical properties of the ECM and adjust their behaviour accordingly. Changes in the stiffness of the ECM can have effects on cell morphology, differentiation and behaviour and cells can follow stiffness gradients in a process called durotaxis. Here we introduce a detailed protocol for the assembly of 3D matrices consisting of collagen I/fibronectin and embedding cells for live cell imaging. Further, we will show how the matrix can be stiffened via non-enzymatic glycation and how collagen staining with fluorescent dyes allows simultaneous imaging of both matrix and cells. This approach can be used to image cell migration in 3D microenvironments with varying stiffness, define cell-matrix interactions and the cellular response to changing ECM, and visualize matrix deformation by the cells.

Keywords: 3D collagen matrix, 3D imaging, Cell-matrix interaction, Cancer cell migration, Filopodia, Live cell imaging

[Background] Cells and the surrounding extracellular matrix (ECM) build functional entities that rely on dynamic adjustments of both, the matrix and the cells, to prevent disease. For years it was thought that the ECM solely provides structural support for embedded cells. However, recent research has highlighted the pivotal functions of the ECM beyond its scaffold function. Modifications of the ECM have been linked to disease progression, and particularly in the context of cancer, in metastasis initiation and subsequent links to clinical prognosis and patient survival.

On one hand, the ECM can create a barrier that impedes cell migration. Spatial confinement in the matrix provokes cell adaptations, such as cell body deformation, nuclear deformation and active ECM remodelling by matrix metalloproteinases (Bonnans *et al.*, 2014; Jayo *et al.*, 2016; Yamada and Sixt, 2019). Conversely, fibrous structures built by a network of collagen and matrix-associated proteins can support cell migration by providing a three-dimensional fibrillary physical scaffold to guide directed motility. ECM components, such as fibronectin provide anchor points for cell adhesion, which is important for mesenchymal migration modes. Cell migration in 2D has been extensively studied and the basic principles include repeated cycles of membrane protrusion at the leading edge, adhesion, F-actin retrograde flow, and actomyosin-driven cell retraction (Abercrombie, 1980, Yamada and Sixt, 2019). Cell migration in 3D is emerging to be a more complex process and cells have been reported to

use mesenchymal, amoeboid, lobopodial and collective cell migration and can also interconvert between these forms depending on the mechanical properties of the microenvironment (van Helvert *et al.*, 2018, Yamada and Sixt, 2019). Invasive cancer cells align along and attach to ECM tension fibres during migration and often leave behind tunnels due to MMP degradation at the front (Yamada and Sixt, 2019). Before the onset of locomotion, many migratory cells explore the ECM with actin-rich membrane protrusions, such as filopodia or lamellipodia, a prerequisite for successful navigation through 3D environments. This allows sensing of dynamic changes in the microenvironment and direct adaptation to the topography, stiffness and anchor points within the matrix (Leithner *et al.*, 2016, Pfisterer *et al.*, 2020).

Recent development of novel imaging tools and advanced microscopes with high resolution and frame rates allow the visualization of these processes in real-time with limited photo-toxicity. Various models have been used, including organotypic, cell-derived or 3D matrices, to investigate cell behaviour in a more physiological 3D environment. However, a detailed general 3D matrix protocol for broad applicability of cancer cell-ECM interaction studies has not been published, to our knowledge. We recently developed a 3D system with variable mechanical properties to monitor the phenotype of cancer cells and the role of the filopodia stabilizing protein fascin within this by live cell imaging (Pfisterer *et al.*, 2020). Our system allows analysis of any protein of interest in living cells embedded into a collagen-fibronectin matrix. Further, we show how the matrix can be stiffened via non-enzymatic glycation to investigate the impact of matrix stiffening on cell or molecule behaviour. Finally, we provide a simple method for collagen staining with fluorescent dyes for simultaneous imaging of the matrix and the cells that allows to draw conclusions on reciprocal forces between the ECM and interacting cells and to predict correlations between cell morphology and behaviour and matrix deformation.

Materials and Reagents

1. Imaging chambers 8-well, glass bottom (Nunc, Lab-Tek, catalog number: 155411PK)
2. Coverslips, glass d = 5 mm, 0.13-0.16 mm thickness (Fisher Scientific, catalog number: 11888372)
3. 10 cm Petri dishes (Fisher Scientific, Nunc, catalog number: 150350)
4. Culture flasks T25 (Greiner Bio One, catalog number: 690160)
5. Glass beaker for dialysis
6. Dialysis tubes for small volume dialysis; dialysis membrane with MWCO 8,000 Da (GE Healthcare, catalog number: 11520694)
7. DMEM – high glucose, 4500 mg/L glucose (Sigma-Aldrich, catalog number: D5796)
8. Fetal calf serum, FCS (Fisher Scientific, Gibco, catalog number: 26140079)
9. L-Glutamine (Sigma, catalog number: G7513)
10. Penicillin-Streptomycin (Sigma, catalog number: P4333)
11. Trypsin-EDTA (Sigma, catalog number: 59427C)

12. Rat tail collagen I, in 0.02N acetic acid, conc. approx. 10 mg/ml (Corning, catalog number: 354249), stored at 4 °C
13. HEPES solution (Sigma, catalog number: H3662)
14. Fibronectin (Merck Millipore, catalog number: FC010)
15. Sodium Bicarbonate (NaHCO_3), powder (Sigma, catalog number: S5761)
16. Sodium Bicarbonate 7.5% solution for cell culture (Fisher Scientific, Gibco, catalog number: 25080094)
17. 1 M Sodium hydroxide (NaOH) solution (Sigma, catalogue number: S2770)
18. Acetic acid, glacial (Sigma, catalogue number: A6283)
19. 1x PBS; deficient of CaCl_2 and MgCl_2 (Gibco, catalog number: 14190-094)
20. D(-)-Ribose (AppliChem, Biochemica, catalog number: A2219.0050)
21. Cy5 monoreactive dye (Amersham, GE Healthcare, catalog number: PA25001)
22. Full Medium (see Recipes)
23. 0.5 M ribose stock solution (see Recipes)
24. 0.1 M Sodium bicarbonate (see Recipes)
25. 0.1% acetic acid (see Recipes)
26. Cy5-labeled collagen (see Recipes)
27. Soft and stiff collagen matrices (see Recipes)

Equipment

1. Overhead tube rotator (Fisher Scientific, catalog number: 11496548)
2. Magnetic mixer (Fisher Scientific, catalog number: 11936558)
3. Centrifuge (Starlab, catalog number: SLN2631-0007)
4. Ice bucket
5. Inverted confocal microscope (e.g., Nikon A1R on Ti Eclipse) with appropriate wavelength lasers (488 nm, 561 nm)
6. Water immersion objective (e.g., 40x Nikon Apochromat LWD WI, 1.15 NA)
7. Lattice Light Sheet microscope (we used the instrument within the AIC, Advanced Imaging Center, Janelia Research Campus)

Software

1. Nikon NIS Elements Software to operate Nikon A1R on Ti Eclipse
2. LabView to operate Lattice Light Sheet Microscope prototype at the AIC

Procedure

Please see also Figure 1 for a timeline of Steps A to F.

Timeline

The main steps of the procedure are summarized in the timeline shown in Figure 1 below.

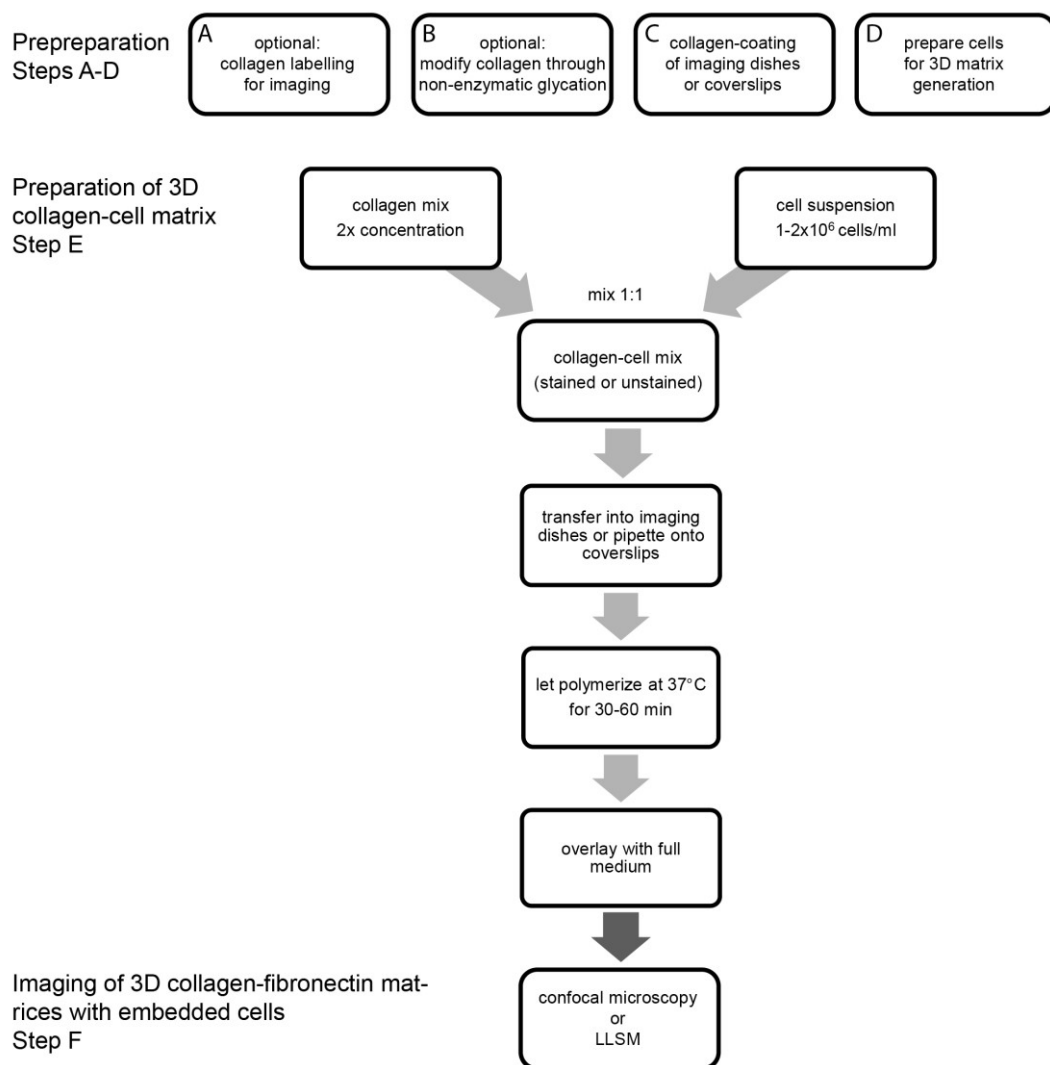


Figure 1. Timeline of the main protocol steps. This timeline summarizes the main steps of the protocol. Optional steps are highlighted. LLSM, lattice light sheet microscopy.

- A. Collagen labeling for imaging (Figure 2, see also Recipe section, Table 1)
 1. Prepare 0.1 M sodium bicarbonate (pH = 9.3) and cool to 4 °C.
 2. Add 900 µl of 0.1 M sodium bicarbonate to one Cy5 tube (contains sufficient dye to label 1 mg of protein) and add 100 µl of collagen stock solution.
 3. Rotate for 30 min at 4 °C on an overhead rotator (cold room, 4 °C).
 4. Transfer collagen-dye solution into precooled dialysis tubes and place the tube in a beaker filled with 500 ml precooled 0.1% acetic acid (prepared with ddH₂O).
 5. Dialyze labeled collagen for 24 h at 4 °C using a magnetic flea and a magnetic mixer at slow speed. Exchange acetic acid solution 4-5 times to fresh 0.1% acetic acid during the 24 h

- dialysis (minimum of 4 changes in 24 h). Keep in the dark.
6. Transfer labeled collagen into 1.5 ml Eppendorf tube and store in the dark at 4 °C. This solution can be stored for up to one week without affecting polymerization and labeling efficiency.
 7. Before 3D matrix preparation, replace 2.5% of unstained collagen (dry weight, see calculation example in Table 1) with Cy5-stained collagen (1:10 dilution of stock) and calculate new concentration (Table 1). Figure 1 illustrates polymerized collagen imaged using a 40x Nikon Apochromat LWD WI objective (1.15 N.A) for confocal reflection microscopy (488 laser for excitation and a 482/35 filter for reflected light; left) and Cy5-labeled collagen (640nm laser for excitation and a Cy5 filter to measure emitted fluorescent light between 670-700; right).

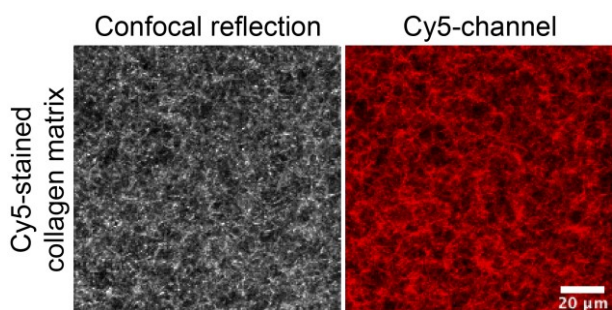


Figure 2. Example of images of 3D matrix containing Cy5-labeled collagen imaged on an inverted confocal microscope. Cy5-labeled collagen was mixed with unlabeled collagen and 2 mg/ml 3D collagen matrix was prepared. Gels were cast in 8-well imaging chambers for imaging using an inverted microscope. Cy5 channel (red) is depicted on the right, and total collagen was visualized using confocal reflection microscopy (left).

B. Modification of collagen through non-enzymatic glycation

Here, the glucose metabolite ribose is used to create intermolecular crosslinks between collagen fibres via glycation to change matrix stiffness (Figure 3).

1. Prepare a 0.5 M ribose stock solution by dissolving ribose in PBS or serum-free phenol-red free DMEM and keep on ice.
2. Determine the change in stiffness you would like to obtain in your 3D matrix. As a guide, 200 mM ribose changes the stiffness from ~200 Pa in unmodified gels to ~800 Pa in ribose modified gels. Increasing concentrations of ribose have been shown to result in a linear increase in stiffness (Roy *et al.*, 2010; Mason *et al.*, 2013).
3. Mix collagen stock solution with ribose solution to obtain a final ribose concentration of e.g., 200 mM and incubate on ice for a minimum of 30 min (recalculate the collagen concentration in the dilution).
4. Keep collagen stock solution on ice until progressing to matrix preparation.

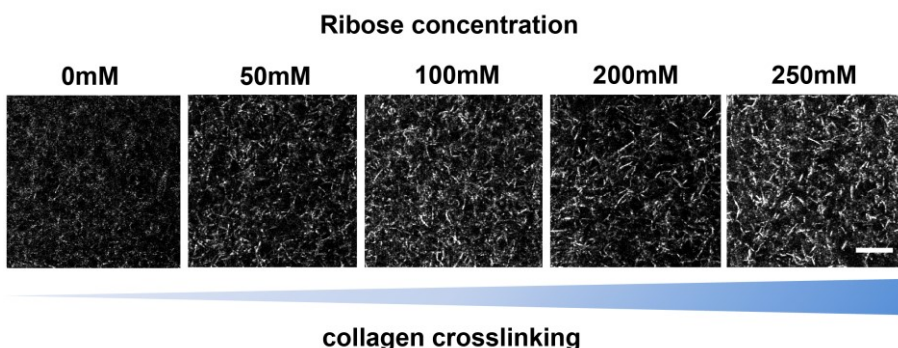


Figure 3. 3D collagen matrix visualized via confocal reflection microscopy. Collagen fibres were crosslinked using ribose-induced glycation and imaged on a confocal microscope. Images highlight increasing matrix modification through glycation-induced crosslinking of collagen fibres. Scale bar = 10 μm .

- C. Coating of glass-bottom chamber slides or glass coverslips to prevent detachment of 3D matrix
 1. Use cleaned glass coverslips or glass-bottom chamber slides before coating with collagen.
 2. Place the coverslips in a 10 cm Petri dish and incubate with a 1:100 dilution of collagen in acetic acid (0.1 mg/ml collagen in 0.1% acetic acid) at 4 °C overnight.
 3. Remove collagen coating solution and wash 2-3 times with 1x PBS.
 4. Store coverslips (in 10 cm Petri dish) or chamber slides covered with PBS at 4 °C (for up to one week), before using as base for 3D matrix preparation.
- D. Cell culture and preparation for imaging
 1. Quickly thaw an aliquot of cancer cells at 37 °C (we used fascin knock-down HeLa cells reconstituted with GFP-fascin, frozen in media plus 10% DMSO) and add 1 ml cells to 6 ml prewarmed phenol-red free high-glucose DMEM supplemented with 10% FCS, 1% Glutamine and 1% Pen/Strep.
 2. Culture cells overnight under standard conditions (37 °C, 5% CO₂ and 95% humidity) and change media next day.
 3. Subculture cells every 2-3 days (at approximately 70-80% confluence) and maintain HeLa cells in a density range of 1 x 10⁶-3 x 10⁶ cells per T25 flask until they recovered from the freeze-thaw process.
 4. To trypsinize cells, remove the media, wash them briefly with 1x PBS and incubate the cells with 1-2 ml of 0.05% Trypsin-EDTA solution at 37 °C (until roughly 80-90% of cells detached from the culture flask).
 5. Add fresh fully supplemented DMEM (> 5 times the volume of Trypsin-EDTA solution), take an aliquot for imaging and subculture the other cells 1:4.
 6. Spin cell aliquot for imaging at 2000 rpm (500 x g) for 4 min and resuspend cell pellet in full medium.

7. Count cells, adjust cell density to 1×10^6 - 2×10^6 cells/ml and put on ice until 3D matrix preparation.
- E. Preparation of 3D collagen-fibronectin matrices with embedded cells (Figure 4, see also Recipe section, Table 2)
1. Choose the desired final volume and characteristics of the matrix/cell solution (stained, unstained, stiffness).
 2. As a general rule, collagen working solutions are made in a twofold concentration and then mixed 1:1 with the cell suspension.
 3. Prepare the 2x collagen working solution containing 40 mM HEPES (final conc. after mixing with cell suspension 20 mM), 40 µg/ml fibronectin (final conc. 20 µg/ml), 0.6% sodium bicarbonate for TC (final percentage 0.3%), serum-free phenol-red free DMEM, and NaOH to neutralize the pH of the solution. Use 20 mM NaOH to neutralize a collagen stock solution in 0.02 N acetic acid (calculated with the volume of collagen stock solution that will be added to prepare collagen working solution) and always calculate in respect to actual acetic acid volume. Please note that the final concentrations will be halved in the collagen-cell solutions (as indicated in brackets).
 4. Mix well and carefully add unstained or stained collagen or ribose-modified collagen to the mix. Try to avoid bubbles! Bubbles can affect the homogeneity of the 3D collagen matrix structure and affect embedded cells. This can have adverse effects on image quality by changes of the refractive index.
 5. Mix final collagen working solution 1:1 with prepared and cooled cell solution by carefully and slowly pipetting up and down.
 6. Keep the final cell density between 5×10^5 - 1×10^6 cells/ml gel to image single cells in 3D matrix (Figure 3 shows a single cancer cell in polymerized collagen matrix).
 7. Immediately transfer the collagen-cell mixture into pre-coated imaging dishes (150-200 µl per 8-well chamber), or pipette 10 µl onto pre-coated 5 mm glass coverslips placed into 12-well plates (one coverslip in each well). Due to the surface tension, the drop of collagen-cell mixture forms a dome on the 5 mm glass coverslip.
 8. Incubate the mixture for 30-60 min at 37 °C in the incubator and allow the collagen to polymerize. Note that the collagen turns turbid when fully solidified. To avoid eventual drying of the collagen-cell mixture, 8-well imaging dishes can be placed into a humidified box, such as a 10 cm dish that contains a water soaked tissue (use sterile water). The incubation time for the coverslips with 10 µl collagen-cell mixture can be limited to 20-30 min.
 9. Gently overlay the collagen-cell matrix with prewarmed full medium.
 10. Incubate collagen-gel matrices at 37 °C for 12 h prior to imaging to allow efficient glycation reactions (only applicable to cells with low matrix degradation activity).
 11. Alternatively, prepare ribose in 0.1% acetic acid and incubate with collagen 2-3 days at 4 °C before matrix preparation (Roy *et al.*, 2010). In this case, the amount of NaOH to neutralize

acetic acid needs to be adjusted to the collagen-ribose solution volume.

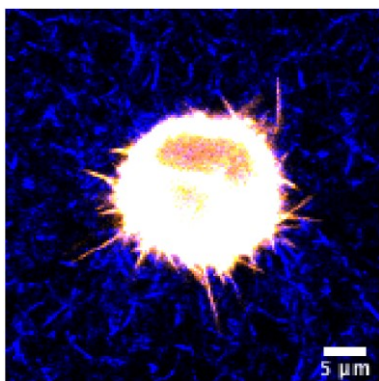


Figure 4. Representative image of a cancer cell in unstained 3D collagen matrix. HeLa cell expressing GFP-fascin (pseudocolored using orange hot LUT) was embedded in 3D collagen-fibronectin matrix and imaged with a water immersion 40x objective on a Nikon Eclipse confocal microscope. Collagen fibres were visualized using confocal reflection microscopy and pseudocolored in blue. Scale bar = 5 μ m.

F. Imaging

1. Prewarm imaging media and exchange media to full medium including 20 mM HEPES, if imaging without CO₂.
2. Preheat imaging chambers and let matrix and cells equilibrate to new environment.
3. Imaging of 3D collagen-cell matrix using confocal microscopy:
 - a. Collagen-cell matrices polymerized in imaging chambers can be imaged at a conventional inverted confocal microscope with heating chamber (37 °C).
 - b. Use a 40x or 60x water immersion objective to allow greater imaging depth in z (imaging depth of ≤ 250 μ m possible, see also section “**Further comments on imaging**”).
 - c. First, focus on the glass coverslip and then move up 50-100 μ m in z (away from coverslip). This minimizes a potential impact of the stiff coverslip on cells.
 - d. Unstained collagen fibres can be visualized using confocal reflection, stained collagen fibres can be visualized using the respective laser and detection setting.
4. Imaging of 3D collagen-cell matrix using a Lattice Light Sheet microscope (LLSM, Figure 5):
 - a. Use collagen-cell matrices on 5 mm coverslips for imaging on the LLSM.
 - b. Coverslips with matrix have to be fixed on the holder before imaging in full medium at 37 °C and 5% CO₂.

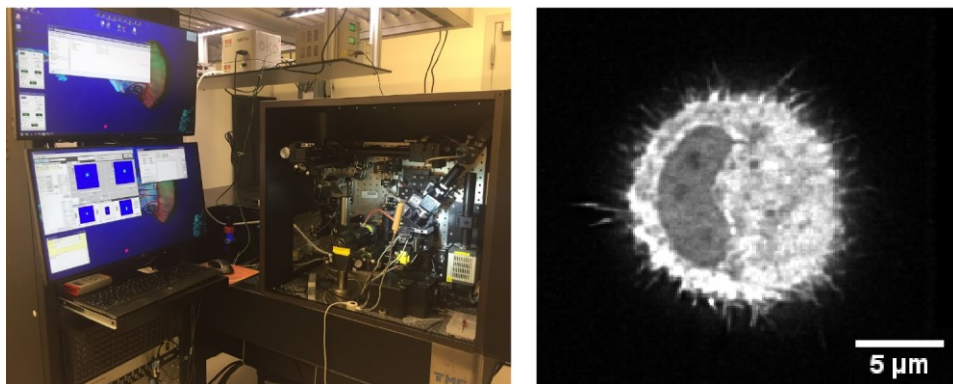


Figure 5. Lattice light sheet microscope imaging. For our experiments we used the Lattice Light Sheet microscope based at the Advanced Imaging Center, Janelia Research campus. The microscope setup is shown on the left, a typical image of a cell in 3D is shown on the right.

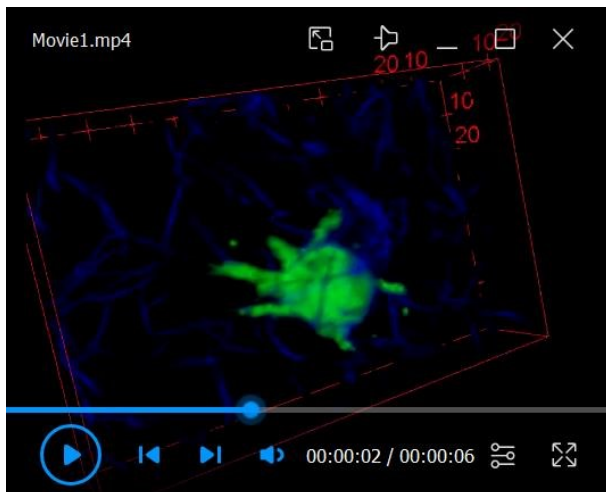
Further comments on imaging

Several microscopes, such as confocal microscopy, structured illumination microscopy (SIM) and light sheet microscopy, can be used to image cells in 3D collagen matrices and all techniques have their own limitations and benefits. We have successfully used confocal microscopy for short time movies (up to 20 min) of cells expressing fluorescently labeled proteins in 3D. However, longer imaging was unsuccessful due to photo-bleaching and photo-toxicity. Also, low expression levels of fluorescently tagged protein and high framerate and laser power can further have an adverse effect on imaging length. Lattice light sheet microscopy overcomes some of those problems as the laser illumination is low and the light more focused. This allows long-term imaging of cells (up to several hours) with low photo-bleaching and photo-toxicity. Further, resolution can be increased when using LLSM instead of confocal microscopy. A major drawback of both imaging techniques is the speed at which 3D structures can be resolved, in particular when multiple fluorophores have to be detected in highly dynamic cells in 3D. As an alternative, 3D-SIM can be used as it allows fast 3D imaging and high resolution compared to the other two methods.

Special attention should be paid to the objective and immersion medium used for imaging cells in 3D matrices. To optimize resolution, which is limited by the diffraction of light, the refractive index of the sample (in our case an aqueous collagen-cell matrix) and the immersion medium should be matched. A mismatch results in spherical aberrations due to a change in the refractive index between the immersion medium and the aqueous 3D matrix and ultimately reduces resolution significantly. Several immersion media are available and all have a particular refractive index n , such as silicone oil ($n = 1.4$), glycerol ($n = 1.47$), oil ($n = 1.52$), water ($n = 1.33$) and air ($n = 1$). As 3D collagen matrices are aqueous, water immersion objectives offer an increased resolution in the z dimension (axial direction) and allow a high penetration depth with limited spherical aberrations compared to the others. This is in particular important when cells or collagen fibres that are further away from the coverslip shall be imaged as the distortion of light is increased with increasing imaging depth in z.

Data analysis

For visualization of time-lapse image sequences, movie generation (see Video 1 for example of 3D rendered cell in collagen), 3D rendering and tracking, we would suggest exploring the following software platforms that we found very useful in our own analysis:



Video 1. Movie of 3D rendered cell in collagen gel

Open-source software:

1. ImageJ/Fiji (<https://imagej.net/Fiji>) (Schindelin *et al.*, 2012)
2. ICY (<http://icy.bioimageanalysis.org/>) (de Chaumont *et al.*, 2012)
3. ZeroCostDL4Mic (<https://github.com/HenriquesLab/ZeroCostDL4Mic/wiki>) (von Chamier *et al.*, 2020)
4. CellProfiler (Broad Institute, <https://cellprofiler.org/>)
5. u-shape3D (<https://github.com/DanuserLab/u-shape3D>) (Driscoll *et al.*, 2019)

Commercial software:

1. Imaris Software (Oxford Instruments, <https://imaris.oxinst.com>)
2. Arivis Vision 4D (Arivis AG, <https://www.arivis.com/de/imaging-science/arivis-vision4d>)
3. Volocity Software (Quorum Technologies, <https://quoruntechnologies.com/volocity>)
4. Matlab (MathWorks, <https://de.mathworks.com/products/matlab.html>)

A comprehensive list of tools to analyse and quantify cell shape, high-dimensional morphometric data and deep learning tools has been summarized recently (Bodor *et al.*, 2020).

Notes

1. We used Telocollagen (acid extracted) for our studies. Using Atelocollagen (enzyme extracted)

may prolong the time until collagen matrix is fully polymerized and could also alter the structure.

2. All work with collagen (especially when using Telocollagen) has to be performed on ice, with precooled solutions, tubes and plates. Handling time should be kept to a minimum.
3. Be very careful with pipetting collagen solutions to avoid bubbles!
4. Keep preparation time constant between experiments to guarantee reproducibility. Non-pepsin treated neutralized collagen solutions can already start to polymerize at 4 °C.
5. Be careful when transporting 3D collagen matrices to the microscopes, as they are very fragile!
6. Preheat media and imaging chambers to 37 °C and let cells adjust to new environment for 30 min before imaging.
7. For confocal reflection microscopy, reflected light from objects in the specimen is detected. In our protocol, collagen fibres are illuminated with a 488 nm laser and the reflected light is measured. The filter setting should be set up to filter reflected light in the range of 465-500 nm (we used a 515 LP filter followed by a 482/35 filter).

Recipes

1. Full Medium
500 ml DMEM
50 ml heat-inactivated FCS
5 ml L-Glutamine (100x)
5 ml Pen Strep (100x)
2. 0.5 M ribose stock solution (MW = 150.13 g/mol)
10 ml PBS or DMEM (w/o FCS, w/o phenol-red)
0.75 g D-ribose
3. 0.1 M Sodium bicarbonate (MW = 84.007 g/mol)
4.2 g sodium bicarbonate powder
Add to 500 ml ddH₂O
Adjust pH to 9.3
4. 0.1% acetic acid
999 ml ddH₂O
1 ml acetic acid
5. Cy5-labeled collagen (Table 1):
Calculation example for preparing a spike-in mixture of Cy5-labeled collagen and unlabelled collagen. 2.5% (dry weight) of unlabeled collagen was exchanged with the same amount of labeled collagen.

Table 1. Mixing in stained collagen. Shown is a calculation scheme example to prepare stained collagen to be used for 3D matrix preparation.

Collagen staining calculation	Volume	Collagen dry weight in mg	Final concentration
Unlabeled collagen stock solution	975 µl	9.75 mg	10 mg/ml
2.5% Cy5 labeled collagen	250 µl	0.25 mg	1 mg/ml
Cy5-collagen solution	1225 µl	10 mg	8.16 mg/ml

6. Soft and stiff collagen matrices (Table 2):

Calculation example for preparing a standard 2 mg/ml 3D collagen matrix with embedded cells. Calculations for soft and stiff matrix are shown. Recalculated new collagen concentration after dilution (for example for stiff collagen preparation or labeled collagen, not shown here).

Table 2. Preparation of 3D matrices with varying mechanical properties. Shown is a pipetting scheme for the preparation of collagen-fibronectin matrices with embedded cells. Volumes are shown for the generation of 1 ml of soft and stiff matrix (200 mM).

Collagen matrix calculation scheme	Soft	Stiff
Collagen stock solution	200 µl	200 µl
0.5M ribose solution (in medium)	-	133.3 µl
	leave on ice for 30 min	
HEPES (stock = 1 M)	20 µl	20 µl
Fibronectin (stock = 1mg/ml)	20 µl	20 µl
1 M NaOH	4 µl	4 µl
Sodium bicarbonate (7.5% solution)	40 µl	40 µl
Phenol-red free medium (serum-free)	216 µl	82.7µl
	mix collagen working solution 1:1 with cell suspension	
Cells in medium	500 µl	500 µl
Final volume of collagen-cell mix	1000 µl	

Acknowledgments

Funding for this work was provided by the Medical Research Council (MR/K015664/1). K. Pfisterer was further funded by the Company of Biologists and the Biochemical Society for travel grants to visit the Janelia Research Campus and the FFG Austria. The LLSM imaging experiments were performed at the Advanced Imaging Center at Howard Hughes Medical Institute Janelia Research Campus. The Advanced Imaging Center is a jointly funded venture of the Gordon and Betty Moore Foundation and the Howard Hughes Medical Institute. We would like to acknowledge Henrietta Lacks for HeLa cells.

Competing interests

The authors declare no competing financial interests.

References

1. Abercrombie, M. (1980). [The Croonian Lecture, 1978-The crawling movement of metazoan cells](#). *Proc Royal Soc B* 207(1167): 129-147.
2. Bodor, D. L., Ponisch, W., Endres, R. G. and Paluch, E. K. (2020). [Of Cell Shapes and Motion: The Physical Basis of Animal Cell Migration](#). *Dev Cell* 52(5): 550-562.
3. Bonnans, C., Chou, J. and Werb, Z. (2014). [Remodelling the extracellular matrix in development and disease](#). *Nat Rev Mol Cell Biol* 15(12): 786-801.
4. de Chaumont, F., Dallongeville, S., Chenouard, N., Herve, N., Pop, S., Provoost, T., Meas-Yedid, V., Pankajakshan, P., Lecomte, T., Le Montagner, Y., Lagache, T., Dufour, A. and Olivo-Marin, J. C. (2012). [Icy: an open bioimage informatics platform for extended reproducible research](#). *Nat Methods* 9(7): 690-696.
5. Driscoll, M. K., Welf, E. S., Jamieson, A. R., Dean, K. M., Isogai, T., Fiolka, R. and Danuser, G. (2019). [Robust and automated detection of subcellular morphological motifs in 3D microscopy images](#). *Nat Methods* 16(10): 1037-1044.
6. Jayo, A., Malboubi, M., Antoku, S., Chang, W., Ortiz-Zapater, E., Groen, C., Pfisterer, K., Tootle, T., Charras, G., Gundersen, G. G. and Parsons, M. (2016). [Fascin Regulates Nuclear Movement and Deformation in Migrating Cells](#). *Dev Cell* 38(4): 371-383.
7. Leithner, A., Eichner, A., Muller, J., Reversat, A., Brown, M., Schwarz, J., Merrin, J., de Gorter, D. J., Schur, F., Bayerl, J., de Vries, I., Wieser, S., Hauschild, R., Lai, F. P., Moser, M., Kerjaschki, D., Rottner, K., Small, J. V., Stradal, T. E. and Sixt, M. (2016). [Diversified actin protrusions promote environmental exploration but are dispensable for locomotion of leukocytes](#). *Nat Cell Biol* 18(11): 1253-1259.
8. Mason, B. N., Starchenko, A., Williams, R. M., Bonassar, L. J. and Reinhart-King, C. A. (2013). [Tuning three-dimensional collagen matrix stiffness independently of collagen concentration modulates endothelial cell behavior](#). *Acta Biomater* 9(1): 4635-4644.
9. Pfisterer, K., Levitt, J., Lawson, C. D., Marsh, R. J., Heddleston, J. M., Wait, E., Ameer-Beg, S. M., Cox, S. and Parsons, M. (2020). [FMNL2 regulates dynamics of fascin in filopodia](#). *J Cell Biol* 219(5). doi: 10.1083/jcb.201906111.
10. Roy, R., Boskey, A. and Bonassar, L. J. (2010). [Processing of type I collagen gels using nonenzymatic glycation](#). *J Biomed Mater Res A* 93(3): 843-851.
11. Schindelin, J., Arganda-Carreras, I., Frise, E., Kaynig, V., Longair, M., Pietzsch, T., Preibisch, S., Rueden, C., Saalfeld, S., Schmid, B., Tinevez, J. Y., White, D. J., Hartenstein, V., Eliceiri, K., Tomancak, P. and Cardona, A. (2012). [Fiji: an open-source platform for biological-image analysis](#). *Nat Methods* 9(7): 676-682.

12. van Helvert, S., Storm, C. and Friedl, P. (2018). [Mechanoreciprocity in cell migration](#). *Nat Cell Biol* 20(1): 8-20.
13. von Chamier, L., Jukkala, J., Spahn, C., Lerche, M., Hernández-Pérez, S., Mattila, P. K., Karinou, E., Holden, S., Solak, A. C., Krull, A., Buchholz, T.-O., Jug, F., Royer, L. A., Heilemann, M., Laine, R. F., Jacquemet, G. and Henriques, R. (2020). [ZeroCostDL4Mic: an open platform to simplify access and use of Deep-Learning in Microscopy](#). bioRxiv: 2020.03.20.000133.
14. Yamada, K. M. and Sixt, M. (2019). [Mechanisms of 3D cell migration](#). *Nat Rev Mol Cell Biol* 20(12): 738-752.